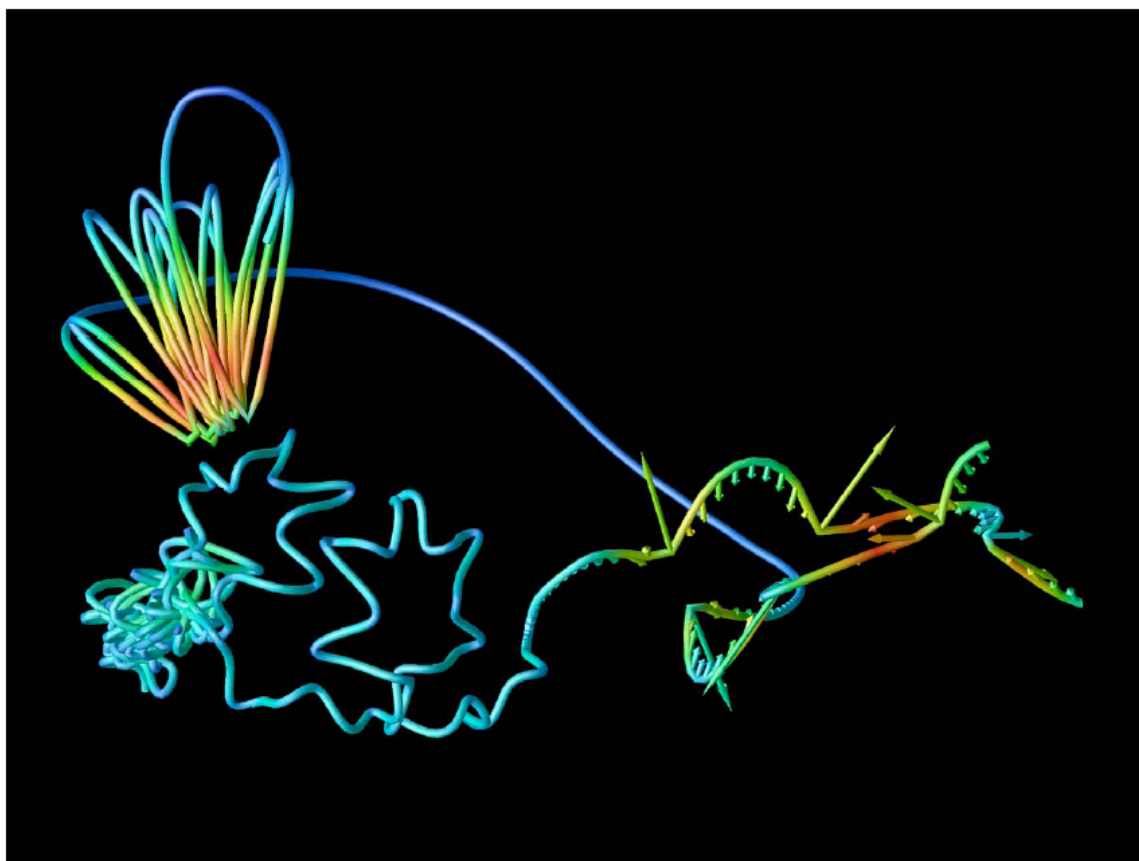


# 27<sup>th</sup> Annual Combustion Research Conference



Wintergreen Conference Center  
Wintergreen, Virginia  
May 30 – June 2, 2006



*Office of Basic Energy Sciences*

Chemical Sciences, Geosciences & Biosciences Division

**Cover Image:** A sample roaming trajectory yielding  $H_{2v}=6$  and  $j_{CO}=5$ . H atom speeds are encoded in trajectory color, and forces (direction and magnitude) are shown in the abstraction region. Only the H atoms are shown. The trajectory begins at left and ends with departure of  $H_2$  at right. **Arthur Suits, pg. 276**

## FOREWORD

The achievement of National goals for energy conservation and environmental protection will rely on technology more advanced than we have at our disposal today. Combustion at present accounts for 85% of the energy generated and used in the U.S. and is likely to remain a dominant source of energy for the coming decades. Achieving energy conservation while minimizing unwanted emissions from combustion processes could be greatly accelerated if accurate and reliable means were at hand for quantitatively predicting process performance. Given current and future fuel costs and climatic impacts, a predictive, science-based approach to energy utilization is necessary.

The reports appearing in this volume present work in progress in basic research contributing to the development of a predictive capability for combustion processes. The work reported herein is supported by the Department of Energy's Office of Basic Energy Sciences (BES) and in large measure by the chemical physics program. The long-term objective of this effort is the provision of theories, data, and procedures to enable the development of reliable computational models of combustion processes, systems, and devices.

The development of reliable models for combustion requires the accurate knowledge of chemistry, turbulent flow, and the interaction between the two at temperatures and pressures characteristic of the combustion environment. In providing this knowledge, the research supported by BES addresses a wide range of continuing scientific issues of long standing.

- For even the simplest fuels, the chemistry of combustion consists of hundreds of reactions. Key reaction mechanisms, the means for developing and testing these mechanisms, and the means for determining which of the constituent reaction rates are critical for accurate characterization are all required.
- For reactions known to be important, accurate rates over wide ranges of temperature, pressure and composition are required. To assess the accuracy of measured reaction rates or predict rates that would be too difficult to measure, theories of reaction rates and means for calculating their values are needed. Of particular importance are reactions involving open shell systems such as radicals and excited electronic states.
- To assess the accuracy of methods for predicting chemical reaction rates, the detailed, state-specific dynamics of prototypical reactions must be characterized.
- Methods for observing key reaction species in combustion environments, for interpreting these observations in terms of species concentrations, and for determining which species control the net reactive flux are all required
- Energy flow and accounting must be accurately characterized and predicted.
- Methods for reducing the mathematical complexity inherent in hundreds of reactions, without sacrificing accuracy and reliability are required. Methods for reducing the computational complexity of computer models that attempt to address turbulence, chemistry, and their interdependence and also needed.

Although the emphasis in this list is on the development of mathematical models for simulating the gas phase reactions characteristic of combustion, such models, from the

chemical dynamics of a single molecule to the performance of a combustion device, require validation by experiment. Hence, the DOE program represented by reports in this volume supports the development and application of new experimental tools in chemical dynamics, kinetics, and spectroscopy.

The success of this research effort will be measured by the quality of the research performed, the profundity of the knowledge gained, as well as the degree to which it contributes to goals of resource conservation and environmental stewardship. In fact, without research of the highest quality, the application of the knowledge gained to practical problems will not be possible.

The emphasis on modeling and simulation as a basis for defining the objectives of this basic research program has a secondary but important benefit. Computational models of physical processes provide the most efficient means for ensuring the usefulness and use of basic theories and data. The importance of modeling and simulation remains well recognized in the Department of Energy and is receiving support through the Scientific Discovery through Advanced Computing (SciDAC) initiative; several work-in-progress reports funded through SciDAC are included in this volume.

During the past year, this program has benefited greatly from the involvement of Dr. Richard Hilderbrandt, program manager for Chemical Physics and for Computational and Theoretical Chemistry, and Dr. Eric Rohlfing, team leader for the Fundamental Interactions programs. Finally, the efforts of Sophia Kitts, Kellye Sliger and Rachel Smith of the Oak Ridge Institute for Science Education and Diane Marceau of the Division of Chemical Sciences, Geosciences, and Biosciences, Office of Basic Energy Sciences in the arrangements for the meeting are also much appreciated.

Frank P. Tully, SC-22.1  
Division of Chemical Sciences, Geosciences, and Biosciences  
Office of Basic Energy Sciences

May 30, 2006



## Wednesday, May 31, 2006

### Evening Session Marsha Lester, Chair

6:15 pm	“Laser Photoelectron Spectroscopy of Ions”, G. Barney Ellison .....	60
6:45 pm	“Detection and Characterization of Free Radicals Relevant to Combustion Processes”, Terry A. Miller .....	193
7:15 pm	“Dynamical Analysis of Highly Excited Molecular Spectra”, Michael E. Kellman .....	131
7:45 pm	<b>Break</b>	
8:00 pm	“Ionization Probes of Molecular Structure and Chemistry”, Philip M. Johnson .....	123
8:30 pm	“Optical Probes of Atomic and Molecular Decay Processes”, Stephen T. Pratt .....	240
9:00 pm	“Time-resolved Structural Probes of Molecular Dynamics”, Peter M. Weber .....	303

## Thursday, June 1, 2006

7:00 am	<b>Breakfast</b> <b>Morning Session</b> Charles Westbrook, Chair	
8:15 am	“Mechanism and Detailed Modeling of Soot Formation”, Michael Frenklach .....	81
8:45 am	“Theoretical Studies of Molecular Systems”, William A. Lester, Jr. ....	158
9:15 am	“Reacting Flow Modeling with Detailed Chemical Kinetics”, Habib N. Najm .....	209
9:45 am	<b>Break</b>	
10:15 am	“Gas Phase Molecular Dynamics: High-Resolution Spectroscopic Probes of Chemical Dynamics”, Gregory E. Hall .....	95
10:45 am	“Universal and State-Resolved Imaging Studies of Chemical Dynamics”, Arthur G. Suits .....	276
11:15 am	“Investigating the Chemical Dynamics of Bimolecular Reactions of Dicarbon and Tricarbon Molecules with Hydrocarbons in Combustion Flames”, Ralf I. Kaiser .....	127
12:00 pm	<b>Lunch</b>	

**Thursday, June 1, 2006**  
**Afternoon and Evening Session**  
*Trevor Sears, Chair*

<b>5:15 pm</b>	<i>“Photoelectron Photoion Coincidence Studies: Heats of Formation of Ions, Molecules, and Free Radicals”</i> , Tomas Baer .....	1
<b>5:45 pm</b>	<i>“Dynamics of Activated Molecules”</i> , Amy S. Mullin .....	205
<b>6:15 pm</b>	<b><i>Break</i></b>	
<b>6:30 pm</b>	<i>“Photoinitiated Reactions of Radicals and Diradicals in Molecular Beams”</i> , Hanna Reisler.....	244
<b>7:00 pm</b>	<i>“State Controlled Photodissociation of Vibrationally Excited Molecules and Hydrogen Bonded Dimers”</i> , F. Fleming Crim.....	41
<b>7:30 pm</b>	<b><i>Cash Bar</i></b>	
<b>8:00 pm</b>	<b><i>Dinner</i></b>	

**Friday, June 2, 2005**

**7:00 am**        ***Breakfast***

**Morning Session**  
***Joe Michael, Chair***

<b>8:15 am</b>	<i>“Kinetics of Combustion-Related Processes at High Temperatures”</i> , John H. Kiefer .....	139
<b>8:45 am</b>	<i>“Spectroscopy and Kinetics of Combustion Gases”</i> , Ronald K. Hanson.....	103
<b>9:15 am</b>	<i>“Chemical Kinetic Data Base for Combustion Modeling”</i> , Wing Tsang.....	296
<b>9:45 am</b>	<b><i>Break</i></b>	
<b>10:00 am</b>	<i>“Kinetics of Elementary Processes Relevant to Incipient Soot Formation”</i> , M. C. Lin .....	165
<b>10:30 am</b>	<i>Closing Remarks</i> , Frank P. Tully	
<b>11:00 am</b>	<b><i>Lunch</i></b>	

## COMBUSTION SIMULATION, VERIFICATION, VALIDATION AND INNOVATION



**Philip J. Smith, professor & chair, Chemical Engineering, The University of Utah**

### **Abstract**

Producing truly predictive simulations of real world processes has been identified by many national panels as the key enabling technology for rapid analysis and deployment of new technologies for addressing the tension between increasing global demand for energy and the increasing concerns over global warming from green-house gases. Producing combustion simulations with quantified uncertainty requires a balance in tensions between the needs of engineering application and the wants of science fundamentals, between quantum scales and equipment scales, between the reality of the cyber infrastructure and the thirst for data, between computer science and physics, and between many other tensions too. This presentation will argue for more widespread development and adoption of formal methods of verification and validation in order to resolve these tensions and to advance the ability of computational science to provide real innovation tools to the combustion community.

### **Biographical Sketch**

Professor Philip J. Smith is a professor of Chemical Engineering at the University of Utah and is the current chair of the Department of Chemical Engineering. He is the director of the Utah Heavy Oil Center (UHOC) and is a member of the directorate of the Center for the Simulation of Accidental Fires and Explosions (CSAFE). He was one of three founding partners of Reaction Engineering International (REI), a consulting firm that uses combustion simulation software originally developed by Phil and his students for problem solving and design of coal and gas combustion boilers, furnaces and gasifiers.

# Table of Contents

<i>Photoelectron Photoion Coincidence Studies: Heats of Formation of Ions, Molecules, and Free Radicals</i> <b>Tomas Baer</b>	1	<i>Scanning Tunneling Microscopy Studies of Chemical Reactions on Surfaces</i> <b>George Flynn</b>	73
<i>Turbulence-Chemistry Interactions in Reacting Flows</i> <b>Robert S. Barlow</b>	5	<i>Quantitative Imaging Diagnostics for Reacting Flows</i> <b>Jonathan H. Frank</b>	77
<i>Theoretical Studies of Combustion Dynamics</i> <b>Joel M. Bowman</b>	9	<i>Mechanism and Detailed Modeling of Soot Formation</i> <b>Michael Frenklach</b>	81
<i>Combustion Chemistry</i> <b>Nancy J. Brown</b>	13	<i>Chemical Dynamics in The Gas Phase: Quantum Mechanics Of Chemical Reactions</i> <b>Stephen K. Gray</b>	85
<i>Probing Radical Intermediates of Bimolecular Combustion Reactions</i> <b>Laurie J. Butler</b>	17	<i>Computer-Aided Construction of Chemical Kinetic Models</i> <b>William H. Green, Jr.</b>	89
<i>Joint Theoretical and Experimental Study of Key Radicals in Hydrocarbon Combustion</i> <b>Barry K. Carpenter</b>	21	<i>Wave Packet Based Statistical Model for Complex-Forming Reactions</i> <b>Hua Guo</b>	93
<i>Ion Imaging Studies of Bimolecular Collision Dynamics</i> <b>David W. Chandler</b>	25	<i>Gas Phase Molecular Dynamics: High-Resolution Spectroscopic Probes of Chemical Dynamics</i> <b>Gregory E. Hall</b>	95
<i>Terascale Direct Numerical Simulation and Modeling of Turbulent Combustion</i> <b>Jacqueline H. Chen, Evatt R. Hawkes, Ramanan Sankaran, David Lignell, and Chun S. Yoo</b>	29	<i>Flame Chemistry and Diagnostics</i> <b>Nils Hansen</b>	99
<i>Dynamics and Energetics of Elementary Combustion Reactions and Transient Species</i> <b>Robert E. Continetti</b>	33	<i>Spectroscopy and Kinetics of Combustion Gases at High Temperatures</i> <b>Ronald K. Hanson and Craig T. Bowman</b>	103
<i>Studies of Flame Chemistry with Photoionization Mass Spectrometry</i> <b>Terrill A. Cool</b>	37	<i>Theoretical Studies of Potential Energy Surfaces</i> <b>Lawrence B. Harding</b>	107
<i>State Controlled Photodissociation of Vibrationally Excited Molecules and Hydrogen Bonded Dimers</i> <b>F.F. Crim</b>	41	<i>Chemical Accuracy From Ab Initio Molecular Orbital Calculations</i> <b>Martin Head-Gordon</b>	111
<i>Spectroscopy and Energy Transfer Dynamics of Highly Vibrationally Excited Molecules and Transient Radicals</i> <b>Hai-Lung Dai</b>	44	<i>Laser Studies of Combustion Chemistry</i> <b>John F. Hershberger</b>	115
<i>Bimolecular Dynamics of Combustion Reactions</i> <b>H. Floyd Davis</b>	48	<i>Terascale High-Fidelity Simulations of Turbulent Combustion With Detailed Chemistry</i> <b>Hong G. Im, Arnaud Trouvé, Christopher J. Rutland, Jacqueline Chen</b>	119
<i>Multiple-Time-Scale Kinetics</i> <b>Michael J. Davis</b>	52	<i>Ionization Probes of Molecular Structure and Chemistry</i> <b>Philip M. Johnson</b>	123
<i>Comprehensive Mechanisms for Combustion Chemistry: Experiment, Modeling, And Sensitivity Analysis</i> <b>Frederick L. Dryer</b>	56	<i>Investigating the Chemical Dynamics of Bimolecular Reactions of Dicarbon and Tricarbon Molecules With Hydrocarbons in Combustion Flames</i> <b>Ralf I. Kaiser</b>	127
<i>Laser Photoelectron Spectroscopy of Ions</i> <b>G. Barney Ellison</b>	60	<i>Dynamical Analysis of Highly Excited Molecular Spectra</i> <b>Michael E. Kellman</b>	131
<i>Hydrocarbon Radical Thermochemistry: Gas-Phase Ion Chemistry Techniques</i> <b>Kent M. Ervin</b>	65	<i>High Energy Processes</i> <b>Alan R. Kerstein</b>	135
<i>Spectroscopic and Dynamical Studies of Highly Energized Small Polyatomic Molecules</i> <b>Robert W. Field</b>	69	<i>Kinetics of Combustion-Related Processes at High Temperatures</i> <b>J. H. Kiefer</b>	129

<i>Theoretical Chemical Kinetics</i> <b>Stephen J. Klippenstein</b>	143	<i>Spectroscopy, Kinetics and Dynamics of Jet-Cooled Combustion Radicals</i> <b>Feng Dong, Chandra Savage, Melanie Roberts, Richard Walters, and David J. Nesbitt</b>	213
<i>Theoretical Modeling of Spin-Forbidden Channels in Combustion Reactions</i> <b>Anna I. Krylov</b>	147	<i>Radical Photochemistry and Photophysics</i> <b>Daniel Neumark</b>	216
<i>Time-Resolved FTIR Emission and Advanced Light Source Studies of Photofragmentation, Radical Reactions, and Aerosol Chemistry</i> <b>Stephen R. Leone</b>	151	<i>Determination of Accurate Energetic Database for Combustion Chemistry by High-Resolution Photoionization and Photoelectron Methods</i> <b>C. Y. Ng</b>	220
<i>Intermolecular Interactions of Hydroxyl Radicals on Reactive Potential Energy Surfaces</i> <b>Marsha I. Lester</b>	155	<i>Large Eddy Simulation of Turbulence-Chemistry Interactions in Reacting Flows</i> <b>Joseph C. Oefelein</b>	224
<i>Theoretical Studies of Molecular Systems</i> <b>William A. Lester, Jr.</b>	158	<i>Kinetics and Dynamics of Combustion Chemistry</i> <b>David L. Osborn</b>	228
<i>Quantum Dynamics of Fast Chemical Reactions</i> <b>John C. Light</b>	161	<i>Large amplitude motion and the birth of novel modes of vibration in energized molecules</i> <b>David S. Perry</b>	232
<i>Kinetics of Elementary Processes Relevant to Incipient Soot Formation</i> <b>M. C. Lin</b>	165	<i>Investigation of Non-Premixed Turbulent Combustion</i> <b>Stephen B. Pope</b>	236
<i>Investigation of Polarization Spectroscopy and Degenerate Four-Wave Mixing for Quantitative Concentration Measurements</i> <b>Robert P. Lucht</b>	169	<i>Optical Probes of Atomic and Molecular Decay Processes</i> <b>Stephen T. Pratt</b>	240
<i>Time-Resolved Infrared Absorption Studies of the Dynamics of Radical Reactions</i> <b>R. G. Macdonald</b>	173	<i>Photoinitiated Reactions of Radicals and Diradicals in Molecular Beams</i> <b>Hanna Reisler</b>	244
<i>Quantum Chemical Studies of Chemical Reactions Related to the Formation of Polyaromatic Hydrocarbons and of Spectroscopic Properties of Their Key Intermediates</i> <b>Alexander M. Mebel</b>	177	<i>High Accuracy Calculation of Electronic Structure, Molecular Bonding and Potential Energy Surfaces</i> <b>Klaus Ruedenberg</b>	248
<i>Flash Photolysis-Shock Tube Studies</i> <b>Joe V. Michael</b>	181	<i>Active Thermochemical Tables – Progress Report</i> <b>Branko Ruscic</b>	252
<i>Particle Diagnostics Development</i> <b>H. A. Michelsen</b>	185	<i>Theoretical Studies of Elementary Hydrocarbon Species and Their Reactions</i> <b>Henry F. Schaefer III and Wesley D. Allen</b>	256
<i>Chemical Kinetics and Combustion Modeling</i> <b>James A. Miller</b>	189	<i>Gas Phase Molecular Dynamics: Spectroscopy and Dynamics of Transient Species</i> <b>Trevor J. Sears</b>	261
<i>Detection and Characterization of Free Radicals Relevant to Combustion Processes</i> <b>Terry A. Miller</b>	193	<i>Picosecond Nonlinear Optical Diagnostics</i> <b>Thomas B. Settersten</b>	264
<i>Reaction Dynamics in Polyatomic Molecular Systems</i> <b>William H. Miller</b>	197	<i>Theoretical Studies of Potential Energy Surfaces and Computational Methods</i> <b>Ron Shepard</b>	268
<i>Gas-Phase Molecular Dynamics: Theoretical Studies of Combustion-Related Chemical Reactions and Molecular Spectra</i> <b>James T. Muckerman</b>	201	<i>Computational and Experimental Study of Laminar Flames</i> <b>M. D. Smooke and M. B. Long</b>	272
<i>Dynamics of Activated Molecules</i> <b>Amy S. Mullin</b>	205	<i>Universal and State-Resolved Imaging Studies of Chemical Dynamics</i> <b>Arthur G. Suits</b>	276
<i>Reacting Flow Modeling With Detailed Chemical Kinetics</i> <b>Habib N. Najm</b>	209	<i>Elementary Reaction Kinetics of Combustion Species</i> <b>Craig A. Taatjes</b>	280

<i>Theoretical Chemical Dynamics Studies of Elementary Combustion Reactions</i> <b>Donald L. Thompson</b>	284
<i>Elementary Reactions of PAH Formation</i> <b>Robert S. Tranter</b>	288
<i>Variational Transition State Theory</i> <b>Donald G. Truhlar</b>	292
<i>Chemical Kinetic Data Base for Combustion Modeling</i> <b>Wing Tsang</b>	296
<i>Single-Collision Studies of Energy Transfer and Chemical Reaction</i> <b>James J. Valentini</b>	300
<i>Time-Resolved Structural Probes of Molecular Dynamics</i> <b>Peter M. Weber</b>	303
<i>Chemical Kinetic Modeling of Combustion Chemistry</i> <b>William J. Pitz and Charles K. Westbrook</b>	307
<i>Probing Flame Chemistry with MBMS, Theory, and Modeling</i> <b>Phillip R. Westmoreland</b>	311
<i>Photoinitiated Processes in Small Hydrides</i> <b>Curt Wittig</b>	315
<i>Theoretical Studies of the Reactions and Spectroscopy of Radical Species Relevant to Combustion Reactions and Diagnostics</i> <b>David R. Yarkony</b>	319
<i>Gas Phase Molecular Dynamics: Quantum Molecular Dynamics of Combustion Reactants and Molecular Spectroscopy Calculations</i> <b>Hua-Gen Yu</b>	322
<i>Experimental Characterization of the Potential Energy Surfaces for Conformational Isomerization in Aromatic Fuels</i> <b>Timothy S. Zwier</b>	326
<b>Author Index</b>	331
<b>Participants</b>	333



***Progress report – March, 2006***  
**Photoelectron Photoion Coincidence Studies: Heats of Formation of Ions,  
Molecules, and Free Radicals**

Tomas Baer ([baer@unc.edu](mailto:baer@unc.edu))  
Department of Chemistry  
University of North Carolina  
Chapel Hill, NC 27599-3290  
DOE Grant DE-FG02-97ER14776

## **Program Scope**

The threshold photoelectron photoion coincidence (TPEPICO) technique is utilized to investigate the dissociation dynamics and thermochemistry of energy selected medium to large organic molecular ions. The reactions include parallel and consecutive steps that are modeled with the statistical theory in order to extract dissociation onsets for multiple dissociation paths. These studies are carried out with the aid of molecular orbital calculations of both ions and the transition states connecting the ion structure to their products. The results of these investigations yield accurate heats of formation of ions, free radicals, and stable molecules. In addition, they provide information about the potential energy surface that governs the dissociation process. Isomerization reactions prior to dissociation are readily inferred from the TPEPICO data.

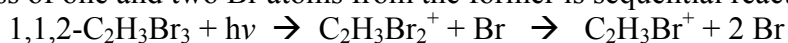
## **The PEPICO Experiment**

The threshold photoelectron photoion coincidence (TPEPICO) experiment in Chapel Hill is carried out with a laboratory H<sub>2</sub> discharge light source. Threshold electrons are collected by velocity focusing them into a 1.5 mm hole on a mask located at the end of the 12 cm drift tube. Some hot electrons pass through a 2x5 mm opening located next to the central 1.5 mm hole. In this fashion, two TPEPICO spectra are simultaneously collected, one for threshold and one for hot electrons. Hot electron free data are obtained by subtracting a fraction of the hot from the threshold TPEPICO data. The ion TOF is either a linear version or a reflectron for studying H loss processes. The electrons provide the start signal for measuring the ion time of flight distribution. When ions dissociate in the microsecond time scale, their TOF distributions are asymmetric. The dissociation rate constant can be extracted by modeling the asymmetric TOF distribution. A high-resolution version of this experiment is currently being constructed in collaboration with Thomas Gerber at the Swiss Light Source (SLS), a synchrotron that will have a gas phase chemical dynamics beamline. Because of the high photon flux, we plan on developing the first multi-start multi-stop coincidence scheme using a master clock as the time base. When combined with coincidence ion detection, the results will permit the measurement of ion dissociation limits to within 1 meV or 0.1 kJ/mol.

## **Recent Results**

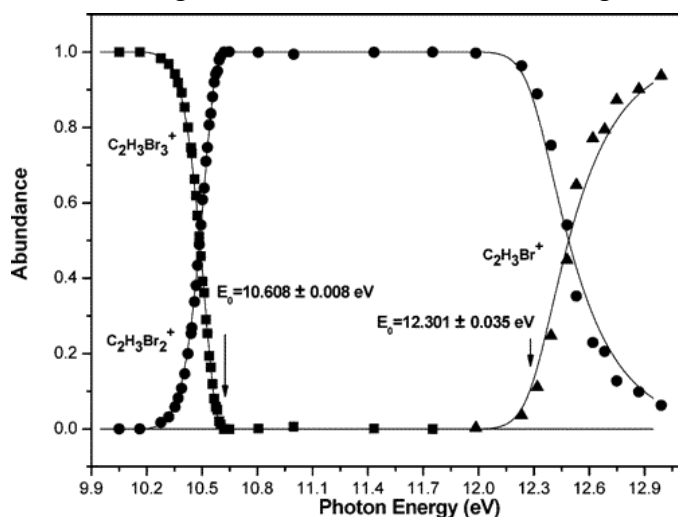
### ***The Heats of Formation of vinyl bromide and vinyl radical***

The threshold photoelectron photoion coincidence (TPEPICO) technique has been used to measure accurate dissociative photoionization onsets of 1,1,2 tribromoethane and vinyl bromide. The loss of one and two Br atoms from the former is sequential reaction:



whose dissociation onsets, modeled by simulating the breakdown diagram are shown in Figure 1.

an interesting feature in this breakdown diagram is the slope at the two cross over energies,

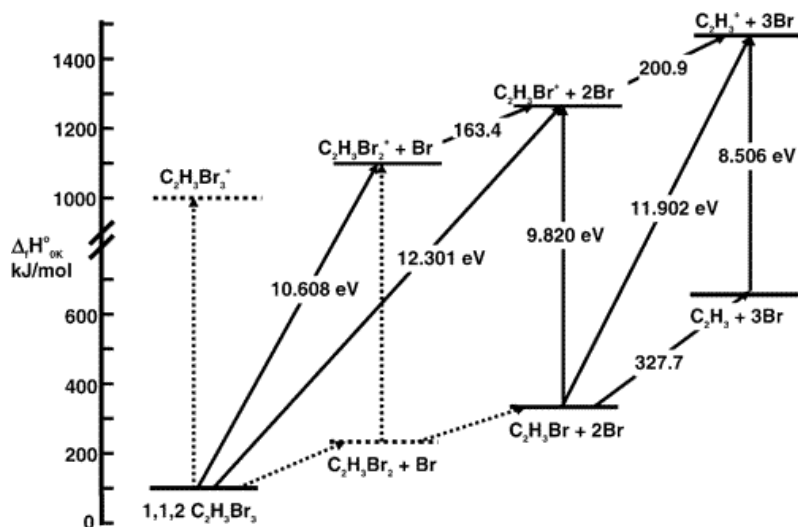


which is steep for the first Br loss and more gentle for the second Br atom loss. The slope for the first one is determined by the thermal energy distribution of our room temperature sample. However, the second reaction is determined by the internal energy distribution of  $C_2H_3Br_2^+$ , which is a product of the first dissociation, and thus has a broader energy distribution because the first Br atom carries off translational energy. This internal energy distribution can be calculated with microcanonical statistical theory:

$$P_{C_2H_3Br_2^+}(E_i) \propto \rho_{C_2H_3Br_2^+}(E_i) \rho_{Br}(E - E_0 - E_i)$$

which assumes that the energy is partitioned statistically among all thermal and external degrees of freedom during the dissociation event. The only input is the set of vibrational frequencies for the product ion. We assume two translational degrees of freedom for the departing fragments. Because the frequencies are known from calculations, the only adjustable parameter for fitting the breakdown diagram is the onset energy for the second Br loss. The fact that it fits so well, indicates that the statistical energy partitioning is near perfect, a conclusion that agrees with results of a number of other sequential ionic reactions that we have investigated.

The loss of two Br atoms from 1,1,2- $C_2H_3Br_3^+$  leads to  $C_2H_3Br^+$  (vinyl bromide). Because our laboratory photon source is limited to  $E < 14$  eV, there was insufficient energy to break the final Br bond to form the vinyl ion. Instead we started from the vinyl bromide neutral and measured the dissociative photoionization onset to produce  $C_2H_3^+ + Br$ , which yielded an onset of  $11.902 \pm .008$  eV. This reaction had also been studied by Ng and co-workers in 2004



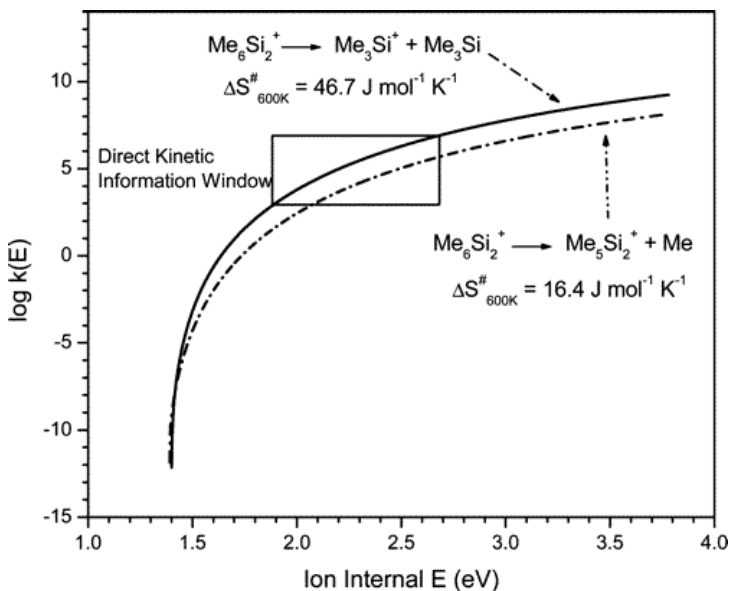
using PFI-PEPICO at the ALS, who reported an onset of  $11.901 \pm .0015$  eV, an onset that agrees very well with our own measurement, although our error bars were much higher. By anchoring the energy to a calculated (W1 theory) value for the vinyl ion ( $\Delta_f H_{298K}^0 = 1116.1 \pm 3.0$  kJ/mol), we were able to determine the heats of formation of a number of species including vinyl bromide ( $53.5 \pm 4.3$ ). The energy diagram shown in Figure 2 summarizes the results. The

dashed lines are not yet measured. However, if someone were to measure the IE of  $C_2H_3Br_2^\bullet$ , both neutral bond energies for the tri-bromoethane would be established.

*Thermochemistry and Dissociative Photoionization of Si(CH<sub>3</sub>)<sub>4</sub>, BrSi(CH<sub>3</sub>)<sub>3</sub>, ISi(CH<sub>3</sub>)<sub>3</sub>, and Si<sub>2</sub>(CH<sub>3</sub>)<sub>6</sub> and their Ge analogues studied by TPEPICO spectroscopy*

In a series of three submitted papers, we investigated the Silane and Germane thermochemistry. One of the results is a very accurate  $\Delta_f H_{298}^{\circ}(\text{Me}_3\text{Si}^{\bullet})$  of  $14.8 \pm 2.0$  kJ/mol, which yields a Si-Si

bond dissociation energy of  $333.3 \pm 5.8$  kJ/mol, whose error limit is determined by the di-silane heat of formation. Among the interesting aspects are the derived rate constants (Figure 3) that we measured over a dynamic range of four orders of magnitude from  $2 \times 10^3 - 2 \times 10^7$  sec<sup>-1</sup>. This permits us to extrapolate this rate down to the onset energy. However, how accurate is this extrapolation, which assumes simple RRKM theory? Because the data are quite self consistent, it seems to work very well. But, we plan on testing this with future experiments on halobenzenes.



## Future Plans

We have begun to carry out temperature controlled TPEPICO experiments (-40 C to +60 C) in order to directly measure a molecule's thermal energy distribution. The goal is to learn about free and hindered rotors in long chain hydrocarbons. Also, we have initiated the measurement of  $k(E)$  curves for halobenzenes because the dissociation to  $\text{C}_6\text{H}_5^+ + \text{X}$  is now well established. We will obtain curves much as those in Figure 3 above, with which we can test RRKM, VTST, and SACM models for rate constants.

Because PEPICO is not part of the Chemical Dynamics Beamline plans, we have begun constructing a new TPEPICO experiment which includes velocity focusing with an imaging detector for electrons at the Swiss Light Source (SLS). It will be possible to carry out these experiments with a resolution of 1 meV (0.1 kJ/mol). A molecular beam free radical source will permit us to obtain threshold photoelectron spectra with 1 meV resolution and thus to determine IE's to a very high precision. Among the molecules planned are a series of organometallic complexes for which we will obtain neutral Metal-Ligand bond energies, as well as solvent molecule binding energies.

### Publications from DOE supported work 2004 – 2006

E.A. Fogleman, H. Koizumi, J. Kercher, B. Sztaray, and T. Baer, The Heats of Formation of the Acetyl radical and Ion obtained by Threshold Photoelectron Photoion Coincidence, *J. Phys. Chem. A* **108** 5288-5294 (2004)

H. Koizumi and T. Baer, The heats of formation of *t*-butyl isocyanide and other alkyl isocyanides by photoelectron photoion coincidence spectroscopy, *J. Phys. Chem. A* **108** 5956-5961 (2004)

A. Bodi, J. P. Kercher, T. Baer, and B. Sztáray On the Parallel Mechanism of the Dissociation of Energy-Selected  $\text{P}(\text{CH}_3)_3^+$  Ions, *J. Phys. Chem. B* **109** 8393-8399 (2005).

Adam Brooks,<sup>a</sup> Kai-Chung Lau,<sup>b</sup> C.Y. Ng,<sup>b</sup> and Tomas Baer<sup>a</sup> The C<sub>3</sub>H<sub>7</sub><sup>+</sup> Appearance Energy from 2-Iodopropane and 2-Chloropropane Studied by Threshold Photoelectron Photoion Coincidence, *European J. of Mass Spectrom.*, **10** 819-828 (2004)

A.F. Lago, J.P. Kercher, A. Bodi, B. Sztáray, B. Miller, D. Wurzelmann, and T. Baer, The heats of formation of the dihalomethanes, CH<sub>2</sub>XY, (X,Y = Cl, Br, and I), by threshold photoelectron photoion coincidence, *J.Phys.Chem.A* **109** 1802-1809 (2005)

J.P. Kercher, E.A. Fogleman, H. Koizumi, B. Sztáray, and T. Baer, The Heats of Formation of the Propionyl ion and Radical and 2,3 Pentanedione by Threshold Photoelectron Photoion Coincidence Spectroscopy, *J. Phys. Chem. A* **109** 939-946 (2005)

T. Baer, B. Sztáray, J. P. Kercher, A.F. Lago, A. Bödi, C. Skull, and D. Palathinkal, Threshold Photoelectron Photoion Coincidence Studies of Parallel and Sequential Dissociation Reactions, *Phys. Chem. Chem. Phys.* **7** 1507-1513 (2005)

J.Z. Davalos, A.F. Lago, and T. Baer, Thermochemical study of the liquid phase equilibrium reaction of dihalomethanes by NMR spectroscopy, *Chem. Phys. Lett.* **409** 230-234 (2005)

Z. Gengeliczki, B. Sztaray, T. Baer, C. Iceman, and P.B. Armentrout, Heats of Formation of Co(CO)<sub>2</sub>NOPR<sub>3</sub>, R = CH<sub>3</sub> and C<sub>2</sub>H<sub>5</sub>, and Its Ionic Fragments, *J. Am. Chem. Soc.* **127** 9393-9402, (2005)

A.F. Lago and T. Baer, A Photoelectron photoion coincidence study of the vinyl bromide and tribromoethane ion dissociation dynamics: Heats of formation of C<sub>2</sub>H<sub>3</sub><sup>+</sup>, C<sub>2</sub>H<sub>3</sub>Br, C<sub>2</sub>H<sub>3</sub>Br<sup>+</sup>, C<sub>2</sub>H<sub>3</sub>Br<sub>2</sub><sup>+</sup> and C<sub>2</sub>H<sub>3</sub>Br<sub>3</sub>, *J. Phys. Chem. A.* (2006) ASAP

M. Hochlaf, T. Baer, X.-M. Qian, and C.Y. Ng, A vacuum ultraviolet pulsed field ionization-photoelectron study of cyanogen cation in the energy range of 13.2-15.9 eV, *J. Chem. Phys.* **123** 144302 (2005)

A. Bodi, B. Sztaray, and T. Baer, Dissociative Photoionization of Mono-, Di- and Trimethylamine Studied by a Combined Threshold Photoelectron Photoion Coincidence Spectroscopy and Computational Approach, *Phys.Chem.Chem.Phys.* **8**, 613-623 (2006)

H. Koizumi, J. Davalos, and T. Baer, Heats of Formation of GeH<sub>4</sub>, GeF<sub>4</sub> and Ge(CH<sub>3</sub>)<sub>4</sub>, *Chem. Phys.* In press (2005)

A. Lago and T. Baer Dissociation dynamics and thermochemistry of chloroform and tetrachloroethane molecules studied by threshold photoelectron photoion coincidence, *Int. J. Mass Spectrom.* (2006) in press

James P. Kercher, Bálint Sztáray, and Tomas Baer, On the dissociation of 2-Pentanone ions by threshold photoelectron photoion coincidence spectroscopy, *Int. J. Mass Spectrom.* **249/250**, 403-411 (2006)

Juan Z. Dávalos and Tomas Baer, Thermochemistry and Dissociative Photoionization of Si(CH<sub>3</sub>)<sub>4</sub>, BrSi(CH<sub>3</sub>)<sub>3</sub>, ISi(CH<sub>3</sub>)<sub>3</sub>, and Si<sub>2</sub>(CH<sub>3</sub>)<sub>6</sub> Studied by Threshold Photoelectron-Photoion Coincidence Spectroscopy, *J.Phys.Chem. A* (2006) ASAP

## Turbulence-Chemistry Interactions in Reacting Flows

Robert S. Barlow  
Combustion Research Facility  
Sandia National Laboratories  
P.O. Box 969, Mail Stop 9051  
Livermore, California 94551  
barlow@ca.sandia.gov

### Program Scope

This program is directed toward achieving a more complete understanding of turbulence-chemistry interactions in flames. In the Turbulent Combustion Laboratory (TCL) at the CRF, simultaneous line imaging of spontaneous Raman scattering, Rayleigh scattering, and two-photon laser-induced fluorescence (LIF) of CO is applied to obtain spatially and temporally resolved measurements of temperature, the concentrations of all major species, and mixture fraction ( $\xi$ ), as well as gradients in these quantities in hydrocarbon flames. The instantaneous three-dimensional orientation of the turbulent reaction zone is also measured by imaging of OH LIF in two crossed planes, which intersect along the laser axis for the multiscale measurements. These combined data characterize both the thermo-chemical state and the instantaneous flame structure, such that the influence of turbulent mixing on flame chemistry may be quantified. Our experimental work is closely coupled with international collaborative efforts to develop and validate predictive models for turbulent combustion. This is accomplished through our visitor program and through an ongoing series of workshops on Turbulent Nonpremixed Flames (TNF). Within the CRF we are collaborating with Joe Oefelein to use highly-resolved large-eddy simulations (LES) of our experimental flames in order to gain greater fundamental understanding of dynamic, multi-scale, flow-chemistry interactions.

### Recent Progress

Recent work has focused on the structure of reacting flows at the smallest scales of turbulence, the dissipation scales, and on the effects of spatial averaging and experimental noise on measurements of scalar dissipation. We have achieved significant progress in this area over the past year and have brought new clarity to both the fundamental understanding of reacting turbulence at the dissipation scales and the experimental techniques used to investigate these issues. We have also been developing a new detection system for multi-scalar line imaging (Raman/Rayleigh/CO-LIF) that will yield significant improvements in spatial resolution, collection efficiency, and rejection of interferences.

#### Scalar Dissipation and the Structure of Reacting Turbulence at the Smallest Scales

Scalar dissipation is a central concept in combustion theory and in several turbulent combustion modeling approaches. Accurate measurements are needed. However, such measurements are challenging because they require high precision and good spatial resolution. Because scalar dissipation,  $\chi = 2D_\xi (\nabla \xi \cdot \nabla \xi)$  or  $\chi_r = 2D_\xi (\partial \xi / \partial r)^2$  for the radial contribution in a jet flame, is determined from the square of the measured gradient in mixture fraction,  $\xi$ , experimental noise in the mixture fraction measurements always increases the apparent measured mean scalar dissipation value. Dissipation occurs at the smallest scales of turbulence. Consequently, the measured dissipation is significantly attenuated when the smallest turbulent scales are not

resolved by the experimental technique. Thus, spatial averaging and noise have opposite effects, and it is necessary to quantify both in order to assess measurement accuracy. We have pursued this by applying Fourier analysis and digital filter theory to line-imaging data from turbulent nonreacting jets and jet flames and comparing results to well established theory for nonreacting turbulent flow. Investigations have been carried out in collaboration with Guanghua Wang (Sandia postdoc), Noel Clemens (UT Austin), and Dirk Geyer (Technical University of Darmstadt), as well as Jonathan Frank and Sebastian Kaiser (Sandia).

Line imaging of Raman/Rayleigh/CO-LIF was used to investigate the energy and dissipation spectra of turbulent fluctuations in temperature, mixture fraction, and their gradients in several flames, including CH<sub>4</sub>/H<sub>2</sub>/N<sub>2</sub> jet flames at Reynolds numbers of 15,200 and 22,800 (DLR-A and DLR-B) and piloted CH<sub>4</sub>/air jet flames at Reynolds numbers of 22,400 and 33,600 (Sandia flames D and E). The high signal-to-noise ratio (SNR) of the one-dimensional (1-D) Rayleigh scattering images enables determination of the turbulent cutoff wavenumber from 1-D thermal dissipation spectra. The local length scale inferred from this cutoff is analogous to the Batchelor scale in nonreacting flows. The measured thermal dissipation spectra in the turbulent flames were shown to be similar to the model spectrum of Pope for turbulent kinetic energy dissipation in nonreacting flow. Furthermore, for these flames with Lewis number near unity, the 1-D dissipation spectra for temperature and mixture fraction were shown to follow nearly the same roll off in the high wavenumber range, such that the cutoff length scale for thermal dissipation is equal to or slightly smaller than the cutoff length scale for mixture fraction dissipation. This suggests that the cutoff length scale determined from Rayleigh scattering measurements may be used to define the local resolution requirements and optimal data processing procedures for accurate determination of the mean mixture fraction dissipation based upon Raman scattering measurements. Additionally, measurements from the piloted CH<sub>4</sub>/air flames were used to demonstrate that a surrogate cutoff scale may be obtained from the dissipation spectrum of the inverse of the Rayleigh signal itself, even when the Rayleigh scattering cross section varies through the flame.

The portion of the turbulent scalar spectra captured in these experiments is illustrated in figure 1, which shows normalized 1-D energy and dissipation spectra, based upon Pope's model spectrum for turbulent kinetic energy. The Rayleigh measurements, which have higher SNR and better spatial resolution than the Raman measurements (0.040 mm or 0.060 mm vs. 0.220 mm), have a spatial dynamic range that includes the peak (in most cases) in the dissipation spectrum and extends beyond the dissipation cutoff, such that the length scale corresponding to the cutoff may be determined at each measurement location. The cutoff wavenumber at  $\kappa^* = 1$  corresponds to 2% of the peak value in the 1-D model dissipation spectrum, as indicated by the large arrow in figure 1.

The normalized 1-D dissipation spectra from the experiments are compared in figure 2 with the 1-D model spectrum from Pope. Here, the wavenumbers of the measured spectra are normalized by the cutoff wavenumber  $\kappa_\beta$  determined from the 2% level in the dissipation spectrum for the inverse Rayleigh signal. The measured and modeled dissipation spectra follow nearly the same exponential roll-off at the high wavenumber region. This indicates that turbulence structure at the dissipation scales in jet flames, as represented by averaged spectra, is similar to that in nonreacting turbulent flows. This is an important experimental observation that should be investigated in a wider range of flames. It is clear that the dissipation spectra from the inverse Rayleigh signal may be used in place of the thermal dissipation spectra, even though the Rayleigh cross section is not constant in these piloted jet flames. It is also clear that the cutoff length scale obtained from the inverse Rayleigh spectra may be used to determine local cutoff length scale for thermal dissipation. Furthermore, this local surrogate length scale may be used to estimate the corresponding length scale for mixture fraction dissipation and resolution requirements for accurate measurement of the mean mixture fraction dissipation.

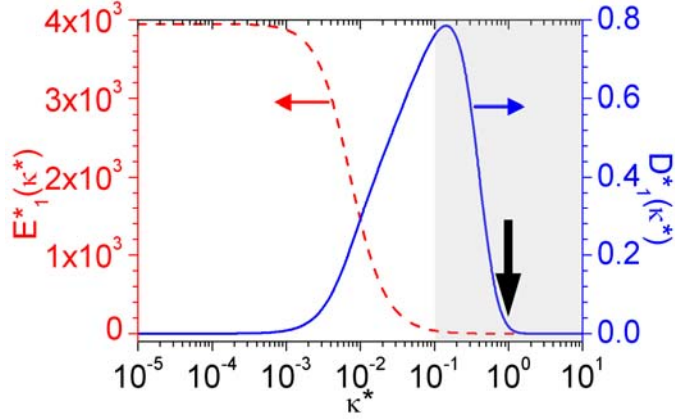


Figure 1. Normalized 1-D energy and dissipation spectra for scalar fluctuations calculated from the model spectrum for turbulent kinetic energy from Pope [Turbulent Flows] with Taylor Reynolds number,  $Re_\lambda = 140$ . The shaded region indicates the wavenumber interval resolved by the current 1-D line Rayleigh imaging measurements, and the large arrow indicates the 2% dissipation cutoff location,  $\kappa\lambda_\beta = \kappa^* = 1$ , where  $\lambda_\beta$  is analogous to the Kolmogorov scale in the model spectrum.

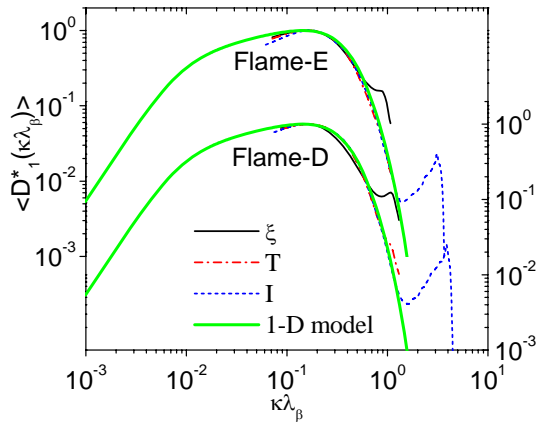


Figure 2. Comparison of the normalized 1-D dissipation spectra of mixture fraction,  $\xi$ , temperature,  $T$ , and the inverse of the Rayleigh signal,  $I$  at  $x/d=15$ ,  $r/d=1.1$  in Sandia flames D and E. The 1-D model spectrum is based on the model spectrum for turbulent kinetic energy from Pope.

Direct measurement of the local scalar spectrum is also expected to be an effective approach for determining local turbulence scales and experimental resolution requirements in complex flames, such as bluff-body or swirl-stabilized flames, where simple scaling laws for estimation of turbulent length scales are not expected to be accurate. The fact that the inverse of the Rayleigh signal may be used directly in this analysis, without the need to know the local Rayleigh scattering cross section, is a significant experimental finding. It suggests that turbulence length scales may be determined in complex reacting flows using relatively simple laser diagnostics. Length scales determined from experiments such as these will also be useful for the design of grids for large eddy simulation (LES) or for the evaluation of the relative resolution of LES results.

### Future Plans

The spectral analysis described above opens a way to remove noise in measurements of the mixture fraction dissipation and also account for effects of spatial averaging when the measurement resolution for Raman scattering is not sufficient to reach the dissipation cutoff. We will use this approach to extract corrected scalar dissipation results from previous jet flame data, allowing quantitative comparisons with model calculations and highly resolved LES (Oefelein). We will

integrate our newly constructed transmission spectrometer for line-imaging of Raman scattering into the multiscale experiments in the Turbulent Combustion Lab and construct a second spectrometer for direct measurement of fluorescence interference in Raman measurements. In collaboration with TU Darmstadt, we will develop a hybrid Raman data analysis approach, combining features of our matrix inversion technique with their spectral fitting technique. These diagnostic advances will allow extension of experiments into flames of more complex fuels. The TNF8 Workshop will be held in Heidelberg, Germany on 3-5 August 2006.

### **BES Supported Publications (2004 - present)**

1. A.N. Karpetsis, T.B. Settersten, R.W. Schefer, and R.S. Barlow, "Laser Imaging System for Determination of Three-Dimensional Scalar Gradients in Turbulent Flames," *Optics Lett.* **29**, 355-357 (2004).
2. A.R. Masri, P.A.M. Kalt, R.S. Barlow, "The compositional structure of swirl-stabilized turbulent nonpremixed flames," *Combust. Flame* **137**, 1-37 (2004).
3. R.S. Barlow, A.N. Karpetsis, "Measurements of Scalar Variance, Scalar Dissipation, and Length Scales in Turbulent Piloted Methane/Air Jet Flames," *Flow Turb. Combust.*, **72**, 427-448 (2004).
4. A.N. Karpetsis and R.S. Barlow, "Measurements of Flame Orientation and Scalar Dissipation in Turbulent Partially Premixed Methane Flames," *Proc. Combust. Inst.* **30**, 665-672 (2005).
5. R.S. Barlow, A.N. Karpetsis, "Scalar Length Scales and Spatial Averaging Effects in Turbulent Piloted Methane/Air Jet Flames," *Proc. Combust. Inst.* **30**, 673-680 (2005).
6. K. Kohse-Hoinghaus, R. S. Barlow, M. Alden, J. Wolfrum, "Combustion at the Focus: Laser Diagnostics and Control," *Proc. Combust. Inst.* **30**, 89-123, (2005) (invited plenary paper).
7. R.S. Barlow, J.H. Frank, A.N. Karpetsis, J.-Y. Chen, "Piloted Methane/Air Jet Flames: Transport Effects and Aspects of Scalar Structure," *Combust. Flame* **143**, 433-449 (2005).
8. R. Cabra, J.-Y. Chen, R.W. Dibble, A.N. Karpetsis, R.S. Barlow, "Lifted Methane-Air Jet Flames in a Vitiated Coflow," *Combust. Flame* **143**, 491-506 (2005).
9. J.C. Oefelein, R.W. Schefer, R.S. Barlow, "Toward Validation of Large Eddy Simulation for Turbulent Combustion," *AIAA J.* **44**, 418-433 (2006).
10. R.S. Barlow, "Laser Diagnostics and their Interplay with Computations to Understand Turbulent Combustion," *Proc. Combust. Inst.* **31** (2006) (invited plenary paper).
11. R.P. Lindstedt, H.C. Ozarovsky, R.S. Barlow, A.N. Karpetsis, "Progression of Localised Extinction in High Reynolds Turbulent Jet Flames," *Proc. Combust. Inst.* **31** (2006) (accepted).
12. D. Wang, C. Tong, R.S. Barlow, A.N. Karpetsis, "Experimental Study of Scalar Filtered Mass Density Function in Turbulent Partially Premixed Flames," *Proc. Combust. Inst.* **31** (2006) (accepted).
13. G.-H. Wang, R. S. Barlow, N.T. Clemens, "Quantification of Resolution and Noise Effects on Thermal Dissipation Measurements in Turbulent Non-premixed Jet Flames," *Proc. Combust. Inst.* **31** (2006) (accepted).

### **Web-Based Information**

<http://www.ca.sandia.gov/CRF/staff/barlow.html>

<http://www.ca.sandia.gov/TNF>

**Theoretical Studies of Combustion Dynamics  
(DE-FG02-97ER14782)**

Joel M. Bowman  
Cherry L. Emerson Center for Scientific Computation and  
Department of Chemistry, Emory University  
Atlanta, GA 30322, jmbowma@emory.edu

**Program Scope**

This program, funded by the Department of Energy grant, is a theoretical and computational one to develop and apply dynamical methods to chemical processes of importance in gas-phase combustion. These include quantum and quasiclassical calculations of bimolecular and unimolecular reactions using *ab initio*-based potentials that govern these processes. Recent work has focused on developing new methods to fit tens of thousands of *ab initio* energies to functional forms that are inherently invariant with respect to any permutation of like nuclei. Dynamics on these potentials, which may contain multiple minima and saddle points, can be done for long times and can reveal new pathways and mechanisms of chemical reactions.

**Recent Progress**

**The “roaming H-atom” in H<sub>2</sub>CO photodissociation**

The photodissociation dynamics of formaldehyde has been of long-standing interest, both experimentally<sup>1-4</sup> and theoretically.<sup>5-9</sup> Previous theoretical work has included high quality *ab initio* calculations of various stationary points of the potential. Potential surfaces have been developed, which however, do not describe the H+HCO radical channel. Classical dynamics have been done on these surfaces, and “direct-classical dynamics” have also been performed with the focus on the product distributions of the CO and H<sub>2</sub> molecular products.

We recently completed a global potential surface for H<sub>2</sub>CO in the ground singlet state, in collaboration with L. B. Harding.<sup>P1</sup> This surface describes both the molecular and H+HCO radical channels. We also completed a semi-global potential energy surface for the triplet state, which leads to H+HCO products.<sup>P2</sup> This surface is based on roughly 10 000 UCCSD(T)/aug-cc-pVTZ calculations. Quasiclassical trajectory calculations were done on both potentials and very interesting and somewhat unexpected results were found. The dynamics on the singlet potential energy surface have revealed an unusual second channel to form the molecular products H<sub>2</sub>+CO. This channel can be described as a “self-reaction” of the incipient H+HCO radical products or a “roaming H-atom” channel. The key experimental signature of this channel, seen by Suits and co-workers, is vibrationally hot H<sub>2</sub> and rotationally cold CO. A joint report of this work appeared in 2004<sup>P3</sup> and a follow-up paper has been submitted.<sup>10</sup>

Reaction dynamics on the triplet and singlet potential energy surfaces have recently been reported in a joint experimental/theoretical work by Scott Kable’s group and my group.<sup>P4</sup> In this work the focus was on the H+HCO products and the internal energy distribution of the HCO product in particular. The experiments found that at photolysis energies below the barrier on the triplet surface the rotational distribution of

HCO is essentially statistical, whereas for energies above the barrier the rotational distribution changes its character suddenly and is much colder. The dynamics calculations agree with this finding, and by considering dynamics separately on the singlet and triplet surface it was shown that at energies above the triplet barrier the H+HCO products are dominated by the triplet surface. These conclusions are in complete agreement with the proposed explanation of similar experimental results made several years ago by Reisler and Wittig and co-workers.<sup>4</sup>

### **A global *ab initio* potential energy surface for H+CH<sub>4</sub>**

Stimulated by recent experimental work of Zare and Schatz and co-workers<sup>11</sup> and pioneering experiments of Valentini and co-workers<sup>12</sup> on hyperthermal scattering studies of the reaction of H with CH<sub>4</sub>, we developed a global *ab initio*-based potential energy surface for this reaction. The need for such a potential was made clear by Schatz and co-workers, who in joint work with Zare, showed that the best available *ab initio*-based potential was inadequate to describe the result of these experiments. Schatz and co-workers did show that quasiclassical trajectory direct dynamics calculations based on Density Functional Theory (B3LYP/6-31G\*\*) calculations did give results in much better agreement with experiment. These calculations do not yield a PES of course and so this motivated us to develop one.

The global potential is based on the new fitting approach to roughly 22 000 CCSD(T)/aug-cc-pVTZ electronic energies.<sup>p5</sup> This fit is quite precise and yields a barrier of 14.8 kcal/mol. This barrier agrees with previous high quality calculations and has been shown in work using semi-global potentials<sup>13,14</sup> to give the thermal rate constant in good agreement with experiment. Thus although we have not calculated the rate constant with the new potential (but plan to do so in the near future) we are confident that we will get good agreement as well with experiment. We have done some preliminary quasiclassical trajectory calculations in the hyperthermal region<sup>p5</sup> and do get very good agreement with the Zare group's results.

### **Future Plans**

We plan to carry out extensive dynamics calculations with the new CH<sub>5</sub> potential, including investigating the effect of exciting the asymmetric stretch on the reaction cross section at collision energies between 1.52 and 2.0 eV. Zare and co-workers reported a relative increase of the cross section by  $3.0 \pm 1.5$  over this energy range. We will also calculate the thermal rate constant using and initial state-selected rate constants using reduced dimensionality quantum approaches that we used earlier<sup>15</sup> on this reaction but with a highly approximate (Jordan-Gilbert) potential.

We also plan to begin studies of the reaction of the reaction of C(<sup>3</sup>P) with C<sub>2</sub>H<sub>2</sub>. This reaction has been extensively studied experimentally by two molecular beam groups.<sup>16,17</sup> This reaction forms *linear*-C<sub>3</sub>H and *cyclic*-C<sub>3</sub>H products and according to one experimental group, singlet C<sub>3</sub>.<sup>17</sup> The singlet C<sub>3</sub> can of course only be formed in a spin changing process. Our plan is to develop global potential energy surfaces for the triplet and singlet states and to study the reaction dynamics on both potentials. We are

stimulated to do this work both by the experimental and previous theoretical work, including *ab initio* calculations of stationary points<sup>18</sup> and rate constant calculations based on statistical<sup>19</sup> or reduced dimensionality approaches.<sup>20,21</sup>

## References

1. For a review up to 1983, see, C. B. Moore and J. C. Weisshaar, *Ann. Rev. Phys. Chem.* **34**, 525 (1983).
2. (a) T. J. Butenhoff, K. L. Carteton and C. B. Moore, *J. Chem. Phys.* **92**, 377 (1990); (b) W. F. Polik, D. R. Guyer and C. B. Moore, *J. Chem. Phys.* **92**, 3453 (1990); (c) R. D. Zee, M. F. Foltz, and C. B. Moore, *J. Chem. Phys.* **99**, 1664 (1993).
3. (a) A. C. Terentis, S. E. Waugh, G. F. Metha, and S. H. Kable, *J. Chem. Phys.* **108**, 3187 (1998); (b) H.-M. Yin, K. Nauta, and S. H. Kable, *J. Chem. Phys.* **122**, 194312 (2005).
4. L. R. Valachovic, M. F. Tuchler, M. Dulligan, Th., Droz-George, M., Zyrianov, A. Kolessov, H. Reisler, and C. J. Wittig, *J. Chem. Phys.* **112**, 2752 (2000).
5. Y. Chang, C. Minichino, and W. H. Miller, *J. Chem. Phys.* **96**, 4341 (1992).
6. Y. Yamaguchi, S. S. Wesolowski, T. J. Huis, H. F. Schaefer, *J. Chem. Phys.* **108**, 5281 (1998).
7. D. Feller, M. Dupuis, and B. C. Garrett, *J. Chem. Phys.* **113**, 218 (2000).
8. (a) X. Li, J. M. Millam and H. B. Schlegel, *J. Chem. Phys.* **113**, 10062 (2000); (b) W. Chen, W. L. Hase, and H. B. Schlegel, *Chem. Phys. Lett.* **228**, 436 (1994).
9. T. Yonehara and S., J. Kato *Chem. Phys.* **117**, 11131 (2002).
10. S. A. Lahankar, S. D. Chambreau, D. Townsend, F. Suits, J. Farnum, X. Zhang, J. M. Bowman, A. G. Suits, The roaming atom mechanism in formaldehyde decomposition, *J. Chem. Phys.*, submitted.
11. (a) J. P. Camden, H. A. Bechtel, D. J. Ankeny Brown, M. R. Martin, R. N. Zare, W. Hu, G. Lendvay, D. Troya, G. C. Schatz, *J. Amer. Chem. Soc.* **127**, 11898 (2005); (b) J. P. Camden, W. Hu, H. A. Bechtel, D. J. Ankeny Brown, M. R. Martin, R. N. Zare, G. Lendvay, D. Troya, and G. C. Schatz, *J. Phys. Chem. A* **110**, 677 (2006); (c) W. Hu, G. Lendvay, D. Troya, G. C. Schatz, J. P. Camden, H. A. Bechtel, D. J. A. Brown, M. R. Martin, and R. N. Zare, *J. Phys. Chem. A* **110**, 3017 (2006).
12. G. J. Germann, Y-D. Huh, and J. J. Valentini, *J. Chem. Phys.* **96**, 1957 (1992).
13. J. Pu and D. G. Truhlar, *J. Chem. Phys.* **116**, 1468 (2002).
14. T. Wu, H-J. Werner, and U. Manthe, *Science* **306**, 2227 (2004).
15. D. Wang and J. M. Bowman, *J. Chem. Phys.* **115**, 2055 (2001).
16. R. I. Kaiser, A. M. Mebel, and Y. T. Lee, *J. Chem. Phys.* **114**, 231 (2001).
17. L. Cartechini, A. Bergeat, G. Capozza, P. Casavecchia, G. G. Volpi, W. D. Geppert, C. Naulin, and M. Costes, *J. Chem. Phys.* **116**, 5603 (2002).
18. A. M. Mebel, W. M. Jackson, A. H. H. Chang, and S. H. Lin, *J. Am. Chem. Soc.* **120**, 5751 (1998).
19. R. Guadagnini, G. C. Schatz, and S. P. Walch, *J. Phys. Chem. A* **102**, 5857 (1998).
20. E. Buonomo, and D. C. Clary, *J. Phys. Chem. A*, **105**, 2694, (2001).
21. T. Takayanagi, *J. Phys. Chem. A* **110**, 361 (2006).

### PUBLICATIONS SUPPORTED BY THE DOE (2004-present)

1. A global *ab initio* potential energy surface for formaldehyde, X. Zhang, S.-L. Zou, L. B. Harding, and J. M. Bowman, *J. Phys. Chem. A* **108**, 8980 (2004).
2. New insights on reaction dynamics from formaldehyde photodissociation, J. M. Bowman and X. Zhang. *Phys. Chem. Chem. Phys.*, invited review, **8** 313 (2006).
3. The roaming atom: Straying from the reaction path in formaldehyde decomposition, D. Townsend, S. A. Lahankar, S. K. Lee, S. D. Chambreau, A. G. Suits, X. Zhang, J. Rheinecker, L. B. Harding and J. M. Bowman, *Science* **306**, 1158 (2004).
4. Signatures of H<sub>2</sub>CO photodissociation from two electronic states, H.M. Yin and S.H. Kable, X. Zhang and J.M. Bowman, *Science*, **311**, 1443 (2006).
5. An *ab initio* potential surface describing abstraction and exchange for H+CH<sub>4</sub>, X. Zhang, B. Braams, J. M. Bowman, *J. Chem. Phys* **124**, 021104 (2006).
6. Calculation of converged rovibrational energies and partition function for methane using vibrational–rotational configuration interaction, A. Chakraborty, D. G. Truhlar, J. M. Bowman, and S. Carter, *J. Chem. Phys.* **121**, 2071 (2004).
7. Construction of a global potential energy surface from novel *ab initio* molecular dynamics for the O(<sup>3</sup>P) + C<sub>3</sub>H<sub>3</sub> reaction, S. C. Park, B. J. Braams, and J. M. Bowman, *J. Theor. Comput. Chem.* **4**, 163 (2005).
8. Quasiclassical trajectory studies of the dynamics of H<sub>2</sub>CO on a global *ab initio*-based potential energy surface, J. L. Rheinecker, X. Zhang, and J. M. Bowman, *Mol. Phys.* **103**, 1067 (2005).
9. Quasiclassical trajectory study of formaldehyde: H<sub>2</sub>CO → H<sub>2</sub>+CO, H+HCO, X. Zhang, J. L. Rheinecker, and J. M. Bowman, *J. Chem. Phys.* **122**, 114313 (2005).
10. Quantum and quasi-classical studies of the O(<sup>3</sup>P) + HCl → OH + Cl(<sup>2</sup>P) reaction using benchmark potential surfaces, T. Xie, J. M. Bowman, J. W. Duff and M. Braunstein, and B. Ramachandran, *J. Chem. Phys.* **122**, 014301 (2005).
11. Enhancement of tunneling due to resonances in pre-barrier wells in chemical reactions, J. M. Bowman, *Chem. Phys.* **308**, 255 (2005).
12. Termolecular kinetics for the Mu+CO+M recombination....J, J. Pan, D. J. Arseneau, M. Senba, D. M. Garner, D. G. Fleming, Ti. Xie and J. M. Bowman, *J. Chem. Phys.*, accepted for publication.

**COMBUSTION CHEMISTRY**  
**Principal Investigator: Nancy J. Brown**  
**Environmental Energy Technologies Division**  
**Lawrence Berkeley National Laboratory**  
**Berkeley, California, 94720**  
**510-486-4241**  
**NJBrown@lbl.gov**

**PROJECT SCOPE**

Combustion processes are governed by chemical kinetics, energy transfer, transport, fluid mechanics, and their complex interactions. Understanding the fundamental chemical processes offers the possibility of optimizing combustion processes. The objective of our research is to address fundamental issues of chemical reactivity and molecular transport in combustion systems. Our long-term research objective is to contribute to the development of reliable combustion models that can be used to understand and characterize the formation and destruction of combustion-generated pollutants. We emphasize studying chemistry at both the microscopic and macroscopic levels. To contribute to the achievement of this goal, our current activities are concerned with three tasks: Task 1) developing models for representing combustion chemistry at varying levels of complexity to use with models for laminar and turbulent flow fields to describe combustion processes; Task 2) developing tools to probe chemistry fluid interactions; and Task 3) modeling and analyzing combustion in multi-dimensional flow fields.

**RECENT PROGRESS**

**Task 1: Developing models for representing combustion chemistry at varying levels of complexity to use with models for laminar and turbulent flow fields to describe combustion processes (with Shaheen R. Tonse and Marcus Day)** Our objective in these studies [Tonse and Brown, 2003 and Tonse et al., 2006] is to develop reduced mechanisms for hydrocarbon fuels that are accurate and efficient because a substantial fraction of computing resources is frequently devoted to solving the chemical rate equations (ODEs) in reactive computational fluid dynamics (CFD) calculations. We observe this fraction to be 93% for a 32 species CH<sub>4</sub>+Air mechanism, GRI-Mech 1.2 embedded in a low Mach number CFD code. The larger dimensionality of these systems requires very large factorial designs, and this renders PRISM (in its previous form) not appropriate. We recently created two approaches for mechanism reduction: an enhanced form of PRISM and DYSSA (Dynamic Steady State Approximation) for reducing chemical mechanisms dynamically. Our method of fast-slow time-scale separation and the framework of hypercube-shaped Chemical Composition Space (CCS) partitions are an essential part of each. PRISM and DYSSA apply their reduction techniques repeatedly and uniquely to each hypercube encountered, and this results in an optimal application of the techniques since species move from the slow category into the fast one as their time scales change during a simulation. The fast/slow species time separation is invariant in a hypercube, is different for each hypercube, and is accomplished dynamically during the simulation.

PRISM constructs polynomial equations in each hypercube, and replaces the ODE system with simpler algebraic polynomials. Earlier versions of PRISM were applied to smaller chemical mechanisms and used *all* chemical species as independent variables in the polynomials. We enhanced PRISM by reducing the dimensionality of its polynomials based on differences in species time scales. DYSSA is an enhancement of the steady-state approximation. As a chemical mixture of the simulation enters different hypercubes, DYSSA uses the fast-slow time-scale separation to determine the set of steady-state species in those hypercubes. A reduced number of chemical kinetic ODEs, equal to the number of non-steady-state species (plus one for temperature), is integrated rather than the set of rate equations associated with the original mechanism. The fast species are approximated accurately and simply in each hypercube.

DYSSA and PRISM are evaluated for simulations of a counter-rotating pair of vortices interacting with a premixed CH<sub>4</sub>/Air laminar flame. We use the adaptive low Mach number algorithm developed by Day and Bell [2000] and their Adaptive Mesh Refinement (AMR) CFD code [Day, 2003]. We replaced their standard chemistry module in the AMR CFD code by either PRISM or DYSSA. DYSSA is shown to be sufficiently accurate for use in combustion simulations. DYSSA's speedup appears to be on the order of three or four for the most accurate simulations (relative error less than 1.0% for all species concentrations) and increases as accuracy requirements are decreased. PRISM does not perform as well as DYSSA with respect to accuracy and efficiency. We also determined the computational burden imposed by the dynamic reduction is quite insignificant. We performed an ad hoc sensitivity study of dynamic reduction to determine the factors that most contribute to its accuracy/efficiency and found that the partitioning of CCS into hypercubes, and how this is accomplished for individual species is very important. We also determined that the partitioning of chemical composition space required by these two approaches affords an opportunity to investigate the chemistry/fluid interactions of a flame interacting with counter-rotating vortices of different strengths.

DYSSA is sufficiently accurate for use in combustion simulations. DYSSA's cost of setting up a surrogate to use in place of the full ODE solution in a hypercube is much reduced relative to PRISM's cost, hence DYSSA has a lower reuse threshold for recovering costs. The modular structure of the code into a hypercube management portion, a Fast/low separation method portion, and a portion used to solve the chemical kinetics rate equations suggests that improvements can be implemented in a straightforward fashion.

The Fast/low method performs well at separating species, and provides a useful means of applying dynamic chemical reduction on the fly when it is applied with the CCS hypercube partitioning concept. The amount of reduction varies considerably over the simulation. In contrast, static reduction, which attempts to maintain suitable accuracy, is limited to a dimensional reduction that is valid over all CCS encountered in a simulation, and it would use the part of CCS with the least reduction as being representative. The static dimensional reduction must be anticipated in advance, and an unexpected access to some other portion of CCS resulting from changes in simulation initial conditions, boundary conditions, and model input would likely result in unanticipated inaccuracies.

A key target for efficiency is creating a reduced mechanism that has a computational burden equal to that of other processes in the reactive CFD simulation so that solving the chemical rate equations is no longer rate limiting. PRISM does not have sufficient accuracy and efficiency to be used in combustion modeling for larger mechanisms (30 species) of the sort treated here. PRISM works well for smaller mechanisms. If the Fast/low approach were applied to H<sub>2</sub>/Air combustion with the Gusset designs, we envision that a factor of 15-20 gain in efficiency might be realized. PRISM might also be useful as part of a hybrid method for that part of CCS where quadratic polynomials are required as a surrogate for the ODE solution. Since DYSSA has both sufficient accuracy and efficiency to be used for combustion modeling. We anticipate devising new strategies for improving DYSSA's efficiency while maintaining accuracy at acceptable levels for various combustion modeling applications. This will be achieved through devising a more sophisticated species separation algorithm, and through algorithmic improvements that result in larger hypercube sizes and greater reuse.

**Task 2. A review of transport property formalisms and their underlying parameterizations is being prepared (Brown).** It is important to properly describe the transport of species, momentum, and energy in flames. Transport coefficients required for the quantification of these processes are diffusion, viscosity, and thermal conductivity coefficients. Our recent sensitivity studies have demonstrated that transport property importance varies according to the dependent variable considered and the flame type. As an important step in improving the representation of transport in combustion modeling, we are currently conducting a review of these transport properties. Major products of this review are suggestions for improving transport property evaluations under combustion conditions as well as improvements in their underlying parameterizations. The review content is discussed in the proposed research section.

**Task 3 Research conducted to examine chemistry fluid mechanical interactions (Brown with Tonse and Day).** We have examined vortex-flame interactions to determine how vortex strength affects chemical pathways. The metric used is the number of hypercubes that are constructed in CCS for a given simulation. The strain field and curvature of the flame surface induced by the impinging vortex leads to a shift in the chemical pathways of methane oxidation. The magnitude of these effects depends strongly on the length and time scales of the perturbing velocity field; the chemistry is not significantly affected if the vortex is weak or moves quickly through the flame zone. Important chemical processes are removed from the dominant methane oxidation pathways for moderate cases of vortex strength and velocity. This effect, observed experimentally [Nguyen and Paul, 1996] and theoretically by Bell et al. [2000], is reproduced in our current simulations. We observe that hypercube numbers increase with velocity to a point, and then decreases. The study also shows that different chemical pathways are emphasized as the velocity increases.

## **FUTURE PLANS**

We will improve the efficiency of DYSSA, while maintaining suitable accuracy for various combustion applications. This and other combustion modeling applications will be undertaken with John Bell's group. We will also extend the data set associated with the potential parameters that support the evaluation of transport properties for species important for H<sub>2</sub> and CH<sub>4</sub> combustion. Our goal is to improve transport properties

important for supporting H<sub>2</sub> and CH<sub>4</sub> combustion. We will work with Michael Frenklach as part of PrIME (<http://primekinetics.org>), an international collaboration concerned with developing reaction models for combustion, which includes kinetics, thermochemistry, and transport. We will also collaborate with Michael Frenklach on the homogeneous nucleation of carbon nanoparticles, and focus on collisions of aromatic-aliphatic linked hydrocarbon compounds.

## REFERENCES

M.S. Day, and J.B. Bell, Numerical Simulation of Laminar Reacting Flows with Complex Chemistry. *Combust. Theory and Modeling*, 4(4), pp. 535-556 (2000). Also LBNL Report 44682.

M.S. Day, <http://seesar.lbl.gov/CCSE/Software> (2003).

J.B. Bell, N.J. Brown, M.S. Day, M. Frenklach, J.F. Grac, and S.R. Tonse, "Effect of Stoichiometry on Vortex-Flame Interactions," *Proceedings of the Combustion Institute* 28, 1933-1939 (2000). Also Lawrence Berkeley National Laboratory Report No. LBNL-44730.

Q.V. Nguyen, and P.H. Paul, "The Time Evolution of a Vortex-Flame Interaction Observed in Planar Imaging of CH and OH," "26<sup>th</sup> Symp. (Intl.) on Combustion, The Combustion Inst., Pittsburgh, PA, 1996, pp.357-364.

## PUBLICATIONS

S.R. Tonse, M.S. Day, and N.J. Brown, 2006. "Dynamic Reduction of a CH<sub>4</sub>/Air Chemical Mechanism Appropriate for Investigating Vortex Flame Interactions." Submitted to *International Journal of Chemical Kinetics*. Also LBNL Report No.59750

N.J. Brown and Revzan, K.L., "Comparative Sensitivity Analysis of Transport Properties and Reaction Rate Coefficients". *International Journal Chemical Kinetics*, 37, pp 538-553 (2005). Also LBNL Report No. 55671

S.R. Tonse and N.J. Brown, "Dimensionality Estimate of the Manifold in Chemical Composition Space for a Turbulent Premixed H<sub>2</sub>+air Flame." *International Journal of Chemical Kinetics* 36, pp 326-336, 2004. Also LBNL Report No. 52058.

Tonse, S.R., Moriarty, N.W., Frenklach, M., and Brown, N.J., "Computational Economy Improvements in PRISM." *International Journal of Chemical Kinetics* 35, pp 438-452 (2003). Also Lawrence Berkeley National Laboratory Report No. LBNL-48858.

Tonse, S.R. and Brown, N.J., "Computational Economy Improvements in PRISM." *Proceedings The 3<sup>rd</sup> Joint Symposium of the U.S. Sections of the Combustion Inst.* Paper-B36 (2003). Also Lawrence Berkeley National Laboratory Report No. LBNL-48858.

# Probing Radical Intermediates of Bimolecular Combustion Reactions

Laurie J. Butler  
The University of Chicago, The James Franck Institute  
5640 South Ellis Avenue, Chicago, IL 60637  
L-Butler@uchicago.edu

## I. Program Scope

Polyatomic radical intermediates play an important role in a wide range of combustion processes. A portion of our DOE-supported work investigates competing product channels in photodissociation processes used to generate radical intermediates important in combustion and develops new methodology to investigate the unimolecular dissociation and isomerization channels of the nascent radicals.<sup>1-3</sup> Our work for DOE in the past two years, described in detail below, focuses on probing the radical intermediates of bimolecular reactions, including the reactions of O atoms and CH radicals with unsaturated hydrocarbons, that proceed through addition/insertion to form an energetically unstable radical intermediate along the reaction coordinate en route to products. Our experiments generate a particular isomeric form of the key unstable radical intermediates along a bimolecular reaction coordinate and investigate the branching between the ensuing product channels of the energized radical as a function of its internal energy under collision-less conditions. The experiments allow us to probe the elementary reaction from the radical intermediate to the competing product channels and determine the energetic barriers in both the entrance and the product channels. The results develop insight on product channel branching in such reactions and provide a key benchmark for emerging electronic structure calculations on polyatomic reactions that proceed through unstable radical intermediates.

## II. Recent Progress

Our work this year completed several studies on bimolecular reactions that proceed through an addition/insertion mechanism. Our velocity map imaging study<sup>4</sup> which resolved the energetic barrier between the lowest energy radical intermediate and the CO + vinyl product channel of the O + propargyl reaction followed earlier work in my group<sup>1</sup> and probed a key portion of the potential surface calculated by Bowman and coworkers. The experiments and analysis were largely complete at the last contractors meeting, so I simply give the reference to our final paper in reference 4. I also give no further details on our collaborative experiments with Steve Pratt, completed this past year, on the photodissociation of propargyl chloride at 193 nm and detailed in reference 5. The experiments described in Section A below outline our investigation of the  $\text{CH}_3\text{O} + \text{CO} \rightarrow \text{CH}_3 + \text{CO}_2$  reaction by accessing the  $\text{CH}_3\text{OCO}$  radical intermediate. This study, done in collaboration with Dr. Jim Lin at Taiwan's National Synchrotron Radiation Research Center (NSRRC) was initiated in the summer of 2004 and finished this year. The results have important implications for the kinetic modeling of oxygenated fuels. The experiments described in Section B below probe the product channels resulting from the propargyl radical intermediate of the  $\text{CH}(X^2\Pi) + \text{C}_2\text{H}_2$  reaction and the  $\text{C}(^3\text{P}) + \text{C}_2\text{H}_3$  reaction. The data evidence the competing  $\text{H} + \text{C}_3\text{H}_2$  and  $\text{H}_2 + \text{C}_3\text{H}$  product channels of the reaction. Unlike most of the other systems we have investigated with this new methodology, the experimental results are not well-predicted by current high-level electronic structure calculations

of the product channel energetics. Finally, Section C describes new experiments we have begun on one of the key radical intermediates of the O + allyl reaction.

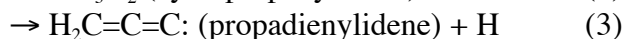
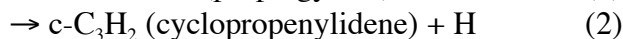
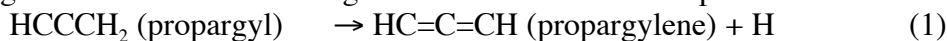
### A. Investigating the $\text{CH}_3\text{O} + \text{CO} \rightarrow \text{CH}_3 + \text{CO}_2$ Reaction by Accessing the $\text{CH}_3\text{OCO}$ Radical Intermediate

The work we completed and published this past year<sup>6</sup> on product branching from the methyl formate radical is key to the chemical kinetic modeling of the effects of oxygenated hydrocarbons on soot emissions from diesel engines (C. K. Westbrook, W. J. Pitz, H. J. Curran, *J. Phys. Chem. A* in press (2006)). While the reaction  $\text{OH} + \text{CO} \rightarrow \text{H} + \text{CO}_2$ , proceeding through the HOCO radical intermediate, has been extensively studied, experimental work on the analogous  $\text{CH}_3\text{O} + \text{CO} \rightarrow \text{CH}_3 + \text{CO}_2$  reaction is relatively limited. A  $\text{CH}_3\text{OCO}$  radical intermediate is indicated both in studies which collisionally stabilize the reaction intermediate and in several theoretical studies of the minima and transition states along the reaction coordinate. Our work, which began in 2004 and was published<sup>6</sup> this past year, investigated the dynamics of this reaction by initiating the reaction from the  $\text{CH}_3\text{OCO}$  radical intermediate. The internal energies of the ground state radicals produced in our experiments allowed access to the low barrier  $\text{CH}_3\text{O} + \text{CO}$  entrance channel of the bimolecular reaction and the exothermic  $\text{CH}_3 + \text{CO}_2$  product channel of the bimolecular reaction, which was predicted to have a higher barrier in several early theoretical papers. An RRKM estimate of the product branching averaged over our ground state radical's internal energy distribution predicted a product branching of  $\text{CH}_3\text{O} + \text{CO} : \text{CH}_3 + \text{CO}_2$  of 280:1 using the barrier energies predicted by B. Wang et al. (B. Wang, H. Hou, and Y. Gu, *J. Phys. Chem. A* **103**, 8021-8029 (1999)). The  $\text{CH}_3 + \text{CO}_2$  channel was also predicted to be the minor one using the early QCISD(T) predictions for the barrier energies and transition state frequencies of Francisco and coworkers. To test these theoretical predictions, our work probed the product channel branching from the ground electronic state  $\text{CH}_3\text{OCO}$  radicals (the photolytic precursor also forms some excited state radicals) using photoionization detection of the  $\text{CH}_3\text{O}$  and CO and the  $\text{CH}_3$  and  $\text{CO}_2$  products (the entrance and exit channels of the bimolecular reaction). Our measured product channel branching from the CO and  $\text{CO}_2$  signal was 1.0 : 2.5 (+/-0.5), in dramatic disagreement with the theoretically predicted  $\text{CH}_3\text{O} + \text{CO} : \text{CH}_3 + \text{CO}_2$  ratio of 280:1; the  $\text{CH}_3 + \text{CO}_2$  products are the major products rather than the minor channel. Our paper includes CCSD(T) calculations to resolve the discrepancy; they show that the reaction proceeds by isomerization of the trans-  $\text{CH}_3\text{OCO}$  radical to the cis- conformer, which can then dissociate via a much lower energy cis- transition state to produce the  $\text{CH}_3 + \text{CO}_2$  products. Using the transition state calculated for this alternate path gives a theoretical prediction in good agreement with experiment. Our results are consistent with the recent work of Glaude et al. (Glaude, P. A.; Pitz, W. J.; Thomson, M. J. *Proc. Combust. Inst.* **2005**, *30*, 1111) which studied the chemical kinetics of dimethyl carbonate, a compound of interest as an oxygenate additive for diesel fuel, and with theoretical work of Good and Francisco (Good, D. A.; Francisco, J. S. *J. Phys. Chem. A* **2000**, *104*, 1171) reporting a lower transition state for the  $\text{CH}_3\text{OCO} \rightarrow \text{CH}_3 + \text{CO}_2$  product channel than in the prior work from that group.

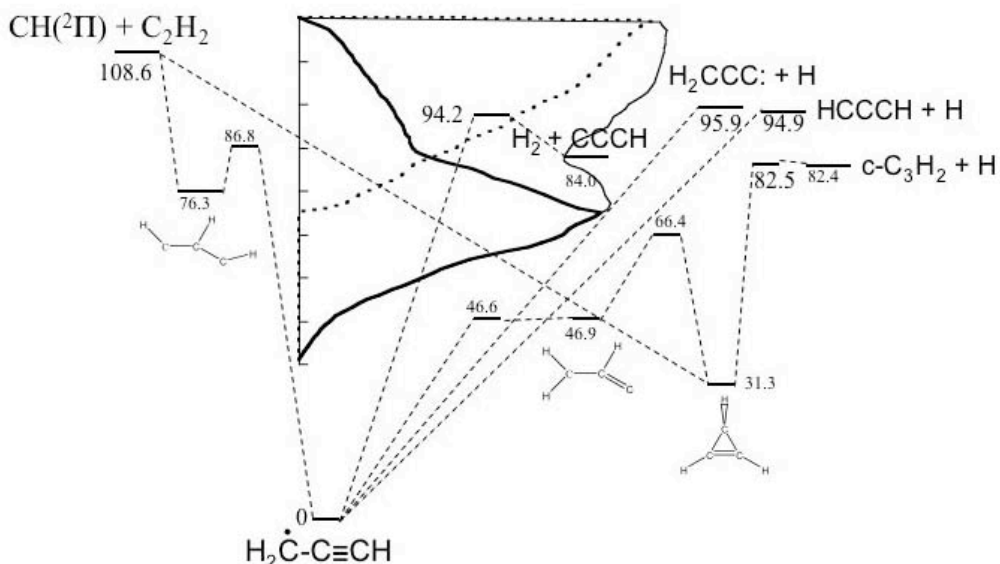
### B. The $\text{CCCH} + \text{H}_2$ and $\text{C}_3\text{H}_2 + \text{H}$ Product Channels from the Propargyl Radical Intermediate of the $\text{CH}(X^2\Pi) + \text{C}_2\text{H}_2$ Reaction and the $\text{C}(^3\text{P}) + \text{C}_2\text{H}_3$ Reaction

In March 2005 we began our investigation of the competing  $\text{H} + \text{C}_3\text{H}_2$  and  $\text{H}_2 + \text{C}_3\text{H}$  product channels of the  $\text{CH}(X^2\Pi) + \text{C}_2\text{H}_2$  reaction and the  $\text{C}(^3\text{P}) + \text{C}_2\text{H}_3$  reaction. We completed

the work this year and submitted the results for publication.<sup>7</sup> Our approach to probing dynamics on the potential energy surface of the  $\text{CH}(X^2\Pi) + \text{C}_2\text{H}_2$  reaction is to investigate the dynamics from the propargyl radical intermediate along the reaction coordinate. The experiments are designed to determine the energetic barriers to each of the product channels:



Several theoretical studies have provided predictions for the barrier energies and, in some cases, branching ratios predicted for these product channels. The lowest energy paths for the  $\text{CH} + \text{acetylene}$  reaction predicted in the most recent theoretical study, A. M. Mebel, S. H. Lin, and R. I. Kaiser, *J. Phys. Chem. A* **105**, 11549-11559 (2001), are shown below:



Importantly, the collisional stabilization of the propargyl intermediate in this nearly gas-kinetic reaction is one of the dominant sources of propargyl radicals in combustion systems, and the self-reaction of the propargyl radicals are key to soot formation.

Our experiments used the photodissociation of propargyl chloride at 157 nm to generate the propargyl radical intermediate of these reactions with internal energies spanning the theoretically-predicted energetic barriers to those product channels. We determine the internal energies and velocities of all the propargyl radicals, those formed with low enough internal energies in the ground state to be below the lowest product channel barrier (or those ones that are stable by virtue of being formed in an excited electronic state or with significant rotational energy) and those formed with higher internal energies that dissociate to the  $\text{CCCH} + \text{H}_2$  or  $\text{C}_3\text{H}_2 + \text{H}$  product channels. Our experiments detected the internal energy onset for dissociation of the nascent propargyl radicals as well as the  $\text{C}_3\text{H}_2$  products in reactions 1-3 and the  $\text{CCCH}$  product of reaction 4 with tunable VUV ionization and simultaneously resolved the velocities of these products. Momentum conservation dictates that the velocity of these heavy partners to  $\text{H}$  and  $\text{H}_2$  products respectively have a nearly identical velocity to the radical intermediate that dissociated to give that product. Thus, our experiments offer the chance to determine the energetic barrier to each of these competing product channels. The most surprising result is that the  $\text{CCCH}$  products are formed from propargyl radicals with an internal energy much lower than that predicted in the

theoretical work. Analysis of the  $\text{H} + \text{C}_3\text{H}_2$  product channels is complicated by an  $\text{HCl}$  elimination channel in the photolytic precursor that also produces  $\text{C}_3\text{H}_2$ , but at higher photoionization energies where the detected  $\text{C}_3\text{H}_2$  product evidences a velocity distribution well characterized by that determined from the unstable portion of the nascent propargyl radicals the data shows that the theoretically predicted energetics are too high by at least 5 kcal/mol. This data thus provides the only experimental benchmark for the theoretically predicted barriers in this important reaction.

### C. Product Branching from a Radical Intermediate of the $\text{O}(^3\text{P}) + \text{Allyl}$ Reaction

We have just initiated new experiments on one of the two key radical intermediates of the  $\text{O} + \text{allyl}$  reaction, using epichlorohydrin as a photolytic precursor for the radical intermediate. Our velocity map imaging studies on the  $\text{C-Cl}$  bond fission process in the precursor determines the internal energy distribution of the radical intermediate and allows us to account for the differing internal energy when the radical is formed in coincidence with the higher spin-orbit state of the  $\text{Cl}$  atom. Data obtained by my student Benj FitzPatrick this month at the NSRRC beamline on the product channel accessed by the radical intermediate of the  $\text{O} + \text{allyl}$  reaction evidences contributions from the competing  $\text{H} + \text{acrolein}$ ,  $\text{CO} + \text{ethyl}$ , and  $\text{HCO} + \text{ethene}$  product channels. The analysis of the results has just begun.

### III. Future Plans

Our work in the coming year will focus on analyzing the reams of data my student Benj FitzPatrick took this month on a key radical intermediate of the  $\text{O} + \text{allyl}$  reaction at the NSRRC, on getting good data in our ongoing velocity map imaging studies of the radical intermediate formed in the  $\text{OH} + \text{allene}$  reaction, and on initiating experiments in our velocity map imaging lab to probe the product channels of radical intermediates with tunable VUV photoionization.

### IV. Publications Acknowledging DE-FG02-92ER14305 (2004 or later)

1. The 193 nm photodissociation of acryloyl chloride to probe the unimolecular dissociation of  $\text{CH}_2\text{CHCO}$  radicals and  $\text{CH}_2\text{CCO}$ , D. E. Szpunar, J. L. Miller, L. J. Butler and F. Qi, *J. Chem. Phys.* **120**, 4223-30 (2004).
2. Competing Pathways in the 248 nm Photodissociation of Propionyl Chloride and the Barrier to Dissociation of the Propionyl Radical, L. R. McCunn, M. J. Krisch, K. Takematsu, L. J. Butler, and J. Shu, *J. Phys. Chem. A* **108**, 7889-7894 (2004).
3.  $\text{C-Cl}$  bond fission dynamics and angular momentum recoupling in the 235 nm photodissociation of allyl chloride, Y. Liu and L. J. Butler, *J. Chem. Phys.* **121**, 11016-11022 (2004).
4. Probing the barrier for  $\text{CH}_2\text{CHCO} \rightarrow \text{CH}_2\text{CH} + \text{CO}$  by the velocity map imaging method, K. -C. Lau, Y. Liu and L. J. Butler, *J. Chem. Phys.* **123**, 054322 (2005).
5. The photodissociation of propargyl chloride at 193 nm, L. R. McCunn, D. I. G. Bennett, L. J. Butler, H. Fan, F. Aguirre, and S. T. Pratt, *J. Phys. Chem. A* **110**, 843-850 (2006).
6. Unimolecular dissociation of the  $\text{CH}_3\text{OCO}$  radical: An intermediate in the  $\text{CH}_3\text{O} + \text{CO}$  reaction, L. R. McCunn, K. -C. Lau, M. J. Krisch, L. J. Butler, J. -W. Tsung, and J. J. Lin, *J. Phys. Chem. A* **110**, 1625-1634 (2006).
7. Unimolecular dissociation of the propargyl radical intermediate of the  $\text{CH} + \text{C}_2\text{H}_2$  reaction, L. R. McCunn, B. L. FitzPatrick, M. J. Krisch, L. J. Butler, C. -W. Liang, and J. J. Lin, submitted to *J. Chem. Phys.* (2006).

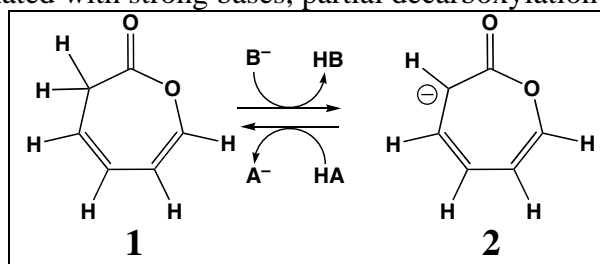
**Joint Theoretical and Experimental Study of  
Key Radicals in Hydrocarbon Combustion  
(DE-FG02-98ER14857)**

PI: Barry K. Carpenter  
Department of Chemistry and Chemical Biology  
Cornell University, Ithaca, NY 14853-1301  
E-mail: [bkcl@cornell.edu](mailto:bkcl@cornell.edu)

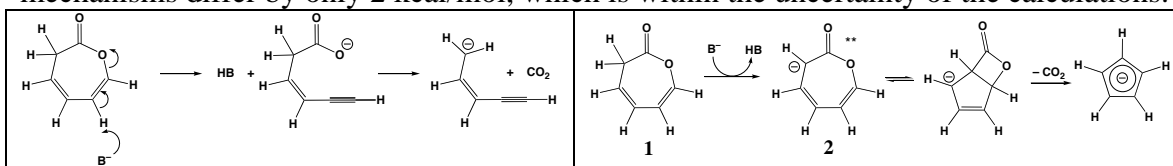
**Towards an Experimental Heat of Formation for the 2-Oxepinoxy Radical**

We have proposed that the 2-oxepinoxy radical could be an important, and possibly detectable, intermediate in the phenyl + O<sub>2</sub> reaction. It is calculated to be the thermodynamically most stable C<sub>6</sub>H<sub>5</sub>O<sub>2</sub> intermediate in our mechanism, and to face substantial barriers to all unimolecular reactions that have so far been investigated. We have embarked on a program to test the theoretical predictions by determining experimental heats of formation and spectroscopic signatures for the radical.

In collaboration with the group of Christopher Hadad at The Ohio State University, we have synthesized 2(3H)-oxepinone (**1**) and have determined its gas-phase acidity in a flowing afterglow. The result is  $\Delta_{298}H_{\text{acid}} = 352 \pm 2$  kcal/mol, which agrees well with the B3LYP/aug-cc-pVTZ value of 349.2 kcal/mol. The anion, **2**, appears to be stable when generated in near-thermoneutral conditions, since acidity measurements determined by both forward (deprotonation of **1**) and reverse (reprotonation of **2**) reactions afford the same value.<sup>4</sup> However, when **1** is deprotonated with strong bases, partial decarboxylation is observed. Two plausible mechanisms have been considered for this process.

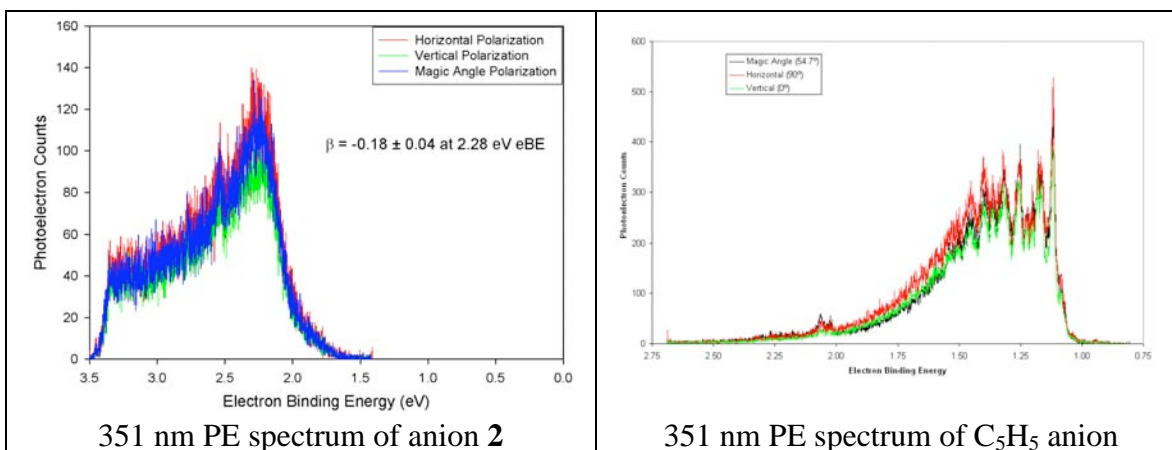


One is that stronger bases open up an E<sub>2</sub>-elimination channel. The other is that the excess internal energy of **2** arising from exothermic deprotonation allows it to surmount a barrier for unimolecular decarboxylation. DFT calculations suggest that the rate-limiting barriers to these two mechanisms differ by only 2 kcal/mol, which is within the uncertainty of the calculations.

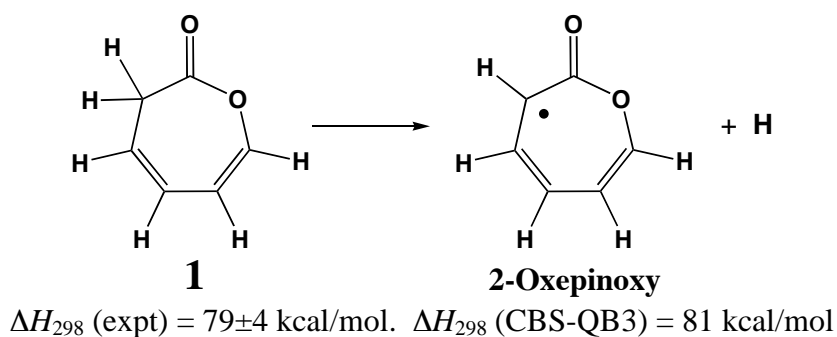


In collaboration with the group of Carl Lineberger at the University of Colorado in Boulder, we have determined the UV photoelectron spectra of both anion **2** and the C<sub>5</sub>H<sub>5</sub> ion produced by its decarboxylation. Both spectra are shown on the next page. Because anion **2** is calculated to be nonplanar, whereas the radical – 2-oxepinoxy– is found to be flat, we anticipated that the (0,0) transition in the photoelectron spectrum could be hard to identify, and that turns out to be the case. Provisionally, the IP of anion **2** seems to be about 1.6 eV, but Franck-Condon calculations are in progress in order to get a more precise estimate. With the provisional value, the combined data from the photodetachment and gas-phase acidity measurements would give the C–H bond

dissociation enthalpy for **1** (in its conversion to 2-oxepinoxy + H) a value of 79 kcal/mol. CBS-QB3 calculations put this value at 81 kcal/mol.



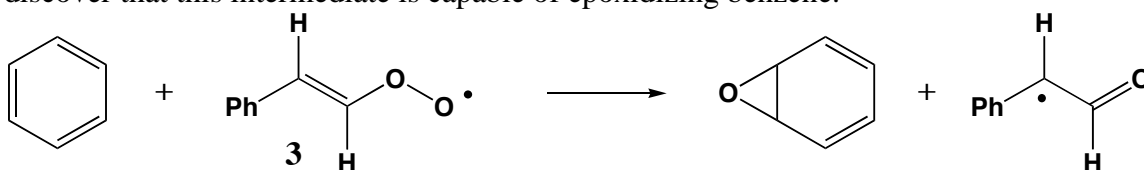
The photoelectron spectrum of the  $C_5H_5^-$  ion shows that it is definitely not cyclopentadienide, whose spectrum is well known and which has been extensively studied in the Lineberger group. This fact rules out the second of the decarboxylation mechanisms shown on the previous page. The (*Z*)-pentenynyl anion that would be generated by the first decarboxylation mechanism has not been previously prepared, and so its photoelectron spectrum is unknown. Franck-Condon calculations are also under way on (*Z*)-pentenynyl anion and radical to determine whether the observed spectrum could be consistent with this structure for the ion.



In addition to the Franck-Condon calculations, completion of the experimental determination for the heat of formation of 2-oxepinoxy requires a calorimetric determination of the heat of formation for the precursor **1**.

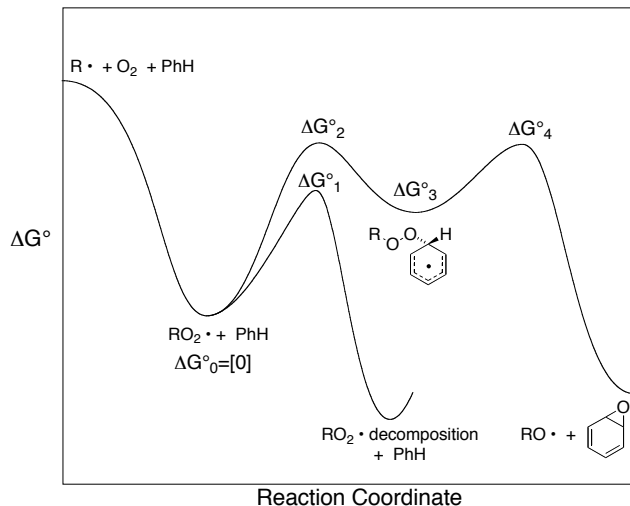
### Oxygen-Transfer Reactions of Unsaturated Peroxy Radicals

During experimental studies on the  $\beta$ -styrylperoxy radical (**3**), we were surprised to discover that this intermediate is capable of epoxidizing benzene.<sup>6</sup>



Several features of this reaction made it worth investigating, in our judgment. First, while there are known conditions for the oxidation of benzene to phenol, this is the only thermal reaction, to our knowledge, that has ever been reported to convert benzene to its epoxide. Second, thermolysis of benzoyl peroxide in O<sub>2</sub>-saturated benzene – conditions that should lead to the formation of phenylperoxy radical – did not result in benzene epoxidation. Hence it appears that not all unsaturated peroxy radicals are capable of effecting this reaction. Third, to our knowledge, oxygen-transfer reactions of peroxy radicals are not included in standard combustion modeling schemes, and so finding out when and why they occur could be important. We investigated these questions with the aid of electronic-structure calculations.

UB3LYP/6-31+G(d,p), G3, and CBS-QB3 calculations on a variety of peroxy radicals supported the mechanism shown in the schematic standard-free-energy profile to the right, and also served to highlight the factors that would make some radicals more effective than others in promoting this reaction. Specifically, it seemed that the TS for addition of the peroxy radical to benzene should have a standard free energy ( $\Delta G^\circ_2$ ) comparable to (or, ideally lower than) the standard free energy ( $\Delta G^\circ_1$ )



of the TS for the most facile unimolecular decomposition pathway for the peroxy radical. In addition, the TS for conversion of the adduct to products should have a TS with a standard free energy ( $\Delta G^\circ_4$ ) comparable to (or, ideally lower than) that for the TS leading to its formation ( $\Delta G^\circ_2$ ). It seemed that both of these requirements would probably be satisfied if the adduct had a weak O–O bond but a strong C–O bond linking the erstwhile peroxy radical and benzene reactants. We further argued, that these properties would probably be reflected in O–O and O–H bond energies of the corresponding hydroperoxides,<sup>6</sup> and that surveys of these quantities might consequently provide an effective way of looking for other radicals that would be good O-atom donors. Table 1, on the next page, summarizes the results of such a survey.

The ability of  $\beta$ -styrylperoxy radical to effect epoxidation of benzene, but the failure of phenylperoxy radical to carry out the reaction, correlate, as expected, with the differences in O–H and O–O BDEs of the corresponding hydroperoxides. DFT calculations on the epoxidation reaction suggested how those factors come into play. At the UB3LYP/6-31+G(d,p) level,  $\Delta G^\circ_2$ ,  $\Delta G^\circ_3$ , and  $\Delta G^\circ_4$  were calculated to be respectively 25.1, 20.7, and 24.9 kcal/mol for oxidation of neat liquid benzene by *E*-PhHC=CHOO•, but 24.6, 20.1, and 27.0 for the corresponding reactions of PhOO•. Thus the addition steps for the two peroxy radicals face similar activation barriers, and lead to adducts of similar stability with respect to the reactants. However, for the PhOO• addition, the stronger O–O bond in the adduct makes its decomposition to the products rate limiting, and raises the overall barrier by 2.4 kcal/mol over that for addition.

**Table 1.** O–H and O–O bond dissociation enthalpies (298K) for selected organic hydroperoxides, ROOH. Values are in kcal/mol. Calculations used the CBS-QB3 model, except where noted.

R	Expt. O–H	Calc. O–H	Expt. O–O	Calc. O–O
H	87.8±0.5	87.8	50.3±0.7	51.3
(CH <sub>3</sub> ) <sub>3</sub> C	84±2	84.8	46±2	47.2
CH <sub>3</sub>	88±1	86.2	44±2	45.6
Ph	–	87.2	–	23.4
H <sub>2</sub> C=CH	–	86.4	–	21.0
<i>E</i> -PhHC=CH	–	86.0 <sup>a</sup>	–	14.9 <sup>a</sup>
NC	–	97.6	–	16.5
BH <sub>2</sub>	–	98.6	–	36.9

a. G3(MP2,B3) result.

These results made it interesting to explore the additions of NCOO• and H<sub>2</sub>BOO• to benzene, since the strong O–H bonds in the corresponding hydroperoxides suggested that the adducts of these radicals to benzene might be relatively stable, and that the barriers to addition might consequently be lower than those for the additions of *E*-PhHC=CHOO• or PhOO•. However NCOO• and H<sub>2</sub>BOO• were not expected to be equally effective oxidants of benzene. The much weaker O–O bond in NCOOH suggested that NCOO• should have the lower overall barrier for the oxidation reaction. The density functional calculations turned out to support that analysis, at least qualitatively, yielding values for  $\Delta G^{\circ}_2$  to  $\Delta G^{\circ}_4$  of 14.5, 6.2, and 17.3 kcal/mol respectively for the H<sub>2</sub>BOO• reaction, and 10.8, 5.0, and 11.1 kcal/mol, respectively for the NCOO• reaction. In order to assess the reliability of the DFT results, the calculations on the NCOO• reaction were repeated at the G3(MP2,B3) level. That model gave values for  $\Delta G^{\circ}_2$  to  $\Delta G^{\circ}_4$  of 13.2, 3.3, and 14.4 kcal/mol, respectively. Thus the calculations suggest that oxidation of benzene by NCOO• should be substantially faster than the observed reaction effected by the  $\beta$ -styrylperoxy radical. More generally, we predict that NCOO• should be a good O-atom donor to essentially any unsaturated hydrocarbon.

### Recent Publications Acknowledging DOE-BES Support

1. “Nonstatistical Dynamics in Thermal Reactions of Polyatomic Molecules,” *Ann. Rev. Phys. Chem.* **2005**, 56, 57.
2. “Reaction of Vinyl Radical with Oxygen: A Matrix Isolation Infrared Spectroscopic and Theoretical Study,” Yang, R.; Yu, L.; Jin, X.; Zhou, M.; Carpenter, B. K. *J. Chem. Phys.* **2005**, 122, 014511.
3. “A Computational Investigation of the Reactivity of a Hexadienyne Derivative,” Litovitz, A. E.; Carpenter, B. K.; Hopf, H. *Org. Lett.* **2005**, 7, 507.
4. “The Gas-Phase Acidity of 2(3H)-Oxepinone: A Step Towards an Experimental Heat of Formation for the 2-Oxepinoxy Radical,” Kroner, S. M.; DeMatteo, M. P.; Hadad, C. M.; Carpenter, B. K. *J. Am. Chem. Soc.* **2005**, 127, 7446.
5. “Factors Controlling the Barriers to Degenerate Hydrogen Atom Transfers,” Isborn, C.; Hrovat, D. A.; Borden, W. T.; Mayer, J. M.; Carpenter, B. K. *J. Am. Chem. Soc.* **2005**, 127, 5794.
6. “Experimental Detection of One Case of Benzene Epoxidation by a Peroxy Radical, and Computational Prediction of Another,” Broyles, D. A.; Carpenter, B. K. *J. Org. Chem.* **2005**, 70, 8642.

## Ion Imaging Studies of Bimolecular Collision Dynamics

David W. Chandler  
Combustion Research Facility  
Sandia National Laboratory  
P.O. Box 969, Mail Stop 9054  
Livermore, CA 94551-0969  
E-mail: chand@sandia.gov

### Program Scope

The goal of this program is to develop new tools for the study of gas phase chemical dynamics and to use them to study the dynamics of fundamental collisional processes. This includes inter and intra molecular energy transfer, photodissociation dynamics and reactive scattering. The primary tool we use to study these processes has been ion imaging. Ion imaging is a technique for the measurement of the velocity (speed and direction) of a laser-produced ion. As such it extends and enhances the sensitivity of Resonant Enhanced Multi-Photon Ionization (REMPI) detection of molecules and atoms. We have been using Ion Imaging to study a new method for the production of ultra-cold molecules, kinematic cooling. We continue to develop the kinematic cooling technique for the production of samples of Ultracold molecules and their use in the study of collisional processes. We are extending this technique to the trapping and guiding of slow molecules for the purpose of collisional studies.

### Recent Progress

From a macroscopic point of view, collisional energy transfer is responsible for the maintenance of thermal equilibrium within a reactive system. From a microscopic point of view, the study of collisional energy transfer is an important way to gain insight about the potential energy surface of the interaction between atomic and molecular species. At high collision energy the transfer is mainly sensitive to the repulsive wall of the interaction potential, but at lower energies or in studying collisions that transfer only a small amount of energy the involvement of the attractive part of the potential energy surface becomes important. In performing previous studies of the differential cross section of inelastic collisional processes, we discovered, in collaboration with Dr. James Valentini of Columbia University, that we could create sample of molecules at sub milliKelvin temperatures. We have studied this process and have extended the study of cooling molecules to several systems beyond NO + Ar collisions. In particular, the HBr +Kr and the NH<sub>3</sub> +Ne systems have been studied since the mass mismatch between the molecule and atom is small, leading to colder samples. We are interested in the possibility of utilizing ultra-cold molecules to study chemical stereo dynamics since this is a tantalizing prospect; however, much experimental capability needs to be developed in order for this to happen. My future work is largely dedicated to developing and characterizing techniques that will lead to such studies.

#### *Ultracold molecule production*

My research focuses on the field of chemical dynamics of gas phase molecular species. Chemical dynamics is the detailed study of the motion of molecules and atoms on potential energy surfaces in order to learn about the details of the surface as

well as the dynamics of their interactions. We have recently produced measurable amounts of cold molecules using a unique crossed molecular beam scattering technique<sup>1</sup>. We are now focusing our efforts on the routine production of samples of ultracold molecules. The routine production of samples of ultracold molecules will provide a potent new tool for the study of many aspects of molecular interactions that are difficult to study with current technologies. Studies of ultra-cold atomic species have already been able to refine the long range potentials of alkali diatomics from the determination of the energy of the highest vibrational state supported in the intermolecular potential by determination of the Feshbach resonance energies<sup>2-3</sup>. This is data spectroscopists have been trying to obtain for a long time and is a very sensitive test of the shape of the intermolecular potential at long range. This success motivates similar sorts of experiments utilizing molecule-atom interactions or molecule-molecule interactions to directly measure the density of quantum states near a dissociation threshold of a polyatomic species<sup>4</sup>. One important aspect to keep in mind about the interaction of two ultra-cold molecules is that the interaction occurs at the top of the intermolecular potential, near the reaction threshold if the molecules are reactive, and therefore is sensitive to the long range part of the potential and not the bottom of the well. I propose to develop the technology and techniques required to produce and manipulate useful densities of ultra-cold molecules and to apply these methods to the study of chemical dynamics.

#### *Rotational and Electronic Inelastic Collisions: NO + Ar*

Our collisional cooling method does not rely on any specific physical property of either colliding species except their masses, because production of a zero velocity sample is a consequence of the experimentally selectable energy and momenta of the collision pair. Moreover, this technique can be used to prepare a single, selectable ro-vibronic quantum state for trapping. We first demonstrated this technique using inelastic collisions between NO molecules in one beam and Ar in the other, specifically  $\text{NO}(^2\Pi_{1/2}, j=0.5) + \text{Ar} \rightarrow \text{NO}(^2\Pi_{1/2}, j'=7.5) + \text{Ar}$ . Using an existing crossed molecular beam experimental apparatus, we generate scattered  $\text{NO}(^2\Pi_{1/2}, j'=7.5)$  with a velocity distribution that is centered about zero, with an upper limit root-mean-square (rms) velocity of  $15 \text{ m s}^{-1}$ . We have more recently made measurements as a function of the velocity of the Ar atomic beam and have shown that as the velocity of the Ar increases the velocity spread of the cold NO is not increased, in accord with our modelling.<sup>5</sup> The probability that an atom-molecule collision will result in an NO molecule that is cooled to within our experimental resolution is small. From an analysis of our data, we estimate that the probability of a molecule having a collision resulting in a laboratory velocity less than  $15 \text{ m s}^{-1}$  is approximately  $10^{-5}$ . In a typical crossed molecular beam experiment, collision frequencies of approximately  $10^{13}$  collisions per second can be achieved. Densities of  $10^7$  to  $10^8$  NO molecules  $\text{cm}^{-3}$  in this single  $(^2\Pi_{1/2}, v', j'=7.5)$  ro-vibrational quantum state with velocities in the laboratory frame of reference rms velocity of 15 meters per second have been achieved.

#### *Collision between NH<sub>3</sub> + Ne.*

More recently, we have scattered NH<sub>3</sub> from Ne in order to cool ammonia in the J=2 rotational state. Because the mass of Ne (20) is close to that of NH<sub>3</sub> (17) the quantum state of NH<sub>3</sub> that is stopped is lower, J=2, than for the NO collision with Ar in which J=7.5 is stopped. A simple equation for determining the amount of energy that must

be put into internal energy in order to stop the molecule was derived and published in reference 5. An image of the ammonia in this state along with the velocity spread measured through the origin is shown in Figure 1. A molecular beam of 5% ammonia seeded in Xe is scattered from a beam of neat Ne gas and the resulting  $\text{NH}_3(J=2)$  is ionized by 2+1 REMPI using  $\sim 334\text{-nm}$  light. The speed of the Xe/ $\text{NH}_3$  molecular beam is measured to be  $420\text{ m s}^{-1}$ , and the speed of the Ne beam is  $760\text{ m s}^{-1}$ . The half width at half maximum velocity distribution that is measured for  $\text{NH}_3$  scattered to the crossing of the molecular beams is approximately  $10\text{ m s}^{-1}$ . Making the artificial relationship  $1/2K_{\text{B}}T = E = 1/2mv^2$  for a one dimensional velocity distribution, we relate the  $10\text{ m s}^{-1}$  to a temperature of approximately  $200\text{ mK}$ . Of course the velocity distribution we obtain with this experiment is not thermal, and the calculated temperature only gives one an order of magnitude sense of the average energy associated with our cold sample for comparison to other techniques.

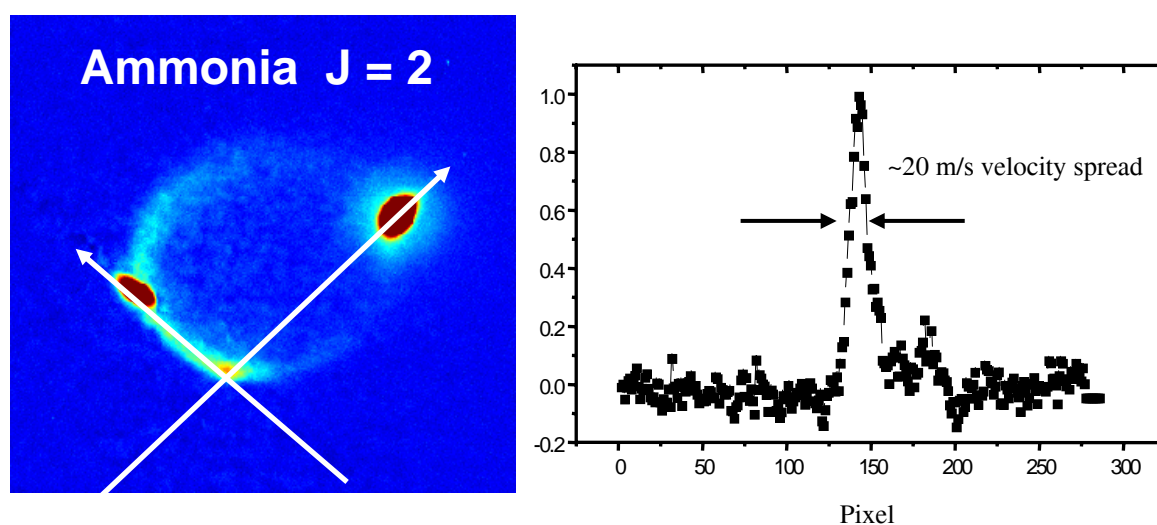


Figure 1, Ion Image of ammonia in the  $J=2$  quantum state recorded after scattering from a beam of Ne. Ionization was through the B-X transition utilizing  $337\text{-nm}$  light. To the right is a velocity distribution associated with the part of the image that is centered around zero velocity in the laboratory reference frame.

### Future Plans

Over the next several years we propose to further develop our collisional cooling technique to produce colder samples and better quantify the velocity distribution we form in the crossed molecular beam apparatus. Additionally, we propose to take advantage of our ability to collisionally cool molecules in a crossed molecular beam apparatus in several ways. First, we will demonstrate the ability to trap cold molecules at the intersection region of the molecular beams with either electrostatic fields or optical fields. Second, we will collect counter-propagating pulses of slowly moving molecules from the atom/molecular beam intersection region into a segmented hexapole storage ring as they exit the interaction region for collisional studies of oriented molecules. Third, we are building an atomic magneto-optical trap (MOT) for the collisional cooling and trapping of molecules by collision with an ultra-cold atom of the same, or similar, mass.

The field of ultracold molecule physical chemistry is in its infancy. To be able to utilize cold molecules for collisional studies as proposed here as well as to study stereochemistry, photochemistry, high resolution spectroscopy, molecular optics, entangled states, tunneling barriers, Feshbach resonances and a host of other possible

research areas, a robust and reliable manner to produce ultracold molecules must be developed. To imagine the potential impact of such a development one needs only to think of the impact of other technologies for cooling molecules and controlling the velocity of molecules: supersonic molecular beams, liquid helium droplet production, or the impact ultracold atom production has had on the Atomic Physics community. This is the science what we are interested in pursuing. As the first step along this path one must learn to reliably produce samples of ultracold molecules and accurately characterize those sources.

## References

- 1) *Subkelvin Cooling NO Molecules via "Billiard-Like" Collisions with Argon*. Elioff, MS; Valentini, JJ; Chandler, DW. Science; vol.302, no.5652, p.1940-3, (2003).
- 2) *Very-high-precision bound-state spectroscopy near a Rb-85 Feshbach resonance*. Claussen, NR; Kokkelmans, SJJMF; Thompson, ST; Donley EA; Hodby, E; Wieman CE; Phys.Rev. A 67, 060701 (2003).
- 3) *High resolution Feshbach spectroscopy of cesium*. Chin C, Vuletic V, Kerman AJ, Chu S. Phys. Rev. Lett., 85 (13): 2717-2720, (2000).
- 4) *Long-Range Scattering Resonances in Strong-Field-Seeking States of Polar Molecules*. Ticknor, C.; Bohn, JL. Physical Review A (Atomic, Molecular, and Optical Physics); vol.72, no.3, p.32717-1-8, (2005).
- 5) *Formation of NO(j'=7.5) Molecules with Subkelvin Translational Energy via Molecular Beam Collisions with Argon Using the Technique of Molecular Cooling by Inelastic Collisional Energy-Transfer*. Elioff, MS; Valentini, JJ; Chandler, DW. European Physical Journal D; vol.31, no.2, p.385-93, (2004).

## Publications for 2004 and 2005

- 1) Probing Spin-Orbit Quenching in Cl(2P)+H<sub>2</sub> via Crossed Molecular Beam Scattering. Parsons B, Strecker K, Chandler DW, European Physical Journal D, accepted for publication April 2006.
- 2) Differential Cross Sections for Collisions of Hexapole State-Selected NO with He. Gijbbersen A, Linnartz H, Rus G, Wiskerke AE, Stolte S, Chandler DW, Klos J, J. Chem. Phys. 123 (22): Art. No. 224305 (2005).
- 3) Simultaneous Time- and Wavelength-Resolved Fluorescence Microscopy of Single Molecules. Luong AK, Gradinaru GC, Chandler DW, Hayden CC, J. Phys. Chem. B. 109 (33): 15691-15698 (2005).
- 4) An Investigation of Nonadiabatic Interactions in Cl(P-2(j))+D-2 via Crossed-Molecular-Beam Scattering, Parsons BF, Chandler DW, J. Chem. Phys. 122 (17): Art. No. 174306 (2005).
- 5) Formation of NO(j'=7.5) Molecules with Sub-Kelvin Translational Energy via Molecular Beam Collisions with Argon Using the Technique of Molecular Cooling by Inelastic Collisional Energy-Transfer. Elioff MS, Valentini JJ, Chandler DW, Euro. Phys. J. D, 31 (2): 385-393 (2004).
- 6) Photodissociation Dynamics of ArNO Clusters. Parsons BF, Chandler DW, Sklute EC, Li SL, Wade EA, J. Phys. Chem A. 108 (45): 9742-9749 (2004).
- 7) Ion Imaging Studies of Product Rotational Alignment in Collisions of NO (X-2 Pi(1/2), j=0.5) with Ar. Wade EA, Lorenz KT, Chandler DW, Barr JW, Barnes GL, Cline JI, Chem. Phys., 301 (2-3): 261-272 (2004)
- 8) Single-Molecule FRET Microscopy of DNA Bending by Bacterial Nucleoid Proteins, Raarup MK, Chandler DW, Dame RT, Goosen N, Schmidt T. Biophys. J., 86 (1): 327A-327A Part 2 Suppl. S, (2004).

## Terascale Direct Numerical Simulation and Modeling of Turbulent Combustion

Jacqueline H. Chen (PI), Evatt R. Hawkes, Ramanan Sankaran, David Lignell, and Chun S. Yoo  
Combustion Research Facility  
Sandia National Laboratories  
P.O. Box 969, Mail Stop 9051  
Livermore, California 94551-0969  
E-mail: [jhchen@sandia.gov](mailto:jhchen@sandia.gov)

### Program Scope

The goal of this research program is to gain fundamental insight into unsteady flow/chemistry interactions that occur in turbulent combustion, and to develop and validate combustion models required in various engineering CFD approaches including Reynolds Averaged Navier-Stokes (RANS) and Large-eddy simulation (LES). In this work a high-fidelity numerical approach known as direct numerical simulation (DNS), which resolves all of the scales in the scalar and velocity fluctuations, is used to efficiently investigate fine-grained physical phenomena associated with interactions between convective and diffusive transport with detailed chemistry in the combustion of hydrogen and hydrocarbon fuels.

### Recent Progress

In the past year, with significant computer allocations from a 2005 DOE Innovative and Novel Computational Impact on Theory and Experiment (INCITE) grant and from NCCS/ORNL, we performed terascale 3D direct numerical simulations of turbulent flames with detailed chemistry. These studies focused on understanding: 1) scalar mixing of reactive and passive scalars in a CO/H<sub>2</sub> jet flame undergoing extinction followed by reignition; 2) the influence of intense turbulence on the flame structure of lean premixed methane-air turbulent flames; and 3) the influence of near-wall turbulent structures and interaction with a premixed hydrogen/air flame on the spatial and temporal patterns of wall heat fluxes. DNS data are also being used to evaluate and improve combustion models. For example, an enthalpy-based flamelet model of autoignition with thermal inhomogeneities was tested against our HCCI DNS data with different initial temperature variance. We have also begun to investigate turbulence coupling with soot production and transport in DNS of sooting ethylene flames. Several of our accomplishments in the past year are summarized below, followed by a description of future research directions.

#### *Scalar Mixing in Direct Numerical Simulations of Temporally-Evolving Plane Jet Flames with Detailed CO/H<sub>2</sub> Kinetics*<sup>13</sup>

To better understand the intricate relationship of turbulence, turbulent mixing and finite-rate chemical reactions, we conducted the first 3D direct numerical simulation of a turbulent nonpremixed H<sub>2</sub>/CO-air flame with detailed chemistry undergoing extinction/reignition with our INCITE grant at NERSC. Also, at MSCF/PNNL and at NCCS/ORNL, we made additional simulations with up to 0.5 billion grid points as part of a parametric study in Reynolds number (Re ranging between 2510 and 9079).

Small-scale turbulence-chemistry interaction phenomena such as extinction and reignition, flow and flame unsteadiness as well as differential diffusion of chemical species are difficult to measure experimentally. Canonical DNS simulations, which resolve all of the temporal and spatial scales of the flow and scalars, uniquely provide structure and statistical information associated with the scalar dissipation rate field, i.e. the dissipation of fluctuations of mixture fraction and reactive scalars in a turbulent flow. Statistics obtained from these calculations are being used to understand the intricate coupling between turbulence, mixing and reaction, and to validate and improve models.

The initial data analysis (of the 30 terabytes of raw data) shows how detailed transport and finite-rate chemistry effects can influence the mixing of passive and reactive scalars. Molecular mixing is the central modeling issue in a key combustion model, the transported probability density function (pdf) approach. In this framework, model predictions are dependent upon the choice of a mixing timescale. Nominally, the

timescale is assumed to be the same for all scalars, and the same order of magnitude as the large scale turbulence timescale. But in flames, differential diffusion between species and the strong interplay between mixing and reaction may degrade these assumptions.

The DNS data show that the turbulence-to-scalar mixing timescale ratio for a conserved scalar (mixture fraction) is close to unity and nearly independent of Reynolds number at sufficiently high Reynolds numbers. On the other hand, non-unity Schmidt numbers and finite-rate chemical effects were found to affect this timescale ratio for reactive species by as much as a factor of three. For major species, there is a decline in the dependence of this timescale ratio on molecular diffusivity with increasing Reynolds number, though a weak dependence exists at the highest Reynolds number simulated,  $Re=9079$ . Chemical reaction effects on reactive scalar mixing were noted for minor species, however, and persist to high Reynolds numbers. The mixing attributes of these species depends not only on their local turbulence production and dissipation balance, but also on reaction.

Simulating different Reynolds numbers illuminated ‘intermittency’— the intense, localized fluctuations in a turbulent flow which can cause localized extinctions and reignition in the combustion process. The results show the link between scalar intermittency and the Reynolds number. As the Reynolds number, and hence, scalar intermittency increases, a greater degree of local extinction is observed and it takes longer to reignite the extinguished regions. Varying degrees of extinction for the different  $Re$  simulations are demonstrated by the conditional pdf of the mass fraction of the OH radical and its conditional Favre mean. The pdf remains monomodal for the CO/H<sub>2</sub> mixture, consistent with earlier experimental observations. The DNS data also show that the high intermittency is manifested by a near log-normally distributed scalar dissipation rate with small negative skewness.

### 3D DNS of the Structure of a Spatially-Developing Lean Methane-Air Turbulent Bunsen Flame<sup>12</sup>

There is strong interest in achieving lean premixed combustion in practical applications of power generation due to high thermal efficiencies and low NO<sub>x</sub> emissions. Because lean flames are thicker and propagate more slowly, these devices operate in the thin reaction zones regime, where intense turbulence can penetrate the broader preheat zone of the flame, but not the reaction zone. There have been contradictory experimental results in this regime, with some reporting thinner flames and others reporting thicker flames. The source of the thickening if it exists is also not clear. To understand the influence of turbulence on the structure of the preheat and reaction zones, we performed the first 3D fully resolved DNS of a spatially-developing lean methane-air turbulent Bunsen flame in the thin reaction zones regime with reduced chemistry. The simulation was advanced long enough to reach statistical stationarity. A reduced chemical mechanism for lean premixed methane-air flames was derived by Lu and Law, Princeton University, customized to the parameter space of the DNS, with minimal temporal stiffness and suitable for vectorization enabling efficient computation on the Cray X1E at ORNL. The reduction was achieved through sequential application of directed relation graph, sensitivity analysis and computational singular perturbation over the GRI-1.2 detailed mechanism.

The DNS results show thickening of the preheat zone due to the action of the turbulent eddies. Despite a mean positive strain rate, the average flame was thicker. Correlations of flame thickness with strain rate and curvature were obtained. A balance equation for the isosurface following derivative of the progress variable gradient was used to determine the sources that affect the flame thickness. Conditional mean reaction rates of the fuel, CO and OH were compared with unstrained and strained laminar reaction rate profiles. The results indicate that while there is considerable thickening of the preheat layer, the turbulent eddies do not significantly disrupt the reaction zone. This may be due to the attenuation of turbulence near the inner layer due to heat release.

### Flamelet-Based Modeling of Autoignition with Thermal Inhomogeneities for Application to HCCI Engines<sup>14</sup>

Homogeneous-Charge Compression Ignition (HCCI) engines have been shown to have higher thermal efficiencies and lower NO<sub>x</sub> and soot emissions than Spark Ignition engines. However, HCCI engines experience very large heat release rates which can result in too rapid an increase in pressure. One method of reducing the heat release rate is to introduce thermal inhomogeneities. DNS with detailed H<sub>2</sub>/air chemistry

(Chen et al. 2006, Hawkes et al 2006, Sankaran et al. 2005) showed that both ignition and deflagration fronts may be present in systems with such inhomogeneities. Collaborating with H. Pitsch and D. Cook of Stanford University, we have developed an enthalpy-based flamelet model and applied it to the DNS test cases in which the temperature variance was varied. The model uses a mean scalar dissipation rate to model mixing between regions of higher and lower enthalpies. The predicted heat release rates agree well with the DNS cases. The model is able to capture spontaneous ignition propagation, deflagrative propagation, as well as mixed-mode propagation. This model shows considerably improved agreement with DNS data over the multizone model, particularly in situations where diffusive transport is important.

#### *DNS of soot growth and transport processes in turbulent nonpremixed ethylene flames*

We have implemented a soot model in the DNS code S3D to study soot growth and transport processes in non-premixed, turbulent flames with complex chemistry. Application of DNS to turbulent sooting flames is an extension to current capabilities intended to increase fundamental understanding of soot-flame-turbulence interactions that do not occur in laminar flames, and to provide high fidelity data that can be used to develop and validate reaction and mixing closure models for LES/RANS calculations. The soot model consists of two transport equations for soot mass fraction and number density with reactive source terms based on a four-step global mechanism including soot nucleation, growth, oxidation and coagulation processes. The soot mechanism was fully integrated with the gas-phase species and energy equations, with detailed transport. A validated, reduced chemistry ethylene mechanism consisting of 19 transported gas-phase species for ethylene combustion was developed by T. Lu and C.K. Law of Princeton University for the DNS simulations.

The testing of the models have been carried out in one- and two-dimensional configurations of increasing complexity: a relaxing non-premixed 1D diffusion flame, a temporal mixing layer with a single vortex-eddy, and flames in 2D decaying isotropic turbulence, with an aim toward a three-dimensional temporal jet simulation. The 2D turbulent cases have yielded important insights into soot formation/oxidation in turbulent flames, such as soot-flame breakthrough in highly curved, burning flame zones, as well as enhanced soot production in regions where soot is convected towards a flame, with a strong correlation to flame curvature.

#### **Future Plans**

The INCITE and NCCS/ORNL projects generated 30 TB of raw DNS data, which are being analyzed to understand turbulent mixing of reactive scalars and extinction and reignition dynamics. To assist with the task of gleaning physical insight from terascale simulated data, we are working closely with computer scientists to develop parallel feature extraction/tracking tools and interactive multi-variate visualization capabilities for spatial and time-varying data that will help us understand how turbulent mixing interacts with chemical reactions. Phenomena we are working to understand include the dynamic behavior at flame edges and cusps, formation of extinction pockets, and the mechanisms by which these pockets reignite. New modules are being developed for flame edge detection and edge speed computation of intersecting passive and reactive scalar isosurfaces. We plan to make qualitative comparisons of the DNS data with measurements of the fine-scale scalar structure with Jonathan Frank and Rob Barlow of SNL. We also plan to perform a priori validation of a multiple-environment conditional PDF model by Raman and Fox 2004 for extinction and reignition in turbulent nonpremixed flames.

In the area of turbulent premixed combustion we plan to perform several more 3D DNS at higher turbulence intensities. The DNS will be instrumented with flame element tracking to determine the transient response of the turbulent burning velocity in the thin reaction zones regime. We have extended the statistical analysis modules for handling three-dimensional data, and new modules are also being added to extract iso-surfaces from the 3D volume data, and to obtain statistical quantities in directions normal and tangential to the iso-surfaces. Analysis in flame-based coordinates will be used to determine the cause of the preheat zone thickening and any modifications to the gradients of heat and mass at the upstream boundary of the fuel consumption layer that affect the burning rate.

Other topics we plan to address include: 1) performing 3D DNS of turbulent nonpremixed sooting ethylene flames to investigate the coupling of turbulent transport with soot formation, oxidation, and transport, such as soot-flame breakthrough in highly curved, burning flame zones; 2) performing joint

computations and experiments of transient counterflow autoignition with Jonathan Frank, SNL to determine the autoignition response of hydrogen and hydrocarbon fuels to unsteady strain rate; 3) performing 3D DNS of turbulent lifted vitiated hydrogen/air flames to investigate the dynamics of flame stabilization in the presence of a vitiated coflow; and 4) performing DNS of multi-stage n-heptane auto-ignition in the presence of thermal stratification in a fixed volume at high pressure.

#### **BES Publications (2004-2006)**

1. E. R. Hawkes and J. H. Chen, "Direct Numerical Simulation of Hydrogen Enriched Lean Premixed Methane/Air Flames," *Combust. Flame*, **138**: 242-258. (2004).
2. S. Liu, J. C. Hewson, J. H. Chen, and H. Pitsch, "Effects of Strain Rate on High-Pressure Nonpremixed N-Heptane Autoignition in Counterflow," *Combust. Flame*, **137**:320-339 (2004).
3. E. R. Hawkes and J. H. Chen, "Evaluation of Models for Flame Stretch in the Thin Reaction Zones Regime," *Proceedings of the Combustion Institute*, **30**, pp. 647-655. (2004).
4. J. C. Sutherland, P. J. Smith, and J. H. Chen, "A Generalized Method for A Priori Evaluation of Combustion Reaction Models," submitted to *Combust. Flame*, (2006).
5. R. Sankaran, H. G. Im, E. R. Hawkes, and J. H. Chen, "The Effects of Nonuniform Temperature Distribution on the Ignition of a Lean Homogeneous Hydrogen-Air Mixture," *Proceedings of the Combustion Institute*, **30**, pp. 875-882. (2004).
6. R. Seiser, J. H. Frank, S. Liu, J. H. Chen, R. J. Sigurdsson, and K. Seshadri, "Ignition of Hydrogen in Unsteady Nonpremixed Flows," *Proceedings of the Combustion Institute*, **30**, pp. 423-430. (2004).
7. E. R. Hawkes and J. H. Chen, "Comparison of Direct Numerical Simulations of Lean Premixed Methane-Air Flames with Strained Laminar Flame Calculations", *Combust. Flame*, **144**: 112-125. (2005).
8. J. C. Sutherland, P. J. Smith, and J. H. Chen, "Quantification of Differential Diffusion in Nonpremixed Systems," *Combust. Theory and Modeling*, **9**:2, pp. 365-383. (2005).
9. J. H. Chen, E. R. Hawkes, R. Sankaran, S. D. Mason, and H. G. Im, "Direct Numerical Simulation of Ignition Front Propagation in a Constant Volume With Temperature Inhomogeneities, Part I: Fundamental Analysis and Diagnostics", *Combust. Flame*, **145**: 128-144. (2006).
10. E. R. Hawkes, R. Sankaran, P. Pebay, and J. H. Chen, "Direct Numerical Simulation of Ignition Front Propagation in a Constant Volume With Temperature Inhomogeneities, Part II: Parametric Study", *Combust. Flame*, **145**: 145-159. (2006).
11. S. Liu, J. C. Hewson, and J. H. Chen, "Nonpremixed n-heptane autoignition in unsteady counterflow," to appear *Combust. Flame*, March (2006).
12. R. Sankaran, E. R. Hawkes, J. H. Chen, T. Lu, and C. K. Law, "Structure of a Spatially-Developing Lean Methane-Air Turbulent Bunsen Flame," to appear *Proceedings of the Combustion Institute*, **31**. (2006).
13. E. R. Hawkes, R. Sankaran, J. Sutherland, and J. H. Chen, "Scalar Mixing in Direct Numerical Simulations of Temporally-Evolving Plane Jet Flames with Detailed CO/H<sub>2</sub> Kinetics," to appear *Proceedings of the Combustion Institute*, **31**. (2006).
14. D. J. Cook, H. Pitsch, J. H. Chen, and E. R. Hawkes, "Flamelet-Based Modeling of Autoignition with Thermal Inhomogeneities for Application to HCCI Engines," to appear *Proceedings of the Combustion Institute*, **31**. (2006).
15. A. Gruber, R. Sankaran, E. R. Hawkes, J. H. Chen, "Wall Heat Fluxes in Turbulent Flame-Wall Interaction at Low Reynolds Number: a DNS Study," in preparation.

**Dynamics and Energetics of Elementary Combustion Reactions and Transient Species  
Grant DE-FG03-98ER14879**

Robert E. Continetti  
Department of Chemistry and Biochemistry  
University of California San Diego  
9500 Gilman Drive  
La Jolla, CA 92093-0340  
[rcontinetti@ucsd.edu](mailto:rcontinetti@ucsd.edu)

April 10, 2006

**Program Scope**

This research program continues studies of the dynamics and energetics of transient species that play important roles in bimolecular combustion reactions involving the hydroxyl radical. Using a photoelectron-photofragment coincidence (PPC) spectrometer, transient neutral species are prepared by photodetachment of corresponding negative ions. The energetics of the nascent neutrals, including dissociative complexes and stable intermediates, is characterized by the photoelectron spectra, while the subsequent dissociation dynamics is probed by recording multiple neutral photofragments from the same photodetachment event in coincidence. In addition, the employment of imaging techniques enables measurement of the angular distributions for both the photoelectrons and photofragments, providing further insights into the dissociative photodetachment (DPD) dynamics.

In the past year, the primary effort focused on extending our previous studies of the  $\text{OH} + \text{CO} \rightarrow \text{HOCO} \rightarrow \text{H} + \text{CO}_2$  potential energy surface by use of a series of lower photon energies in the photodetachment of  $\text{HOCO}^-$ . The study of the HOCO potential well by near-threshold photodetachment and a two-photon detachment process have both been completed. Experiments were also carried at intermediate photon energies to characterize the energy dependence of the  $\text{HOCO} \rightarrow \text{H} + \text{CO}_2$  channel and the threshold behavior of the  $\text{OH} + \text{CO}$  product channel. A new series of experiments to extend our previous studies of the  $\text{OH} + \text{F} \rightarrow \text{O} + \text{HF}$  reaction are also underway. Previous studies of the DPD of  $\text{OHF}^-$  using 258 nm photons (4.80 eV, DOE publication #3) probed the  $\text{O} + \text{HF}$  product channel and provided evidence for a breakdown of vibrational adiabaticity in this system. In the current experiments, first the detailed product angular distributions are being measured at 4.8 eV, followed by a new series of experiments at 230 nm (5.4 eV), that will provide access to the  $\text{OH} + \text{F}$  product channel as well. In addition, in the last year an improvement of the pumping speed in the ion source (by a factor of four) was completed, allowing the production of colder, weakly bound anion precursors.

**Recent Progress**

**1. Probing HOCO free radical by DPD of  $\text{HOCO}^-$**

Recent experiments have concentrated on the DPD dynamics of  $\text{HOCO}^-$  at a number of wavelengths, extending previous studies of this reaction at 258 nm (4.80 eV).<sup>1</sup> Measurement of photoelectrons in coincidence with one of the three neutral product

channels:  $\text{H}+\text{CO}_2$ ,  $\text{OH}+\text{CO}$  and stable  $\text{HOCO}$ , allowed characterization of the potential energy surface and dissociation dynamics of the  $\text{HOCO}$  free radical intermediate in the  $\text{OH} + \text{CO} \rightarrow \text{H} + \text{CO}_2$  reaction.

In recent progress, the bottom of  $\text{HOCO}$  potential well was probed by near-threshold photodetachment of  $\text{HOCO}^-$  at 772 nm (1.6 eV), yielding resolved structure in the photoelectron spectra. The resolved structure may derive from vibrational progressions or the likely existence of *cis*- and *trans*-  $\text{HOCO}^-$  isomers in the ion beam. A two-photon photodetachment process was also observed, with a four-fold symmetry in the photoelectron angular distribution at 772 nm (Figure 1), while the one-photon measurement at 386 nm only shows photoelectrons peaking parallel to the laser electric field. Closer examination reveals that the two-photon signals parallel and perpendicular to the electric vector of the 772 nm radiation exhibit distinct photoelectron spectra (Figure 2), and have different compositions with respect to the  $\text{HOCO}$ ,  $\text{OH}+\text{CO}$  and  $\text{H}+\text{CO}_2$  products. This nearly resonant two-photon detachment process may involve the transient one-photon photodetachment continuum as an important intermediate step. One interesting possibility is that the two-photon detachment process provides a means for separating the *cis*- and *trans*- $\text{HOCO}^-$  contributions to the observed spectra.

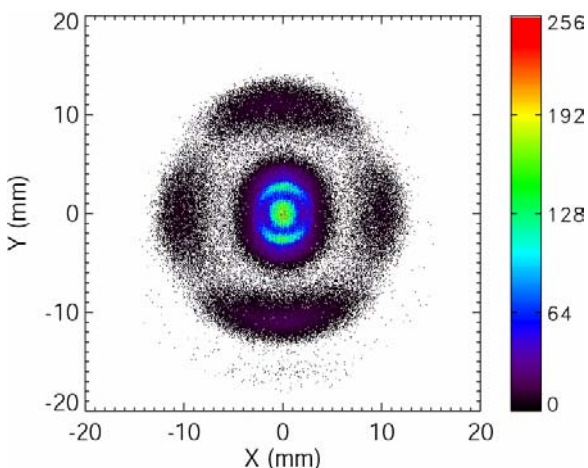


Fig. 1. Photoelectron image of  $\text{HOCO}^-$  at 772 nm. The laser polarization is along the y axis.

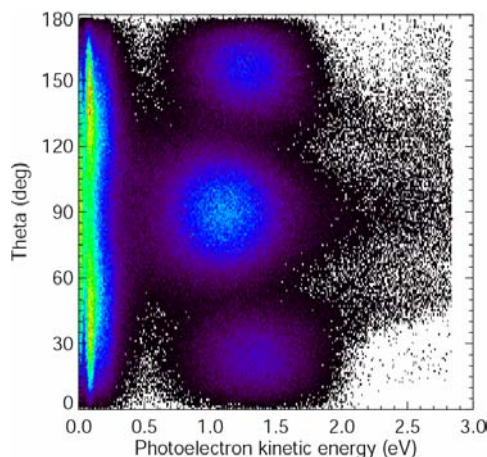


Fig. 2. Photoelectron kinetic energy vs.  $\theta$ .  $\theta$  is defined as photoelectron recoil angle with respect to the laser polarization.

The DPD dynamics of  $\text{HOCO}^-$  have also been studied at several other laser wavelengths, including 386 nm (3.2 eV) and 532 nm (2.3 eV). At all wavelengths studied to date, it is found that the  $\text{H} + \text{CO}_2 + e^-$  channel is open below the calculated dissociation barrier,<sup>2</sup> indicating that quantum mechanical tunneling is important for this channel even near the bottom of the  $\text{HOCO}$  well. In addition, it was found that in the  $\text{H} + \text{CO}_2 + e^-$  channel, the maximum kinetic energy ( $\text{KE}_{\text{max}}$ ) summed for all translational degrees of freedom exhibits a shift to lower energy at 532 nm compared with measurements at other wavelengths. This  $\text{KE}_{\text{max}}$  shift may indicate that excited  $\text{HOCO}^-$  resonant states are populated at this wavelength, mediating vibrational-state-specific tunneling into  $\text{H} + \text{CO}_2$  products at 532 nm. Finally, the measurements at lower photon energies show that the  $\text{OH} + \text{CO}$  product channel is also observed in a more limited range below the calculated

energetic limit. In this case, tunneling is not possible and the most likely explanation are hot bands in the *trans*-HOCO<sup>-</sup> anion that reaches the HOCO neutral surface closest to the OH + CO products, or a problem in the calculated *cis*- / *trans*- energy differences in the HOCO<sup>-</sup> and HOCO wells.

## 2. OHF<sup>-</sup> and the O + HF → OH + F reaction

The O + HF → OH + F reaction is a benchmark system that can be studied by dissociative photodetachment of the OHF<sup>-</sup> anion, as originally shown by the photoelectron spectroscopy measurements by Neumark and co-workers.<sup>3</sup> This system has recently been the subject of extensive theoretical calculations of both the potential energy surfaces and dynamics by Roncero and co-workers,<sup>4,5</sup> focusing on non-adiabatic effects on the reaction dynamics on the neutral potential energy surface. Previously, photoelectron-photofragment coincidence studies of this system have been carried out at a photon energy of 4.8 eV (258 nm), as recently reported in Phys. Chem. Chem. Phys. (DOE publication 3 below). In this earlier work, a vibrationally non-adiabatic process was observed in the O + HF(*v* = 1) channel. The calculations of Roncero and co-workers support the presence of non-adiabatic channels and suggest that these are mediated by conical intersections along the reaction coordinate near the linear configuration. To study this system in the interesting region near the opening of the OH + F channel, where a number of scattering resonances are predicted, it will be essential to use higher photon energies for photodetachment. Efforts to make 230 nm light with the Ti:Sapphire/OPA laser system have been successful and we should thus soon be able to prepare product states in the endothermic OH + F channel. Current studies are recording detailed photoelectron-photofragment angular distributions at 4.8 eV to help deconvolute contributions from different electronic states of the OHF system.

## 3. Improvements of the ion source

Previous efforts to synthesize sufficient quantities of the (H<sub>3</sub>O)<sup>-</sup> and (OHCl)<sup>-</sup> anions in the laboratory have not been successful. These anions have previously been studied by photoelectron spectroscopy, and will provide an important platform to study the fundamental OH + H<sub>2</sub> and O + HCl reactions.<sup>6</sup> During the summer of 2005, a new pumping system was installed, employing an 8000 l/s diffusion pump backed by a roots blower system. This increase of the pumping speed by a factor of four has improved the performance of the anion source considerably and will be essential to studying these reactions using PPC spectroscopy.

## Future plans

Following the study of the DPD dynamics of (OHF)<sup>-</sup> at 230 nm, future experiments are being planned on other hydroxyl radical reactions including the OH+H<sub>2</sub> and OH+Cl systems. With the new pumping system installed, synthesis of the required anion precursors (H<sub>3</sub>O)<sup>-</sup> and (OHCl)<sup>-</sup> in sufficient quantities to carry out these experiments should be possible. The PPC spectrum of (H<sub>3</sub>O)<sup>-</sup> in particular has already been predicted in reaction dynamics calculations,<sup>7</sup> so this system will provide an important test of this fundamental reaction. As these efforts proceed, future research will also extend our previous DPD study of the acetate anion to larger carboxylate anions. Several candidates in this category include benzoate (C<sub>6</sub>H<sub>5</sub>CO<sub>2</sub><sup>-</sup>) and its methyl-

substituted isomers (*o*-, *m*-, *p*-CH<sub>3</sub>C<sub>6</sub>H<sub>5</sub>CO<sub>2</sub><sup>-</sup>), recently studied by photoelectron spectroscopy by Wang and coworkers.<sup>8</sup> The DPD measurement will elucidate the influence of conjugation of the carboxyl radical with the phenyl ring and steric effects of methyl substitution on the stability of corresponding carboxyl radicals. Finally, once the extensive measurements conducted on the HOCO<sup>-</sup> anion have been fully understood, an appropriate wavelength will be chosen to study the effect of deuterium substitution by synthesizing the DOCO<sup>-</sup> anion. This measurement has not been carried out to date as it requires the use of expensive CD<sub>4</sub> for generation of the DOCO<sup>-</sup> anion.

#### DOE Publications: 2004 – Present

1. R.E. Continetti and C.C. Hayden, "Coincidence imaging techniques," in Modern Trends in Reaction Dynamics, ed. X. Yang and K. Liu, World Scientific (Singapore), 2004.
2. Z. Lu and R.E. Continetti, "Dynamics of the acetyloxyl radical studied by dissociative photodetachment of the acetate anion.", *J. Phys. Chem. A* **108**, 9962-9969 (2004).
3. H.J. Deyerl and R.E. Continetti, "Photoelectron-photofragment coincidence study of OHF<sup>-</sup>: transition state dynamics of the reaction OH + F → O + HF.", *Phys. Chem. / Chem. Phys.* **7**, 855-860 (2005).

#### References Cited

---

1. T.G. Clements, R.E. Continetti and J.S. Francisco, *J. Chem. Phys.* **117**, 6478 (2002).
2. H.-G. Yu, J.T. Muckerman and T. Sears, *Chem. Phys. Lett.* **349**, 547 (2001).
3. S.E. Bradforth, D.W. Arnold, R.B. Metz, A. Weaver and D.M. Neumark, *J. Phys. Chem.* **95**, 8066 (1991).
4. L. González-Sánchez, S. Gómez-Carrasco, A. Aguado, M. Paniagua, M. L. Hernández, J. M. Alvarino and O. Roncero, *J. Chem. Phys.* **121**, 309 (2004). ; S. Gómez-Carrasco, L. González-Sánchez, A. Aguado, O. Roncero, J. M. Alvarino, M. L. Hernández and M. Paniagua, *J. Chem. Phys.* **121**, 4605 (2004).
5. L. González-Sánchez, S. Gómez-Carrasco, A. Aguado, M. Paniagua, M. Luz Hernández, J. M. Alvarino and O. Roncero, *J. Chem. Phys.* **121**, 9865 (2004).
6. E. de Beer, E.H. Kim, D.M. Neumark, R.F. Gunion and W.C. Lineberger, *J. Phys. Chem.* **99**, 13627 (1995); M.J. Davis, H. Koizumi, G.C. Schatz, S.E. Bradforth and D.M. Neumark, *J. Chem. Phys.* **101**, 4708 (1994).
7. D.H. Zhang, M.A. Collins and S-Y. Lee, *Proc. Nat. Acad. Sci.* **99**, 11579 (2002).
8. H.-K. Woo, X.-B. Wang, B. Kiran, L.-S. Wang, *J. Phys. Chem. A* **109**, 11395 (2005).

## Studies of Flame Chemistry with Photoionization Mass Spectrometry

Terrill A. Cool  
School of Applied and Engineering Physics  
Cornell University, Ithaca, New York 14853  
[tac13@cornell.edu](mailto:tac13@cornell.edu)

### Project Scope

Studies of flame chemistry leading to an understanding of the kinetic mechanisms responsible for the formation of undesirable combustion byproducts including NO<sub>x</sub>, soot particles, and hazardous emissions, (e.g., polycyclic aromatic hydrocarbons (PAH)) are critically important in efforts to minimize environmental pollution associated with hydrocarbon combustion. Principal themes of our current research are (1) develop further understanding of the chemical mechanisms that are precursors to the formation of PAHs and soot, and (2) study the flame chemistry of oxygenated fuels or fuel additives (dimethyl ether, ethanol, alkyl esters) proposed as clean burning alternatives to conventional liquid hydrocarbon fuels derived from petroleum.

Kinetic model development in all of these reaction systems requires direct measurements of the absolute concentrations of combustion intermediates in laboratory flames chosen to reveal underlying reaction mechanisms. Photoionization mass spectrometry (PIMS) using monochromated synchrotron radiation, applied to the selective detection of flame species, is uniquely suited for the development and testing of kinetic models of combustion chemistry. A flame-sampling PIMS instrument, developed at the Advanced Light Source of the Lawrence Berkeley National Laboratory in a collaborative effort between investigators at Cornell, the Sandia Combustion Research Facility, the University of Massachusetts, and the ALS Chemical Dynamics group, is leading to major advances in the detection of reaction intermediates in laboratory flames and the measurement of their concentrations. These advances yield improved kinetic models for the combustion of the major classes of modern fuels and fuel blends, and measurements of fundamental properties (photoionization cross sections and ionization energies) of selected reaction intermediates. This instrument is the first to use easily tunable vacuum ultraviolet synchrotron radiation for PIMS studies of flame species.

### Recent Progress

The past year has been exceptionally productive, with work completed for a variety of fuel-rich hydrocarbon and oxygenated hydrocarbon flames. Our research has focused on several studies:

1. The identification of isomers of C<sub>3</sub>, C<sub>4</sub>, and C<sub>5</sub> unsaturated hydrocarbon radicals in fuel-rich hydrocarbon flames in studies of precursor reaction mechanisms leading to the formation of polycyclic aromatics (PAHs) and soot.

2. A systematic search for ethenol and higher enols in 24 different flames of 14 prototypical fuels representing the major classes of chemicals appearing in modern fuel blends: alkanes, alkenes, alkynes, cyclic hydrocarbons, aromatics, and alcohols.
3. Initial mole fraction measurements of reaction intermediates in alkyl ester (e.g., methyl acetate, ethyl formate) flames. These studies are directed toward a mechanistic understanding of the reductions in PAHs and particulate matter (soot) achieved when biodiesel fuels are used as petroleum diesel replacements.
4. Several oxygenated hydrocarbon flames, with ethanol, propene/ethanol, and dimethyl ether (DME) fuels have been comprehensively studied to characterize reaction pathways that lead to reductions in PAHs and soot.
5. Photoionization cross sections were measured for several reaction intermediates. These results will appear in the repository for photoionization cross sections in the Collaboratory for Multiscale Chemical Systems (CMCS).

These studies are collaborative efforts with researchers at Sandia (Hansen, Taatjes, Miller), at Argonne (Klippenstein), the University of Bielefeld (Kohse-Höinghaus), the University of Massachusetts (Westmoreland) and Princeton University (Dryer).

Flames fueled by allene ( $\text{CH}_2\text{CCH}_2$ ) and propyne ( $\text{CH}_3\text{CCH}$ ) are under study, as both molecules are potential precursors for propargyl radicals, thus enhancing the importance of the propargyl self-recombination reaction. Our work on other rich flames fueled with  $\text{C}_3$  species (propene and propane) will continue.

Pure flames of toluene ( $\text{C}_7\text{H}_8$ ), never previously studied, are a high priority for immediate investigation. Preliminary measurements for a fuel-rich ( $\Phi=1.8$ ) toluene/ $\text{O}_2$ /Ar flame reveal a large and complex assortment of stable and radical reaction intermediates with 46 m/z values ranging from 15 to 168.

Other work in progress includes newly initiated studies of non petroleum-based fuels such as ethanol, ethers, and alkyl esters (biodiesel fuels), which are potentially important replacements for conventional gasoline and diesel fuels that may provide substantial energy security and environmental benefits. We have begun studies of ethanol, propene/ethanol fuel blends, dimethyl ether, methyl acetate, and ethyl formate flames to provide mechanistic data for modeling studies that will clarify the role of such replacement fuels in reducing PAH and soot formation. The research program will be expanded from pure fuel/ $\text{O}_2$  oxidation processes to real fuel/ $\text{N}_2$ / $\text{O}_2$  combustion systems, to explore the unknown reaction mechanisms responsible for observed *increases* in  $\text{NO}_x$  pollutants with biodiesel fuels.

Substantial reductions in particulate emissions are possible when dimethyl ether or dimethyl carbonate are used as additives to, or replacements for, petroleum diesel. When our studies of dimethyl ether for flames of several stoichiometries are completed, we will undertake similar investigations of low-pressure flames fueled by dimethyl carbonate. Dimethyl carbonate has a key chemical kinetic feature that makes it of interest in the investigation of oxygenate chemistry: It leads to the formation of the

methoxy formyl radical ( $\text{CH}_3\text{OCO}$ ), a member of the key alkyLOCO moiety in oxygenate chemistry. This structure provides a pathway to  $\text{CO}_2$  or  $\text{CO}$ .

There are many other interesting oxygenates, but mechanistic studies of flames of aldehydes and ketones seem especially pertinent; we plan to study  $\text{CH}_3\text{CHO}/\text{O}_2/\text{Ar}$  flames in the near future.

## Future Plans

Several papers are in preparation for publication. These include studies of flames of cyclohexane, propene, propene/ethanol, DME, methyl acetate and ethyl formate and measurements and calculations ionization energies for several higher polyacetylenes  $\text{C}_{2n}\text{H}_2$ . Much more work is planned on biodiesel fuel surrogates (e.g., methyl acetate, ethyl formate) and oxygenated hydrocarbons (propene/DME and propene/ethanol mixed fuels). We are placing greater emphasis on kinetic modeling with the addition of Fred Dryer and co-workers at Princeton to complement the efforts of Phil Westmoreland and James Miller.

The  $\text{C}_5$  species present in a variety of rich flames have been analyzed. Now, we plan to extend our work to investigate the isomeric composition of  $\text{C}_6$  ( $\text{C}_6\text{H}_4$  to  $\text{C}_6\text{H}_{12}$ ) and  $\text{C}_7$  ( $\text{C}_7\text{H}_6$  to  $\text{C}_7\text{H}_{14}$ ) species in fuel-rich flames more thoroughly. Of special interest will be a quantitative understanding of the isomeric composition of  $\text{C}_6\text{H}_6$  and  $\text{C}_7\text{H}_8$  species, but other stable and radical species that may be important in molecular growth reactions may attract our attention as well. A comparison of the experimentally determined isomeric composition of  $\text{C}_6\text{H}_6$  with a hydrocarbon combustion kinetics model will ultimately clarify the importance of even ( $\text{C}_2 + \text{C}_4$ ) and odd ( $\text{C}_3 + \text{C}_3$ ) cyclization processes for a variety of different fuels.

Finally, we will continue our measurements of photoionization cross sections to fill in gaps in our CMCS data repository. Knowledge of absolute photoionization cross sections is required for quantitative measurements of flame species mole fractions. We have completed cross section measurements for 20 key reaction intermediates, mainly in the  $\text{C}_1$ - $\text{C}_3$  range. For the next beam cycles we plan to measure absolute cross sections for  $\text{C}_4$ - $\text{C}_6$  species. These data are critically needed not just for a quantitative analysis, but also because ion fragments of a given mass-to-charge ( $m/z$ ) ratio may interfere with the detection of parent ions with the same  $m/z$  value. Hence partial photoionization cross sections for many dissociative ionization channels are required for successful strategies for quantitative measurements of flame species composition. In general, as we consider heavier species, the number of isomers becomes larger and the ability to identify species by their ionization thresholds through photoionization efficiency (PIE) measurements becomes critical.

An interesting example is the identification of  $\text{C}_6\text{H}_6$  isomers of benzene that may be intermediates in molecular weight growth processes leading to the formation of PAH and soot. Both fulvene and benzene have been identified by their ionization thresholds recorded with PIMS, but the potential presence others among the 12  $\text{C}_6\text{H}_6$  isomers with thresholds ranging from 8.3 to 9.9 eV is still an open question. To assist in the interpretation of PIE data, we plan to measure absolute photoionization cross sections for fulvene and 1,5-hexadiyne.

## DOE Publications for 2004-2005

- C. A. Taatjes and D. L. Osborn (Sandia National Laboratories) and T. A. Cool and K. Nakajima (Cornell University) "Studies of Flame Chemistry with Photoionization Mass Spectrometry" Science Highlight, 2004 ALS Activity Report
- C. A. Taatjes, N. Hansen, A. McIlroy, J. A. Miller, J. P. Senosiain, S. J. Klippenstein, F. Qi, L. Sheng, Y. Zhang, T. A. Cool, J. Wang, P. R. Westmoreland, M. E. Law, T. Kasper, and K. Kohse-Höinghaus, "Enols are Common Intermediates in Hydrocarbon Oxidation", *Science* **308**, 1887-1889 (2005), online 12 May 2005 (10.1126/science.1112532).
- T. A. Cool, A. McIlroy, F. Qi, P. R. Westmoreland, L. Poisson, D. S. Peterka and M. Ahmed, "A photoionization mass spectrometer for studies of flame chemistry with a synchrotron light source", *Rev. Sci. Instrum.* (2005) **76**, 094102.
- C. A. Taatjes, D. L. Osborn, T. A. Cool, and K. Nakajima, "Synchrotron Photoionization Measurements of Combustion Intermediates: The Photoionization Efficiency of HONO", *Chem. Phys. Lett.*, **394**, (2004) 19-24.
- T. A. Cool, Juan Wang, K. Nakajima, C. A. Taatjes, and A. McIlroy, "Photoionization cross sections for reaction intermediates in hydrocarbon combustion", *Intl J. Mass Spectrom.*, **247** (2005) 18-27.
- C. A. Taatjes, S. J. Klippenstein, N. Hansen, J. A. Miller, T. A. Cool, J. Wang, M. E. Law, and P. R. Westmoreland, "Synchrotron Photoionization Measurements of Combustion Intermediates: Photoionization Efficiency of C<sub>3</sub>H<sub>2</sub> Isomers", *Phys. Chem. Chem. Phys.* **7**, (2005) 806-813.
- T. A. Cool, K. Nakajima, C. A. Taatjes, A. McIlroy, P. R. Westmoreland, M. E. Law and A. Morel, "Studies of a Fuel-Rich Propane Flame with Photoionization Mass Spectrometry", *Proc. Combust. Inst.* **30**, 1631-1638 (2004).
- C. A. Taatjes, N. Hansen, J. A. Miller, T. A. Cool, J. Wang, P. R. Westmoreland, M. E. Law, T. Kasper, K. Kohse-Höinghaus, "Combustion Chemistry of Enols: Possible Ethenol Precursors in Flames", *J. Phys. Chem. A*, **110**, 3254-3260 (2006).
- N. Hansen, S. J. Klippenstein, C. A. Taatjes, J. A. Miller, J. Wang, T. A. Cool, B. Yang, R. Yang, L. Wei, C. Huang, J. Wang, F. Qi, M. E. Law, P. R. Westmoreland, "Identification and Chemistry of C<sub>4</sub>H<sub>3</sub> and C<sub>4</sub>H<sub>5</sub> Isomers in Fuel-Rich Flames", *J. Phys. Chem. A*, **110**, 3670-3678, (2006).
- N. Hansen, S.J. Klippenstein, J.A. Miller, J. Wang, T.A.Cool, M.E.Law, P.R.Westmoreland, T. Kasper, and K. Kohse-Höinghaus, "Identification of C<sub>5</sub>H<sub>x</sub> Isomers in fuel-rich flames by photoionization mass spectrometry and electronic structure calculations", *J. Phys. Chem A*, **110**, 4376-4388 (2006).
- N. Hansen, J. A. Miller, C. A. Taatjes, J. Wang, T. A. Cool, M. E. Law, P.R. Westmoreland, "Photoionization Mass Spectrometric Studies and Modeling of Fuel-Rich Allene and Propyne Flames", *Proc. Combust. Inst.* **31**, accepted.
- K. Kohse-Höinghaus, P. Osswald, U. Struckmeier, T. Kasper, N. Hansen, C. A. Taatjes, J. Wang, T. A. Cool, S. Gon, P.R. Westmoreland, "The Influence of Ethanol Addition on a Premixed Fuel-Rich Propene-Oxygen-Argon Flame", *Proc. Combust. Inst.* **31**, accepted.
- M. E. Law, P.R. Westmoreland, T.A. Cool, J. Wang, N. Hansen, C. A. Taatjes, T. Kasper, K. Kohse-Höinghaus, "Benzene precursors and formation routes in a stoichiometric cyclohexane flame", *Proc. Combust. Inst.* **31**, accepted.
- T. A. Cool, J. Wang, N. Hansen, P. R. Westmoreland, F. L. Dryer, Z. Zhao, A. Kazakov, T. Kasper and K. Kohse-Höinghaus, "Photoionization mass spectrometry and modeling studies of the chemistry of fuel-rich dimethyl ether flames", *Proc. Combust. Inst.* **31**, accepted.

# STATE CONTROLLED PHOTODISSOCIATION OF VIBRATIONALLY EXCITED MOLECULES AND HYDROGEN BONDED DIMERS

F.F. Crim  
Department of Chemistry  
University of Wisconsin–Madison  
Madison, Wisconsin 53706  
fcrim@chem.wisc.edu

Our research investigates the chemistry of vibrationally excited molecules. The properties and reactivity of vibrationally energized molecules are central to processes occurring in environments as diverse as combustion, atmospheric reactions, and plasmas and are at the heart of many chemical reactions. The goal of our work is to unravel the behavior of vibrationally excited molecules and to exploit the resulting understanding to determine molecular properties and to control chemical processes. A unifying theme is the preparation of a molecule in a specific vibrational state using one of several excitation techniques and the subsequent photodissociation of that prepared molecule. Because the initial vibrational excitation often alters the photodissociation process, we refer to our double resonance photodissociation scheme as *vibrationally mediated photodissociation*. In the first step, fundamental or overtone excitation prepares a vibrationally excited molecule and a second photon, the photolysis photon, excites the molecule to an electronically excited state. Vibrationally mediated photodissociation provides new vibrational spectroscopy, measures bond strengths with high accuracy, alters dissociation dynamics, and reveals the properties of and couplings among electronically excited states.

Several recent measurements illustrate the scope of the approach and point to new directions. We have completed an extensive study the spectroscopy and non-adiabatic dissociation dynamics of ammonia ( $\text{NH}_3$ ), have published new results on the vibrationally mediated photodissociation of methanol ( $\text{CH}_3\text{OH}$ ), have made our first ion imaging measurements on  $\text{NH}_3$ , and have begun studying the vibrationally mediated photodissociation of formic acid dimers. In each case, the goals are understanding and exploiting vibrations in the ground electronic state, studying the vibrational structure of the electronically excited molecule, and probing and controlling the dissociation dynamics of the excited state.

## Vibrationally Mediated Photodissociation of Ammonia ( $\text{NH}_3$ )

Ammonia is a famously well-studied molecule that holds interesting opportunities for vibrationally mediated photodissociation experiments because it has both a nonadiabatic dissociation to yield ground state  $\text{NH}_2 + \text{H}$  and an adiabatic dissociation to form excited state  $\text{NH}_2^* + \text{H}$ . Our previous studies, in which we observed excited state vibrations and monitored reaction products, provided new insights into the non-adiabatic dynamics that set the stage for our most recent ion imaging experiments. The most interesting observation is for initially excited stretching vibrations in the electronically excited state. Dissociation from the state containing one quantum of symmetric stretch ( $\nu_1$ ) produces a distribution with both fast and slow components that are similar to that for the origin. Dissociation from the antisymmetric N-H stretch state ( $\nu_3$ ), however, produces dramatically different results. It forms *only* slow hydrogen atoms, likely reflecting preferential decomposition to make solely the excited state product. New calculations by D. Yarkony (J. Chem. Phys. **121**, 628 (2004)) seem consistent with molecules that have excited asymmetric

N-H stretching vibrations preferentially remaining on the excited state surface, apparently avoiding one conical intersection by moving toward another intersection for which the crossing probability is smaller. It seems that the coupled electronic surfaces of ammonia provide a challenging target for theory (Nangia and Truhlar, J. Chem. Phys. **124**, 124309 (2006)) and that careful experiments provide a useful point of comparison.

### Ion Imaging

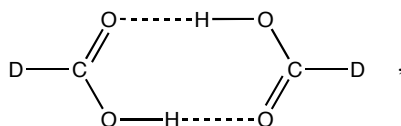
Implementing ion imaging in vibrationally mediated photodissociation experiments has been a focus of our effort during the past year. We have modified our apparatus and tested the system by obtaining velocity mapped images of molecules such as NO and O<sub>2</sub> and have made our first measurements on one-photon dissociation of NH<sub>3</sub>. Adding vibrational excitation for the ammonia experiments is demanding on both the detection scheme, particularly with regards to spurious background ionization, and on the infrared generation system, but we have now performed the first vibrationally mediated photodissociation experiments with ion imaging detection .

### Ammonia

The quantum state populations of the NH<sub>2</sub> fragment that we obtain by ion imaging of the H-atom product of the one-photon dissociation of ammonia agree with earlier measurements using Rydberg tagged H-atom detection. Even though the signal is much smaller in the vibrationally mediated photodissociation experiments, we are able to observe the products of the decomposition from molecules with excited umbrella and excited bending vibrations. The distribution of energy among the NH<sub>2</sub> product states is again consistent with the recoil energy distributions we measured earlier. Photodissociation through stretching vibrations is the most challenging experiment, and there are several complicating background signals that we have now sorted out. The NH<sub>2</sub> product from dissociation through the *symmetric* stretching state is similar to that for one-photon photolysis. By contrast, images for the dissociation through the *antisymmetric* stretching state show that there is much less energy in translation, in agreement with our previously measured H-atom Doppler profiles. The state structure and its variation with total energy are consistent with the formation of the electronically product, NH<sub>2</sub>\*. We are completing the analysis of these data including understanding several competing multiphoton dissociation and excitation processes.

### Formic Acid and Formic Acid Dimers

One of the primary goals of our work is understanding the dissociation dynamics in vibrationally excited dimers, and we have applied our newly developed capabilities to studying formic acid and its hydrogen bonded dimer,



shown here for partially deuterated formic acid. We have developed schemes for distinguishing the monomer from the dimer in both one-photon dissociation and vibrationally mediated photodissociation. Exciting either the O-H or C-H stretch while observing the H-atom product from the undeuterated dimer gives vibrational action spectra that agree with the absorption spectrum a supersonic expansion. Using the partially deuterated molecule and exciting the C-D stretch while detecting the D atom product gives the

first vibrational spectrum of the cold partially deuterated dimer. Cooling reveals new structure that we are analyzing. We are studying the vibrational excitation and energy dependence of the yield of H atoms (from the hydrogen bonds) compared to that of D atoms upon excitation of either the C–D or the O–H stretch. The usual advantage of being able to obtain spectra of cold molecules and explore their dissociation dynamics with vibrationally mediated photodissociation opens many possibilities for studying these strongly bound dimers.

### **FUTURE DIRECTIONS**

Now that we can perform vibrationally mediated photodissociation of strongly bound dimers, our primary goal is to refine the study of formic acid and extend our measurements and analysis to other carboxylic acid dimers. We can now capitalize on the investment in the development of these new experimental capabilities. We intend to obtain both spectra that reveal couplings in the dimers and to learn about their excited state decomposition dynamics for different initial vibrational states.

### **PUBLICATIONS SINCE 2004 ACKNOWLEDGING DOE SUPPORT**

*Action spectroscopy and photodissociation of vibrationally excited methanol.* J. Matthew Hutchison, Robert J. Holiday, Andreas Bach, Shizuka Hsieh, and F. Fleming Crim, *J. Phys. Chem. A* **108**, 8115 (2004).

# Spectroscopy and Energy Transfer Dynamics of Highly Vibrationally Excited Molecules and Transient Radicals

Hai-Lung Dai

Department of Chemistry, University of Pennsylvania  
Philadelphia, PA 19104-6323; [dai@sas.upenn.edu](mailto:dai@sas.upenn.edu)

## I. Program Scope

The primary goal of this project is to characterize the structure and dynamics of highly vibrationally excited species in combustion processes. Specifically, we have been focusing on detecting the previously unknown vibrational modes of transient radicals and characterizing collision energy transfer from highly excited molecules.

To tackle the vibrational spectroscopy of radicals that can only be generated in small quantities with short life times, we have applied the nanosecond time resolved Fourier Transform IR Emission Spectroscopy (TR-FTIRES) to the study. The transient radical species is produced with high vibrational excitation through UV photolysis of a precursor molecule. IR emission from the highly excited species through its IR active vibrational modes is detected with fast time resolution. Inert buffer gas is used for collision quenching of the radicals so that IR emission observed at later times is from the fundamental levels. Isotope substitution, multiple precursors, time-dependence of the emission signal, and theoretical calculations are used to assist spectral assignment. In addition, a two-dimensional cross-spectra correlation technique has been developed for analyzing the time-resolved FTIR emission spectra. This approach allows the previously unknown vibrational modes be detected as emission transitions with modest resolution. The spectroscopic approach also allows the reactions of the excited radical and the photolysis reaction of the precursor molecules to be characterized. The radicals we choose for study at present are small radicals that are known or proposed to play important roles in combustion reactions. So far, we have reported all nine vibrational modes of the vinyl radical, two vibrational modes and the structure of cyanovinyl, two modes of OCCN, the CH stretch mode of HCCO, and the vibrational modes of deuterated vinyl and cyanovinyl.

The nanosecond TR-FTIRES technique has also enabled the characterization of the vibrational energy content of excited molecules during a collision quenching process. The energy distribution of an ensemble of highly vibrationally excited molecules as a function of number of collisions can be determined which allow the amount of energy transferred per collision to be measured. Information on collision energy transfer of highly excited radicals is important to the characterization of combustion processes but little is known on this subject.

## II. Recent Progress

### A. The Ketenyl Radical (HCCO)

The  $\nu_1$  CH stretch, a previously uncharacterized mode of the ketenyl (HCCO) radical was detected at  $3208\text{ cm}^{-1}$  through sub-microsecond time resolved Fourier transform infrared emission spectroscopy. HCCO was produced with excess vibrational excitation through 193 nm photodissociation of the precursor ethyl ethynyl ether (Krisch, Miller, and Butler, *J. Chem. Phys.* 119, 176 (2003)). IR emission from the photolysis products was detected with time- and frequency resolution. Spectral assignments were made based on comparison with theoretical

calculations and the time-dependence of the emission intensity which allows differentiation of emission from photolysis products such as HCCO vs. that from secondary reaction products.

This work also provides spectroscopic evidence for the detection of the quartet state of HCCO. According to the Butler and coworkers' study the radical generated through the 193 nm dissociation of EEE exists with majority as HCCO( $\tilde{a}^4A''$ ). IR emission from the CO stretch of the quartet state has been identified. The quartet state has initially sufficient energy for dissociation into CH and CO. Collision with buffer gas causes both internal vibrational relaxation and intersystem crossing to the lower quartet state surface where dissociation may also occur. The rate of collision induced intersystem crossing can be extracted from integrated intensity time-profiles obtained using three different collision partners: He, Ar and Xe. Since helium is a light and fast atom, collision with He is more efficient for vibrational relaxation within the quartet state potential surface and less efficient in inducing the intersystem crossing to the lower doublet state. Collision with He provides effectively a means to trap HCCO( $\tilde{a}^4A''$ ) for a longer period of time than with argon or xenon. Both heavier atoms are efficient at inducing intersystem crossing that allows the ISC rate constants to be extracted from the appearance of diatomic CO in the time-resolved IR emission spectra. This work also allows the determination of the fundamental transition of the  $\nu_2$  stretch of HCCO( $\tilde{a}^4A''$ ) at  $\sim 1923\text{ cm}^{-1}$ .

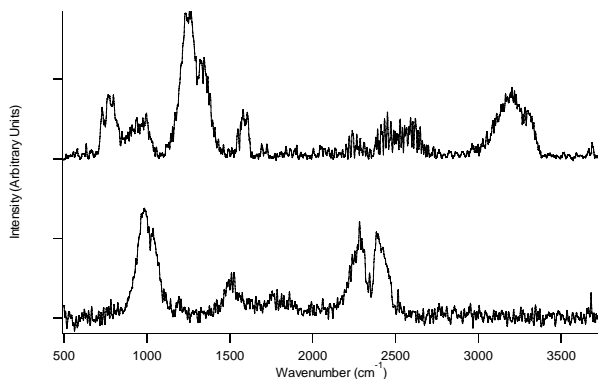
## B. Two-Dimensional Cross Spectral Correlation Analysis

A spectral analysis method, based on the generalized two-dimensional vibrational spectra correlation analysis, is developed for deciphering the correlation among the spectral peaks of two *different* spectra. This 2D *cross*-spectral correlation (2DCSC) analysis is aimed at revealing the vibrational features associated with a common species in two spectra, each obtained from a system containing multiple species with at least one common species. The cross-spectral correlation is based on the premise that the spectral features of the same species should have the same time- and frequency-response toward similar perturbations. The effectiveness of the cross-spectral correlation analysis is first illustrated with model systems, with spectral peaks decaying linearly or exponentially with time, before being applied to analyzing time-resolved emission spectra obtained, by a Fourier transform IR spectrometer, for samples consisting of the vibrationally excited transient cyanooxomethyl radical (OCCN). 2DCSC among the three different sets of time-resolved spectra collected following the photodissociation of three different precursor molecules of OCCN, respectively, allows the identification of the CN and CO stretching modes of this radical.

## C. Deuterated Vinyl

Experimentally determined vibrational frequencies for the hydrogenated vinyl molecule (Letendre, Liu, Pibel, Halpern and Dai, *J. Chem. Phys.*, 112, 9209 (2000)) were in good agreement with theoretically predicted values (such as the ones in Sattelmeyer and Schaefer, *J. Chem. Phys.* 117, 7914 (2002)) with a single exception, the  $\nu_5$  vibrational mode – the assigned position lie more than  $150\text{ cm}^{-1}$  from the theoretical value with an order of magnitude more intensity. In principle, isotopic substitution allows for the alteration of atomic masses without changing the potential in which the atoms move. In the case of deuterium substituted vinyl, the ratio of the experimentally determined frequencies of the non-deuterated/deuterated molecules can be used for comparison with theoretical normal mode estimations and confirm the normal mode assignments.

We have performed a TR-FTIRES study of vinyl-d<sub>3</sub> produced from 193 nm photodissociation of vinyl bromide-d<sub>3</sub>. The photodissociation also generates acetylene-d<sub>2</sub>, DBr, and Br\*. The C-D stretch of acetylene appears at 2439 cm<sup>-1</sup> and its C-D bend combination (4+5) can be seen at 1042 cm<sup>-1</sup>. The highly vibrationally excited DBr exhibits partially resolved rotational lines centered at 1839 cm<sup>-1</sup>. A sharp feature at 3685 cm<sup>-1</sup> arises from the electronic transition of excited Br\*  $^2P_{3/2} \leftarrow ^2P_{1/2}$ . The peaks at 2420, 2346 and 2264 cm<sup>-1</sup> correspond to emission in the C-D stretch region. There is also a very intense peak located at 984 cm<sup>-1</sup>. These four peaks with similar time dependence in intensity decay can be assigned to vinyl. The figure shown here compares the emission spectra from the non-deuterated vinyl bromide photodissociation (upper trace) and the deuterated vinyl bromide (lower trace). The two spectra were taken 2.5 μs after photolysis. The strongest peak in the vinyl bromide spectrum at 1277 cm<sup>-1</sup> (ν<sub>5</sub>) corresponds well to the peak at 984 cm<sup>-1</sup> (ν<sub>5</sub> CD<sub>2</sub> asymmetric bent) of the deuterated vinyl bromide spectrum. The CH<sub>2</sub> asym. stretch at 3235 cm<sup>-1</sup>, the CH<sub>2</sub> sym. stretch at 3164 cm<sup>-1</sup>, and the αCH stretch at 3103 cm<sup>-1</sup> of vinyl can all be identified in correspondence with their CD counterparts in this comparison.



Two other partially deuterated vinyl, CD<sub>2</sub>CH and CH<sub>2</sub>CD, will be examined using their respective deuterated vinyl bromide precursors and ab initio calculations will be conducted for all the isotopically substituted vinyl for comparison to ensure a correct understanding of its vibrational structure.

#### D. Photodissociation of Acrylonitrile

A photofragment translational energy spectroscopy study of acrylonitrile, also known as vinyl cyanide, (Blank, Suits, Lee, North, and Hall, *J. Chem. Phys.*, 108, 5784 (1998)) has found a major photolysis product with m/e=27. Based on the detected photoionization threshold, this species was tentatively assigned to HCN. The presence of internal excitation energy in the product molecule, however, may result in a lower ionization threshold and affect the interpretation of the experimental observation, causing uncertainty for distinguishing in between HCN and HNC. We have used TR-FTIRES to detect the IR emission from excited products from the 193 nm photodissociation of vinyl cyanide. Since the vibrational frequencies of both HCN and HNC have been accurately reported in the literature, the identification of a given geometric isomer can be accomplished through assignment of observed emission peaks. Furthermore, the relative populations of the two species can be obtained from a comparison of the peak intensities. Our time resolved emission spectra clearly show the presence of the HNC(ν<sub>1</sub>) and HNC(ν<sub>3</sub>) features at 3652 cm<sup>-1</sup> and 2023 cm<sup>-1</sup> respectively. Intensity ratios of these two peaks can be compared with the prominent HCCH(ν<sub>3</sub>) feature at 3289 cm<sup>-1</sup> to determine in what ratio HNC is formed with respect to HCCH. Our modeling of the spectra shows that though HCN may appear as a product, HNC is the dominate isomer as product. This observation is consistent with recent findings from Robert Field's laboratory at MIT using millimeter wave spectroscopy in detecting the low lying vibrational level populations of the product molecules.

### **E. V-T Energy Transfer from Highly Vibrationally Excited Molecules**

We have applied TR-FTIR emission spectroscopy, which can be used to determine the vibrational energy content of the emitting molecules (Pibel, Sirota, Brenner and Dai, *J. Chem. Phys.* 108, 1297 (1998)), to characterize collision energy transfer from highly excited molecules. It has been shown that collision energy transfer from highly excited molecules, particularly in the energy region of strong vibronic coupling (Hartland, Qin, and Dai, *J. Chem. Phys.* 102, 8677 (1995)), is dominated by transition dipole mediated long range interactions (Hartland, Qin, Dai and Chen, *J. Chem. Phys.*, 107, 2890 (1997); Qin, Hartland and Dai, *J. Phys. Chem. A*, 104, 10460 (2000)). Recently we have focused on the V-T process from highly excited molecules.

We have measured the amount of energy transferred per L-J collision as a function of the excitation energy in NO<sub>2</sub>, following its initial excitation at 22,000 cm<sup>-1</sup>, by ambient inert gases. It is found that when NO<sub>2</sub> is excited below this threshold energy, the collision removal rate is about 0.1 to 5 cm<sup>-1</sup> per collision with He as the most efficient quencher. This observation is in compliance with the expected V-T transfer behavior from the SSH theory where repulsive collision dominates the energy transfer interaction. However, when NO<sub>2</sub> is excited above the threshold, the energy removal rate has increased by about two orders of magnitude and He has become the least efficient quencher. Instead, the removal rate increases approximately with the size of the inert gas atoms.

The appearance of the threshold in V-T transfer efficiency at ~9,000 cm<sup>-1</sup> is very similar to cases with other molecular colliders for which V-V dominates in energy transfer. This threshold can be understood in that the first two excited electronic states of NO<sub>2</sub> start at 9,800 and 13,000 cm<sup>-1</sup> respectively and there is substantial vibronic coupling between these electronic states and the ground state. Enhanced vibronic coupling results in more electronic character in the high vibrational levels of the X state and enhances their transition dipoles for energy transfer. This observation, together with the one showing that above threshold V-T transfer is more efficient for the larger inert gases, suggest that long range interaction is significant in contributing to V-T transfer from highly vibrationally excited NO<sub>2</sub>.

#### **Publications since 2004 acknowledging support from this grant**

The  $\nu_1$  and  $\nu_2$  Vibrational Bands of The OCCN Radical Detected Through Time-Resolved Fourier Transform IR Emission Spectroscopy, *Can. J. Chem.* [Herzberg Memorial Issue], 82(6), 925-933 (2004) W. McNavage, W. Dailey and H. L. Dai

Two-Dimensional Cross-Spectra Correlation Analysis of Time-Resolved Fourier Transform IR Emission Spectra, *J. Chem. Phys.*, 123, 184104-15 (2005), W. McNavage and H. L. Dai

Time-Resolved FTIR Emission Spectroscopy of Transient Radicals, *J. Chinese Chem. Soc. (Taipei)*, [K. C. Lin special issue] (2005), L. T. Letendre, W. McNavage, C. Pibel, D.-K. Liu, and H. L. Dai

Time-Resolved FTIR Emission Spectroscopy of the  $\nu_1$  CH Stretch Mode of the Ketenyl (HCCO) Radical, *J. Chem. Phys.*, submitted, W. McNavage, M. J. Wilhelm, R. R. Groller and H. L. Dai

# Bimolecular Dynamics of Combustion Reactions

H. Floyd Davis

Department of Chemistry and Chemical Biology  
Baker Laboratory, Cornell University, Ithaca NY 14853-1301  
hfd1@Cornell.edu

## I. Program Scope:

The aim of this project is to better understand the mechanisms and product energy disposal in bimolecular reactions fundamental to combustion chemistry. Using the crossed molecular beam method, a molecular beam containing highly reactive free radicals is crossed at right angles with a second molecular beam. The angular and velocity distributions of the products from single reactive collisions are measured, primarily using Rydberg tagging methods.

## II. Recent Progress:

### i. Crossed Beam Study of the $\text{CN} + \text{O}_2 \rightarrow \text{NCO} + \text{O}({}^3\text{P}_2)$ Reaction

The oxidation reactions of CN and NCO radicals can lead to formation of  $\text{NO}_x$ , and are therefore relevant to combustion processes. The reaction exhibits a mild negative temperature dependence, suggesting that it proceeds on a barrierless attractive potential energy surface.<sup>1</sup> The  $\text{CN} + \text{O}_2$  reaction is one of the simplest 4-atom systems containing “heavy” atoms, and represents a prototypical reaction between two open-shell species:



We used oxygen Rydberg time-of-flight (ORTOF) spectroscopy to carry out a crossed beam study of the  $\text{CN} + \text{O}_2$  reaction at collision energies of 3.1 and 4.1 kcal/mol. The  $\text{NCO} + \text{O}$  translational energy distribution was broad, with forward-backward symmetric center of mass (CM) angular distributions (Fig. 1), indicating the participation of NCOO intermediates with lifetimes comparable to or longer than their picosecond rotational timescales. The product flux contour map is shown in Fig. 2.

We carried out RRKM calculations using calculated NCOO intermediate and  $\text{NCO} + \text{O}$  transition state geometries to estimate the decay rate for NCOO complexes. An NC-OO binding energy of  $\geq 38$  kcal/mol appears to be consistent with our measured angular distribution if the transition state for O-O bond fission is tight. A tight transition state for  $\text{NCO} + \text{O}$  production appears to lend support to the mechanism for the  $\text{NO} + \text{CO}$  channel postulated by Mohammed and coworkers involving a secondary collision between the departing O atom and the N within NCOO.<sup>2</sup> Since the 4-center transition state for  $\text{NO} + \text{CO}$  production is energetically inaccessible, this

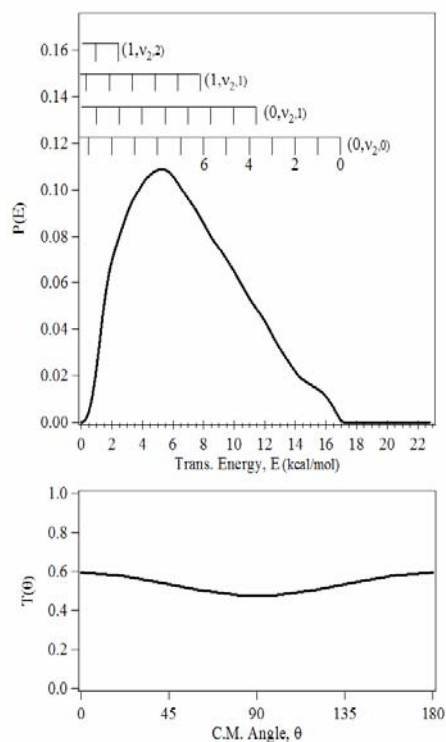


**Fig. 1:** Center of Mass translational energy,  $P(E)$  and angular,  $T(\theta)$  distributions for  $\text{NCO} + \text{O}$  from  $\text{CN} + \text{O}_2$  reaction.

intramolecular reaction likely involves a “wandering” O atom, analogous to that proposed recently by Suits and coworkers in the unimolecular decomposition of  $\text{H}_2\text{CO}$  near threshold for  $\text{H} + \text{HCO}$  formation.<sup>3</sup> Indeed, Rim and Hershberger have found that the quantum yield for  $\text{CO} + \text{NO}$  production from  $\text{CN} + \text{O}_2$  is  $0.22 \pm 0.02$  at 296 K; they suggest that this actually becomes the dominant channel at low temperatures.<sup>4</sup>

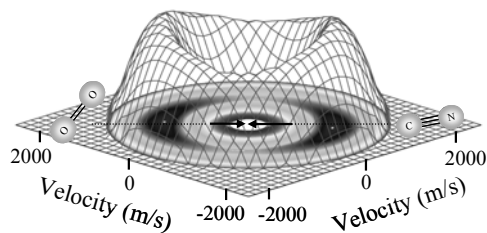


**Fig. 2:** O atom product flux contour map for  $\text{CN} + \text{O}_2 \rightarrow \text{NCO} + \text{O}$  reaction

## ii. Reactive Quenching of $\text{OH}(\text{A}^2\Sigma^+)$ + $\text{D}_2$ Studied by Crossed Beams

It has been known for many years that electronically excited hydroxyl radicals are rapidly quenched by collisions with small molecules. The  $\text{OH}(\text{A}^2\Sigma^+)$  quenching rate constants for many different atomic and molecular partners have been measured as a function of temperature. In most studies, the quenching was monitored through the disappearance of  $\text{OH}(\text{A}^2\Sigma^+)$ ; the products resulting from the quenching events were not identified. For quenching of  $\text{OH}(\text{A}^2\Sigma^+)$  by molecules containing hydrogen (RH), both physical quenching forming  $\text{OH}(\text{X}^2\Pi) + \text{RH}$ , as well as bimolecular reaction forming  $\text{H}_2\text{O} + \text{R}$ , are possible.<sup>5</sup>

The  $\text{OH}(\text{A}^2\Sigma^+) + \text{H}_2(\text{D}_2)$  reaction has become a benchmark system for examining nonadiabatic quenching processes. The crossing regions between the ground state and excited state potential energy surfaces for  $\text{OH}(\text{A}^2\Sigma^+) + \text{H}_2(\text{D}_2)$  lead to conical intersections.<sup>5</sup> We have studied the quenching reaction using crossed molecular beams, employing the Rydberg time-of-flight method. The OH beam was produced by 193 nm photodissociation of anhydrous nitric acid seeded in a pulsed supersonic expansion of hydrogen at 2 atm. Due to the relatively short fluorescence lifetime of  $\text{OH}(\text{A}^2\Sigma)$ , excitation from the ground state was carried out in the beam crossing region by a dye laser using the  $\text{Q}_1(1)$  transition near 308 nm.

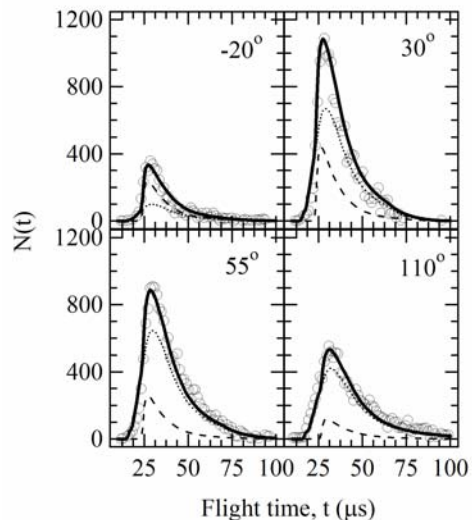


**Fig. 3:** D atom time-of-flight spectra at four laboratory angles (circles) with fits (solid line).

The time-of-flight spectra for D atoms from the title reaction are shown in Fig. 3, and the product flux contour map is shown in Fig. 4. The D atom products are preferentially forward-scattered relative to the incident  $\text{D}_2$  molecules. This implies that the dominant reaction mechanism is direct, occurring on timescales shorter than that for rotation of the  $\text{OH}-\text{D}_2$  pair, *i.e.*, on subpicosecond timescales.

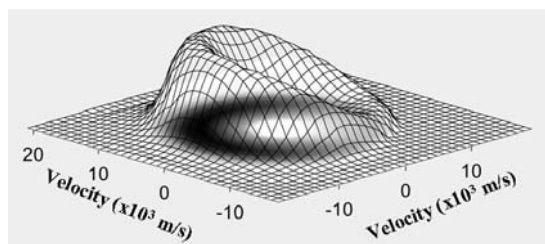


**Fig. 4:** D atom product flux contour map for  $\text{OH}(\text{A}) + \text{D}_2$  quenching reaction.

The preferential forward-scattering is a signature of a mechanism in which the incoming  $\text{OH}(\text{A}^2\Sigma^+)$  reactant picks up a D atom from  $\text{D}_2$  at relatively large impact parameters, with the newly-formed HOD continuing in nearly the same direction as the incident OH (A). This behavior is exactly the

opposite to that for the ground state reaction, which involves small-impact parameter collisions with the D atoms backward-scattered relative to the incident  $D_2$  molecules (*i.e.*, HOD is backward-scattered relative to OH). The  $OH(A^2\Sigma^+, v=0) + D_2 \rightarrow HOD + D$  is exoergic by 451 kJ/mol. The translational energy distribution peaks at  $\sim 55$  kJ/mol, but includes contributions up to  $\sim 340$  kJ/mol. Thus, the most probable internal energy of the HOD product is  $\sim 410$  kJ/mol, which at the collision energy of this experiment corresponds to  $\sim 88\%$  of the total available energy.

We hope that these initial results stimulate new theoretical work on this system.

### III. Future Plans:

#### i. $H + O_2 \rightarrow OH(^2\Pi) + O(^3P_J)$ .

We developed the ORTOF method largely with the intention of studying  $H + O_2 \rightarrow OH(^2\Pi) + O(^3P_J)$ , a reaction considered to be among the most important in combustion. The OH is preferentially formed in high-N levels. Prior to our recent upgrade of the apparatus, we attempted to study this reaction in crossed beams using fast photolytic H atoms produced by photodissociation of HI at 248 nm. However, we were unsuccessful in observing signal. This is largely due to the small cross section for reaction, and also because the H atom source, although very monoenergetic, is relatively weak. During the course of these experiments, we were able to assess the feasibility of using ORTOF on this system by carrying out “single beam” experiments involving coexpansion of 5% HI with 30%  $O_2$  in He. The configuration is similar to that in Zare’s “photoloc” experiments. The HI was photolyzed by the residual 212 nm light used for VUV generation; resulting H atoms react with  $O_2$  within the beam producing  $OH + O$ . A representative TOF spectrum is shown in Fig. 5. From energy and momentum conservation, and because they disappear when the H atom beam is turned off, we believe the peaks correspond to formation of OH in  $J = 25, 26,$  and  $27$  from  $H + O_2$ . Since our signal to noise ratio has been increased by a factor of 30 since these experiments were done, we believe that our upcoming study of  $H + O_2$  under true crossed beam conditions will be successful.

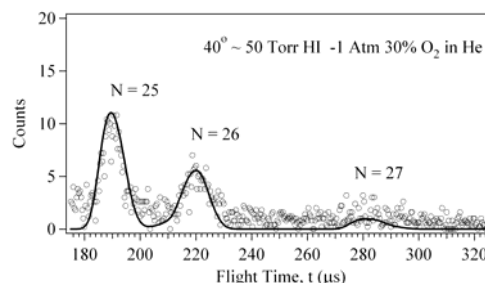


Fig. 5: O Rydberg TOF spectrum for  $H + O_2$  reaction carried out in single beam.

The configuration is similar to that in Zare’s “photoloc” experiments. The HI was photolyzed by the residual 212 nm light used for VUV generation; resulting H atoms react with  $O_2$  within the beam producing  $OH + O$ . A representative TOF spectrum is shown in Fig. 5. From energy and momentum conservation, and because they disappear when the H atom beam is turned off, we believe the peaks correspond to formation of OH in  $J = 25, 26,$  and  $27$  from  $H + O_2$ . Since our signal to noise ratio has been increased by a factor of 30 since these experiments were done, we believe that our upcoming study of  $H + O_2$  under true crossed beam conditions will be successful.

#### ii. Studies of $OH + D_2(v = 1) \rightarrow HOD + D$

The  $OH + D_2$  reaction is important in combustion, and is the simplest member of the family of abstraction reactions involving OH. It involves a substantial potential energy barrier, leading to a small reaction cross section even at relatively high collision energies. The OH moiety acts much like a spectator, and is not appreciably excited in the product HOD. On the other hand, the D-D bond in  $D_2$  is broken during the course of the reaction; vibrational excitation of this reactant is thus expected to strongly enhance reactivity.<sup>6</sup>

The most challenging aspect of this experiment is vibrational excitation of an appreciable fraction of  $D_2$  molecules. We have constructed a home-made narrow band optical parametric oscillator (OPO) for NSF-supported studies of reactions involving vibrationally-excited hydrocarbons with transition metal atoms in crossed beams. The OPO, based on the original design by Bosenberg and Guyer,<sup>7</sup> is based on the use of KTP (potassium titanyl phosphate), and

facilitates production of high energy pulsed light in the 700 – 900 nm range, as well as at 1.4 – 4.0  $\mu\text{m}$ . Following the approach of Lucht and coworkers,<sup>8</sup> we have been able to obtain near transform-limited pulses through injection seeding with a narrow bandwidth distributed feedback (DFB) diode laser. The DFB lasers are inexpensive (particularly when purchased as surplus), and, when controlled using an appropriate power and temperature controller, produce extremely narrow bandwidth (1 MHz) continuous wave (CW) radiation (20 mW) in the 1.55  $\mu\text{m}$  range commonly used in the telecom industry. We plan to use the tunable narrowband near IR radiation from this device for SRP of  $\text{D}_2$ . By seeding at the idler wavelength using a DFB laser operating at 1.55  $\mu\text{m}$ , the 532 nm pumped nonresonant oscillator produces several mJ of near-transform-limited 807 nm radiation as the signal. This 807 nm light will be amplified in an available multipass titanium sapphire amplifier to produce  $\approx 50$  mJ/pulse of near-transform-limited radiation. The SRP process in  $\text{D}_2$  to be used will employ this beam and the residual narrowband 1064 nm fundamental from the Nd:YAG pump laser.

#### IV. Publications since 2004:

1. Crossed Beams Study of the Reaction  ${}^1\text{CH}_2 + \text{C}_2\text{H}_2 \rightarrow \text{C}_3\text{H}_3 + \text{H}$ , H. F. Davis, J. Shu, D.S. Peterka, and M. Ahmed, *J. Chem. Phys.* **121**, 6254 (2004).
2. Photodissociation Dynamics of  $\text{N}_2\text{O}$  at 130 nm: The  $\text{N}_2(\text{A } {}^3\Sigma_u^+, \text{B } {}^3\Pi_g) + \text{O}({}^3\text{P}_{J=2,1,0})$  Channels, Mark F. Witinski, Mariví Ortiz-Suárez, and H. Floyd Davis, *J. Chem. Phys.* **122**, 174303 (2005).
3. Reaction Dynamics of  $\text{CN} + \text{O}_2 \rightarrow \text{NCO} + \text{O}({}^3\text{P}_2)$ , Mark F. Witinski, Mariví Ortiz-Suárez, and H. Floyd Davis, *J. Chem. Phys.*, 124, 094307 (2006).
4. Reactive Quenching of  $\text{OH}(\text{A } {}^2\Sigma^+) + \text{D}_2$  Studied by Crossed Molecular Beams, Mariví Ortiz-Suárez, Mark F. Witinski, and H. Floyd Davis, submitted to *J. Chem. Phys.*

#### V. References:

- 
1. I. W. M. Smith, *Chemical Dynamics and Kinetics of Small Radicals Part I*, edited by K. Liu and A. F. Wagner (World Scientific, Singapore, 1995).
  2. F. Mohammad, V. R. Morris, W. H. Fink, and W. M. Jackson, *J. Phys. Chem.* **97**, 11590 (1993).
  3. D. Townsend, S.A. Lahankar, S.K. Lee, S.D. Chambreau, A.G. Suits, X. Zhang, J. Rheinecker, L.B. Harding, and J.M. Bowman, *Science* **306**, 1158 (2004).
  4. K. T. Rim and J. F. Hershberger, *J. Phys. Chem.* **103**, 3721 (1999).
  5. D. T. Anderson, M. W. Todd, and M. I. Lester, *J. Chem. Phys.* **110**, 11117 (1999).
  6. M. J. Lakin, D. Troya, G. Lendvay, M. Gonzalez and G.C. Schatz, *J. Chem. Phys.* **115**, 5160 (2001).
  7. W.R. Bosenberg and D. Guyer, *J. Opt. Soc. Am. B.* **10**, 1716 (1993).
  8. W.D. Kulatilaka, T.N. Anderson, T.L. Bougher, and R.P. Lucht, *Appl. Phys. B.* **80**, 669 (2005).

## Multiple-time-scale kinetics

Michael J. Davis

Chemistry Division  
Argonne National Laboratory  
Argonne, IL 60439  
Email: davis@tcg.anl.gov

Research in this program focuses on three interconnected areas. The first involves the study of intramolecular dynamics, particularly of highly excited systems. The second area involves the use of nonlinear dynamics as a tool for the study of molecular dynamics and complex kinetics. The third area is the study of the classical/quantum correspondence for highly excited systems, particularly systems exhibiting classical chaos.

### Recent Progress

In the past year, most of the progress has focused on the rational reduction of chemical systems with reaction and transport. Such systems can be studied under transient or steady conditions, and most of the work in the past year involved steady problems. In this type of problem the reduction of the chemical kinetics occurs along the spatial domain. Our approach to reduction is geometric and depends on the resolution of low-dimensional manifolds. The work described here includes collaborations with Tomlin (Leeds) and Zagaris and Kaper (Boston University).

There are several methods available for generating steady one-dimensional flames. These include Newton's methods and the solution of the transient problem to reach steady conditions. These two methods are implemented in the Chemkin program "Premix". A third method involves casting the steady problem as a set of first order ordinary differential equations and studying the steady problem as a dynamical system.<sup>1</sup> It is well known that this latter method can generally be implemented only for rather simple kinetics and is not a viable method for generating steady solutions for systems with multiple-time-scale kinetics. Therefore, the other two methods are the methods of choice for such problems. Although, it may be difficult to generate the spatial dependence of a steady flame using the dynamical systems approach, it is useful for generating and understanding reduced descriptions of the chemistry-transport process and we have implemented this approach for several systems.

To understand how low-dimensional manifolds appear in steady problems, consider the phase space structure of the reaction-diffusion equations for the reaction  $C_2H_6 \rightleftharpoons CH_3 + CH_3$  ( $A \equiv \rho_{C_2H_6}$ ,  $B \equiv \rho_{CH_3}$ ):

$$\frac{\partial A}{\partial t} = -k_f A + k_r B^2 + D \frac{\partial^2 A}{\partial x^2} \quad (1a)$$

$$\frac{\partial B}{\partial t} = 2k_f A - 2k_r B^2 + D \frac{\partial^2 B}{\partial x^2} \quad (1b)$$

Under steady conditions, with,  $c = 2\rho_{C_2H_6} + \rho_{CH_3}$ , and  $u \equiv \frac{dB}{dx}$ , the system can be written as a Hamiltonian system with the spatial coordinate “x” the independent variable:

$$\frac{dB}{dx} = u \quad (2a)$$

$$\frac{du}{dx} = \frac{k_f}{D} B + \frac{2k_r}{D} B^2 - \frac{k_f c}{D} \quad (2b)$$

The system has an equilibrium point and a saddle point. The phase space structure is pictured on the left in the figure below.

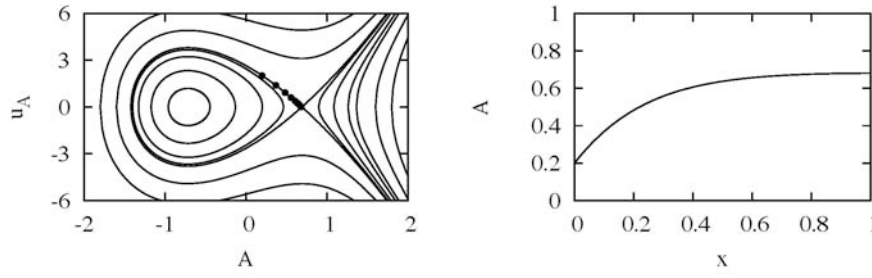


Fig. 1

Two models for the steady solutions of such a problem are asymptotically stable solutions of initial value problems and solutions to two-point boundary value problems. An asymptotically stable solution starts on one of the level curves and stays finite over the rest of its spatial extent. The only solutions like this in Fig. 1 that are physically realizable (all A's > 0) start on the separatrix and approach the saddle over the infinite spatial domain. The separatrix is a one-dimensional stable manifold and may be written as the level curve for H:

$$H = 0 = -\frac{k_f}{2D} B^2 - \frac{2k_r}{3D} B^3 + \frac{k_f c}{D} B$$

A typical solution of the two-point boundary value problem lies near the asymptotically stable solution along a portion of one of the phase space curves, and one is shown as a series of dots on the phase space structure. Its spatial profile is shown on the right in Fig. 1. Such solutions are unstable outside the spatial domain set by the two boundaries. An alternative model of the steady structure results for the asymptotically stable solutions described above and it is this latter model that we are studying in all the cases presented here. Generally, the two-point boundary solution and the asymptotically stable solutions are very similar, especially if the right hand boundary of the two-point boundary problem is at large distance.

Figure 1, although overly simple, describes the type of phase space that describes steady solutions of flames. Although these systems are generally not Hamiltonian, they

sometimes are volume-preserving. Even when neither condition is met, the basic structure pictured in Fig. 1 persists and an asymptotically stable solution is found along the stable manifold of an otherwise unstable system. From our experience, the dimension of the stable manifold is similar to the number of species. Because the systems are unstable, some extra care is necessary for deducing reduced kinetics compared to pure chemical-kinetic systems.

We have adapted two methods for finding low-dimensional manifolds to the asymptotic solutions of the steady problems, the ILDM method of Maas and Pope<sup>2</sup> and the iterative method of Fraser.<sup>3</sup> Our implementation of the Maas-Pope algorithm is similar to Ref. 4. The iterative method of Fraser allows for more accurate computation of manifolds. We first tested our algorithms on a model system that has an exact solution. In general, the two algorithms agree, but under some conditions, the Maas-Pope is inaccurate. Figure 2 shows an example of this.

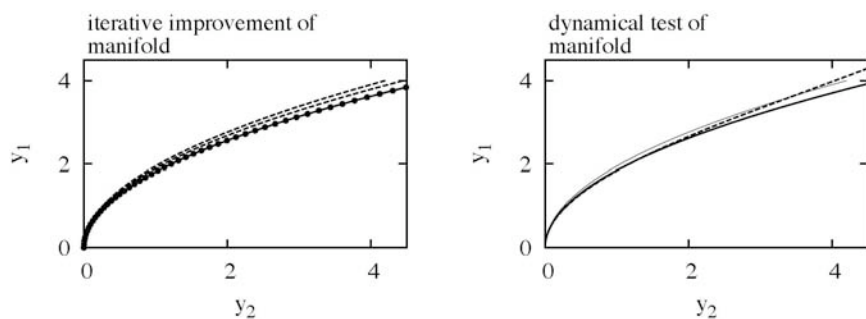


Fig. 2

The thick solid line with the dots in the left panel shows the exact stable manifold of the model system. The upper most dashed line shows the Maas-Pope estimate of the manifold, which is the first guess in the iterative procedure. The lower dashed curve shows one of the iterates to the manifold and the dots drawn on the exact manifold demonstrate the fully converged iterative result. On the right panel, a typical steady solution of the system is plotted in species space and it is demonstrated that the exact manifold is a more accurate representation of the asymptotic dynamics than the Maas-Pope estimate, plotted as a dotted line.

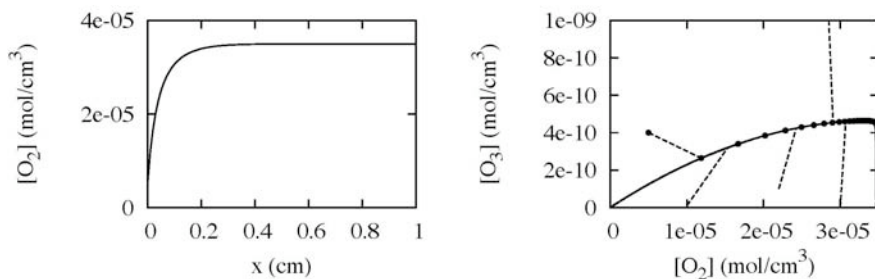


Fig. 3

We have applied the manifold methods to two other systems. Fig. 3 shows results for an ozone combustion system in the presence of diffusion only. The left panel shows a profile of the  $O_2$  concentration as a function of a spatial coordinate. The right panel repeats this as a series of dots along with several other steady solutions. These are

plotted in species space with the  $O_2$  and  $O_3$  concentrations. The thick solid curve shows a Maas-Pope estimate of a one-dimensional stable manifold and it demonstrates that this algorithm gives an accurate estimate of the reduced dynamics.

Figure 4 shows results for a 1-D premixed  $H_2/O_2$  flame generated from the Chemkin program “Premix”. The left panel shows a spatial profile of the mole fraction of  $H_2$  and the right panel shows a species space plot of the mole fractions of  $H_2$  and  $O_2$  plotted as a dashed curve. The dots on the curve correspond to the last seven dots in the profile on the left. The thick solid line shows an estimate of a 1-D manifold using the Maas-Pope algorithm, and the results are encouraging. We have not implemented the iterative algorithm for this case as yet, and improvements are expected.

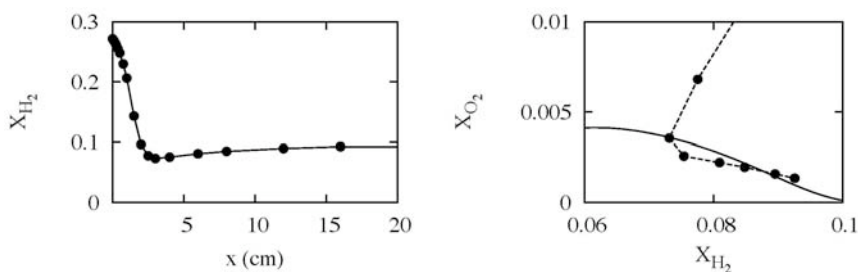


Fig. 4

## Future Plans

In the near term, it is expected that reduction methods for steady problems will be improved and be made more efficient so that they can be more readily applied to hydrocarbon combustion, including methane oxidation. We also expect to broaden the study of reduction. The reduction of chemical systems undergoing transport involves three cases. Two are transient cases and the third is the steady case outlined here. One of the transient cases was the subject of the two papers in press. In the future we will address the second transient case, which we have referred to as “species reduction”.

## References

- <sup>1</sup>For example, J. O. Hirschfelder and C. F. Curtiss, *Adv. Chem. Phys.* **3**, 59 (1961).
- <sup>2</sup>U. Maas and S. B. Pope, *Combust. Flame* **88**, 239 (1992).
- <sup>3</sup>Fraser, S. J. *J. Chem. Phys.* **88**, 4732 (1988).
- <sup>4</sup>H. Bongers, J.A. Van Oijen, and L.P.H. De Goey, *Proc. Combust. Inst.* **29**, 1371, Part I (2002).

## Publications

M. J. Davis, “Low-dimensional manifolds in reaction-diffusion equations. 1. Fundamental aspects”, *J. Phys. Chem. A* (in press).

M. J. Davis, “Low-dimensional manifolds in reaction-diffusion equations. 2. Numerical analysis and method development”, *J. Phys. Chem. A* (in press).

# COMPREHENSIVE MECHANISMS FOR COMBUSTION CHEMISTRY: EXPERIMENT, MODELING, AND SENSITIVITY ANALYSIS

Frederick L. Dryer

*Department of Mechanical and Aerospace Engineering  
Princeton University, Princeton, New Jersey 08544 5263*

fldryer@princeton.edu

Grant No. DE FG02 86ER 13503

## Program Scope

Experiments conducted in a Variable Pressure Flow Reactor (VPFR) at pressures from 0.3 to 20 atm and temperatures from 500 K to 1200 K, with observed reaction times from  $0.5 \times 10^{-2}$  to 2 seconds, and laminar flame speed measurements at atmospheric pressure are combined with literature data and numerical studies to develop and validate chemical kinetic reaction mechanisms and to improve determinations of important elementary rates. Continuing efforts are: (1) utilizing the perturbations of the H<sub>2</sub>/O<sub>2</sub> and CO/H<sub>2</sub>O/Oxidant reaction systems by the addition of small amounts of other species to further clarify elementary reaction properties; (2) further elucidating the reaction mechanisms for the pyrolysis and oxidation of hydrocarbons (alkanes, olefins) and oxygenates (aldehydes, alcohols, and ethers).

## Recent Progress

In the work summarized below, we investigate the complex kinetic behavior associated with hydrocarbon two-stage ignition and provide a conclusive explanation for the onset of the second ignition stage. We also report on recent experimental and modeling results using our newly developed DME kinetic model.

### *CSP Analysis of Ignition Phenomena*

Two-stage ignition and other related phenomena such as cool flames and negative temperature coefficient (NTC) ignition are of practical importance to, for example, engine technologies (HCCI, diesel ignition, cetane ratings, engine knock) and industrial processes. To date, however, an unambiguous interpretation of the underlying mechanisms responsible for this well-established behavior is lacking and is a subject of continuous debate (Westbrook, C.K., *Proc. Combust. Inst.*, **28**, 1563-1577). The analysis outlined below conclusively explains and confirms some of the postulated theories related to two-stage ignition.

Computational Singular Perturbation (CSP) analysis (Lam, S.H., *Combust. Sci. Tech.*, **89**, 1993, 375-404) is a commonly used tool to generate reduced kinetic models (Lam, S.H. and Goussis, D.A., *Int. J. Chem. Kinet.*, **26**, 1994, 461-486; Massias, A., et al., *Combust. Flame*, **117**, 1999, 685-708; Lu, T., et al., *Combust. Flame*, **126**, 2001, 1445-1455). In this study we have extended the CSP methodology and applied it to the analysis of the two-stage ignition behavior observed in large hydrocarbon molecules such as *n*-heptane. As opposed to other typical sensitivity analysis methods, the CSP method utilized here treats the entire thermokinetically coupled system directly so that factors controlling observed macroscopic behavior (such as two-stage ignition) can be determined unambiguously. A chemical kinetic reaction system may be represented as a set of ordinary differential equations,  $dz/dt = \mathbf{g}(\mathbf{z})$ , where  $\mathbf{z}$  is the state variable vector, containing the normalized temperature and species mass fractions, and  $\mathbf{g}$  the overall reaction rate vector. The inclusion of temperature as one of the CSP state variables is essential for the direct analysis of thermokinetic feedback during autoignition; many previous CSP applications interested in model reduction have not treated temperature as an independent variable. At any given time  $t$  the rate vector can be differentiated (i.e. "perturbed") with respect to time,  $d\mathbf{g}/dt = \mathbf{J} \cdot \mathbf{g}$ , so that a local Jacobian matrix is defined,  $\mathbf{J} = d\mathbf{g}/dt$ . One can, thus, perform a decomposition of the form:  $\mathbf{J} = \mathbf{V}\mathbf{\Lambda}\mathbf{V}^{-1}$ , where  $\mathbf{V}$  is the matrix of eigenvectors ( $\mathbf{v}_i$ ) and  $\mathbf{\Lambda}$  the diagonal matrix containing eigenvalues. The differentiation essentially yields a system of linear ordinary differential equations for  $\mathbf{g}$ . Using the decomposition above, the rate vector can be represented as a sum of individual modes:

$$\mathbf{g}(t + \Delta t) \approx \sum_{i=1}^{n+1} f_i \mathbf{v}_i \exp(\lambda_i \Delta t),$$
 where  $f_i$  is the mode amplitude (indicating the mode importance) and  $\lambda_i$  the

corresponding eigenvalue (indicating the mode time scale and physical behavior). The identified modes can be classified according to the sign of the real component of the system eigenvalues,  $\text{Re}(\lambda_i)$ . The modes with negative  $\text{Re}(\lambda_i)$  are referred to as *stable* (decaying) modes, while the modes with positive  $\text{Re}(\lambda_i)$  are *unstable* (explosive) modes. These explosive modes are of importance for the present analysis as they control the ignition behavior of the kinetic system. Reactions contributing to the identified explosive modes were identified using the concept of Participation Index as explained by Lam (*Combust. Sci. Tech.*, **89**, 1993, 375-404). Further details on the developed CSP method can be found in Refs. 1 and 2.

The above methodology was applied to the study of premixed *n*-heptane/air homogeneous ignition under stoichiometric conditions at a pressure and temperature of 13.5 bar and 850 K, respectively. Under these conditions, *n*-heptane exhibits two-stage ignition (Ciezki, H. and Adomeit, G., *Combust. Flame*, **93**, 1993, 421-433). Detailed (H.J. Curran et al., *Combust. Flame*, **114**, 1998, 149-177) and skeletal (N. Peters et al., *Combust. Flame*, **128**, 2002, 38-59) chemical kinetic models were considered in the analysis. Figures 1 and 2 show the main participating reactions associated with the explosive modes identified during the first and second ignition stages. The first stage (Fig. 1) is governed by a low-temperature branching sequence (S.W. Benson, *Prog. Energy Combust. Sci.* **7**, 1981, 125-134) driven by the internal isomerization reactions of alkylperoxy radicals. Due to the simplifications made in generating the skeletal scheme, it is seen that alkyl radical decomposition competes with alkylperoxy isomerization, which should not be expected at the intermediate temperatures observed during the first stage. The results obtained when analyzing the second ignition stage and shown in Fig. 2 are of most importance here. Figure 2 shows that for both detailed and skeletal models the single explosive mode responsible for the second stage is nearly exclusively driven by the decomposition of H<sub>2</sub>O<sub>2</sub>. This result is consistent with some proposed schemes (F. Battin-Leclerc, et al., European Combustion Meeting; Louvain-la-Neuve, Belgium, 2005, paper 16) but contradicts the earlier interpretations by Peters et al. using the same model above. Peters et al. incorrectly attributed the runaway at the second stage as the sudden release of OH into the system once the fuel is fully depleted. Figure 2 shows that no fuel reactions are important during the second stage.

Moreover, the present results also show that though the predicted overall heat release and ignition delay are similar for both detailed and skeletal models, the product speciations as functions of time are extremely different. The skeletal reduced model produces a pool of small carbon number molecules dominated by ethylene and formaldehyde, whereas the detailed model yields significant fraction of initial fuel along with large olefins and partially oxygenated species. Such differences are to be expected as shortcomings in the generation of skeletal models based on limited validation targets.

#### *Dimethyl Ether*

As we reported here in 2005, an updated high-temperature model for DME pyrolysis and oxidation has been developed [3]. The model includes revised sub-models and thermochemistry for hydrogen as well as C<sub>1</sub>-C<sub>2</sub> reactions developed in recent experimental and modeling studies of ethanol pyrolysis and oxidation. The H<sub>2</sub>-O<sub>2</sub> and C<sub>1</sub>-C<sub>2</sub> subsets were hierarchically assembled and comprehensively tested against a large volume of high temperature data from shock tubes, flow reactors, and flames involving hydrogen, carbon monoxide, formaldehyde, and methanol as initial reactants. Significant modifications were made to important reactions such as fuel H-atom abstraction by H, OH and CH<sub>3</sub> and the termination reaction between formyl and methyl radicals, HCO+CH<sub>3</sub> = CO+CH<sub>4</sub>. The high-temperature DME reaction model consists of 46 species undergoing 263 reversible elementary reactions. The new DME model predictions compare well with high-temperature flow reactor, jet-stirred reactor, shock-tube ignition, burner-stabilized flames, and laminar premixed flame speed experimental data.

More recently, a molecular-beam flame-sampling photoionization mass spectrometer (PIMS), employing VUV synchrotron radiation, was applied to the measurement of 21 flame species in low-pressure premixed fuel-rich ( $\Phi=1.2, 1.68$ ) DME/O<sub>2</sub>/Ar flat flames [4]. The new DME model was used to predict the species profiles measured in these DME flames. Reaction path analyses were performed using predicted mole fractions to establish the contributions of individual formation and destruction reactions using an in-house code developed at Princeton. As shown in Fig. 3, major species profiles measured by the PIMS are found to agree with profiles predicted by the kinetic model within the range of experimental uncertainties ( $\pm 10$ -20%). No systematic differences are apparent. Intermediate species present at the highest concentrations (CH<sub>2</sub>O, CH<sub>4</sub>, C<sub>2</sub>H<sub>6</sub>, C<sub>2</sub>H<sub>4</sub>, and C<sub>2</sub>H<sub>2</sub>) are satisfactorily predicted within experimental uncertainties, while minor species (CH<sub>3</sub>OH, CH<sub>3</sub>CHO, CH<sub>2</sub>CO, CH<sub>3</sub>, HCO) exhibit much larger discrepancies, with the predicted mole fractions typically exceeding the measurements by factors of 2 to 3. The relative mole fractions measured for O, H and OH, normalized to the model predictions, exhibit spatial profiles similar to those predicted by the model. The new model exhibits a better prediction of flame species profiles than a previously published model (S.L. Fischer et al., *Int. J. Chem. Kinet.*, **32**, 2000, 713-740) or its recent updates (H.J. Curran, personal communication, 2005).

The new DME model has also been shown to reproduce laminar flame speed measurements of DME-doped CH<sub>4</sub>/air premixed flames at atmospheric pressure [5], as shown in Fig. 4. An analysis utilizing the CSP methodology described above to investigate the ignition behavior of these mixtures successfully explains the dramatic enhancement of high temperature ignition by the addition of DME to both premixed and non-premixed CH<sub>4</sub>-air systems [5]. DME additions as small as 2% of the overall fuel concentration substantially shorten the time required for early radical pool development as a result of the rapid unimolecular decomposition of DME (in comparison to the generation and growth of radicals from the CH<sub>4</sub>+O<sub>2</sub> reaction, see Fig. 5). Radical pool growth is also no longer limited by the rate at which methyl radicals alone can produce more reactive species since DME decomposition yields CH<sub>3</sub>O and CH<sub>3</sub>, providing additional channels for generating radicals (e.g. through CH<sub>3</sub>O decomposition/oxidation).

## Plans

Reaction systems presently under investigation and of continuing interest over the coming year, include the pyrolyses and oxidations of acetaldehyde, acetone, and toluene, all over a range of pressures and temperatures similar to our previous work.

## Publications

1. A. Kazakov, M. Chaos, Z. Zhao, and F.L. Dryer, "Computational Singular Perturbation Analysis of Two-Stage Ignition of Large Hydrocarbons," J. Phys. Chem. A, 2006; in press. (available electronically as an ASAP article at: <http://pubs3.acs.org/acs/journals/toc.page?incoden=jpcfah&indecade=0&involume=0&inissue=0>).
2. A. Kazakov, Z. Zhao, B.D. Urban, and F. L. Dryer, "Do We Understand How Two-Stage Hydrocarbon Ignition Mechanisms Work?" Poster L15, 6th International Conference on Chemical Kinetics, Gaithersburg, MD, July 25-29, 2005.
3. Z. Zhao, J. Li, A. Kazakov, and F.L. Dryer, "Thermal Decomposition Reaction and a High Temperature Kinetic Model of Dimethyl Ether", Joint Meeting of the U.S. Sections of the Combustion Institute, Drexel University, Philadelphia, PA, March 22-24, 2005, paper C14.
4. T.A.Cool, J. Wang, N. Hansen, P.R. Westmoreland, F.L. Dryer, Z. Zhao, A. Kazakov, T. Kasper, K. Kohse-Höinghaus, "Photoionization Mass Spectrometry and Modeling Studies of Fuel-Rich Dimethyl Ether Flames," Proc. Combust. Inst., 31, 2006; in press.
5. Z. Chen, X. Qin, Y. Ju, Z. Zhao, M. Chaos, and F.L. Dryer, "High Temperature Ignition and Combustion Enhancement by Dimethyl Ether Addition to Methane-Air Flames," Proc. Combust. Inst., 31, 2006; in press.

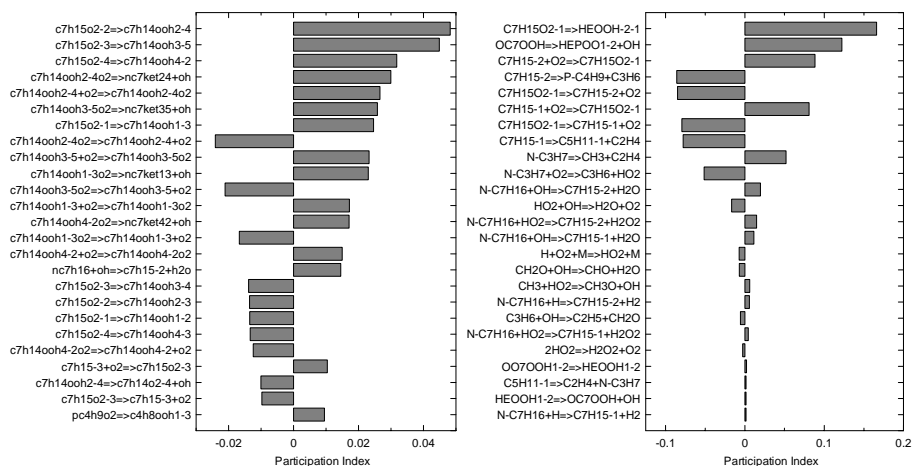


**Fig. 1.** Reaction make-up of explosive modes driving the first ignition stage for the detailed (left) and skeletal (right) models.

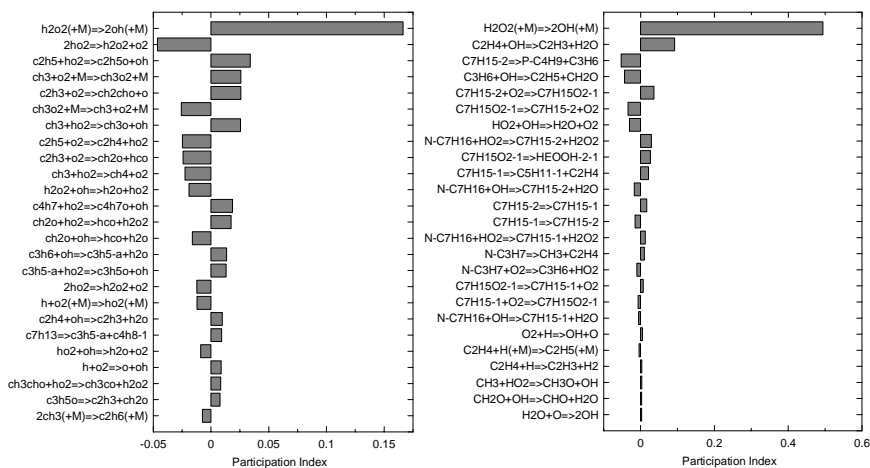


**Fig. 2.** Reaction make-up of explosive modes driving the second ignition stage for the detailed (left) and skeletal (right) models.

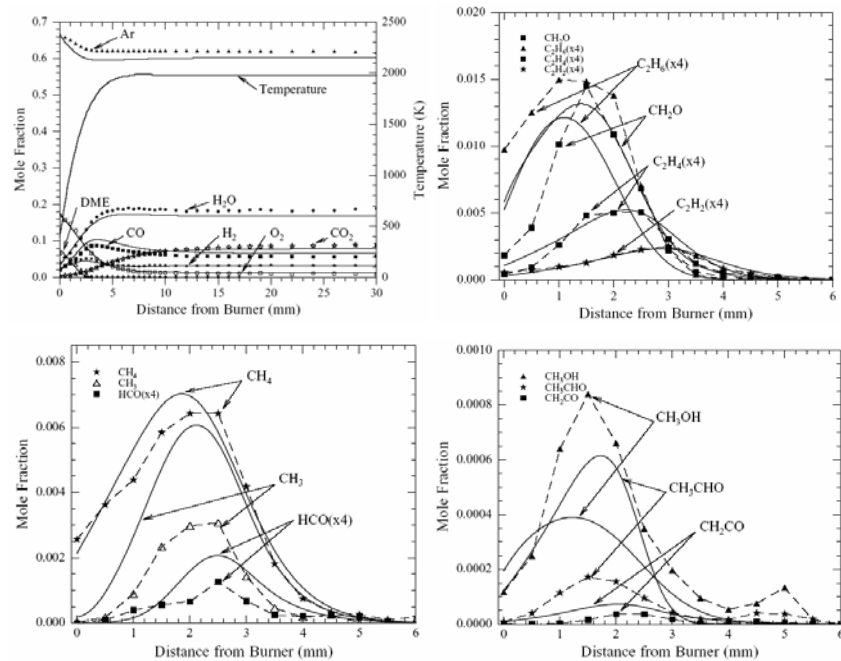


**Fig. 3.** Comparison of experimental (T.A. Cool et al., 2006) (symbols) and computed (lines) species profiles in DME-O<sub>2</sub>-Ar burner stabilized flame ( $P = 4.0$  kPa,  $\phi = 1.2$ ).

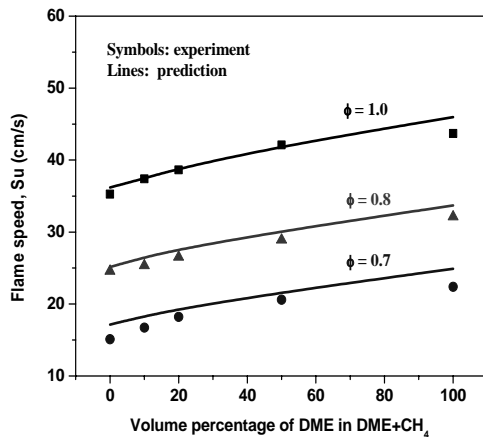


**Fig. 4.** Variation of laminar flame speeds of DME/CH<sub>4</sub>-air mixtures with DME blending at different equivalence ratios at 298K, atmospheric pressure, compared with model predictions.

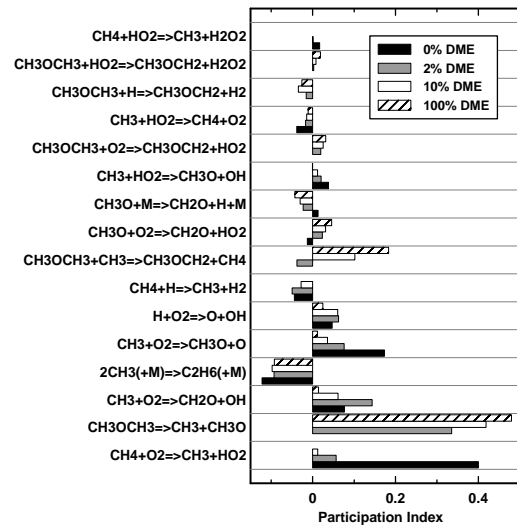


**Fig. 5.** Dominant reactions during initial radical build-up (DME/CH<sub>4</sub>-air;  $P = 1$ atm,  $\phi = 1.0$ ,  $T = 1,200$ K) obtained from CSP analysis

# LASER PHOTOELECTRON SPECTROSCOPY OF IONS

G. Barney Ellison  
Department of Chemistry & Biochemistry  
University of Colorado  
Boulder, CO 80309-0215  
Email: [barney@JILA.colorado.edu](mailto:barney@JILA.colorado.edu)

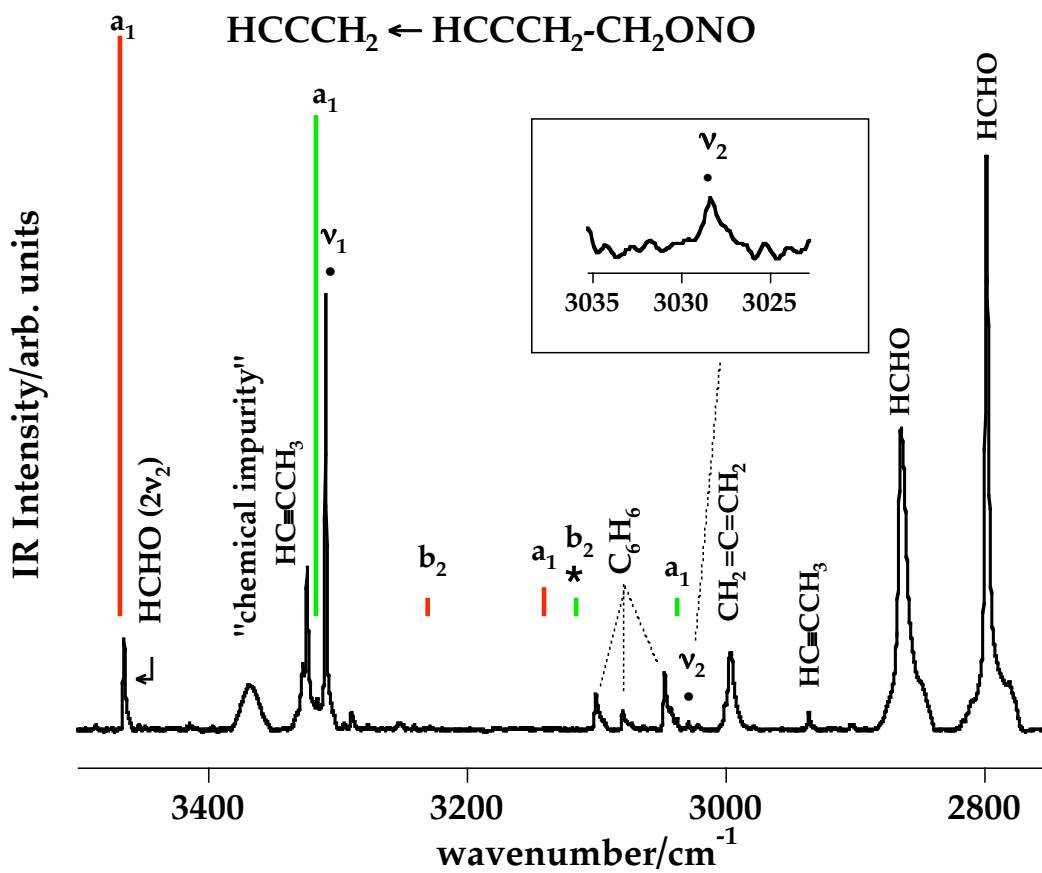
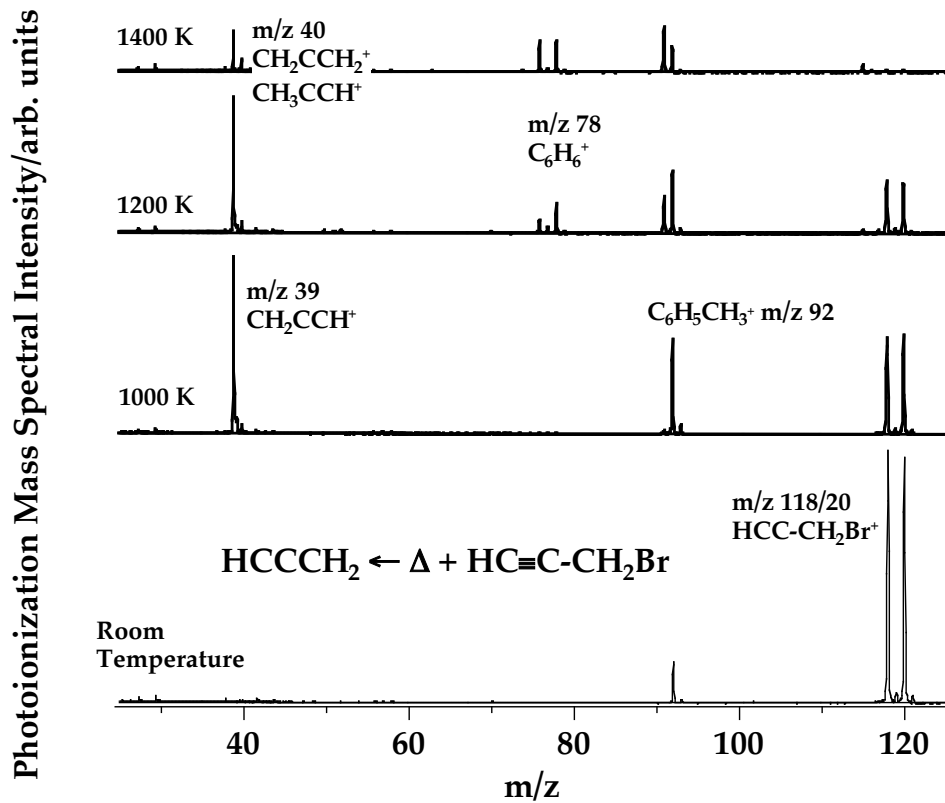
## Propargyl Radical: *ab initio* Anharmonic Modes and the Polarized Infrared Absorption Spectra of Matrix-Isolated HCCCH<sub>2</sub>

The propargyl radical has twelve fundamental vibrational modes,  $\Gamma_{\text{vib}}(\text{HCCCH}_2) = 5a_1 \oplus 3b_1 \oplus 4b_2$ , and nine have been detected in a cryogenic matrix.<sup>1</sup> *Ab initio* coupled-cluster anharmonic force field calculations were used to help guide some of the assignments. The experimental HC≡C-CH<sub>2</sub> matrix frequencies (cm<sup>-1</sup>) and polarizations are: a<sub>1</sub> modes — 3308.5 ± 0.5, 3028.3 ± 0.6, 1935.4 ± 0.4, 1440.4 ± 0.5, 1061.6 ± 0.8; b<sub>1</sub> modes — 686.6 ± 0.4, 483.6 ± 0.5; b<sub>2</sub> modes — 1016.7 ± 0.4, 620 ± 2. We recommend a complete set of gas-phase vibrational frequencies for the propargyl radical, HC≡C-CH<sub>2</sub>  $\tilde{X}^2B_1$ . From an analysis of the vibrational spectra, the small electric dipole moment,  $\mu_{\text{D}}(\text{HCCCH}_2) = 0.150$  D, and the large resonance energy(HCCCH<sub>2</sub>) = roughly 11 kcal mol<sup>-1</sup>, we conclude that propargyl is a completely delocalized hydrocarbon radical, and is best written as HC≡C-CH<sub>2</sub>.

As part of the study of the spectroscopy and bonding of propargyl radical, our experiment also revealed that these HC≡C-CH<sub>2</sub> radicals were dimerizing in the nozzle to produce the simplest aromatic ring, benzene: HCCCH<sub>2</sub> + HCCCH<sub>2</sub> → C<sub>6</sub>H<sub>6</sub>. In the PIMS spectrum below, propargyl bromide is thermally dissociated to generate propargyl, HCC-CH<sub>2</sub>Br + Δ → HCCCH<sub>2</sub> + Br. As the nozzle is heated, Br atoms are not observed since *IE*(Br) is 11.8 eV while the VUV laser is only 10.487 eV ( $\hbar\omega_{118.2\text{nm}}$ ). Heating the nozzle to 1000 K induces dissociation of propargyl bromide and HCCCH<sub>2</sub><sup>+</sup> is clearly observed at *m/z* 39. The feature at *m/z* 92 belongs to C<sub>6</sub>H<sub>5</sub>CH<sub>3</sub><sup>+</sup> which derives from the toluene stabilizer added to the commercial supply of HC≡CCH<sub>2</sub>Br. At a nozzle temperature of 1200 K, two HC≡C-CH<sub>2</sub> radicals appear to dimerize to form C<sub>6</sub>H<sub>6</sub> *m/z* 78. The IR spectra (*vide infra*) clearly shows that the C<sub>6</sub>H<sub>6</sub> adduct is benzene. At higher nozzle temperatures (1400 K), the HC≡C-CH<sub>2</sub> radicals are abstracting H atoms in the nozzle and producing CH<sub>2</sub>=C=CH<sub>2</sub> and HC≡C-CH<sub>3</sub>. The IR spectra (*vide infra*) permit us to identify both allene and methylacetylene as reaction products.

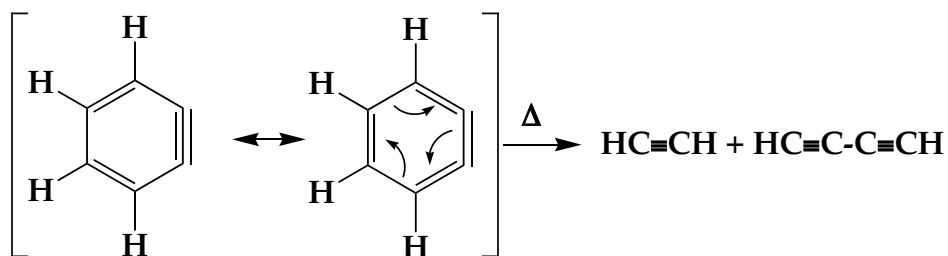
---

<sup>1</sup> Evan B. Jochowitz, Xu Zhang, Mark R. Nimlos, Mychel Elizabeth Varner, John F. Stanton, and G. Barney Ellison, "Propargyl Radical: *ab initio* Anharmonic Modes and the Polarized Infrared Absorption Spectra of Matrix-Isolated HCCCH<sub>2</sub>", *J. Phys. Chem. A*, **109**, 3812-3821 (2005).

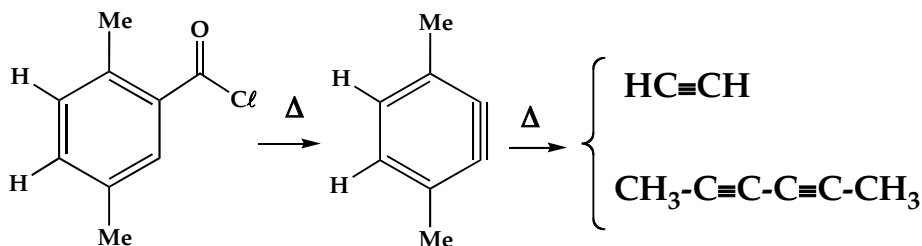


## Unimolecular thermal fragmentation of *ortho*-benzyne

The generation of the *ortho*-benzyne diradical,  $o\text{-C}_6\text{H}_4$ , and its subsequent thermal decomposition has been carried out in a supersonic hyperthermal nozzle.<sup>2</sup> As the temperature of the nozzle is increased, benzyne undergoes further fragmentation. The thermal dissociation products were detected using three different experimental methods: (1) time-of-flight photoionization mass spectrometry, (2) matrix-isolation Fourier transform infrared absorption spectroscopy, and (3) chemical ionization mass spectrometry. At the threshold dissociation temperature, *o*-benzyne cleanly decomposes into acetylene and diacetylene *via* an apparent retro-Diels-Alder process:  $o\text{-C}_6\text{H}_4 + \Delta \rightarrow \text{HC}\equiv\text{CH} + \text{HC}\equiv\text{C}-\text{C}\equiv\text{CH}$ .

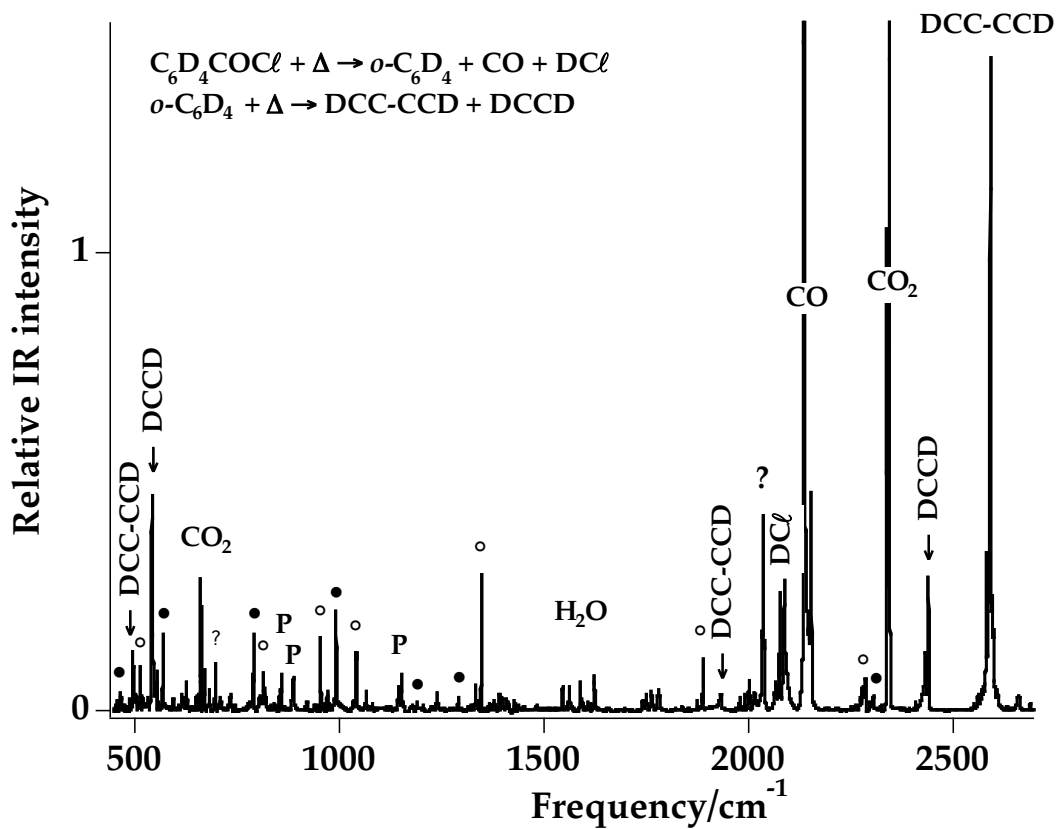
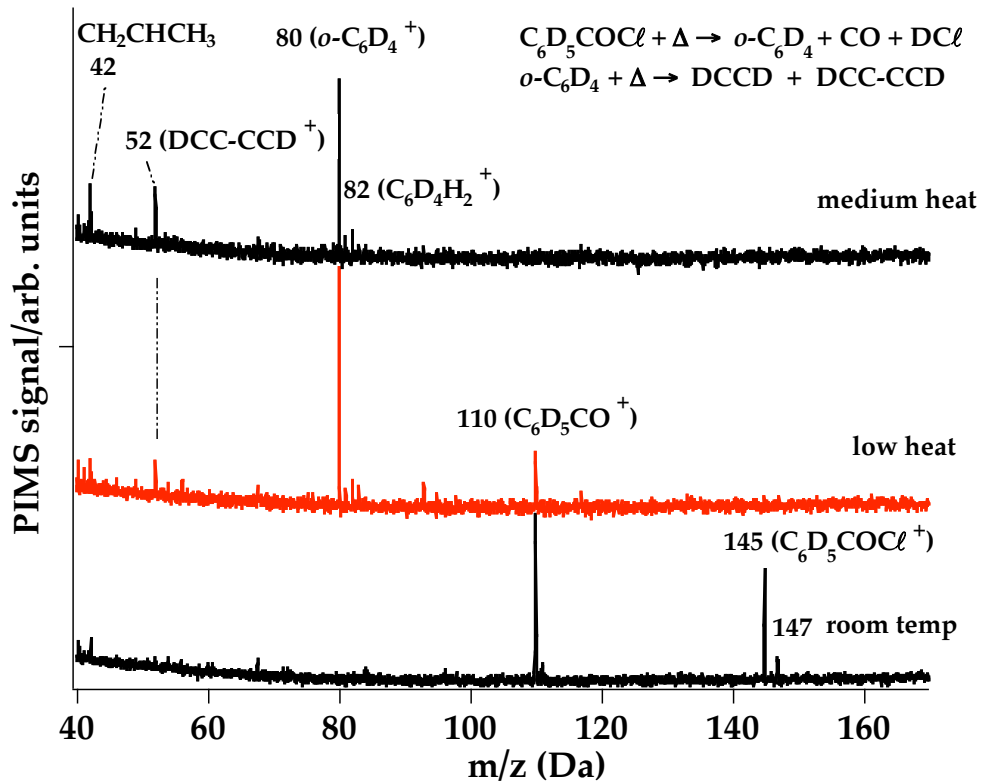


Below are representative PIMS and IR spectra for decomposition of the deuterated benzoyl chloride:  $\text{C}_6\text{D}_5\text{COCl} + \Delta \rightarrow [o\text{-C}_6\text{D}_4] + \Delta \rightarrow \text{DC}\equiv\text{CD} + \text{DC}\equiv\text{C}-\text{C}\equiv\text{CD}$ . To demonstrate the proper regio-chemistry of a Diels-Alder fragmentation, we examined the decomposition of 2,5-dimethylbenzoyl chloride. For a concerted retro-Diels Alder fragmentation of the 2,5-dimethylbenzyne, one would expect formation of  $\text{HC}\equiv\text{CH}$  and  $\text{CH}_3\text{C}\equiv\text{C}-\text{C}\equiv\text{CCH}_3$  only. This is what is observed.



At higher nozzle temperatures, the fragmentation mechanism becomes more complicated. A careful assessment of the thermochemistry for the high temperature fragmentation of benzene is presented:  $\text{C}_6\text{H}_6 \rightarrow \text{H} + [\text{C}_6\text{H}_5] \rightarrow \text{H} + [o\text{-C}_6\text{H}_4] \rightarrow \text{HC}\equiv\text{CH} + \text{HC}\equiv\text{C}-\text{C}\equiv\text{CH}$ . *Ab initio* electronic structure calculations have been used to calculate the barrier for the classical retro-Diels-Alder fragmentation. A CCSD(T)/cc-pVQZ calculation finds  $E_a(o\text{-C}_6\text{H}_4 + \Delta \rightarrow \text{HCCH} + \text{HCC-CCH}) = 88 \pm 2 \text{ kcal mol}^{-1}$ . A barrier of this magnitude is consistent with the operating temperatures of our supersonic hyperthermal nozzle.

<sup>2</sup> Xu Zhang, Alan T. Maccarone, Mark R. Nimlos, Shuji Kato, Veronica M. Bierbaum, Barry K. Carpenter, G. Barney Ellison, Branko Ruscic, Andrew C. Simmonett, Wesley D. Allen, and Henry F. Schaefer III, "Unimolecular thermal fragmentation of *ortho*-benzyne," J. Chem. Phys. (submitted, 2006).



## DOE Publications

- Xu Zhang, Veronica M. Bierbaum, G. Barney Ellison, and Shuji Kato, "Gas-Phase Reactions of Organic Radicals and Diradicals with Ion", J. Chem. Phys., **120**, 3531-3534 (2004).
- G. Barney Ellison, John M. Herbert and Anne B. McCoy, Péter G. Szalay and John F. Stanton, "Unimolecular Rearrangement of *trans*-FONO to FNO<sub>2</sub>. A Possible Model System for Atmospheric Nitrate Formation", J. Phys. Chem. A, **108**, 7639-7642 (2004).
- Xu Zhang, Shuji Kato, Veronica M. Bierbaum, Mark R. Nimlos, and G. Barney Ellison, "The Use of a Flowing Afterglow-SIFT Apparatus to Study the Reactions of Ions with Organic Radicals", J. Phys. Chem. A, **108**, 9733-9741 (2004).
- Evan B. Jochowitz, Xu Zhang, Mark R. Nimlos, Mychel Elizabeth Varner, John F. Stanton, and G. Barney Ellison, "Propargyl Radical: *ab initio* Anharmonic Modes and the Polarized Infrared Absorption Spectra of Matrix-Isolated HCCCH<sub>2</sub>", J. Phys. Chem. A, **109**, 3812-3821 (2005).
- Xu Zhang, Mark R. Nimlos and G. Barney Ellison, Mychel E. Varner and John F. Stanton, "The Infrared Absorption Spectra of Matrix-Isolated *cis*, *cis*-HOONO and its *ab initio* CCSD(T) Anharmonic Vibrational Bands", J. Chem. Phys., **124**, 1 (2006).

# Hydrocarbon Radical Thermochemistry: Gas-Phase Ion Chemistry Techniques

Kent M. Ervin  
Department of Chemistry/216  
University of Nevada, Reno  
Reno, Nevada 89557  
E-mail: ervin @ chem.unr.edu

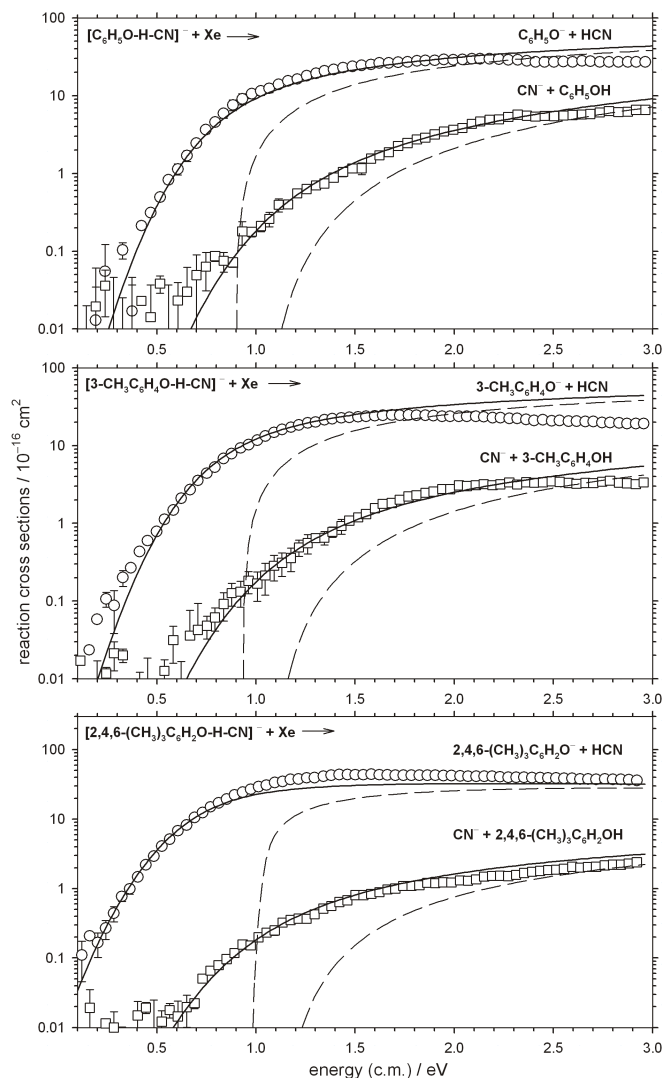
## Project Scope

Gas phase negative ion chemistry methods are employed to determine enthalpies of formation of hydrocarbon radicals that are important in combustion processes and to investigate the dynamics of ion–molecule reactions. Guided ion beam tandem mass spectrometry is used to measure the activation of endoergic ion-molecule reactions as a function of kinetic energy. Modeling the measured reaction cross sections using statistical rate theory or empirical reaction models allows extraction of reaction threshold energies. These threshold energies yield relative gas-phase acidities, proton affinities, or hydrogen-atom affinities, which may then be used to derive neutral R–H bond dissociation enthalpies using thermochemical cycles involving established electron affinities or ionization energies. The reactive systems employed in these studies include endoergic bimolecular proton transfer reactions, hydrogen-atom transfer reactions, and collision-induced dissociation of heterodimer complex anions and cations. Electronic structure calculations are used to evaluate the possibility of potential energy barriers or dynamical constrictions along the reaction path, and as input for RRKM and phase space theory calculations.

## Recent Progress

### *O-H bond dissociation energy of phenol*

In recently published work,<sup>1</sup> we used competitive threshold collision-induced dissociation (TCID) techniques to determine the bond dissociation energy of phenol,  $D(\text{C}_6\text{H}_5\text{O}-\text{H})$ , for which recent literature determinations are not in agreement. We produced the proton-bound heterodimer  $[\text{C}_6\text{H}_5\text{O}.. \text{H}.. \text{CN}]^-$ , which upon collisional activation dissociates into either  $\text{C}_6\text{H}_5\text{O}^- + \text{HCN}$  or  $\text{C}_6\text{H}_5\text{OH} + \text{CN}^-$ . Using statistical rate theories, we quantitatively model the branching ratio between these two product channels as a function of the available energy to obtain the threshold energy difference between the two channels. Using HCN as a reference acid, this yields the gas-phase acidity of phenol, which can be combined with the electron affinity of phenoxy radical from photoelectron spectroscopy<sup>2</sup> to give the O–H bond dissociation energy of phenol. Our results yielded  $D_{298}(\text{C}_6\text{H}_5\text{O}-\text{H}) = 359 \pm 8$  kJ/mol, smaller than the values reported from proton transfer energy thresholds by both in early experiments in our group ( $\text{Cl}^- + \text{C}_6\text{H}_5\text{OH}$ )<sup>3</sup> and by Anderson and coworkers ( $\text{ND}_3 + \text{C}_6\text{H}_5\text{OH}^+$ )<sup>4</sup>. Since our more recent publication,<sup>1</sup> two other groups have published disparate theoretical/experimental re-evaluations of the bond dissociation energy of phenol,  $D_{298}(\text{C}_6\text{H}_5\text{O}-\text{H}) = 363 \pm 3$  kJ/mol by Mulder and coworkers<sup>5,6</sup> and  $D_{298}(\text{C}_6\text{H}_5\text{O}-\text{H}) = 373$  kJ/mol by Canuto and coworkers.<sup>7,8</sup> Because phenoxy



radical is important in combustion and because the gas-phase acidity scale is deficient in the region of phenol, we have now extended our experimental work on the phenol system by using additional reference acids besides HCN, namely  $\text{H}_2\text{S}$  and  $\text{HOO}$ , and by including several cresols into a local thermochemical network of relative acidities for a more precise determination. For example, the cross sections for TCID of proton-bound complexes of  $\text{CN}^-$  with phenol, para-methylphenol and 2,4,6-trimethylphenol are shown in the figure at left. The fits to the cross sections employ RRKM theory to model the product branching fractions as a function of available energy. To construct the local thermochemical network, 48 independent measurements of 16 different complexes were undertaken. Our new bond dissociation energy [preliminary value pending final fits] is  $D_{298}(\text{C}_6\text{H}_5\text{O}-\text{H}) = 361 \pm 4 \text{ kJ/mol}$ , i.e., very close to the value of  $359 \pm 8 \text{ kJ/mol}$  we obtained previously based upon TCID of just the single  $[\text{C}_6\text{H}_5\text{O}\cdots\text{CN}]^-$  complex. Our value agrees with the lower prediction of Mulder and coworkers,<sup>5,6</sup> which is based upon both theory and photoacoustic calorimetry measurements in solution corrected to the gas phase, but

does not agree well with the higher value advocated by Canuto and coworkers,<sup>7,8</sup> which is based upon complete-basis-set extrapolated coupled-cluster calculations and supported by a 1998 literature evaluation by Santos and Simões.<sup>9</sup> The still-higher experimental values of  $381 \pm 4 \text{ kJ/mol}$  by Anderson and co-workers<sup>4</sup> and  $\leq 377 \pm 13 \text{ kJ/mol}$  in early work in our lab,<sup>3</sup> both based on threshold energies for bimolecular proton transfer reactions, can be definitely excluded.

### Hydrogen sulfide/Hydrogen cyanide

We recently examined the  $\text{HCN}/\text{H}_2\text{S}$  system.<sup>10</sup> These two acids have well-established gas-phase acidities, are well characterized spectroscopically, and  $\text{H}_2\text{S}$  and  $\text{HCN}$  have very similar gas-phase acidities. Therefore, the energy-resolved competitive collision-induced dissociation of the proton-bound complex  $[\text{HS}\cdots\text{H}\cdots\text{CN}]^-$  serves as a good test of the TCID method and our data modeling procedures. The cross sections for the  $\text{HS}^- + \text{HCN}$  and the  $\text{CN}^- + \text{H}_2\text{S}$  product channels, exhibit nearly the same threshold energy as expected. However, the  $\text{HS}^- + \text{HCN}$  channel has a cross section up to a factor of fifty larger than  $\text{CN}^- + \text{H}_2\text{S}$  at higher energies. The cross sections are modeled using both RRKM theory and microcanonical phase space theory

(PST). Modeling the systems requires a loose transition state for the  $\text{HS}^- + \text{HCN}$  channel and a tight transition state for  $\text{CN}^- + \text{H}_2\text{S}$ . Theoretical calculations show that the proton-transfer potential energy surface has a single minimum and that the hydrogen bonding in the complex is strongly unsymmetrical, with an ion-molecule complex of the form  $\text{HS}^- \cdots \text{HCN}$  rather than  $\text{CN}^- \cdots \text{H}_2\text{S}$  or an intermediate structure. The requirement for proton transfer before dissociation to  $\text{CN}^- + \text{H}_2\text{S}$  and curvature along the reaction path impedes that product channel. Although these issues complicate the extraction of energetic information, the relative gas-phase acidity can be obtained with reasonable precision (within  $\pm 4$  kJ/mol). As an aside, detailed comparisons of the results of our code for PST using the classical formulation of Chesnavich and Bowers<sup>11</sup> to the VARIFLEX code for quantum PST<sup>12</sup> showed that the approximation in the former using spherical rotors instead of symmetric tops leads to small but significant errors in the calculations of densities of states. We are therefore pursuing improvements in our implementation of the PST models.

### ***Collision-induced dissociation of $\text{O}_2^-$***

The energetics and dynamics of collision-induced dissociation of  $\text{O}_2^-$  with Ar and Xe targets have been studied experimentally using guided ion-beam tandem mass spectrometry and modeled theoretically by classical trajectory calculations.<sup>13</sup> The collisionally activated dissociation process is surprisingly inefficient. Experimental threshold energies are 2.1 and 1.1 eV in excess of the thermochemical  $\text{O}_2^-$  bond dissociation energy for argon and xenon, respectively. Classical trajectory calculations confirm the observed threshold behaviour and the dependence of cross sections on the relative kinetic energy. Representative trajectories reveal the bond dissociation taking place on a short time scale of about 50 fs in strong collisions. Collision-induced dissociation is found to be remarkably restricted to the perpendicular approach of Ar/Xe to the molecular axis of  $\text{O}_2^-$ , while collinear collisions do not result in dissociation.

### **Future Directions**

Because of the importance of oxygen-containing species in combustion, especially with oxygenated fuels, we will target the O–H bond dissociation enthalpies of unsaturated alcohols, carboxylic acids, and peroxides. Work is currently underway examining the gas-phase acidities of formic acid, acetic acid, and benzoic acid. We will examine additional ions for their suitability as proton transfer and hydrogen atom transfer reagents. For proton affinity measurements, the experimental apparatus is being modified to allow the positive ion reactions as well as negative ions.

<sup>1</sup>L. A. Angel and K. M. Ervin, *J. Phys. Chem. A* **108**, 8345 (2004).

<sup>2</sup>R. F. Gunion, M. K. Gilles, M. L. Polak, and W. C. Lineberger, *Int. J. Mass Spectrom. Ion Processes* **117**, 601 (1992).

<sup>3</sup>V. F. DeTuri and K. M. Ervin, *Int. J. Mass Spectrom.* **175**, 123 (1998).

<sup>4</sup>H.-T. Kim, R. J. Green, J. Qian, and S. L. Anderson, *J. Chem. Phys.* **112**, 5717 (2000).

<sup>5</sup>P. Mulder, H.-G. Korth, D. A. Pratt, G. A. DiLabio, L. Valgimigli, G. F. Pduilli, and K. U. Ingold, *J. Phys. Chem. A* **109**, 2647 (2005).

<sup>6</sup>G. A. DiLabio and P. Mulder, *Chem. Phys. Lett.* **417**, 566 (2006).

<sup>7</sup>B. J. Costa Cabral and S. Canuto, *Chem. Phys. Lett.* **406**, 300 (2005).

<sup>8</sup>B. J. Costa Cabral and S. Canuto, *Chem. Phys. Lett.* **417**, 570 (2006).

- <sup>9</sup>R. M. Borges dos Santos and J. A. Martinho Simoes, *J. Phys. Chem. Ref. Data* **27**, 707 (1998).
- <sup>10</sup>F. A. Akin and K. M. Ervin, *J. Chem. Phys.* **110**, 1342 (2006).
- <sup>11</sup>W. J. Chesnavich and M. T. Bowers, *J. Chem. Phys.* **66**, 2306 (1977).
- <sup>12</sup>S. J. Klippenstein, A. Wagner, S. Roberstson, R. Dunbar, and D. M. Wardlaw, VariFlex, version 1.0, 1999.
- <sup>13</sup>F. A. Akin, J. Ree, K. M. Ervin, and H. K. Shin, *J. Chem. Phys.* **123**, 064308 (2005).

### **Publications, 2004–present**

“Collision-Induced Dissociation of HS<sup>-</sup>(HCN): Unsymmetrical Hydrogen Bonding in a Proton-Bound Dimer Anion”, F. A. Akin and Kent M. Ervin, *J. Phys. Chem. A*, **110**, 1342-1349 (2006).

“Threshold collision-induced dissociation of diatomic molecules: A case study of the energetics and dynamics of O<sub>2</sub><sup>-</sup> collisions with Ar and Xe”, F. A. Akin, J. Ree, K. M. Ervin and H. K. Shin, *J. Chem. Phys.* **123**, 064308:1-12 (2005).

“Photoelectron spectroscopy of phosphorus hydride anions”, K. M. Ervin and W. C. Lineberger, *J. Chem. Phys.* **122**, 194303:1-11 (2005).

“Systematic and random errors in ion affinities and activation entropies from the extended kinetic method”, K. M. Ervin and P.B. Armentrout, *J. Mass Spectrom.* **39**, 1004-1015 (2004).

“Competitive threshold collision-induced dissociation: Gas-phase acidity and O-H bond dissociation enthalpy of phenol”, L. A. Angel and K. M. Ervin, *J. Phys. Chem. A*, **108**, 8345-8352 (2004).

PESCAL, Fortran program for Franck-Condon analysis of photoelectron spectra, K. M. Ervin, (revised 2004).

ODRFIT, Fortran program for analysis of extended kinetic method data using orthogonal distance regression analysis, K. M. Ervin and P. B. Armentrout, (2004).

CRUNCH, Fortran program for analysis of reaction cross sections with RRKM and PST models, K. M. Ervin and P. B. Armentrout, version 5.10 (revised 2005).

# Spectroscopic and Dynamical Studies of Highly Energized Small Polyatomic Molecules

**Robert W. Field**

Massachusetts Institute of Technology

Cambridge, MA 02139

[rwfield@mit.edu](mailto:rwfield@mit.edu)

## Program Definition

The fundamental goal of this program is to develop the experimental techniques, diagnostics, interpretive concepts, and pattern-recognition schemes needed to reveal and understand how large-amplitude motions are encoded in the vibration-rotation energy level structure of small, gas-phase, combustion-relevant polyatomic molecules. We are focusing our efforts on three areas: (i) a spectroscopic study of HNC  $\leftrightarrow$  HCN isomerization on the  $S_0$  potential energy surface, starting from the HNC side of the barrier and exploiting millimeter-wave spectroscopy and the Stark effect to identify barrier-proximal states; (ii) a spectroscopic study of acetylene  $\leftrightarrow$  vinylidene isomerization on the  $S_0$  potential energy surface, exploiting the Stark effect and identical atom permutation doublings as markers of barrier-proximal states; and (iii) the use of millimeter-wave pure rotational spectroscopy to measure absolute species- and vibrational level-populations of combustion-relevant molecules formed in nonequilibrium sources, such as a discharge jets, pyrolysis jets, and photolysis jets.

## Recent Progress

### *HNC $\leftrightarrow$ HCN Isomerization*

The  $S_0$  HNC-HCN potential energy surface is a prototype for high-barrier, bond-breaking isomerization. One of the primary goals of this research program is to observe and identify barrier-proximal states, i.e. the states that are energetically located near the isomerization barrier and have amplitude localized along the minimum energy isomerization path (MEIP). The large amplitude motion embodied in the barrier-proximal states provides the basis for their detectability. When a large amplitude motion alters the molecular geometry, the electronic structure of the molecule inevitably changes as well. Thus, electronic properties, such as the Stark effect, can serve as universal markers to distinguish the rare barrier proximal states from the vastly more numerous states in which excitation is divided among many modes. In the HNC $\leftrightarrow$ HCN system, the magnitude of the dipole moment is a sensitive diagnostic because the barrier-proximal states have significantly reduced dipole moments ( $\sim 1$  D) due to cancellation from the two oppositely signed dipole moments in the HCN ( $\sim +3$  D) and HNC ( $\sim -3$  D) configurations.

Hyperfine structure, which arises from the interaction of the nuclear quadrupole moment of the nitrogen nucleus with the gradient of the field due to the electronic wavefunction, is another nuclear dynamics-sensitive electronic property. For HCN in the ground vibrational state, the quadrupole coupling constant is large and negative,  $(eQq)_N = -4.7$  MHz, whereas for HNC in the ground vibrational state, it is small and positive  $(eQq)_N = 0.26$  MHz. Recent electronic structure calculations in our group have demonstrated that the quadrupole coupling constant is strongly dependent on the bond angle and therefore on the extent of bend excitation. As a consequence, measurements of the quadrupole-coupling constant, in addition to the dipole moment, could be used as a sensitive probe for the onset of isomerization. Hyperfine splitting measurements, however, have the additional benefit of being able to determine in which potential well the vibrational wavefunction is localized.

In the  $J=1-0$  rotational transition of HCN or HNC, hyperfine splitting gives rise to a triplet of lines. In HCN, this structure is clearly resolved under normal Doppler broadened conditions. In HNC, however, the hyperfine structure is unresolved and appears as a single line. We have recently improved the resolution of our mm-wave jet spectrometer by propagating the mm-wave radiation coaxially with the molecular beam (see Figure 1). This geometry substantially reduces Doppler and transit-time broadening, allowing all members of the HNC hyperfine triplet to be resolved (see Figure 2). We believe these measurements to be the first laboratory

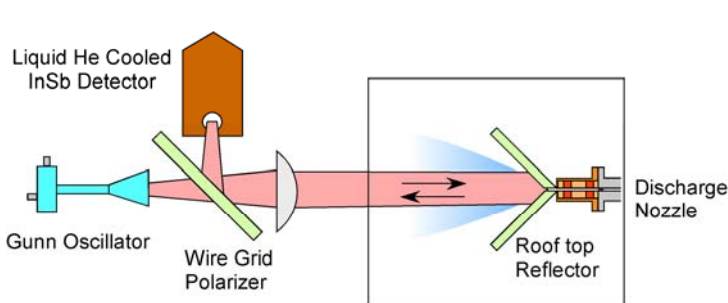


**Figure 1.** Experimental schematic of coaxial mm-wave discharge jet spectrometer. The coaxial geometry leads to a Doppler splitting (see Figure 2) of the lines caused by the mm-wave radiation counter propagating and co-propagating with the molecular beam.

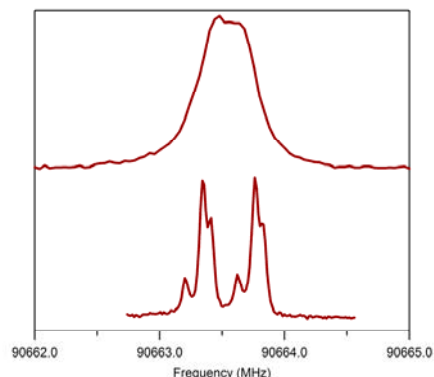


**Figure 2.** HNC ( $J=1-0$ ) rotational transition. *Upper trace:* Doppler broadened; *Lower trace:* observed in coaxial geometry.

measurements of the hyperfine splitting in HNC. Moreover, the increased resolution of our spectrometer gives us additional sensitivity to the onset of isomerization.

### *Acetylene* $\leftrightarrow$ *Vinylidene* Isomerization

As in the HNC $\leftrightarrow$ HCN system, the goal of our studies on the acetylene  $\leftrightarrow$  vinylidene system is to observe barrier-proximal states. Large-amplitude motion on the acetylene  $S_0$  surface, however, is considerably more complicated than in HCN, due both to the increased number of vibrational modes and to the inversion symmetry of the molecule. This symmetry results in normal modes of vibration that are either symmetric (g) or antisymmetric (u) with respect to inversion through the center of the molecule. Many studies have demonstrated that the vibrational eigenstates of acetylene and similar molecules undergo a normal-to-local transition in which the normal modes appropriate to describe small deviations from the equilibrium geometry evolve into local modes in which the excitation is isolated in a single C-H bond. The evolution of vibrational character is of particular interest in the acetylene bending system because the local bending vibration bears a strong resemblance to the reaction coordinate for isomerization from acetylene to vinylidene (see Figure 3) with one hydrogen migrating a large distance off the C-C bond axis, while the other hydrogen remains relatively stationary.

Despite the large number of studies of the vibrational overtone spectrum of acetylene, very little information is available regarding the effect of an electric field on the vibrational levels of the  $S_0$  state of this molecule. This lack of information is perhaps not surprising considering the symmetric nature of the acetylene molecule. Not only does the definite g/u symmetry of every rovibrational level dictate that there can be no permanent dipole moment in any eigenstate, but the inversion symmetry of the molecule further restricts the action of the dipole operator to off-diagonal in the vibrational quantum numbers. That is, there is no electric dipole moment in acetylene that can lead to a pure rotational transition.

The large amplitude motion associated with the local stretching and bending vibrations, however, lead to changes in the electronic properties of acetylene, which result in a transition dipole between rotational levels of the two nearly degenerate g/u vibrational eigenstates. This g/u degeneracy is a signature of local mode behavior. This transition dipole moment gives rise to a Stark effect and the ability to observe pure rotational transitions in acetylene. We have recently utilized a one-dimensional reaction path-like Hamiltonian to put predictions of these dipole moments on a quantitative basis. Calculations performed at the CCSD(T) level of theory with a cc-pVQZ basis predict an approximately linear dependence of the dipole moment on the number of quanta in either the local stretching or local bending excitation. In the local mode limit, one quantum of stretching excitation leads to an increase of 0.039 D in the a-axis dipole moment and one quantum of bending vibration leads to an increase of 0.068 D (see Figure 4). The use of a one-dimensional model for the local bend is justified by comparison to the well-established polyad model that reveals a decoupling of the large amplitude bending from other degrees of freedom in the range of  $N_{\text{bend}} = 14 - 22$ . We find that the same one-dimensional large amplitude bending motion emerges from these two profoundly different representations, the full *ab initio* derived seven-dimensional Hamiltonian and the three-dimensional ( $\ell = 0$ ) pure-bending experimentally parameterized spectroscopic Hamiltonian.

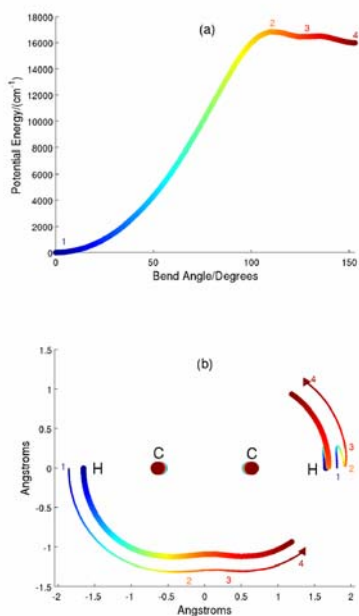


**Figure 3.** (a) One-dimensional potential for the acetylene-vinylidene isomerization as a function of the HCC valence bend angle. A transition state structure is labeled by the number 2, and local minima are denoted by numbers 3 and 4. (b) Depicts the spatial positions of the acetylene coordinates color-coded to match their corresponding location on the one-dimensional potential.

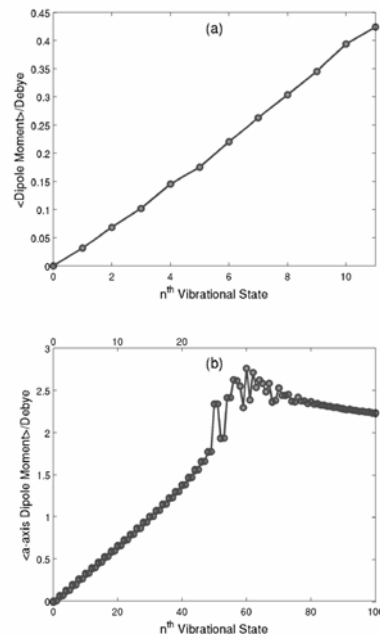


**Figure 4.** Vibrationally averaged *ab initio* dipole moments computed (a) for a local C-H stretch and (b) for a local bend. The bottom axis of (b) is numbered according to the vibrational level in the fully permutational symmetric isomerization path, and the top axis labels only the symmetric vibrational levels. Both averaged dipole moments are reported relative to the lowest vibrational quantum state.

### *Mm-wave Rotational Spectroscopy*

Many probes of photodissociation dynamics, such as laser induced fluorescence (LIF), resonance enhanced multiphoton ionization (REMPI), or time-resolved Fourier transform infrared absorption (TR-FTIR), suffer from spectral congestion and an enormous spectroscopic burden to convert observable transition strengths into populations. Pure rotational spectroscopy, however, does not suffer from these problems because the high resolution and the dependence of the rotational constant on vibrational level ( $\sim 1\%$  change per vibrational quantum) assure that rotational lines of different vibrational levels are well resolved. Moreover, population measurements are simplified because the permanent electric dipole moment can be accurately calculated or measured for each species or vibrational state. Despite the quantitative, species-selective, and nearly universal properties of rotational spectroscopy, it is seldom used as a probe of photodissociation dynamics.

We are currently using mm-wave spectroscopy to investigate the branching ratio of the HCN and HNC products from acrylonitrile photolysis at 193 nm (see Figure 5). Although we have demonstrated that millimeter-wave spectroscopy is capable of measuring vibrational distributions and branching ratios of photolytic products, one of the shortcomings of the technique is the mm-wave signal dependence on temperature. Because mm-wave signals are proportional to the population difference between rotational levels rather than the population of the initial state, mm-wave signals are proportional to  $1/T^2$ . Thus, to achieve maximum sensitivity, the rotational temperature of the photoproducts must be reduced by supersonic-jet cooling. In theory, rotational cooling can be achieved in a molecular beam without significantly altering the vibrational temperature by photolyzing in the higher density region of the expansion and detecting in the lower density region after rotational cooling has taken place. Our results, however, indicate that additional processes, such as collisionally enhanced multiphoton excitation (see Figure 6), are enhanced by photolyzing in the higher density region.

### **Future Plans**

Our future plans involve the continued monitoring of the changes in electronic properties caused by large amplitude vibrational motion. We are in the process of measuring the hyperfine structure of HNC in the lowest vibrational levels. Ultimately, we plan to measure the hyperfine structure in highly excited bending levels that are

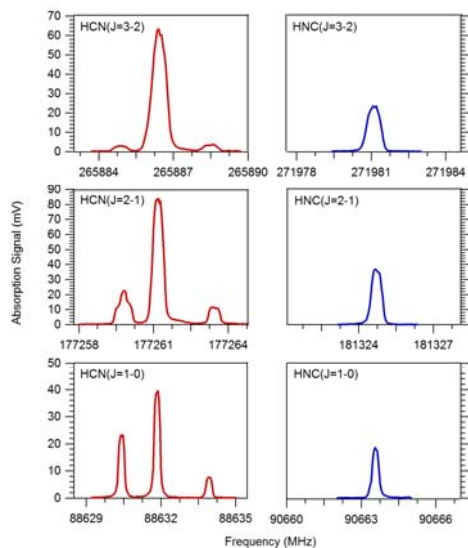


**Figure 5.** Pure rotational spectra of HCN and HNC products from photolysis of acrylonitrile at 193 nm. The measured branching ratio between the two products is approximately 3 and is independent of rotational transition.

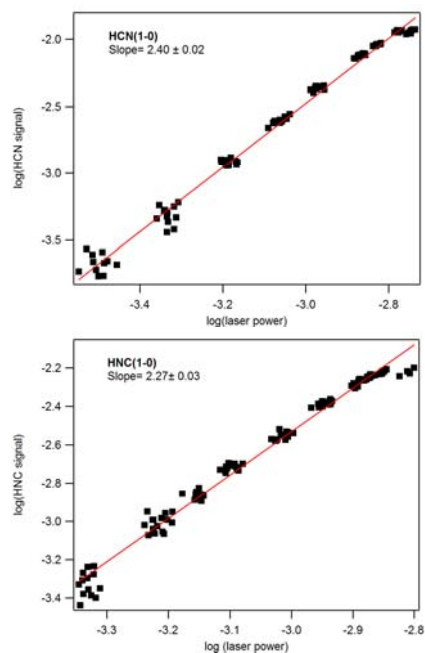


**Figure 6.** Photolysis laser power law study on the HCN and HNC products, indicating that the products are from a multiphoton process.

prepared by stimulated emission pumping (SEP). Before we can accomplish this goal, however, we must locate and characterize the first excited electronic state of HNC, which has not been observed. The lack of experimental information about the HNC  $S_1$  state stems from several reasons: 1) HNC is not stable and must be continuously generated in a suitable source, 2) the theoretical FC factors between the vibrationless level of the ground electronic state and the lowest lying vibrational levels of the  $S_1$  state are extremely small due to the large increase in CN bond length in the  $S_1$  state relative to the  $S_0$  state, and 3) the  $S_1$  vibrational levels with useful FC factors ( $>10^{-3}$ ), by analogy to HCN, are expected to be rapidly predissociated. We have already characterized several sources of HNC and plan to circumvent the predissociation problem by observing  $S_1$ - $S_0$  transitions with a photofragment fluorescence excitation (PHOFEX) scheme, in which the fluorescence of the CN photofragments is monitored.

The acetylene  $\leftrightarrow$  vinylidene system also requires considerable spectroscopic investigations of the  $S_1$  surface before barrier-proximal eigenstates on the  $S_0$  potential energy surface can be observed. Specifically, a comprehensive understanding of the anharmonic and Coriolis couplings on the  $S_1$  surface is necessary to locate special eigenstates that have the unique characteristic of being able to serve as “local-bender plucks” of the extreme local-bender (ELB) states on the  $S_0$  surface. Once these eigenstates on the  $S_1$  surface are found, the Stark effect will be used to identify the extreme local-bend excited barrier-proximal states among the many SEP-populated vibrational levels of the electronic ground state.

### Recent DOE-supported Publications (since 2004)

1. A. H. Steeves, H. A. Bechtel, S. L. Coy, and R. W. Field, “Millimeter wave polarization detected millimeter wave optical double resonance spectroscopy of CS,” *J. Chem. Phys.* **123**, 141102 (2005).
2. Z. Duan, N. Yamakita, S. Tsuchiya, and R. W. Field, “Differential Temperature Laser Induced Fluorescence Spectroscopy,” *Chem. Phys.*, accepted.
3. B. M. Wong, A. H. Steeves, and Robert W. Field, “Electronic Signatures of Large Amplitude Motions: Dipole Moments of Vibrationally Excited Local-Bend and Local-Stretch States of  $S_0$  Acetylene,” *J. Phys. Chem. A*, submitted.

## Scanning Tunneling Microscopy Studies of Chemical Reactions on Surfaces

George Flynn, Department of Chemistry, Columbia University  
Mail Stop 3109, 3000 Broadway, New York, New York 10027  
flynn@chem.columbia.edu

### Introduction and Overview

Our Department of Energy sponsored work is now focused on fundamental chemical events taking place on graphite, modified graphite, and metal surfaces with the intent of shedding light on the role of these surfaces in mediating the formation of polycyclic aromatic hydrocarbons (PAHs) and the growth of soot particles.<sup>1-11</sup> Interest in soot is ultimately driven by the environmental and health implications arising from its formation in combustion reactions (particularly those involving heavier, diesel fuels), which are nearly ubiquitous throughout our society.<sup>1</sup> Of the four phases of soot formation,<sup>3,4</sup> the work being pursued here is focused on surface reactions that lead to growth and oxidation of these particles.

Our experimental system employs Scanning Tunneling Microscopy and other surface science techniques to study reactions on a well-defined graphite, modified graphite, or metal surface (rather than the more complex soot particle) interacting with vapor phase or adsorbed molecules. This experimental method provides a powerful tool with which to follow the behavior of reaction processes on surfaces and complements gas phase spectroscopic studies of PAH formation.<sup>1-11</sup> Scanning Tunneling Microscopy can be used to identify surface defects and step edges, as well as to resolve and probe individual molecules on surfaces. The convenience and importance of being able to probe single molecules and/or single sites on surfaces probably cannot be overemphasized. Graphite itself is largely inert and reactive events are likely to occur when individual molecules are at or near dangling surface bonds typically found only at defect sites or step edges.

The long range experimental program that we are pursuing<sup>12-16</sup> can be divided into two parts. First, we deposit small to medium sized molecules and simple PAH moieties on a relatively cool (25-400 K) graphite, modified graphite, or metal surface in an ultrahigh vacuum system, trigger reaction between different chemical species (using electrons from the STM tip, photons or thermal energy), and use STM and other surface techniques to probe both the pre-reaction and post-reaction species. Minimally, we expect such studies to provide fundamental information about the reactions of hydrocarbons on surfaces, the role of surface defects and step edges in mediating these reactions, and the effect of temperature on the chemical mechanisms of importance for such reactions. Second, by taking advantage of the high temperature capability of our UHV STM, we plan to pre-heat samples to high temperatures (800-1200 K), characterize the surface with STM, and impinge potential PAH/soot precursor molecules onto the sample. The surface will then be re-characterized with STM after growth of carbonaceous material is initiated in order to identify the species forming at the surface-vacuum interface.

### Results: Chemistry and Imaging of Hexabenzocoronene on Ruthenium

Hexabenzocoronene (HBC) is a moderate size PAH of the type that might be expected to be seen in the early stages of soot growth. The molecule, which consists of a coronene core surrounded by 6 benzene rings, is not planar because some of the outer H atoms on

the molecule interact sterically to push alternate benzene units above and below the plane of the basic central coronene structure.

On an electron-rich metal surface, molecules of this type are likely to react by losing their H atoms and forming a structure with alternating 5 and 6 membered rings around the outer edge. (This structure resembles the “end cap” of a carbon nanotube). Further reactions of this species, either with or mediated by the surface, might be expected to occur at higher temperatures. For example, if a surface such as ruthenium decorated with HBC is dosed with acetylene, growth of carbon nanotubes is possible. Aside from its intrinsic interest, the behavior of HBC on metals is related to soot chemistry since many soot particles, especially those formed from diesel fuel, are impregnated with heavy metal atoms, which are very likely to affect the rate and mechanism of soot growth.

In collaboration with our colleague Colin Nuckolls, whose group has provided the non-planar HBC molecules, we have deposited HBC on a clean Ru(0001) surface in a UHV vacuum chamber. The single-crystal Ru was cleaned by ion bombardment and heating to 1200 K. Its cleanliness and surface order were checked with AES and LEED, respectively. HBC was deposited onto the room temperature metal surface at sub-monolayer coverage using a vacuum evaporation oven and a quartz crystal microbalance. The HBC-decorated ruthenium was then imaged using our UHV Omicron V-T STM at room temperature. Following this treatment and study, the metal substrate with HBC on it was warmed to 900 K, returned to room temperature and imaged again.

A height profile taken along a line across a molecular feature in the STM topograph shows that the overall size of the HBC image (a bright spot plus a “fuzzy” cloud) is about 15 Å, consistent with the known dimensions of the HBC molecule. A bright region approximately 6 Å wide, located off center on one side of the molecular image is likely the signature of covalent bonding between Ru and the HBC adduct. The asymmetry of the tunneling image suggests that the HBC is only attached to the surface along one side or one edge of the molecule. Repeated scans of the surface do not reveal any obvious mobility of the HBC adduct for surface temperatures near 300 K suggesting reasonably tight adsorbate-surface bonding. Heating the adsorbate decorated Ru surface to 900 K induces easily observed changes in the STM images. The bright spots in the molecular images (apparent topographical elevations) become symmetrically centered in the fuzzy background that is the HBC adduct, and topographical features appear that are clearly characteristic of dimer and trimer formation. The symmetrical images observed after heating the surface are consistent with a model structure in which the HBC is symmetrically bonded to the Ru surface at the edges. These preliminary results suggest that the HBC adducts are mobile at temperatures above 300 K and form an intermediate capable of further chemistry leading to clusters. Future experiments on the HBC-Ru system will be aimed at the identification of the species formed, using Scanning Tunneling Spectroscopy,<sup>17-20</sup> and the addition of acetylene to determine if soot particle growth can be achieved and detected for single sites. Many of the proposed mechanisms for soot growth consist of successive additions of acetylene (a suspected surface growth precursor) to a radical followed by cyclization.<sup>1</sup> The temperature dependence of these

growth processes will likely provide a convenient parameter with which to control the surface chemistry mechanism.

### **Present and Future Experimental Program**

These STM images have provided preliminary evidence for chemical reactions of a polycyclic aromatic hydrocarbon, hexabenzocoronene, on a ruthenium surface. Future work will focus on further development of techniques to identify molecules on a surface using STM methods; investigations of the chemistry and growth of PAHs on metal surfaces; the chemistry of PAHs and their precursors on graphite surfaces with defects induced by plasma etching; chemistry on metal atom impregnated graphite; and the physical and chemical behavior of PAHs on graphene sheets (single layers of graphite) as well as the electronic structure of graphene sheets themselves.

### **References**

1. J. A. Miller and G. A. Fisk, "Combustion Chemistry", *Chem. & Eng. News*, **65** (35), 22-46, August 31, 1987
2. C. S. McEnally, A. G. Robinson, L. D. Pfefferle and T. S. Zwier, "Aromatic Hydrocarbon Formation in Nonpremixed Flames Doped with Diacetylene, Vinylacetylene, and Other Hydrocarbons: Evidence for Pathways Involving C<sub>4</sub> Species", *Combustion and Flame* **123**, 344-357 (2000)
3. M. Frenklach, "Reaction mechanism of soot formation in flames", *Phys. Chem. Chem. Phys.* **4**, 2028-2037 (2002)
4. M. Frenklach and H. Wang, "Detailed modeling of soot particle nucleation and growth", *Proc. Combust. Inst.* **23**, 1559-1566 (1991)
5. H. Richter and J. B. Howard, "Formation of Polycyclic Aromatic Hydrocarbons and their Growth to Soot – A Review of Chemical Reaction Pathways", *Prog. Energy and Combust. Sci.* **26**, 565-608 (2000)
6. C. F. Melius, M. E. Colvin, N. M. Marinov, W. J. Pitz and S. M. Senkan, "Reaction mechanisms in aromatic hydrocarbon formation involving the C<sub>5</sub>H<sub>5</sub> cyclopentadienyl moiety", *Proc. Combust. Inst.* **26**, 685-692 (1996)
7. P. R. Westmoreland, A. M. Dean, J. B. Howard and J. P. Longwell, "Forming benzene in flames by chemically activated isomerization", *J. Phys. Chem.* **93**, 8171-8180 (1989)
8. M. Frenklach, N. W. Moriarty and N. J. Brown, "Hydrogen migration in polyaromatic growth", *Proc. Combust. Inst.* **27**, 1655-1661 (1998)
9. M. Frenklach, "On surface growth mechanism of soot particles", *Proc. Combust. Inst.* **26**, 2285-2293 (1996)
10. C. A. Arrington, C. Ramos, A. D. Robinson and T. S. Zwier, "Aromatic ring-forming reactions of metastable diacetylene with 1, 3-butadiene", *J. Phys. Chem. A* **102**, 3315-3322 (1998)
11. N. M. Marinov, W. J. Pitz, C. K. Westbrook, M. J. Castaldi and S. M. Senkan, "Modeling of aromatic and polycyclic aromatic hydrocarbon formation in premixed methane and ethane flames", *Combust. Sci. Technol.* **116**, 211-287 (1996)
12. Gina M. Florio, Tova L. Werblowsky, Thomas Mueller, Bruce J. Berne, and George W. Flynn, "The Self-Assembly of Small Polycyclic Aromatic

- Hydrocarbons on Graphite: A Combined STM and Theoretical Approach”, J. Phys. Chem. B, 109, 4520-4532 (2005)
13. Markus Lackinger, Thomas Müller, T.G. Gopakumar, Falk Müller, Michael Hietschold and George W. Flynn, “Tunneling Voltage Polarity Dependent Submolecular Contrast of Naphthalocyanine on Graphite – a STM Study of Close Packed Monolayers under Ultrahigh-Vacuum Conditions”, J. Phys. Chem. 108, 2279-2284 (2004)
  14. Kwang Taeg Rim, Jeffrey P. Fitts, Thomas Müller, Kaveh Adib, Nicholas Camillone, III, Richard M. Osgood, S. A. Joyce, and George W. Flynn, “CCl<sub>4</sub> Chemistry on the Reduced Selvege of a  $\alpha$ -Fe<sub>2</sub>O<sub>3</sub>(0001) Surface: A Scanning Tunneling Microscopy Study”, Surf. Sci. 541, 59-75, (2003).
  15. K. Rim, M. Myers, L. Liu, C. Su, M. Steigerwald, M. S. Hybertsen, C. Nuckolls, and G. W. Flynn, “Scanning Tunneling Microscopy Probe of the Polycyclic Aromatic Hydrocarbon Hexabenzocoronene on a Ruthenium Surface: Evidence for Catalytic Formation of Carbon Nanotube End Caps”, in preparation.
  16. Leanna C. Giancarlo and George W. Flynn, “Scanning Tunneling and Atomic Force Microscopy Probes of Self-Assembled, Physisorbed Monolayers: Peeking at the Peaks”, Annu. Rev. Phys. Chem., 49, 297-336 (1998)
  17. K.W. Hips, D.E. Barlow, U. Mazur, J. Phys. Chem. B 104, 2444-2447 (2000)
  18. J. Gaudioso, H. J. Lee and W. Ho, “Vibrational Analysis of Single Molecule Chemistry: Ethylene Dehydrogenation on Ni(110)”, J. Am. Chem. Soc., 121, 8479-8485 (1999).
  19. B. C. Stipe, M. A. Rezaei, and W. Ho, “Single-molecule Vibrational Spectroscopy and Microscopy”, Science, 280, 1732-1735 (1998). on NiAl(110)”. J. Chem. Phys. 119, 2296-2300 (2003).
  20. W. Ho, “Single Molecule Chemistry”, J. Chem. Phys. 117, 11033-11061(2002)

#### **DOE Publications: (2003-2006)**

1. Natalie Seiser, Kavita Kannappan, George Flynn, “Long Range Collisional Energy Transfer from Highly Vibrationally Excited Pyrazine to CO Bath Molecules: Excitation of the  $\nu=1$  CO Vibrational Level”, J. Phys. Chem., 107, 8191-97, (2003)
2. Markus Lackinger, Thomas Müller, T.G. Gopakumar, Falk Müller, Michael Hietschold and George W. Flynn, “Tunneling Voltage Polarity Dependent Submolecular Contrast of Naphthalocyanine on Graphite – a STM Study of Close Packed Monolayers under Ultrahigh-Vacuum Conditions”, J. Phys. Chem. 108, 2279-2284 (2004)
3. Gina M. Florio, Tova L. Werblowsky, Thomas Mueller, Bruce J. Berne, and George W. Flynn, “The Self-Assembly of Small Polycyclic Aromatic Hydrocarbons on Graphite: A Combined STM and Theoretical Approach”, J. Phys. Chem. B, 109, 4520-4532 (2005)
4. K. Rim, M. Myers, L. Liu, C. Su, M. Steigerwald, M. S. Hybertsen, C. Nuckolls, and G. W. Flynn, “Scanning Tunneling Microscopy Probe of the Polycyclic Aromatic Hydrocarbon Hexabenzocoronene on a Ruthenium Surface: Evidence for Catalytic Formation of Carbon Nanotube End Caps” in preparation.

# Quantitative Imaging Diagnostics for Reacting Flows

**Jonathan H. Frank**

Combustion Research Facility  
Sandia National Laboratories  
P.O. Box 969, MS 9051  
Livermore, CA 94551-0969  
email: jhfrank@ca.sandia.gov

## Program Scope

The primary objective of this project is the development and application of laser-based imaging diagnostics for studying the interactions of fluid dynamics and chemical reactions in reacting flows. Imaging diagnostics provide temporally and spatially resolved measurements of species, temperature, and velocity distributions over a wide range of length scales. Multi-dimensional measurements are necessary to determine spatial correlations, scalar and velocity gradients, flame orientation, curvature, and connectivity. Current efforts in the Advanced Imaging Laboratory focus on planar laser-induced fluorescence (PLIF) and Rayleigh scattering techniques for probing the detailed structure of both isolated flow-flame interactions and turbulent flames. The investigation of flow-flame interactions is of fundamental importance in understanding the coupling between transport and chemistry in turbulent flames. These studies require the development of new imaging diagnostic techniques to measure key species in the hydrocarbon-chemistry mechanism as well as to image rates of reaction and dissipation.

## Recent Progress

Recent research has continued to emphasize imaging diagnostics for probing the detailed structure of reaction zones during flow-flame interactions. Research activities have included: i) Highly spatially resolved dissipation imaging in the near field of turbulent jet flames where traditional scaling laws from self-similar nonreacting flows may not apply, ii) Studies of edge-flame dynamics in transient flows.

### *Two-Dimensional Dissipation Measurements in Turbulent Flames*

In turbulent flows, the scalar dissipation rate is a fundamental quantity governing the rate of molecular mixing and is prominent in theoretical analysis, models, and numerical simulations of turbulent flames. The scalar dissipation rate,  $\chi = 2D(\nabla\xi \cdot \nabla\xi)$ , where  $D$  is the mass diffusivity and  $\xi$  is the mixture fraction, is challenging to measure because it requires simultaneous multi-dimensional measurements of multiple scalars. Two-dimensional imaging provides simultaneous measurements of the radial and axial contributions to the dissipation rate,  $\chi = 2D((\partial\xi/\partial x)^2 + (\partial\xi/\partial r)^2)$ , and gives unique insight into the spatial structures of the dissipation field. In previous efforts, we developed a multi-scalar imaging technique for measuring mixture fraction in turbulent flames using a combination of LIF and Rayleigh scattering. The need to combine multiple diagnostic techniques places inherent limitations on the signal-to-noise ratio and the spatial resolution of the scalar dissipation measurements. Highly spatially resolved dissipation measurements are required because dissipation occurs at the smallest scales of turbulence. Noise reduction is critical to accurate dissipation measurements because noise in the scalar measurements artificially increases the measured dissipation rates.

Our recent experiments used high-resolution 2-D Rayleigh imaging to measure the thermal dissipation structures in turbulent jet flames. Rayleigh scattering is a relatively strong scattering process that provides thermal dissipation measurements with high spatial resolution and relatively large signal-to-noise ratios. Figure 1 shows an example of instantaneous measurements of temperature fluctuations,  $T'$ , and the square of the temperature-fluctuation gradient,  $|\nabla T'|^2$ , which is proportional to the thermal dissipation rate. The measurements were performed at two different radial locations in a turbulent nonpremixed jet flame with a  $\text{CH}_4/\text{H}_2/\text{N}_2$  fuel mixture and a jet-exit Reynolds number of 15,200. This jet flame is a target flame for an international collaboration between modelers and experimentalists via the TNF Workshop. The fuel mixture was chosen such that variations in the effective Rayleigh cross-section were limited to approximately  $\pm 3\%$  across the flame. Consequently, the temperature was determined directly from the inverse of the Rayleigh signal without the need to correct for variations in the local composition.

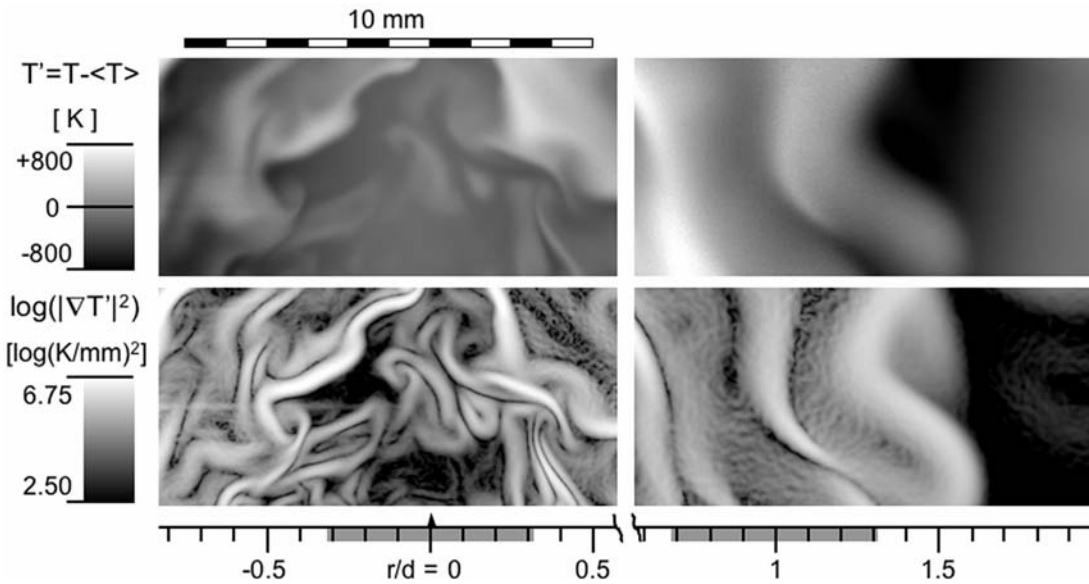


Fig. 1 Temperature fluctuations and the square of the temperature-fluctuation gradient, which provides a measure of the thermal dissipation. The images are centered at  $x/d = 10$  ( $d = 8$  mm) in a turbulent  $\text{CH}_4/\text{H}_2/\text{N}_2$  jet flame with jet-exit  $\text{Re}=15,200$  (DLR-A). The two sets of images show the dissipative scales near the jet axis ( $r/d=0$ ) and in the high-temperature region.

The significant effect of heat release on the dissipation length scales is evident from a comparison of the cold fuel mixing region near the jet axis ( $r/d=0$ ) and the region containing hot combustion products near  $r/d=1$ . The dissipation length scales were quantified by both spectral and spatial analyses. For the spectral analysis, we demonstrated an interlacing technique that significantly suppressed the noise and allowed three orders of magnitude to be resolved in the average power spectral density (see Fig. 2). The dynamic range of the power spectrum without interlacing was limited to approximately a factor of 50. The interlacing approach exploits the spatial redundancy of the data, assuming that the relevant scales are over-resolved. We have shown that similar noise cancellation can be achieved using two cameras with identical imaging optics to record the Rayleigh scattering on opposite sides of the flame. The improved dynamic range is a significant advancement that provides fully resolved spectra from dissipation images.

The analysis of dissipation structures in the spatial domain was performed by determining PDFs of the dissipation layer thickness,  $\lambda_d$  (full width at 20% of the local peak dissipation). The Rayleigh imaging system was capable of measuring  $\lambda_d$  with less than a 10% relative error for dissipation structures wider than  $62 \mu\text{m}$ . Figure 3 illustrates the progression of dissipation layer thickness PDFs as a function of temperature. These conditional PDFs illustrate the temperature-dependent scaling behavior, which is required for determining the relevant length scales within a turbulent flame. Theoretical analysis of 1-D dissipation spectra suggest that the majority of the mean dissipation occurs above a cutoff spatial frequency that is defined at the 2% power level. Our results are consistent with this analysis. However, the PDFs of  $\lambda_d$  indicate that the spatial resolution required for measuring the detailed structure of the dissipation field and resolving the narrowest dissipation layers is significantly finer than the Nyquist criterion for measuring the cutoff frequency. These dissipation studies are being conducted in collaboration with Sebastian Kaiser (Sandia postdoc), and comparisons with the line-imaging measurements of Rob Barlow and Guanghua Wang (Sandia) are ongoing.

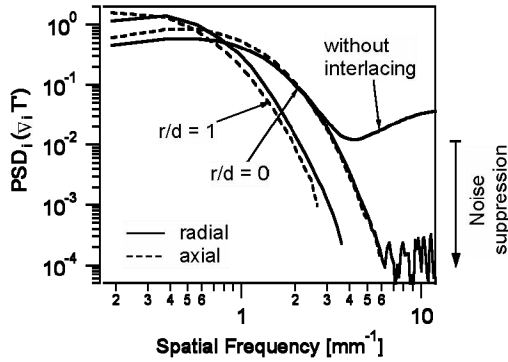


Fig. 2. Radial and axial power spectra of the temperature-fluctuation gradient using interlacing to suppress noise. Radial spectrum at  $r/d=0$  is calculated with and without interlacing.

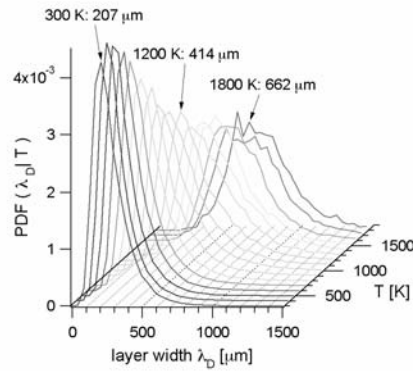


Fig. 3. Progression of PDFs of dissipation layer thickness as a function of temperature.

### Edge-flame Dynamics

Edge-flame dynamics are important in diffusion flame stabilization and in extinction/ignition processes. We have made significant progress on a joint experimental/computational investigation of edge-flame behavior in transient flows. An edge flame was formed as counter-propagating toroidal vortices impinged on an axisymmetric counterflow diffusion flame. In the initial stages of the edge-flame formation, the extinction front receded away from the axis of symmetry at a negative propagation speed that was several times that of a freely propagating stoichiometric laminar flame. At later stages, the edge flame propagated into the cold mixing layer with a positive propagation speed, and eventually the original diffusion flame was reestablished. Figure 4 illustrates the detailed agreement between the numerical simulations and measurements. This research is a collaboration with Mitchell Smooke, Alessandro Gomez, and Giuliano Amantini (postdoc) at Yale University.

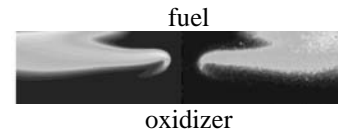


Fig. 4. Comparison of predicted (left) and measured (right) CO-LIF signals from a propagating edge flame in an axisymmetric counterflow burner.

## Future Plans

High-resolution 2-D thermal dissipation measurements will be applied to several TNF target flames and will be combined with measurements of reaction rates to better understand the relationship between dissipation structures and chemical reactions. Our experimental results will be coupled with large-eddy simulations (LES) by Joe Oefelein (Sandia) to determine the necessary resolution for simulating turbulent nonpremixed flames. An uncertainty quantification analysis of the dissipation measurements and the development of adaptive smoothing algorithms will be pursued in collaboration with Habib Najm (Sandia) and Roger Ghanem (USC).

We have added a regeneratively amplified 100-ps pulsed Nd:YAG laser to the Advanced Imaging Laboratory and have begun constructing a tunable picosecond dye laser for PLIF imaging of atomic oxygen and atomic hydrogen. This effort builds upon our demonstration of interference-free imaging of two-photon O-atom LIF using a ps pulsed laser for excitation. As part of this ongoing study to quantify and minimize the effects of photolysis interference, we will measure the quantum yield for the photodissociation of thermally excited CO<sub>2</sub>. We will also investigate two-photon H-atom LIF excitation with ps lasers ( $\lambda_{\text{excitation}}=205 \text{ nm}$ ,  $3d^2D \leftarrow \leftarrow 1s^2S$ ) as a potential method for H-atom detection ( $\lambda_{\text{detection}}=656 \text{ nm}$   $3d^2D \rightarrow 2p^2P$ ) without photolytic interference. These studies will be conducted in collaboration with Tom Settersten (Sandia).

We are currently constructing a counterflow burner with a heated oxidizer flow to study the effects of unsteady flows on ignition kernels. We will investigate hydrogen and hydrocarbon ignition and study edge-flame propagation that occurs as the ignition kernel spreads. These experiments will be coupled with direct numerical simulations (DNS) by Jackie Chen (Sandia).

## DOE Supported Publications (2004–present)

J.H. Frank, X. Chen, B.D. Patterson, T.B. Settersten, “Comparison of Nanosecond and Picosecond Excitation for Two-Photon LIF Imaging of Atomic Oxygen in Flames,” *Appl. Opt.*, 43:2588 (2004).

J.H. Frank and T.B. Settersten, “Two-photon LIF Imaging of Atomic Oxygen in Flames with Picosecond Excitation,” *Proc. Combust. Inst.* 30:1527-1534 (2004).

C.M. Vagelopoulos and J.H. Frank, “An Experimental and Numerical Study on the Adequacy of CH as a Flame Marker in Premixed Methane Flames,” *Proc. Combust. Inst.* 30:241-249 (2004).

R. Seiser, J.H. Frank, S. Liu, J.H. Chen, R.J. Sigurdsson, K. Seshadri, “Ignition of Hydrogen in Unsteady Nonpremixed Flows,” *Proc. Combust. Inst.* 30:423-430 (2004).

G. Amantini, J.H. Frank, A. Gomez, “Experiments on Standing and Traveling Edge Flames around Flame Holes in Both Ignition and Extinction Modes,” *Proc. Combust. Inst.* 30:313-321 (2004).

S. A. Kaiser, J. H. Frank, M. B. Long, “Use of Rayleigh Imaging and Ray Tracing to Correct for Beam-Steering Effects in Turbulent Flames,” *Appl. Opt.*, 44:6557-6564 (2005).

R. S. Barlow, J. H. Frank, A. N. Karpetis, J.-Y. Chen, “Piloted Methane/Air Jet Flames: Transport Effects and Aspects of Scalar Structure,” *Combust. Flame* 143:433-449 (2005).

J. H. Frank, S. A. Kaiser, M. B. Long, “Multiscalar Imaging in Partially Premixed Jet Flames with Argon Dilution,” *Combust. Flame*, 143:507-523 (2005).

S. A. Kaiser and J. H. Frank, “Imaging of Dissipative Structures in the Near Field of a Turbulent Non-premixed Jet Flame,” *Proc. Combust. Inst.* 31 (Accepted).

## MECHANISM AND DETAILED MODELING OF SOOT FORMATION

Principal Investigator: Michael Frenklach

Department of Mechanical Engineering

The University of California

Berkeley, CA 94720-1740

Phone: (510) 643-1676; E-mail: myf@me.berkeley.edu

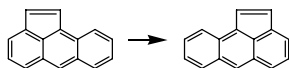
**Project Scope:** Soot formation is one of the key environmental problems associated with operation of practical combustion devices. Mechanistic understanding of the phenomenon has advanced significantly in recent years, shifting the focus of discussion from conceptual possibilities to specifics of reaction kinetics. However, along with the success of initial models comes the realization of their shortcomings. This project focuses on fundamental aspects of physical and chemical phenomena critical to the development of predictive models of soot formation in the combustion of hydrocarbon fuels, as well as on computational techniques for the development of predictive reaction models and their economical application to CFD simulations. The work includes theoretical and numerical studies of gas-phase chemistry of gaseous soot particle precursors, soot particle surface processes, particle aggregation into fractal objects, and development of economical numerical approaches to reaction kinetics.

### Recent Progress:

*Graphene Layer Growth: Collision of Migrating Five-Membered Rings* (with R. Whitesides, A. C. Kollias, D. Domin, W. A. Lester, Jr)

There are a variety of carbonaceous materials whose growth is envisioned through the extension of aromatic edges; familiar examples may include pyrolytic graphite, carbon black, combustion soot, interstellar “dust”, fullerenes, and nanotubes. In combustion, it is estimated that nearly 80% of soot mass comes from surface growth. Recent modeling and interpretation of soot surface growth has been done mostly by assumption of chemical similarity to reactions of gaseous aromatic species and, specifically, by invoking the HACA mechanism. This surface growth model is a repetitive reaction sequence of edge surface activation by gaseous hydrogen followed by addition of a gaseous hydrocarbon precursor (acetylene) to the surface radical site formed.

The initial surface HACA model was based on the armchair edges of aromatics, yet our recent work, under the present project, has explored growth on zigzag edges, which can be formed by the filling of armchair edge boat sites. A gaseous acetylene molecule can adsorb onto an H-activated zigzag edge (i.e., add to a surface radical formed by H abstraction) and then react to form a five-membered, cyclopenta edge ring. Theoretical investigation of zigzag edge reactions identified the possibility of migration of cyclopenta rings along the zigzag edge



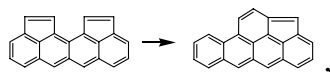
The overall step consists of a series of unimolecular transformations of the chemisorbed  $C_2H_2$  surface moiety mediated by hydrogen atoms.

During the past couple of years, under the present program, we undertook a detailed analysis of the migration reaction: energetics were examined at several levels of quantum-chemical theory (DFT, MP2, and PM3), the elementary reaction rates of the migration process were

obtained by solving energy transfer master equations (with the MultiWell code), and graphene edge growth rates and evolving surface morphologies were obtained in sterically-resolved kinetic Monte Carlo (KMC) simulations by augmenting the migration kinetics with estimated rates for eight additional surface steps describing adsorption, desorption, and transformation of the cyclopenta rings.

The reaction rates showed values sufficiently high to compete with, and even dominate, other surface reactions. The kinetics results indicated that the rate-limiting step of the migration sequence is the  $\beta$ -scission of the five-member ring after the addition of H atom, with the rest of the steps reaching partial equilibrium at higher temperatures. The KMC results provided further support to the critical role of the five-member ring migration in the growth of graphene layers. Also, the molecular structures produced in the KMC simulations are consistent with recent spectroscopic observations of PAH species in interstellar clouds.

One of the consequences of rapid surface migration is that two migrating cyclopenta rings could react with one another to form a relatively stable surface species such as



possibly leading to graphene layer curvature. The latter phenomenon has mechanistic implications for the evolution of soot particle surface morphology, which has been receiving increasing attention, as well as to growth of fullerene materials and carbon nanotubes.

During the last year, we investigated this possibility, namely, the existence of an elementary-reaction pathway of combination of “colliding” cyclopenta rings on an aromatic zigzag edge. The process is initiated by H addition to a five-membered ring, followed by opening of that ring and the formation of a six-membered ring adjacent to another five-membered ring. The elementary steps of the migration pathway were analyzed using density functional theory, B3LYP/6-311G(d,p), to examine the region of the potential energy surface associated with the pathway (Fig. 1). The calculations were performed on a substrate modeled by the zigzag edge of tetracene. Based on the obtained energetics, the dynamics of the system were analyzed by solving the energy transfer master equations.

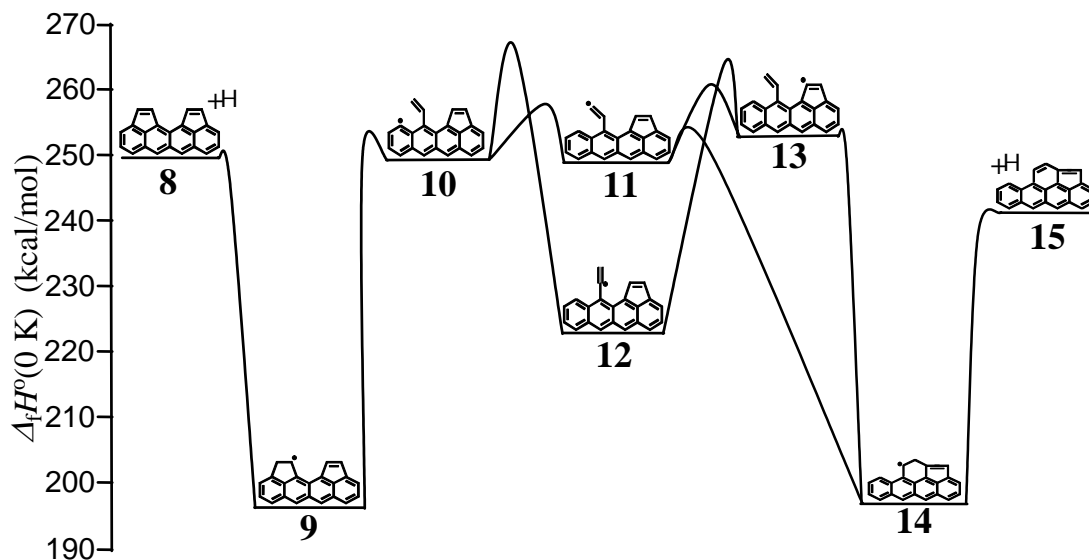


Figure 1. Potential energy diagram of the cyclopenta combination reaction pathway.

The results identified two new mechanistic features of aromatic-edge growth: (1) combination of (migrating) cyclopenta rings forms a relatively thermodynamically stable species that can serve as a middle-edge nucleating site, and (2) desorption of migrating cyclopenta rings is intrinsically coupled to the migration reaction pathway. Both of these new processes are comparable in rate to cyclopenta migration, which calls for establishing these mechanisms in fuller detail. The latter knowledge will bring us closer to detailed kinetic Monte Carlo simulations of graphene edge buildup, the rate of appearance of surface defects, and the amount of surface curvature.

## Future Plans

*Developing Models for Representing Combustion Chemistry at Varying Levels of Complexity to Use with Models for Laminar and Turbulent Flow Fields to Describe Combustion Processes:* The collaboration with the Sandia group of Habib Najm will continue on the combination of the CSP-slow-manifold projection method and PRISM to construct an adaptive reduced-order model for stiff dynamical systems.

*Pre-nucleation Chemistry:* The collaboration with William Lester's group will continue on quantum ab initio, DFT, and Quantum Monte Carlo (QMC) analysis of reactions that are critical to the development of kinetic models of aromatic growth. The QMC analysis for the C<sub>4</sub> and C<sub>5</sub> hydrocarbon species is in progress.

*Soot Particle Aggregation:* We will continue collaboration with Markus Kraft (Cambridge University) and Michael Balthasar (Volvo) on detailed Monte Carlo simulations of aggregate-aggregate collisions. Our present interest is in performing "benchmark calculations" for the testing and further development of the method of moments under extreme condition, as well as exploration of different regimes of particle aggregation.

*Soot Particle Surface Reactions:* Our goal is to gain fundamental understanding of evolution of soot particles, including their atomistic structures and surfaces. This discovered phenomenon of migration of five-membered ring along the zigzag edge alters significantly the framework for surface chemistry of graphene layer, and introduces a large number of possible elementary reaction steps that could take place on an evolving surface. One such example is the "collision" of migrating rings examined by us during the past funding period, and discussed above. During the next period we will examine equally important reaction steps: the "reverse" of the five-membered-ring collision that removes the five-six-membered-ring complex from the surface, "collision" of the migrating five-membered ring with the "stationary" six-membered ring, its reverse, combination of migrating and gaseous species, and so on. This work will be performed in collaboration with William Lester's group, performing DFT analysis of the reaction systems and then QMC analysis on most critical reaction steps identified in the prior DFT studies. For every reaction system, a complete set of rate coefficients will be established in master-equation solutions.

*Homogeneous Nucleation of Carbon Nanoparticles:* We will continue exploration of clustering of aromatic species through molecular dynamics simulations with on-the-fly quantum forces. The significance of our prior results, obtained under the previous funding period of this program, can be summarized as following: a) Aromatic molecules can, in principle, form dimers at temperatures as high as 1600 K, associated with soot particle inception in hydrocarbon combustion, and b) The mechanism explaining the phenomenon is the formation of internal rotors upon molecular collision that trap the excess energy. These conclusions lead to the following reasoning. If the formation of internal rotors is the critical factor in particle

nucleation, then collisions of molecular structures that form more of such rotors should be effective in forming dimers. Our objective for the next period is to perform a similar analysis for aromatic-aliphatic-linked hydrocarbons (AALH) compounds. As before, we will examine the pattern of energy transfer during binary collisions of such AALH structures. We will also examine binary collisions of AALH molecules and radicals with the peri-condensed-ring aromatics, such as benzene, phenyl, naphthalene, etc. After that, we will focus on formation and behavior of clusters larger than dimers. The work will be performed in collaboration with Nancy Brown.

### Publications (2004-2006)

1. "On the Role of Surface Migration in the Growth and Structure of Graphene Layers," M. Frenklach and J. Ping, *Carbon* **42**, 1209–1211 (2004).
2. "Towards a CSP and PRISM Tabulation Based Adaptive Chemistry Models," J. C. Lee, H. N. Najm, M. Frenklach, M. Valorani, and D. A. Goussis, Spring Technical Meeting of the Western States Section of the Combustion Institute, UC Davis, CA, March 29-30, 2004, Paper No. 04S-28.
3. "Monte-Carlo Simulations of Soot Particle Formation Including Aggregate-Aggregate Collisions," M. Balthasar, M. Kraft, and M. Frenklach, Poster No. 2F1-01, 30th International Symposium on Combustion, Chicago, IL, July 25-30, 2004.
4. "Detailed Kinetic Modeling of Soot Aggregate Formation in Laminar Premixed Flames," M. Balthasar and M. Frenklach, *Combust. Flame* **140**, 130–145 (2005).
5. "Migration Mechanism of Aromatic-edge Growth," M. Frenklach, C. A. Schuetz, and J. Ping, *Proc. Combust. Inst.* **30**, 1389–1396 (2005).
6. "Monte-Carlo Simulation of Soot Particle Coagulation and Aggregation: The Effect of a Realistic Size Distribution," M. Balthasar and M. Frenklach, *Proc. Combust. Inst.* **30**, 1467–1475 (2005).
7. "Kinetic Monte Carlo Simulations of Soot Particle Aggregation," M. Balthasar, M. Kraft, and M. Frenklach, *Prepr. Pap.-Am. Chem. Soc., Div. Fuel Chem.* **50**(1), 2005, pp. 135–136.
8. "On Chain Branching and Its Role in Homogeneous Ignition and Premixed Flame Propagation," J. C. Lee, H. N. Najm, S. Lefantzi, J. Ray, M. Frenklach, M. Valorani, and D. Goussis, in *Computational Fluid and Solid Mechanics 2005*, K. J. Bathe, Ed., Elsevier, New York, 2005, pp. 717–720.
9. "Quantum Monte Carlo Study of Heats of Formation and Bond Dissociation Energies of Small Hydrocarbons," A. C. Kollias, D. Domin, G. Hill, M. Frenklach, D. M. Golden, and W. A. Lester, Jr., *Int. J. Chem. Kinet.* **37**, 583–592 (2005).
10. "The Role of Explosive Modes in Homogeneous Ignition and Premixed Flames," J. C. Lee, H. N. Najm, S. Lefantzi, J. Ray, M. Frenklach, M. Valorani, and D. A. Goussis, Proceedings of the *20th International Colloquium on the Dynamics of Explosions and Reactive Systems*, Montreal, 2005.
11. "An Adaptive Reduced-Order Chemical Model," J. C. Lee, H. N. Najm, S. Lefantzi, J. Ray, M. Frenklach, M. Valorani, and D. A. Goussis, Proceedings of the *20th International Colloquium on the Dynamics of Explosions and Reactive Systems*, Montreal, 2005.
12. "Graphene Layer Growth: Collision of Migrating 5-Member Rings," R. Whitesides, A. C. Kollias, D. Domin, W. A. Lester, Jr., and M. Frenklach, Fall Meeting of the Western States Section of the Combustion Institute, Stanford, CA, October 17-18, 2005, paper 05F-62.
13. "Quantum Monte Carlo Study of Small Hydrocarbon Atomization Energies," A. C. Kollias, D. Domin, G. Hill, M. Frenklach, W. A. Lester, Jr., *Mol. Phys.* **104**, 467 (2006).
14. "Graphene Layer Growth: Collision of Migrating Five-Membered Rings," R. Whitesides, A. C. Kollias, D. Domin, W. A. Lester, Jr., and M. Frenklach, *Prepr. Pap.-Am. Chem. Soc., Div. Fuel Chem.* **51**, 174 (2006).
15. "A CSP and Tabulation Based Adaptive Chemistry Model," J. C. Lee, H. N. Najm, S. Lefantzi, J. Ray, M. Frenklach, M. Valorani, and D. A. Goussis, *Combust. Theory Model.*, submitted.
16. "Transforming Data into Knowledge—Process Informatics for Combustion Chemistry," M. Frenklach, *Proc. Combust. Inst.* **31**, Invited Topical Review.
17. "Graphene layer growth: Collision of migrating five-member rings," R. Whitesides, A. C. Kollias, D. Domin, W.A. Lester, Jr., and M. Frenklach, *Proc. Combust. Inst.* **31**, accepted.
18. "Numerical Simulations of Soot Aggregation in Premixed Laminar Flames," N. Morgan, M. Kraft, D. Wong, M. Frenklach, P. Mitchell, *Proc. Combust. Inst.* **31**, accepted.

# CHEMICAL DYNAMICS IN THE GAS PHASE: QUANTUM MECHANICS OF CHEMICAL REACTIONS

Stephen K. Gray

Chemistry Division  
Argonne National Laboratory  
Argonne, IL 60439

Email: [gray@tcg.anl.gov](mailto:gray@tcg.anl.gov)

## PROGRAM SCOPE

This program focuses on theoretical chemical reaction dynamics. It involves primarily the development and application of accurate quantum mechanical methods to study the spectroscopy and dynamics of experimentally relevant and combustion important gas phase systems. Rigorous time-dependent quantum methods (wave packets) and iterative time-independent quantum methods are often used. The results obtained allow one to gauge the quality of potential energy surfaces, and to infer the validity of more approximate theoretical methods such as quasiclassical trajectories and statistical theories. The results also can provide important mechanistic insights into the dynamics.

## RECENT PROGRESS

The  $\text{CH} + \text{H}_2 \rightarrow \text{CH}_2 + \text{H}$  reaction was studied theoretically using rigorous, six-dimensional quantum dynamics, quasiclassical trajectories (QCTs), and capture/phase space theory (C/PST) models [1]. This combustion-relevant system has been the focus of experimental attention, e.g., Refs. [2-5], and is dynamically interesting because of the presence of an intermediate potential well corresponding to excited methyl complexes. This work was carried out in collaboration with Goldfield, Gonzalez and coworkers. We employed a global potential function based on thousands of high-level ab initio points determined by Harding. This surface was used in an earlier study of the vibrational levels of the methyl radical, which showed it to yield vibrational energy levels in very good agreement with experiment [6]. The C/PST model involved a wavepacket-based estimate of the probability to form complexes, coupled with a PST calculation of the complex breakup, and represents a simplified variation of recent approaches of Lin and Guo [7]. The quantum mechanical calculations were carried out for zero total angular momentum,  $J = 0$ , and reaction probabilities were contrasted with the corresponding QCT and PST results in the  $J = 0$  limit. The many  $J$  values required for a full QM rate constant make a completely rigorous QM rate constant computationally challenging for this reaction, and so more approximate approaches, such as the QCT method, need to be considered. However, we find severe zero-point energy violation occurs at the lower collision energies in the QCT results, leading to completely incorrect threshold behavior. Consequently, QCT-based rate constants, which we also estimated by allowing for  $J > 0$  and running many trajectories are inaccurate for  $T < 1000\text{K}$ . However, as indicated

in Figure 1, we find reasonable agreement between (corrected) QM and the C/PST  $J = 0$  results, suggesting that pursuing a C/PST estimate of the rate constant would be worthwhile.

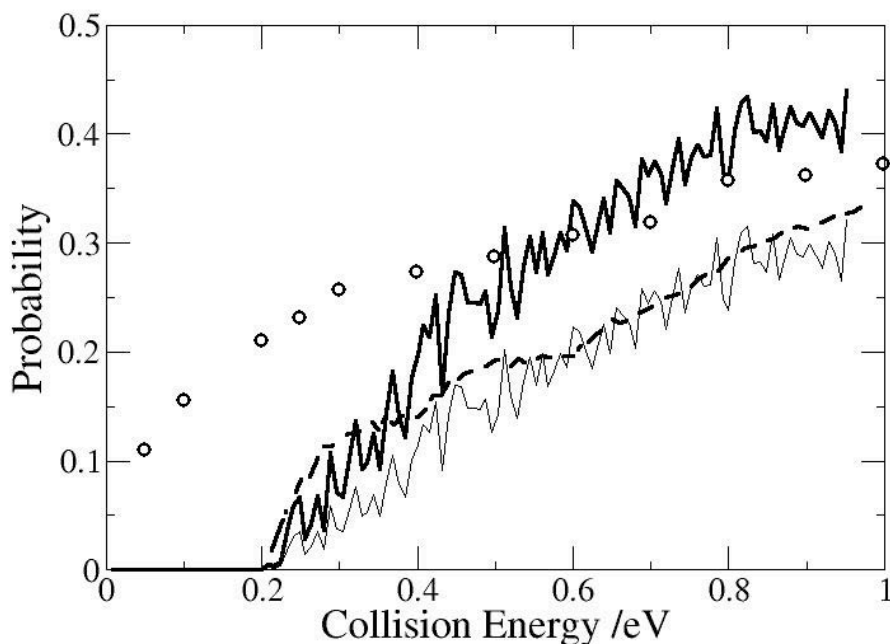


Figure 1. Comparison of QCT (symbols), quantum (heavy and light lines), and capture/phase space theory reaction probabilities for  $\text{CH} + \text{H}_2 \rightarrow \text{CH}_2 + \text{H}$  with zero total angular momentum. The original quantum calculation (heavy line) did not allow the reactant CH bond to break, and the lighter line is the result of applying a simple correction to those results (see Ref. [1] for more details).

In collaboration with Goldfield, we completed the first phase of quantum dynamics calculations on the photodetachment of electrons from HOCO anions,  $\text{HOCO}^-$ , which have been studied experimentally by Continetti and co-workers [8]. It is possible to form stable HOCO,  $\text{H} + \text{CO}_2$  and  $\text{OH} + \text{CO}$  from such a process, and the theoretical results should be useful since the theoretical results involve no contributions from excited electronic states, whereas that may be a complicating issue in the experiments. Our results, including relative total amounts of products, product and electron translational energy distributions, turn out to agree reasonably well with experiment.

The four-atom real wavepacket code, based on diatom plus diatom reactants, which has been developed and used over the past few years was generalized to the case of atom plus triatomic reactants. Work with Gonzalez and coworkers is in progress on validation of the code with a study of the  $\text{H} + \text{H}_2\text{O} \rightarrow \text{H}_2 + \text{OH}$  reaction.

## FUTURE PLANS

We will continue to explore the CH + H<sub>2</sub> system. In particular, we will make quantum mechanical estimates of the rate constant by carrying out a variety of J > 0 wavepacket calculations to obtain capture probabilities and invoking variations of the C/PST model [1] or related wavepacket-based capture models [7]. The reverse reaction, CH<sub>2</sub> + H, will also be studied with the aid of our newly developed atom plus triatom wavepacket code. We will also continue to investigate aspects of HOCO dissociative photodetachment, by extending our work to the deuterated analogue, which is also of experimental relevance. Finally, the resonance decay of formyl radical, HCO, will be revisited with the aid of a recently developed, high-level potential surface by Harding.

## REFERENCES

- [1] J. Mayneris, A. Saracibar, E. M. Goldfield, M. Gonzalez, E. Garcia, and S. K. Gray, *J. Phys. Chem. A*, *in press* (2006).
- [2] R. G. Macdonald and K. Liu, *J. Chem. Phys.* **89**, 4443 (1988).
- [3] A. McIlroy and F. P. Tully, *J. Chem. Phys.* **99**, 3597 (1993).
- [4] R. A. Eng, G. E. Goos, H. Hippler, and C. Kachiani, *Phys. Chem. Chem. Phys.* **3**, 2258 (2001).
- [5] R. A. Brownsword, A. Canosa, B. R. Rowe, I. R. Sims, I. W. M. Smith, D. W. A. Stewart, A. C. Symonds and D. Travers, *J. Chem. Phys.* **106**, 7662 (1997).
- [6] D. M. Medvedev, L. B. Harding, and S. K. Gray Methyl radical: ab initio global potential energy surface, vibrational levels, and partition function, *Mol. Phys.* **104**, 73-82(2006).
- [7] S. Y. Lin and H. Guo, *J. Chem. Phys.* **120**, 9907 (2004).
- [8] T. G. Clements, R. E. Continetti, and J. S. Francisco, *J. Chem. Phys.* **117**, 6478 (2002).

## DOE COMBUSTION PROGRAM SUPPORTED PUBLICATIONS (2004-2006)

1. D. M. Medvedev and S. K. Gray, A new expression for the direct quantum mechanical evaluation of the thermal rate constant, *J. Chem. Phys.* **120**, 9060-9070 (2004).
2. D. M. Medvedev, S. K. Gray, E. M. Goldfield, M. J. Lakin, D. Troya, and G. C. Schatz, Quantum wave packet and quasiclassical trajectory studies of OH + CO: Influence of the reactant channel well on thermal rate constants, *J. Chem. Phys.* **120**, 1231-1238(2004).
3. Y. He, E. M. Goldfield, and S. K. Gray, Quantum dynamics of vibrationally activated OH-CO reactant complexes, *J. Chem. Phys.* **121**, 823-828 (2004).
4. D. M. Medvedev, E. M. Goldfield, and S. K. Gray, An OpenMP/MPI approach to the parallelization of iterative four-atom quantum mechanics, *Comp. Phys. Comm.* **166**, 94-108 (2005).
5. D. M. Medvedev, L. B. Harding, and S. K. Gray Methyl radical: ab initio global potential energy surface, vibrational levels, and partition function, *Mol. Phys.* **104**, 73-82(2006).
6. E. M. Goldfield and S. K. Gray, An accurate approach to quantum reaction dynamics, *Adv. Chem. Phys.*, *in press* (2006).
7. J. Mayneris, A. Saracibar, E. M. Goldfield, M. Gonzalez, E. Garcia, and S. K. Gray, Theoretical study of the complex-forming  $\text{CH} + \text{H}_2 \rightarrow \text{CH}_2 + \text{H}$  reaction, *J. Phys. Chem. A*, *in press* (2006).

**This work was supported by the Office of Basic Energy Sciences, Division of Chemical Sciences, Geosciences, and Biosciences, U.S. Department of Energy under Contract No. W-31-109-ENG-38.**

# Computer-Aided Construction of Chemical Kinetic Models

William H. Green, Jr., MIT Department of Chemical Engineering,  
77 Massachusetts Ave., Cambridge, MA 02139. email: whgreen@mit.edu

## Project Scope

The combustion chemistry of even simple fuels can be extremely complex, involving hundreds or thousands of kinetically significant species. The most reasonable way to deal with this complexity is to use a computer not only to numerically solve the kinetic model, but also to construct the kinetic model in the first place. We are developing the methods needed to make computer-construction of accurate combustion models practical, as well as tools to make it feasible to handle and solve the resulting large kinetic models, even in multidimensional reacting flows. Many of the parameters in the models are derived from quantum chemistry, and the models are compared with experimental data measured by our collaborators or in our lab.

## Recent Progress

We have applied the automated reaction mechanism-construction tools we have developed to several technologically important problems, including pyrolysis and oxidative chemistry of molecules with 4 to 8 carbons, and to predict the performance of homogeneous charge compression-ignition (HCCI) engines. We also have begun to address the serious human-interface issues associated with these large-scale simulations: developing methods to document the large mechanisms constructed using computer-aided modeling software, and to make it feasible for humans to see (and so be able to check) the assumptions underlying the kinetic simulation. We have focused considerable effort on data models and software architecture, to make it practical for other scientists to easily and correctly extend the software and databases to address new systems. (The computer-science-oriented aspects of this effort are financially supported primarily by NSF and DOE's MICS division; the combustion aspects are supported primarily by DOE's BES division.)

The research necessarily spans the range from quantum chemical calculations on individual molecules and elementary-step reactions, through the development of improved rate/thermo estimation procedures based on generalizations, to the creation of algorithms and software for constructing and solving the simulations, including methods for model-reduction and for correctly using reduced models in reacting-flow simulations.

Notable accomplishments during this grant period include:

- 1) Distribution of the first automated reaction-mechanism generation software that is easily extensible to incorporate new chemistry knowledge, along with extensive documentation and databases, and a graphical interface.
- 2) Use of the above software to construct models for the hexane pyrolysis data measured in Marin's lab [15], and for the neo-pentane oxidation experiments conducted in Taatjes's lab. In both cases the accurate detailed models reveal features of the chemistry that were unexpected and difficult to infer from the experimental data alone.
- 3) Development of the first rigorous method for controlling the error associated with use of reduced chemistry models in CFD reacting-flow simulations.[18]

- 4) Development of the first automated method for constructing a reduced kinetic model guaranteed to be accurate to any user-specified error tolerance over any user-specified range of reaction conditions (*Combust. Theory & Modelling*, submitted).
- 5) Demonstration (in collaboration with Paul Barton) of new global optimization algorithms useful in combustion modeling and kinetics, e.g. [9,16,18]. Most importantly, we presented the first algorithm guaranteed to find the global best-fit to the nonlinear least-squares problems that arise when interpreting flash-photolysis kinetics [16].
- 6) Extension of our method for more accurately estimating PAH thermochemistry [6] to furans and arynes.[17]
- 7) Development of kinetic models for supercritical water oxidations, including rate constants and thermochemistry for organophosphorus compounds derived from quantum chemistry.[14]

### **Future Plans**

We are currently distributing the beta version of our model-construction software for user testing. We are in the midst of publishing all the journal papers, examples, and other documentation, and will post version 1.0 of this open-source software on SourceForge in the next few months. We plan to integrate this software with the PrIME and Active Tables projects, so that the models constructed will always be using the best current values for thermochemistry and rate constants.

We are currently adding the capability to compute uncertainty estimates for the model predictions, make it much easier to sensibly test the models vs. data. The uncertainty estimates are critical so users will know how much credence to give the model predictions in cases where there are no data available.

We are developing reacting-flow simulation methods that automatically reduce the chemical kinetic models where that introduces errors negligible compared to other errors in the simulations. So far we have developed methods that work for steady-state laminar flames using reaction-elimination; we will extend this to dynamic simulations and to models with reduced numbers of chemical species.

We will incorporate NO<sub>x</sub> and organic nitrogen chemistry into the model-construction software, and improve its treatment of chemically-activated and fall-off reactions. We are also modeling combustion synthesis of inorganic nanoparticles, and the high temperature chemistry measured in doped flames in Lisa Pfefferle's research group.

### **Publications Resulting from DOE Sponsorship (Since 2004)**

1. P.E. Yelvington, M. Bernat i Rollo, S. Liput, J. Yang, J.W. Tester, & W.H. Green, "Predicting Performance Maps for HCCI Engines", *Combust. Sci. & Tech.* **176**, 1243-1282 (2004).
2. W.H. Green, C.D. Wijaya, P.E. Yelvington, & R. Sumathi, "Predicting Chemical Kinetics with Computational Chemistry: Is QOOH = HOQO Important in Fuel Ignition?", *Mol. Phys.* **102**, 371-380 (2004).
3. Patricia A. Sullivan, Raman Sumathi, William H. Green, and Jefferson W. Tester, "Ab initio modeling of Organophosphorus Combustion Chemistry", *Physical Chemistry Chemical Physics* **6**(17), 4296-4309 (2004).

4. Patricia A. Sullivan, Jason M. Ploeger, William H. Green, and Jefferson W. Tester, "Elementary Reaction Rate Model for MPA Oxidation in Supercritical Water", *Physical Chemistry Chemical Physics* **6**(17), 4310-4320 (2004)
5. J.W. Taylor, G. Ehlker, H.-H. Carstensen, L. Ruslen, R.W. Field, & W.H. Green, "Direct Measurement of the Fast Reversible Addition of Oxygen to Cyclohexadienyl Radicals in Nonpolar Solvents", *J. Phys. Chem. A* **108**, 7193-7203 (2004).
6. Joanna Yu, Raman Sumathi, and William H. Green, Jr., "Accurate and Efficient Method for Predicting Thermochemistry of Polycyclic Aromatic Hydrocarbons", *Journal of the American Chemical Society* **126**(39), 12685-12700 (2004).
7. H. Richter, S. Granata, W.H. Green, & J.B. Howard, "Detailed Modeling of PAH and Soot Formation in a Laminar Premixed Benzene/Oxygen/Argon Low-Pressure Flame", *Proc. Combust. Inst.* **30**(1), 1397-1405 (2005).
8. H. Ismail, J. Park, B.M. Wong, W.H. Green, & M.C. Lin, "A Theoretical and Experimental Kinetic Study of Phenyl Radical Addition to Butadiene", *Proc. Combust. Inst.* **30**(1), 1049-1056 (2005).
9. B. Bhattacharjee, P. Lemonidis, W.H. Green and P.I. Barton "Global Solution of Semi-infinite Programs", *Mathematical Programming (Series A)* **103**(2), 283-307 (2005).
10. O.O. Oluwole and W.H. Green, "Rigorous Error Control in Reacting Flow Simulations Using Reduced Chemistry Models", in *Computational Fluid and Solid Mechanics 2005*, ed. by K.J. Bathe (Elsevier, 2005).
11. B.M. Wong & W.H. Green, "Effects of Large-Amplitude Torsions on Partition Functions: Beyond the Conventional Separability Assumption", *Mol. Phys.* **103**, 1027-1034 (2005).
12. Karen Schuchardt, Oluwayemisi Oluwole, William Pitz, Larry A. Rahn, William H. Green, David Leahy, Carmen Pancerella, Magnus Sjoberg, and John Dec, "Development of the RIOT Web Service and Information Technologies to Enable Mechanism Reduction for HCCI Simulations", *Journal of Physics: Conference Series* **16**, 107-112 (2005).
13. Jose Luis Chesa Rocafort, Morgan Andreae, William H. Green, Wai K. Cheng, and Jim S. Cowart, "A Modeling Investigation into the Optimal Intake and Exhaust Valve Event Duration and Timing for a Homogeneous Charge Compression Ignition Engine", *SAE 2005-01-3746* (2005).
14. Jason M. Ploeger, Patricia A. Bielenberg, Joanna L. DiNaro-Blanchard, Russell P. Lachance, Joshua D. Taylor, William H. Green, and Jefferson W. Tester, "Modeling Oxidation and Hydrolysis Reactions in Supercritical Water – Free Radical Elementary Reaction Networks and their Applications", *Combustion Science and Technology* **177**, 1-35 (2005).
15. Kevin Van Geem, Marie Françoise Reyniers, Guy Marin, Jing Song, David M. Matheu, and William H. Green, "Automatic Reaction Network Generation using RMG for Steam Cracking of n-Hexane", *A.I.Ch.E. Journal* **52**(2), 718-730 (2006).
16. Adam B. Singer, James W. Taylor, Paul I. Barton, and William H. Green, "Global Dynamic Optimization for Parameter Estimation in Chemical Kinetics", *Journal of Physical Chemistry A* **110**(3), 971-976 (2006).

17. Joanna Yu, R. Sumathi, and William H. Green, "Accurate and Efficient Estimation Method for Predicting the Thermochemistry of Furans and ortho-Arynes -- Expansion of the Bond-Centered Group Additivity Method", *Journal of Physical Chemistry A* (2006, in press, available online).
18. Oluwayemisi O. Oluwole, Binita Bhattacharjee, John E. Tolsma, Paul I. Barton, William H. Green, "Rigorous Valid Ranges for Optimally-Reduced Kinetic Models", *Combustion and Flame* (2006, in press).

## Wave packet based statistical model for complex-forming reactions

*PI: Hua Guo*

*Department of Chemistry, University of New Mexico*

*Albuquerque, NM 87131*

*hguo@unm.edu*

### ABSTRACT

Chemical reactions can either be direct or proceed via the formation of a reaction complex. Direct reactions are ideally suited for time-dependent quantum studies because of the short reaction time. On the other hand, complex-forming reactions pose a challenge for quantum characterization because of the long lifetime of the reaction intermediate and the large number of quantum states supported by the potential energy well.

It has been realized long ago that one can take advantage of the long lifetime of the intermediate in a complex-forming reaction to simplify the theoretical treatment of the dynamics. This is because the formation and decay of a reaction intermediate with a sufficiently long lifetime are dominated by statistics, in other words, by the availability of open channels. The early statistical models, represented by the Phase Space Theory (PST), have been found to be very successful in describing barrierless complex-forming reactions. Recently, Manolopoulos and co-workers<sup>1,2</sup> demonstrated that a quantum mechanical version of the statistical model is capable to predict semi-quantitatively the integral and differential cross-sections of several prototypical insertion reactions dominated by long-lived intermediates.

Following Pechukas and Light,<sup>3-5</sup> the state-resolved reaction probability for a statistical reaction can be expressed as follows:

$$p_{f \leftarrow i}(E) = p_i^{(c)}(E) \times \frac{p_f^{(c)}(E)}{\sum_l p_l^{(c)}(E)}, \quad (1)$$

where  $p_i^{(c)}(E)$  represents the probability of being captured by the deep well for a particular channel ( $l$ ), which can be computed using a quantum mechanical method. The summation in the denominator of Eq. (1) runs over all the open channels at energy  $E$ . The statistical model is expected to be valid if the lifetime of the intermediate is sufficiently long.

There are several important features in the quantum mechanical calculation of the capture probabilities. Above all, the quantum treatment of the dynamics allows the capturing of all quantum effects in the entrance and exit channels, such as tunneling and zero-point energy. Since the capture is a quasi-inelastic event, no coordinate transform is necessary. Only potentials in the dissociation channels need be accurately determined. In addition, the coupled-state (or centrifugal sudden) approximation has been shown to work

well for reactions that are known to have a strong Coriolis coupling in the interaction region.

Recently, we have developed a wave packet based statistical model.<sup>6</sup> In the wave packet implementation, the capture probabilities are computed using a flux method for the incoming wave packets.<sup>6</sup> The numerical advantage of the wave packet implementation is many-fold. First, wave packet propagation has better scaling laws than time-independent methods, so it might be amenable to large systems. Second, the capture is a short time process and the wave packet propagation needs not be carried out for a long time. Third, Fourier transform of the wave packets allows the determination of capture probabilities in the entire energy range. The latter feature is important for understanding the energy dependency of the cross-sections and for rate constant calculations.

The performance of the wave packet based statistical model has been very encouraging. Cross-sections and rate constants obtained from the quantum statistical model have been shown to agree well with exact results and with experimental data for insertion reactions between H<sub>2</sub> and C(<sup>1</sup>D),<sup>7</sup> S(<sup>1</sup>D),<sup>8</sup> and N(<sup>2</sup>D).<sup>9</sup> The latter case is particularly interesting because the lifetime of the NH<sub>2</sub> intermediate is not very long. The statistical model has also been used to study the OH + O  $\leftrightarrow$  O<sub>2</sub> + H reaction,<sup>10,11</sup> which is considered to be the most important combustion reaction, and the O<sub>2</sub> + O  $\leftrightarrow$  O + O<sub>2</sub> isotope exchange reactions.<sup>12</sup> These studies help to establish the statistical limits in these important complex-forming reactions.

For the near future, statistical studies of polyatomic systems will be carried out. In particular, we are constructing potential energy surfaces for the O + CO<sub>2</sub>  $\rightarrow$  O + CO<sub>2</sub> exchange reaction, which has been found to be dominated by a long-lived reaction intermediate.<sup>13</sup> We plan to treat the dynamics using an atom-linear molecule model.

#### References:

- <sup>1</sup> E. J. Rackham, F. Huarte-Larranaga, and D. E. Manolopoulos, *Chem. Phys. Lett.* **343**, 356 (2001).
- <sup>2</sup> E. J. Rackham, T. Gonzalez-Lezana, and D. E. Manolopoulos, *J. Chem. Phys.* **119**, 12895 (2003).
- <sup>3</sup> J. C. Light, *J. Chem. Phys.* **40**, 3221 (1964).
- <sup>4</sup> P. Pechukas and J. C. Light, *J. Chem. Phys.* **42**, 3281 (1965).
- <sup>5</sup> P. Pechukas, J. C. Light, and C. Rankin, *J. Chem. Phys.* **44**, 794 (1966).
- <sup>6</sup> S. Y. Lin and H. Guo, *J. Chem. Phys.* **120**, 9907 (2004).
- <sup>7</sup> S. Y. Lin and H. Guo, *J. Phys. Chem.* **A108**, 10060 (2004).
- <sup>8</sup> S. Y. Lin and H. Guo, *J. Chem. Phys.* **122**, 074304 (2005).
- <sup>9</sup> S. Y. Lin and H. Guo, *J. Chem. Phys.* **124**, 031101 (2006).
- <sup>10</sup> S. Y. Lin, E. J. Rackham, and H. Guo, *J. Phys. Chem.* **110**, 1534 (2006).
- <sup>11</sup> C. Xu, D. Xie, D. H. Zhang, S. Y. Lin, and H. Guo, *J. Chem. Phys.* **122**, 244305 (2005).
- <sup>12</sup> S. Y. Lin and H. Guo, *J. Phys. Chem.* (in press).
- <sup>13</sup> M. J. Perri, A. L. V. Wyngarden, K. A. Boering, J. J. Lin, and Y. T. Lee, *J. Chem. Phys.* **119**, 8213 (2003).

# GAS PHASE MOLECULAR DYNAMICS: HIGH-RESOLUTION SPECTROSCOPIC PROBES OF CHEMICAL DYNAMICS

Gregory E. Hall (gehall@bnl.gov)

*Chemistry Department, Brookhaven National Laboratory, Upton, NY 11973-5000*

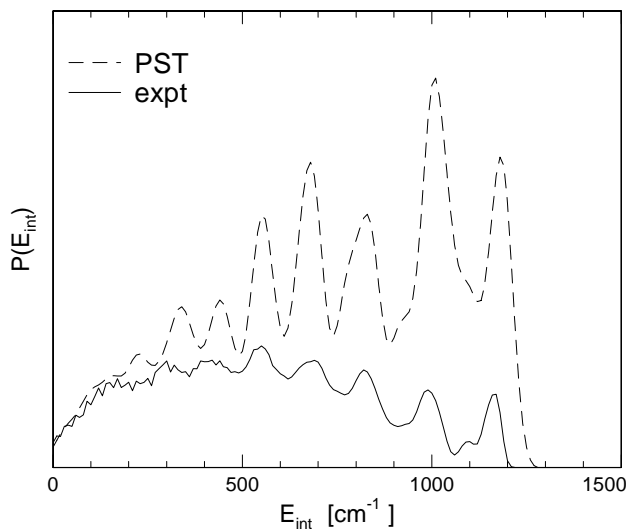
## PROGRAM SCOPE

This research is carried out as part of the Gas Phase Molecular Dynamics group program in the Chemistry Department at Brookhaven National Laboratory. High-resolution spectroscopic tools are developed and applied to problems in chemical dynamics. Recent topics have included the state-resolved studies of collision-induced electronic energy transfer, dynamics of barrierless unimolecular reactions, and the kinetics and spectroscopy of transient species.

## RECENT PROGRESS

### Correlated photochemistry: CH<sub>2</sub>CO

In collaboration with Arthur Suits (now at Wayne State University), time sliced, velocity-mapped images of CO photofragments from ketene dissociation have been measured to characterize the correlated product distributions of this benchmark unimolecular dissociation. Despite the relatively low and nearly continuous distribution of recoil velocities for the CO fragments, multiple rings in the CO images can be resolved, corresponding to the irregular density of CH<sub>2</sub> rotational states. The importance of finite slicing



in the analysis of the images has been considered quantitatively, and an inversion method has been developed to account for the variable resolution for faster and slower ions in the image. The high resolution features allow for a detailed analysis of the product correlations, to compare with theory and previous work in the laboratories of Wodtke<sup>1</sup> (UCSB) and Hall<sup>2</sup> (BNL). In contradiction with some features of both these previous studies, we find the difference between the observed correlated product distributions and those of the zero-order predictions of Phase Space Theory are restricted to the highest internal energy states of CH<sub>2</sub>. The figure shows an example of the internal energy distribution in the CH<sub>2</sub> fragment coincident with a selected CO rotational state (J=24), derived from the sliced image of that CO state. The dashed line

illustrates the PST prediction for this row of the correlated state distribution matrix, after degrading the resolution to match the experiment. The peaks and valleys in the energy distribution correspond to the spectroscopically known clumps and gaps in the rotational density of states. The energy-dependent ratio of experimental to PST  $P(E_{\text{int}})$  is well represented by an exponential function of the available energy, in the spirit of a linear surprisal. Similar patterns were obtained for all observed CO states, as well as in the direct dynamics theoretical study of this unimolecular reaction in collaboration with Klippenstein and Gray.<sup>3</sup> These calculations reproduced the trends in the product state distributions. The deviations from PST could be attributed to anisotropic exit channel interactions, starting at a variational transition state. Previous measurements in the Wodtke lab and at BNL were inconsistent with both the calculations and with these new experimental results, and different types of non-statistical effects were considered to explain the earlier experiments. These non-statistical explanations are unnecessary with the revised experimental data. (with Suits and Komissarov)

## Double-resonance energy transfer studies in CH<sub>2</sub>

Because of the close connection between collision-induced intersystem crossing and rotational energy transfer in the sparse mixed-state limit, we have been performing a double resonance study of collisional energy transfer in CH<sub>2</sub>. In these experiments, individual CH<sub>2</sub> rotational levels are bleached by a tunable ns dye laser or OPO, while monitoring the populations of the same or nearby rotational levels with near-infrared transient FM spectroscopy. Saturation recovery experiments have characterized the rotational energy transfer rates as the rotational population hole is filled in by collisions of CH<sub>2</sub> with rare gases and ketene. We observe that the rotational alignment of the hole decays several times faster than the population hole itself. State-to-state propensities for rotational energy transfer can be assessed with the more challenging saturation transfer experiments, in which the bleached state and the probed state differ, but are connected by single or multiple collisions. The diffusion of a population hole among all rotational levels of the same nuclear spin symmetry is observed, with differing transfer kinetics depending on the strength and directness of coupling between bleached and probed rotational levels.

Compared to the behavior of rotational energy transfer among “normal” singlet CH<sub>2</sub> states, the saturation transfer behavior of singlet-triplet mixed states is revealing. The mixed states come in pairs, sharing the oscillator strength of the zero-order singlet. The pairs are typically observed as a strong line, perturbed from its predicted frequency, and a weaker extra line, arising from a near-degenerate triplet state level, made bright by partial mixing with the zero-order singlet level. The two components of mixed state pairs are typically separated by several cm<sup>-1</sup> and can be independently depleted in the saturation transfer experiment. We find extremely rapid collisional sharing of the population depletion between the two components of a mixed state pair, followed by a slower diffusion of the hole among other detected states. (with Sears and Kim)

## Double-resonance spectroscopy studies

The same experiment used for energy transfer studies in CH<sub>2</sub> has recently provided confirmation of a theoretical assignment<sup>4</sup> of some sharp lines observed but never assigned by Herzberg in the near-ultraviolet *c-a* system. With a visible dye laser tuned to a known transition in the *b-a* spectrum, the near-ir FM laser is scanned in the region of the predicted *c-b* transition, seeking a transient FM absorption signal with zero background, in a pump-probe ladder scheme, contrasted with the probe-pump “V” scheme used for saturation recovery measurements. Most of the tentative assignments of Bunker and co-workers have been confirmed and published. (with Sears and Kim).

## FUTURE WORK

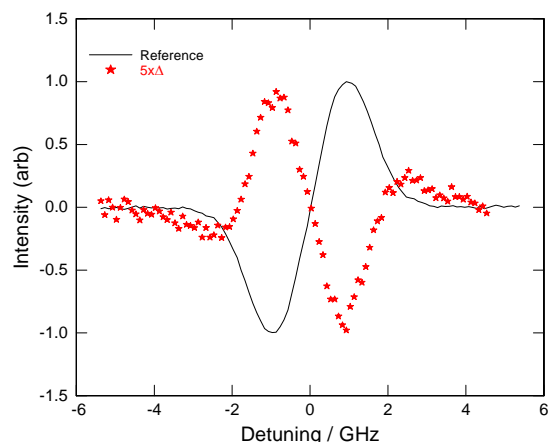
### Nonequilibrium kinetics of singlet CH<sub>2</sub>

We have in hand temperature-dependent kinetic measurements of singlet CH<sub>2</sub> in both *ortho* and *para* nuclear spin modifications, as well as careful decay studies of vibrationally excited CH<sub>2</sub> *a* (010) to compare to the (000) level. This work requires final analysis and integration to publish along with our earlier work on methylene relaxation kinetics and reversible intersystem crossing.

Following clarification of the intersystem crossing kinetics with rare gases, similar measurements in the presence of reactive gases such as H<sub>2</sub>O, O<sub>2</sub> and H<sub>2</sub> will be performed. Compared to the rare gases, we will look for differences in the evolution of the state distribution and total singlet survival probability as the nascent CH<sub>2</sub> ensemble thermalizes, reacts, and interconverts with triplet. Recent work from the laboratories of Hancock<sup>5</sup> (Oxford) and Pilling<sup>6</sup> (Leeds) on the <sup>1</sup>CH<sub>2</sub> + O<sub>2</sub> reaction indicating that quenching to <sup>3</sup>CH<sub>2</sub> is the only significant channel implies that mixed states have little to do with this much more efficient intersystem crossing process. Our preliminary measurements with O<sub>2</sub> show strongly curved semi-logarithmic decays, and require open-minded interpretation. We have the tools in hand to explore these interesting questions.

## Probe-pump double-resonance studies in CH<sub>2</sub>

Searching for unknown bands with a high resolution ring laser is far more tedious than confirming predicted assignments. Particularly with the availability of an easily tunable OPO, we have been investigating double resonance schemes combining a fixed frequency FM measurement and a scanning OPO. Setting the cw laser to an assigned *b-a* transition, and scanning the OPO across a region with suspected *c-b* lines, one might hope to see some effect due to depopulation of the *b* state population



produced by the cw laser with an unusual probe-pump ladder sequence. This effect turns out to be unobservable, but instead, an easily detected double resonance FM transient is observed, which we can attribute to an AC Stark broadening of the *b-a* transition when the resonant *c-b* field is present. We have tested this on some of the same double-resonance transitions we have previously observed in the more intuitive pump-probe ladder scheme, described above. A few mJ of unfocused light from the OPO generates a perturbation on the FM signal whose probe lineshape can be modeled with a transient and reversible increase of about 5-10% in the linewidth of the *b-a* transition. This has a dramatic effect on the derivative spectrum,

corresponding to a 10-20% transient change in the peak FM signal, which can be measured with high signal/noise ratio, as shown in the figure above. The solid reference spectrum is obtained by scanning the cw probe laser across a CH<sub>2</sub> rotational transition in the near infrared, with a time gate just before the pump pulse fires. The symbols are a five times expanded spectrum of the peak transient signal only observed during the ~10 ns when the pump pulse is fired at the peak of the *c-b* resonant transition, during the same probe laser scan used to produce the reference spectrum. This non-intuitive probe-pump sequence shows good sensitivity, and its size and shape relative to the reference spectrum characterizes the pump-induced shift of the *b* state level to be no more than about 50 MHz, while the Doppler-broadened reference spectrum has an additional AC Stark broadening of about 150-200 MHz induced by the double resonance pump laser. The pump lineshapes measured at the peak probe frequency, about 1 GHz from line center, are symmetrical and approximately Doppler-limited. These very new results are still somewhat surprising to us, and may enable several new types of spectroscopy and dynamics investigations, as discussed in the abstract of Trevor Sears.

## Cited References

- 1 G. C. Morgan, M. Drabbels, and A. M. Wodtke, *J. Chem. Phys.* **104**, 7460 (1996).
- 2 M. L. Costen, H. Katayanagi, and G. E. Hall, *J. Phys. Chem. A* **104**, 10 247 (2000).
- 3 K. M. Forsythe, S. K. Gray, S. J. Klippenstein, and G. E. Hall, *J. Chem. Phys.* **115**, 2134 (2001).
- 4 S. N. Yurchenko, P. Jensen, Y. Li, R. J. Buenker, and P. R. Bunker, *J. Mol. Spectrosc.* **208**, 136 (2001).
- 5 G. Hancock and V. Haverd, *Chem. Phys. Lett.* **372**, 288 (2003).
- 6 M. A. Blitz, K. W. McKee, M. J. Pilling, and P. W. Seakins, *Chem. Phys. Lett.* **372**, 295 (2003).

## DOE SPONSORED PUBLICATIONS SINCE 2004

The spectrum of CH<sub>2</sub> near 1.36 and 0.92 microns: Re-evaluation of rotational level structure and perturbations in *a* (010)

K. Kobayashi, G. E. Hall and T. J. Sears  
*J. Chem. Phys.* (in press, 2006)

Correlated product distributions from ketene dissociation measured by DC sliced ion imaging

A. V. Komissarov, M. P. Minitti, A. G. Suits, and G. E. Hall  
*J. Chem. Phys.* **124**, 014303 (2006)

Rotationally resolved spectrum of the *A* (060) – *X* (000) band of HCB<sub>r</sub>

G. E. Hall, T. J. Sears and H-G. Yu  
*J. Mol. Spectr.* **235**, 125-131 (2006)

Reflectron velocity map ion imaging

B. D. Leskiw, M. H. Kim, G. E. Hall and A. G. Suits  
*Reviews of Scientific Instruments*, **76**, 104101; Erratum 129901 (2005)

Observation of the *c*<sup>1</sup>A<sub>1</sub> state of methylene by optical-optical double resonance

Y. Kim, A. Komissarov, G. E. Hall and T. J. Sears  
*J. Chem. Phys.* **123**, 024306 (2005)

Hyperfine quantum beats from photolytic orientation and alignment

M. L. Costen and G. E. Hall  
*Phys. Chem. Chem. Phys.*, **7** 1408-13 (2005)

Doppler-resolved spectroscopy as an assignment tool in the spectrum of singlet methylene

G. E. Hall, A. Komissarov and T. J. Sears  
*J. Phys. Chem. A*, **108** 7922-27 (2004)

The photodissociation of bromoform at 248 nm: Single and multiphoton processes

P. Zou, J. Shu, T. J. Sears, G. E. Hall and S. W. North  
*J. Phys. Chem. A*, **108**, 1482-8 (2004)

Superexcited state dynamics probed with an extreme-ultraviolet free electron laser

W. Li, R. Lucchese, A. Doyuran, Z. Wu, H. Loos, G. E. Hall and A. G. Suits  
*Phys. Rev. Lett.*, **92**, 083002 (2004)

---

This work was performed at Brookhaven National Laboratory under Contract No. DE\_AC02\_98CH10886 with the U.S. Department of Energy and supported by its Division of Chemical Sciences.

# Flame Chemistry and Diagnostics

Nils Hansen

*Combustion Research Facility, Sandia National Laboratories*

*P.O. Box 969, Livermore, CA 94551-0969*

E-mail: [nhansen@sandia.gov](mailto:nhansen@sandia.gov)

## SCOPE OF THE PROGRAM

The goal of this program is to provide a rigorous basis for the elucidation of chemical mechanisms of combustion, combining experimental measurements employing state of the art combustion diagnostics with detailed kinetic modeling. The experimental program concentrates on the development and application of combustion diagnostics for measurements of key chemical species concentrations. These measurements are carried out in low-pressure, one-dimensional laminar flames and are designed to serve as benchmarks for the validation of combustion chemistry models. Comparison of experimental data to models employing detailed chemical kinetics is critical to determining important chemical pathways in combustion and in pollutant formation in combustion systems. As turbulent combustion models become increasingly sophisticated, accurate chemical mechanisms will play a larger role in computations of realistic combustion systems. Verification of detailed chemistry models against a range of precise measurements under thoroughly-characterized steady conditions is necessary before such flame models can be applied with confidence in turbulent combustion calculations.

## PROGRESS REPORT

### Molecular Beam Mass Spectrometry at the Advanced Light Source

In collaboration with Terrill A. Cool of Cornell University and Phillip R. Westmoreland of the University of Massachusetts, great progress has been made measuring low pressure flames using molecular beam mass spectrometry with synchrotron photoionization at the Advanced Light Source at Lawrence Berkeley National Laboratory. The molecular-beam photoionization mass spectrometer is now in full operation. In the past year, different flames over a wide range of stoichiometry using the following fuels have been characterized: allene, benzene, cyclohexane, cyclopentene, dimethylether, ethanol, ethylene, ethylformate, methane, methylacetate, propene, propyne, and toluene. The data is currently being reduced for comparison to detailed models.

### Identification of the Isomeric Composition of C<sub>4</sub>H<sub>3</sub> and C<sub>4</sub>H<sub>5</sub> Radicals

In collaboration with F. Qi at the University of Science and Technology, Hefei, China, and S. J. Klippenstein of Argonne National Laboratory we identified the resonantly stabilized *i*-C<sub>4</sub>H<sub>3</sub> and *i*-C<sub>4</sub>H<sub>5</sub> isomers ( $\text{CH}_2=\text{C}\cdot-\text{C}\equiv\text{CH} \leftrightarrow \text{CH}_2=\text{C}=\text{C}=\cdot\text{CH}$  and  $\cdot\text{CH}_2-\text{CH}=\text{C}=\text{CH}_2 \leftrightarrow \text{CH}_2=\text{CH}-\cdot\text{C}=\text{CH}_2$ ) in fuel-rich allene, propyne, cyclopentene, and benzene flames.

Identification has been accomplished by comparing experimental photoionization efficiency spectra with simulated curves based on calculated adiabatic ionization energies and Franck-Condon factor analysis. The simulations employed force-constant matrices, unscaled frequencies, and normal mode displacement coordinates as calculated with high-level *ab initio* methods for the neutral and cation of various isomers.

For  $C_4H_5$ , the Franck-Condon analysis also suggested the presence of  $CH_3CCCH_2$  ( $CH_3-\bullet C=C=CH_2 \leftrightarrow CH_3-C\equiv C-\bullet CH_2$ ) and/or  $CH_3CHCCH$  isomers ( $CH_3-\bullet CH-C\equiv CH \leftrightarrow CH_3-CH=C-\bullet CH$ ). The detection of the *i*-isomers suggests that their reactions with acetylene is a plausible cyclization step. The role in soot formation of  $CH_3CCCH_2$  and/or the  $CH_3CHCCH$  isomer, which are currently absent from most flame models, requires further investigation. No clear evidence for the less-stable *n*- $C_4H_3$  ( $\bullet CH=CH-C\equiv CH$ ) and *n*- $C_4H_5$  isomers ( $\bullet CH=CH-CH=CH_2$ ) was found. The small amounts together with large differences in vertical and adiabatic ionization energies may make it difficult to detect them.

### Determination of Isomeric Composition of $C_5$ Intermediates

Due to the lack of knowledge about their respective chemistry, most  $C_5$  combustion intermediates are absent from current flame chemistry models. Therefore the importance of most  $C_5$  species in the growth of higher hydrocarbons in combustion is at this point rather unclear.

In recent work, we thoroughly investigated the isomeric composition of  $C_5H_x$  ( $x = 2 - 8$ ) intermediates in several fuel-rich flames. For  $C_5H_2$ , the analysis revealed the presence of the *cyclo*- $CCHCCCH$ -, a five-membered ring which was observed as a weak signal in a fuel-rich cyclopentene flame. At least two  $C_5H_3$  isomers have been clearly identified. Both,  $CH_2CCCCH$  (*i*- $C_5H_3$ ) and  $CHCCHCCH$  (*n*- $C_5H_3$ ) are present in fuel-rich flames, while the presence of the *cyclo*- $CCHCHCCH$ -needs further investigation. For  $C_5H_4$ , contributions from  $CH_2CCCCH_2$ ,  $CH_2CCHCCH$ , and  $CHCCCCH_3$  were evident, as were some contributions from  $CHCCH_2CCH$  in the cyclopentene and benzene flames. Signal at  $m/z = 65$  ( $C_5H_5$ ) originated mainly from the cyclopentadienyl radical, although signal from a linear isomer was clearly detected. Contributions from cyclopentadiene,  $CH_3CCCHCH_2$ ,  $CH_3CHCHCCH$ , and  $CH_2CHCH_2CCH$  have been observed at  $m/z = 66$  ( $C_5H_6$ ). At  $m/z = 68$  ( $C_5H_8$ ) cyclopentene,  $CH_2CHCHCHCH_3$ ,  $CH_3CCCH_2CH_3$ , and  $CH_2CHCH_2CHCH_2$  were contributing to the signal.

### Propyne and Allene Flame Studies

It is of particular interest to study fuel-rich allene and propyne flames, as both molecules are potential precursors for propargyl radicals. More than 40 species have been identified in both fuel-rich allene and propyne flames. Quantitative mole fraction profiles for more than 30 flame species with ion masses ranging from 2 to 78 have been determined. J. A. Miller (Sandia National Laboratories) has modeled these flames and the calculated mole fraction profiles have been compared with experimental results. Determined mole fractions for the common combustion intermediates are quantitatively similar in both flames. Although the model predicted the mole fractions of the major species quite accurately, some discrepancies were observed for minor species.

### $C_2$ -Species diagnostics

In collaboration with J. H. Frank (Sandia National Laboratories) we are developing a laser-induced fragmentation fluorescence (LIFF) technique for probing vinyl ( $C_2H_3$ ) and acetylene ( $C_2H_2$ ) in premixed laminar low-pressure flames. As part of the development, we conducted a series of low-pressure flame experiments to quantify the temperature dependence of the LIFF signal by combining LIFF measurements with photoionization mass spectrometry in a low-pressure flame at the ALS. The mass spectrometer will provide quantitative measurements of the vinyl and acetylene profiles in the flames which will then be compared with the LIFF signal profiles.

## FUTURE DIRECTIONS

In recent work, different C<sub>6</sub>H<sub>6</sub> isomers have been identified in fuel-rich allene and propyne flames. Besides benzene, fulvene is clearly identified by its ionization energy of 8.3 eV. The limitations on identifying more isomers appear to be uncertainties about the shapes of their PIE curves. It is planned to measure those during one of the next beam cycles.

To improve the resolution of the time-of-flight mass spectrometer used in the described ALS experiments a reflectron will be installed. Early calculations predict an improvement of the resolution by one order of magnitude. This will help to separate accidentally overlapped species like CO and ethylene, formaldehyde and ethane, or ketene and propene.

One key immediate task is the analysis of the large body of ALS data accumulated in the past year, which may compel further or confirmatory measurements during subsequent beam cycles. However, several new areas of investigation are planned for the ALS flame experiments. Studies of oxygenated fuel chemistry will continue with investigations of aldehydes (ethanal, propanal) and ketones. In addition, esters, as contents in biodiesel, are of considerable interest. Doping these fuels in a well-characterized H<sub>2</sub>/O<sub>2</sub> flame may be an attractive alternative or complement to pure-fuel studies. The isomeric selectivity of the ALS photoionization will have a large impact in unraveling chemical pathways; therefore we want to compare hexene flames with previous measured cyclohexane flames. Hexenes exist in 13 different isomers. We will continue our studies of the influence of oxygenated fuels on fuel-rich flames.

In collaboration with L. A. Rahn we will incorporate the ALS flame data into the web based “Collaboratory for Multi-Scale Chemical Science – CMCS” (<http://cmcs.org>). This will make the data widely available for the interested scientific community – especially theorists will be able to compare their flame models with the data.

## PUBLICATIONS ACKNOWLEDGING BES SUPPORT 2004-PRESENT

1. T. A. Cool, K. Nakajima, C. A. Taatjes, A. McIlroy, P. R. Westmoreland, M. E. Law and A. Morel, “Studies of a Fuel-Rich Propane Flame with Photoionization Mass Spectrometry”, *Proc. Combust. Inst.* **30**, 1631-1638 (2004).
2. C. A. Taatjes, D. L. Osborn, T. A. Cool, K. Nakajima, “Synchrotron Photoionization of Combustion Intermediates: The Photoionization Efficiency of HONO”, *Chem. Phys Lett.* **394**, 19-24 (2004).
3. C. A. Taatjes, S. J. Klippenstein, N. Hansen, J. A. Miller, T. A. Cool, J. Wang, M. E. Law, and P. R. Westmoreland, “Synchrotron Photoionization Measurements of Combustion Intermediates: Photoionization Efficiency of C<sub>3</sub>H<sub>2</sub> Isomers”, *Phys. Chem. Chem. Phys.* **7**, 806-813 (2005).
4. C. A. Taatjes, N. Hansen, A. McIlroy, J. A. Miller, J. P. Senosiain, S. J. Klippenstein, F. Qi, L. Sheng, Y. Zhang, T. A. Cool, J. Wang, P. R. Westmoreland, M. E. Law, T. Kasper, and K. Kohse-Höinghaus, “Enols are Common Intermediates in Hydrocarbon Oxidation”, *Science* **308**, 1887-1889 (2005), online 12 May 2005 (10.1126/science.1112532).
5. A. McIlroy and F. Qi, “Identifying Combustion Intermediates via Tunable Vacuum Ultraviolet Photoionization Mass Spectrometry”, *Combust. Sci. Technol.* **177**, 2021-2037 (2005).
6. N. Hansen, A. M. Wodtke, J. C. Robinson, N. E. Sveum, S. J. Goncher, D. M. Neumark, “Photofragment Translational Spectroscopy of ClN<sub>3</sub>: Determination of the primary and secondary Dissociation Pathways”, *J. Chem. Phys.* **123**, 104305-1-104305-11 (2005).
7. C. A. Taatjes, N. Hansen, J. A. Miller, T. A. Cool, J. Wang, P. R. Westmoreland, M. E. Law, T. Kasper, K. Kohse-Höinghaus, “Combustion Chemistry of Enols: Possible Ethenol Precursors in Flames”, *J. Phys. Chem. A*, **110**, 3254-3260 (2006).
8. N. Hansen, S. J. Klippenstein, C. A. Taatjes, J. A. Miller, J. Wang, T. A. Cool, B. Yang, R. Yang, L. Wei, C. Huang, J. Wang, F. Qi, M. E. Law, P. R. Westmoreland, “Identification and Chemistry of C<sub>4</sub>H<sub>3</sub> and C<sub>4</sub>H<sub>5</sub> Isomers in Fuel-Rich Flames”, *J. Phys. Chem. A*, **110**, 3670-3678 (2006).

9. N. Hansen, S. J. Klippenstein, J. A. Miller, J. Wang, T. A. Cool, M. E. Law, P. R. Westmoreland, T. Kasper, K. Kohse-Höinghaus, "Identification of C<sub>5</sub>H<sub>x</sub> Isomers in Fuel-Rich Flames by Photoionization Mass Spectrometry and Electronic Structure Calculations", *J. Phys. Chem A*, **110**, 4376-4388 (2006).
10. A. McIlroy, A. H. Steeves and J. W. Thoman, Jr. "Chemical Intermediates in Low-Pressure Dimethyl Ether/Oxygen/Argon Flames," *Combustion and Flame*, accepted.
11. N. Hansen, J. A. Miller, C. A. Taatjes, J. Wang, T. A. Cool, M. E. Law, P. R. Westmoreland, "Photoionization Mass Spectrometric Studies and Modeling of Fuel-Rich Allene and Propyne Flames", *Proc. Combust. Inst.*, accepted.
12. M. E. Law, P. R. Westmoreland, T. A. Cool, J. Wang, N. Hansen, C. A. Taatjes, T. Kasper, "Benzene Precursors and Formation Routes in a Stoichiometric Cyclohexane Flame", *Proc. Combust. Inst.*, accepted.
13. T. A. Cool, J. Wang, N. Hansen, P. R. Westmoreland, F. L. Dryer, Z. Zhao, A. Kazakov, T. Kasper, K. Kohse-Höinghaus, "Photoionization Mass Spectrometry and Modeling Studies of the Chemistry of fuel-rich Dimethyl Ether Flames", *Proc. Combust. Inst.*, accepted.
14. K. Kohse-Höinghaus, P. Oßwald, U. Struckmeier, T. Kasper, N. Hansen, C. A. Taatjes, J. Wang, T. A. Cool, S. Gon, P. R. Westmoreland, "The Influence of Ethanol Addition on a premixed fuel-rich Propene-Oxygen-Argon Flame", *Proc. Combust. Inst.*, accepted.

## SPECTROSCOPY AND KINETICS OF COMBUSTION GASES AT HIGH TEMPERATURES

Ronald K. Hanson and Craig T. Bowman  
Department of Mechanical Engineering  
Stanford University, Stanford, CA 94305-3032  
[rkhanon@stanford.edu](mailto:rkhanon@stanford.edu), [ctbowman@stanford.edu](mailto:ctbowman@stanford.edu)

### **Program Scope:**

This program involves two complementary activities: (1) development and application of cw laser absorption methods for the measurement of concentration time-histories and fundamental spectroscopic parameters for species of interest in combustion; and (2) shock tube studies of reaction kinetics relevant to combustion. Species investigated in the spectroscopic portion of the research include benzyl ( $C_6H_5CH_2$ ),  $CO_2$ , CH,  $HO_2$ , HCO and NCN using narrow-linewidth ring dye laser absorption. Reactions of interest in the shock tube kinetics portion of the research include:  $C_6H_5CH_2 \rightarrow C_7H_6 + H$ ; toluene  $\rightarrow$  products;  $CO_2 + M \rightarrow CO + O(^3P) + M$ ;  $CH_3 + M \rightarrow$  products; and  $CH+N_2 \rightarrow NCN + H$ .

### **Recent Progress: Shock Tube Chemical Kinetics**

**Benzyl and Toluene Decomposition:** We have begun studying the pyrolysis and oxidation reactions of aromatic species. The decomposition of benzyl,  $C_6H_5CH_2 \rightarrow C_7H_6 + H$ , was studied behind reflected shock waves at temperatures of 1461 to 1730 K and pressures of 1.47 to 1.67 atm with mixtures of 50 and 100 ppm benzyl iodide dilute in argon using ultraviolet laser absorption for detection of benzyl at 266 nm. The low concentrations provided excellent isolated sensitivity to the benzyl decomposition reaction. The rate coefficient at 1.5 atm can be expressed as  $k(T) = 8.20 \times 10^{14} \exp(-40600 K/T)[s^{-1}]$ , where the RMS experimental scatter about the fit is  $\pm 11\%$  and the overall uncertainty of the rate coefficient  $\pm 25\%$ .

Comparison of the results of the current study with the results of four previous shock tube studies is shown in Fig. 1. The current data agree very well with the UV absorption study of Hippler et al. (1990) ( $\sim 0.5$  atm) and the H-atom ARAS study of Braun-Unkhoff et al. (1990) ( $\sim 2$  atm), although the scatter of the current data is significantly reduced from that of these previous studies. In addition, the current data for  $k$  are in agreement with the IUPAC review recommendation, Baulch et al. (2005). The rate coefficient results of the UV absorption study of Jones et al. (1997) ( $\sim 10$ -12 atm) and the H-atom ARAS study of Rao and Skinner (1986) ( $\sim 0.6$  atm) are approximately an order-of-magnitude lower than the current results. Our rate coefficient determinations have significantly less uncertainty due to the low concentrations used and high sensitivity of the laser absorption technique.

The decomposition of toluene was also investigated in reflected shock wave experiments. Mixtures of 200 and 400 ppm of toluene dilute in argon were shock-heated behind reflected shock waves and absorption at 266 nm, primarily due to benzyl radicals, was monitored. Reflected shock conditions ranged from 1398 to 1782 K and 1.44 to 1.58 atm. Toluene is known to decompose via two parallel channels  $C_6H_5CH_3 \rightarrow C_6H_5CH_2 + H$  (a) and  $\rightarrow C_6H_5 + CH_3$  (b). The temporal variation of the benzyl concentration with the overall decomposition rate coefficient and the branching ratio allows separation of these two parameters. As in the case of benzyl decomposition, the absorption of benzyl, benzyl fragments, and toluene was accounted for.

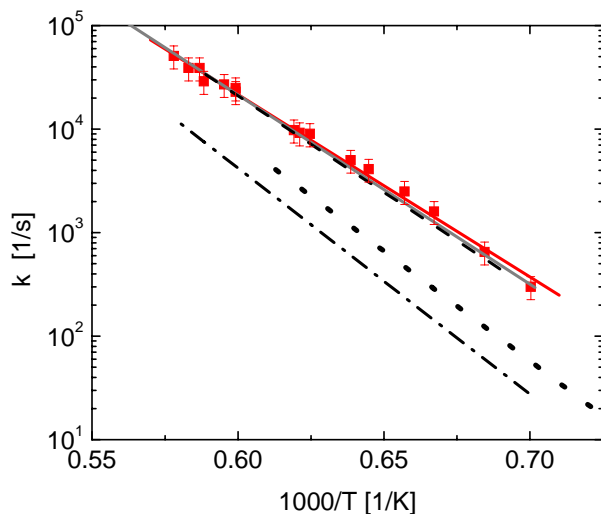


**Fig. 1.** Rate coefficient for benzyl decomposition: filled squares with error bars, current experimental results (~1.5 atm); heavy solid line (red), fit to current data; solid gray line, Hippler et al. (1990) (~0.5 atm); dashed line, Braun-Unkhoff et al. (1990) (~2 atm) and Baulch et al. (2005); dotted line, Jones et al. (1997) (~10-12 atm); dash-dot line, Rao and Skinner (1986) (~0.6 atm).

Expressions for the rate coefficients of toluene decomposition at 1.5 atm given by the least-squares fits are

$$k_a(T) = 2.09 \times 10^{15} \exp(-44040 \text{ K}/T) [\text{s}^{-1}]$$

$$k_b(T) = 2.66 \times 10^{16} \exp(-49260 \text{ K}/T) [\text{s}^{-1}]$$

where the RMS experimental scatter about the fits is  $\pm 13\%$  and  $\pm 17\%$  and the overall uncertainties are estimated to be  $\pm 35\%$  and  $\pm 35\%$  for  $k_a$  and  $k_b$  respectively.

The current findings for the overall decomposition rate coefficient agree with the previous results of Eng et al. (2002), Braun-Unkhoff et al. (1988), and Luther et al. (1990), but are significantly different than the results of Pammidimukkala et al. (1987) and Rao and Skinner (1989).

The current findings for the branching ratio agree with the H-atom ARAS experiments of Eng et al. (2002) and with the study of Luther et al. (1990) that clearly show the toluene decomposition channel leading to benzyl dominates the channel leading to phenyl, but are in disagreement with the results of Pammidimukkala et al. (1987), Rao and Skinner (1989), and Braun-Unkhoff et al. (1988).

**CH<sub>3</sub> Thermal Decomposition:** The methyl radical plays an important role in hydrocarbon combustion and pyrolysis and is directly relevant to high-temperature studies of the CH+N<sub>2</sub> reaction system that are currently underway in our laboratory. We are studying the overall decomposition rate and branching ratio of the two-channel thermal decomposition of the methyl radical, CH<sub>3</sub> + M → CH + H<sub>2</sub> + M (a) and → CH<sub>2</sub> + H + M (b), in shock tube experiments at temperatures of 2400 to 3500 K and pressures between 0.1 and 4 atm. Continuous-wave laser absorption diagnostics for CH and OH radicals are being employed to infer rate coefficient data for reactions (a) and (b), respectively. Reaction (b) is studied by measuring OH in shock heated mixtures of C<sub>2</sub>H<sub>6</sub> or CH<sub>3</sub>I and O<sub>2</sub> (0.1-0.5%) dilute in argon. H-atoms that are generated via reaction (b) rapidly react with O<sub>2</sub>, which is present in excess, forming OH.

**CO<sub>2</sub> Thermal Decomposition and Incubation:** The decomposition of carbon dioxide was investigated behind reflected shock waves at temperatures from 3200 to 4600 K and pressures between 0.45 and 1 atm. The progress of the reaction was monitored by observing ultraviolet laser absorption by CO<sub>2</sub> at 216.5 and 244 nm. Incubation prior to the thermal decomposition of CO<sub>2</sub> was observed for the first time in reflected shock wave experiments (see Fig. 2).

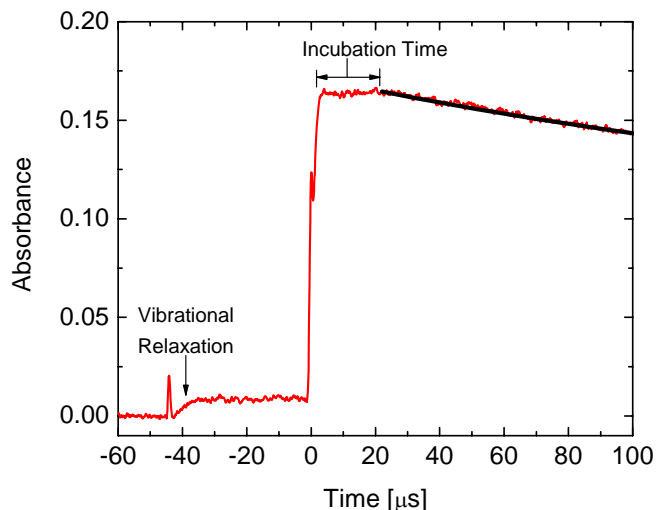


**Fig. 2.** Example experiment and fit (dark line): CO<sub>2</sub> absorbance ( $\ln(I_0/I)$ ) at 216.5 nm. Initial mixture 2% CO<sub>2</sub>/Ar. Vibrationally equilibrated incident shock conditions: 1812 K and 0.16 atm. Initial (prior to decomposition) vibrationally equilibrated reflected shock conditions: 3838 K, 0.83 atm.

Master equation simulations, with a simple model for collisional energy transfer, were carried out to describe the measured incubation times and unimolecular rate coefficient. The second order rate coefficient for CO<sub>2</sub> dissociation was found to be  $3.14 \times 10^{14} \exp(-51300 \text{ K} / T) [\text{cm}^3 \text{mol}^{-1} \text{s}^{-1}]$ . The current findings agree very well with the studies of Burmeister and Roth (1990), Ebrahim and Sandeman (1976), and Hardy et al. (1974). The number of incubation collisions was found to range from  $7 \times 10^3$  at 4600 K to  $3.5 \times 10^4$  at 3200 K. The master equation simulations suggest that the energy transferred per collision must have a greater than linear dependence on energy.

### **Recent Progress: Spectroscopy**

**Benzyl Spectroscopy:** Benzyl radicals have strong broadband absorption in the ultraviolet from 245 to 275 nm allowing detection of benzyl at 266 nm. Continuous-wave laser radiation was generated at 266 nm (1.5 mW) by the single pass of a focused laser beam at 532 nm (Nd:YVO<sub>4</sub> at 5 W) through an angle-tuned BBO crystal; the generated 266 nm harmonic was separated from the 532 nm fundamental beam in a Pellin-Broca prism. Determination of the absorption coefficient for benzyl radicals was performed using the fast decomposition of benzyl iodide as a benzyl source.

**CH Spectroscopy:** As part of the investigation of the reaction of CH+N<sub>2</sub> we have investigated sources and the high temperature kinetics of the CH radical. CH is detected using cw laser absorption at 431 nm generated in a ring dye laser cavity. Both azomethane and ethane have been used to generate CH<sub>3</sub> radicals which decompose to CH and CH<sub>2</sub> radicals.

**NCN Spectroscopy:** Current work focuses on developing a CW laser absorption system for the NCN radical. A detailed survey of NCN spectroscopy has identified the X<sup>3</sup>Σ - A<sup>3</sup>Π transition near 329 nm as well-suited to monitoring the NCN radical at shock tube conditions. Light at 329 nm is generated by doubling 658 nm radiation generated in a ring dye laser cavity with an external-cavity frequency doubler with a BBO crystal. To the best of our knowledge, a quantitative absorption analysis of this transition has not been carried out previously. The relative absorption spectrum for this transition is being mapped out using a microwave discharge as a source of NCN. An extensive literature survey was performed to identify strategies to quantitatively calibrate the NCN laser absorption diagnostic. A kinetic calibration scheme using the reaction between CN and N<sub>2</sub>O shows promise. This reaction occurs via two pathways that form NCN+NO and NCO+N<sub>2</sub>, respectively.

### **Future Plans:**

1) Continue development of external-cavity frequency-doubling methods for the generation of laser radiation in the deep ultraviolet. Apply these frequency-doubling methods to wavelengths of interest including the detection of benzyl at 266 nm, NCN at 329 nm, HCO at 230 and 258 nm, and HO<sub>2</sub> at 230 nm. 2) Develop experimental approaches to measure the overall rate and product branching ratio of the reaction  $\text{CH} + \text{N}_2 \rightarrow \text{NCN} + \text{H}$  using laser absorption. 3) Investigate the oxidation reactions of aromatics including toluene + O<sub>2</sub> and benzyl + O<sub>2</sub>. 4) Begin to apply the CO<sub>2</sub> UV laser-based scheme to measure high temperatures in shock tube reaction rate measurement experiments, and to use tunable diode lasers at 2.0 or 2.7 μm IR absorption of CO<sub>2</sub> for low-temperature measurements.

### **Recent Publications of DOE Sponsored Research: 2004-2006**

M. A. Oehlschlaeger, D. F. Davidson and R. K. Hanson, "High Temperature Thermal Decomposition of Benzyl Radicals," *Journal of Physical Chemistry A*, in press.

M. A. Oehlschlaeger, D. F. Davidson and R. K. Hanson, "Thermal Decomposition of Toluene: Overall Rate and Branching Ratio," Submitted to *Proceedings of the Combustion Institute*, November (2005); and presented as Paper 05F-59, Fall Meeting of the Western States Section of the Combustion Institute, Stanford CA, October (2005).

D. F. Davidson, M. A. Oehlschlaeger, and R. K. Hanson, "Methyl Concentration Time Histories During Iso-Octane and N-Heptane Oxidation," Paper 05F-61, Fall Meeting of the Western States Section of the Combustion Institute, Stanford CA, October (2005).

M. A. Oehlschlaeger, D. F. Davidson and J. B. Jeffries, "Temperature Measurements Using Ultraviolet Laser Absorption of Carbon Dioxide behind Shock Waves," *Applied Optics* 44, 6599-6605 (2005).

V. Vasudevan, D.F. Davidson, R.K. Hanson, "High Temperature Measurement of the Reactions of OH with Toluene and Acetone," *Journal of Physical Chemistry A* 109, 3352-3359 (2005); also presented at the 25<sup>th</sup> *International Symposium on Shock Waves*, Bangalore, India (2005).

V. Vasudevan, D. F. Davidson and R. K. Hanson, "High Temperature Measurements of OH Radical Reactions," Joint Meeting of the US Sections of the Combustion Institute Philadelphia PA, March (2005).

M. A. Oehlschlaeger, D. F. Davidson and R. K. Hanson, "High Temperature UV Absorption of Methyl Radicals behind Shock Waves," *Journal of Quantitative Spectroscopy and Radiative Transfer* 92: 393-402 (2005).

J.T. Herbon, R.K. Hanson, C.T. Bowman, and D.M. Golden, "The Reaction of CH<sub>3</sub>+O<sub>2</sub>: Rate Coefficients for the Product Channels at High Temperatures," *Proceedings of the Combustion Institute* 30, 955-963 (2005).

M. A. Oehlschlaeger, D. F. Davidson, and R. K. Hanson, "High-Temperature Ethane and Propane Decomposition," *Proceedings of the Combustion Institute* 30, 1119-1127 (2005).

M. A. Oehlschlaeger, D. F. Davidson, J. B. Jeffries, and R. K. Hanson, "Carbon Dioxide Thermal Decomposition: Observation of Incubation," *Zeitschrift für Physikalische Chemie* 219, 555-567 (2005).

## Theoretical Studies of Potential Energy Surfaces\*

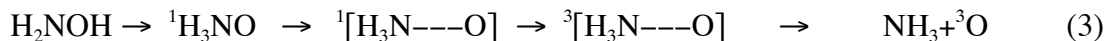
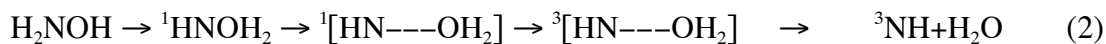
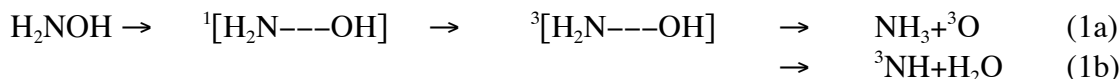
Lawrence B. Harding  
Chemistry Division  
Argonne National Laboratory  
Argonne, IL 60439  
harding@anl.gov

### Program Scope

The goal of this program is to calculate accurate potential energy surfaces for both reactive and non-reactive systems. Our approach is to use state-of-the-art electronic structure methods (CASPT2, MR-CI, CCSD(T), etc.) to characterize multi-dimensional potential energy surfaces. Depending on the nature of the problem, the calculations may focus on local regions of a potential surface (for example, the vicinity of a minimum or transition state), or may cover the surface globally. A second aspect of this program is the development of techniques to fit multi-dimensional potential surfaces to convenient, global, analytic functions that can then be used in dynamics calculations. Finally a third part of this program involves the use of direct dynamics for high dimensional problems to by-pass the need for surface fitting.

### Recent Results

**H<sub>2</sub>NOH:** The dominant pathway for the high temperature, thermal decomposition of H<sub>2</sub>NOH is dissociation to NH<sub>2</sub>+OH. However, recent shock tube studies by Michael et al, indicate that a second channel contributes significantly at lower temperatures. This second pathway has a lower activation energy and a lower A-factor than the dominant NH<sub>2</sub>+OH channel. Formation of HNO+H<sub>2</sub> is exothermic with respect to NH<sub>2</sub>+OH and thus is a possible candidate for the new pathway. However a recent theoretical study<sup>1</sup> reports the barrier for H<sub>2</sub>NOH→HNO+H<sub>2</sub> is significantly higher than the threshold for formation of NH<sub>2</sub>+OH. There are no other spin-allowed products exothermic with respect to NH<sub>2</sub>+OH. There are two possible spin-forbidden pathways exothermic with respect to NH<sub>2</sub>+OH, <sup>3</sup>NH+H<sub>2</sub>O and NH<sub>3</sub>+<sup>3</sup>O. This year we began a theoretical study of the H<sub>2</sub>NOH potential surface with the goal of identifying the second decomposition pathway. To date we have focused on spin-forbidden paths leading to either <sup>3</sup>NH+H<sub>2</sub>O or NH<sub>3</sub>+<sup>3</sup>O. Two mechanisms have been examined for each set of products:



Mechanisms (1a) and (1b) involve the initial formation of an H<sub>2</sub>N---OH hydrogen bonded complex which crosses to a triplet surface and then undergoes an internal hydrogen abstraction to form final products. Although singlet-triplet crossings for the hydrogen bonded complex are found at energies below that of the NH<sub>2</sub>+OH asymptote, the subsequent internal hydrogen abstractions are predicted to have barriers above the NH<sub>2</sub>+OH asymptote. Thus (1a) and (1b) are

not viable candidates for the second decomposition path. Mechanisms (2) and (3) both begin with (1,2) hydrogen migrations followed by N-O bond cleavage. In these mechanisms singlet-triplet crossings occur as the NO bond lengthens. For mechanism (2) the initial hydrogen migration is predicted to have a barrier in excess of the  $\text{NH}_2+\text{OH}$  asymptote. For mechanism (3) the hydrogen migration barrier is well below the  $\text{NH}_2+\text{OH}$  asymptote. Singlet and triplet MEP calculations for  $\text{H}_3\text{NO} \rightarrow \text{NH}_3+\text{O}$  demonstrate the existence of singlet-triplet crossings below the  $\text{NH}_2+\text{OH}$  asymptote (see Figure 1). A CCSD(T)/aug-cc-pvtz search for the minimum singlet-

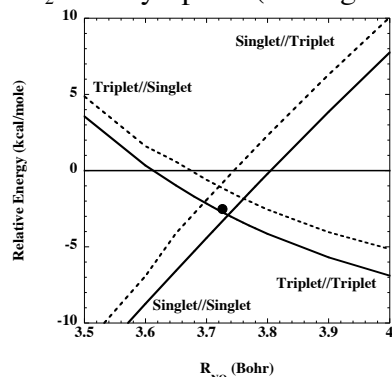
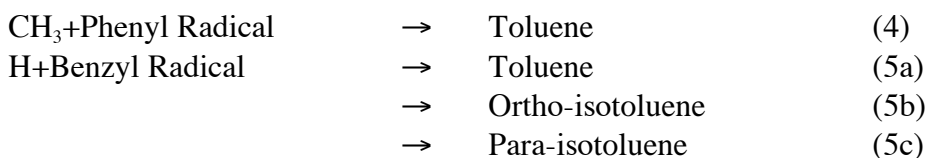


Figure 1. CCSD(T)/aug-cc-pvtz minimum energy paths (MEP's) for  $\text{H}_3\text{NO} \rightarrow \text{NH}_3+\text{O}$ . The solid line with positive slope is the singlet state MEP, the solid line with negative slope is the triplet state MEP. The dashed lines are the singlet state energies at the triplet state geometries and vice versa. The dot near the center is the location of the lowest intersection of the singlet and triplet surfaces. The horizontal line represents the energy of the  $\text{NH}_2+\text{OH}$  asymptote.

triplet crossing point in this region, using the Lagrangian method of Koga and Morokuma,<sup>2</sup> yields an energy of -2.5 kcal/mole, relative to  $\text{NH}_2+\text{OH}$ . We conclude then that mechanism (3) is the only viable candidate for the second decomposition channel identified to date. More work on this system is planned (in collaboration with Stephen Klippenstein) with the goal of determining whether or not the rate of (3) is consistent with that needed to explain the shock tube experiments.

**Radical-Radical Association Reactions:** This year we completed a study of the following radical-radical association reactions on the  $\text{C}_7\text{H}_8$  potential surface:



using the CASPT2-based, direct, variable reaction coordinate transition state theory technique we have developed over the last few years. More details concerning the rates of these reactions are given in Stephen Klippenstein's abstract.

We also undertook an extensive survey of the  $\text{C}_7\text{H}_8$  potential surface to address questions of competition between the above association/dissociation reactions and isomerizations amongst the various  $\text{C}_7\text{H}_8$  isomers. A number of processes with barriers at or below the dissociation threshold have been identified (see Figure 2). For example, the calculations predict that the barrier for isomerization from ortho-isotoluene to para-isotoluene (via meta-isotoluene) is lower than the H+benzyl radical dissociation limit. However, at combustion temperatures the dissociation rates are predicted to greatly exceed the isomerization rates, and therefore the kinetics of each isomer can be treated as simple, uncoupled association/dissociation equilibria.

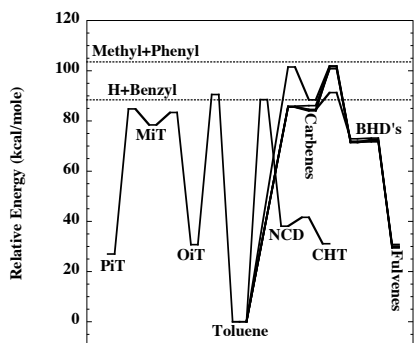
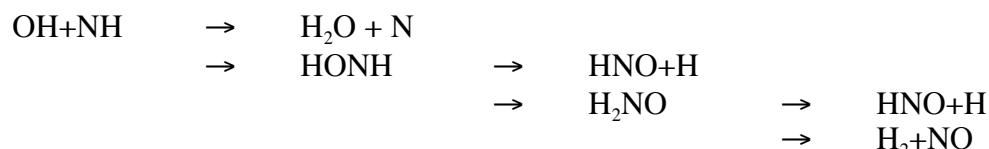


Figure 2. Relative energies for stationary points on the  $C_7H_8$  potential surface from CCSD(T)/aug-cc-pvtz//B3LYP/6-31G\* calculations. The nomenclature is as follows: OiT, MiT, and PiT refer to ortho, meta and para isotoluene, respectively, NCD to norcaradiene, CHT to cycloheptatriene, and BHD's to various methyl substituted [3.1.0]-bicyclohexadiene's.

**Future Work:** We intend to continue our studies of radical-radical reactions focusing on reactions involving resonance stabilized radicals and disproportionation reactions. The work on resonance stabilized radicals will initially focus on H atoms reacting with propargyl, allyl,  $CH_2CCCH$ ,  $CH_3CCCH_2$ ,  $CH_2CHCCH_2$ ,  $CH_3CHCCH$ , cyclic- $C_4H_5$ ,  $CH_2CCCCH$ ,  $CHCCHCCH$ , cyclic- $C_5H_5$ .

We also plan to fit global surfaces for both the lowest doublet and quartet states of  $H_2NO$ . These surfaces will allow us to then calculate rates for the reactions,



The reaction of OH with NH has been cited as an important reaction in combustion systems although no experimental data is yet available.

Finally, in collaboration with Stephen Gray, we plan new calculations on HCO. The best potential surface available today still yields large errors in the lifetimes of some of the low-lying resonance states. We plan to fit a new surface using CCSD(T)/aug-cc-pvqz calculations in an attempt to resolve this discrepancy between theory and experiment.

## References:

- (1) J. C. Mackie and G. B. Bacskay, *J. Phys. Chem. A* **109**, 11967 (2005)
- (2) N. Koga and K. Morokuma, *Chem. Phys. Lett.* **119**, 371 (1985)

**Acknowledgement:** This work was performed under the auspices of the Office of Basic Energy Sciences, Division of Chemical Sciences, Geosciences and Biosciences, U.S. Department of Energy, under Contract W-31-109-Eng-38.

## PUBLICATIONS (2004 - Present):

### Speciation of $C_6H_6$ Isomers by GC-Matrix Isolation FTIR-MS

K.B. Anderson, R.S. Trantor, W. Tang, K. Brezinsky and L.B. Harding  
*J. Phys. Chem. A* **108**, 3403-3405 (2004)

### A Global Analytic Potential Surface for Formaldehyde

X. Zhang, S. Zou, L.B. Harding and J.M. Bowman  
*J. Phys. Chem A* **108**, 8980-8986 (2004)

**The Roaming Atom: Straying from the Reaction Path in Formaldehyde Decomposition**

D. Townsend, S.A. Lahankar, S.K. Lee, S.D. Chambreau, A.G. Suits, X. Zhang,  
J. Rheinecker, L.B. Harding, and J.M. Bowman  
*Science* **306**, 1158 (2004)

**Reaction of Oxygen Atoms with Hydrocarbon Radicals: A Priori Kinetic Predictions for the CH<sub>3</sub>+O, C<sub>2</sub>H<sub>5</sub>+O and C<sub>2</sub>H<sub>3</sub>+O Reactions**

L.B. Harding, S.J. Klippenstein and Y. Georgievskii  
*Proc. Combust. Inst.*, **30**, 985-993 (2005)

**Rate Constants for the D+C<sub>2</sub>H<sub>4</sub> → C<sub>2</sub>H<sub>3</sub>D+H at High Temperature: Implications to the High Pressure Rate Constant for H+C<sub>2</sub>H<sub>4</sub> → C<sub>2</sub>H<sub>5</sub>**

J.V. Michael, M.-C. Su, J.W. Sutherland, L.B. Harding and A.F. Wagner  
*Proc. Combust. Inst.*, **30**, 965-973 (2005)

**Predictive Theory for Hydrogen Atom – Hydrocarbon Radical Association Kinetics**

L. B. Harding, Y. Georgievskii and S. J. Klippenstein  
*J. Phys. Chem. A* **109**,4646-4656(2005)

**The Determination of molecular properties from MULTIMODE with an application to the calculation of Franck-Condon factors for photoionization of CF<sub>3</sub> to CF<sub>3</sub><sup>+</sup>**

J. M. Bowman, X. Huang, L.B. Harding and S. Carter  
*Mol. Phys.* **104**, 33-45(2006)

**Methyl Radical: Ab Initio Global Potential Surface, Vibrational Levels, and Partition Function**

D. M. Medvedev, L.B. Harding and S. K. Gray  
*Mol. Phys.* **104**, 73-81(2006)

**Predictive Theory for the Association Kinetics of Two Alkyl Radicals**

S.J. Klippenstein, Y. Georgievskii, L.B. Harding  
*Phys. Chem. Chem. Phys.* **8**,1133-1147 (2006)

**Initiation in CH<sub>4</sub>/O<sub>2</sub>: High Temperature Rate Constants for CH<sub>4</sub>+O<sub>2</sub> → CH<sub>3</sub>+HO<sub>2</sub>**

N.K. Srinivasan, J.V. Michael, L.B. Harding and S.J. Klippenstein  
31<sup>st</sup> Symposium (International) on Combustion (accepted)

**Pyrolysis of Acetaldehyde, Rates for Dissociation and Following Chain Decomposition**

K.S. Gupte, J.H. Kiefer, R.S. Tranter, S.J. Klippenstein and L.B. Harding  
31<sup>st</sup> Symposium (International) on Combustion (accepted)

**On the Formation and Decomposition of C<sub>7</sub>H<sub>8</sub>**

S.J. Klippenstein, L.B. Harding and Y. Georgievskii  
31<sup>st</sup> Symposium (International) on Combustion (accepted)

# CHEMICAL ACCURACY FROM AB INITIO MOLECULAR ORBITAL CALCULATIONS

Martin Head-Gordon

Department of Chemistry, University of California, Berkeley, and,  
Chemical Sciences Division, Lawrence Berkeley National Laboratory,  
Berkeley, CA 94720.  
mhg@cchem.berkeley.edu

## 1. Scope of Project.

Short-lived reactive radicals and intermediate reaction complexes are believed to play central roles in combustion, interstellar and atmospheric chemistry. Due to their transient nature, such molecules are challenging to study experimentally, and our knowledge of their structure, properties and reactivity is consequently quite limited. To expand this knowledge, we develop new theoretical methods for reliable computer-based prediction of the properties of such species. We apply our methods, as well as existing theoretical approaches, to study prototype radical reactions, often in collaboration with experimental efforts. These studies help to deepen understanding of the role of reactive intermediates in diverse areas of chemistry. They also sometimes reveal frontiers where new theoretical developments are needed in order to permit better calculations in the future.

## 2. Summary of Recent Major Accomplishments.

### 2.1 *Time-dependent density functional theory calculations.*

Time-dependent density functional theory (TDDFT) is an in-principle exact framework for calculating excitation energies. We have recently published a major review of this approach and other methods for treating the excited states of large molecules [23]. Such calculations are feasible on systems up to about 100 non-hydrogen atoms on PC's.

We applied TDDFT to study excited states in biological systems [10,20,23], as well as other compounds [6,16,24]. Perhaps the most interesting results were on excited states of models of chlorophyll and associated carotenoids that are found in the photosynthetic light-harvesting complex. Our calculations [20,23] are relevant to the mechanism of non-photochemical quenching (NPQ); the process by which excited chlorophyll molecules are directly relaxed under high-light conditions to prevent damage to the reaction center. We showed that both direct singlet-singlet excitation energy transfer, and also a novel electron transfer reaction are energetically feasible. If the latter process is operative, we suggested that it may be experimentally probed by seeking the spectral signature of the carotenoid radical cation under high-light conditions. Such detection has subsequently been accomplished in Graham Fleming's group at LBNL.

### 2.2 *Failure of TDDFT for charge-transfer excited states.*

While TDDFT calculations are clearly often useful, they are far from perfect. For instance various reports suggest poor results for charge-transfer excited states. We have

examined the charge-transfer problem in considerable detail [1,23], and, for the first time clarified both the nature of the problem, and its origin. The long-range Coulomb attraction between donor and acceptor is *entirely absent* in TDDFT using local and gradient corrected functionals. A correct description requires 100% non-local exact exchange. Thus the popular B3LYP functional, which includes 20% exact exchange, has 20% of the correct Coulomb attraction! We also suggested a simple work-around which uses a hybrid of single excitation CI (CIS) (which has 100% exact exchange) for charge-transfer excited states, and regular TDDFT for the localized excitations. Finding more satisfactory solutions to this fundamental problem is an important issue, which we are actively engaged in.

### 2.3 *Electron correlations in molecules.*

For molecular ground states, the highest levels of accuracy currently possible come from wavefunction-based calculations, such as CCSD(T) (which are dramatically more expensive than DFT). Yet for radicals, CCSD(T) quite often performs more poorly than for closed shell molecules. In addition to new (more expensive) alternatives, we have found that the poor CCSD(T) results can be greatly improved by using Kohn-Sham orbitals. These effects are particularly dramatic for systems that contain transition metals, as we have recently demonstrated [13]. We have also addressed the problem of identifying and visualizing the most important correlations from the CCSD doubles amplitudes [4], using a singular value decomposition.

### 2.4 *Characterizing unpaired electrons in radicals.*

We have proposed a new definition of the unpaired electrons in molecules [8]. This approach is based on characterizing radical, diradical and polyradical character in molecules by manipulating the wavefunction itself to find the orbitals which have the highest probability of single occupancy (for radical character) or simultaneous single occupancy (for diradical character, and higher). These method may be useful in helping to qualitatively characterize complex wavefunctions, and to visualize strong correlations in molecules.

### 2.5 *Application to radicals and radical-radical coupling reactions.*

Radicals such as the neutral PAH, C<sub>13</sub>H<sub>9</sub> (phenalenyl), and the TCNE anion are known experimentally to form stable pi dimers, characterized by stacking distances of about 3 Angstroms; too short for van der Waal complexes, and yet far too long for a conventional chemical bond. We have recently attempted to understand the nature of this fascinating bonding [2,6], which we find to be a dispersion-assisted diradicaloid bond. Weak bonding interactions between the monomers together with dispersion-driven attraction are sufficient to overcome Pauli repulsions between filled levels and permit approach inside the usual van der Waals radius. Upon ionization of the phenalenyl dimer, there are significant electrostatic perturbations that, remarkably, cause the “1-electron bond” to be stronger than the “2-electron bond”. Almost equally remarkably, the alternative mode of dimerization, which is the formation of a sigma linkage between the (phenalenyl) radicals

has a bond strength that is almost exactly the same as the pi dimer: about 16 kcal/mol [24,26]. This reflects the large loss of aromaticity associated with sigma dimerization.

### 3. Summary of Research Plans.

- Exploration of ways to solve the charge-transfer problem in TDDFT, by functionals that include 100% exact exchange at long-range, while leaving the short-range interactions essentially unmodified.
- Development and testing of simplified coupled cluster methods for radicals and diradicals. We are seeking to extend the imperfect pairing model, which has only been defined for closed shell systems hitherto, to radicals. We are also exploring ways to overcome some unwanted artifacts such as symmetry breaking.
- Studies of the properties of reactive radicals and radical reactions. Since many of our computational tools are developed in-house, we have capabilities that are not broadly available to treat unsaturated radical and diradicaloid molecules.

### 4. Publications from DOE Sponsored Work, 2004-present.

- [1] "Failure of time-dependent density functional theory for long-range charge-transfer excited states: the zincbacteriochlorin-bacteriochlorin and bacteriochlorophyll-spheroidene complexes", A. Dreuw and M. Head-Gordon, *J. Am. Chem. Soc.* 126, 4007-4016 (2004).
- [2] "What is the nature of the long bond in the (TCNE)<sub>2</sub><sup>(2-)</sup> π dimer?", Y. Jung and M. Head-Gordon, *Phys. Chem. Chem. Phys.* 6, 2008-2011 (2004).
- [3] "The spatial size of Fe(II) spin states and the spin-dependence of the structure of Fe(II)-porphyrins", J.M. Ugalde, B. Dunietz, A. Dreuw, M. Head-Gordon and R.J. Boyd, *J. Phys. Chem. B* 108, 4653-4657 (2004)
- [4] "Extracting dominant pair correlations from many-body wavefunctions", G.J.O. Beran and M. Head-Gordon, *J. Chem. Phys.* 121, 78-88 (2004).
- [5] "Initiation of electro-oxidation of CO on Pt-based electrodes at full coverage conditions simulated by ab initio electronic structure calculations", B.D. Dunietz, N. Markovic, G. Somorjai, P.N. Ross and M. Head-Gordon, *J. Phys. Chem B* 108, 9888-9892 (2004).
- [6] "Intermolecular π-to-π bindings between stacked aromatic dyads. Experimental and theoretical binding energies and NIR optical transitions for phenalenyl radical/radical versus radical/cation dimerization", D. Small, Vladimir Zaitsev, Yousung Jung, Sergiy V. Rosokha, Martin Head-Gordon and Jay K. Kochi, *J. Am. Chem. Soc.* 126, 13850-13858 (2004).
- [7] "An efficient method for calculating maxima of homogeneous functions of orthogonal matrices: Applications to localized occupied orbitals", J.E. Subotnik, Y. Shao, W. Liang and M. Head-Gordon, *J. Chem. Phys.* 121, 9220-9229 (2004).
- [8] "An orbital-based definition of radical and multi-radical character", A.D. Dutoi, Y. Jung, and M. Head-Gordon, *J. Phys. Chem. A* 108, 10270-10279 (2004).
- [9] "Scaled opposite spin second order correlation energy: An economical electronic structure method", Y. Jung, R. Lochan, A.D. Dutoi, and M. Head-Gordon, *J. Chem. Phys.* 121, 9793-9802 (2004).
- [10] "Ultra-fast photo-initiated long-range electron transfer in cyclophane-bridged zincporphyrin-quinone complexes via conical intersections", A. Dreuw, G.A. Worth, M. Head-Gordon, and L.S. Cederbaum, *J. Phys. Chem. B* 108, 19049-19055 (2004)
- [11] "A localized basis that allows fast and accurate second order Moller-Plesset calculations", J.E. Subotnik and M. Head-Gordon, *J. Chem. Phys.* 122, 034109 (2005) (9 pages).

- [12] "Auxiliary basis expansions for large-scale electronic structure calculations", Y. Jung, A. Sodt, P.M.W. Gill and M. Head-Gordon, Proc. Nat. Acad. USA 102, 6692-6697 (2005).
- [13] "Nitrogen activation via 3-coordinate molybdenum complexes: Comparison of density functional theory performance with wave function based methods", D.C. Graham, G.J.O. Beran, M. Head-Gordon, G. Christian, R. Stranger, and B.F. Yates, J. Phys. Chem. A 109, 6762-6772 (2005).
- [14] "Scaled opposite spin second order Moller-Plesset theory with improved physical description of long-range dispersion interactions", R.C. Lochan, Y. Jung, and M. Head-Gordon, J. Phys. Chem. A 109, 7598-7605 (2005).
- [15] "Decay behavior of least-squares expansion coefficients", P.M.W. Gill, A.T.B. Gilbert, S.W. Taylor, G. Friesecke, and M. Head-Gordon, J. Chem. Phys. 123, 061101 (2005)
- [16] "Search for stratospheric bromine reservoir species: theoretical study of the photostability of mono-, tri-, and pentacoordinated bromine compounds", T.J. Lee, C.N. Mejia, G.J.O. Beran, and M. Head-Gordon, J. Phys. Chem. A 109, 8133-8139 (2005).
- [17] "A local correlation model that yields intrinsically smooth potential energy surfaces", J.E. Subotnik and M. Head-Gordon, J. Chem. Phys. 123, 064108 (2005).
- [18] "Fast electronic structure methods for strongly correlated molecular systems", M. Head-Gordon, G.J.O. Beran, A. Sodt, and Y. Jung, J. Phys.: Conf. Ser. 16, 233-242 (2005).
- [19] "A Resolution-Of-The-Identity Implementation of the Local Triatomics-In-Molecules Model for Second Order Møller-Plesset Perturbation Theory with Application to Alanine Tetrapeptide Conformational Energies", R.A. DiStasio Jr, Y. Jung, and M. Head-Gordon, J. Chem. Theor. Comput. 1, 862-876 (2005).
- [20] "Role of electron-transfer quenching of chlorophyll fluorescence by carotenoids in non-photochemical quenching of green plants", A. Dreuw, G.R. Fleming and M. Head-Gordon, Biochem. Soc. Trans. 33, 858-862 (2005).
- [21] "Fast localized orthonormal virtual orbitals which depend smoothly on nuclear coordinates", J.E. Subotnik, A.D. Dutoi, and M. Head-Gordon, J. Chem. Phys. 123, 114108 (2005) (9 pages).
- [22] "Unrestricted perfect pairing: The simplest wave-function-based model chemistry beyond mean field", G.J.O. Beran, B. Austin, A. Sodt, and M. Head-Gordon, J. Phys. Chem. A 109, 9183-9192 (2005)
- [23] "Single reference ab initio methods for the calculation of excited states of large molecules", A. Dreuw and M. Head-Gordon, Chem. Rev. 105, 4009-4037 (2005).
- [24] "Characterizing the dimerizations of phenalenyl radicals by ab initio calculations and experiments:  $\sigma$ -bond formation vs resonance  $\pi$ -stabilization", D. Small, S.V. Rosokha, J.K. Kochi and M. Head-Gordon, J. Phys. Chem. A 105, 11261-11267 (2005).
- [25] "Accuracy and limitations of second order many-body perturbation theory for predicting vertical detachment energies of solvated-electron clusters", J.M. Herbert and M. Head-Gordon, Phys. Chem. Chem. Phys. 8, 68-78 (2006).
- [26] "Steric modulations in the reversible dimerizations of phenalenyl radicals via unusually weak  $\pi$ - and  $\sigma$ - carbon-centered bonds", V. Zaitsev, S.V. Rosokha, M. Head-Gordon, and J.K. Kochi, J. Org. Chem. 71, 520-526 (2006).
- [27] "A fast implementation of perfect pairing and imperfect pairing using the resolution of the identity approximation", A. Sodt, G.J.O. Beran, Y. Jung, B. Austin, and M. Head-Gordon, J. Chem. Theor. Comput. 2, 300-305 (2006).
- [28] "Second order correction to perfect pairing: an inexpensive electronic structure method for the treatment of strong electron-electron correlations", G.J.O. Beran, M. Head-Gordon, and S.R. Gwaltney, J. Chem. Phys. 124, 114107 (2006) (15 pages).
- [29] "The localizability of valence space electron-electron correlations in pair-based coupled cluster models", G.J.O. Beran and M. Head-Gordon, Mol. Phys. 104, 1191-1206 (2006).

## Laser Studies of Combustion Chemistry

John F. Hershberger

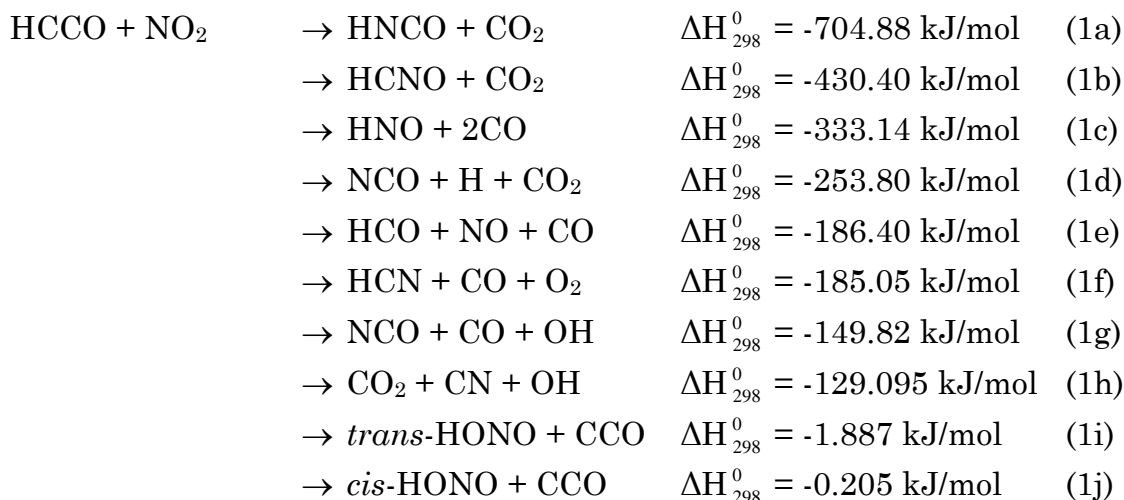
Department of Chemistry  
North Dakota State University  
Fargo, ND 58105  
john.hershberger@ndsu.edu

Time-resolved infrared absorption and laser-induced fluorescence spectroscopy are used in our laboratory to study the kinetics and product channel dynamics of chemical reactions of importance in the gas-phase combustion chemistry of nitrogen-containing radicals. This program is aimed at improving the kinetic database of reactions crucial to the modeling of NO<sub>x</sub> control strategies such as Thermal de-NO<sub>x</sub>, RAPRENO<sub>x</sub>, and NO-reburning. The data obtained is also useful in the modeling of propellant chemistry. The emphasis in our study is the quantitative measurement of both total rate constants and product branching ratios.

### HCCO+NO<sub>2</sub> Reaction

#### A. HCCO+NO<sub>2</sub>

Experimental studies on the HCCO+NO<sub>2</sub> reaction were reported in a previous abstract (for the 2005 Combustion meeting). Many possible exothermic product channels exist:

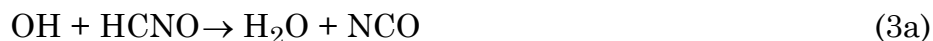


The primary product channels observed were HCNO+CO<sub>2</sub> ( $\phi=0.40$ ) and HCO+NO+CO ( $\phi=0.60$ ).<sup>1</sup> The second product channel was inferred somewhat indirectly from the CO and CO<sub>2</sub> yields, assuming any HCO formed would quickly react with NO<sub>2</sub>. Although the assumptions made were reasonable, we felt that it was important to examine this reaction with computational methods, primarily to investigate whether a low energy pathway to HCO+NO+CO products exists on the potential energy surface. Therefore, we have performed ab initio calculations of the potential energy surface of this reaction. Intermediates and transition states were optimized at the CCSD(T)/6-31G(d,p) level of theory, and single-point energy calculations at the CCSD(T)/6-311++G(2d,p) level were performed. We find that formation of a C-N bonded HC(NO<sub>2</sub>)CO intermediate followed by a four-center transition state to an HC(NO)C(O)O intermediate represents a facile pathway to the HCNO+CO<sub>2</sub> products. Alternatively, formation of an initial OCC(H)ONO intermediate may result in sequential NO and CO loss to form HCO+NO+CO products. Other pathways to this product channel were found as well. Pathways to other channels (such as HNCO+CO<sub>2</sub> and HNO+2CO) were found, but they involved multiple rearrangements, one of which is via a fairly high energy three-center transition state. In general, our calculations provide evidence that HCO+NO+CO is a reasonable product channel, in agreement with our interpretation of the experiments. Other workers have performed similar studies,<sup>2</sup> although at different level of theory, and have obtained similar conclusions.

One issue that may warrant re-investigation involves the HNO channel. When we performed the experimental study, we did not have the right diode laser for sensitive detection of HNO. More recently, we have acquired a diode laser near  $\sim 2700$  cm<sup>-1</sup> which can detect HNO, and have developed a method of calibrating such signals.

## HCNO Kinetics

There is virtually no literature data available on the kinetics of HCNO, the fulminic acid molecule. After recent work in our laboratory to synthesize pure HCNO for infrared absorption coefficient calibration purposes, we are in a position to examine reaction kinetics of this species. The HCNO synthesis is slow and inefficient, but our reaction cell geometry is ideally suited to dealing with reagents that are only available in small quantities. We have recently completed a study of the kinetics and product branching of the OH+HCNO reaction, which plays an important role in NO-reburning mechanisms:<sup>3</sup>





Initially, we produced OH using 193 nm photolysis of N<sub>2</sub>O to produce O(<sup>1</sup>D), followed by reaction with H<sub>2</sub>O. We have verified that the small amount of H<sub>2</sub>O does not significantly increase the rate of HCNO decomposition in our cell. More recently, we have used 248 nm photolysis of H<sub>2</sub>O<sub>2</sub> to directly form OH. This approach is preferable because the UV absorption of HCNO is much smaller at 248 nm than at 193 nm. Secondary reactions involving HCNO photofragments are therefore less prevalent when using 248 nm photolysis. Our measured total rate constants are the same using either method, but only the 248 nm photolysis is suitable for product detection.

For total rate constant measurements, OH is detected by laser-induced fluorescence at 307.966 nm. We obtain a rate constant of:

$$k(T) = (2.69 \pm 0.41) \times 10^{-12} \exp[(750.2 \pm 49.8)/T] \text{ cm}^3 \text{ molecule}^{-1} \text{ s}^{-1}$$

over the temperature range 298-386 K. At 296 K, the rate constant is  $k = (3.39 \pm 0.3) \times 10^{-11} \text{ cm}^3 \text{ molecule}^{-1} \text{ s}^{-1}$ . The measurements are restricted to a limited temperature range because of the instability of HCNO at high temperatures. The 296 K rate constant is somewhat higher than the preliminary value reported in last year's report. The primary improvement in our experiments is that we have optimized the conditions necessary for reliable synthesis of high-purity HCNO.

This is the first experimental measurement reported on this reaction, and the 296 K rate constant is in excellent agreement with an estimate of  $3.32 \times 10^{-11} \text{ cm}^3 \text{ molecule}^{-1} \text{ s}^{-1}$  used in a modeling study.<sup>4</sup>

Infrared diode absorption spectroscopy was used to detect CO, CO<sub>2</sub>, NO, N<sub>2</sub>O, CH<sub>2</sub>O, and HNO products. N<sub>2</sub>O was formed by NCO+NO secondary chemistry when NO reagents were included in the reaction mixture. HCNO photolysis produces background signals that were substantial for some but not all of the detected products. Subtraction of product yields obtained without the H<sub>2</sub>O<sub>2</sub> precursor was used to correct for this effect. After consideration of possible secondary chemistry, we conclude that channel (3f) and (3c) predominate, with branching fractions of  $0.61 \pm 0.06$  and  $0.35 \pm 0.06$ , respectively. Channel (3e) also appears as a minor contribution, with  $\phi = 0.04 \pm 0.02$ . Surprisingly, channel (3a) appears to not be significant.

We have also begun work on the CN + HCNO reaction:





CN is produced by photolysis of ICN or C<sub>2</sub>N<sub>2</sub>, and detected by LIF at ~388 nm. We have obtained the following rate constants:

$$k = (3.95 \pm 0.53) \times 10^{-11} \exp[(287 \pm 45)/T] \text{ cm}^3 \text{ molecule}^{-1} \text{ s}^{-1} \text{ (T=298-388 K)}$$

$$k \text{ (296 K)} = (1.03 \pm 0.04) \times 10^{-10} \text{ cm}^3 \text{ molecule}^{-1} \text{ s}^{-1}$$

Work on identifying product channels is ongoing. Preliminary data suggests that NCO+HCN and HCCN+NO are the major channels.

Future plans include kinetic measurements of other radical species reacting with HCNO, including NCO+HCNO, NH+HCNO, etc.

## References

1. J.P. Meyer and J.F. Hershberger, *J. Phys. Chem. A* **109**, 4772 (2005).
2. M.T. Hien, T.L. Nguyen, S.A. Carl, and M.T. Nguyen, *Chem. Phys. Lett.* **416**, 199 (2005).
3. J.A. Miller, S.J. Kilppenstein, and P. Glarborg, *Comb. Flame* **135**, 357 (2003).

## Publications acknowledging DOE support (2004-present)

“Kinetics of the CCO+NO and CCO+NO<sub>2</sub> Reactions”, W.D. Thweatt, M.A. Erickson, and J.F. Hershberger, *J. Phys. Chem. A* **108**, 74 (2004).

“Product Channels of the HCCO+NO Reaction”, J.P. Meyer and J. F. Hershberger, *J. Phys. Chem. B* **109**, 8363 (2005).

“Kinetics of the HCCO+NO<sub>2</sub> Reaction”, J.P. Meyer and J.F. Hershberger, *J. Phys. Chem. A* **109**, 4772 (2005).

“Kinetics of the OH+HCNO Reaction”, W. Feng, J.P. Meyer, and J.F. Hershberger, *J. Phys. Chem. A* **110**, 4458 (2006).

“Ab Initio Study of the HCCO+NO<sub>2</sub> Potential Energy Surface”, J.P. Meyer and J.F. Hershberger, *Chem. Phys.*, accepted.

## **Terascale High-Fidelity Simulations of Turbulent Combustion with Detailed Chemistry (TSTC) <http://purl.org/net/tstc>**

SciDAC: Computational Chemistry  
(DOE Office of Science, BES: Chemical Sciences, Program Manager: R. Hilderbrandt)  
Work-in-Progress Report – *Period from 04/01/05 to 03/31/06*

### **Principal Investigators**

- Hong G. Im (University of Michigan, UMI, [hgim@umich.edu](mailto:hgim@umich.edu))
- Arnaud Trouvé (University of Maryland, UMD, [atrouve@eng.umd.edu](mailto:atrouve@eng.umd.edu))
- Christopher J. Rutland (University of Wisconsin, UW, [rutland@engr.wisc.edu](mailto:rutland@engr.wisc.edu))
- Jacqueline Chen (Sandia National Laboratories, SNL, [jhchen@ca.sandia.gov](mailto:jhchen@ca.sandia.gov))

### **Project Summary**

The TSTC project is a multi-university collaborative effort to develop a high-fidelity turbulent reacting flow simulation capability utilizing terascale, massively parallel computer technology. The main paradigm of our approach is direct numerical simulation (DNS) featuring highest temporal and spatial accuracy, allowing quantitative observations of the fine-scale physics found in turbulent reacting flows as well as providing a useful vehicle towards description of sub-models needed in device-level simulations. The new S3D software is enhanced with new numerical algorithms and physical models to provide predictive capabilities for spray dynamics, combustion, and pollutant formation processes in turbulent combustion.

### **Program Scope**

The primary goal of the SciDAC TSTC project for FY04-07 is to extend the S3D code with enhanced physical and algorithmic modules, and undertake several large-scale simulations to investigate important scientific issues. The specific objectives of this project include:

- To enhance the computational architecture and numerical algorithms in order to allow more robust, accurate, and efficient simulations of multi-dimensional turbulent combustion in the presence of strong turbulence and chemical stiffness. The efforts include new algorithms for characteristic boundary condition treatment and improved code architecture for various hardware platforms.
- To expand and upgrade the physical submodels to describe the underlying mechanisms in greater detail. The existing modules of radiation, soot, and spray evaporation models are being further enhanced to reproduce realistic combustion processes. In particular, advanced soot formation model to account for detailed soot precursors and improved spray model to incorporate droplet distortion effects are being developed.
- To demonstrate the capability of the terascale DNS code in investigating fundamental science issues by several pilot simulations of canonical flames that can be reproduced in the laboratory. The pilot configurations proposed for TSTC Phase II include turbulent counterflow and jet flames, and turbulent spray jet evaporation and ignition problems. The large scale simulation data will be analyzed for science discovery by incorporating efficient data-mining and visualization tools through the partnership with other projects sponsored by the SciDAC program.

## **Recent Progress**

We present here a summary of progress made during the past 12 months work period of this project extending from 04/01/05 to 03/31/06.

### ***Computational developments:***

- As part of the 2005 Joule Software Effectiveness study, S3D have been ported to the Cray X1 and XT3 platforms at the NCCS/ORNL. Furthermore, several key modules of S3D were optimized and rewritten to improve the performance of the code on different platforms. As a result, the performance improved by 45% on the scalar architectures. The new modules were also suitable for vectorization, which enabled a terascale combustion science simulation on the Cray X1E (SNL).

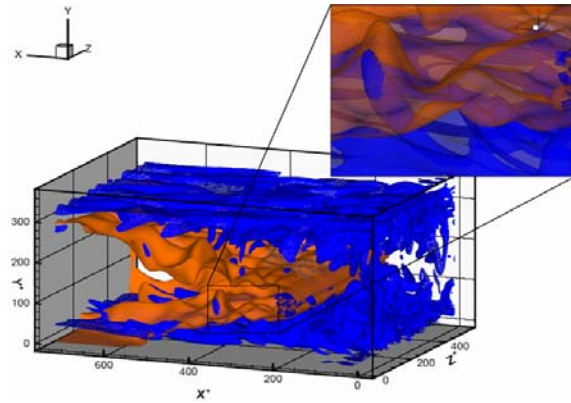


Figure 1: 3D simulation of the flame-wall interaction in a spatially developing configuration where the premixed flame is anchored at the center of the channel.

- A new turbulence injection procedure have been developed, which allows time evolving turbulence from an ancillary cold non-reacting DNS to be fed in at the inflow of the main reacting DNS. This procedure was used in the DNS of a spatially developing flame-wall interaction problem (Figure 1), where a realistic wall-bounded turbulence inflow was necessary for accuracy (SNL).
- The characteristic boundary conditions have been further extended to account for multi-dimensional, viscous, and reaction effects in nonreflecting and solid surface boundaries. The new development shows great promise in successful simulations of many challenging problems such as turbulent counterflow flames, spray combustion, and wall-bounded combustion problems (UMI/UMD).

### ***Physical model developments:***

- As ongoing efforts under the Joule Software Effectiveness Study, two alternative radiative heat transfer models, discrete ordinate method (DOM) and discrete transfer method (DTM) have been validated and tested for their performance metrics in multi-dimensional DNS (UMI/UMD). The spray module has also been tested for its effectiveness in conjunction with the improved outflow characteristic boundary conditions (UWI/UMI).

### ***New combustion science:***

- Using the developed radiation and soot models, characteristics of soot formation in turbulent nonpremixed flames have been studied, in which the effects of turbulent transport on the transient soot dynamics and their impact on the overall soot production have been examined in

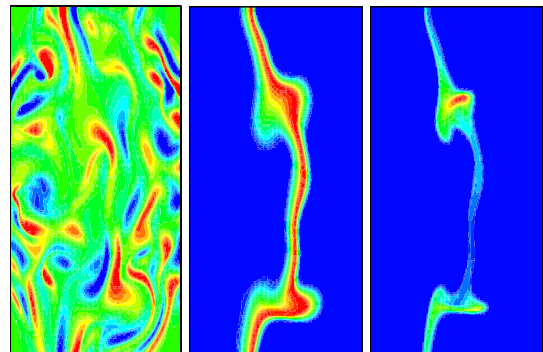


Figure 2: Simulations of turbulent nonpremixed ethylene-air flames, showing from left to right the vorticity, temperature, and soot volume fraction.

detail (Figure 2). The study revealed the importance of detailed information of the local and transient flow-chemistry interaction in accurate prediction of the soot formation characteristics (UMI).

- 2D simulations have been performed on the basic interaction of a turbulent ethylene-air jet diffusion flame with cold solid wall boundaries. The results revealed flame extinction events due to excessive wall cooling, and convective heat transfer up to  $100 \text{ kW/m}^2$ . The structure of the simulated wall flames is studied in terms of a classical fuel-air-based mixture fraction and an excess enthalpy variable. The current simulations account for soot (using a semi-empirical soot formation model) and thermal radiation (using the gray gas assumption and DOM or DTM) (UMD).
- 2D simulations of a fuel spray jet were performed to investigate the ignition and propagation of the flame front. Figure 3 shows the temperature contours in an evolving fuel spray jet, where the black line denotes the stoichiometric line. It is seen that ignition first occurs at the edges of the spray jets rather than the tip region which is subjected to stronger evaporative cooling. The improved characteristic boundary conditions and enhance code efficiency with a large number of droplets have enabled successful demonstration of accurate and robust realization of fuel spray combustion (UWI).

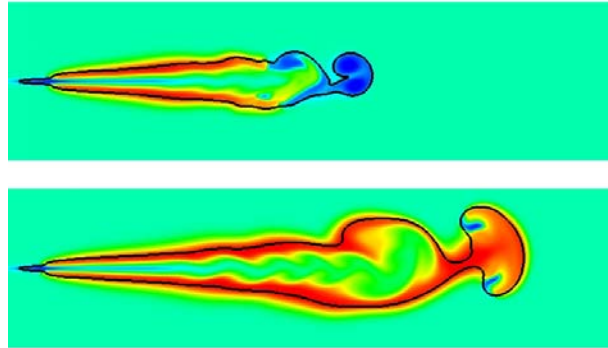


Figure 3: Temperature contours of combustion in the evolving fuel spray jet.

### **Future Plans**

- As the first pilot demonstration case study incorporating all the physical models developed under this project, large scale 3D simulations will be conducted for turbulent nonpremixed flames in the presence of mean flow strain and fine water droplets. The targeted science issue to be addressed is fundamental characteristics of flame suppression by the complex interaction between turbulence, chemistry, radiation, and water spray. The high quality simulation data with full consideration of multi-physics processes will allow understanding of the key mechanisms in the flame quenching behavior (UMI/UMD/UWI/SNL).
- A parallel particle tracking algorithm will be implemented into S3D to study the temporal evolution of fluid parcels undergoing turbulence-chemistry interaction. A further extension of this tool will be made in the form of an iso-surface elements tracking algorithm which will track elements of a chosen iso-surface as it propagates against the flow (SNL).
- 3D simulations will be conducted on two-stage ignition behavior in a three-dimensional jet flow with fuel spray. In the simulation, some 20 million computational meshes will be used and half million liquid droplets will be included (UWI).
- Improved characteristic boundary conditions will be developed for open and solid boundaries (UMI/UMD).
- Advanced soot models will be developed based on the method of moments (UMI).

## **Publications**

### ***Journals (2004-2006)***

1. E. R. Hawkes, R. Sankaran, J. Sutherland, and J. H. Chen (2006), "Scalar mixing in direct numerical simulations of temporally-evolving plane jet flames with detailed CO/H<sub>2</sub> kinetics," *Proc. Combust. Inst.*, **31**, accepted.
2. R. Sankaran, E. R. Hawkes, J. H. Chen, T. Lu, and C. K. Law (2006), "Structure of a spatially-developing lean methane-air turbulent bunsen flame," *Proc. Combust. Inst.*, **31**, accepted.
3. Yoo, C. S. and Im, H. G. (2006), "Transient soot dynamics in turbulent nonpremixed ethylene-air counterflow flames," *Proc. Combust. Inst.*, **31**, accepted.
4. Chen, J. H., Hawkes, E. Sankaran, R., Mason, S. D., and Im, H. G. (2006), "Direct numerical simulation of ignition front propagation in a constant volume with temperature inhomogeneities, Part I: Fundamental analysis and diagnostics," *Combustion and Flame*, **145**:128-144.
5. Hawkes, E., Sankaran, R., Pébay, P. P., and Chen, J. H. (2006), "Direct numerical simulation of ignition front propagation in a constant volume with temperature inhomogeneities, Part II: Parametric Study," *Combustion and Flame*, **145**:145-159.
6. Wang, Y. and Trouvé A. (2006), "Direct numerical simulation of non-premixed flame-wall interactions", *Combustion and Flame, Combust. Flame*, **144**:461-475.
7. Yoo, C. S., Wang, Y., Trouvé A. and Im, H. G. (2005), "Characteristic boundary conditions for direct simulations of turbulent counterflow flames", *Combust. Theory Modelling*, **9**:617-646.
8. Sankaran, R., Im, H. G., Hawkes, E. R. and Chen, J. H. (2004), "The effects of nonuniform temperature distribution on the ignition of a lean homogeneous hydrogen-air mixture," *Proc. Combust. Inst.*, **30**:875-882.
9. Yoo, C. S. and Im, H. G. (2004), "Transient dynamics of edge flames in a laminar nonpremixed hydrogen-air counterflow," *Proc. Combust. Inst.*, **30**:349-356.
10. Wang, Y. and Rutland, C. J. (2004), "Effects of temperature and equivalence ratio on the ignition of n-heptane fuel droplets in turbulent flow," *Proc. Combust. Inst.*, **30**:893-900.
11. Wang, Y. and Trouvé, A. (2004), "Artificial acoustic stiffness reduction in fully compressible, direct numerical simulation of combustion," *Combust. Theory Modelling*, **8**:633-660.

### ***Selected Recent Communications***

1. Sankaran, R., Hawkes, E. R., Chen, J. H., Lu, T., and Law, C. K. (2006), "Study of premixed flame thickness using direct numerical simulation in a slot burner configuration," *44th AIAA Aerospace Sciences Meeting and Exhibit*, January 9-12, Reno, NV., Paper No. 2006-0165.
2. Wang, Y. and Rutland, C. J. (2005), "On the ignition of turbulent liquid fuel spray jets using direct numerical simulation," *58th APS Annual Meeting of the Division of Fluid Dynamics*, Chicago, IL, November 20-22.
3. Yoo, C. S. and Im, H. G. (2005), "Transient dynamics of soot in ethylene-air nonpremixed counterflow flames," *Technical Meeting of the Eastern States Section*, The Combustion Institute, University of Central Florida, Orlando, FL, November 13-15.
4. Im, H. G. (2005), "High-speed, high-fidelity simulation of reacting flows towards energy and environmental research," *The 2005 US-Korea Conference on Science, Technology and Entrepreneurship*, August 11-13, Irvine, California.
5. Yoo, C. S., Im, H. G., Wang, Y. and Trouvé A. (2005), "Improved Navier-Stokes characteristic boundary conditions for direct simulations of compressible reacting flows", *3rd MIT Conf. Computational Fluid and Solid Mech.*, Cambridge, MA, June 13-16.
6. Williamson, J., McGill, J., Hu, Z., Kohout, A., Wang, Y., and Trouve, A. (2005), "Direct and large-eddy simulation for fire safety applications," *Computational Engineering and Science Conference*, Washington, DC, April 26-27, Poster Presentation.
7. Im, H. G., Rutland, C. J., Trouve, A., Chen, J. H., Yoo, C. S., Wang, Y., Wang, Y., Hawkes, E. R., Sankaran, R. (2005), "Terascale high-fidelity simulations of turbulent combustion with detailed chemistry," *Computational Engineering and Science Conference*, Washington, DC, April 26-27, Poster Presentation.
8. Hawkes, E. R., Chen, J. H., Sankaran, R., and Im, H. G. (2005), "Direct numerical simulations of ignition front propagation in a constant volume with thermal stratification," *European Combustion Meeting 2005*, Louvain-la-Neuve, April 3-6, 2005.
9. Wang, Y. (2005), "A general approach to creating FORTRAN interface for C++ application libraries," *International High Performance Computing and Applications Conference*, Shanghai, China, August 8-10.

# IONIZATION PROBES OF MOLECULAR STRUCTURE AND CHEMISTRY

Philip M. Johnson  
Department of Chemistry  
Stony Brook University, Stony Brook, NY 11794  
Philip.Johnson@sunysb.edu

## PROGRAM SCOPE

Photoionization processes provide very sensitive probes for the detection and understanding of molecules and chemical pathways relevant to combustion processes. Laser based ionization processes can be species-selective by using resonances in the excitation of the neutral molecule under study or by exploiting different sets of ionization potentials of different molecules. Therefore the structure and dynamics of individual molecules can be studied, or species monitored, even in a mixed sample. We are continuing to develop methods for the selective spectroscopic detection of molecules by ionization, to use these spectra for the greater understanding of molecular structure, and to use these methods for the study of some molecules of interest to combustion science.

## RECENT PROGRESS

The introduction of a high resolution CW pulse-amplified dye laser into our laboratory has given us the capability of studying the spectroscopy and photophysics of larger, less symmetric molecules with rotational resolution. To exploit this capability, recently we have been looking at various interesting properties of the molecules benzonitrile and phenylacetylene. These molecules have both singlet-singlet and photoinduced Rydberg ionization (PIRI) transitions in the wavelength range of the high resolution CW pulse-amplified dye laser, enabling a more controlled examination of the spectroscopy and energy dynamics of both the neutral and cationic species.

## Calculations of the vibrational structure of symmetry forbidden electronic transitions

Vibronic coupling is a relatively old topic, and over the years many theoretical groups have developed the capability to calculate the effects of vibrational-electronic coupling, even including sophisticated treatments of conical intersections and Jahn-Teller coupling. In particular there have been many attempts to analyze the vibrational spectral structure of a forbidden electronic transition. These have mostly been applied to systems where there are only a few possible inducing modes in the spectrum, such as the  $S_1 \leftarrow S_0$  transition of benzene.

It turns out that the  $\tilde{B}-\tilde{X}$  PIRI transition of the benzonitrile cation is forbidden electronically. This is a  $C_{2v}$  molecule, however, and there are 21 different vibrations that can induce transition intensity. We have recorded the vibrational spectrum of this molecule from three different lower vibrational levels of differing symmetry, and wished to be able to assign the vibrational structure we observe.

The revolution in electronic spectroscopy caused by the use of electronic structure programs by experimentalists has been impressive. The capability of non-specialists to be able to calculate fairly accurate vibrational frequencies has greatly reduced the guesswork involved in assigning vibrational structure. More recently, good programs have become available that

calculate Franck-Condon factors from the vibrational vectors produced by the electronic structure programs. These have enabled even better results, because now the intensities of the experimental lines provide verifiable information, at least for allowed transitions. We have analyzed the vibrational structure of the allowed  $\tilde{C}-\tilde{X}$  transition of phenylacetylene cation, and find a remarkable agreement between the spectrum and the calculated vibrational positions and intensities.

However, for forbidden transitions the vibrational frequencies are less reliable, and intensities are greatly affected by the vibronic coupling. For a molecule with as many vibrational modes as benzonitrile, a correct vibrational assignment would be pure luck without having guidance from good theoretical intensity information. We have therefore employed a relatively simple method of calculating vibronic intensities using information from readily available electronic structure and Franck-Condon programs.

In most cases the intensity in forbidden transitions comes from simple lowering of the symmetry of the molecule by the various non-symmetric vibrational modes. Non-adiabatic coupling by the kinetic energy terms in the Hamiltonian is mostly important in states with conical intersections or degeneracies. Therefore, for non-pathological cases, vibronic intensities should be able to be calculated from integration of the transition moment over the vibrational wave functions.

As is usual in this kind of a problem, one can expand the electronic transition moment in a Taylor series in the normal coordinate space:

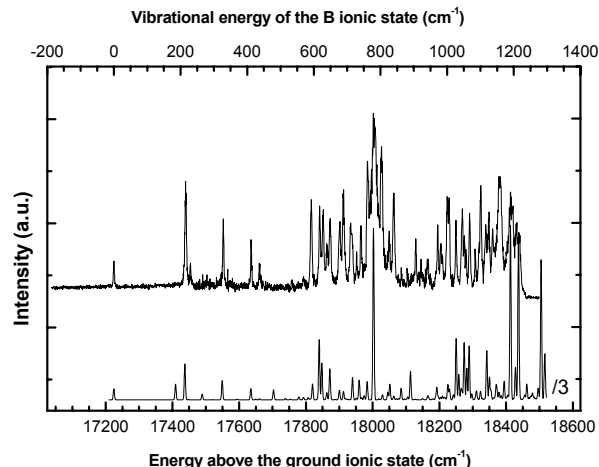
$$M(Q) = M(0) + \sum_i \left( \frac{\partial M}{\partial Q_i} \right)_0 Q_i + \frac{1}{2} \sum_{i,j} \left( \frac{\partial^2 M}{\partial Q_i \partial Q_j} \right)_0 Q_i Q_j + \frac{1}{6} \sum_{i,j,k} \left( \frac{\partial^3 M}{\partial Q_i \partial Q_j \partial Q_k} \right)_0 Q_i Q_j Q_k + \dots$$

Almost universally, this series has been terminated after the linear term in previous treatments of vibronic coupling. However, that precludes the proper treatment of combination bands that contain more than one non-symmetric mode. In order to include the highest order non-zero term for every combination band, one needs to include derivatives up to an order that varies with the point group of the molecule. For example, for  $C_{2v}$ ,  $D_2$ , and  $D_{2d}$  one can safely terminate after the quadratic sum, but for  $D_{2h}$  one should include up to the third order cross terms, and  $D_{6h}$  needs fourth derivatives if Franck-Condon factors for such complicated combinations are substantial.

For a forbidden transition, the first term on the right side of this equation is zero, and the intensity of any vibronic transition is simply proportional to the square of the integral of  $M(Q)$  over the upper and lower vibrational wave functions. Using recurrence properties of harmonic oscillator functions, all integrals over vibrational functions reduce to sums of Franck-Condon factors, which automatically take into account such difficult features as changes in geometry and rotation of the normal coordinate space between the two electronic states.

The end result is that vibronic intensities can be simply computed by combining calculations from available programs. The transition moments can be obtained from SAC-CI calculations (a module of the Gaussian package), and derivatives estimated by finite differences. Franck-Condon factors are calculated with the program MolFC, written and distributed by Andrea Peluso and Raffaele Borrelli. Geometries and vibrational vectors are produced by a variety of Gaussian and Gamess methods.

We have successfully applied this procedure to understanding the vibrational structure of the B-X transition of benzonitrile cation. It is, of course, subject to the accuracy of the vibrational vectors and transition moments, and neglects important things like Fermi resonance and Born-Oppenheimer breakdown, so it is not perfect. However, we feel the procedure should be of great use to experimentalists needing some guidance for difficult assignments. The spectrum at right shows the transition from a non-symmetric vibration in the lower state (upper trace), along with a simulated spectrum below it. Most of the strong lines in this spectrum involve more than one inducing mode.

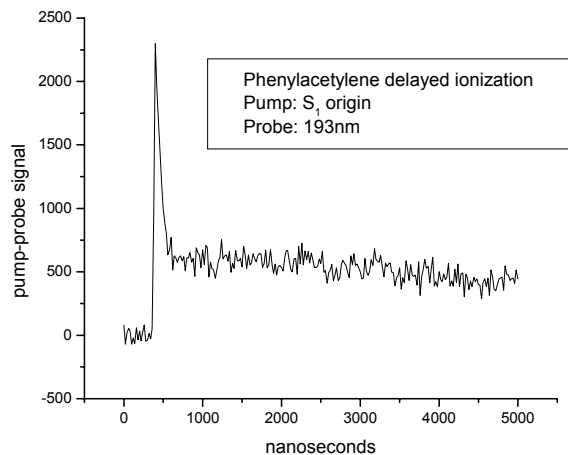


### Radiative decay in the triplet manifold of large molecules

In radiationless transition theory, it is assumed that the wavefunction of an isolated excited singlet state of a large molecule can mix with the high density of isoenergetic triplet and ground singlet states. This mixing can be experimentally followed in time by ionizing the molecule at various times after its excitation, since when the system evolves into the high vibrational levels of the ground state, the Franck-Condon factors prevent ionization and the signal disappears. In this way, one can measure the lifetimes of the triplet states isoenergetic with the pumped singlet state. These are typically on the order of hundreds of nanoseconds to a few microseconds in substituted benzenes.

While measuring the pump-probe decays of benzonitrile and phenylacetylene, in addition to the excited triplet decays we saw very long lived decays (longer than we can measure accurately). This was not unexpected since we have seen similar things in other molecules. There we attributed it to the dissociation of clusters removing energy from the molecules, allowing them to drop down to the lower vibrational levels of the lowest triplet state where the excited state lifetimes are quite long. This time, however, we were exciting with a pulse-amplified CW laser system and able to scan over the rotational structure of the transition. The action spectrum of the long-lived component shows that the active molecules are strictly monomers, thus eliminating the cluster mechanism from possibility.

The long lived states are clearly triplet states. We determined their ionization threshold by scanning the probe laser and found it to be consistent with the triplet state energies, the latter determined from the phosphorescence of these molecules in low temperature solution. However, how could an isolated monomer in a collisionless beam lose energy to drop down



into the lower levels of the triplet state?

The only viable mechanism is that the molecules are losing energy by radiation. Conventional wisdom is that the emission lifetimes for excited vibrational states are too long for their emission to play a part in molecular decay in the triplet manifold, and there is no evidence in the literature that this is not the case. However, there is nothing to prevent an electronic transition from playing a role if there is an excited triplet state just below the excited singlet. We have done calculations to show that there is an excited triplet state in the vicinity of the singlet, with sufficient oscillator strength. We therefore believe that in these two molecules there is considerable radiative decay in the triplet manifold. It may be that some of the other long-lived decays we saw in the past are also due to this mechanism, but a proof would require redoing those experiments with the high resolution laser. A discovery that the occurrence of radiative triplet-triplet transitions in larger molecules is general may require some rethinking about aspects of energy flow in these species.

## FUTURE PLANS

Since the present evidence for triplet-triplet emission is indirect, we are going to look directly for the emission in the near infrared. In phenylacetylene the quantum yield of the long lived product is quite high, and the emission intensity should be comparable to singlet fluorescence. We are also going to examine the radiationless transition properties of some classic systems like pyrazine with the high resolution pulsed laser. Another project involves a puzzling broadening of the line width of transitions when the laser pulse is modulated in time.

## DOE PUBLICATIONS

Andrew Burrill, Jia Zhou and Philip Johnson, "The Mass Analyzed Threshold Ionization Spectra of  $C_6H_6^+$  and  $C_6D_6^+$  obtained via the  $^3B_{1u}$  Triplet State," J. Phys. Chem. A, **107**, 4601-4606 (2003).

James Lightstone, Heather Mann, Ming Wu, Philip Johnson and Michael White, "Gas-phase production of molybdenum carbide, nitride, and sulfide clusters and nanocrystallites," J. Phys. Chem. B, **107**, 10359-10366 (2003).

Andrew. B. Burrill, You K. Chung, Heather. A. Mann, and Philip M. Johnson, "The Jahn-Teller effect in the lower electronic states of benzene cation: Part III The ground state vibrations of  $C_6H_6^+$  and  $C_6D_6^+$ ," J. Chem. Phys. **120**, 8587-8599 (2004).

Haifeng Xu, Trevor Sears, and Philip Johnson, "Photoinduced Rydberg Ionization spectroscopy of Phenylacetylene: Vibrational assignments of the  $\tilde{C}$  state of the cation," J. Phys. Chem., to be published.

# Investigating the chemical dynamics of bimolecular reactions of dicarbon and tricarbon molecules with hydrocarbons in combustion flames

Ralf I. Kaiser  
Department of Chemistry  
University of Hawai'i at Manoa  
Honolulu, HI 96822  
[kaiser@gold.chem.hawaii.edu](mailto:kaiser@gold.chem.hawaii.edu)

## 1. Program Scope

The goal of this project is to untangle experimentally the energetics and the dynamics of reactions of dicarbon,  $C_2(X^1\Sigma_g^+/a^3\Pi_u)$ , and tricarbon molecules,  $C_3(X^1\Sigma_g^+)$ , with unsaturated hydrocarbons acetylene ( $C_2H_2(X^1\Sigma_g^+)$ ), ethylene ( $C_2H_4(X^1A_g)$ ), methylacetylene ( $CH_3CCH(X^1A_1)$ ), allene ( $H_2CCCH_2(X^1A_1)$ ), and benzene ( $C_6H_6(X^1A_{1g})$ ) on the most fundamental, microscopic level. These reactions are of crucial importance to understand the formation of carbonaceous nanostructures as well as of polycyclic aromatic hydrocarbons and their hydrogen deficient precursors in combustion flames. The closed shell hydrocarbons serve as prototype reaction partners with triple (acetylene), double (ethylene), and aromatic (benzene) carbon-carbon bonds; methylacetylene and allene are chosen as the simplest representatives of closed shell hydrocarbon species to investigate how the reaction dynamics change from one structural isomer to the other. The experiments are carried out under single collision conditions utilizing a crossed molecular beams machine at The University of Hawai'i. Highlighted results of these studies are an identification of the reaction products and the determination of the energetics and entrance barriers of the reaction, the intermediates involved, of the reaction mechanisms of small carbon clusters with unsaturated hydrocarbons, and of the branching ratios - data which are very much required by the combustion chemistry community. The experiments are pooled together with electronic structure calculations to verify the elucidated reaction mechanisms theoretically. All findings will be then incorporated into chemical reaction networks to examine the influence of dicarbon and tricarbon molecules on the growth of carbonaceous nanostructures and of polycyclic aromatic hydrocarbons together with their hydrogen deficient precursors in combustion flames.

## 2. Recent Progress

We summarize this prior work below in chronological order. Firstly, the specifications of the crossed beams together with the newly designed components were/are published in publications 1, 2, 4, 10, and 11. Briefly, our machine operates completely hydrocarbon free, reaches excellent pressures in the main chamber ( $10^9$  torr range) and detector ( $10^{-11}$  torr range with an option to achieve lower pressures down to the high  $10^{-13}$  torr range with a high power Sumitomo cold head). The universal mass spectrometric detector utilizes electron impact ionization of the neutral species. We also upgraded the detector system by incorporating additional housings and electrostatic lenses. This enhances the detection efficiency by a factor of about 20-30 compared to currently operating 'universal' crossed beams machines as demonstrated in scattering experiments (elastic, inelastic, and reactive scattering) by comparison of the signal of these systems with previous studies by the PI. The newly developed electronics to conduct the experiments are i) an air cooled resistance-based voltage divider chain for the photomultiplier tube (publication 1), ii) a high stability oscillator driven chopper wheel motor controller to achieve steady dicarbon and tricarbon pulsed beams (publication 2), iii) a universal pulse shaper for the pulsed valve to optimize the beam profile of the supersonic reactant beams (publication 11), iv) an ultra high vacuum compatible laser ablation source to generate dicarbon and tricarbon reactants species (publication 10), and v) a novel interlock system to protect ultra high vacuum machines from power failure, pump failure, pressure increase, temperature increase, and humidity damage (publication 4).

This setup enabled us to conduct crossed molecular beams studies and to focus on the energetics and the dynamics of reactions of dicarbon,  $C_2(X^1\Sigma_g^+/a^3\Pi_u)$ , and tricarbon molecules,  $C_3(X^1\Sigma_g^+)$ , with unsaturated hy-

dicarbon acetylene ( $C_2H_2(X^1\Sigma_g^+)$ ), ethylene ( $C_2H_4(X^1A_g)$ ), allene ( $H_2CCCH_2(X^1A_1)$ ), methylacetylene ( $CH_3CCH(X^1A_1)$ ), and benzene ( $C_6H_6(X^1A_{1g})$ ). During the award period, crossed beams experiments were carried at 34 collision energies in the ranges of 10 – 50  $\text{kJmol}^{-1}$  and 72 - 128  $\text{kJmol}^{-1}$  for dicarbon and tricarbon, respectively; 14 additional experiments with (partially) deuterated (D3-methylacetylene; D1-ethylene; D2-ethylene (cis, trans, gem); D4-ethylene; D6-benzene; D1-acetylene, D2-acetylene) and  $^{13}\text{C}$ -substituted reactants ( $^{13}\text{C}$ -acetylene) were conducted to investigate the position of the deuterium versus hydrogen loss and the influence of the symmetry of the reaction intermediates on the center-of-mass angular distributions and hence on the reaction dynamics. All data have been analyzed and could be fit. The following dicarbon systems have been published/in press/submitted for publication: acetylene (publications 3, 9, 12, 14), ethylene (publications 6, 9, 14), methylacetylene (7, 8, 9, 14), and allene (publications 9, 13, 14).

## 2.1. The Reaction of Dicarbon with Acetylene

The reaction of dicarbon molecules in their electronic ground,  $C_2(X^1\Sigma_g^+)$ , and first excited state,  $C_2(a^3\Pi_u)$ , with acetylene,  $C_2H_2(X^1\Sigma_g^+)$ , to form the 1,3-butadiynyl,  $C_4H(X^2\Sigma^+)$ , plus a hydrogen atom was investigated under single collision conditions at six different collision energies between 10.6  $\text{kJmol}^{-1}$  and 47.5  $\text{kJmol}^{-1}$ . Augmented by electronic structure calculations, dicarbon was found to react with acetylene on the  $^1A$  surface without entrance barrier via complex formation through an addition process involving two initial intermediates. The latter undergoes ring opening to the diacetylene molecule which decomposes via a loose exit transition state by an emission of a hydrogen atom to form the 1,3-butadiynyl radical  $C_4H(X^2\Sigma^+)$ ; the overall reaction was found to be exoergic by about 33  $\text{kJmol}^{-1}$ . The  $D_{\infty h}$  symmetry of the decomposing diacetylene intermediate results in collision-energy invariant, isotropic (flat) center-of-mass angular distributions of this microchannel. On the triplet surface, the reaction involves three feasible addition complexes. Following the  $^3A$  surface, the reaction strongly depends on the impact parameter. These dynamics result in forward-scattered contour plots of the heavy 1,3-butadiynyl radical  $C_4H(X^2\Sigma^+)$  at lower collision energies; as the collision energy rises, the distributions switch to a pronounced backward scattering. The definite detection of the 1,3-butadiynyl radical,  $C_4H(X^2\Sigma^+)$ , as the sole reaction product of the dicarbon versus hydrogen exchange pathway in the bimolecular collision with acetylene represents an important mechanism to build up a hydrogen-deficient organic radical and can account for the hitherto unexplained formation of the 1,3-butadiynyl radical in combustion flames.

## 2.2. The Reaction of Dicarbon with Methylacetylene

The chemical dynamics to synthesize the 2,4-pentadiynyl-1 [ $C_5H_3(X^2B_1)$  HCCCCCH<sub>2</sub>] and 1,4-pentadiynyl-3 radical [ $C_5H_3(X^2B_1)$  HCCCHCCH], via the neutral – neutral reaction of dicarbon with methylacetylene, were examined in crossed molecular beams experiments. Based on the energetics alone, we could not decide if the 2,4-pentadiynyl-1 [ $C_5H_3(X^2B_1)$ , HCCCCCH<sub>2</sub>] and/or 1,4-pentadiynyl-3 [ $C_5H_3(X^2B_1)$  HCCCHCCH] radical were formed under single collision conditions. Recall that the enthalpies of formation of these isomers differ only by 1  $\text{kJmol}^{-1}$ ; this difference is lower than the error limits of the experimentally determined reaction energy of  $\pm 12 \text{kJmol}^{-1}$ . The potential involvement of a third isomer,  $H_5CCCCC(X^2A)$ , complicates the interpretation of the data even further. Here, the reaction to form this structure plus atomic hydrogen was determined to be exoergic by 39 and 48  $\text{kJmol}^{-1}$ , respectively. To facilitate the identification on the product isomer, we also carried out an experiment utilizing  $CD_3CCH$  to investigate explicitly if the hydrogen atom was released from the methyl group or from the acetylenic carbon atom. Here, the decomposition of a  $CD_3C_4H$  intermediate ( $m/z = 67$ ) could form  $CD_2C_4H$  (D atom loss;  $m/z = 65$ ) or  $C_5D_3$  ( $m/z = 66$ ; H atom loss). Experimentally, we only observed signal at  $m/z = 65$ , but not at  $m/z = 66$ . This verifies explicitly that the released atom is a deuterium atom. We can compare these experimental observations now with the computed singlet and triplet surfaces. On the singlet surface, the formation of the  $H_5CCCCC(X^2A)$  isomer requires the existence of a methyldiacetylene intermediate. Considering partially deuterated methylacetylene (d3-methylacetylene), this translates into a  $CD_3-C\equiv C-C\equiv C-H$  structure which had to lose a hydrogen atom

forming  $D_3CCCC(X^2A)$ . Since only a deuterium loss was observed experimentally, we can exclude the formation of  $D_3CCCC(X^2A)$  on the singlet surface. On the triplet surface, the synthesis of the  $H_3CCCC(X^2A)$  isomer had to involve the presence of an intermediate. Again, in case of a d3-methylacetylene reactant ( $CD_3CCH$ ), this process would lead to the emission of a hydrogen atom from the acetylenic group giving signal solely at  $D_3CCCC(X^2A)$ . Similar to the singlet surface, no hydrogen emission was observed, and the formation of  $D_3CCCC(X^2A)$  and hence – in case of methylacetylene -  $H_3CCCC(X^2A)$  can be ruled out. The exclusion of the hydrogen loss pathway has additional consequences for the triplet surface and helped us to identify the existence of a second isomer, the 1,4-pentadiynyl-3 radical [ $C_5H_3(X^2B_1)$ , HCCCHCCH].

### 2.3. The Reaction of Dicarbon with Allene

The reactions dynamics of the dicarbon molecule  $C_2$  in the  $^1\Sigma_g^+$  singlet ground state and  $^3\Pi_u$  first excited triplet state with allene,  $H_2CCCH_2(X^1A_1)$ , were investigated under single collision conditions using the crossed molecular beam approach at four collision energies between  $13.6 \text{ kJmol}^{-1}$  and  $49.4 \text{ kJmol}^{-1}$ . The experiments were combined with *ab initio* electronic structure calculations of the relevant stationary points on the singlet and triplet potential energy surfaces. Our investigations imply that the reactions are barrier-less and indirect on both the singlet and the triplet surfaces and proceed through bound  $C_5H_4$  intermediates via addition of the dicarbon molecule to the carbon-carbon double bond (singlet surface) and to the terminal as well as centered carbon atoms of the allene molecule (triplet surface). The initial collision complexes isomerize to form triplet and singlet pentatetraene intermediates ( $H_2CCCCCH_2$ ) which decompose via atomic hydrogen loss to yield the 2,4-pentadiynyl-1 radical, HCCCCCH $_2(X^2B_1)$ . These channels result in symmetric center-of-mass angular distributions. On the triplet surface, a second channel involves the existence of a non-symmetric reaction intermediate which fragments through atomic hydrogen emission to the 1,4-pentadiynyl-3 radical [ $C_5H_3(X^2B_1)$  HCCCHCCH]; this pathway was found to account for the backward-scattered center-of-mass angular distributions at higher collision energies. The identification of two resonance-stabilized free  $C_5H_3$  radicals, i.e. 2,4-pentadiynyl-1 and 1,4-pentadiynyl-3, suggest that these molecules can be important transient species in combustion flames.

### 2.4. The Reaction of Dicarbon with Ethylene

The dicarbon-ethylene system was found to show more complicated reaction dynamics on the singlet and triplet surfaces. Our experimental data clearly reveal the presence of a dicarbon versus atomic hydrogen leading to the formation of the  $C_s$  symmetric 1-butene-3-yne-2-yl radical [ $i-C_4H_3(X^2A')$ ,  $H_2CCCCCH$ ] via bound  $C_4H_4$  intermediates. The dynamics of this system are currently under investigation; we conducted additional experiments utilizing partially deuterated ethylene reactants D1-ethylene and D2-ethylene (gem, cis, and trans). The reaction with D1-ethylene was aimed to investigate if the forward-backward center-of-mass angular distribution at lower collision energies was the result of a long lived reaction intermediate of purely the outcome of *symmetric* reaction intermediates decomposing to the 1-butene-3-yne-2-yl radical; the reactions with three D2-ethylene isotopomers were carried out to elucidate the involvement of distinct rotational excitations of the reaction intermediates and their influence on the shape of the center-of-mass angular distributions. These data are currently being analyzed.

## 3. Future Plans

The write-up of the dicarbon – benzene and tricarbon reactions is currently ongoing.

## 4. Acknowledgements

This work was supported by US Department of Energy (Basic Energy Sciences; DE-FG02-03ER15411).

## 5. Publications

1. X. Gu, Y. Guo, E. Kawamura, R.I. Kaiser, *Design of a compact, air-cooled cluster-based resistor chain for photomultiplier tubes*. Rev. Sci. Instr. 76 083115-1-6 (2005).
2. X. Gu, Y. Guo, H. Chan, E. Kawamura, R.I. Kaiser, *Design and Characteristics of a High Precision Chopper Wheel Motor Driver*. Rev. Sci. Instr. 76, 116103-1-3 (2005).
3. X. Gu, Y. Guo, R.I. Kaiser, *Mass Spectrum of the Butadiynyl Radical ( $C_4H$ ;  $X^2\tilde{a}^+$ )*. Int. J. Mass Spectr. Ion Processes 246, 29-34 (2005).
4. Y. Guo, X. Gu, E. Kawamura, R.I. Kaiser, *A versatile interlock system for ultra high vacuum machines – A crossed molecular beams setup as a case study*. Rev. Sci. Instr. 77, 034701-9 (2006).
5. A. M. Mebel, V. V. Kislov, R. I. Kaiser, *Potential Energy Surface and Product Branching Ratios for the Reaction of Dicarbon,  $C_2(X^1S_g^+)$ , with Methylacetylene,  $CH_3CCH(X^1A_1)$ : An Ab Initio/RRKM Study*, JPCA 110, 2421-2433 (2006).\* cover page
6. Y. Guo, X. Gu, R.I. Kaiser, *Mass Spectrum of the 2-Buten-1-yn-3-yl Radical ( $i-C_4H_3$ ;  $X^2A'$ )*. Int. J. Mass Spectrometry 249-250, 420-425 (2006).
7. Y. Guo, X. Gu, N. Balucani, R.I. Kaiser, *Formation of the 2,4-pentadiynyl-1 radical ( $H_2CCCCCH$ ,  $X^2B_1$ ) in the Crossed Beams Reaction of Dicarbon Molecules with Methylacetylene*. JPCA (in press 2006).\* cover page
8. X. Gu, Y. Guo, F. Zhang, R.I. Kaiser, *Unimolecular Decomposition of Singlet and Triplet Methylacetylene – A Crossed Molecular Beams Study*. PCCP (in press 2006).
9. X. Gu, Y. Guo, F. Zhang, A.M. Mebel, R.I. Kaiser, *Reaction Dynamics of Carbon-Bearing Radicals*. Faraday Discussion 133 (in press 2006).
10. X. Gu, Y. Guo, E. Kawamura, R.I. Kaiser, *Characteristics and Diagnostics of a UHV Compatible Laser Ablation Source for Crossed Molecular Beams Experiments*. J. Vac. Science & Technology A (in press 2006).
11. Y. Guo, X. Gu, E. Kawamura, R.I. Kaiser, *Design of a Low Cost, Dual Pulse Shaper for Pulsed, Crossed Molecular Beams Experiments*. J. Vac. Science & Technology A (submitted 2005).
12. X. Gu, Y. Guo, A.M. Mebel, R.I. Kaiser, *Investigating the Reaction Dynamics of Dicarbon Molecules,  $C_2(X^1S_g^+/a^3P_u)$ , with Acetylene,  $C_2H_2(X^1S_g^+)$* . PCCP (submitted 2005).
13. Y. Guo, X. Gu, F. Zhang, R.I. Kaiser, *Unimolecular Decomposition of Chemically Activated Pentatetraene ( $H_2CCCCCH_2$ ) Intermediates – A Crossed Beams Study of Dicarbon Molecule Reactions with Allene*. J. Chem. Phys (submitted 2005).
14. X. Gu, Y. Guo, R.I. Kaiser, *Formation of hydrogen-deficient, carbon-bearing radicals in extraterrestrial environments via reactions of dicarbon molecules with unsaturated hydrocarbons*, ApJ (submitted 2006).
15. Y. Guo, X. Gu, R.I. Kaiser, *Mass Spectrum of the 2,4-Pentadiynylidyne Radical ( $C_5H$ ;  $X^2P$ )*. Int. J. Mass Spectrometry (submitted 2006).

## DYNAMICAL ANALYSIS OF HIGHLY EXCITED MOLECULAR SPECTRA

Michael E. Kellman

Department of Chemistry, University of Oregon, Eugene, OR 97403

[kellman@uoregon.edu](mailto:kellman@uoregon.edu)

### PROGRAM SCOPE:

Spectra and internal dynamics of highly excited molecules are essential to understanding processes of fundamental importance for combustion, including intramolecular energy transfer and isomerization reactions. The goal of our program is to develop new theoretical tools to unravel information about intramolecular dynamics encoded in highly excited experimental spectra. We want to understand the formation of “new vibrational modes” when the ordinary normal modes picture breaks down in highly excited vibrations. We want in addition to predict experimental signatures of the new dynamics. For these purposes we use bifurcation analysis of semiclassical versions of the effective Hamiltonians used by spectroscopists to fit complex experimental spectra.

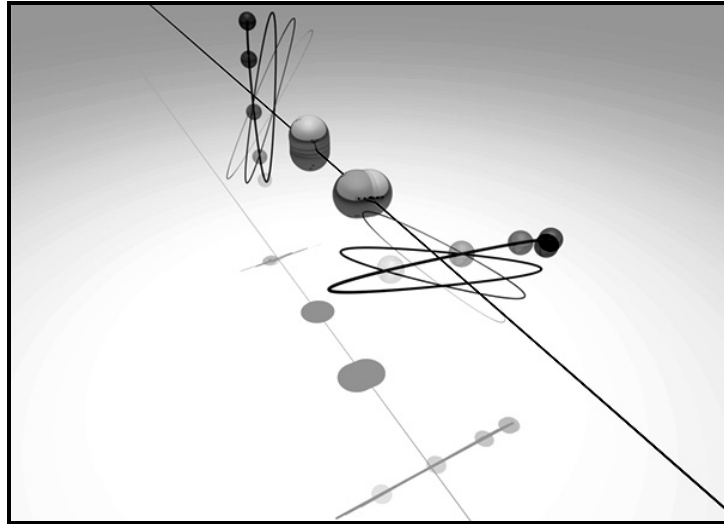
The acetylene/vinylidene system is of great importance in combustion, acetylene as an intermediate, and the vinylidene isomer as precursor of the radical pool formed by reaction with O<sub>2</sub>. We have completed an effort to gain a systematic understanding of the bending dynamics of the acetylene system. We are in the midst of the difficult but crucial problems of treating the full stretch-bend degrees of freedom, and treating full rotation-vibration dynamics. We have begun to make progress in incorporating multiple potentials and above-barrier dynamics, with the goal of extending our methods to encompass isomerization phenomena.

In the near future, the goals are (1) to continue the development of our bifurcation methods to systems of greater number of degrees of freedom, in particular, the full stretch-bend vibrational dynamics of acetylene; (2) to continue current progress on the bifurcation analysis for rotation-vibration dynamics; and (3) to develop effective Hamiltonians for analysis of isomerizing systems.

### RECENT PROGRESS: DYNAMICS FROM SPECTRA OF HIGHLY EXCITED ACETYLENE APPROACHING ISOMERIZATION.

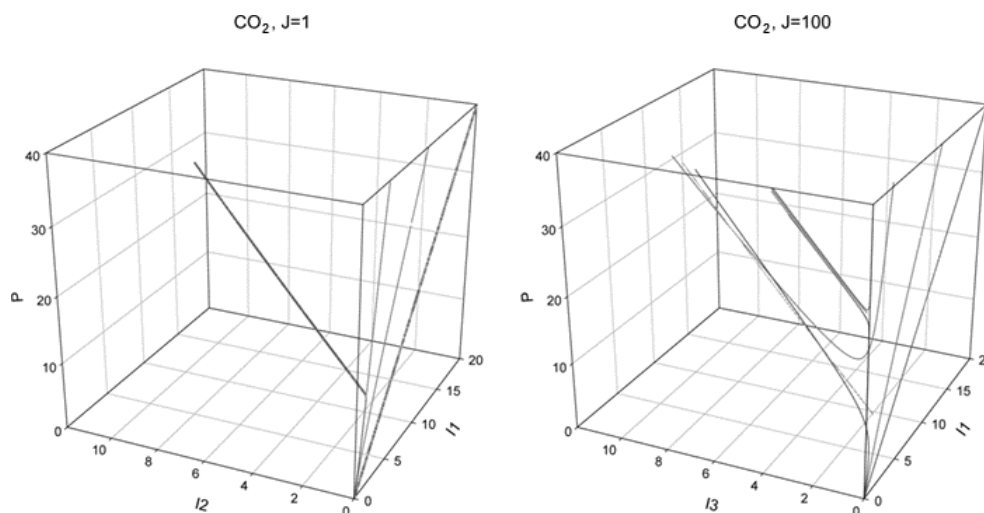
**Bifurcation analysis: Branchings of the normal modes into new anharmonic modes.** Our approach to highly excited vibrational spectra uses bifurcation analysis of the classical version of the effective Hamiltonian used to fit spectra. We have applied this to a bifurcation analysis of the bend degrees of freedom of acetylene. This work is now complete and is in press as Ref. 2 below.

**Higher  $\mathbf{l}$  -vibrational angular momentum states of acetylene.** The bifurcation analysis of the pure bends system described above is for spectra with vibrational angular momentum  $\mathbf{l} = 0$  in the fitting Hamiltonian. Obviously, it is of great interest to extend the analysis to systems with  $\mathbf{l} > 0$ . We have performed the bifurcation analysis for  $\mathbf{l}$  up to 20. We find that there are four new modes born in bifurcations, as for the  $\mathbf{l} = 0$  case. However, these new modes are precessing orbits, due to the  $\mathbf{l}$  excitation. The figure shows one of these, the precessing Orthogonal mode.



**Experimental signature of bifurcation.** An important problem is prediction of experimental phenomena associated with bifurcation behavior. For the  $\mathbf{l} > 0$  states described above, we have found that the spectroscopic Hamiltonian predicts a fascinating phenomenon associated with a bifurcation sequence (not seen earlier for  $\mathbf{l} > 0$ ) in which the Local bending mode turns into the Orthogonal mode in the figure above. This phenomenon of “moment of inertia backbending” is analogous to a similar phenomenon associated in deformed nuclei with phase transitions, and recently predicted for a phase transition from nuclear to quark matter in rotating neutron stars!

**Rotation-vibration spectra and dynamics:** The analysis above starts with bending dynamics with  $\mathbf{l} = 0$ , then progressed to include vibrational angular momentum, with  $\mathbf{l} > 0$ . The next step is to go beyond pure vibrational angular momentum, to include full rotation-vibrations dynamics. This includes new, rotation-vibration couplings due to Coriolis effects. In the bifurcation analysis, this takes us to three non-trivial degrees of freedom (after factoring out all “polyad” constants). This move to higher degrees of freedom is really the “big step” in furthering the program of bifurcation analysis. (More on the technical aspects is described below under “future plans”.) We have succeeded in performing the bifurcation analysis for full rotation-vibration dynamics of triatomics. Results are shown below for  $\text{CO}_2$  for  $J = 1$  and  $J = 100$ . A notable feature is that the bifurcation structure is intelligible and relatively simple, having the nature of a basic “tree” that grows “branches” as rotation-vibration couplings grow with  $J$ .



### **FUTURE PLANS: FULL STRETCH-BEND DYNAMICS, ABOVE BARRIER MOTION AND ISOMERIZATION DYNAMICS.**

The bifurcation analysis completed so far is for pure bends spectra. It is of great interest to extend this to systems with combinations of stretch and bend excitation, for which fitting Hamiltonians of existing experimental spectra are available. A related goal is to extend the bifurcation methodology to rotation-vibration spectra. Another major goal is to extend the bifurcation approach to isomerizing systems. The challenge, however, is to extend the bifurcation analysis of real spectroscopic Hamiltonian to multiple potential wells, and very large-amplitude motion above two or more wells.

#### **The challenge of higher dimensions: Analytically scalable bifurcation analysis.**

Existing spectra of the acetylene system access states in which the stretches and bends are coupled in a highly complex way. As the dimensionality of the problem becomes larger, one of the challenges is whether our analysis can be performed, in a way that is still understandable and useful.

The key to making tractable larger systems such as the full stretch-bend degrees of freedom is use of the polyad quantum number, which is an integral part of the standard spectroscopic fitting Hamiltonian. A fact rarely utilized outside our group is that the polyad Hamiltonian makes possible determination of the mode bifurcation structure by *analytic* means, i.e. by solution of simple algebraic equations related to the Hamiltonian function, rather than numerical solution of the equations of motion. Specifically, in our approach we seek the critical points or “flat spots” of the polyad Hamiltonian. Because the critical points are obtained analytically, it is not necessary to perform numerical integration of Hamilton's equations and analysis of surfaces of section. This is expected to become extremely advantageous as the number of degrees of freedom and phase space dimensions increase. -

**Full rotation-vibration spectra dynamics of acetylene including bends, stretches, and rotations:** As described above, a major achievement has been the performance of the bifurcation analysis for full rotation-vibration dynamics of triatomics. We now want to develop this analysis for acetylene. With four atoms, this makes the problem yet a higher-dimensional challenge. In particular, the Coriolis couplings in acetylene necessarily couple the bending to the stretching modes. The acetylene rotation-vibration problem therefore necessitates the full effective Hamiltonian, with all degrees of freedom – bend vibrations, stretch vibrations, rotations, and all their couplings.

**Spectroscopic Hamiltonians for multiple wells and above barrier spectroscopy.**

Isomerization dynamics are of extreme interest in combustion. In particular, the vinylidene-acetylene isomerization problem continues to attract major emphasis. From our point of view, the challenge in performing bifurcation analysis related to “isomerization spectra” is to build an effective spectroscopic Hamiltonian. Nobody has yet done this, but developments in experiment and theory make the time ripe to face this challenge. The familiar spectroscopic Hamiltonian consists of two parts: a zero-order part which is diagonal in the zero-order quantum numbers; and a coupling part consisting of a sum of resonance coupling operators.

For systems with multiple wells and above-barrier motion, there are two problems in building an effective resonance Hamiltonian. The first is to define separate zero-order quantum numbers for each of the well regions and for the above-barrier region. The second is to define coupling operators that couple the zero-order states. Most challenging of all is to devise cross-barrier couplings that act above and below the barrier, and between wells.

**Recent publications (in print, in press, in preparation since 2003) related to DOE supported research:**

1. S. Yang and M.E. Kellman, “Semiclassical wave function from a quantizing cantorus”, *Chem. Phys.*, 322, 30 (2006).
2. V. Tyng and M.E. Kellman, “Bending Dynamics of Acetylene: New Modes Born in Bifurcations of Normal Modes”, in press, *J. Phys. Chem.*
3. M.E. Kellman and V. Tyng, “Dances with Molecules”, in press, *Accounts of Chemical Research*.

## High Energy Processes

Alan R. Kerstein  
Combustion Research Facility  
Sandia National Laboratories  
P.O. Box 969, Mail Stop 9051  
Livermore, CA 94551-0969  
E-mail: [arkerst@sandia.gov](mailto:arkerst@sandia.gov)

### Project Scope

This project pursues the development, demonstration, and application of new mathematical and conceptual paradigms for capturing the interplay of complexity and randomness in advection/diffusion/reaction processes. The perspective that is adopted is that these processes and their couplings should be represented in a manner that is faithful to the underlying physics and chemistry rather than subsuming important phenomenology in parameterizations designed to represent outcomes rather than pathways and mechanisms. Accordingly, the goal of this research is the formulation of numerical models that combine physical fidelity and computational efficiency, and their use for physics discovery as well as interpretation of known phenomenology.

A longstanding topical focus of this effort has been 1D unsteady simulation of turbulent reacting flows, with emphasis on combustion applications. Modeling based on reduction of spatial dimensionality is a widely used strategy for simplification and reduction of computational cost. In particular, 2D turbulent combustion simulations are commonplace. The governing equations carry over straightforwardly from 3D to 2D, but the flow physics changes qualitatively. Vortex stretching, which is the mechanism of length-scale reduction in the 3D turbulent cascade, does not occur in 2D because all vortices are aligned in the out-of-plane direction. In fact, 2D turbulence has an inverse cascade (amalgamation of small structures into large scale motions).

In contrast, reduction to a 1D representation requires not only a reformulation but a paradigm change. Advection is now viewed as a sequence of maps applied to the spatial domain. Advection as prescribed by the exact governing equations can be approximated to arbitrary accuracy by a suitably defined map sequence, and in fact this approach is used in Lagrangian numerical implementations. In the present context, the utility of this perspective is that it extends naturally to 1D, albeit requiring a modeling approach that is not formally equivalent to the exact evolution. The most significant accomplishment of this effort to date has been the formulation of a 1D approach that emulates the 3D turbulent cascade, and in this regard represents 3D turbulence more accurately than more costly 2D methods [A].

This accomplishment has provided the impetus for a wide range of scientific and technological advances, including physics discoveries subsequently verified experimentally, theoretical explanations of phenomena not previously understood, and new predictive capabilities, as reported in numerous publications by the P.I., coworkers, and other research groups that have adopted the methodology. Areas of application include turbulent combustion, multiphase flows, geophysical flows, and spontaneous structure formation in turbulence. Recent accomplishments and planned efforts related to the 1D approach are outlined in subsequent sections.

A method for studying complexity and stochastic effects in advection/diffusion/reaction processes that has obvious benefits if it proves tractable is analysis of the governing equations based on systematic mathematical approximations. This requires consideration of the ensemble of flow realizations as a whole. In fact, this is the most common form of engineering analysis of turbulence. Namely, the governing equations are averaged, yielding an unclosed system due to nonlinearities, and modeling is used to close the formulation.

The modeling involves parameterizations that are known to be physically and mathematically problematic. However, there is an entirely different analysis strategy that avoids such parameterizations yet addresses the full ensemble of flow realizations. It involves the path-integral representation of the ensemble, a formulation originating in quantum field theory [B].

The strategy is as follows. The governing equations are supplemented by assumed stochastic noise processes. By construction, these noises determine the statistical weight of each possible flow realization, which is a path through the space of all possible flow states. On this basis, the expectation value of any observable can be determined by evaluating it for each path and then forming the sum over paths based on the prescribed weighting. Because this is a sum over a continuous rather than discrete set of possibilities, it is formally a path integral. This procedure often yields consistency conditions that constrain or uniquely determine the noise processes, thereby eliminating the arbitrariness of their specification. For such cases, fully self-contained solutions are obtained. For other cases, useful results are inferred from study of the dependence of the solution on assumptions about the noise. For still other cases, the noise represents a physical stochastic forcing, so it is part of the physical problem specification.

Brute-force numerical implementation of this approach corresponds to direct numerical simulation (DNS) of the full problem. A huge gain in cost-performance is achieved for cases in which mathematical analysis of the noise-driven nonlinear evolution allows systematic approximation of the entire path integral. One of the most remarkable achievements of the human intellect has been the development of mathematical methods for doing this [B].

P.I. previously performed analysis and simulation of problems that can be formally cast in this framework, but were instead addressed heuristically [C,D,E]. Recent developments in quantum field theory [F] indicate the possibility of addressing these problems within the path-integral framework. Efforts to date and future plans in this regard are outlined in subsequent sections.

### **Recent Progress**

The development of the map-based representation of advection was motivated by the goal of formulating an economical yet physically valid 1D method for turbulence simulation. Recent efforts have resulted in progress in the development of two distinctly different ways of using this concept to improve fully three-dimensional turbulence simulations.

One such application is specific to a multiphase flow problem. The rate of agglomeration of particles in turbulent flow is controlled by their collision rate. This rate depends on the square of the local number density, analogous to a second order chemical reaction. This quadratic dependence implies that number-density fluctuations enhance collisions and hence agglomeration.

At scales below the smallest scales of turbulent flow structure, local fluctuations of the number density of advected inertial particles are far greater than expected based on independent particle motions. This particle clustering phenomenon, a subtle consequence of fluid-particle relative motion (particle ‘slip’), has been modeled from several perspectives [G,H]. However, it has not been incorporated into computational models [I] that couple particle motion to other effects (e.g., condensational growth in the case of coagulating droplets) in scientifically interesting regimes due to the huge numerical cost of resolving clustering at small scales on a spatial domain that is large enough to capture other relevant processes.

Mathematical analysis based on a version of map-based advection that is applicable in any number of spatial dimensions [6] provides an intuitive geometrical interpretation of the clustering phenomenon and establishes an efficient method for incorporating it into numerical simulations. A recently initiated application of the new method is discussed in the next section.

Another application of map-based advection to 3D simulations involves 1D map implementation, but now on each 1D domain within three arrays of such domains, where each array is oriented in one of the three Cartesian coordinate directions. The 1D simulation model evolves on each domain, resolving the smallest space and time scales, but on a slower time scale the domain evolutions are coupled to capture 3D motion. In appropriate limits of this formulation, conventional 3D flow simulation is recovered.

A preliminary implementation of this strategy [J] yielded encouraging results. In this implementation, treatment of some problematic issues was postponed in order to reduce the effort required for an initial test of the approach. The success of the initial test motivated subsequent efforts to obtain a more robust formulation.

The outcome was a formulation based on an all-Mach-number rather than a zero-Mach-number time-advancement strategy that eliminates the need to evolve coarse-grained variables. Concurrent coupled evolution of resolved and coarse-grained variables introduces some of the drawbacks of conventional parameterization (mentioned in the previous section), hence the impetus to avoid coarse-graining. In addition, the physical scope of the formulation has been broadened, e.g. as in [3]. Plans to implement the improved approach are discussed in the next section.

Previous work by the P.I. on front propagation in heterogeneous media (e.g., composite-propellant combustion) and advected media (e.g., turbulent premixed combustion) identified novel physical regimes and a potentially rich phenomenology that merits further exploration [C,D,E]. Path-integral analysis (see the previous section) is a promising tool for putting this investigation on a firmer mathematical and conceptual foundation as well as broadening its scope. Initial application of this approach has revealed the mathematical origin of results previously obtained heuristically and computationally and has identified parameter dependencies not previously noted.

### Future Work

The new 3D formulation of map-based advection is being used to study rain formation. Existing models under-predict raindrop formation rates [I]. Explicit coupling of droplet clustering and other relevant processes, enabled by the new formulation, might reduce or eliminate the discrepancy and thereby resolve a conundrum of widely recognized climatological significance.

The newly formulated 3D simulation method based on coupled 1D domains will be implemented computationally. The initial target problem is Rayleigh convection, which is well represented in some respects on a single 1D domain, but in other respects requires a 3D representation [4].

A variant of this approach, in which the coupled 1D domains are imbedded in a 3D steady-state turbulence computation, is also being implemented. This reduces fidelity somewhat, but for some combustion applications may prove to be the most cost-effective simulation approach.

Basic studies involving a single 1D domain are continuing. One initiative is investigation of the eigenvalues of complex chemical reaction mechanisms coupled to 1D advection-diffusion in order to assess the implications of this coupling with regard to chemical mechanism reduction.

The path-integral analysis performed to date is restricted to the regime of small amplitude random fluctuations. The analysis will be extended to large amplitude fluctuations. One focus will be the improvement of a turbulent flame speed formula, widely used for parameterization in simulations, that was derived using field-theoretic methods but has some apparent conceptual flaws.

### References

1. A. R. Kerstein, *J. Fluid Mech.* **392**, 277 (1999).
2. M. E. Peskin and D. V. Schroeder, *An Introduction to Quantum Field Theory* (Westview Press, 1995).
3. A. R. Kerstein, *Combust. Flame* **69**, 95 (1987).
4. A. R. Kerstein and Wm. T. Ashurst, *Phys. Rev. Lett.* **68**, 934 (1992).
5. A. R. Kerstein and Wm. T. Ashurst, *Phys. Rev. E* **50**, 1100 (1994).
6. A. Crisanti and U. M. B. Marconi, *Phys. Rev. E* **51**, 4237 (1995).
7. E. Balkovsky, G. Falkovich, and A. Fouxon, *Phys. Rev. Lett.* **86**, 2790 (2001).
8. J. Chun, D. L. Koch, S. L. Rani, A. Ahluwalia, and L. R. Collins, *J. Fluid Mech.* **536**, 219 (2005).
9. H. R. Pruppacher and J. D. Klett, *Microphysics of Clouds and Precipitation*, 2<sup>nd</sup> Ed. (Kluwer, 1997).
10. R. C. Schmidt, R. McDermott, and A. R. Kerstein, "ODTLES: A Model for 3D Turbulent Flow Based on One-dimensional Turbulence Modeling Concepts," Sandia National Laboratories Report SAND2005-0206 (2005).

#### **Publications Since 2004**

1. S.E. Woosley, S. Wunsch, and M. Kuhlen, "Carbon Ignition in Type Ia Supernovae: An Analytic Model," *Astrophys. J.* **607**, 921 (2004).
2. S. Wunsch and S.E. Woosley, "Convection and Off-Center Ignition in Type Ia Supernovae," *Astrophys. J.* **616**, 1102 (2004).
3. Wm. T. Ashurst and A. R. Kerstein, "One-Dimensional Turbulence: Variable-Density Formulation and Application to Mixing Layers," *Phys. Fluids* **17**, 025107 (2005).
4. S. Wunsch and A. R. Kerstein, "A Stochastic Model for High Rayleigh Number Convection," *J. Fluid Mech.* **528**, 173 (2005).
5. R. J. McDermott, A. R. Kerstein, R. C. Schmidt, and P. J. Smith, "The Ensemble Mean Limit of the One-Dimensional Turbulence Model and Application to Residual Stress Closure in Finite Volume Large-Eddy Simulation," *J. Turb.* **6**, 1 (2005).
6. A. R. Kerstein and S. K. Krueger, "Clustering of Randomly Advected Low-Inertia Particles: A Solvable Model," *Phys. Rev. E* **73**, 025302 (2006).
7. A. R. Kerstein and S. Wunsch, "Simulation of a Stably Stratified Atmospheric Boundary Layer Using One-Dimensional Turbulence," *Bound. Layer Meteorol.*, in press (2006).
8. J. Cuxart, A. A. M. Holtslag, A. R. Kerstein, S. Wunsch, *et al.*, "Single-Column Model Intercomparison for a Stably Stratified Atmospheric Boundary Layer," *Bound. Layer Meteorol.*, in press (2006).

# KINETICS OF COMBUSTION-RELATED PROCESSES AT HIGH TEMPERATURES

**J. H. Kiefer**

**Department of Chemical Engineering**

University of Illinois at Chicago  
Chicago, IL 60607  
([kiefer@uic.edu](mailto:kiefer@uic.edu))

## **Program Scope**

This program involves the use of the shock tube with laser-schlieren (LS), and now time-of-flight mass spectrometry, as diagnostics for the exploration of reaction rates and energy relaxation processes over an extremely wide range of temperatures and pressures. We are interested in both energy transfer and the kinetics of reactions at combustion temperatures and above. We emphasize the phenomena of unimolecular reaction including incubation and falloff for whose observation LS provides a unique capability.

## **Relaxation**

In a continuing effort to understand our observation of non-RRKM dissociation in 1,1,1-trifluoroethane [pub.#2, below], we have embarked on a study of relaxation and dissociation in the closely related 1,1-difluoroethane, as was briefly mentioned in the last abstract. This project was difficult but now seems complete and we do have good dissociation and relaxation data. As usual we first looked at the relaxation, and found that it is not double as it is in the trifluoroethane. The relaxation is nonetheless very rapid; the derived  $\langle \Delta E \rangle_{\text{down}}$  larger than the lowest frequency.

The product of HF elimination in 1,1-difluoroethane is vinyl fluoride, whose own HF elimination interferes. We have accordingly investigated this species as well. For this we have also been to establish accurate relaxation times for both molecule and rare gas diluent, and these nicely extrapolate to the room-T ultrasonic relaxation rate for the pure gas (see Fig. 1, below). We also have good relaxation data in pentafluoroethane and the symmetric 1,1,2,2-tetrafluoroethane. The latter is remarkably rapid, with  $P\tau$  values below 10 nsec-atm. We will add data on the monofluoroethane and then do some more analysis' finally publishing our extensive relaxation results on these 2-carbon fluoro-compounds this year.

## **Dissociation in fluoroethanes**

We have completed and analyzed a large series of experiments on the HF elimination from 1,1-difluoroethane. Here the analysis is very dependent on the rate of decomposition of the product vinyl fluoride and we have made a considerable effort to determine rates for this in the range of the 1,1-difluoroethane experiments. This project is now also complete and we have what seem to be solid rate measurements and a good fit RRKM model of the HF elimination in vinylfluoride (see Fig. 2.). This dissociation is complicated by the presence of two channels with the same products, a 1,1-HF

elimination to vinylidene and then to acetylene, and a 1,2-elimination leading directly to acetylene. These two paths have very similar barriers, according to G3B3 calculations (the 1,1- is 74.51 kcal/mol and 1,2-, 72.94 kcal/mol), so there is little effect of falloff on the branching ratio. Nonetheless, we have used a two-channel analysis of these reactions in a master-equation program (Chemrate [1]) for our fit, which uses a total TST  $k_{\infty} = 5.62 \times 10^{15} \exp(-78.068 \text{ kcal/mol/RT})$ . The calculations do indicate a rather large  $\langle \Delta E \rangle_{\text{down}}$  of  $1200 \text{ cm}^{-1}$ , but this is similar to, if somewhat larger than, what is needed in the fluoroethanes. The calculated rate is in excellent agreement with the Tschuikow-Roux group's [2] single pulse data for their low-T, high-P conditions. Unfortunately, the heat of dissociation is too small for LS observation in the monofluoroethane and 1,2-difluoroethane.

### **The acetaldehyde decomposition**

This project is now complete and we have a complete RRKM model of the C-C bond-fission at high temperatures as illustrated in Fig. 3., below. This paper has been submitted for presentation at the 31<sup>st</sup> Combustion Symposium to be held this July.

### **Incubation times in CO<sub>2</sub>**

Quite convincing incubation times for the  $\text{CO}_2 \rightarrow \text{CO} + \text{O}$  reaction have recently been presented by the Stanford group [3]. Because these were obtained in the reflected shock wave, while much of the relaxation occurs in the prior incident wave, we decided to see if there were any differences between these and direct incident wave measurements. We have now obtained relaxation, incubation and rate measurements to extremely high temperatures (to  $> 6000\text{K}$ ) and, overall, we find close agreement with the Stanford results on rate and incubation.

### **Time-of-flight mass spectrometer TOF construction and testing**

Please see the abstract of R.S. Tranter for the current situation on this. We plan to collaborate with Tranter and B. Giri on this machine in some of our projects listed below.

### **New and planned work**

We have started the examination of the dissociation of the six-member oxygen heterocycles, where we include cyclohexane as the "zero oxygen" member. So far we have data on both cyclohexane and 1,4-dioxane. We will be doing the 1,3-dioxane and tetrahydropyran (one oxygen) shortly. The products of these decompositions are quite uncertain. Although much can actually be discerned from LS measurements, a full understanding will undoubtedly require TOF analysis. This is also in the works.

### **References**

1. V. M. Bedanov, W. Tsang, and M. R. Zachariah, *J Phys. Chem.* 99, 11452 (1995), W. Tsang, V. Bedanov, and M. R. Zachariah, *J. Phys. Chem.* 100, 4011 (1996).
2. E. Tschuikow-Roux, W. J. Quiring, and J. M. Simmie, *J. Phys. Chem.* 74, 2449 (1970).

3. M. A. Oehlschlager, D. F. Davidson, J.B. Jeffries, and R. K. Hanson, *Z. Phys. Chem.* **219**, 555 (2005).

### Publications

1. “Vibrational Relaxation in Methyl Hydrocarbons at High Temperatures: Propane, Isobutene, Isobutane, Neopentane and Toluene”, J. H. Kiefer, G. C. Sahukar, S. Santhanam, N. K. Srinivasan., and R.S. Tranter, *J. Chem. Phys.*, **120**, 918 (2004).

2. “A Shock-Tube, Laser-Schlieren Study of the Dissociation of 1, 1, 1-Trifluoroethane: An Intrinsic non-RRKM Process”, J. H. Kiefer, C. Katopodis, S. Santhanam, N. K. Srinivasan, and R. S. Tranter, *J. Phys. Chem.* **108**, 2443 (2004).

3. “Dissociation, Relaxation, and Incubation in the High-Temperature Pyrolysis of Ethane, and a Successful RRKM Modeling”, J. H. Kiefer, S. Santhanam, N. K. Srinivasan, R.S. Tranter, and S. J. Klippenstein, *Proc. Combust. Inst.* **30**, 1129 (2005).

4. “Decomposition of Acetaldehyde: Experiment and Theory”, K. S. Gupte, J. H. Kiefer, R.S. Tranter, S. J. Klippenstein, and L.B. Harding, *Proc. Combust. Inst.* **31**, submitted.

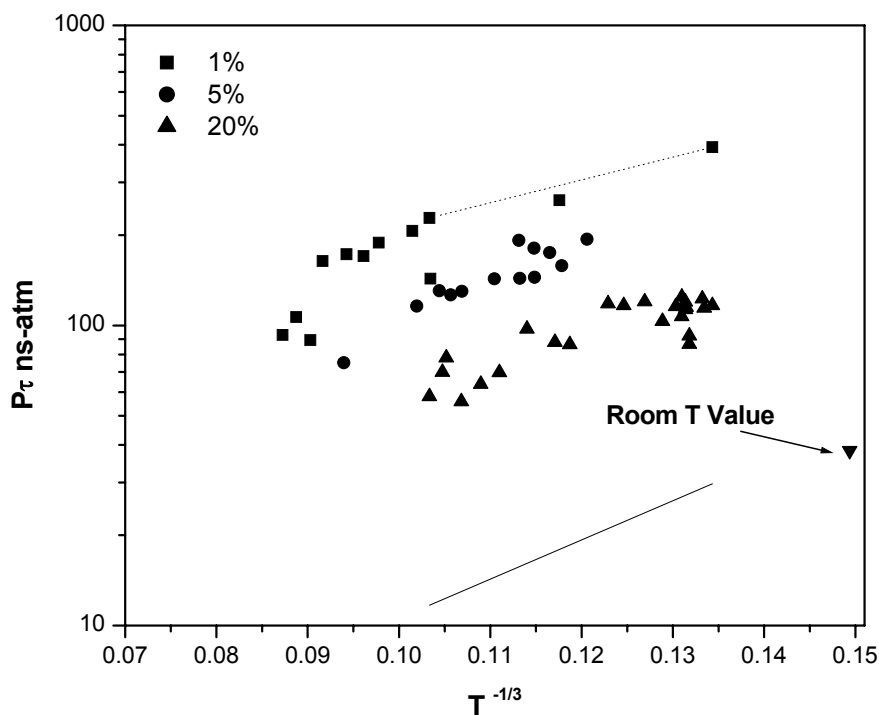


Fig. 1. Relaxation times in vinyl fluoride. The solid line shows extrapolated pure gas values.

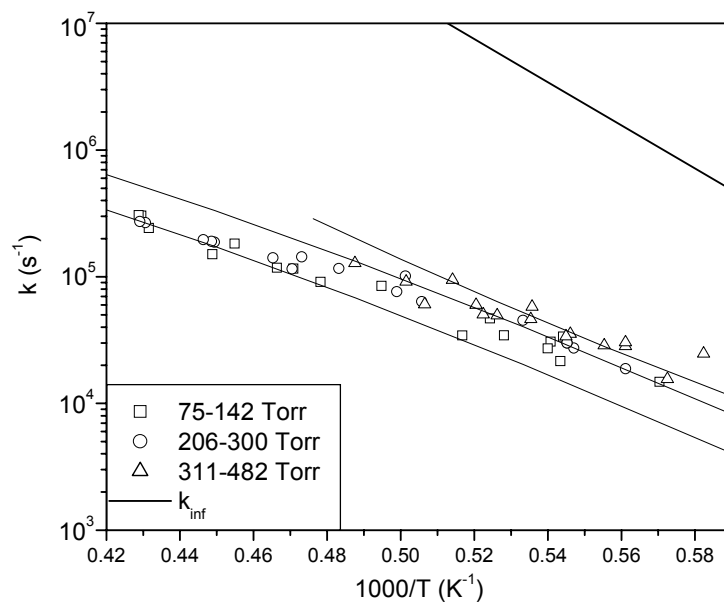


Fig. 2. HF elimination rates in vinyl fluoride. The lines show RRKM master-equation calculations described in the text for closely similar pressures.

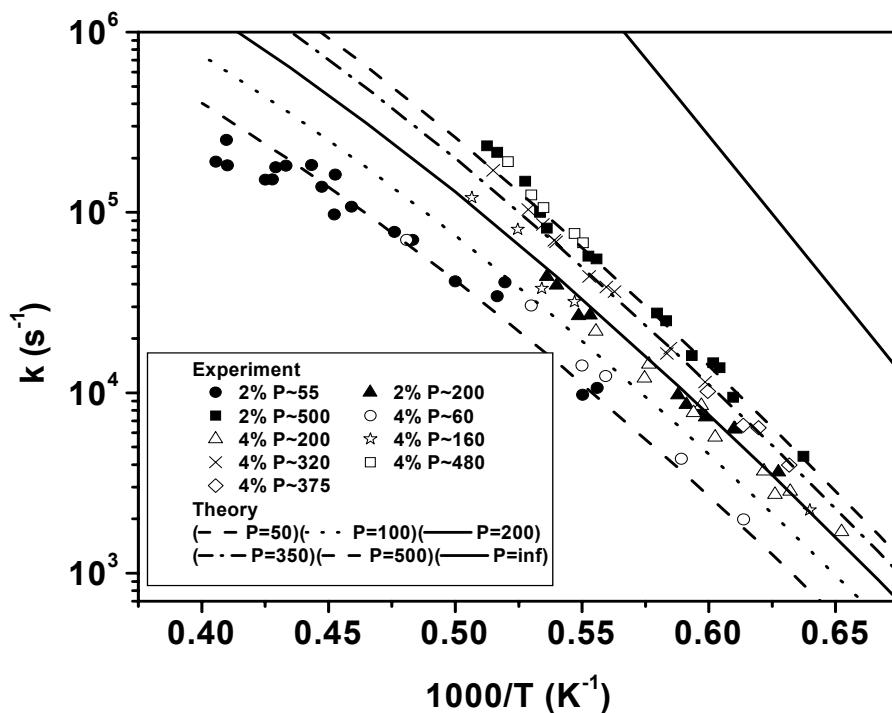


Fig. 3. Arrhenius plot of laser-schlieren rates for C-C fission in  $\text{CH}_3\text{CHO}$ . Pressure groups in torr are indicated on the figure. The solid lines show variable reaction coordinate RRKM calculations whose  $\langle \Delta E \rangle_{\text{down}}$  have been chosen to fit the experiments

## THEORETICAL CHEMICAL KINETICS

Stephen J. Klippenstein  
Chemistry Division  
Argonne National Laboratory  
Argonne, IL, 60439  
[sjk@anl.gov](mailto:sjk@anl.gov)

### Program Scope

The focus of this program is the theoretical estimation of the kinetics of elementary reaction steps of importance in combustion chemistry. The research involves a combination of *ab initio* quantum chemistry, variational transition state theory, direct dynamics, and master equation simulations. The emphasis of our current applications is on (i) reactions of importance in soot formation, (ii) radical oxidation reactions, and (iii) NO<sub>x</sub> chemistry. We are also interested in a detailed understanding of the limits of validity of and, where feasible, improvements in the accuracy of specific implementations of transition state theory. Detailed comparisons with experiments, and with other theoretical methods are used to explore and improve the predictive properties of the transition state theory models. Direct dynamics simulations are being performed as a means for testing the statistical assumptions, for exploring reaction mechanisms, and for generating theoretical estimates where statistical predictions are clearly inadequate. Master equation simulations are used to study the pressure dependence of the kinetics and to obtain phenomenological rate coefficients for use in kinetic modeling.

### Recent Progress

#### *Soot Formation (in collaboration with Larry Harding)*

Our work on delineating the kinetics of reactions related to soot formation has focused this year on two key aspects. First, we have generalized our CASPT2/dz based direct VRC-TST based procedure to treat the recombination kinetics of resonantly stabilized alkyl radicals. This generalization involves the inclusion of CASPT2/adz calculated minimum energy path corrections together with the consideration of larger active spaces. Analyses of the recombination of H atoms with triplet propargylene, propargyl, allyl, CH<sub>2</sub>CCCH, CH<sub>3</sub>CCCH<sub>2</sub>, CH<sub>2</sub>CHCCH<sub>2</sub>, CH<sub>3</sub>CHCCH, cyclic-C<sub>4</sub>H<sub>5</sub>, CH<sub>2</sub>CCCCH, CHCCHCCH, cyclic-C<sub>5</sub>H<sub>5</sub>, and benzyl radicals are now nearing completion. Comparisons with the available experiment data for the propargyl, allyl, and benzyl radical reactions affirm the accuracy of the present approach.

These studies serve as an important prelude to studies of the full pressure and temperature dependent kinetics on the corresponding molecular surfaces. We have just completed a master equation based analysis of the pressure and temperature dependent kinetics of reactions on the C<sub>7</sub>H<sub>8</sub> surface, employing the reactive fluxes obtained in the abovementioned analysis of the H + benzyl reaction, and from a related analysis of the C<sub>6</sub>H<sub>5</sub> + CH<sub>3</sub> reaction. For the H + benzyl addition reaction, the branching to *o*-isotoluene and *p*-isotoluene, which had been ignored in prior SACM studies, was found to be roughly equal to the branching to toluene. The theoretical predictions were found to be in reasonably satisfactory agreement with the available experimental data for the photodissociation of toluene, the temperature and pressure dependent

dissociation of toluene, and the reaction of benzyl radical with H. For the  $C_6H_5 + CH_3$  recombination, the theoretical predictions exceed the experimental measurements of Lin and coworkers by a factor of 2 or more for all temperatures.

### *Hydrocarbon Oxidation*

In collaboration with Jim Miller, we have completed master equation simulations of the temperature and pressure dependent kinetics of the reactions of OH with ethylene and diacetylene. These studies were preceded by high-level *ab initio* mappings of the potential energy surface. For both cases, modest adjustments in a key energy barrier ( $< 1$  kcal/mol) yields agreement with most of the experimental data, including the temperature and pressure dependence of the rate coefficients. For the  $C_2H_4 + OH$  reaction, we confirm the importance of the abstraction channel above 800 K and find that a significant fraction of the total rate coefficient ( $\sim 10\%$ ) is due to the formation of vinyl alcohol above this temperature. Calculations of the vinyl alcohol channel are consistent with the observation of this molecule in low-pressure flames by the ALS flame team. For the  $C_4H_2 + OH$  reaction, at low temperatures, the reaction proceeds mostly to the addition product, as well as to CO and propargyl. Above 1200 K, direct hydrogen abstraction and production of H atoms become important.

In collaboration with John Kiefer and Larry Harding we have applied our direct CASPT2 based variable reaction coordinate RRKM approach to the study of the classic pyrolytic decomposition of acetaldehyde. The RRKM predictions were then incorporated in 2-dimensional master equation fits of the strong falloff seen in the laser-schlieren experiments, and also that shown in some previous shock-tube results using UV absorption of the acetaldehyde as diagnostic. Theory and experiment provide a consistent and reasonable model for the dissociation of acetaldehyde.

### *Radical Identification (in collaboration with ALS Flame Team)*

Quantitative identification of isomers of hydrocarbon radicals in flames is critical to understanding soot formation. In some recent studies we have demonstrated that many isomers can be effectively identified via the comparison of observed photoionization efficiencies (obtained in experiments that combine molecular-beam mass spectrometry with photoionization by tunable vacuum-ultraviolet synchrotron radiation) with theoretical simulations based on calculated ionization energies and Franck-Condon factors. The theoretical simulations employ the rovibrational properties obtained with B3LYP/6-311++G(d,p) density functional theory and electronic energies obtained from QCISD(T) *ab initio* calculations extrapolated to the complete basis set limit. In this last year we have applied this approach to the identification of  $C_4H_x$  and  $C_5H_x$  species. For the  $C_4H_x$  species, we identified *i*- $C_4H_3$  and *i*- $C_4H_5$  in various flames, and described the lack of evidence for *n*- $C_4H_3$  and *n*- $C_4H_5$  coupled with the possible difficulties in observing them. For the  $C_5H_x$  species, we identified a number of  $C_5H_3$ ,  $C_5H_4$ ,  $C_5H_5$ , and  $C_5H_6$  isomers and identified a possible contributor to the minor signal for  $C_5H_2$ . In all but one instance the calculated ionization energies were within the error bars of the experimental observations.

### *NOx chemistry*

We are currently in the process of examining the  $NH_2 + OH$  (in collaboration with Larry Harding and Joe Michael) and  $H + NCN$  reactions (in collaboration with Larry Harding and Jim Miller).

## Future Directions

We will continue our studies of radical-radical reactions in collaboration with Larry Harding. These studies will consider the recombination of (i) CH<sub>3</sub> radical with resonantly stabilized alkyl radicals, (ii) two resonantly stabilized alkyl radicals, (iii) alkyl radicals with OH and OOH, (iv) alkyl radicals with O<sub>2</sub>, and (v) halogen substituted hydrocarbons. Bill Pitz, Henry Curran and Charlie Westbrook have also suggested a particular set of large saturated alkyl radical recombinations for further study. We are also interested in studying series of radical-radical abstraction reactions. Preliminary results from our analysis of the reaction of vinyl radical with O<sub>2</sub> have led us to some novel indications of the importance of supercollisions in kinetics that we expect to pursue. Our contributions to the radical identification efforts of the ALS flame team continue with quantum chemical studies of the ionization energies of various polyynes and of various oxygenated species related to the combustion of methyl acetate and ethyl formate.

## DOE Supported Publications, 2004-Present

1. James A. Miller and Stephen J. Klippenstein, *The H + C<sub>2</sub>H<sub>2</sub> (+M) ↔ C<sub>2</sub>H<sub>3</sub> (+M) and H + C<sub>2</sub>H<sub>4</sub> (+M) ↔ C<sub>2</sub>H<sub>5</sub> (+M) Reactions: Electronic Structure, Variational Transition State Theory, and Solutions to a Two-Dimensional Master Equation*, Phys. Chem. Chem. Phys., **6**, 1192-1202 (2004).
2. Frank Striebel, Leonard E. Jusinski, Askar Fahr, Joshua B. Halpern, Stephen J. Klippenstein, and Craig A. Taatjes, *Kinetics of the Reaction of Vinyl Radicals with NO: Ab Initio Theory, Master Equation Predictions, and Laser Absorption Measurements*, Phys. Chem. Chem. Phys., **6**, 2216-2223 (2004).
3. Juan P. Senosiain, Stephen J. Klippenstein and James A. Miller, *A Complete Statistical Analysis of the Reaction of OH with CO*, Proc. Comb. Inst., **30**, 945-953 (2004).
4. Lawrence B. Harding, Stephen J. Klippenstein, and Yuri Georgievskii, *Reaction of Oxygen Atoms with Hydrocarbon Radicals: A Priori Predictions for the CH<sub>3</sub> + O, C<sub>2</sub>H<sub>5</sub> + O, and C<sub>2</sub>H<sub>3</sub> + O Reactions*, Proc. Comb. Inst., **30**, 985-993 (2004).
5. J. H. Kiefer, S. Santhanam, N. K. Srinivasan, R. S. Tranter, S. J. Klippenstein, and M. A. Oehlschlaeger, *Dissociation, Relaxation, and Incubation in the High-Temperature Pyrolysis of Ethane, and a Successful RRKM Modeling*, Proc. Comb. Inst. **30**, 1129-1135 (2004).
6. James A. Miller and Stephen J. Klippenstein, *Some Observations Concerning Detailed Balance in Association/Dissociation Reactions*, J. Phys. Chem. A, **108**, 8296-8306 (2004).
7. T. D. Jaeger, D. van Heijnsbergen, S. J. Klippenstein, G. von Helden, G. Meijer, and M. A. Duncan, *Vibrational Spectroscopy and Density Functional Theory of Transition Metal Ion-Benzene and Di-benzene Complexes in the Gas Phase*, J. Am. Chem. Soc., **126**, 10981-10991 (2004).
8. Craig A. Taatjes, Stephen J. Klippenstein, Nils Hansen, James A. Miller, Terrill A. Cool, Juan Wang, Matthew E. Law, and Phillip R. Westmoreland, *Synchrotron Photoionization Measurements of Combustion Intermediates: Photoionization Efficiency of C<sub>3</sub>H<sub>2</sub> Isomers*, Phys. Chem. Chem. Phys., **7**, 806-813, (2005).
9. Edgar G. Estupinan, Stephen J. Klippenstein, and Craig A. Taatjes, *Measurements and Modeling of HO<sub>2</sub> Formation in the Reactions of n-C<sub>3</sub>H<sub>7</sub> and i-C<sub>3</sub>H<sub>7</sub> Radicals with O<sub>2</sub>*, J. Phys. Chem. B, **109**, 8374-8387 (2005).
10. Yuri Georgievskii and Stephen J. Klippenstein, *Transition State Theory for Long-Range Potentials*, J. Chem. Phys., **122**, 194103;1-17 (2005).

11. Stephen J. Klippenstein and James A. Miller, *The Addition of Hydrogen Atoms to Diacetylene and the Heats of Formation of *i*-C<sub>4</sub>H<sub>3</sub> and *n*-C<sub>4</sub>H<sub>3</sub>*, *J. Phys. Chem. A*, **109**, 4285-4295 (2005).
12. Larry B. Harding, Yuri Georgievskii, and Stephen J. Klippenstein, *Predictive Theory for Hydrogen Atom-Hydrocarbon Radical Association Kinetics*, *J. Phys. Chem. A*, feature article, **109**, 4646-4656 (2005).
13. Keiji Matsumoto, Stephen J. Klippenstein, Kenichi Tonokura, and Mitsuo Koshi, *Channel Specific Rate Constants Relevant to Thermal Decomposition of Disilane*, *J. Phys. Chem. A*, **109**, 4911-4920 (2005).
14. Peng Zou, Stephen J. Klippenstein, and David L. Osborn, *The Vinyl + NO Reaction: Determining the Products with Time-Resolved Fourier Transform Spectroscopy*, *J. Phys. Chem. A*, **109**, 4921-4929, (2005).
15. Craig A. Taatjes, Nils Hansen, Fei Qi, Andrew McIlroy, James A. Miller, Juan P. Senosiain, Stephen J. Klippenstein, Terrill A. Cool, Juan Wang, Phillip R. Westmoreland, Matthew E. Law, Tina Kasper, and Katharina Kohse-Hoinghaus, *Enols are Common Intermediates in Hydrocarbon Oxidation*, *Science*, **308**, 1887-1889 (2005).
16. Erin E. Greenwald, Simon W. North, Yuri Georgievskii, and Stephen J. Klippenstein, *A Two Transition State Model for Barrierless Radical-Molecule Reactions: A Case Study of the Addition of OH to C<sub>2</sub>H<sub>4</sub>*, *J. Phys. Chem. A*, **109**, 6034-6044 (2005).
17. Juan P. Senosiain, Stephen J. Klippenstein and James A. Miller, *The Reaction of Acetylene with Hydroxyl Radicals*, *J. Phys. Chem. A*, **109**, 6045-6055 (2005).
18. Stephen J. Klippenstein, Yuri Georgievskii, and Larry B. Harding, *Predictive Theory for the Association Kinetics of Two Alkyl Radicals*, *Phys. Chem. Chem. Phys.*, invited article, **8**, 1133-1147 (2006).
19. Nils Hansen, Stephen J. Klippenstein, Craig A. Taatjes, James A. Miller, Juan Wang, Terrill A. Cool, Bin Yang, Rui Yang, Lixia Wei, Chaoqun Huang, Jing Wang, Fei Qi, Matthew E. Law, and Phillip R. Westmoreland, *Identification and Chemistry of C<sub>4</sub>H<sub>3</sub> and C<sub>4</sub>H<sub>5</sub> Isomers in Fuel Rich Flames*, *J. Phys. Chem. A*, **110**, 3670-3678, (2006).
20. Nils Hansen, Stephen J. Klippenstein, James A. Miller, Juan Wang, Terrill A. Cool, Matthew E. Law, Phillip R. Westmoreland, Tina Kasper, and Katharina Kohse-Hoinghaus, *Identification of C<sub>5</sub>H<sub>x</sub> Isomers in Fuel-Rich Flames by Photoionization Mass Spectrometry and Electronic Structure Calculations*, *J. Phys. Chem. A*, **110**, 4376-4388 (2006).
21. Juan P. Senosiain, Stephen J. Klippenstein, and James A. Miller, *Pathways and Rate Coefficients for the Decomposition of Vinyloxy and Acetyl Radicals*, *J. Phys. Chem. A*, in press (2006).
22. Juan P. Senosiain, Stephen J. Klippenstein, and James A. Miller, *The Reaction of Ethylene with Hydroxyl Radicals: A Theoretical Study*, *J. Phys. Chem. A*, in press (2006).
23. N. K. Srinivasan, J. V. Michael, L. B. Harding, and S. J. Klippenstein, *Initiation in CH<sub>4</sub>/O<sub>2</sub>: High Temperature Rate Constants for CH<sub>4</sub> + O<sub>2</sub> → CH<sub>3</sub> + HO<sub>2</sub>*, *Proc. Comb. Inst.*, **31**, in press (2006).
24. Stephen J. Klippenstein, Lawrence B. Harding, and Yuri Georgievskii, *On the Formation and Decomposition of C<sub>7</sub>H<sub>8</sub>*, *Proc. Comb. Inst.*, **31**, in press (2006).
25. K. S. Gupte, J. H. Kiefer, R. S. Tranter, S. J. Klippenstein, and L. B. Harding, *Decomposition of Acetaldehyde: Experiment and Detailed Theory*, *Proc. Comb. Inst.*, **31**, in press (2006).
26. Juan P. Senosiain, Stephen J. Klippenstein, and James A. Miller, *Oxidation Pathways in the Reaction of Diacetylene with OH Radicals*, *Proc. Comb. Inst.*, **31**, in press (2006).

# Theoretical modeling of spin-forbidden channels in combustion reactions

Anna I. Krylov

Department of Chemistry, University of Southern California,  
Los Angeles, CA 90089-0482  
krylovusc.edu

April 10, 2006

## 1 Scope of the project

The goal of our research is to develop predictive theoretical methods, which can provide crucial quantitative data (e.g., rate constants, branching ratios, heats of formation), identify new channels and refine reaction mechanisms. Specifically, we are developing tools for computational studies of spin-forbidden and non-adiabatic pathways of reactions relevant to combustion, and applying these tools to study electronic structure and reactions of open-shell and electronically excited species involved in these processes.

## 2 Summary of recent major accomplishments

### 2.1 Beyond vinyl: Electronic structure of unsaturated propen-1-yl, propen-2-yl, 1-buten-2-yl, and trans-2-buten-2-yl hydrocarbon radicals

Hydrocarbon radicals are major players in the combustion of hydrocarbon fuels. We applied state-of-the-art electronic structure methods to characterize unsaturated hydrocarbon radicals derived from vinyl[1]. Vertical excitation energies and oscillator strengths for several valence and Rydberg electronic states of vinyl, propen-1-yl, propen-2-yl, 1-buten-2-yl, and trans-2-buten-2-yl radicals were calculated using equation-of-motion coupled cluster methods with single and double substitutions (EOM-CCSD). Systematic changes in the geometries, excitation energies, and Rydberg state quantum defects within this group of radicals were discussed.

The electronic spectrum of these species was found to be very dense and dominated by Rydberg transitions. The electronic structure and energetics of the valence low-lying excited states are similar in all the radicals, except for the  $n \leftarrow \sigma$  states, which change substantially with the number of adjacent  $\sigma$ -bonds. The excitation energies for the Rydberg states, however, depend strongly on the size and the structure of the radicals. The major

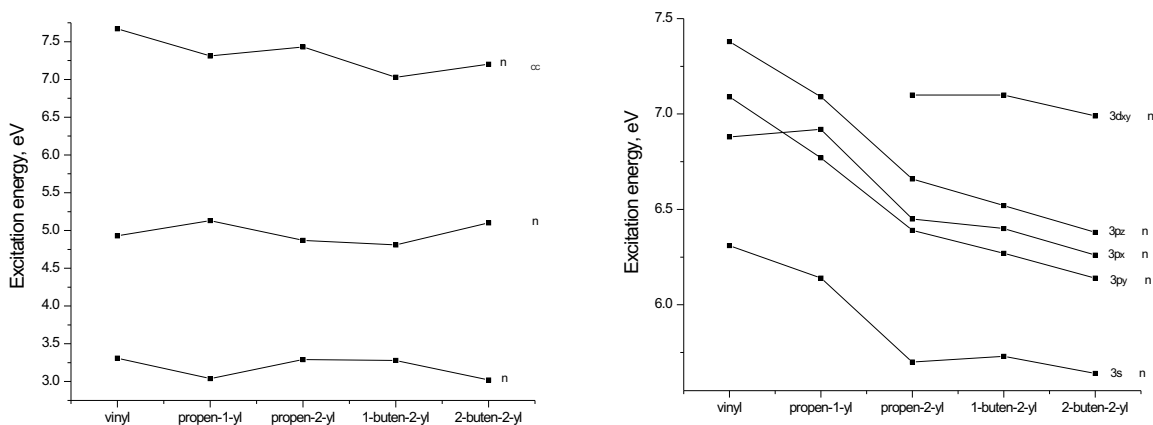


Figure 1: Changes in the valence  $n \leftarrow \pi$ ,  $\pi^* \leftarrow n$ , and  $n \leftarrow \sigma_{CC}$  (left panel), and in the Rydberg  $nl_m \leftarrow n$  (right panel) vertical excitation energies.

factor responsible for the changes in the Rydberg states' energies is the strong dependence of the ionization potentials on the size and geometric structure. Our results suggest that the quantum defect  $\delta$  for the  $3p_x$ ,  $3p_y$ , and  $3p_z$  Rydberg states is determined by the geometry dependent charge distribution within the cation core.

Based on the results of accurate *ab initio* calculations, we derived the qualitative picture encompassing the effects of substitution of hydrogens with methyl or ethyl groups in unsaturated hydrocarbons. Our results helped to interpret the experimental data of Prof. Laurie Butler, who found that the C-Br fission, the primary channel of 2-bromo-1-butene photodissociation, produces about 10-20% of electronically excited 1-buten-2-yl radicals. Based on our calculations, this state was assigned to the  $n \leftarrow \pi$  transition. Similar behavior was observed for 2-chloro-2-butene. We hope that the qualitative understanding of the electronic structure of unsaturated radicals will help in predicting excited state properties and reaction pathways of other related species.

## 2.2 Conical and glancing Jahn-Teller intersections in the cyclic trinitrogen cation

Characterization of crossings between potential energy surfaces is essential for understanding the dynamics of electronic transitions. We applied EOM-CC methods to study excited states in the cyclic  $N_3$  cation at the equilibrium  $D_{3h}$  geometry and along the Jahn-Teller distortions (submitted to J. Chem. Phys.). Lowest excited states are derived from single excitations from the doubly degenerate HOMO to the doubly degenerate LUMO, which gives rise to two exactly and two nearly degenerate states. The interaction of two degenerate states with two other states eliminates linear terms and results in a glancing rather than conical Jahn-Teller intersection. HOMO-2  $\rightarrow$  LUMO excitations give rise to two regular Jahn-Teller states. This result is of fundamental importance. We predict that a similar pattern would occur in other species with doubly degenerate HOMO and LUMO, e.g., benzene.

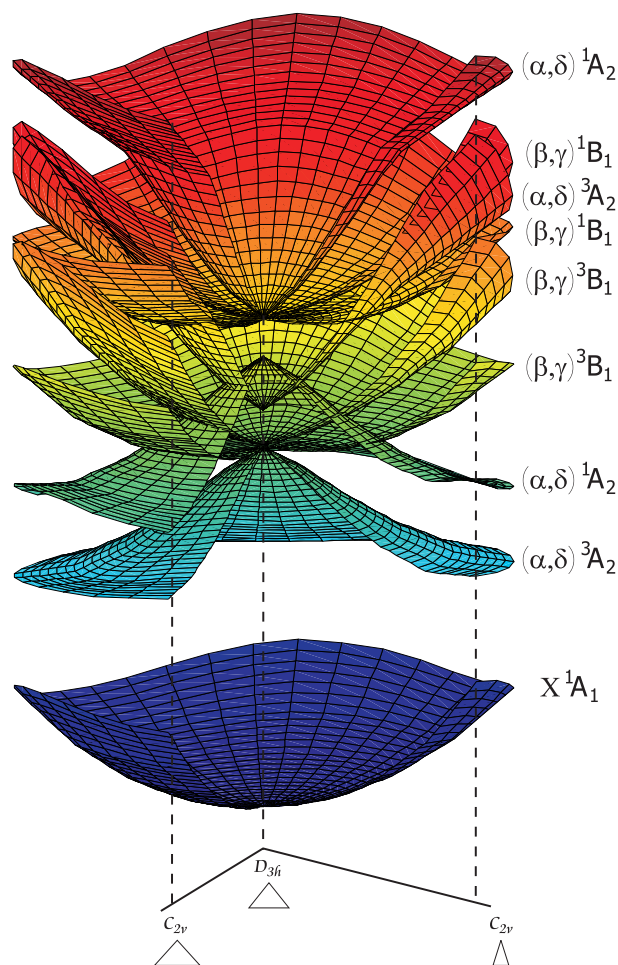


Figure 2: PESs of the ground (X) and the first eight excited states of  $N_3^+$ . Three out of four states in each multiplicity are almost degenerate in  $D_{3h}$ , two being exactly degenerate.

### 2.3 Benchmark study of the performance of spin-flip methods for bond-breaking

In collaboration with Stephen Klippenstein and Larry Harding, we performed a benchmark study of the spin-flip (SF) methods (anuscript in preparation). We considered bond-breaking in methylene and ethane, and tested SF methods against FCI and MR-CI. We found that the EOM-SF-CCSD curves are within 1 kcal/mol from the MR-CI data of Klippenstein and Harding.

## 3 Current research and future plans

Currently, we are implementing algorithms developed by Prof. David Yarkoni for characterizing intersections between PESs of the same and different multiplicity within EOM methods. Immediate applications include characterization of singlet-triplet crossings in formaldehyde (in collaboration with Prof. Joel Bowman), and in the  $C_2H_4O$  diradical (in collaboration with Prof. Hai Wang). We are also collaborating with Prof. Hanna Reisler on characterizing the electronic structure of diazomethane, a precursor for producing triplet and singlet methylene.

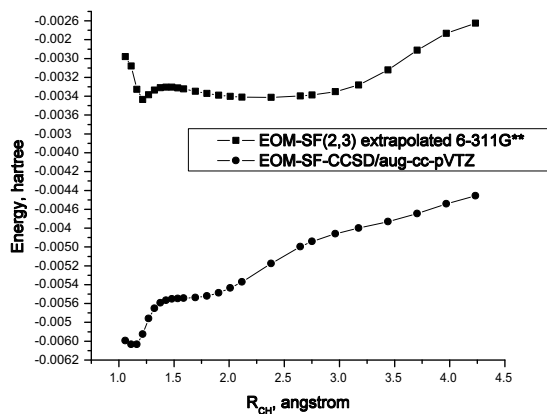


Figure 3: Errors of EOM-SF-CCSD and extrapolated EOM-SF(2,3) against MR-CISD results in aug-cc-pVTZ basis set. The corresponding non-parallelity errors are 0.99 and 0.51 kcal/mol, respectively.

## References

- [1] L. Koziol, S.V. Levchenko, and A.I. Krylov, Beyond vinyl: Electronic structure of unsaturated propen-1-yl, propen-2-yl, 1-buten-2-yl, and trans-2-buten-2-yl hydrocarbon radicals, *J. Phys. Chem. A* **110**, 2746 (2006).

# TIME-RESOLVED FTIR EMISSION AND ADVANCED LIGHT SOURCE STUDIES OF PHOTOFRAGMENTATION, RADICAL REACTIONS, AND AEROSOL CHEMISTRY

*Stephen R. Leone*  
*Departments of Chemistry and Physics*  
*and Lawrence Berkeley National Laboratory*  
*University of California*  
*Berkeley, California 94720*  
*(510) 643-5467 srl@berkeley.edu*

## Scope of the Project

Combustion is a complex process involving short-lived radical species, highly excited states, kinetics, transport processes, heterogeneous chemistry and aerosols such as soot, fluid dynamics, and energy transfer. Detailed measurements of microscopic reaction pathways, rate coefficients, vibrational and rotational product state distributions, and thermochemistry have resulted in considerable information to aid in the understanding of combustion processes. Infrared and visible emissions are used together with a Fourier transform spectrometer to explore laser-initiated radical reactions, radical-radical reactions, photofragmentation events, and energy transfer processes. Vibrationally excited and low-lying visible electronically excited species generated in chemical dynamics processes are investigated. The current research involves the study of several important radical reactions (e.g.  $C_2H + O$ ,  $HCCO + O$ ,  $C_2H + O_2$ ,  $O + C_2H_2$ ) to determine the nascent product species and states as well as the mechanisms and kinetic pathways. Vacuum ultraviolet light at the Chemical Dynamics Beamline of the Advanced Light Source provides a tool to measure the energetics and photoionization spectroscopy of important combustion species. For example, at the Chemical Dynamics Beamline there are efforts to study photoionization spectroscopy of carbon cluster species (new work performed by Mike Duncan and our postdoc Christophe Nicolas). To facilitate this, a laser ablation apparatus has been developed at the beamline with Musa Ahmed to produce and study  $C_1$ , through  $C_{10}$  and higher species in photoionization. The same source has also been applied to biomolecules by M. Ahmed and to metal oxide species with Ricardo Metz. Ongoing work also involves interactions with Terry Cool, Craig Taatjes (Combustion Research Facility), and Phil Westmoreland in their pursuit of studies in flame chemistry. We are working with Taatjes and David Osborn (Combustion Research Facility) on a new kinetics apparatus that uses single photon VUV ionization detection. A new theme has been initiated to study aerosol formation, light scattering, and aerosol reactive chemistry. The latter effort will explore aerosol species and their roles and production in combustion, and the resulting soot species from combustion.

## Time-Resolved FTIR and FT-VIS Studies of Combustion Dynamics

### Product State Distributions of $C_2H + O$ , $C_2H + O_2$ reactions

The reactions of ethynyl radical ( $C_2H$ ) play a key role in hydrocarbon combustion processes, as well as in the chemistry of interstellar space and planetary atmospheres. One of the important reactions is the radical-radical reaction with  $O(^3P)$  atom to produce a CO molecule and either  $CH(X^2\Pi)$  or  $CH(A^2\Delta)$ , the two major electronic product channels. The  $CH(A^2\Delta)$  emission from this reaction is substantially responsible for the blue flame emission in combustion. We recently investigated the mechanism of this reaction first by measuring time-resolved vibrational emission spectra of the  $CO(v)$  product.  $C_2H$  and  $O(^3P)$  radicals were produced by 193 nm pulsed laser photolysis of an acetylene/ $SO_2$  mixture. A bimodal distribution of the  $CO(v)$  vibrationally excited products was observed (Fig. 1), assigned to the CO from each of the two electronic channels of the reaction. Simulation of the spectra allows extraction of a relative branching between the two channels, indicating a  $CH(A^2\Delta):CH(X^2\Pi)$  ratio of  $\sim 3:2$  for the  $CO + CH$  branch, seemingly greater than previously expected from the overall  $CH(A)$  reaction pathway by Josef Peeters' group. This has led Shaun Carl to suggest the possibility of formation of a  $C_2O + H$  channel as well. Surprisal analysis indicates that energy from the reaction is

preferentially deposited into CO vibrations, consistent with a short-lived HCCO transition state for the reaction, in agreement with earlier studies.

Second, we investigated the mechanism of the  $C_2H + O(^3P)$  reaction by observing the rotationally resolved electronic emission spectrum of the  $CH(A^2\Delta)$  product at  $\sim 430$  nm, by operating the FTIR in the visible mode (FT-VIS). The nascent rotational and vibrational population distributions for the  $CH(A^2\Delta)$  product were determined by fitting the experimentally measured spectrum to a simulated spectrum. The vibrational temperature of the  $CH(A^2\Delta)$  product is found to be appreciably hotter ( $\sim 2800 \pm 100$  K) than the rotational temperature ( $\sim 1250 \pm 250$  K). This also supports the assignment of the HCCO radical as an intermediate in the reaction, perhaps in an electronically excited bent state. A study of the photodissociation of the HCCO radical at high excitation energies will be valuable to clarify the mechanism of the  $C_2H + O(^3P)$  reaction.

Another important reaction of the ethynyl radical in hydrocarbon flames is  $C_2H + O_2$ . The room temperature rate constant of the  $CH(A^2\Delta) + CO_2$  producing channel of this reaction is  $1/500^{\text{th}}$  that of the  $C_2H + O(^3P) \rightarrow CH(A^2\Delta) + CO$  reaction described above, making its detection with the FT-VIS considerably more challenging under the low pressure experimental conditions required to obtain a nascent product distribution. This reaction was studied in our lab by observing the rotationally-resolved electronic emission spectrum of the  $CH(A^2\Delta)$  product at  $\sim 430$  nm.  $C_2H$  was produced by 193 nm photolysis of acetylene. Extraction of the rotational and vibrational populations by fitting simulated spectra to the experimental spectra reveal rotationally and vibrationally excited  $CH(A^2\Delta)$  products, with a rotational temperature of  $\sim 1150$  K and a vibrational temperature of  $\sim 1600$  K. The mechanism of this reaction is complex, involving multiple intermediates and an electronic surface crossing. Our results suggest that the final step of this reaction involves dissociation from a bent state intermediate to form the  $CH(A^2\Delta)$  and  $CO_2$  products.

#### **Dynamics of Acetylene Oxidation: CO(v) from $C_2H_2 + O(^3P)$ and HCCO + $O(^3P)$ reactions**

Acetylene oxidation is of great importance in combustion chemistry as well as the chemistry of certain planetary atmospheres. Since acetylene is readily formed in fuel rich hydrocarbon flames, a detailed understanding of acetylene oxidation is essential for understanding hydrocarbon combustion chemistry. We measured the vibrational distributions of the CO(v) products from the reactions of  $C_2H_2$  and HCCO with  $O(^3P)$  atoms using FTIR emission spectroscopy.  $C_2H_2$  was reacted with  $O(^3P)$  formed by microwave discharge of  $O_2$ . The vibrational distribution of CO(v) from the  $C_2H_2 + O(^3P)$  oxidation process exhibits a bimodal distribution corresponding to reactions of two different radicals produced in the initial oxidation steps,  $CH_2 + CO$  and  $HCCO + H$  (where HCCO subsequently reacts with  $O(^3P)$  to form  $2CO + H$ ). Using simultaneous 193 nm photodissociation of ethyl ethynyl ether and  $SO_2$ , further results were obtained for CO(v) from the individual reaction of HCCO with  $O(^3P)$ . This reaction also shows a bimodal CO(v) vibrational distribution with vibrational temperatures  $2320 \pm 40$  K and  $10300 \pm 600$  K. This result, along with previous theoretical work, suggests a sequential dissociation process of  $HC(O)CO^{\ddagger} \rightarrow CO + HCO$ ;  $HCO \rightarrow H + CO$ . The results strongly hint at the possibility that the two CO vibrational distributions could be formed by the two CO product mechanisms. However, the ratios of the two components of the vibrational emission are not at all equal (85% cold, 15% hot), precluding a simple assignment to the two CO formation processes and instead requiring the possible participation of electronically excited surfaces. The close fit of the vibrational populations to Boltzmann-like temperatures does suggest a longer-lived intermediate mechanism.

#### **Photoionization Measurements**

At the Advanced Light Source, a novel laser vaporization source has been developed to produce carbon cluster species for photoionization spectral studies. Such investigations provide basic thermodynamic and structural information for these fundamental species. The cluster source was

used to produce  $C_1 - C_{10}$  and higher by vaporization of a graphite rod, and the ionization potentials for each of these species are in the process of being measured. F. Schaefer is working on calculations for comparison to experiment. The detailed photoionization efficiency data for species such as  $C_3$ , coupled with CAS-SCF calculations on the resulting  $C_3^+$  ion states, performed by our collaborator M. Hochlaf, suggest that additional intensity maxima in the photoionization efficiency versus energy data can be attributed to identifiable electronically excited states of  $C_3^+$ .

### **Aerosol Chemistry**

Using a newly constructed aerosol machine at the Chemical Dynamics Beamline, we have undertaken fundamental studies of the optical properties of aerosol particles using VUV radiation. Silica particles, chemically synthesized online, are size-selected by a differential mobility analyzer and introduced into vacuum through a set of aerodynamic lenses. The angular distributions of scattered photons originating from 70, 100, 200 nm diameter silica particles are measured with 145.9 and 118.1 nm synchrotron radiation. As predicted by Mie Theory, these angular distributions show strong forward scattering. A careful comparison of scattered fluxes at both visible and VUV wavelengths clearly shows enhanced size sensitivity at shorter wavelengths. A collaborative effort initiated with Prof. Eckart Rühl (University of Würzburg) began investigations of the fundamental electronic properties of nanoparticles for the first time using velocity map imaging (VMI) of the ejected photoelectrons. A pronounced asymmetry in the photoelectron angular distributions is observed for insulator particles and correlated with particle size. The asymmetry is most pronounced for 500 nm diameter particles and decreases with particle size down to 45 nm, suggesting that for insulating particles the light is absorbed on the illuminated surface and the electrons ejected from that surface. However, the magnitude of this asymmetry with particle size is dependent upon the electronic properties. Gold particles, which are conducting, show very little asymmetry compared to an insulator like NaCl. This is presumably due to differences in low energy (1 eV) electron dynamics and the field interactions with a conductor vs. an insulator. George Schatz (Northwestern University) is helping with computations to understand the electron dynamics within the particles to consider these results.

The capability to study aerosol composition and chemistry using VUV photoionization was also initiated. This “soft” ionization technique has been shown to yield near “fragment free” mass spectra of a variety of organic molecules. Aerosol particles are flash vaporized (50-500°C) and the resulting molecules are photoionized near threshold and then analyzed using time of flight (TOF) mass spectrometry. In this way, the chemical composition of aerosol particles can be monitored in the course of a chemical reaction. The first studies of aerosol chemistry using this technique were conducted in collaboration with Prof. Tom Baer and Erin Mysak (University of North Carolina). Oleic acid aerosol particles are generated in urban areas as a by-product of meat grilling in the fast food industry. Oleic acid particles were generated in situ and the resulting mass spectrum after the oleic acid aerosol was vaporized and ionized at 9 eV photon energy contains a single parent peak at 284 amu. In contrast, electron impact ionization results in extensive fragmentation that prohibits a detailed investigation of more complex aerosol chemistry due to interference between reactant and product fragmentation peaks in the electron impact mass spectrum. Oleic acid aerosols were also reacted with  $O_3$  (a ubiquitous atmospheric oxidant). The VUV photoionization mass spectrum showed a decrease of the parent ion with  $O_3$  addition as well as an increase in the particle phase products located at lower masses. Additional studies are aimed at probing the reactivity of surface-bound polyaromatic hydrocarbon molecules with the ultimate goal to understand oxidative aging of soot particles in the troposphere. To accomplish this, binary nanometer-sized particles are made with monolayer coatings of anthracene on various inorganic (e.g. NaCl) and organic (stearic acid) seed particles. Upon reaction with ozone a variety of new particle phase oxidation products are clearly identified by VUV single photon ionization mass spectrometry. Detailed studies of how the oxidation rate of anthracene depends on coating thickness and seed particle size are currently underway.

Correlating changes in particle size with oxidation chemistry will also be used to a better understand of how chemistry is influenced by particle morphology.

### Future Plans

New studies will explore radical reactions such as  $C_2H$  with  $NO$  (parallel to  $C_2H + O_2$ ),  $CH_3 + N$ , kinetic energy-enhanced reactions such as  $OH +$  propane, radical-radical reactions of  $NCO$  with  $O$  and  $H$  atoms and radical-molecule reactions such as  $NCO +$  carbon/hydrogen species. Experiments are also being considered to use the time-resolved FTIR method to examine heterogeneous processes with aerosol surface reactions. Other investigations are ongoing to explore the  $CH(A)$  state formed by photodissociation of bromoform with vacuum ultraviolet light at the Advanced Light Source. Major studies will exploit the aerosol generation and detection instrumentation, described above, and the new kinetics machine developed with Sandia National Laboratory, which is being tested in detail. As an example, the production and VUV ionization of soot-containing aerosols can be investigated in the future.

### Recent Publications Citing DOE Support

V. Chikan, B. Nizamov and S. R. Leone, "Product state distributions of vibrationally excited  $CO(v)$  for the  $CH(X^2\Pi)$  and  $C(A^2\Delta)$  channels of the  $C_2H+O(^3P)$  reaction," *J. Phys. Chem. A* **108**, 10770 (2004).

V. Chikan and S. R. Leone, "Vibrational distributions of the  $CO(v)$  products of the  $C_2H_2 + O(^3P)$  and  $HCCO + O(^3P)$  reactions studied by FTIR emission," *J. Phys. Chem. A* **109**, 2525 (2005).

V. Chikan, S. R. Leone, "Vibrational and rotational distributions of the  $CH(A^2\Delta)$  product of the  $C_2H + O(^3P)$  reaction studied by Fourier transform visible (FTVIS) emission spectroscopy," *J. Phys. Chem. A* **109**, 10646 (2005).

V. Chikan, B. Nizamov, and S. R. Leone, "State-resolved dynamics of the  $CH(A^2\Delta)$  channels from single and multiple photon dissociation of bromoform in the 10–20 eV energy range," *J. Phys. Chem. A* **110**, 2850 (2006).

J. Shu, D. S. Peterka, S. R. Leone, and M. Ahmed, Tunable synchrotron vacuum ultraviolet ionization, time-of-flight investigation of the photodissociation of trans-crotonaldehyde at 193 nm," *J. Phys. Chem. A* **108**, 7895 (2004).

J. Shu, K. R. Wilson, A. N. Arrowsmith, M. Ahmed, and S. R. Leone, "Light scattering of ultrafine silica particles by VUV synchrotron radiation," *Nano Letters* **5**, 1009 (2005).

R. B. Metz, C. Nicolas, M. Ahmed, and S. R. Leone, "Direct determination of the ionization energies of  $FeO$  and  $CuO$  with VUV radiation," *J. Chem. Phys.* **123**, 114313 (2005).

J. Shu, K. R. Wilson, M. Ahmed, S. R. Leone, C. Graf, and E. Rühl, "Elastic light scattering from nanoparticles by monochromatic vacuum-ultraviolet radiation," *J. Chem. Phys.* **124**, 034707 (2006).

K. R. Wilson, M. Jimenez-Cruz, C. Nicolas, L. Belau, S. R. Leone, and M. Ahmed, "Thermal vaporization of biological nanoparticles: Fragment-free vacuum ultraviolet photoionization mass spectra of tryptophan, phenylalanine-glycine-glycine and  $\beta$ -carotene," *J. Phys. Chem. A* **110**, 2106 (2006).

C. Nicolas, J. Shu, D. S. Peterka, M. Hochlaf, L. Poisson, S. R. Leone, and M. Ahmed, "Vacuum ultraviolet photoionization of  $C_3$ ," *J. Amer. Chem. Soc.* **128**, 220 (2006).

K. R. Wilson, L. Belau, C. Nicolas, M. Jimenez-Cruz, S. R. Leone, and M. Ahmed, " Direct determination of the ionization energy of histidine with VUV synchrotron radiation," *Int. J. Mass Spectrosc.* **249**, 155 (2006).

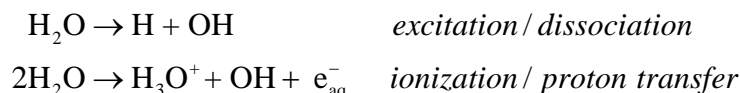
# INTERMOLECULAR INTERACTIONS OF HYDROXYL RADICALS ON REACTIVE POTENTIAL ENERGY SURFACES

Marsha I. Lester  
Department of Chemistry  
University of Pennsylvania  
Philadelphia, PA 19104-6323  
milester@sas.upenn.edu

## PROGRAM SCOPE

The primary objective of the DOE-sponsored research in this laboratory is to characterize the interactions of hydroxyl radicals with reactive partners of combustion relevance (e.g. H<sub>2</sub>/D<sub>2</sub>, CH<sub>4</sub>, CO, and C<sub>2</sub>H<sub>2</sub>). In the current grant period, we are focusing our efforts on the solvation of hydroxyl radicals as a prototype for interactions of radicals in aqueous environments. In particular, we are examining the binary interaction of an open-shell OH X <sup>2</sup>Π radical with a water molecule as well as the characteristics of an OH radical embedded in small water clusters. Our goal is to understand the solvation structures, energetics, dynamics, and reactions of OH radicals in aqueous systems. In addition, we are examining the origin of quenching of electronically excited OH A <sup>2</sup>Σ<sup>+</sup> radicals by water, a process known to be efficient in gaseous and condensed phase environments. As a first step toward understanding such processes, we have extended our investigation of collisional quenching of OH A <sup>2</sup>Σ<sup>+</sup> by molecular hydrogen,<sup>1-3</sup> which has emerged as a benchmark system for investigation of the nonadiabatic processes that lead to quenching.

The DOE relevance of this research has been highlighted in a recent workshop report.<sup>4</sup> Hydroxyl radicals are important products of electron-driven processes in water as evident from the primary pathways for the decomposition of water by ionizing radiation:



A starting point for understanding the reactive behavior of radical species in aqueous environments is to examine the structure and energetics of isolated radical species with solvent molecules.

## RECENT PROGRESS

Extensive *ab initio* calculations have shown that the global minimum on the OH + H<sub>2</sub>O potential energy surface is a C<sub>s</sub> structure, H<sub>2</sub>O-HO, in which hydrogen bonding occurs between the H atom of the hydroxyl radical (donor) and the O atom in the water molecule (acceptor),<sup>5</sup> as shown in Fig. 1. The energy of the planar structure is calculated to be less than 40 cm<sup>-1</sup> higher, and the two equivalent structures, with the water tilted “up” and “down” are likely to be connected by large amplitude, zero-point motion through this small barrier, as found for the analogous closed shell species.

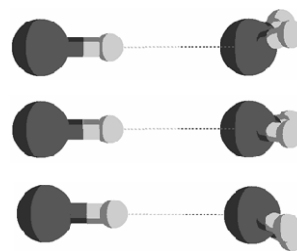


**Fig. 1** Minimum energy structures of the binary OH-water complex.

The computed well depth of  $\sim 5.7$  kcal mol<sup>-1</sup> for the OH-water complex is somewhat greater than that for the water dimer.

We have predicted that the rotational band structure of microwave and infrared transitions of the OH-water complex, typically used for spectral identification, would be quite complicated and very different from analogous closed-shell systems.<sup>6</sup> The rotational band structure is expected to be strongly affected by the coupling between the spin and/or orbital angular momenta of the open-shell OH radical with the overall rotation of the complex. These predictions are built on our experimental and theoretical studies of the OH-acetylene complex,<sup>7-9</sup> which displays analogous behavior. Our predictions<sup>6</sup> have since been confirmed by microwave measurements,<sup>10,11</sup> and provide the theoretical basis for analysis of rotationally resolved infrared spectra of the OH-water complex.

As shown for other OH containing complexes, there are two relevant potentials of <sup>2</sup>A'' and <sup>2</sup>A' symmetry, differing only by the orientation of the half-filled pπ orbital of OH with respect to the nuclear framework. Various *ab initio* calculations indicate an energy difference between the <sup>2</sup>A'' and <sup>2</sup>A' surfaces, termed the difference potential ρ, of -110 and -190 cm<sup>-1</sup> for OH-water at its equilibrium geometry.<sup>5,12,13</sup> A recent microwave study indicates an intermediate value of -147 cm<sup>-1</sup>.<sup>11</sup> These values are sufficiently large, relative to the spin-orbit coupling constant for the OH monomer (*a* = -139 cm<sup>-1</sup>), to partially quench the electronic orbital angular momentum of the OH radical and with it the magnetic field responsible for coupling the OH radical's electron spin to the *a* inertial axis.

We have carried out model calculations that predict the evolution of the rotational energy levels for the interacting pair of molecules between the limits of completely unquenched to fully quenched OH orbital angular momentum in the complex.<sup>6</sup> The rotational energy levels of the OH-water complex group into manifolds according to the value for the projection of the angular momentum along the *a* inertial axis of the complex in both limiting cases. Fig. 2 shows a correlation diagram of the energies of the rotational manifolds for OH-water as a function of the difference potential ρ. The first few rotational levels of each manifold on the left are labeled with half integer projection quantum number *P* of the total angular momentum (including rotation, orbital and spin angular momenta). As the difference potential increases, the electronic orbital angular momentum is quenched, and the manifolds evolve into the limiting case on the right in which rotational levels are characterized by the integer projection quantum number *K<sub>a</sub>* of the rotational angular momentum. Our calculations also indicate how these changes in the rotational energy levels will be manifested in the microwave and infrared spectra of the OH-water complex.<sup>6</sup>

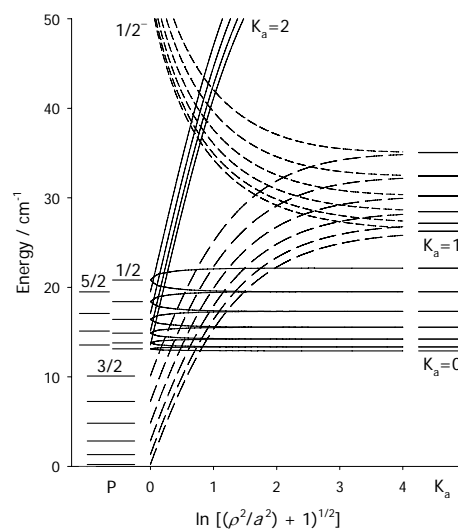


**Fig. 2** Correlation diagram of rotational energy levels for OH-water complex.

### FUTURE PLANS

Our primary focus is infrared spectroscopic studies of the binary OH-water complex and OH embedded in small water clusters using action spectroscopy. Towards this end, we have

developed a dual pulsed valve source to separately introduce nitric acid, the precursor for OH radicals, and water vapor. Spectroscopic searches in the OH radical stretch and H<sub>2</sub>O asymmetric stretch regions are currently underway. Spectral identification of the OH-water complex will require explicit consideration of the partial quenching of the electronic orbital angular momentum of the OH radical as discussed above. We will also measure the OH product state distributions following infrared excitation to determine the binding energy of the OH-water complex.

#### REFERENCES

- <sup>1</sup> D. T. Anderson, M. W. Todd, and M. I. Lester, *J. Chem. Phys.* **110**, 11117 (1999).
- <sup>2</sup> M. W. Todd, D. T. Anderson, and M. I. Lester, *J. Phys. Chem. A* **105**, 10031 (2001).
- <sup>3</sup> I. B. Pollack, Y. Lei, T. A. Stephenson, and M. I. Lester, *Chem. Phys. Lett.* **421**, 324 (2006).
- <sup>4</sup> B. C. Garrett, D. A. Dixon, D. M. Camaioni, D. M. Chipman, M. A. Johnson, et al., *Chem. Rev.* **105**, 355 (2005).
- <sup>5</sup> Y. Xie and H. F. Schaefer, *J. Chem. Phys.* **98**, 8829 (1993).
- <sup>6</sup> M. D. Marshall and M. I. Lester, *J. Phys. Chem. B* **109**, 8400 (2005).
- <sup>7</sup> J. B. Davey, M. E. Greenslade, M. D. Marshall, M. I. Lester, and M. D. Wheeler, *J. Chem. Phys.* **121**, 3009 (2004).
- <sup>8</sup> M. D. Marshall, J. B. Davey, M. E. Greenslade, and M. I. Lester, *J. Chem. Phys.* **121**, 5845 (2004).
- <sup>9</sup> M. D. Marshall and M. I. Lester, *J. Chem. Phys.* **121**, 3019 (2004).
- <sup>10</sup> Y. Ohshima, K. Sato, Y. Sumiyoshi, and Y. Endo, *J. Am. Chem. Soc.* **127**, 1108 (2005).
- <sup>11</sup> C. S. Brauer, G. Sedo, E. M. Grumstrup, K. R. Leopold, M. D. Marshall, and H. O. Leung, *Chem. Phys. Lett.* **401**, 420 (2005).
- <sup>12</sup> P. D. Cooper, H. G. Kjaergaard, V. S. Langford, A. J. McKinley, T. I. Quickenden, and D. P. Schofield, *J. Am. Chem. Soc.* **125**, 6048 (2003).
- <sup>13</sup> D. P. Schofield and H. G. Kjaergaard, *J. Am. Chem. Soc.* **120**, 6930 (2004).

#### DOE SUPPORTED PUBLICATIONS 2004-2006

1. J. B. Davey, M. E. Greenslade, M. D. Marshall, M. I. Lester, and M. D. Wheeler, "Infrared Spectrum and Stability of a  $\pi$ -type Hydrogen-Bonded Complex between the OH and C<sub>2</sub>H<sub>2</sub> Reactants", *J. Chem. Phys.* **121**, 3009-3018 (2004).
2. M. D. Marshall and M. I. Lester, "Spectroscopic Implications of the Coupling of Unquenched Angular Momentum to Rotation in OH-Containing Complexes", *J. Chem. Phys.* **121**, 3019-3029 (2004).
3. M. D. Marshall, J. B. Davey, M. E. Greenslade, M. I. Lester, "Evidence for Partial Quenching of Orbital Angular Momentum upon Complex Formation in the Infrared Spectrum of OH-Acetylene", *J. Chem. Phys.* **121**, 5845-5851 (2004).
4. M. D. Marshall and M. I. Lester, "Spectroscopic Implications of Partially Quenched Orbital Angular Momentum in the OH-Water Complex", *J. Phys. Chem. B* **109**, 8400-8406 (2005).

# Theoretical Studies of Molecular Systems

William A. Lester, Jr.  
Chemical Sciences Division,  
Ernest Orlando Lawrence Berkeley National Laboratory and  
Kenneth S. Pitzer Center for Theoretical Chemistry  
Department of Chemistry, University of California, Berkeley  
Berkeley, California 94720-1460  
walester@lbl.gov

## Program Scope

This research program is directed at extending fundamental knowledge of atoms and molecules. The approach combines the use of ab initio basis set methods and the quantum Monte Carlo (QMC) method to describe the electronic structure and energetics of systems of primarily combustion interest.

## Recent Progress

**Hydrocarbon Benchmark Study** (with A. C. Kollias, D. Domin, G. Hill, M. Frenklach, D. M. Golden) A quantum Monte Carlo (QMC) benchmark study of 22 small hydrocarbons using DMC was completed. Heats of formation at 298 K, bond dissociation energies (BDEs), and atomization energies were computed using simple product trial wave functions consisting of a single determinant and correlation function. DMC results were compared to experiment and to other theory including a version of complete basis set theory (CBS-Q) and density functional theory (DFT) with the B3LYP functional.

**Graphene Layer Growth: Collision of Five-Membered Rings** (with R. Whitesides, A.C. Kollias, D. Domin, and M. Frenklach). Research of the past couple of years has led to identification of a new reaction pathway for the five-member ring migration along a graphene edge. The migration sequence is initiated by H-atom addition to an adsorbed cyclopenta group. Earlier simulation results showed that the evolving surface morphology and ensuing growth rate are determined by competition between the migration of five-member rings and other gas-surface and surface processes such as “nucleation” of six-member rings at surface corners and their desorption. Further comments on this work can be found in the abstract of Michael Frenklach.

**DMC Study of the n and i isomers of C<sub>4</sub>H<sub>3</sub>** (with D. Domin, M. Y. Frenklach)

Recently large basis set spin-restricted open-shell coupled-cluster calculations through triple excitations—ROCCSDT— and QCISD(T) have yielded an energy difference between the i and n isomers larger than that reported previously using the DMC method. The basis of this difference is important for mechanisms of formation of the first aromatic molecule and has implications for the procedures used in the earlier DMC calculations for these systems. Computations are nearing completion to clarify this situation..

## Future Plans

Selected systems from the recently completed DMC benchmark studies of atomization energies of small hydrocarbons will be studied further owing to their importance for combustion mechanisms. The benchmark study was limited to the use of single-determinant trial functions, which are not always adequate for establishment of combustion mechanisms. Key systems for further study include C<sub>2</sub>H, C<sub>2</sub>H<sub>2</sub>, C<sub>4</sub>H<sub>3</sub>, C<sub>4</sub>H<sub>5</sub>. The two leading systems in this list are pertinent to experiments at the ALS (Advanced Light Source). Alternative trial function types found to be successful previously in this laboratory including natural orbitals from CASSCF expansions will be investigated for the present systems. In addition, valence bond forms will be pursued owing to their compactness.

Efforts will return to the study of the pathways leading to formation of the first aromatic and subsequent reaction to form polyaromatic hydrocarbons (PAHs) in collaboration with Michael Frenklach's group. This direction was slowed in order to ascertain the dependence of DMC energies on walker populations. It is now clear that larger walker populations are needed to remove ambiguities that can arise in computed energies. This aspect appears to be as important, if not more so, than the form of the trial function chosen.

The collaborative effort with M. Frenklach on the growth of carbonaceous systems will continue. Frenklach has discussed the role of "collision" between migrating cyclopenta groups. The plan is to explore this and other related reactions using quantum chemical methods (ab initio, DFT, and QMC), and then determine reaction rates from the solution of master equations.

Efforts will continue in the pursuit of approaches for the accurate calculation of forces in DMC in collaboration with Roland Assaraf, CNRS (Paris). Although methods for the evaluation of forces have been pursued in this and other laboratories for a number of years, there is still no approach that can be routinely applied that yields accuracy of predictive merit.

## DoE Supported Publications (2004-2006)

1. A. Aspuru-Guzik, O. El Akramine, J. C. Grossman, and W. A. Lester, Jr., "Quantum Monte Carlo for Electronic Excitations of Free-Base Porphyrin," *J. Chem. Phys.* **120**, 3049 (2004).
2. A. C. Kollias, O. Couronne, and W. A. Lester, Jr., "Quantum Monte Carlo Study of the Reaction: Cl + CH<sub>3</sub>OH → CH<sub>2</sub>OH + HCl," *J. Chem. Phys.* **121**, 1357 (2004).
3. A. Aspuru-Guzik and W. A. Lester, Jr., "Quantum Monte Carlo: Theory and Application to Molecular Systems," Proceedings of the International Conference on Computational and Mathematical Methods in Science and Engineering, CMMSE-2004, Uppsala, June 4-8, 2004, p. 100.
4. W. A. Lester, Jr., Commentary on "Quantum Monte Carlo Studies on Be and LiH," in *Molecular Quantum Mechanics, Selected papers of N. C. Handy, D. C. Clary, S. M. Colwell, and H. F. Schaefer III*, eds, 2004, p. 145.
5. A. Aspuru-Guzik, A. C. Kollias, R. Salomon-Ferrer, and W. A. Lester, Jr. "Quantum Monte Carlo: Theory and Applications to Atomic, Molecular and Nano Systems," in the Handbook of

Theoretical and Computational Nanotechnology, eds. M. Rieth and W. Schommers, American Scientific Publishers (2005).

6. A. C. Kollias, D. Domin, G. Hill, M. Frenklach, D. M. Golden, and W. A. Lester, Jr., "Quantum Monte Carlo Study of Heats of Formation and Bond Dissociation Energies of Small Hydrocarbons," *Int. J. Chem. Kinetics* **37**, 583 (2005).
7. A. Aspuri-Guzik, R. Salomon-Ferrer, and W. A. Lester, Jr., "A Sparse Algorithm for the Evaluation of the Local Energy in Quantum Monte Carlo," *J. Comput. Chem.* **26**, 708 (2005).
8. A. Aspuri-Guzik and W. A. Lester, Jr., "Quantum Monte Carlo: Theory and Application to Molecular Systems," *Adv. Quant. Chem.* **49**, 209 (2005).
9. A. C. Kollias, D. Domin, G. Hill, M. Frenklach, and W. A. Lester, Jr., "Quantum Monte Carlo Study of Small Hydrocarbon Atomization Energies," *Mol. Phys.* **104**, 467 (2006).
10. A. Aspuri-Guzik, R. Salomon-Ferrer, B. Austin, R. Perusquia-Flores, M. A. Griffin, R. A. Oliva, D. Skinner, D. Domin, and W. A. Lester, Jr., "Zori 1.0: A Parallel Quantum Monte Carlo Electronic Structure Package," *J. Comp. Chem.* **26**, 856 (2005).
11. R. Whitesides, A.C. Kollias, D. Domin, W.A. Lester, Jr., and M. Frenklach, "Graphene Layer Growth: Collision of Migrating 5-Member Rings," Fall Meeting of the Western States Section of the Combustion Institute, Stanford, CA, October 17-18, 2005, paper 05F-62.
12. R. Whitesides, A. Kollias, D. Domin, W. A. Lester, Jr., and M. Frenklach, "Graphene layer growth: Collision of migrating five-membered rings," Symposium on *Nanoparticles in Energy Processes: Friend and Foe: Combustion Synthesis: From Pollutants to Advanced Materials*, 231st National Meeting of the American Chemical Society, Atlanta, GA, March 26-30, 2006.
13. R. Whitesides, A. Kollias, D. Domin, W. A. Lester, Jr., and M. Frenklach, "Graphene Layer Growth: Collision of Migrating Five-Membered Rings", *Prepr. Pap.-Am. Chem. Soc., Div. Fuel Chem.* **51**(1), 2006, pp. 174-175.
14. W. A. Lester, Jr. and R. Salomon-Ferrer, "Some Developments in Quantum Monte Carlo for Electronic Structure: Methods and Application to a Bio System," THEOCHEM, accepted.
15. R. Whitesides, A. C. Kollias, D. Domin, W. A. Lester, Jr., and M. Frenklach, "Graphene Layer Growth: Collision of Migrating Five-Member Rings," *Proc. Comb. Inst.* **31**, accepted.

# Quantum Dynamics of Fast Chemical Reactions

DE-FG02-87ER13679

Progress Report 3/2005 - 3/2006

John C. Light

The James Franck Institute and Department of Chemistry  
The University of Chicago  
Center for Integrative Science  
929 E 57th St., CIS E127  
Chicago, Illinois 60637  
email: j-light@uchicago.edu

The aims of this research are to develop a theoretical understanding and predictive ability for a variety of processes occurring in the gas phase. These include bimolecular chemical exchange reactions, photodissociation, predissociation resonances, unimolecular reactions and recombination reactions. Our focus on accurate quantum dynamics of small system is important for many reactions related to combustion and atmospheric chemistry involving light atom transfer reactions and, for example, resonances in dissociation and recombination reactions.

A major impediment to extension of these techniques to large or heavier molecular systems is the poor scaling of quantum methods with number of atoms treated accurately quantum mechanically and with the number of vibrational basis functions per degree of freedom. The scaling for straightforward quantum solutions is between  $n^{3d}$  and  $n^d$  where  $d = 3N - 6$ ,  $N$  is the number of atoms, and "n" the number of points or basis functions required to describe the motions in *each* dimension accurately – perhaps 10 to 100. For heavier atoms (e.g. O atoms in ozone) as many as 250 per degree of freedom are required.

We focus on developing substantially improved approaches and applying them to larger systems of interest. The techniques developed and used are primarily quantum mechanical (sometimes combined with classical mechanics) which permits us to focus on the effects of the internal states of reactants on reactions, and the internal state distributions, isotopic ratios, and branching ratios for products.

## I. RECENT PROGRESS

During the past two years we have refined computational methods to make the calculation of bound states and resonances of small systems easier and have applied them to molecular systems relevant to combustion such as ozone. Improved methods for examining resonances have been developed.

Our theoretical approach to the quantum dynamics of such "floppy" molecules has utilized three recent important innovations: the generation and use of reduced dimensionality *minimum* PES's to define the basis functions for each subset of the coordinates [1–3]; the combination of these reduced dimensional basis functions to form an *energy selected* non-direct product basis [2–4]; and the use of an iterative (IRLM) solution method for determining eigenvalues, eigenfunctions of the molecule [1,3,4]. Optimized grids for each of the degrees of freedom may also be used [5]. These

improvements are synergistic, with the minimum potentials assuring appropriate coordinate ranges for the bases, the energy selected basis reducing both the basis size and, perhaps more important, the spectral range, and the iterative (IRLM) solution providing excellent scaling as well as eigenfunction evaluation. Earlier we reported an improved grid approach for problems with several angular degrees of freedom as well as applications to important tetra-atomic and triatomic systems [5].

### A. Bound States of Ozone

The very highly excited vibrational levels of ozone are of interest for photodissociation and recombination particularly in the atmosphere. In addition the highly excited vibrations and resonance states of ozone for the  $(^{16}\text{O})_3$  and  $(^{16}\text{O}_2\ ^{18}\text{O})$  isotopomers are probably responsible for the observed "isotopic anomaly" of atmospheric ozone in which the isotopic ratios are not in the expected chemical equilibrium.

In the ozone calculation we determined all the bound states, including the long range van der Waals states, of  $^{48}\text{O}_3$  and  $^{50}\text{O}_3$  [6]. The accurate PES of Babikov [7] was used. This calculation resolved a discrepancy between the calculations of Grebenshchikov et al. and Babikov, *J. Chem. Phys.* **119**, 6512 and 6564 (2003) respectively. Since the high lying vdW states are likely to be strongly involved in the anomalous isotope effect in the ozone recombination process, resolution of the discrepancy was important. Our results agreed extremely well with a subset of the results (corresponding to the proper  $A_2$  vibrational symmetry) of Greabenschikov (within about  $0.04\text{ cm}^{-1}$ ) [3].

## II. CONTINUING PROJECTS: REACTIONS OF OZONE AND OF $\text{H}_3^+ + \text{H}_2$

Both the recombination of  $\text{O}_2 + \text{O}$  in the atmosphere and the low energy reactions of  $\text{H}_3^+$  and  $\text{H}_2$  proceed via complexes which have deep attractive wells. In both cases quantum effects will be important, via resonances, tunneling, and nuclear symmetry effects. The understanding of ozone recombination is important for atmospheric chemistry whereas the understanding of the ortho-para exchange processes and rotational relaxation in the low energy  $\text{H}_3^+$  collision system is important for interstellar chemistry.

### A. Ozone:

Ozone recombination in the atmosphere occurs by  $\text{O} + \text{O}_2$  collisions to form a metastable resonance state followed by collision with an atmospheric molecule to de-excite the system to a stable  $\text{O}_3$  molecule. The apparent kinetic preference (over and above thermodynamic equilibrium) for  $^{18}\text{O}$  enhanced ozone [8,9] presumably is a result of selective enhancement by resonances.

We are continuing calculations on the ozone system in two stages, first to determine the resonance states which might participate in the three body association process; then to calculate the thermal collisional relaxation rates from each resonance

state and then the final relaxation to stable ozone via a master equation. This will require the determination of the state specific energy transfer and dissociation rates for collisions of  $O_3^*$  with atmospheric gases. This will be a mixed quantum-classical calculation similar to our Ar + HCO calculation done some time ago [10].

This requires determining not only the eigenvalues of ozone but the wave functions of the stable states and lifetimes and eigenfunctions of metastable and scattering states. We have initiated this using "Ozone Lite", where the masses are reduced by a factor of 4 from real ozone. This permits the techniques for the above calculations to be evaluated and the approach to be made efficient *before* the very large final calculations are started. We use hyperspherical coordinates to permit easy symmetrization and "stretched" sinc DVR's for the hyperspherical radius permitting a dense grid at small  $\rho$  and a larger grid at large values where the asymptotic processes occur. We also use an efficient energy selected basis based on minimum marginal potentials [1,3]. We have solved the  $L^2$  problem for both bound and (discrete) unbound states by iterative methods. Scattering wave functions and resonance lifetimes are now being found using the "artificial boundary inhomogeneity" method [11,12].

When the ozone "lite" calculations near completion, we will proceed with the real ozone problem. It will, however, be interesting to see the isotope effects in ozone "lite" although the specific positions of the resonances are expected to play a significant role.

### B. $H_3^+ + H_2$ reaction:

The low energy  $H_3^+ + H_2$  ion-molecule reaction is one of the only relaxation mechanisms for ortho-para exchange in interstellar space, both for the  $H_2$  and for the  $H_3^+$ . We have just completed the statistical theory calculations using both the isotropic average interaction potential and the anisotropic interaction potentials which depend explicitly on the rotational quantum state of the  $H_2$ . At high energy or temperature where many rotational states are occupied the statistical theory is straightforward and has been done by Quack [13] and Oka [14]. However, at low temperatures characteristic of some interstellar molecular clouds the branching ratios for spin exchange reactions may differ substantially from the purely statistical predictions due to the sparsity of open rotational levels.

We have calculated the cumulative reaction probabilities using a relatively simple (average isotropic potential) statistical theory approach (Ref [15,16]. We have also included the long range effects of the anisotropic interactions dependent on the rotational state of the  $H_2$  [17]. In each case we considered both the full "scrambling" of the five nuclei in the complex and the "restricted" case in which the  $H_2$  bond is retained in the complex. The branching ratios for specific state-to-state reactions show very strong energy dependence at low collision energies (below about  $300\text{ cm}^{-1}$ .)

This five nucleus system is difficult because of the nuclear symmetry and large quantum effects but is fascinating for the same reasons. This work is now being written up for publication.

PUBLICATIONS supported by this DOE Grant, 2004-2006: References 2,3,and 6 below.

## REFERENCES

- [1] H. S. Lee and J. C. Light. Molecular vibrations: Iterative solution with energy selected bases. *J. Chem. Phys.*, 118:3458, 2003.
- [2] Hee-Seung Lee and J. C. Light. Iterative solutions with energy selected bases for highly excited vibrations of tetra-atomic molecules. *J. Chem. Phys.*, 120:4626, 2004.
- [3] J. C. Light and H. S. Lee. *Molecular dynamics: energy selected bases*. Kluwer Academic Publishers, 2004.
- [4] X.G. Wang and T.C. Carrington, Jr. The utility of constraining basis function indices when using the lanczos algorithm to calculate vibrational energy levels. *J. Phys. Chem. A*, 105:2575, 2001.
- [5] Hua Chen H. S. Lee and J. C. Light. Symmetry adapted direct product discrete variable representation for the coupled angular momentum operator: Application to the vibrations of  $(\text{CO}_2)_2$ . *J. Chem. Phys.*, 119:4187, 2003.
- [6] Hee-Seung Lee and J. C. Light. Vibrational energy levels of ozone up to dissociation revisited. *J. Chem. Phys.*, 120:5862, 2004. Communication.
- [7] D. Babikov, B. K. Kendrick, R. B. Walker, R. T. Pack P. Fleurat-Lesard and R. Schinke. *J. Chem. Phys.*, 118:6298, 2003.
- [8] Y. Q. Gao and R. A. Marcus. Strange and unconventional isotope effects in ozone formation. *Science*, 293:259–263, 2001.
- [9] C. Jansssen, J. Guenther, D. Krankowsky, and K. Mauersberger. Relative formation rates of  $^{50}\text{O}_3$  and  $^{52}\text{O}_3$  in  $^{16}\text{O}$ - $^{18}\text{O}$  mixtures. *J. Chem. Phys.*, 111:7179–7182, 1999.
- [10] G. S. Whittier and J. C. Light. Quantum/classical time-dependent self-consistent field treatment of Ar-HCO. *J. Chem. Phys.*, 110:4280, 1999.
- [11] Hyo Weon Jang and J. C. Light. Finite range scattering wave function method for scattering and resonance lifetime. *J. Chem. Phys.*, 99:1057, 1993.
- [12] G. S. Whittier and J. C. Light. Calculation of resonances of HCO by the artificial boundary inhomogeneity method. *J. Chem. Phys.*, 107:1816, 1997.
- [13] M. Quack. *Mol. Phys.*, 34:477, 1977.
- [14] T. Oka. *J. Mol. Spectrosc.*, 228:635, 2004.
- [15] P. Pechukas and J. C. Light. On detailed balancing and statistical theories of chemical kinetics. *J. Chem. Phys.*, 42:3281, 1965.
- [16] J. C. Light. Statistical theory of bimolecular exchange reactions. *Discuss. Faraday Soc.*, 44:14, 1967.
- [17] E. J. Rackham, T. Gonzalez-Lezana, and D. E. Manolopoulos. A rigorous test of the statistical model for atom–diatom insertion reactions. *J. Chem. Phys.*, 119:12895, 2003.

## Kinetics of Elementary Processes Relevant to Incipient Soot Formation

Principal Investigator: M. C. Lin  
Department of Chemistry  
Emory University, Atlanta, GA 30322  
chemmcl@emory.edu

### I. Program Scope

Soot formation and abatement processes are some of the most important and challenging problems in hydrocarbon combustion. The key reactions involved in the formation of polycyclic aromatic hydrocarbons (PAH's), the precursors to soot, remain elusive. Small aromatic species such as  $C_5H_5$ ,  $C_6H_6$  and their derivatives are believed to play a pivotal role in incipient soot formation.

The goal of this project is to establish a kinetic database for elementary reactions relevant to soot formation in its incipient stages. In the past year, our major focus has been placed on the experimental studies on the reactions of  $C_6H_5$  with small alcohols; their mechanisms have been elucidated computationally by quantum-chemical calculations. A similar theoretical analysis on the effects of temperature and pressure on the reaction of  $C_6H_5$  with  $C_3H_6$  has been carried out. In addition, several reactions involving OH with  $CH_2O$  and  $C_2H_4$ , and HCO with NO as well as the decomposition of  $C_6H_5OH$  have been computationally studied.

### II. Recent Progress

#### 1. $C_6H_5C_2H_2 + O_2 \rightarrow C_6H_5C_2H_2O_2 \rightarrow C_6H_5CHO + CHO$ (ref. # 1)

$C_6H_5C_2H_2$  is the key product of the  $C_6H_5 + C_2H_2$  reaction under high pressure conditions. The effects of temperature and pressure on the formation and decomposition of  $C_6H_5C_2H_2O_2$  in the  $C_6H_5C_2H_2 + O_2$  reaction (which competes with the formation of PAHs) have been investigated at temperatures from 298 - 358 K by directly monitoring the  $C_6H_5C_2H_2O_2$  radical in the visible region with CRDS. The rate constant for the  $C_6H_5C_2H_2 + O_2$  association and that for fragmentation of  $C_6H_5C_2H_2O_2$  were found to be respectively

$$k_1 (C_6H_5C_2H_2 + O_2 \rightarrow C_6H_5C_2H_2O_2) = (2.84 \pm 1.21) \times 10^{11} \exp(+780/T) \text{ cm}^3 \text{ mol}^{-1} \text{ s}^{-1}$$
$$k_2 (C_6H_5C_2H_2O_2 \rightarrow C_6H_5CHO + HCO) = (1.68 \pm 0.10) \times 10^4 \text{ s}^{-1}$$

$k_1$  was found to be weakly dependent on pressure in the range of 40 – 150 Torr Ar, whereas  $k_2$  was found to be independent of pressure. The mechanism for this very fast reaction has been elucidated quantum-chemically by B3LYP/6-31G(d,p) calculations. The result of the calculations indicate that the reaction effectively occur by two competitive association paths giving 3- and 4-member-ring peroxide intermediates which fragment rapidly to  $C_6H_5CHO + CHO$  with a predicted 382 kJ/mol exothermicity in agreement with experimental value. Additional kinetic measurements by pulsed-laser photolysis/mass spectrometry (PLP/MS) and a more detailed computational study of the mechanism and associated kinetics are underway for interpretation of measured temperature and pressure dependent data. In the PLP measurement, the  $C_6H_5CHO$  product has been directly detected.

#### 2. $C_6H_5 + CH_3OH (CH_3OD) \rightarrow C_6H_6 (C_6H_5D) + \text{other products}$ (ref. # 2)

The kinetics of aromatic radical reactions with alcohols in the gas phase is important to the alternate fuel chemistry. The rate constant for the  $C_6H_5 + CH_3OH$  reaction has been measured by PLP/MS in the temperature range of 300 - 767 K. In this experiment, the  $C_6H_5$

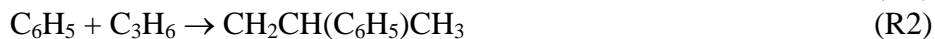
radical was generated by the photolysis of  $C_6H_5COCH_3$  at 193 nm in the presence of  $CH_3OH$ . The  $C_6H_5 + CH_3OH$  rate constant was determined by kinetically modeling the absolute yields of  $C_6H_6$  and  $C_6H_5CH_3$  products. In order to differentiate the reactivity of the radical toward the hydroxyl group from the primary alkyl group, we used  $CH_3OD$  as a reactant and its reaction rate reaction was determined by kinetic modeling the absolute yields of  $C_6H_5D$  and  $C_6H_5CH_3$  products. The results of these two reactions can be represented by the following Arrhenius expressions:

$$k(C_6H_5+CH_3OH \rightarrow C_6H_6+products) = 6.69 \times 10^{11} \exp(-750/T) \text{ cm}^3 \text{ mol}^{-1} \text{ s}^{-1}$$

$$k(C_6H_5+CH_3OD \rightarrow C_6H_5D+CH_3O) = 1.60 \times 10^{11} \exp(-550/T) \text{ cm}^3 \text{ mol}^{-1} \text{ s}^{-1}$$

### 3. $C_6H_5 + C_3H_6$ (ref. # 3)

The detailed density functional theory and G2M(RCC) calculations for the  $C_6H_5 + C_3H_6$  reaction have been carried out to assist our interpretation of the previously measured kinetic data in our lab and predict a product distribution of the title reaction at combustion temperatures. In this study we have focused our computational efforts on establishing the mechanisms for three major reaction modes of the phenyl radical attack on propylene:



The result of our statistical-theory calculations predicts that the addition to the terminal  $=CH_2$  site is dominant and that the total bimolecular rate constant is in reasonable agreement with experimental value for the temperature range studied. The branching rate constants in the second order region have been predicted for combustion applications by the following expressions (in units of  $\text{cm}^3 \text{ mol}^{-1} \text{ s}^{-1}$ ) at  $T = 250 - 2500 \text{ K}$ :

$$k_{R1} = 1.695 \times 10^4 T^{2.47} \exp[-370/T]$$

$$k_{R2} = 1.603 \times 10^3 T^{2.64} \exp[-847/T]$$

$$k_{R3} = 1.359 T^{3.82} \exp[-723/T]$$

### 4. $C_6H_5OH \rightarrow CO + C_5H_6$ (ref. # 4)

$C_6H_5OH$  is a key intermediate of benzene and toluene oxidation reactions. The unimolecular decomposition of  $C_6H_5OH$  on its singlet state potential energy surface has been studied at the G2M//B3LYP/6-311G(d, p) level of theory. The PES and the predicted rate constants show that the most favorable reaction channel to produce  $C_5H_6 + CO$  is phenol isomerization to M1 (2,4-cyclohexadienone) followed by isomerization/decomposition processes involving other low-lying isomers. Our result supports the earlier assumption on the important role of M1 in  $C_5H_6$  formation.

The rate constants have been predicted by the microcanonical RRKM and/or variational transition state theories in the temperature range of 800 – 2000 K at Ar pressure below 100 atm. The predicted pressure-independent rate constant for CO production agrees very well with available experimental data in the temperature range studied.<sup>5,6</sup> The predicted result for H-atom production was found to be much smaller than the estimated value by Lovell et al.<sup>7</sup>, although our predicted values for  $k_{CO}$  and  $k_H$  at 1500 - 1600 K, giving  $k_H/k_{CO} = 0.13 - 0.14$  (for 2.5 atm Ar) are

consistent with the estimation of Horn and coworkers<sup>6</sup>,  $k_{\text{H}}/k_{\text{CO}} < 0.15$ , based on direct measurements of CO and H atoms by resonance absorption.

The rate constants for the production of CO (which is independent of pressure) and H for high- and low-pressure limits can be represented by:

$$\begin{aligned}k_{\text{CO}} &= 1.15 \times 10^{17} T^{-0.953} \exp(-37567/T) \text{ s}^{-1} \\k_{\text{H}}^{\infty} &= 3.33 \times 10^{17} T^{-0.51} \exp(-46100/T) \text{ s}^{-1} \\k_{\text{H}}^0 &= 2.56 \times 10^{94} T^{-28.21} \exp(-63400/T) \text{ cm}^3 \text{ molecule}^{-1} \text{ s}^{-1}\end{aligned}$$

## 5. OH + CH<sub>2</sub>O (ref. # 8)

The reaction of OH radical with formaldehyde (CH<sub>2</sub>O) is one of the most critical reactions in the combustion of hydrocarbons, [C,H,O,N]-containing nitramine propellants and nitrate ester oxidizers. In this presentation, we report the result obtained by a high-level quantum chemical and statistical theory calculation, which correlates reasonably well with the experimental data. The geometries of all species involved have been optimized at the B3LYP/6-311+G(3df,2p) and CCSD/6-311++G(d,p) levels, respectively. Their relative energies improved by single-point calculations at the CCSD(T)/6-311+G(3df,2p) level based on the geometries optimized at the B3LYP/6-311+G(3df,2p) (CCSD(T)-1) and CCSD/6-311++G(d,p) (CCSD(T)-2) levels. The rate constants of reaction channel (1) producing H<sub>2</sub>O + HCO and (2) giving the hydroxylmethoxy radical are calculated by the Variflex code based on the PES calculated using the CCSD(T)-1 and CCSD(T)-2 methods with the corresponding the optimized geometries and frequencies.



The existence of the molecular complex at the entrance channel has a significant effect on the predicted rate constant due to multiple reflections above the well of the complex, particularly for reaction (1). The predicted values with multiple reflections based on the PES calculated using the CCSD(T)-2 method are in good agreement with the experimental data for the whole temperature region within the scatters of the data.<sup>9,10</sup> The predicted individual rate constants given in units of cm<sup>3</sup> molecule<sup>-1</sup> s<sup>-1</sup> can be represented by

$$\begin{aligned}k_1 &= 2.45 \times 10^{-21} T^{2.98} \exp(1750/T) \quad (200 - 400 \text{ K}) \\ &= 3.22 \times 10^{-18} T^{2.11} \exp(849/T) \quad (400 - 3000 \text{ K}) \\ k_2 &= 1.05 \times 10^{-17} T^{1.63} \exp(-2156/T) \quad (200 - 3000 \text{ K}).\end{aligned}$$

The result indicates that  $k_2$  accounts for 1% of the total rate constant at T = 1000 – 1600 K. The predicted total rate constants with multiple reflections based the PES calculated using CCSD(T)-1 method are lower 10-20% than the experimental data.

## 6. OH + C<sub>2</sub>H<sub>4</sub> addition kinetics and mechanism (ref. # 11):

C<sub>2</sub>H<sub>4</sub> is a model olefin fuel whose combustion kinetics has been studied extensively. We have predicted the rate constant for the addition of OH to C<sub>2</sub>H<sub>4</sub> for the first time. The low energy paths for the reaction of HO with C<sub>2</sub>H<sub>4</sub> have been studied at the PMP2/aug-cc-PVQZ//MP2/cc-PVTZ level of theory. The rate constants for the production of C<sub>2</sub>H<sub>4</sub>OH, CH<sub>2</sub>CHOH + H and

$C_2H_3 + H_2O$  calculated with variational RRKM theory indicated that below 500 K, the formation of  $C_2H_4OH$  ( $k_1$ ) via an  $OH\cdots\pi$  complex with 1.9 kcal/mol binding energy is the major product channel exhibiting a negative-temperature dependence; between 800 - 1000 K, the formation of  $CH_2CHOH + H$  ( $k_2$ ) and  $C_2H_3 + H_2O$  ( $k_3$ ) becomes competitive; at  $T > 1000$  K,  $k_3$  becomes dominant.  $k_1$  was found to be strongly affected by multiple reflections above the well of the  $OH\cdots\pi$  complex. The predicted results are in close agreement with available experimental data.

### III. Future plans:

The study on the reaction of  $C_6H_5$  with  $C_2H_5OH/C_2H_5OD$  will be completed by PLP/MS and CRDS measurements. Focus will be placed on the spectroscopy and kinetics of naphthyl radicals in the coming months. In addition, full kinetic analyses on the reactions of  $C_6H_5$  with  $O_2$  and  $a-C_3H_4$  will be carried out by multi-channel RRKM/master equation calculations.

### IV. References (DOE publications denoted by \*)

1. "Formation and Decomposition of Phenylvinylperoxy Radicals in the  $C_6H_5C_2H_2 + O_2$  Reaction", J. Park, Z. F. Xu, Y. M. Choi, and M. C. Lin, in preparation.\*
2. J. Park, Z. F. Xu, K. Kun, and M. C. Lin, in preparation.\*
3. "Experimental and Theoretical Studies of the Phenyl Radical Reaction with Propene," J. Park, I. Tokmakov, G. Nam and M. C. Lin, in preparation.\*
4. Z. F. Xu and M. C. Lin, *J. Phys. Chem., A*, (2006), 110(4), 1672-1677.\*
5. Manion, J. A.; Louw, R. *J. Phys. Chem.* **1989**, 93, 3563.
6. C. Horn, K. Roy, P. Frank, Just, Th. 27<sup>th</sup> *Symposium (International) on Combustion*, 1998, 321.
7. Lovell, A. B.; Brezinsky, K.; Glassman, I. *Int. J. Chem. Kinet.* 21, 547 (1989).
8. Shucheng Xu, R. S. Zhu, and M. C. Lin, "Ab Initio Study of the OH +  $CH_2O$  Reaction: The Effect of the  $OH\cdots OCH_2$  Complex on the H-Abstraction Kinetics", *Int. J. Chem. Kinet.*, accepted.\*
9. Vasudevan, V.; Davidson, D. F.; Hanson, R. K. *Int. J. Chem. Kinet.* 2005, 37, 98-109.
10. Sivakumaran, V.; Hoelscher, D.; Dillon, T. J.; Crowley, J. N. *Phys. Chem. Chem. Phys.* 2003, 5, 4821-4827.
11. R. S. Zhu, J. Park, M. C. Lin, *Chem. Phys. Letter.* 408(1-3), 25-30 (2005).\*

### Other DOE publications not cited in the text:

1. J. Park, Liming Wang and M. C. Lin, *Int. J. Chem. Kinet.*, **36**, 49-56 (2004).
2. I. V. Tokmakov, L. V. Moskaleva, and M. C. Lin, *Int. J. Chem. Kinet.*, **36**, 139-51 (2004).
3. Y. M. Choi and M. C. Lin, *ChemPhysChem.*, **5**, 225-32 (2004).
4. Y. M. Choi and M. C. Lin, *ChemPhysChem.*, **5**, 661-68 (2004).
5. Z. F. Xu, J. Park and M. C. Lin, *J. Chem. Phys.*, **120**, 6593 - 99 (2004).
6. R. S. Zhu, Z. F. Xu and M. C. Lin, *J. Chem. Phys.*, **120**, 6566 - 73 (2004).
7. I. V. Tokmakov and M. C. Lin, *J. Phys. Chem., A*, **108**, 9697-714 (2004).
8. Y. M. Choi, J. Park, Liming Wang, and M. C. Lin, *ChemPhysChem*, **5**, 1231-34 (2004).
9. Huzeifa Ismail, Joonbum Park, Bryan M. Wong, W. H. Green, Jr. and M. C. Lin, *Proc. Combust. Inst.*, **30**, 1049 - 56 (2005).
10. Y. M. Choi and M. C. Lin, *Int. J. Chem. Kinet.*, **37**, 261-74 (2005).
11. Shucheng Xu and M. C. Lin, *J. Phys. Chem., B*, **109**, 8367-8373 (2005).
12. Chih-Wei Lu and Shen-Long Chou, Yuan-Pern Lee, Shucheng Xu, Z. F. Xu and M. C. Lin, *J. Chem. Phys.*, **122**, 244314/1-244314/11 (2005).
13. I.V. Tokmakov, G.-S. Kim, V. V. Kislov, A. M. Mebel and M. C. Lin, *J. Phys. Chem. A*, **109**, 6114-27 (2005).
14. Z. F. Xu and M. C. Lin, *J. Phys. Chem., A*, **109**, 9054-60 (2005).
15. Z. F. Xu, C.-H. Hsu and M. C. Lin, *J. Chem. Phys.* 122(23), 234308/1-234308/11, (2005).
16. Cheng-Ming Tzeng, Y. M. Choi, Cheng-Liang Huang, Chi-Kung Ni, Yuan T. Lee, and M. C. Lin, *J. Phys. Chem., A*, **108**, 7928-35, (2004).

# INVESTIGATION OF POLARIZATION SPECTROSCOPY AND DEGENERATE FOUR-WAVE MIXING FOR QUANTITATIVE CONCENTRATION MEASUREMENTS

Principal Investigator: Robert P. Lucht  
School of Mechanical Engineering, Purdue University, West Lafayette, IN 47907-2088  
(Lucht@purdue.edu)

## I. PROGRAM SCOPE

Nonlinear optical techniques such as laser-induced polarization spectroscopy (LIPS) and resonant wave mixing (RWM) are techniques that show great promise for sensitive measurements of transient gas-phase species, and diagnostic applications of these techniques are being pursued actively at laboratories throughout the world. Over the last few years we have also begun to explore the use of three-laser electronic-resonance-enhanced (ERE) coherent anti-Stokes Raman scattering (CARS) as a minor species detection method with enhanced selectivity.

The objective of this research program is to develop and test strategies for quantitative concentration measurements using these nonlinear optical techniques in flames and plasmas. We are investigating the physics of these processes by direct numerical integration (DNI) of the time-dependent density matrix equations for the resonant interaction. Significantly fewer restrictive assumptions are required using this DNI approach compared with the assumptions required to obtain analytical solutions. Inclusion of the Zeeman state structure of degenerate levels has enabled us to investigate the physics of LIPS and of polarization effects in DFWM. We have incorporated the effects of hyperfine structure in our numerical calculations of LIPS signal generation. We are concentrating on the accurate simulation of two-photon processes, including Raman transitions, where numerous intermediate electronic levels contribute to the two-photon transition strength.

During the last year we continued our studies of two-photon LIPS of atomic hydrogen. We have investigated in detail the effects of pump polarization on LIPS signal generation, and we are still trying to resolve some differences between our experimental results and our theoretical predictions. We performed numerical simulations of our high-resolution two-photon-induced laser-induced fluorescence (LIF) measurements of NO. We have incorporated an effective intermediate electronic level in our calculations to account for the effects of the numerous intermediate electronic levels for the  $A^2\Sigma^+-X^2\Pi$  two-photon resonances. We have also performed a detailed investigation of ERE CARS spectroscopy of nitric oxide, and have demonstrated the capability of measuring NO at concentrations of 50 ppm in atmospheric pressure flames.

## II. RECENT PROGRESS

### A. *Investigation of Polarization Effects in Two-Photon Laser-Induced Polarization Spectroscopy of Atomic Hydrogen*

In collaboration with Thomas Settersten at the Combustion Research Facility at Sandia National Laboratories, we investigated in detail the effects of pump beam polarization on two-photon LIPS signal generation for atomic hydrogen; these effects were also investigated for resonant six-wave mixing spectroscopy of atomic hydrogen. The experiments were performed in the CRF Picosecond Laser Facility using two separately tunable distributed feedback dye lasers to generate the 243-nm two-photon pump beam and the 656-nm probe beam. For the LIPS measurements, we used a quarter-wave plate to change the polarization of the pump beam from linear to elliptical to circular, and carefully characterized the linear and circular polarization states of the pump beam. The dependence of both the LIPS and LIF

signals from atomic hydrogen on the polarization state of the 243-nm two-photon pump beam is shown in Fig. 1.

We have developed a detailed numerical model for resonant interaction of pulsed laser radiation with atomic hydrogen, and have used this code to model the LIPS process. In particular, we have been concentrating on the effect of the polarization of the two-photon 243-nm pump beam on LIPS signal generation. The results of these calculations are shown in Fig. 2. Comparing Figs. 1 and 2, it can be seen that we predict, in agreement with experiment, that there is no LIPS signal generation for circular polarization of the pump beam because the two-photon  $1S-2S$  transition is not allowed due to destructive interference between different excitation pathways. Theoretically, we predict LIPS signal generation for an elliptically polarized pump beam. This signal generation, after detailed investigation of the numerical results, can be attributed to a phase anisotropy induced in the Zeeman states of the  $2S$  level. However, we do not predict a LIPS signal for linear pump beam polarization, in sharp disagreement with the experimental results. We are continuing to investigate this disagreement between theory and experiment.

We also performed resonant six-wave mixing measurements of atomic hydrogen, and the signals were approximately two orders of magnitude higher than for LIPS. The numerical model has been modified for resonant six-wave mixing calculations for comparison with the experimental results.

### ***B. High-Resolution Two-Photon-Induced Fluorescence Spectroscopy of Nitric Oxide***

As an initial demonstration of the use of our optical parametric generator (OPG)/optical parametric amplifier (OPA) system, we performed two-photon-excited fluorescence of the NO molecule for both a single-beam configuration and a two-beam counterpropagating configuration. Following two-photon excitation of transitions within the (0,0) band of the  $A^2\Sigma^+ - X^2\Pi$  electronic transition, ultraviolet fluorescence was monitored from this same band. The measurements were performed in a room-temperature gas cell at pressures of 0.8-3.0 kPa for a mixture of 3000 ppm NO in  $N_2$  buffer gas. In the single-beam configuration, the two lines were not resolved and a single line with a width of 1.5 GHz is observed, corresponding to the expected Doppler width of 3 GHz in the ultraviolet. For the counterpropagating configuration, the two-photon absorption process is Doppler-free when a single-photon is absorbed from each of the pump beams, and the transitions were resolved to approximately 200 MHz. Saturation and Stark shifting of the transitions starts to become apparent when the pulse energy is increased to 2 mJ for a beam diameter of approximately 3mm.

We have developed a computer code for numerical simulation of this process and have investigated the saturation and Stark shifting of the two-photon line shape in detail. Because of our interest in LIPS, two-photon LIF, and ERE CARS measurements of NO, we have concentrated on developing a realistic model of these processes for the NO molecule. The two-photon absorption and Raman processes both proceed through intermediate levels that are single-photon-coupled with both the initial and final transition levels. The intermediate levels that are important in this process lie in excited electronic levels such as the  $B^2\Pi$ ,  $C^2\Pi$ ,  $D^2\Sigma^+$ , and  $E^2\Sigma^+$  levels. The number of these electronic levels and the lack of electronic transition strength data made it impractical to include all of these levels in our numerical model. Instead, we have included a single intermediate electronic level and have adjusted the oscillator strengths of the transitions between this intermediate level and the  $A^2\Sigma^+$  and  $X^2\Pi$  electronic levels for best agreement between theory and experiment. Modeling the two-photon process in this manner enables us to obtain accurate values of the two-photon cross sections and to calculate accurate polarization properties for the transitions.

### ***C. Electronic-Resonance-Enhanced CARS Spectroscopy of Nitric Oxide***

We have also investigated the physics and explored the diagnostic potential of ERE CARS for measurements of nitric oxide. The motivation for the work is to determine whether ERE CARS can be

used to measure NO in high-pressure environments, where LIF measurements are very difficult because of interfering LIF signals from species such as O<sub>2</sub>, H<sub>2</sub>O, and CO<sub>2</sub>. ERE CARS is inherently more selective because of the requirement for both electronic Raman resonance for signal generation. Our initial NO ERE CARS measurements were reported in 2003 [1]. At that time our measurements were degraded because of unstable injection-seeding of our pulsed Nd:YAG laser. Over the last few months we have obtained results that are far superior to these early results, and have detected NO in flames down to concentration levels of 50 ppm. With further system development, we should be able to measure concentration levels of 10 ppm or lower. In addition, we have shown that the ERE CARS signal from NO is essentially independent of the quenching collision rate, as shown in Fig. 3. The ERE CARS signal level was unaffected when the N<sub>2</sub> in the buffer gas with CO<sub>2</sub>, even though the quenching cross section for CO<sub>2</sub> is a factor of 1000 higher. We have also investigated in detail the pressure dependence of the ERE CARS signal, as shown in Fig. 4. The ERE CARS signal from a room temperature cell increases until pressures of approximately 3 atm and then is essentially constant up to 8 atm.

### III. FUTURE WORK

Our investigation of the physics of two-photon, two-color LIPS will continue. We will continue to explore the physics of this process using our direct numerical integration (DNI) code. We will use the injection-seeded optical parametric (OP) system for LIPS measurements of the NO molecule. We will also develop a second OP system, and then use this system to investigate two-photon, two-color LIPS technique for measurements of the O-atom and of the C-atom. Further collaboration with Thomas Settersten at Sandia on LIPS and RWM spectroscopy of atomic hydrogen is also planned.

We plan to pursue further theoretical and experimental investigations of the ERE CARS process for NO and C<sub>2</sub>H<sub>2</sub>, especially at higher pressures where collisional narrowing may result in significant improvement in the detection limits. The DNI code for ERE CARS has been developed and will be used to explore the physics of the ERE CARS process. We will also use this DNI code for numerical modeling of the femtosecond CARS process.

We will further develop and characterize the injection-seeded OP systems. In particular, we plan to use diode lasers in the wavelength range from 760 nm to 1000 nm as injection seeding lasers for our OPG. Using these diode lasers to seed at the idler wavelength, the signal radiation will be generated at wavelengths from 667 nm to 550 nm for 355-nm pumping of the BBO crystals in the OPG stage. The signal radiation from the OPG can then be amplified using pulsed dye amplifiers with Rhodamine dyes. The use of pulsed dye amplification is expected to simplify the system alignment, improve beam quality, and increase the output power. This OP source technology will enhance greatly the potential for quantitative application of pulsed cavity ring-down spectroscopy and nonlinear techniques such as LIPS, DFWM, dual-pump CARS, and ERE CARS spectroscopy.

### IV. REFERENCES

1. S. F. Hanna, W. D. Kulatilaka, Z. Arp, T. Opatrný, M. O. Scully, J. P. Kuehner, and R. P. Lucht, "Electronic-Resonance-Enhanced (ERE) Coherent Anti-Stokes Raman Scattering (CARS) Spectroscopy of Nitric Oxide," *Applied Physics Letters* **83**, 1887-1889 (2003).

### V. BES-SUPPORTED PUBLICATIONS 2004-2006

1. W. D. Kulatilaka, R. P. Lucht, S. F. Hanna, and V. R. Katta, "Two-Color, Two-Photon Laser-Induced Polarization Spectroscopy Measurements of Atomic Hydrogen in Near-Adiabatic, Atmospheric Pressure Hydrogen/Air Flames," *Combustion and Flame*, **137**, 523-537 (2004).
2. R. P. Lucht, S. Roy, and J. R. Gord, "Nonperturbative Modeling of Two-Photon Absorption in a Three-State System," *Journal of Chemical Physics* **121**, 9820-9829 (2004).

- W. D. Kulatilaka, T. N. Anderson, T. L. Bougher, and R. P. Lucht "Development of an Injection-Seeded, Pulsed Optical Parametric Generator for High-Resolution Spectroscopy," *Applied Physics B* **80**, 669-680 (2005).
- S. Roy, W. D. Kulatilaka, S. V. Naik, N. M. Laurendeau, R. P. Lucht, and J. R. Gord, "Effect of Quenching on Electronic-Resonance-Enhanced CARS of Nitric Oxide," *Applied Physics Letters*, submitted for publication (2006).

Graduate Students Supported at Present Time: Waruna D. Kulatilaka (PhD student at Purdue University)

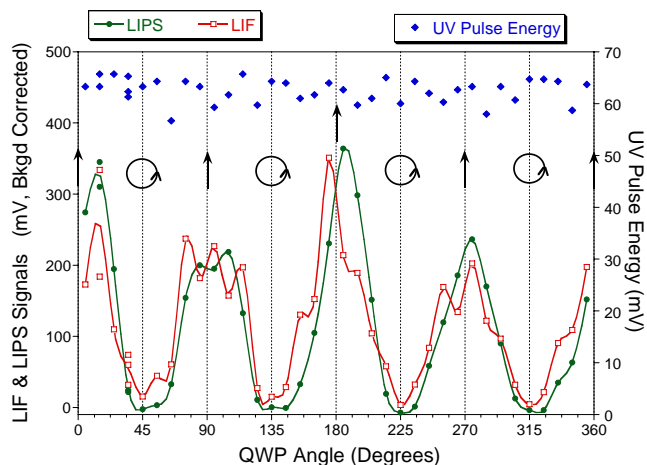


Fig. 1. LIFS and LIF signals from atomic hydrogen versus quarter-wave plate angle. The polarization state of the pump beam is circular at 45°, 135°, 225°, and 315°. The polarization is linear at 0°, 90°, 180°, 270°, and 360°.

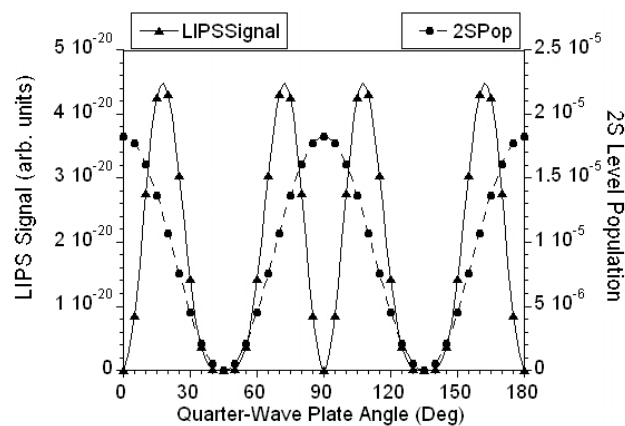


Fig. 2. DNI calculations of the LIFS signal and the population of the 2S level of atomic hydrogen as a function of the quarter-wave plate angle. The polarization of the pump beam is circular at 45°, and 135°. The polarization is linear at 0°, 90°, and 180°.

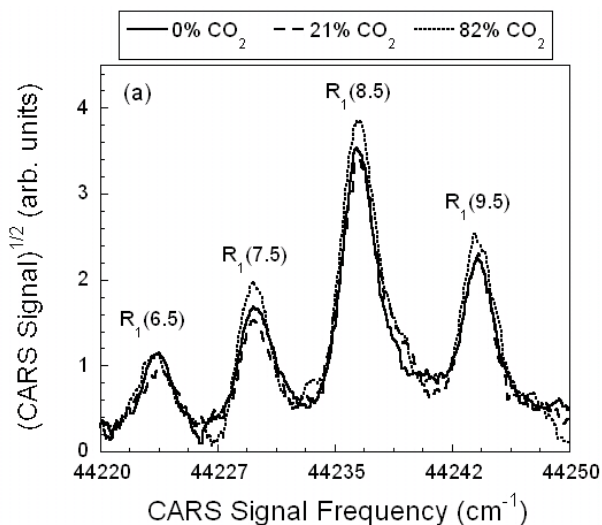


Fig. 3. ERE CARS signal from 1000 ppm of NO in a buffer gas of N<sub>2</sub> and CO<sub>2</sub>.

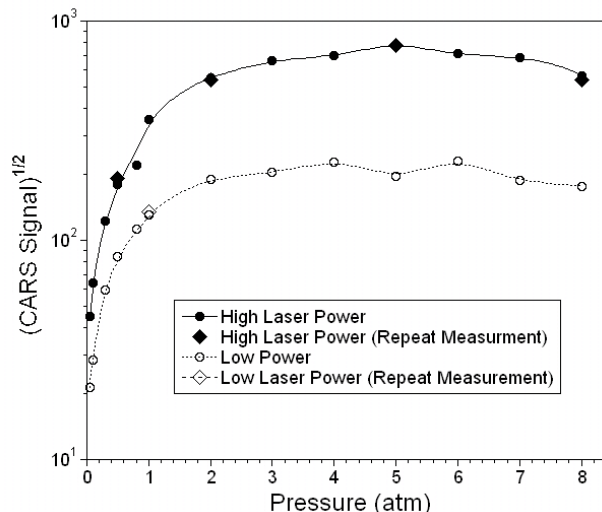


Fig. 4. ERE CARS signal from 300 ppm of NO in a buffer gas of N<sub>2</sub> as a function of cell pressure.

# Time-Resolved Infrared Absorption Studies of the Dynamics of Radical Reactions

R. G. Macdonald  
Chemistry Division  
Argonne National Laboratory  
Argonne, IL 60439  
Email: rgmacdonald@anl.gov

## Background

There is very little information available about the dynamics of radical-radical reactions. These processes are important in combustion being chain termination steps as well as processes leading to new molecular species. For almost all radical-radical reactions, multiple product channels are possible, and the determination of product channels will be a central focus of this experimental effort. Two approaches will be taken to study radical-radical reactions. In the first, one of the species of interest will be produced in a microwave discharge flow system with a constant known concentration and the second by pulsed-laser photolysis of a suitable photolyte. The rate constant will be determined under pseudo-first order conditions. In the second approach, both transient species will be produced by the same photolysis laser pulse, and both followed simultaneously using two different continuous-wave laser sources. This approach allows for the direct determination of the second-order rate constant under any concentration conditions if the appropriate absorption cross sections have been measured. In both approaches, the time dependence of individual ro-vibrational states of the reactants and/or products will be followed by frequency- and time-resolved absorption spectroscopy. In order to determine branching ratios and second-order rate constants, it is necessary to measure state-specific absorption coefficients and transition moments of radicals and these measurements will play an important role in this experimental study.

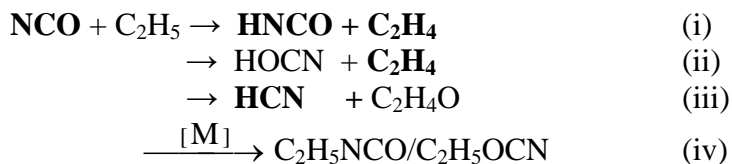
## Recent Results

In the current work, the above difficulty was dealt with by either monitoring the concentration of the two reacting radical species using time-resolved infrared absorption spectroscopy or by monitoring one of the reacting species and inferring the concentration of the other from a stoichiometric relationship between the two species. These experiments also illustrate the utility of the time-resolved absorption technique, and the power of infrared spectroscopy to probe a variety of molecular and/or transient species at the individual ro-vibration state level of detail.

Over the past few years, this laboratory has concentrated on the study of the reaction on the NCO radical with simple alkyl radicals, H, CH<sub>3</sub> and C<sub>2</sub>H<sub>5</sub>. The NCO radical is an important intermediate in the chemistry of NO<sub>x</sub> generation and several NO<sub>x</sub> abatement strategies, such as the RAPRENOX and NOXOUT processes. In general, the chemistry of the NCO radical has not been extensively explored, and in particular, there are few studies of the interaction between NCO and other open shell species. In many cases, the NCO radical appears to behave as a pseudohalogen abstracting an H atom from hydrogen donors. Over this past period, work has been completed on the analysis of the NCO + CH<sub>3</sub> and C<sub>2</sub>H<sub>5</sub> reaction systems. Further experimental work is needed on the

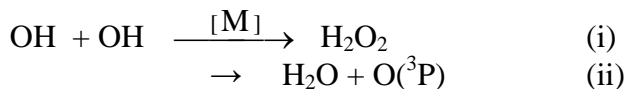
NCO + H reaction to resolve some questions on the products of this reaction, and will be delayed until the delivery of a new infrared laser system.

(a)  $\text{NCO}(^2\Pi) + \text{C}_2\text{H}_5(^2\text{A}')$ . The reaction between the NCO and  $\text{C}_2\text{H}_5$  radicals has four product channels:



The species in bold were detected by time-resolved infrared absorption spectroscopy in the 2.6 to 3.3 micron range. The reaction was initiated by photolyzing CINCO at 248 nm generating equal concentrations of NCO and Cl atoms. The  $\text{C}_2\text{H}_5$  radical was produced with little vibrational energy by the subsequent rapid reaction of the Cl atom with  $\text{C}_2\text{H}_6$ . The rate constants and branching ratios were determined by comparing the experimental temporal concentration profiles to predictions of model calculations. An appropriate rate constant was varied in the model simulations until the deviation between experiment and model predictions of the concentration profile was minimized, as illustrated in figure 1. Absolute concentrations of the detected species were measured. The infrared absorption coefficients of NCO and HNCO were measured in separate experiments and those for other species taken from literature tabulations. The reaction was studied over the pressure range from about 2 to 4 Torr in an excess of  $\text{N}_2\text{O}$  or  $\text{C}_2\text{H}_6$ . The rate constants for complicating secondary reactions,  $\text{C}_2\text{H}_5 + \text{CINCO}$  and  $\text{NCO} + \text{C}_2\text{H}_6$  were also measured. Two interesting features emerged from these studies. One, the total removal rate constant for  $\text{NCO} + \text{C}_2\text{H}_5$  was fast and pressure dependent, increasing from  $2.5 \times 10^{-10}$  to  $3.9 \times 10^{-10} \text{ cm}^3 \text{ molecule}^{-1} \text{ s}^{-1}$ , as the pressure increased from 2 to 4 Torr. Two, channels i, ii and iii were found to be independent of pressure, indicating they proceeded through a direct bimolecular reactive encounter. At 2 Torr, the H atom abstraction channels accounted for 50% of the products with channel i giving the more stable HNCO isomer, accounting for 90% of the H atom abstraction products. Channel iii was a very minor channel accounting for less than 0.3% of the total rate constant.

(b)  $\text{OH}(^2\Pi) + \text{OH}(^2\Pi)$ . Work has been initiated on the study of this simple but important radical-radical reaction. This reaction is prototypical of the interaction of two radicals possessing both spin and electronic angular momentum, and is simple enough to be amenable to detailed theoretical calculations (L. B. Harding, J. Phys. Chem. **95**, 8653 (1991)). There are four singlet and triplet electronic surfaces correlating to singlet and triplet products



The reaction was initiated by photolysis of  $\text{N}_2\text{O}$  at 193 nm to generate  $\text{O}(^1\text{D})$  atoms and the reaction of  $\text{O}(^1\text{D})$  with  $\text{H}_2\text{O}$  to produce two OH radicals. The OH radical in  $v=0$  and 1 was monitored on rotational transitions of the first vibrational overtone transitions around 1.47 microns. To date, the experiments have been conducted at low pressures to determine the rate constant for the abstraction channel, channel ii. Preliminary results

indicate that the real time measurements of this rate constant, carried out in this work, are almost a factor of two larger than recent measurements (H. Sun and Z. Li, Chem. Phys. Lett. **399**, 33 (2004)).

### **Future Work**

Work will continue on the study of the OH + OH reaction. Current effort is to conduct the low pressure measurements in various inert gases, He, Ne and Ar, to validate the present procedure for measuring the loss of OH by diffusion and flow. Once the rate constant for channel ii has been established, the measurements will be extended to higher pressure.

Work will also begin on the investigation of the  $\text{CH}_3(^2\text{A}_2'') + \text{OH}(^2\Pi)$ , radical – radical reaction. As in the CN + OH work, both species will be interrogated on the same photolysis laser pulse using different laser sources. The product branching ratio into the  $^1\text{CH}_2 + \text{H}_2\text{O}$  channel will be probed using time-resolved absorption spectroscopy of  $^1\text{CH}_2$  using the vibronic transitions of the  $^1\text{CH}_2(b\ ^1\text{B}_1) \leftarrow (a\ ^1\text{A}_2)$  transition in the near infrared. The formation of other product channels will be probed using infrared vibrational spectroscopy.

### **Publications 2004-2006.**

*Determination of the rate constants for the  $\text{NCO}(X^2\Pi) + \text{Cl}(^2\text{P})$  and  $\text{Cl}(^2\text{P}) + \text{CINCO}(X^2\text{A}')$  reactions at 293 and 345 K.*

-Y. Gao and R. G. Macdonald

J. Phys. Chem. 109A, 5388-5397 (2005).

*Determination of the rate constant for the  $\text{NCO}(X^2\Pi) + \text{CH}_3(X^2\text{A}_2'')$  reaction at 293 K and an estimate of possible product channels.*

-Y. Gao and R. G. Macdonald

J. Phys. Chem. 110A, 977-989 (2006).

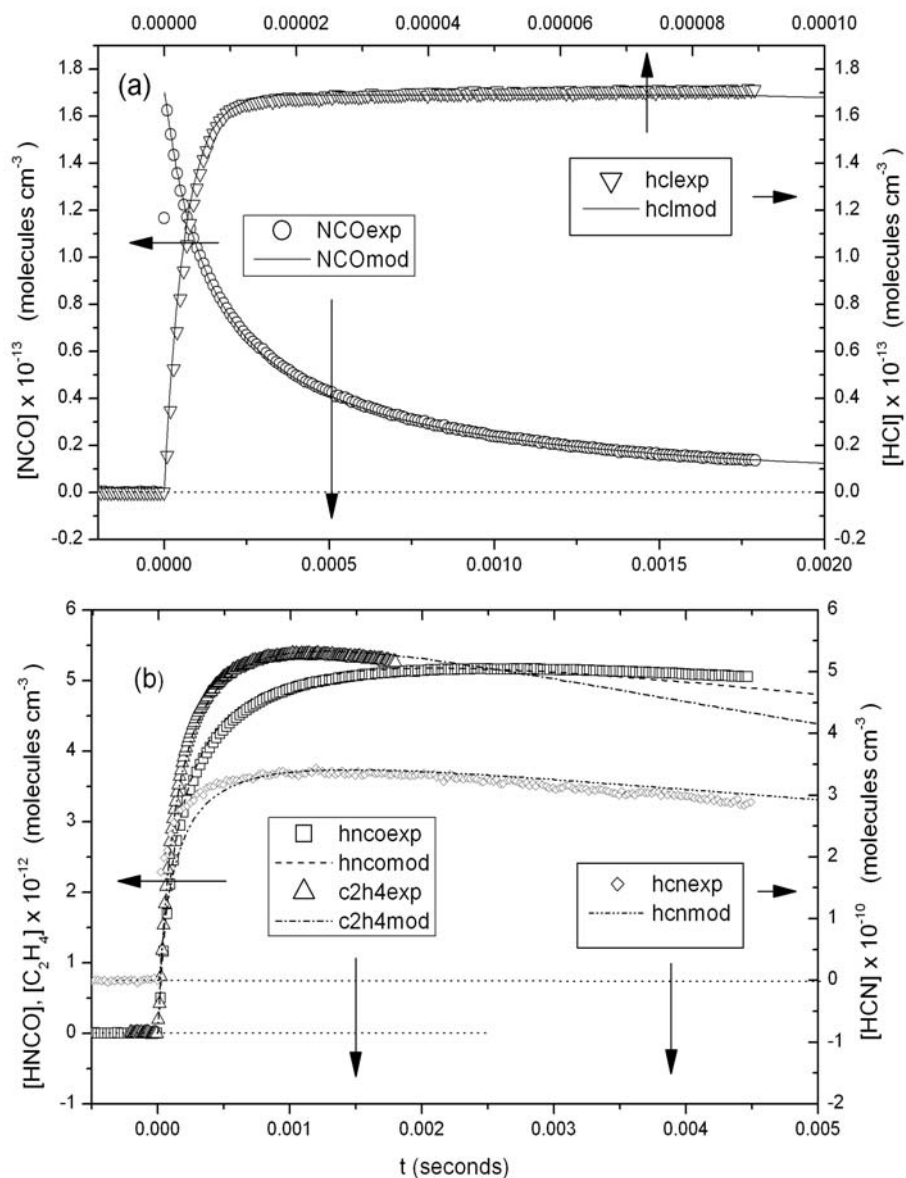


Figure 1(a). Comparison between experimental and model predictions for NCO and HCl. The rapid rise in the HCl concentration provides a convenient measure of the initial NCO and  $\text{C}_2\text{H}_5$  radical concentrations. The rate constant for the  $\text{NCO} + \text{C}_2\text{H}_5$  reaction depended on the total pressure. For this experiment, it was found to be  $3.8 \times 10^{-10} \text{ cm}^3 \text{ molecules}^{-1} \text{ s}^{-1}$ . The conditions of the experiment were  $P_{\text{N}_2\text{O}} = 3.813$ ,  $P_{\text{Ar}} = 0.384$ ,  $P_{\text{C}_2\text{H}_6} = 0.172$ , and  $P_{\text{CINCO}} = 0.013$  Torr, at a temperature of 293 K. 1(b) Same experiment as (a) except showing the detected products of the  $\text{NCO} + \text{C}_2\text{H}_5$  reaction. Note the different temporal dependence for HNCO and  $\text{C}_2\text{H}_4$  products due to channel (ii) and the reaction  $\text{NCO} + \text{C}_2\text{H}_6 \rightarrow \text{HNCO} + \text{C}_2\text{H}_5$ . The rate constants for the various channels were determined to be  $k(\text{i}) = 1.28 \times 10^{-10}$ ,  $k(\text{ii}) = 3.1 \times 10^{-11}$ , and  $k(\text{iii}) = 1.0 \times 10^{-12}$ .

# Quantum chemical studies of chemical reactions related to the formation of polyaromatic hydrocarbons and of spectroscopic properties of their key intermediates

Alexander M. Mebel

Department of Chemistry and Biochemistry, Florida International University  
Miami, Florida 33199. E-mail: mebel@fiu.edu

**Program Scope.** The goal of this project is to theoretically investigate the mechanism of formation of polyaromatic hydrocarbons (PAHs) from smaller ring and chain hydrocarbons, of the key reactions of PAH oxidation, and the reactions of dicarbon and tricarbon molecules with simplest unsaturated hydrocarbons leading to hydrogen-deficient resonance-stabilized radicals relevant to the PAH growth. We use chemically accurate *ab initio* calculations to predict reaction potential energy surfaces and statistical theories to compute absolute reaction rate constants and product branching ratios. An additional goal is to calculate spectroscopic properties of most important reaction intermediates and products in order to facilitate their experimental spectroscopic identification and monitoring.

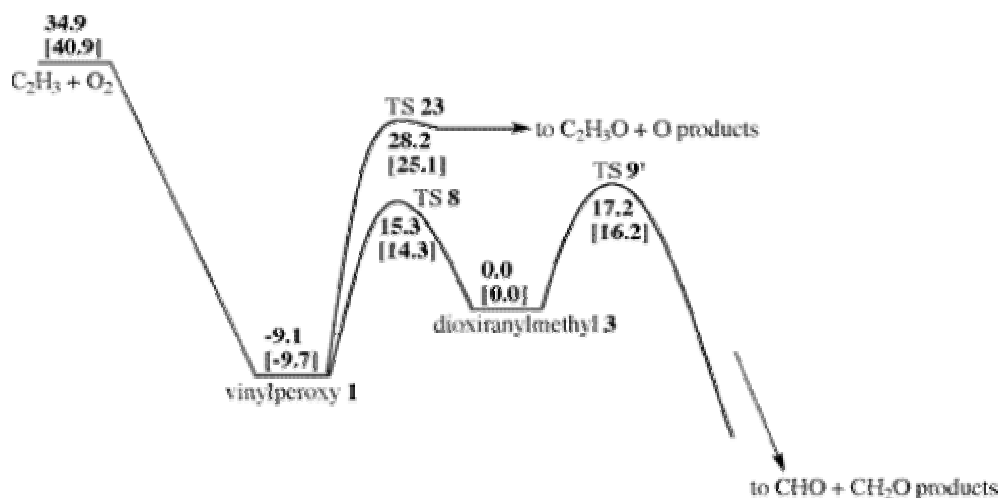
## Recent Progress

### 1. *Ab initio*/RRKM study of photodissociation of naphthalene, azulene, and their cations

The *ab initio*/RRKM approach has been applied to investigate the photodissociation mechanism of the simplest PAHs, naphthalene and azulene, at various laser wavelengths. A broad variety of reaction pathways for the naphthalene-azulene isomerization and dissociation leading to different products have been mapped out at the G3(MP2,CC)/B3LYP level and then the RRKM and microcanonical variational transition state theories have been applied to compute rate constants for individual reaction steps. Relative product yields (branching ratios) for the dissociation products have been calculated using the steady-state approach. The results show that photoexcited azulene can readily isomerize to naphthalene and the dominant reaction pathway is the one-step norcaradiene-vinylidene (Dewar-Becker) mechanism, in which the rearrangement of two carbon rings and a hydrogen shift occur in a concerted manner. The major dissociation channel is elimination of an H atom from naphthalene (99% of the total product yield at 193 nm). The branching ratio of this channel decreases with an increase of the photon energy. Acetylene elimination is the most probable minor reaction channel and its branching ratio rises as the photon energy increases. The main C<sub>8</sub>H<sub>6</sub> fragments at 193 nm are found to be phenylacetylene and pentalene and the yield of the latter grows fast with the increasing excitation energy. A similar theoretical approach was also used to study the photodissociation mechanism of naphthalene and azulene cations. The dominant isomerization pathway of photoexcited azulene cation is the norcaradiene-vinylidene mechanism, which provides about 50% of naphthalene. Once cationic naphthalene is formed, it can decompose mostly through elimination of a hydrogen atom, H<sub>2</sub> molecule, or acetylene. The major acetylene elimination channel, pentalene<sup>+</sup> + C<sub>2</sub>H<sub>2</sub>, occurs from azulene<sup>+</sup> and the other two channels, benzocyclobutadiene<sup>+</sup> + C<sub>2</sub>H<sub>2</sub> and phenylacetylene<sup>+</sup> + C<sub>2</sub>H<sub>2</sub>, start from naphthalene<sup>+</sup>. The branching ratio of the H elimination channel decreases with an increase of the photon energy, whereas those for the acetylene elimination and H<sub>2</sub> elimination rise as the photon energy increases. The main C<sub>8</sub>H<sub>6</sub><sup>+</sup> fragment at all photon energies considered is the pentalene cation.

## 2. High-accuracy reinvestigation of PES of the $C_2H_3 + O_2$ reaction

The reaction of vinyl radicals with molecular oxygen is of immense importance in the combustion of hydrocarbon fuels, as it represents a key step in the high-temperature oxidation of  $C_2H_4$  in ethylene and acetylene flames. Successive reaction products of vinyl radicals with unsaturated hydrocarbons have been shown to be a potential source of benzene, the initial building block of PAHs. The  $C_2H_3 + O_2$  reaction retards soot formation by competing with the reactions of vinyl radicals with unsaturated hydrocarbons. Therefore, to model PAH formation in combustion, it is critical to accurately predict the reaction rate constants and product branching ratios as functions of combustion conditions, i.e., temperature and pressure. According to the G2M(RCC,MP2) calculated PES, the reaction mechanism can be briefly outlined as follows:

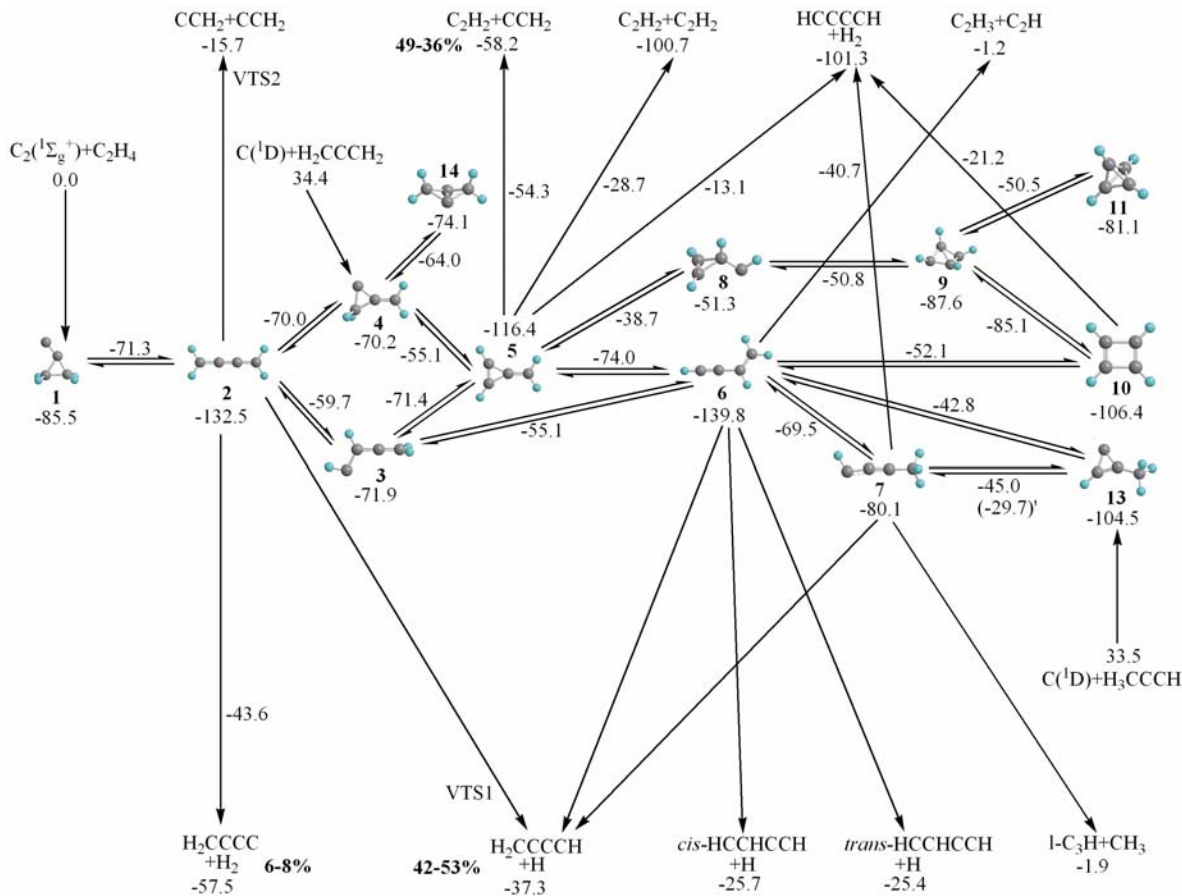


The reaction initiates by barrierless addition of  $O_2$  to the radical site of  $C_2H_3$  to produce the vinylperoxy radical. The latter can either lose the terminal oxygen atom to yield the  $C_2H_3O + O$  products via TS **23** or rearrange to the dioxiranylmethyl radical **3** via TS **8**. At the next reaction step, **3** undergoes an O-atom insertion into the C-C bond via TS **9'** (it can be also described as ring opening of dioxiranylmethyl radical) and then, eventually, the  $CHO + CH_2O$  products are formed. The O-insertion reaction step is strongly exothermic and its reverse barrier is very high,  $\sim 94$  kcal/mol, making this step practically irreversible. Thus, if the ring opening via TS **9'** does occur,  $CHO + CH_2O$  will be the dominant products. Therefore, branching ratios of the major products,  $C_2H_3OO$ ,  $C_2H_3O + O$ , and  $CHO + CH_2O$ , will be mostly controlled by relative energies and molecular parameters of five stationary points on the PES, intermediates **1** and **3** and transition states **23**, **8**, and **9'**. The product branching ratios are expected to be very sensitive to their thermodynamical parameters and there has been discussion in the literature concerning the accuracy of our earlier G2M calculated relative energies of these species and, in general, about applicability of the single reference coupled cluster method to chemical systems of this type. Therefore, we have revisited this reaction and recalculated energies of the critical intermediates and transition states at the CCSD(T) and multireference MRCI levels with extrapolation to the complete basis set limit. We found that the energy difference between two crucial transition states, **8** and **9'**, is about 2 kcal/mol both at the MRCI and CCSD(T) levels. The deviation from the earlier G2M(RCC,MP2) value ( $\sim 7$  kcal/mol) is caused by a deficiency of the 6-311+G(3df,2p) basis set as compared to

correlation-consistent Dunning's basis sets, but the CCSD(T) method is reconfirmed as an efficient, generally reliable, and uniform alternative to multireference calculations.

### 3. Theoretical study of potential energy surfaces, rate constants, and product branching ratios for the reactions of $C_2$ with unsaturated hydrocarbons

In conjunction with experiments carried out in crossed molecular beams by R. I. Kaiser at the University of Hawaii, we have studied PES for the reactions of dicarbon with acetylene, ethylene, methylacetylene, and allene using ab initio calculations at the G2M level and RRKM theory for prediction of reaction rate constants and product branching ratios. The calculations showed that  $C_2$  adds to double and triple bonds of unsaturated hydrocarbons without a barrier to form  $C_4H_2$ ,  $C_4H_4$ , and  $C_5H_4$  intermediates in singlet and triplet states depending on the electronic state of the attacking  $C_2$  molecule. After the formation of initial intermediates, the reactions proceed by  $C_2$  insertion into the attacked C-C bond followed by isomerizations involving H migrations and ring opening/closure processes. Under single-collision conditions, the  $C_4H_2$ ,  $C_4H_4$ , and  $C_5H_4$  species can dissociate through a loss of a hydrogen atom,  $H_2$  molecule, or decompose to a pair of heavy fragments. According to RRKM calculations, the dominant dissociation channel is the H loss producing the  $C_4H$ ,  $C_4H_3$ , and  $C_5H_3$  radicals, respectively. These calculations, together with the crossed molecular beams experiments, clearly demonstrate that the reactions of dicarbon with unsaturated hydrocarbons open routes to the formation of resonance-stabilized hydrocarbon radicals, which, in turn, can play a significant role in the formation and growth of PAHs in combustion flames (and in the interstellar medium). The  $C_2(^1\Sigma_g^+) + C_2H_4$  reaction exploring the singlet  $C_4H_4$  PES is peculiar. If this reaction follows a statistical RRKM behavior, *i*- $C_4H_3 + H$  are not the dominant products as their



branching ratio varies in the range of 42-53% when the collision energy increases from 0 to 10 kcal/mol. The other major products should be acetylene + vinylidene (50-36%) and a significant amount (6-8%) of  $\text{H}_2\text{CCCC} + \text{H}_2$  should be also produced.

### Future Plans

We will complete a detailed study of the reactions leading to indene and compute thermal rate constants for the pathways involving benzene (phenyl), toluene (benzyl), cyclopentadiene (cyclopentadienyl), fulvene (fulvenyl), and naphthalene (naphthyl) reacting with abundant small hydrocarbon molecules and their radicals ( $\text{CH}_3$ ,  $\text{C}_3\text{H}_3$ ,  $\text{C}_2\text{H}_2$ ,  $\text{C}_4\text{H}_4$ ) and with  $\text{O}_2$ . We will also continue to investigate potentially important channels of naphthalene formation in combustion, such as the  $\text{C}_5\text{H}_5 + \text{C}_5\text{H}_5$ ,  $\text{C}_6\text{H}_5 + \text{C}_4\text{H}_4$ , and  $\text{C}_7\text{H}_7 + \text{C}_3\text{H}_3$  reactions. In parallel with experimental crossed molecular beam measurements in R. I. Kaiser's group at the University of Hawaii, we will investigate the  $\text{C}_5\text{H}_2$ ,  $\text{C}_5\text{H}_4$ , and  $\text{C}_6\text{H}_4$  PESs in order to understand mechanisms and to predict collision energy dependent product branching ratios for the reactions of tricarbon,  $\text{C}_3$ , with acetylene, ethylene, methylacetylene, and allene. We will proceed with calculations of electronic/vibrational spectra for hydrogen-deficient, resonance-stabilized  $\text{C}_4\text{H}_3$  and  $\text{C}_5\text{H}_3$  radicals.

### DOE/BES sponsored publications (since 08/2004)

1. L. Wang, V. V. Kislov, A. M. Mebel, X. Yang, X. Wang, "Potential energy surface and product branching ratios for the reaction of  $\text{F}(^2\text{P})$  with the methyl radical: An ab initio/RRKM study," *Chem. Phys. Lett.* 406, 60 (2005).
2. I. V. Tokmakov, G.-S. Kim, V. V. Kislov, A. M. Mebel, M. C. Lin, "The reaction of phenyl radical with molecular oxygen: A G2M study of the potential energy surface," *J. Phys. Chem. A* 109, 6114 (2005).
3. V. V. Kislov, A. M. Mebel, "The  $\text{C}_2\text{H}_3 + \text{O}_2$  reaction revisited: Is multireference treatment of the wave function really critical?," *J. Phys. Chem. A* 109, 6993 (2005).
4. V. V. Kislov, N. I. Islamova, A. M. Kolker, S. H. Lin, A. M. Mebel, "Hydrogen abstraction acetylene addition and Diels-Alder mechanisms of PAH formation: A detailed study using first principles calculations," *J. Chem. Theory and Comput.* 1, 908 (2005).
5. Y. A. Dyakov, C. K. Ni, S. H. Lin, Y. T. Lee, A. M. Mebel, "Photodissociation of azulene at 193 nm: Ab initio and RRKM study," *J. Phys. Chem. A* 109, 8774 (2005).
6. A. M. Mebel, V. V. Kislov, R. I. Kaiser, "Potential energy surface and product branching ratios for the reactions of dicarbon  $\text{C}_2(\text{X}^1\Sigma_g^+)$  with methylacetylene,  $\text{CH}_3\text{CCH}(\text{X}^1\text{A}_1)$ : An ab initio/RRKM study," *J. Phys. Chem. A* 110, 2421 (2006).
7. Y. A. Dyakov, A. M. Mebel, S. H. Lin, Y. T. Lee, C. K. Ni, "Acetylene elimination in photodissociation of neutral azulene and its cation: An ab initio and RRKM study," *J. Chin. Chem. Soc.* 53, 161 (2006).
8. Y. A. Dyakov, C. K. Ni, S. H. Lin, Y. T. Lee, A. M. Mebel, "Ab initio and RRKM study of photodissociation of azulene cation," *Phys. Chem. Chem. Phys.* 12, 1404 (2006).
9. Y. Guo, X. Gu, F. Zhang, A. M. Mebel, R. I. Kaiser, "Unimolecular decomposition of chemically activated pentatetraene ( $\text{H}_2\text{CCCCCH}_2$ ) intermediates – a crossed beams study of dicarbon molecule reactions with allene," *J. Chem. Phys.*, in press.
10. Y. Guo, X. Gu, F. Zhang, A. M. Mebel, R. I. Kaiser, "Unimolecular decomposition of singlet and triplet methylidyne acetylene – a crossed molecular beams study," *Phys. Chem. Chem. Phys.*, in press.
11. Y. Guo, X. Gu, F. Zhang, A. M. Mebel, R. I. Kaiser, "Reaction dynamics of carbon bearing radicals in circumstellar envelopes of carbon stars," *Faraday Discuss.*, in press.

## FLASH PHOTOLYSIS-SHOCK TUBE STUDIES

Joe V. Michael

Gas Phase Chemical Dynamics Group, Chemistry Division  
Argonne National Laboratory, Argonne, IL 60439  
e-mail: jmichael@anl.gov

The scope of the program is to measure high-temperature thermal rate constants with shock tube techniques for use in high-temperature combustion. As described earlier, we have used a multi-pass optical system for detecting OH-radicals.<sup>1</sup> The new configuration is similar to that described previously.<sup>2-4</sup>

During the past year, the reflected shock tube technique using OH-radical absorption at 308 nm has been used to study two unimolecular reactions,  $\text{H}_2\text{O} \rightarrow \text{H} + \text{OH}$  and  $\text{CH}_3\text{OH} \rightarrow \text{products}$  at path lengths of  $\sim 1.75$  and  $4.90$  m, respectively. The temporal concentration build up of OH was determined from measured absorbance,  $(ABS)_t = \ln[I_0/I_t] = [\text{OH}]_t l \sigma_{\text{OH}}$ , through an earlier determination<sup>1</sup> of the absorption cross-section at 308 nm ( $\sigma_{\text{OH}} = (4.516 - 1.18 \times 10^{-3} T) \times 10^{-17} \text{ cm}^2 \text{ molecule}^{-1}$ ).

The thermal decomposition of water



was studied between 2196 and 2792 K using 0.3, 0.5, and 1%  $\text{H}_2\text{O}$ , diluted in Kr. As a result of the increased sensitivity for OH-radical detection, the existing database for this reaction could be extended downward by 500 K. Combining the present work with that of Homer and Hurle,<sup>5</sup> the composite rate expression for water dissociation in either Ar or Kr bath gas is

$$k_{1,\text{Ar(or Kr)}} = (2.43 \pm 0.57) \times 10^{10} \exp(-47117 \pm 633 K/T) \text{ cm}^3 \text{ molecule}^{-1} \text{ s}^{-1} \quad (2)$$

for the  $T$ -range of 2196-3290 K. Applying the Troe factorization method to data for both forward and reverse reactions, the rate behavior could be expressed to within  $<\pm 18\%$  over the  $T$ -range, 300-3400 K, by the three-parameter expression

$$k_{1,\text{Ar}} = 1.007 \times 10^4 T^{-3.322} \exp(-60782 K/T) \text{ cm}^3 \text{ molecule}^{-1} \text{ s}^{-1} \quad (3)$$

A large enhancement due to  $\text{H}_2\text{O}$  with  $\text{H}_2\text{O}$  collisional activation has been noted previously, and both absolute and relative data have been considered allowing us to suggest

$$k_{1,\text{H}_2\text{O}} = 1.671 \times 10^2 T^{-2.440} \exp(-60475 K/T) \text{ cm}^3 \text{ molecule}^{-1} \text{ s}^{-1} \quad (4)$$

for the rate constants with  $\text{H}_2\text{O}$  bath gas over the  $T$ -range, 300-3400 K.

Fifty-eight experiments have been carried out to investigate the thermal decomposition of  $\text{CH}_3\text{OH}$  in the reflected shock wave regime over the  $T$ -range, 1591 to 2865 K, and reflected shock pressures between 0.3 and 1.1 atm. Four mixtures were used varying from 6.4 – 27.9 ppm  $\text{CH}_3\text{OH}$  diluted in Kr bath gas. The present sensitivity for

OH-radical detection is significantly higher with fifty-six optical passes than in the previous work.<sup>1</sup>

There are six decompositions, two of which dominate under the present high-T conditions, reactions (4) and (5).



In our lower-T regime, 1590-1700 K, sensitivity analysis shows that the only important reactions affecting [OH] are reaction (4) and the process,



Reaction (6) is composite since the initially formed  $\text{CH}_2\text{OH}$  or  $\text{CH}_3\text{O}$  radicals instantaneously decompose to  $\text{CH}_2\text{O}$  and H. Hence, rate constants for both (4) and (6) can be determined. The present values for  $k_6$  are plotted in Fig. 1. Our  $k_6$  values, the most direct to date, along with earlier lower-T determinations have been used in a three parameter evaluation giving

$$k_6 = 6.87 \times 10^{-16} T^{1.3348} \exp(-133 \text{ K/T}) \text{ cm}^3 \text{ molecule}^{-1} \text{ s}^{-1}. \quad (7)$$

Eqn. (7) is also plotted in Fig. 1 along with the data from earlier studies,<sup>6-10</sup> including the single point of Bott and Cohen,<sup>11</sup> that were used to derive it. As seen in the figure, Eqn. (7) agrees to within  $\pm 20\%$  with all previous determinations. There are two flame studies<sup>12,13</sup> where  $k_6$  is estimated from fits to complex mechanisms, and our evaluation falls squarely between these two.

In addition to the  $T < 1700$  K values for (4), both  $k_4$  and the branching ratio,  $k_4/(k_4 + k_5)$ , can be determined at  $T > 1700$  K from OH yields and simulations with a 29 step mechanism. Only a few of the reactions exhibit OH sensitivity. We find

$$k_4 = 9.29 \times 10^{-9} \exp(-30851 \text{ K/T}), \quad (8)$$

and

$$k_5 = 3.27 \times 10^{-10} \exp(-25946 \text{ K/T}), \quad (9)$$

both in  $\text{cm}^3 \text{ molecule}^{-1} \text{ s}^{-1}$ . For the two reactions, the present results are plotted in Fig. 2 along with lines calculated from (8) and (9). The points in Fig. 2 are within  $\pm 32$  and  $\pm 48\%$  at one standard deviation of the lines determined from Eqns. (8) and (9), respectively. Summing the values for  $k_4$  and  $k_5$  for each experiment gives  $k_{\text{total}}$  as a function of temperature, and these follow the linear-least-squares equation over the T-range, 1591-2385 K,

$$k_{\text{total}} = 5.73 \times 10^{-9} \exp(-29171 \text{ K/T}). \quad (10)$$

The summed points are within  $\pm 26\%$  of Eqn. (10) at the one standard deviation level.

There are several earlier studies on the thermal decomposition of  $\text{CH}_3\text{OH}$ ,<sup>14</sup> and rate constants vary by about a factor of forty over the present temperature range. The present

result summarized by Eqn. (10) is about a factor of two lower than the earlier determination from this laboratory<sup>15</sup> and is slightly outside the combined experimental error of the present and earlier study. The 1979 estimate by Westbrook and Dryer<sup>16</sup> is in substantial agreement with the present result up to ~1700 K but then diverges to higher values as temperature increases. The results of Cribb et al.<sup>17</sup> are 2 - 2.5 times higher whereas the results of Dombrowsky et al.<sup>18</sup> give values that agree best with the present work being within  $\sim\pm 25\%$  of Eqn. (10). Probably preferring the results of Cribb et al., the 1994 Baulch et al.<sup>19</sup> evaluation suggests values  $\sim 2 - 2.5$  times higher than the present value. These results will be compared to theoretical models based on RRKM calculations.

Additional atom and radical with molecule reaction studies (e. g. Cl + hydrocarbons, OH + hydrocarbons, CF<sub>2</sub> + O<sub>2</sub>, etc.) and, also, thermal decomposition investigations (e. g. C<sub>2</sub>H<sub>5</sub>, C<sub>2</sub>H<sub>3</sub>, etc.) are in the planning stage at the present time.

This work was supported by the U. S. Department of Energy, Office of Basic Energy Sciences, Division of Chemical Sciences, Geosciences and Biosciences, under Contract No. W-31-109-ENG-38.

## References

1. Srinivasan, N. K.; Su, M.-C.; Sutherland, J. W.; Michael, J. V. *J. Phys. Chem. A* **2005**, *109*, 1857.
2. Su, M.-C.; Kumaran, S. S.; Lim, K. P.; Michael, J. V. *Rev. Sci. Inst.* **1995**, *66*, 4649.
3. Su, M.-C.; Kumaran, S. S.; Lim, K. P.; Michael, J. V.; Wagner, A. F.; Dixon, D. A.; Kiefer, J. H.; DiFelice, J. *J. Phys. Chem.* **1996**, *100*, 15827.
4. Su, M.-C.; Kumaran, S. S.; Lim, K. P.; Michael, J. V.; Wagner, A. F.; Harding, L. B.; Fang, D.-C. *J. Phys. Chem. A* **2002**, *106*, 8261.
5. Homer, J. B.; Hurle, I. R. *Proc. R. Soc. London A* **1970**, *314*, 585.
6. Hagele, J.; Lorenz, K.; Rhasa, D.; Zellner, R. *Ber. Bunsenges. Phys. Chem.* **1983**, *87*, 1023.
7. Meier, U.; Grotheer, H.-H.; Riekert, G.; Just, Th. *Ber. Bunsenges. Phys. Chem.* **1985**, *89*, 325.
8. Greenhill, P. G.; O'Grady, B. V. *Aust. J. Chem.* **1986**, *39*, 1775.
9. Hess, W. P.; Tully, F. P. *J. Phys. Chem.* **1989**, *93*, 1944.
10. Jimenez, E.; Gilles, M. K.; Ravishankara, A. R. *J. Photochem. Photobio. A Chem.* **2003**, *157*, 237.
11. Bott, J. G.; Cohen, N. *Int. J. Chem. Kinet.* **1991**, *23*, 1075.
12. Vandooren, J.; Van Tiggelen, P. J. *Proc. Combust. Inst.* **1981**, *18*, 473.
13. Li, S. C.; Williams, F. A. *Proc. Combust. Inst.* **1996**, *26*, 1017.
14. *NIST Chemical Kinetics Database*, NIST Standard Reference Database 17, Gaithersburg, MD, (2000).
15. Krasnoperov, L. N.; Michael, J. V. *J. Phys. Chem. A* **2004**, *108*, 8317.
16. Westbrook, C. K.; Dryer, F. L. *Combust. Sci. Technol.* **1979**, *20*, 125.
17. Cribb, P. H.; Dove, J. E.; Yamazaki, S. *Combust. Flame* **1992**, *88*, 169.
18. Dombrowsky, Ch.; Hoffman, A.; Klatt, M.; Wagner, H. Gg. *Ber. Bunsenges. Phys. Chem.* **1991**, *95*, 1685.
19. Baulch, D. L.; Cobos, C. J.; Cox, R. A.; Frank, P.; Hayman, G.; Just, Th.; Kerr, J. A.; Murrells, T.; Pilling, M. J.; Troe, J.; Walker, R. W.; Warnatz, J. *J. Phys. Chem. Ref. Data* **1994**, *23*, 847.

## **PUBLICATIONS FROM DOE SPONSORED WORK FROM 2004-2006**

- *New Rate Constants for D + H<sub>2</sub> and H + D<sub>2</sub> between ~1150 and 2100 K*, J. V. Michael, M.-C. Su, and J. W. Sutherland, *J. Phys. Chem. A* **108**, 432 (2004).
- *Shock Tube Studies Using a Novel Multi-pass Absorption Cell: Rate Constant Results for OH + H<sub>2</sub>, and OH + C<sub>2</sub>H<sub>6</sub>*, L. N. Krasnoperov and J. V. Michael, *J. Phys. Chem. A* **108**, 5643 (2004).

■ *High Temperature Shock Tube Studies Using Multi-pass Absorption: Rate Constant Results for OH + CH<sub>3</sub>, OH + CH<sub>2</sub>, and the Dissociation of CH<sub>3</sub>OH*, L. N. Kransnoperov and J. V. Michael, *J. Phys. Chem. A* **108**, 8317 (2004).

■ *Rate Constants for D + C<sub>2</sub>H<sub>4</sub> → C<sub>2</sub>H<sub>3</sub>D + H at High Temperature: Implications to the High Pressure Rate Constant for H + C<sub>2</sub>H<sub>4</sub> → C<sub>2</sub>H<sub>5</sub>*, J. V. Michael, M.-C. Su, J. W. Sutherland, L. B. Harding, and A. F. Wagner, *Proc. Combust. Inst.* **30**, 965 (2005).

■ *Reflected Shock Tube Studies of High-Temperature Rate Constants for OH + CH<sub>4</sub> → CH<sub>3</sub> + H<sub>2</sub>O and CH<sub>3</sub> + NO<sub>2</sub> → CH<sub>3</sub>O + NO*, N. K. Srinivasan, M.-C. Su, J. W. Sutherland, and J. V. Michael, *J. Phys. Chem. A* **109**, 1857 (2005).

■ *Reflected Shock Tube Studies of High-Temperature Rate Constants for CH<sub>3</sub> + O<sub>2</sub>, H<sub>2</sub>CO + O<sub>2</sub>, and OH + O<sub>2</sub>*, N. K. Srinivasan, M.-C. Su, J. W. Sutherland, and J. V. Michael, *J. Phys. Chem. A* **109**, 7902 (2005).

■ *The Thermal Decomposition of Water*, N. K. Srinivasan and J. V. Michael, *Int. J. Chem. Kinet.* **38**, 211 (2006).

■ *Active Thermochemical Tables: Accurate Enthalpy of Formation of Hydroperoxyl Radical, HO<sub>2</sub>*, B. Ruscic, R. E. Pinzon, M. L. Morton, N. K. Srinivasan, M.-C. Su, J. W. Sutherland, and J. V. Michael, *J. Phys. Chem. A*, in press.

■ *Reflected Shock Tube Studies of High-Temperature Rate Constants for OH + NO<sub>2</sub> → HO<sub>2</sub> + O<sub>2</sub> and OH + HO<sub>2</sub> → H<sub>2</sub>O + O<sub>2</sub>*, N. K. Srinivasan, M.-C. Su, J. W. Sutherland, J. V. Michael, and B. Ruscic., *J. Phys. Chem. A*, in press.

■ *Initiation in CH<sub>4</sub>/O<sub>2</sub>: High Temperature Rate Constants for CH<sub>4</sub> + O<sub>2</sub> → CH<sub>3</sub> + HO<sub>2</sub>*, N. K. Srinivasan, J. V. Michael, L. B. Harding, and S. J. Klippenstein, *Proc. Combust. Inst.* **31**, accepted.

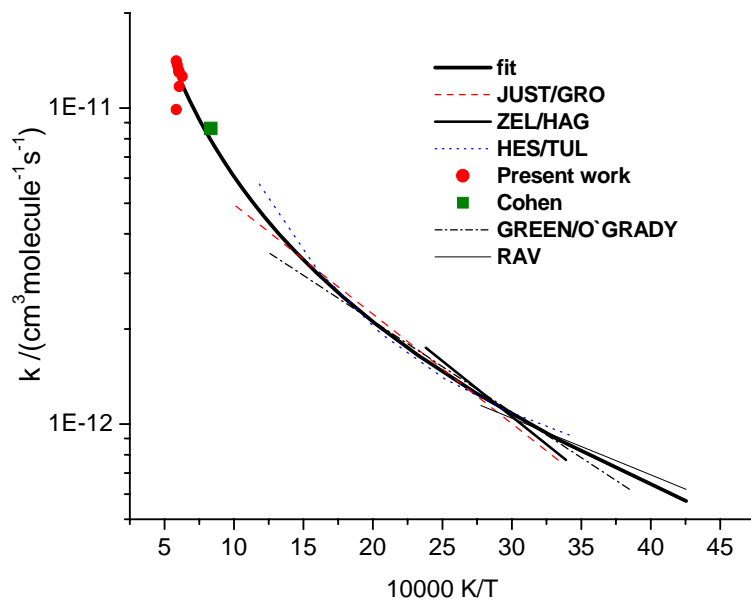


Fig .1

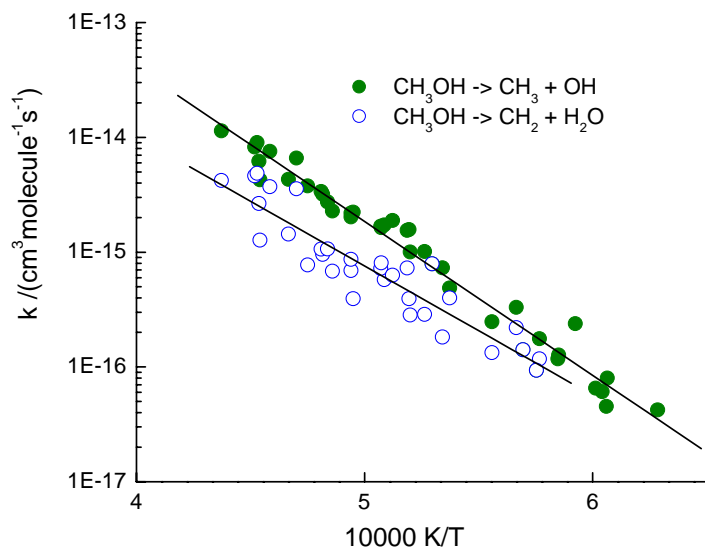


Fig .2

## Particle Diagnostics Development

H. A. Michelsen

Sandia National Laboratories, P. O. Box 969, MS 9055, Livermore, CA 94551

hamiche@ca.sandia.gov

### 1. Program Scope

Small (sub-micron) particulates are believed to pose a greater health risk than larger soot particles<sup>1</sup> and are expected to have a significant impact on the Earth's climate.<sup>2</sup> A growing concern about adverse health and environmental effects of small particles has prompted strict regulations of fine particulate emissions and has intensified research on the formation and impact of combustion-generated particles.<sup>3</sup> Studies of particle formation and evolution, however, are hindered by a lack of sensitive, accurate, noninvasive measurements of their physical characteristics. The research program described here focuses on the development of optical diagnostics for particles, primarily soot particles, in combustion environments and combustion exhaust plumes. The goal of this work is in situ measurements of volume fraction, size, composition, and morphology of such particles with fast time response and high sensitivity.

### 2. Recent Progress

Our work has focused on developing a detailed understanding of the chemical and physical mechanisms that influence the applicability of laser-induced incandescence (LII) for soot detection under a wide range of conditions. In order to understand these mechanisms, we have coupled experimental studies with the development of a model that predicts the temporal behavior of LII from soot on a nanosecond time scale. The model accounts for particle heating by laser absorption, oxidation, and annealing and cooling by sublimation, conduction, and radiation. The model also includes mechanisms for convective heat and mass transfer, melting, and nonthermal photodesorption of carbon clusters.<sup>4</sup> Initial experimental results used in the development of the model were collected in a coflow diffusion flame with fresh, mature, dry soot as the sample.

In our recent work we have used a flow-tube system to study the effects of laser radiation on the morphology and fine structure of dry soot aggregates. We have performed these studies in collaboration with Mary Gilles and Alexei Tivanski at the Lawrence Berkeley National Laboratory Advanced Light Source (ALS) and with Peter Buseck and Laura van Poppel at Arizona State University (ASU).

We have also performed experiments designed to isolate fast (picosecond timescale) laser-particle mechanisms from processes that are expected to evolve over longer (nanosecond) timescales. Fast processes, such as laser absorption and photolytic desorption, can have an influence on LII and elastic laser scattering (ELS). These experiments were performed using a regeneratively amplified modelocked Nd:YAG laser with a pulse duration at 532 nm of ~65 ps and a streak camera with a temporal resolution of ~8 ps. These measurements have been compared with those made using a YAG laser with a 6.9-ns pulse duration to heat the particles. The results will be used to revise and refine the LII model and our understanding of the mechanisms involved in LII detection.

#### *2.1. The effects of laser radiation on the morphology and fine structure of soot aggregates.*

Soot is composed of dendritic aggregates of small (15-50 nm diameter) carbon spheroids called primary particles. Previous work has suggested that, during laser irradiation, these aggregates can break apart into primary particles.<sup>5</sup> Transmission electron microscopy (TEM) images of laser-heated soot, however, have demonstrated substantial changes to particle fine structure and morphology without the appearance of small fragments.<sup>6,7</sup> This result suggests that

either mass loss occurred via laser-induced sublimation of carbon clusters or that any primary particles lost from the aggregates were not retained on the grids.

In collaboration with Peter Buseck and his group at ASU and Mary Gilles and her group at the ALS, we have used particle electric mobility sizing, TEM techniques, and near edge X-ray absorption fine structure (NEXAFS) spectroscopy to investigate the physical and chemical changes induced in soot aggregates exposed to laser radiation at 532 and 1064 nm. In these experiments, soot particles were measured with a scanning mobility particle sizer (SMPS) and were concurrently collected on TEM grids and Si<sub>3</sub>N<sub>4</sub> windows prior to and following exposure to laser radiation over a wide range of laser fluences (0.01-1 J/cm<sup>2</sup>).

The initial soot particles produced by the flame during these experiments were polydisperse and followed a log-normal size distribution with a median electric mobility diameter of ~100 nm. TEM images of these particles revealed typical fractal-like branched-chain aggregates consisting of approximately 50 spherical primary particles. The average geometric diameter of the primary particles was 25 nm. The aggregate fractal dimension was  $d_f = 1.7$ , which is typical of dry, mature soot.

No change in particle electric mobility diameter, morphology, fine structure, or chemical structure (carbon hybridization) was observed when the particles were exposed to laser radiation at low fluences (<~0.12 J/cm<sup>2</sup> at 532 nm and <~0.22 J/cm<sup>2</sup> at 1064 nm). At higher fluences, a new size mode (centered at 8 – 20 nm in electric mobility diameter) was observed. These smaller particles grew in size and particle number density with increasing fluence. NEXAFS showed predominantly graphitic (sp<sup>2</sup>-hybridized) carbon in the non-irradiated particles and a mixture of sp<sup>2</sup>- and sp<sup>3</sup>-hybridized carbon (consistent with amorphous carbon) in the irradiated particles. In TEM images small (~30 nm diameter) particles produced by irradiation of soot consisted of extended regions without any obvious long-range order and smaller isolated regions of carbon with significant long-range order. These ordered regions contain small graphite crystallites or partially annealed carbon that forms small, layered carbon rings or ribbons. Large particles (~100 nm diameter) irradiated at fluences above the threshold fluence for new particle formation consist of primary particles that appear to be similar in size and structure to the non-irradiated primary particles. These large particles can also include primary particles with denser layered carbon rings, which may result from partial annealing.

These results suggest that particle growth proceeds through recondensation of small carbon clusters (e.g., C, C<sub>2</sub>, and C<sub>3</sub>) by homogeneous nucleation, heterogeneous nucleation onto graphitic fragments of primary particles, or a combination of both homogeneous and heterogeneous nucleation. Nanoparticle growth via homogeneous or heterogeneous nucleation of small carbon clusters is consistent with model predictions of the onset and extent of carbon volatilization by sublimation and photodesorption mechanisms. The efficiency for laser-induced nanoparticle production was significantly smaller at 1064 nm than at 532 nm at all fluences above 0.12 J/cm<sup>2</sup>. Reduced efficiency of new particle formation at the longer wavelength is likely due to a smaller absorption coefficient and lower photodesorption efficiency at the longer wavelength. These results are consistent with previous studies of laser irradiation of soot particles and bulk graphite. The onset of soot fragmentation at 0.12 J/cm<sup>2</sup> at 532 nm is consistent with energetic requirements for carbon sublimation observed experimentally and predicted by the LII model.<sup>4</sup>

## ***2.2. Laser-induced incandescence on a picosecond timescale.***

LII involves heating the soot particles with a high-power pulsed laser to temperatures (2500-4000 K) at which they incandesce and measuring the emitted light. Interpretation of LII signals for quantitative measurements is hampered by an incomplete understanding of the physical mechanisms that influence signal evolution during and after the laser pulse. Previous

experimental work has shown that, at low fluences ( $< \sim 0.15 \text{ J/cm}^2$ ), temporally resolved LII signals increase during the laser pulse and slowly decay with decay times on the order of a few hundred nanoseconds at atmospheric pressure and flame temperatures.<sup>4,8-12</sup> Decay times decrease with increasing fluence, particularly at fluences above  $0.2 \text{ J/cm}^2$ .<sup>4,5,8-10,13,14</sup> These studies were performed using laser systems with pulse durations in the range of 7-8 ns.

Because the LII signal is approximately proportional to  $T^5$  (i.e., for a Rayleigh particle with an emissivity proportional to  $1/l$ ), particle cooling leads to a decrease in signal. LII signals also depend on particle size and decrease approximately linearly with a decrease in particle volume. Model results suggest that, on nanosecond to microsecond timescales, laser-heated soot particles cool predominantly by sublimation and conduction to the surrounding atmosphere.<sup>4,5,11,12,14-18</sup> Sublimation also causes particles to shrink. Further evidence indicates that an unknown mechanism leads to a significant loss of signal within the first few nanoseconds of the laser pulse at fluences above  $\sim 0.2 \text{ J/cm}^2$ .<sup>4,10</sup> In order to gain an understanding of this latter process, experiments were performed on a picosecond timescale. A picosecond laser was used to heat the soot, and a streak camera was used to collect the emitted light.

Soot was produced in an atmospheric laminar co-flow diffusion flame and was heated with the 532-nm output from a picosecond Nd:YAG laser with a pulse duration of 65 ps. The signal was recorded on a streak camera with a temporal resolution of  $\sim 8$  ps. Similar measurements were made using the 532-nm output from a Nd:YAG with a 6.9-ns pulse duration to heat the soot and a photodiode with a rise time of  $< 0.3$  ns to record the signal. Relative to the laser timing, the temporal characteristics of the picosecond and nanosecond signals are qualitatively very similar.

The results of both experiments were compared with an LII model that has been optimized using data from a nanosecond LII system. As has been demonstrated previously,<sup>4,10</sup> the LII model gives good agreement with the nanosecond data at fluences  $\leq 0.2 \text{ J/cm}^2$  and underpredicts the signal decay rates at higher fluences. The model does not agree as well with the picosecond data. The picosecond temporal profiles increase significantly faster and earlier in the laser pulse than predicted by the model. This disagreement between the model and picosecond LII data may be attributable to perturbations to the signal by laser-induced fluorescence (LIF) from polycyclic aromatic hydrocarbons (PAHs) or another class of large organic species that fluoresces in the range of 633-900 nm in which the signal was detected. The power dependence of the signal enhancement suggests that the excited state or states responsible for this fluorescence are accessed via a two-photon transition, which would explain the enhanced sensitivity to this interference with the shorter pulse duration. These states are short-lived and are estimated to have an effective lifetime of  $\sim 55$  ps.

### 3. Future plans

Current work builds on these results and extends it to combustion-generated particles with inorganic and organic coatings representative of particles found in exhaust plumes. In order to simulate exhaust-plume particulates, we have modified our flow-tube system to allow controlled deposition of a coating with low volatility on flame-generated soot. The thickness of the coating can be varied and the particles collected for analysis by TEM and NEXAFS. Coatings investigated to date have been selected for diagnostic development for diesel exhaust and include sulfuric acid, heptamethylnonane, and oleic acid. These experiments are currently limited by our inability to determine the mass loading of particle coatings. Developing an understanding of the cause and magnitude of the effects of coatings will require characterization of the particle coatings. Coating the particles increases the mean aggregate size as measured by the SMPS, but measurements of electric mobility diameter provided by the SMPS do not provide a quantitative measure of the volatile coating fraction either by volume or by mass. In order to measure the volatile fraction, we will build a chamber that includes a temperature-controlled oscillating

crystal microbalance on which we can deposit the particles. Heating the particles will force vaporization of the volatile component and enable us to determine its mass relative to that of the nonvolatile portion. This chamber will also be equipped with a residual gas analyzer for additional coating characterization through mass spectrometric speciation and temperature programmed desorption measurements.

We will also extend our studies of fast processes that are important during laser heating of soot. In order to identify the source of the fast signal seen in the picosecond experiments, we will perform these experiments in regions of the flame where PAH concentrations should be higher and soot concentrations lower. We will also perform these experiments at 1064 nm, which would reduce any contribution from a multiphoton LIF process. We will use these results to refine the LII model. Experiments at 1064 nm on both nanosecond and picosecond timescales will allow us to modify the model to run at this wavelength.

#### 4. References

- 1) Horvath, H. *J. Environ. Radioactivity* **2000**, *51*, 5.
- 2) IPCC *Climate Change 2001: The Scientific Basis. Contribution of Working Group I to the Third Assessment Report of the Intergovernmental Panel on Climate Change*; Cambridge University Press: Cambridge, UK and New York, NY, 2001.
- 3) NRC *Research Priorities for Airborne Particulate Matter: IV. Continuing Research Progress*; National Academy Press: Washington, DC, 2004.
- 4) Michelsen, H. A. *J. Chem. Phys.* **2003**, *118*, 7012.
- 5) Filippov, A. V.; Markus, M. W.; Roth, P. *J. Aerosol Sci.* **1999**, *30*, 71.
- 6) Vander Wal, R. L.; Ticich, T. M.; Stephens, A. B. *Appl. Phys. B* **1998**, *67*, 115.
- 7) Vander Wal, R. L.; Choi, M. Y. *Carbon* **1999**, *37*, 231.
- 8) Ni, T.; Pinson, J. A.; Gupta, S.; Santoro, R. J. *Appl. Opt.* **1995**, *34*, 7083.
- 9) Witze, P. O.; Hochgreb, S.; Kayes, D.; Michelsen, H. A.; Shaddix, C. R. *Appl. Opt.* **2001**, *40*, 2443.
- 10) Michelsen, H. A.; Witze, P. O.; Kayes, D.; Hochgreb, S. *Appl. Opt.* **2003**, *42*, 5577.
- 11) Snelling, D. R.; Liu, F.; Smallwood, G. J.; Gülder, Ö. L. *Combust. Flame* **2004**, *136*, 180.
- 12) Schittkowski, T.; Mewes, B.; Brüggemann, D. *Phys. Chem. Chem. Phys.* **2002**, *4*, 2063.
- 13) Vander Wal, R. L.; Weiland, K. J. *Appl. Phys. B* **1994**, *59*, 445.
- 14) Allouis, C.; Beretta, F.; D'Alessio, A. *Exp. Thermal Fluid Sci.* **2003**, *27*, 455.
- 15) Weeks, R. W.; Duley, W. W. *J. Appl. Phys.* **1974**, *45*, 4661.
- 16) Eckbreth, A. C. *J. Appl. Phys.* **1977**, *48*, 4473.
- 17) Melton, L. A. *Appl. Opt.* **1984**, *23*, 2201.
- 18) Liu, F.; Smallwood, G. J.; Snelling, D. R. *J. Quant. Spectrosc. Radiat. Transfer* **2005**, *93*, 301.

#### 5. BES-supported, peer-reviewed publications

- 1) C. Schulz, B. Kock, M. Hofmann, H. Michelsen, S. Will, B. Bougie, R. Suntz, and G. Smallwood, "Laser-induced incandescence: Recent trends and current questions", *Appl. Phys. B*, in press (2006).
- 2) H. A. Michelsen, "Laser-induced incandescence of flame-generated soot on a picosecond timescale", *Appl. Phys. B*, in press (2006).
- 3) L. Nemes, A. M. Keszler, C. G. Parigger, J. O. Hornkohl, H. A. Michelsen, and V. Stakhursky, "The C<sub>3</sub> puzzle: Formation of and spontaneous emission from the C<sub>3</sub> radical in carbon plasmas", *Int. Elect. J. Mol. Design*, in press (2006).
- 4) P. O. Witze, M. Y. Gershenson, and H. A. Michelsen, "Dual-laser LIDELS: An optical diagnostic for time-resolved volatile fraction measurements of diesel particulate emissions", *Proc. SAE*, SAE paper #2005-01-3791 (2005).
- 5) B. K. Pun, C. Seigneur, and H. A. Michelsen, "Atmospheric Transformations", in *Air Pollution Modeling: Theories, Computational Methods, and Available Software, 2nd edition, Vol. 2*, P. Zannetti, Ed., Van Nostrand Reinhold, New York, Chapter 12 (2005).

# Chemical Kinetics and Combustion Modeling

James A. Miller

Combustion Research Facility, Sandia National Laboratories

MS 9055, Livermore, CA, 94551-0969

email: jamille@sandia.gov

## Program Scope

The goal of this project is to gain qualitative insight into how pollutants are formed in combustion systems and to develop quantitative mathematical models to predict their formation and destruction rates. The approach is an integrated one, combining theory, modeling, and collaboration with experimentalists to gain as clear a picture as possible of the processes in question. My efforts and those of my collaborators are focused on problems involved with the nitrogen chemistry of combustion systems and the formation of soot and PAH in flames, as well as on general problems in hydrocarbon combustion. Current emphasis is on determining phenomenological rate coefficients from the time-dependent, multiple-well master equation for reactions involved in the pre-cyclization and cyclization chemistry of flames burning aliphatic fuels.

## Recent Results

*The Reaction of Ethylene with Hydroxyl Radicals: A Theoretical Study* (with Juan Senosiain and Stephen Klippenstein)

*Ab initio* electronic-structure calculations were used to determine the portions of the C<sub>2</sub>H<sub>5</sub>O potential energy surface critical to the title reaction. These calculations are based on QCISD geometries and frequencies and RQCISD(T) energies extrapolated to the complete-basis-set limit. Rate coefficients for the reaction of C<sub>2</sub>H<sub>4</sub> with OH were calculated using this surface and the two transition-state model of Greenwald and co-workers [*J. Phys. Chem. A* **2005**, *109*, 6031] for the association of OH with C<sub>2</sub>H<sub>4</sub>. The present calculations reproduce most of the experimental data, including the temperature and pressure dependence of the rate coefficients, with only a small (0.4 kcal/mol) adjustment to the energy barrier for direct hydrogen abstraction. We confirm the importance of this channel above 800 K and find that a significant fraction of the total rate coefficient (~10%) is due to the formation of vinyl alcohol above this temperature. Calculations of the vinyl alcohol channel are consistent with the observation of this molecule in low-pressure flames [Taatjes, C. A.; Hansen, N.; McIlroy, A.; Miller, J. A.; Senosiain, J. P.; Klippenstein, S. J.; Qi, F.; Sheng, L.; Zhang, Y.; Cool, T. A.; Wang, J.; Westmoreland, P. R.; Law, M. E.; Kasper, T.; Kohse-Höinghaus, K. *Science* **2005**, *308*, 1887] and suggest that this reaction should be included in hydrocarbon oxidation mechanisms.

*Oxidation Pathways in the Reaction of Diacetylene with OH Radicals* (with Juan Senosiain and Stephen Klippenstein)

In this work we determined a portion of the potential energy surface of the reaction of diacetylene with OH radicals; the calculations were performed using RQCISD(T) and two basis-set extrapolation schemes. Based on this surface, we performed calculations of the rate coefficients using RRKM theory and a master equation formulation. After a small (1 kcal/mol) adjustment to the energy barrier of the association reaction, our calculations agree with direct kinetic measurements near room temperature. However, our calculations at high temperatures are smaller than the values of the rate coefficients inferred from indirect experiments by more than an order of magnitude. We found strong non-Arrhenius behavior (and a significant pressure dependence) of the rate coefficients above 800 K

due to the competition between stabilization, abstraction, and addition/elimination channels. The abundance of low-energy isomerization pathways available to the initial adduct results in a complex mechanism with several decomposition products, many of them producing H atoms. At low temperatures and pressures, the reaction proceeds mostly to CO and propargyl. Above 1200 K, direct hydrogen abstraction and production of H atoms become important.

*Pathways and Rate Coefficients for the Decomposition of Vinyloxy and Acetyl Radicals* (with Juan Senosiain and Stephen Klippenstein)

The potential in the vicinity of the stationary points on the surface for the decomposition of ground-state vinyloxy and acetyl radicals was calculated using the RQCISD(T) method extrapolated to the infinite-basis-set limit. Rate coefficients for the decomposition pathways of these two radicals were computed using the master equation and variational transition-state theory. Agreement between our calculated rate coefficients for  $\text{H} + \text{CH}_2\text{CO} \rightarrow \text{CH}_3 + \text{CO}$  and experimental data is very good, without the need for empirical adjustments to the *ab initio* energy barriers. Multireference, configuration-interaction calculations indicate two competitive channels for vinyloxy decomposition, with the channel leading to  $\text{H} + \text{CH}_2\text{CO}$  being preferred at photodissociation energies. However, at typical combustion conditions vinyloxy decomposes primarily to CO and methyl. In contrast, decomposition of acetyl shows only one decomposition channel, leading to CO and methyl. The implications of a low-lying exit channel for the calculation of theoretical rate coefficients were also addressed in this work.

*Quantum Chemistry Methods for Use in Chemical Kinetics* (with Juan Senosiain)

Quantum chemistry calculations are becoming ubiquitous in the field of chemical kinetics. The choice of method for treatment of electron correlation normally depends on the size of the system being studied and the computational resources available. Most quantum chemistry methods have been tested and/or parameterized for their ability to reproduce a set of atomization, ionization, and reaction energies. However, there is little information about the relative performance of these methods in calculating classical energy barriers, partly because these quantities cannot be measured directly. In this work we compared the performance of six popular methods (B3LYP, KMLYP, MPW1K, MP2, QCISD(T), and CCSD(T)) for calculating a series of energy barriers reported by Lynch et al. (*J. Phys. Chem. A* **2000**, *104*, 4811-4815) that are considered to be well known. We find that the best agreement is obtained with the (spin-restricted) QCISD(T) method, closely followed by the related CCSD(T) method. The MPW1K method, which was parameterized for this set of reactions, provides a good compromise between performance and computational cost.

## Future Directions

We shall continue our work on the chemical kinetics of rich flames of aliphatic fuels, particularly that concerned with the formation of the first aromatics containing one or two rings. In the next year or 2 we expect to focus attention on the reaction of allyl with propargyl, on the reactions of various  $\text{C}_4\text{H}_3$  and  $\text{C}_4\text{H}_5$  isomers with acetylene, and on a number of reactions on the  $\text{C}_3\text{H}_5$  potential, particularly allyl dissociation. The work on allyl + propargyl is being pursued in collaboration with Wesley Allen and co-workers at the University of Georgia. We shall continue to develop our chemical kinetic model, particularly in conjunction with the flame experiments at the Advanced Light Source. We shall also continue to maintain our interest in the nitrogen chemistry of combustion, particularly that concerned with  $\text{NO}_x$  control technologies such as reburning, Thermal De- $\text{NO}_x$ , and RAPRENO $_x$ .

## Publications of James A. Miller 2004-present

- J.A. Miller and S.J. Klippenstein, "Master Equation Methods in Gas-Phase Chemical Kinetics", feature article for *J. Phys. Chem. A*, submitted (2006)
- A. Fernandez-Ramos, J.A. Miller, S.J. Klippenstein, and D.G. Truhlar, "Modeling the Kinetics of Bimolecular Reactions," *Chemical Reviews*, submitted (2006)
- J.P. Senosiain, S.J. Klippenstein, and J.A. Miller, "The Reaction of Ethylene with Hydroxyl Radicals: A Theoretical Study", *J. Phys. Chem. A*, in press (2006)
- J.P. Senosiain, S.J. Klippenstein, and J.A. Miller, "Oxidation Pathways in the Reaction of Diacetylene with OH Radicals", *Proc. Combust. Inst.* **31**, in press (2006)
- N. Hansen, J. A. Miller, J. Wang, T. A. Cool, M.E. Law, P. R. Westmoreland, T. Kasper, and K. Kohse-Höinghaus, "Photoionization Mass Spectrometric Studies and Modeling of Fuel-Rich Allene and Propyne Flames," *Proc. Combust. Inst.* **31**, in press (2006)
- N. Hansen, S. J. Klippenstein, J. A. Miller, J. Wang, T. A. Cool, M.E. Law, P. R. Westmoreland, T. Kasper, and K. Kohse-Höinghaus, "Identification of C<sub>5</sub>H<sub>x</sub> (x=3-6,8) Isomers in Fuel-Rich Flames by Photoionization Mass Spectrometry and Electronic Structure Calculations", *J. Phys. Chem. A* **110**, 4376-4388 (2006)
- J.P. Senosiain, S.J. Klippenstein, and J.A. Miller, "Pathways and Rate Coefficients for the Decomposition of Vinyloxy and Acetyl Radicals", *J. Phys. Chem. A*, in press (2006)
- C.A. Taatjes, N. Hansen, J.A. Miller, T.A. Cool, J. Wang, P.R. Westmoreland, M.E. Law, T. Kasper, and K. Kohse-Höinghaus, "Combustion Chemistry of Enols: Possible Ethenol Precursors in Flames", *J. Phys. Chem. A* **110**, 3254-3260 (2006)
- N. Hansen, S. J. Klippenstein, C. A. Taatjes, J. A. Miller, J. Wang, T. A. Cool, F. Qi, M.E. Law, and P. R. Westmoreland, "The Identification and Chemistry of C<sub>4</sub>H<sub>3</sub> and C<sub>4</sub>H<sub>5</sub> Isomers in Fuel-Rich Flames", *J. Phys. Chem. A* **110**, 3670-3678 (2006)
- J.A. Miller, M.J. Pilling, and J. Troe, "Unravelling Combustion Mechanisms Through a Quantitative Understanding of Elementary Reactions", *Proc. Combust. Inst.* **30**, 43-88 (2005)
- S.J. Klippenstein and J.A. Miller, "The Addition of Hydrogen Atoms to Diacetylene and the Heats of Formation of i-C<sub>4</sub>H<sub>3</sub> and n-C<sub>4</sub>H<sub>3</sub>", *J. Phys. Chem. A* **109**, 4285-4295 (2005)
- J.P. Senosiain, S.J. Klippenstein, and J.A. Miller, "The Reaction of Acetylene with Hydroxyl Radicals", *J. Phys. Chem. A* **109**, 6045-6055 (2005)
- C.A. Taatjes, N. Hansen, A. McIlroy, J.A. Miller, J.P. Senosiain, S.J. Klippenstein, F. Qi, L. Sheng, Y. Zhang, T.A. Cool, J. Wang, P.R. Westmoreland, M.E. Law, T. Kasper, and K. Kohse-Höinghaus, "Enols are Common Combustion Intermediates in Hydrocarbon Oxidation", *Science* **308**, 1887-1889 (2005)
- C. A. Taatjes, S. J. Klippenstein, N. Hansen, J. A. Miller, T. A. Cool, J. Wang, M.E. Law, and P. R. Westmoreland, "Synchrotron Photoionization Measurements of Combustion

Intermediates: Photoionization Efficiency and Identification of C<sub>3</sub>H<sub>2</sub> Isomers”, *Phys. Chem. Chem. Phys.* **7**, 806-813 (2005)

- J.P. Senosiain, S.J. Klippenstein, and J.A. Miller, "A Complete Statistical Analysis of the Reaction Between OH and CO," *Proc. Combust. Inst.* **30**, 945-953 (2005)
- J.A. Miller and S.J. Klippenstein, "Some Observations Concerning Detailed Balance in Association /Dissociation Reactions", *J. Phys. Chem. A* **108**, 8296-8306 (2004)
- J.A. Miller and S.J. Klippenstein, "The H+C<sub>2</sub>H<sub>2</sub>(+M)↔C<sub>2</sub>H<sub>3</sub>(+M) and H+C<sub>2</sub>H<sub>4</sub>(+M)↔C<sub>2</sub>H<sub>5</sub>(+M) Reactions: Electronic Structure, Variational Transition-State Theory, and Solutions to a Two-Dimensional Master Equation", *Physical Chemistry Chemical Physics* **6**, 1192-1202 (2004).

# Detection and Characterization of Free Radicals Relevant to Combustion Processes

Terry A. Miller

Laser Spectroscopy Facility, Department of Chemistry  
The Ohio State University, Columbus OH 43210, email: tamiller+@osu.edu

## 1 Program Scope

The chemistry of combustion is well-known to be extremely complex. Modern computer codes are now available that employ hundreds of reaction steps and a comparable number of chemical intermediates. Nonetheless the predictions of such models can be no better than the fundamental dynamical and mechanistic data that are their inputs. Spectroscopic identifications and diagnostics for the chemical intermediates in the reaction mechanisms constitute an important experimental verification of the models. Such spectroscopic investigations also provide experimental “gold standards” against which quantum chemistry computations of molecular properties may be judged.

Our spectroscopic work has centered upon two families of reactive radical intermediates that are of key importance in combustion processes. These families are the organic peroxy radicals,  $\text{RO}_2$ , and the corresponding alkoxy radicals,  $\text{RO}$ .

## 2 Recent Progress

Our recent research has involved the spectroscopy of both the peroxy and alkoxy species. Indeed our work on large primary alkoxy radicals such as 1-hexoxy and 1-heptoxy is described in reference 3. Our initial work on the cycloalkoxies, e.g., cyclohexoxy, is described in reference 2. However given the limitation on the length of this report, we will concentrate here on our recent progress on the peroxy radicals. This is particularly appropriate since we are now reaching a global understanding of the spectroscopy of the simple alkyl peroxy radicals and the relation between their isomeric and conformeric molecular structure and their spectra.

Few free radical intermediates are more important to combustion processes than the organic peroxy radicals,  $\text{RO}_2$ . For many years most spectroscopic diagnostics for the peroxy radicals utilized their UV absorption spectrum to the excited  $\tilde{B}$  state. This approach benefitted from the strong UV absorption cross-section. However it was limited by the fact that the  $\tilde{B}$  state is repulsive; hence most  $\text{RO}_2$  radicals have a roughly 40 nm wide absorption centered around 240 nm, largely independent of the R group.

It has long been known that the peroxy radicals have an  $\tilde{A}$  state with a near infrared (NIR) absorption that might be expected to yield sharp, structured spectra that would be distinguishable for different R groups. However the  $\tilde{A} - \tilde{X}$  transition is based on the highly forbidden  $a^1\Delta_g - X^3\Sigma_g^-$  transition of the  $\text{O}_2$  chromophore. Thus the NIR cross-section is  $10^4 - 10^5$  times smaller than for the UV transition. For the most part the  $\tilde{A} - \tilde{X}$  transition

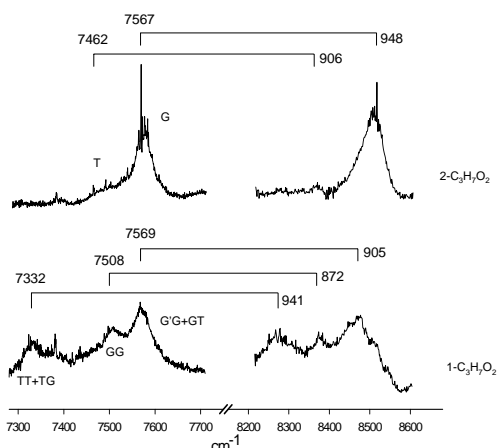


Figure 1: Cavity ringdown absorption spectra of 1-propyl and 2-propyl peroxy radicals. The absolute frequencies ( $\text{cm}^{-1}$ ) are given for the assigned origin bands and the separation ( $\omega_0$ ) of the O–O stretching bands. Assignments of bands to given conformers are noted.

was simply too weak to detect, given the relatively low concentrations of peroxy radical intermediates present during chemical reactions of interest. Cavity ringdown spectroscopy (CRDS), however, is particularly appropriate for weak transitions such as the  $\tilde{A} - \tilde{X}$  one of peroxy radicals because the large number, typically  $10^4 - 10^5$ , of photon passes through the cavity effectively compensates for the low probability of absorption per pass.

The simplest of the organic peroxy radicals are with R equals an alkyl group and of course methyl is the simplest alkyl group. Our first successful CRDS experiment on peroxy radicals involved the detection of the  $\tilde{A} - \tilde{X}$  NIR spectrum of  $\text{CH}_3\text{O}_2$ . While methyl peroxy is the prototype of the alkyl peroxy radicals, it is also unique. There is only one peroxy radical isomer of  $\text{CH}_3\text{O}_2$ . While one could imagine staggered (*s*) and eclipsed (*e*) (due to H-bonding to the O atom) conformers for  $\text{CH}_3\text{O}_2$ , our quantum chemistry calculations indicate that the *e* conformer corresponds to a saddle point in the potential and only the *s* form exists as a stable minimum. This is consistent with the observation of the spectrum of only one species.

When R increases in size beyond  $\text{CH}_3$ , then structure diversity is possible. There is a good deal of evidence that the chemistry of different  $\text{RO}_2$  isomers is often very different. While there is little evidence one way or the other concerning whether different conformers have different chemistry, we would certainly expect them to have different spectra. Understanding the spectral differences in different isomers and conformers is critical to developing useful spectral diagnostics for these radicals to aid in unraveling their chemistry and for comparison to computations.

The ethyl peroxy radical,  $\text{C}_2\text{H}_5\text{O}_2$ , also has only one isomer. However, our quantum chemistry calculations indicate two minima in the potential, called *trans* (T) and *gauche* (G) conformations corresponding respectively to O-O-C and O-C-C dihedral angles of  $0^\circ$  and  $\pm 120^\circ$  (spectrally unresolvable  $G \pm$  enantiomers). The T conformation has  $C_s$  symmetry. However our NIR  $\tilde{A} - \tilde{X}$  spectral observations so far have identified only one species. Efforts are continuing to observe the other conformer.

In propyl peroxy,  $\text{C}_3\text{H}_7\text{O}_2$ , full structural diversity becomes possible. There are two peroxy isomers, 1- $\text{C}_3\text{H}_7\text{O}_2$  and 2- $\text{C}_3\text{H}_7\text{O}_2$ . Following similar arguments as with ethyl peroxy, stable conformations for 1- $\text{C}_3\text{H}_7\text{O}_2$  are expected for the dihedral angle between the O-O- $\text{C}_1$  and O- $\text{C}_1$ - $\text{C}_2$  planes at  $0^\circ$  (T) and  $\pm 120^\circ$  (G and G' enantiomers). Considering 1- $\text{C}_3\text{H}_7\text{O}_2$  to be formed by the substitution of a  $\text{C}_2\text{H}_5\text{O}_2$  terminal H by a methyl group at any of the 3 possible positions (O- $\text{C}_1$ - $\text{C}_2$  and  $\text{C}_1$ - $\text{C}_2$ - $\text{C}_3$  dihedral angles of  $0^\circ$ ,  $\pm 120^\circ$ ), each substitution leads to a stable minimum for both the T and G conformations of ethyl peroxy. This results in a total of 5 unique conformations,  $\text{T}_1\text{T}_2$ ,  $\text{T}_1\text{G}_2$ ,  $\text{G}_1\text{T}_2$ ,  $\text{G}_1\text{G}_2$ ,  $\text{G}_1\text{G}'_2$ , where the subscripts 1 and 2 refer, respectively, to the two dihedral angles indicated above. By similar arguments, it is deduced that there should be two stable conformers (T and G) of 2- $\text{C}_3\text{H}_7\text{O}_2$ . Fig. 1 shows the spec-

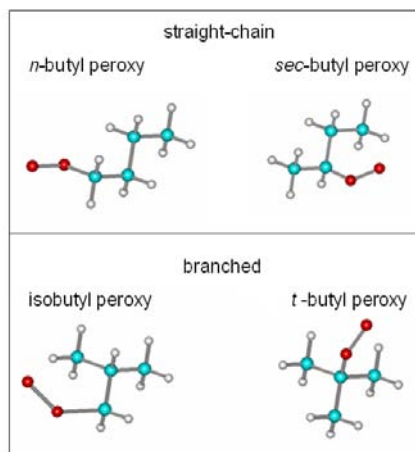


Figure 2: The four isomers of butyl peroxy radical,  $\text{C}_4\text{H}_9\text{O}_2$ .

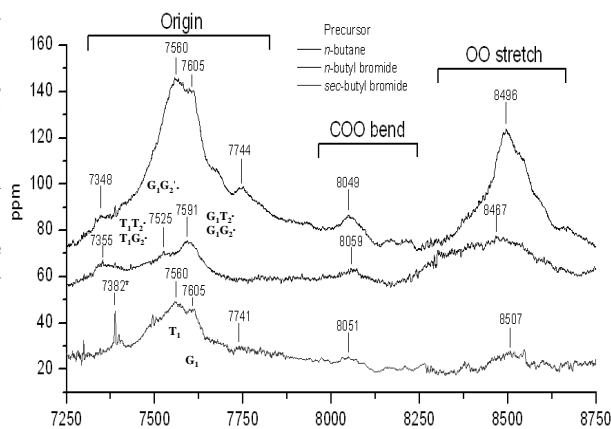


Figure 3: CRDS spectra of *n*-butyl and *sec*-butyl peroxy radicals. The top trace is the CRDS spectrum of *n*-butyl and *sec*-butyl peroxy radicals produced by the hydrogen abstraction of *n*-butane by Cl, followed by  $\text{O}_2$  reaction and is offset by 30 ppm. The middle trace is the CRDS spectra of *n*-butyl peroxy radical produced by the direct photolysis of *n*-butyl bromide, offset by 30 ppm. The bottom trace is the CRDS spectra of *sec*-butyl peroxy radical produced by the direct photolysis of *sec*-butyl bromide, with no offset. The peak labelled with an asterisk belongs to methyl peroxy radical. Approximate frequencies in  $\text{cm}^{-1}$  are indicated for the major peaks. Assignments of bands to given conformers are indicated.

Fig. 1 shows the spec-

tra of 1- and 2-propyl peroxy radicals with the bands labelled by conformer. Conformer identifications were facilitated by comparison to spectral shifts and vibrational frequencies from quantum chemistry calculations.

A similar but more complicated pattern is present for butyl peroxy. Fig. 2 shows there are 4 isomers possible. The *n*-butyl and *sec*-butyl radicals can be formed by Cl atom attack on *n*-butane followed by reaction with O<sub>2</sub>, while isobutyl and *t*-butyl radicals are generated similarly except isobutane is substituted as the precursor.

Fig. 3 shows the resulting spectra for *n*-butyl and *sec*-butyl peroxy. Similar spectra are available for isobutyl and *t*-butyl peroxy but not shown for brevity. While the spectra of Fig. 3 appear quite complicated, the extension of the previous analyses of the propyl peroxy spectra yields some relatively simple results from the butyl spectra. For *n*-butyl peroxy 3 distinct conformer bands are observed and by comparison of the spectral shifts to those of propyl peroxy, can be assigned to T<sub>1</sub>T<sub>2</sub>.+T<sub>1</sub>G<sub>2</sub>., G<sub>1</sub>G<sub>2</sub>., and G<sub>1</sub>T<sub>2</sub>.+G<sub>1</sub>G<sub>2</sub>. conformers as is shown in Fig. 3. The dot denotes T<sub>3</sub>, G<sub>3</sub> or G<sub>3</sub>' which indicates the orientation of the third dihedral angle at the "end" of the hydrocarbon tail away from the O<sub>2</sub> chromophore. Not unexpectedly, at the present resolution, transitions from these conformers are not resolved.

Present work is focussed upon extending our understanding of the isomers and conformers of the alkyl peroxy radicals with the examination of the pentyl peroxy radicals. Fig. 4 compares the spectrum of the isobutyl peroxy with the neopentyl peroxy radical, the latter being of particular interest, since neopentane has been used as a model compound for studying oxidation chemistry because of its unique structural characteristics. While neopentyl peroxy is the largest alkyl peroxy studied thus far, the spectrum shown in Fig. 4 is relatively simple. Firstly only one isomeric peroxy radical results from Cl atom attack on neopentane. Secondly Fig. 4 shows the spectrum of only one conformer clearly. Two conformers might be expected but like ethyl peroxy, from which neopentyl peroxy can be derived by substitution of the β H atoms by methyl groups, only one spectrum has been so far identified.

Transitions in trace (A) of Fig. 4 are marked with *i* for isobutyl peroxy and *t* for butyl peroxy, both of which can be formed in the abstraction reaction. (The asterisk marks the methyl peroxy origin.) Three distinct conformer origin transitions for isobutyl peroxy are identified, while only one is identified for *t*-butyl peroxy. The region  $\geq 8000$  cm<sup>-1</sup> shows bands attributable to the O-O stretch and possibly other vibrations. In trace (B) a relatively strong origin and an O-O stretch band of a single conformer are indicated by *n* for neopentyl peroxy. The transitions just below 7800 cm<sup>-1</sup> may be a C-O-O bending vibration of neopentyl peroxy and/or the origin of *t*-butyl peroxy, which is known to be formed by neopentyl peroxy radical reactions.

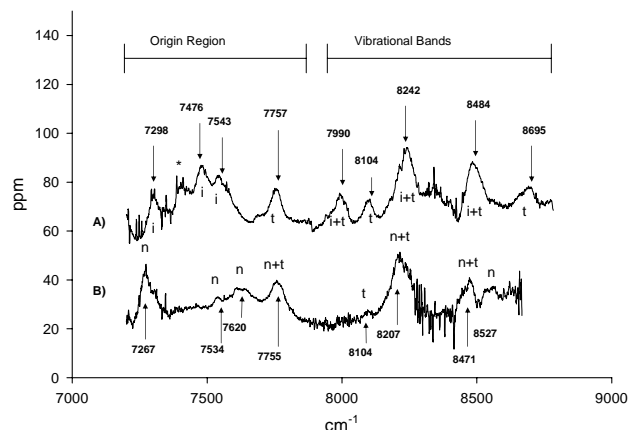


Figure 4: Peroxy radical spectra. Trace (A) shows the spectrum obtained using H atom extraction of isobutane followed by combination with O<sub>2</sub> while in trace (B) the precursor is neopentane. Approximate frequencies of major peaks are indicated.

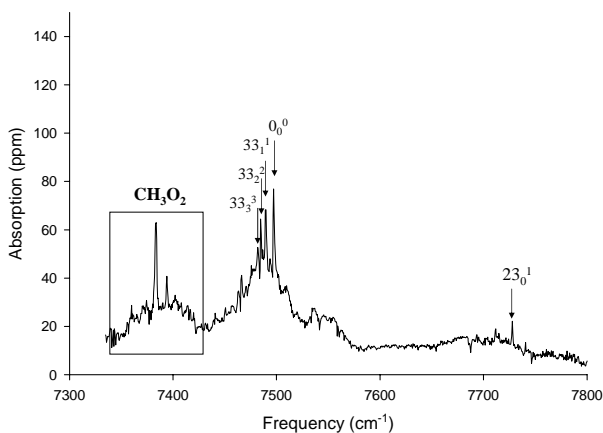


Figure 5: The spectrum of the  $\tilde{A} - \tilde{X}$  electronic transition of phenyl peroxy radical, produced by photolyzing acetophenone with subsequent oxidation. The boxed region labelled CH<sub>3</sub>O<sub>2</sub> matches the previously reported experimental spectrum of the  $\tilde{A} - \tilde{X}$  electronic transition of the methyl peroxy radical. The indicated band assignments for phenyl peroxy are discussed in the text.

Efforts will continue to record the spectra of other pentyl peroxy isomers and conformers. We would expect that the propyl and butyl peroxy analyses can be extended to understand all the pentyl peroxy spectra, and that the totality of the data taken will produce generic patterns that are pervasive and explain all the larger alkyl peroxy spectra.

Before closing we should point out that we have now extended our CRDS observations to unsaturated peroxies, namely phenyl peroxy. Again this radical is of importance in hydrocarbon combustion, as its production is believed to impede the formation of soot. A scan in the origin region of phenyl peroxy is shown in Fig. 5. Transitions identified include the  $0_0^0$  band and a hot band sequence in the low-lying  $\nu_{33}$  mode (hindered rotation of O-O). Further details of the phenyl peroxy analysis can be found in Ref. 6.

### 3 Future Plans

Our immediate efforts will be focussed upon three areas for which we have already made initial progress. (1) We wish to “wrap up” the alkyl peroxy work with the analysis of the pentyl peroxy radicals. At this point we believe that we will have sufficient data to establish trends in spectral characteristics, e.g., origin and vibrational frequencies, and correlate them with structural changes, e.g., site of  $O_2$  addition, primary, secondary, or tertiary, size of alkyl group, its degree of branching, and its conformation near the  $O_2$ . (2) We plan to pursue the spectra of unsaturated peroxy radicals beyond phenyl peroxy to other aromatic species like benzoyl peroxy and non-aromatic species like vinyl and propargyl peroxy. (3) We have already performed some kinetic measurements using the CRDS spectra to monitor butyl peroxy radical recombination reactions as a function of isomer and conformer. Similar measurements are on-going on the neopentyl peroxy radical reaction to form *t*-butyl peroxy. Such measurements can be extended to other organic peroxy radical reactions.

### List of Publications Supported by DOE

- [1] “Near-IR Cavity Ringdown Spectroscopy and Kinetics of the Isomers and Conformers of the Butyl Peroxy Radical,” B. G. Glover and T. A. Miller, *J. Phys. Chem. A* **109**, 11191 (2005).
- [2] “Jet-Cooled LIF Spectra of Cyclohexoxy Radical,” L. Zu, J. Liu, G. Tarczay, P. Dupre, and T. A. Miller, *J. Chem. Phys.* **120**, 10579 (2004).
- [3] “The Rotationally Resolved Electronic Spectra of Several Conformers of 1-Hexoxy and 1-Heptoxy,” L. Zu, J. Liu, S. Gopalakrishnan, and T. A. Miller, *Can. J. Chem. (Herzberg Memorial Issue)* **82**, 854 (2004).
- [4] “Dispersed Fluorescence Spectroscopy of Primary and Secondary Alkoxy Radicals,” J. Jin, I. Sioutis, G. Tarczay, S. Gopalakrishnan, A. Bezant, and T. A. Miller, *J. Chem. Phys.* **121**, 11780 (2004).
- [5] “Conformational Analysis of the 1- and 2-Propyl Peroxy Radicals,” G. Tarczay, S. Zalyubovsky, and T. A. Miller, *Chem. Phys. Lett.* **406**, 81 (2005).
- [6] “Cavity Ringdown Spectroscopy of the  $\tilde{A} - \tilde{X}$  Electronic Transition of the Phenyl Peroxy Radical,” G. M. P. Just, E. N. Sharp, S. J. Zalyubovsky, and T. A. Miller, *Chem. Phys. Lett.* **417**, 378 (2005).
- [7] “Spectroscopic Probing and Diagnostics of the Geometric Structure of the Alkoxy and Alkyl Peroxy Radical Intermediates,” T. A. Miller, *Mol. Phys.* (invited review, accepted).

## Reaction Dynamics in Polyatomic Molecular Systems

William H. Miller

Department of Chemistry, University of California, and  
Chemical Sciences Division, Lawrence Berkeley National Laboratory  
Berkeley, California 94720-1460  
millerwh@berkeley.edu

### Program Scope or Definition

The goal of this program is the development of theoretical methods and models for describing the dynamics of chemical reactions, with specific interest for application to polyatomic molecular systems of special interest and relevance. There is interest in developing the most rigorous possible theoretical approaches and also in more approximate treatments that are more readily applicable to complex systems.

### Recent Progress

There are only a few computational methodologies that are available for treating molecular systems with *many degrees of freedom*, primarily methods based on integrating the classical equations of motion (i.e., classical trajectory calculations = molecular dynamics simulations), and those based on evaluating Feynman path integrals (by Monte Carlo or other statistical sampling methods) for the Boltzmann operator,  $\exp(-\beta\hat{H})$ . This research program has been focusing in recent years on developing theoretical approaches to chemical dynamics that leverage these two computational methodologies.

Over the last two years most effort has focused on exploiting the latter two of these methodologies, namely the ability to evaluate the Boltzmann operator,  $\exp(-\beta\hat{H})$ , fully quantum mechanically, for large molecular systems. This has taken place within the *quantum instanton* (QI) model for thermal rate constants for chemical reactions,  $k(T)$ . The name is due to the relation to a much older semiclassical (SC) approximation<sup>1</sup> for thermal rates that came to be known as the instanton model. The SC instanton model has many qualitatively correct features and insights, but the SC approximation to the Boltzmann operator that is inherent to it was not sufficiently quantitative in early test calculations.<sup>2</sup> The present QI model incorporates the physical ideas of the SC instanton model but is expressed wholly in terms of the *quantum* Boltzmann operator, thus alleviating most of the quantitative deficiencies of the SC version. Its evaluation thus involves (Monte Carlo) evaluation of the path integral expression for the Boltzmann operator, but no real time dynamics. The basic result for the thermal reaction rate is

$$k(T) = Q_r^{-1} \frac{\hbar\sqrt{\pi}/2}{\Delta H(T)} C_{ff}(0), \quad (1a)$$

where  $C_{ff}(0)$  is the zero time flux-flux autocorrelation function

$$C_{ff}(0) = \text{tr} \left[ e^{-\beta\hat{H}/2} \hat{F} e^{-\beta\hat{H}/2} \hat{F} \right], \quad (1b)$$

and  $\Delta H(T)$  is a particular kind of energy variance (also expressed wholly in terms of the Boltzmann operator). The important practical aspect of Eq. (1) is that its evaluation only requires that of the Boltzmann operator and quantities related to it, and as emphasized above, this can be performed fully quantum mechanically for quite large molecular systems. Most of the papers in the 2004-2006 list below have to do with technical developments related to evaluating the QI rate expression and to its applications to various test reactions.

Paper 3 on the list below, for example, describes the application of the QI approximation to the  $H + CH_4 \rightarrow H_2 + CH_3$  reaction; excellent results are obtained over a wide temperature range (up to 2000 K and down to 200 K). Of special significance is that the calculations were carried out in the 3d Cartesian coordinates of all the atoms ( $2 \times 6 = 18$  degrees of freedom), not even taking out the overall center-of-mass translation of the 6 atom system. This means that no approximation based on small fluctuations about a minimum energy path (MEP) are incorporated, and that no sum over individual total angular momentum J states is involved. This implementation of the QI model is thus applicable to quite general molecular systems (provided, of course, that one has a sufficiently accurate Born-Oppenheimer potential energy surface).

Paper 6 describes the application to a model of proton transfer in a polar solvent,  $AH + B \rightarrow A^- + H^+B$  solvated by 255 methyl chloride molecules (the Azzouz-Borgis model<sup>3</sup>), this calculation also being carried out using the 3d Cartesian coordinates of all the atoms. Of particular interest here, too, is the isotope effect in the rate constant upon replacement of the H atom by D. This model problem is important since it is characteristic of H atom transfer reactions in condensed phases, and also because many different theoretical approaches has been applied to it. Unfortunately, the results of the various approaches differ from each other in various respects, so even though we believe the QI calculations to be the most accurate to date, there is no way at present to be certain of this, for this non-trivial example lies beyond the possibility of a brute-force 'exact' calculation.

Paper 11 shows how the QI rate theory can be put into a particularly convenient form for calculating *kinetic isotope effects* (such as the  $H \rightarrow D$  isotope effect noted above in paper 6). This makes use of free-energy perturbation methods in Monte Carlo simulation technology, and it yields an approach for calculating the *ratio* of two rate constants for different isotopic species that is much more efficient than the calculation of the rate constant for either species alone. This should be a particularly useful feature of the QI model.

Papers 8 and 14 deal with the important problem in any transition state-type theory of reaction rates (of which the QI model is one), namely how to choose the best *dividing surface* (DS) for defining the flux operators that appear in the rate expression. Paper 14 shows how the one parameter family of DS's that are normal to the MEP at various distances along it can be used in the QI model. This is a simple but general approach that should be applicable to a wide range of polyatomic systems. It should be emphasized that in this approach the MEP is used solely for the purpose of defining a family of DS's; the dynamical coordinates in which the path integrals are evaluated are still the Cartesian coordinates of all the atoms. Thus the "reaction coordinate", the distance along the MEP, is simply a *parameter* that specifies the particular DS, and is not one of the dynamical coordinates of the system.

## Future Plans

Future efforts will be focused on further development of this QI model for thermal rate constants, as well as further developing semiclassical methods that exploit the fact that one can carry out classical molecular dynamics simulations for a wide variety of molecular processes. These SC approaches are more general than the QI model, which only applies to thermal rate constants — an important problem but not ‘everything’; semiclassical methods can in principle describe quantum effects in *any* dynamical quantity.

## References

1. W. H. Miller, J. Chem. Phys. **62**, 1899 (1975).
2. S. Chapman, B. C. Garrett, and W. H. Miller, J. Chem. Phys. **63**, 2710 (1975).
3. H. Azzouz and D. Borgis, J. Chem. Phys. **98**, 7361 (1993); J. Mol. Liq. **61**, 17 (1994); **63**, 89 (1995).

## 2004 - 2006 (to date) DOE Publications

1. C. Venkataraman and W. H. Miller, “The Quantum Instanton (QI) Model for Chemical Reaction Rates: the ‘Simplest’ QI with One Dividing Surface,” J. Phys. Chem. A **108**, 3035-3039 (2004). LBNL-53815.
2. T. Yamamoto and W. H. Miller, “On the Efficient Path Integral Evaluation of Thermal Rate Constants within the Quantum Instanton Approximation,” J. Chem. Phys. **120**, 3086-3099 (2004). LBNL-53821.
3. Y. Zhao, T. Yamamoto and W. H. Miller, “Path Integral Calculation of Thermal Rate Constants within the Quantum Instanton Approximation: Application to the H+CH<sub>4</sub> & H<sub>2</sub>+CH<sub>3</sub> Hydrogen Abstraction Reaction in Full Cartesian Space,” J. Chem. Phys. **120**, 3100-3107 (2004). LBNL-53881.
4. M. Ceotto and W. H. Miller, “Test of the Quantum Instanton Approximation for Thermal Rate Constants for Some Collinear Reactions,” J. Chem. Phys. **120**, 6356-6362 (2004). LBNL-54170.
5. Y. Li and W. H. Miller, “Different Time Slices for Different Degrees of Freedom in Feynman Path Integration,” Molec. Phys. **103**, 203-208 (2005). LBL-56194.
6. T. Yamamoto and W. H. Miller, “Path Integral Evaluation of the Quantum Instanton Rate Constant for Proton Transfer in a Polar Solvent,” J. Chem. Phys. **122**, 044106.1-13 (2005). LBNL-56319.
7. M. Ceotto, S. Yang and W. H. Miller, “Quantum Reaction Rate from Higher Derivatives of the Thermal Flux-Flux Autocorrelation Function at Time Zero,” J. Chem. Phys. **122**, 044109.1-7 (2005). LBNL-56546.

8. C. Predescu and W. H. Miller, "Optimal Choice of Dividing Surface for the Computation of Quantum Reaction Rates," *J. Phys. Chem. B* **109**, 6491-6499 (2005). LBNL-56195.
9. W. H. Miller, "Quantum Dynamics of Complex Molecular Systems", Proceedings of the National Academy of Sciences **102**, 6660-6664 (2005). LBNL-56664.
10. M. S. Small, C. Predescu and W. H. Miller, "Quantifying the Extent of Recrossing Flux for Quantum Systems," *Chem. Phys.* **322**, 151-159 (2006). LBNL-57467.
11. J. Vanicek, W. H. Miller, J. F. Castillo and F. J. Aoiz, Quantum Instanton Evaluation of the Kinetic Isotope Effects, *J. Chem. Phys.* **123**, 054108.1-14 (2005). LBNL-57468.
12. J. Vanicek and W. H. Miller, "Path Integral Evaluation of the Kinetic Isotope Effects Based on the Quantum Instanton Approximation," in Proceedings of the 8<sup>th</sup> International Conference on "Path Integrals, from Quantum Information to Cosmology," (JINR Publishing, Dubna, Moscow, Russia) pp. XX-XX (2005). LBNL-58733.
13. S. Yang, T. Yamamoto, and W. H. Miller, "Path-Integral Virial Estimator for Reaction Rate Calculation Based on the Quantum Instanton Approximation," *J. Chem. Phys.* **124**, xxx-xxx (2006). LBNL-59146.
14. Y. Li and W. H. Miller, "Using a Family of Dividing Surfaces Normal to the Minimum Energy Path for Quantum Instanton Rate Constants," *J. Chem. Phys.* (submitted). LBNL-59735.

## GAS-PHASE MOLECULAR DYNAMICS: THEORETICAL STUDIES OF COMBUSTION-RELATED CHEMICAL REACTIONS AND MOLECULAR SPECTRA

James T. Muckerman  
Chemistry Department, Brookhaven National Laboratory  
Upton, NY 11973-5000  
muckerma@bnl.gov

### Program Scope

This project explores the energetics, dynamics and kinetics of chemical reactions resulting from molecular collisions in the gas phase. The goal of this work is a fundamental understanding of chemical processes related to combustion. We are interested in the microscopic factors affecting the structure, dynamics and reactivity of short-lived intermediates such as free radicals in gas-phase reactions. There is a very strong coupling between the theoretical and experimental efforts in all of the group's work. From the phenomenon of axis-switching in halocarbenes, dynamical aspects of the rovibronic spectrum of methylene to the spectroscopy of coordinatively unsaturated transition-metal-containing species, the interplay between state-of-the-art theory and experiment has provided deep new insights. The theoretical work in spectroscopy seeks to generate extremely accurate benchmark calculations of the electronic structure of systems at the small end of the size scale of interest for comparison with (and as a guide to) high-resolution experimental studies carried out in this program. There is also a strong focus in the theoretical work on the direct dynamics of the reactions of polyatomic molecules involving species being studied in the experimental part of the program.

### Recent Progress

#### **Energetics and dynamics of the reaction of OH with HOCO.**

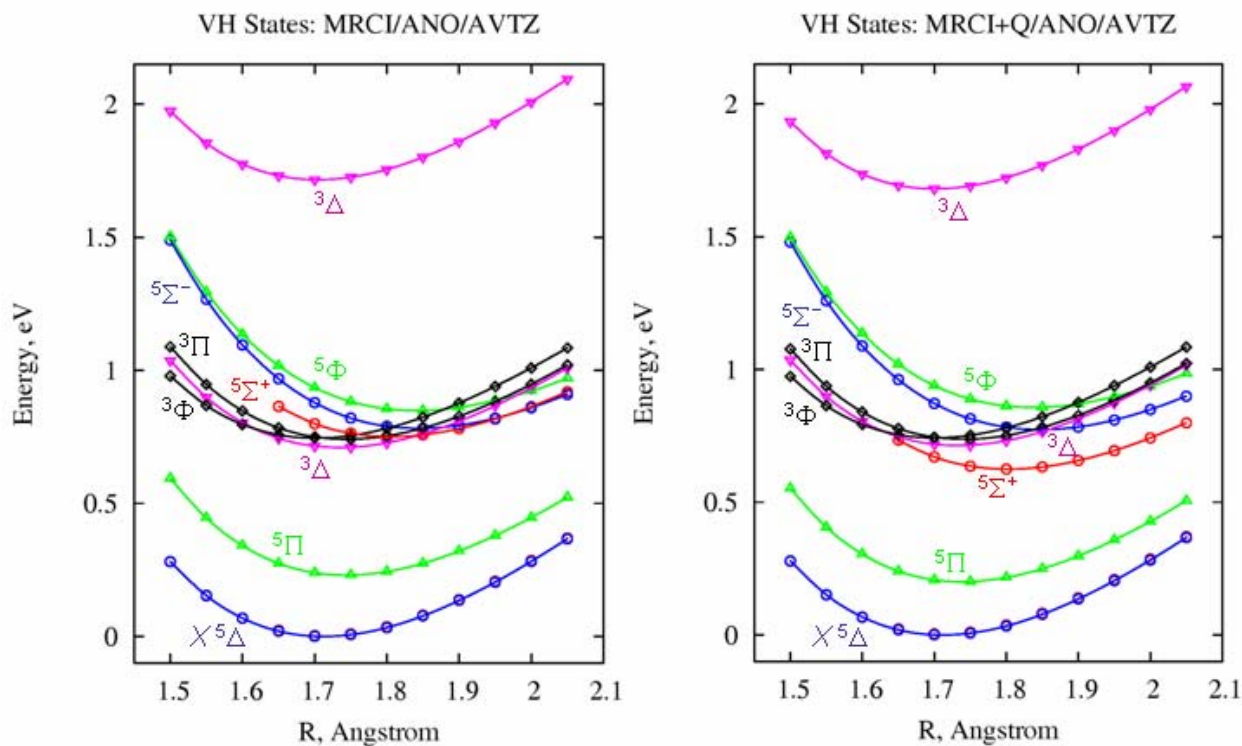
In another application of our *ab initio* direct dynamics approach, in collaboration with J. Francisco (Purdue Univ.), we have mapped out the properties (energies, geometries, vibrational frequencies) of the stationary points on the ground-state singlet potential energy surface for the reaction of OH and HOCO using high-level *ab initio* electronic structure methods with basis set extrapolation to the complete basis set (CBS) limit. This was the first study of any kind of this reaction despite both OH and HOCO being important molecules in both combustion and atmospheric science. In a manner similar to our treatment of the singlet methanol reaction, we have performed a direct dynamics study on the OH + HOCO reaction using a SAC/MP2 method. Results show that the reaction produces H<sub>2</sub>O + CO<sub>2</sub> as final products via an HOC(O)OH intermediate. The lifetime of the HOC(O)OH complex is estimated to be short. In particular, dynamics trajectories reveal that hydrogen bonding plays an important role during the initial stages of the reaction. The OH + HOCO reaction is found to be nearly temperature-independent at lower temperature, and at 300 K, the thermal rate constant is predicted to be  $1.03 \times 10^{-11} \text{ cm}^3 \text{ molecule}^{-1} \text{ s}^{-1}$ . It is a fast radical reaction (with Yu & J. Francisco).

#### **Calculation of ground and excited states of transition metal hydrides.**

We have calculated the energies and dipole moments for the low-lying electronic states of several first transition metal series hydrides at a very high level of theory (MRCI-SD from a very large CASSCF reference function). The results for FeH are compared to the experimental results for this, the best characterized of these small, but very complicated, systems. The state ordering and relative energies compare very well with experiment. More importantly, the wavefunctions also correctly predict observed electric dipole moments, where they have been measured. Previously published calculations have poor agreement with the experimentally measured dipole moments, because they take insufficient account of

the low-lying  $3d^7 4s^1$  excited configuration of the Fe atom which is important in the description of the bonding in the lowest states of the FeH molecule. Similar calculations on VH predict a similarly complicated set of low-lying states. No experimental data exist and we are preparing to search for its electronic spectrum based on the computational results, using a newly constructed apparatus (with Sears & Wang).

**MRCI and MRCI+Q Calculations of the Low-Lying States of VH**  
 based on CAS(6,14) reference functions  
 Basis: V, Bauschlicher-ANO(spdfg); H, aug-cc-pVTZ(sp)



**Renner-Teller and spin-orbit effects on the vibronic energies of DCCI and HCCI.**

Halomethylenes, H<sub>2</sub>CX, are prototypes for unsymmetrical carbenes. It is believed that HCCI plays a role in ozone depletion pathways in the chemistry of the earth's atmosphere. In coordination with the experimental measurements of the HCCI spectra carried out at our GPMD group, we have carried out a parallel theoretical investigation. The potential energy surfaces of three low-lying electronic states of HCCI were calculated with an *ab initio* multi-reference configuration interaction (MRCI) method. The three-dimensional potential energy surfaces were interpolated using a general DVR technique from thousands of MRCI energy points. Finally, we applied a variational method to compute the vibronic energy levels of the DCCI and HCCI molecules using a *K*-dependent quantum dynamics approach in hyperspherical coordinates. In this study, we especially focused on the Renner-Teller effect and the spin-orbit coupling in the system. As a result, we were able to predict the position of the triplet state of HCCI relative to the singlet ground state (with Yu & Sears).

**Energetics and dynamics of the reaction of O<sub>2</sub> with HOCO.**

We have carried out a study of another important combustion reaction, that of O<sub>2</sub> with HOCO using an *ab initio* direct dynamics method based on the UB3PW91 density functional theory (DFT). This DFT

method was selected by minimizing the errors of the relative energies of the stationary points on the ground-state electronic surface of HOC(O)O<sub>2</sub> with respect to the best *ab initio* values of Poggi and Francisco (J. Chem. Phys. 120 (2004) 5073). Our results show that the reaction can occur via two mechanisms: direct hydrogen abstraction and an addition reaction through a short-lived HOC(O)O<sub>2</sub> intermediate. The lifetime of the intermediate is predicted to be 660 ± 30 fs. Although this is an activated reaction, the activation energy is only 0.71 kcal/mol. At room temperature, the obtained thermal rate coefficient is  $2.1 \times 10^{-12} \text{ cm}^3 \text{ molecule}^{-1} \text{ s}^{-1}$ , in good agreement with experimental results (with Yu).

## Future Plans

### Quantum force molecular dynamics study of radical-radical reactions.

We will continue to develop our quantum force molecular dynamics program, and to apply it to some important combustion reactions. Of particular interest are the dynamics and kinetics of the radical-radical reactions. One application to the O + HOCO reaction, in collaboration with J. Francisco (Purdue Univ.), is in progress. This research mainly addresses the energies, geometries, and vibrational frequencies of the stationary points on the ground-state doublet potential energy surface for the O + HOCO reaction as well as the reaction mechanism studied using a SAC method (probably the SAC/UCCD variant). The temperature dependence of the thermal rate constants will be calculated (with Yu & J. Francisco).

### Triplet channel in CH<sub>2</sub> + HCCH.

One aspect of the reaction of methylene with acetylene that was neglected in the previous quantum force trajectory studies is the possible role of the triplet state of the adduct. Reaction dynamics were computed under the influence of the ground singlet surface, yet the triplet state of the biradical obtained by transient ring-opening of the cyclopropene intermediate is known to be lower in energy than the singlet biradical, as is the asymptotic <sup>3</sup>CH<sub>2</sub> + HCCH channel lower in energy than the <sup>1</sup>CH<sub>2</sub>+HCCH asymptote. It is unclear where the surface crossings occur or what influence they may have on this reaction. Further investigation of this reaction is warranted by both experimental and computational means. Experimentally, the marginal effect of added HCCH on the double-exponential decays of singlet methylene in rare gas can probe the <sup>3</sup>CH<sub>2</sub> channel. Theoretically, the stationary points of the lowest triplet potential energy surface will be computed at a high level of theory and their relative energies fit with a cheaper method with analytic gradients by scaling the computed correlation energy by a global constant. New direct dynamics trajectories will then be computed on the singlet surface and the energies of both the singlet and triplet surface will be monitored along each trajectory to determine where crossings occur. Finally, we will compute surface-hopping trajectories to estimate the importance of non-adiabatic effects due to spin-orbit coupling in the dynamics of the reaction (with Hall & Yu).

## Acknowledgment

This work was performed at Brookhaven National Laboratory under Contract DE-AC02-98CH10886 with the U.S. Department of Energy and supported by its Division of Chemical Sciences, Office of Basic Energy Sciences.

## Publications since 2004

*MRCI calculations of the lowest potential energy surface for CH<sub>3</sub>OH and direct ab initio dynamics calculations of the O(<sup>1</sup>D) + CH<sub>4</sub> and OH + CH<sub>3</sub> reactions*, H.-G. Yu and J.T. Muckerman, J. Phys. Chem. A **108**, 8615 (2004).

*Exploring the multiple reaction pathways for the H + cyc-C<sub>3</sub>H<sub>6</sub> reaction*, H.-G. Yu and J.T. Muckerman, J. Phys. Chem. A **108**, 10844 (2004).

- Ab initio and direct dynamics studies of the reaction of singlet methylene with acetylene, and the lifetime of the cyclopropene complex*, H.-G. Yu and J.T. Muckerman, *J. Phys. Chem. A* **109**, 1890 (2005).
- Ab initio and direct dynamics studies of the reaction of singlet methylene with acetylene, and the lifetime of the cyclopropene complex*, H.-G. Yu and J.T. Muckerman, *J. Phys. Chem. A* **109**, 1890-1896 (2005).
- Product Study of the Reaction of CH<sub>3</sub> with OH Radicals at Low Pressures and Temperatures*, C. Fockenberg, R.A. Weston, Jr. and J.T. Muckerman, *J. Phys. Chem. B* **109**, 8415-8427 (2005).
- Direct Ab Initio Dynamics Study of the OH + HOCO Reaction*, H.-G. Yu, J.T. Muckerman and J.S. Francisco, *J. Phys. Chem. A* **109**, 5230-5236 (2005).
- Potential energy surfaces and vibrational energy levels of DCCL and HCCL in three low-lying states*, H.-G. Yu, T.J. Sears and J.T. Muckerman, *Mol. Phys.* **104**, 47 (2006).
- Quantum molecular dynamics study of the reaction of O<sub>2</sub> with HOCO*, H.-G. Yu and J.T. Muckerman, *J. Phys. Chem. A* (in press, 2006).
- Multi-reference configuration interaction calculations of the low-lying states of iron and vanadium monohydride, FeH and VH*, Z. Wang, T. J. Sears and J. T. Muckerman, *J. Chem. Phys.* (submitted).
- Related publications in Nanocatalysis and the Hydrogen Fuel Initiative**
- Why is Re-Re bond formation/cleavage in [Re(bpy)(CO)<sub>3</sub>]<sub>2</sub> different from that in [Re(CO)<sub>5</sub>]<sub>2</sub>? Experimental and theoretical studies on the dimmers and fragments*, E. Fujita and J.T. Muckerman, *Inorg. Chem.* **43**, 7636 (2004).
- Desulfurization of SO<sub>2</sub> and thiophene on surfaces and nanoparticles of molybdenum carbide: unexpected ligand and steric effects*, P. Liu, J.A. Rodriguez and J.T. Muckerman, *J. Phys. Chem. B* **108**, 15662-15670 (2004).
- The Ti<sub>8</sub>C<sub>12</sub> metcar: A new model catalyst for hydrodesulfurization*, P. Liu, J.A. Rodriguez and J.T. Muckerman, *J. Phys. Chem. B* **108**, 18796-18798 (2004).
- The Chemical Activity of Metal Compound Nanoparticles: Importance of Electronic and Steric Effects in M<sub>8</sub>C<sub>12</sub> (M=Ti, V, Mo) Metcars*, P. Liu, J.A. Rodriguez and J.T. Muckerman, *J. Chem. Phys.* **121**, 10321-10324 (2004).
- Sulfur Adsorption and Sulfidation of Transition Metal Carbides as Hydrotreating Catalysts*, P. Liu, J.A. Rodriguez and J.T. Muckerman, *J. Mol. Catal. A: Chem.* **239**, 116-124 (2005).
- First-principles study of Ti-catalyzed hydrogen chemisorption on an Al surface: A critical first step for reversible hydrogen storage in NaAlH<sub>4</sub>*, S. Chaudhuri and J.T. Muckerman, *J. Phys. Chem. B* **109**, 6952 (2005).
- A Density Functional Theory Study of the Catalytic Role of Ti Atoms in Reversible Hydrogen Storage in the Complex Metal Hydride NaAlH<sub>4</sub>*, S. Chaudhuri and J.T. Muckerman, in "Materials and Technology for Hydrogen Storage and Generation," edited by G-A. Nazri, C. Ping, R.C. Young, M. Nazri, and J. Wang (Mater. Res. Soc. Symp. Proc. 884E, Warrendale, PA, 2005) GG2.1.
- Hydrogen Oxidation and Production Using Nickel-Based Molecular Catalysts with Positioned Proton Relays*, A.D. Wilson, R.H. Newell, M.J. McNevin, J.T. Muckerman, M. Rakowski DuBois, and D.L. DuBois, *J. Am. Chem. Soc.* **128**, 358-366 (2006).
- Kinetic Studies of the Photoinduced Formation of Transition Metal-Dinitrogen Complexes Using Time-Resolved Infrared and UV-vis Spectroscopy*, D.C. Grills, K.-W. Huang, J.T. Muckerman and E. Fujita, *Coord. Chem. Rev.* (in press, 2006).
- Transition State Characterization for the Reversible Binding of Dihydrogen to Bis(2,2'-bipyridine)rhodium(I) from Temperature- and Pressure-Dependent Experimental and Theoretical Studies*, E. Fujita, B.S. Brunschwig, C. Creutz, J.T. Muckerman, N. Sutin, D. Szalda and R. van Eldik, *Inorg. Chem.* (in press).
- Adsorption of platinum on the stoichiometric RuO<sub>2</sub>(110) surface*, P. Liu, J.T. Muckerman and R.R. Adzic, *J. Chem. Phys.* (in press).
- Reaction of thiophene with metcar Ti<sub>8</sub>C<sub>12</sub><sup>+</sup> nanoparticles*, P. Liu, J.M. Lightstone, J.A. Rodriguez, J.T. Muckerman and M.G. White, *J. Phys. Chem. B* (in press).
- Ground state electronic properties of Na<sub>3</sub>*, R. Requist, T. Baruah, J.T. Muckerman and P.B. Allen, *Phys. Rev. B* (submitted).
- Understanding the role of Ti in reversible hydrogen storage as sodium alanate: A combined experimental and first-principles theoretical approach*, S. Chaudhuri, J. Graetz, A. Ignatov, J.T. Reilly and J.T. Muckerman, *J. Am. Chem. Soc.* (submitted).

## Dynamics of Activated Molecules

Amy S. Mullin  
Department of Chemistry and Biochemistry  
University of Maryland  
College Park, MD 20742  
mullin@umd.edu

### Program Scope

The goal of this program is to study the state-resolved pathways by which polyatomic molecules with large amounts of internal energy dissipate their energy through inelastic and reactive collisions. Highly vibrationally excited molecules are generated by pulsed UV excitation and serve as prototypes for studying the dynamics of molecules with internal temperatures of 1000-4000 K. The high state densities and complex spectra of the highly excited molecules make direct probing of their dynamics unrealistic. The primary tool for these studies is high resolution transient IR diode and/or F-center laser absorption to monitor energy gain and/or formation of small molecules that undergo collisions with the highly excited molecules. The high resolution of the IR probe lasers allows measurement of individual quantum states as well as velocity distributions for diatomic and small polyatomic collision partners and reaction products. The current research involves elucidating the underlying forces that determine energy partitioning in the collisional relaxation of highly excited molecules and developing methods for state-resolved probing of both weak and strong collisions.

### Recent Progress

At the beginning of this progress cycle, the principal investigator moved her research labs to the University of Maryland, College Park. After a period of down-time, two transient absorption spectrometers are now set up and fully operational at Maryland. Our efforts this year have continued to focus on the dynamics of collisional energy transfer of highly vibrationally excited molecules.

#### **“Supercollisions” of alkylated pyridines with CO<sub>2</sub>**

A recent study was performed to investigate collisional relaxation of highly vibrationally excited alkylated molecules ( $E_{\text{vib}} \sim 38500 \text{ cm}^{-1}$ ) with CO<sub>2</sub>. Previously, we showed that in the relaxation of aromatic donor molecules such as pyrazine, pyridine and methylpyridine, the shape of the high energy tail of the energy transfer distribution function  $P(\Delta E)$  correlates with the energy dependence of the donor vibrational state density. The shape of the  $P(\Delta E)$  tail for each donor/CO<sub>2</sub> pair is described by a shape parameter ( $\beta_{\text{obs}}$ ) by fitting the experimental data to a single exponential decay using

$P(\Delta E) = \alpha_{\text{obs}} e^{-\beta_{\text{obs}} \Delta E}$ . In addition, the energy dependence of the vibrational state density is fit using  $\rho(E - \Delta E) = \alpha_{\text{p}} e^{-\beta_{\text{p}} \Delta E}$ . Such a correlation between  $\beta_{\text{obs}}$  and  $\beta_{\text{p}}$  has important predictive ramifications for modeling the relaxation of highly excited molecules. The goal of the current study is to learn how floppiness and size in vibrationally hot donor molecules affect the strong collisions (also called “supercollisions”) and the correlation with state density. Our approach is to use sequentially alkylated pyridine molecules, where the pyridine component acts as the UV chromophore allowing for single photon vibrational excitation at 266 nm. The donors in this study are 2-ethylpyridine, 2-propylpyridine and 2-t-butylpyridine. The nascent rotational and translational energy gain profiles for CO<sub>2</sub> that result from collisions with the hot donors are collected using diode laser transient absorption at 4.3  $\mu\text{m}$ . The resulting  $\beta_{\text{obs}}$  values for the alkylated donors indicate that the strong collisions pathway is reduced relative to the non-alkylated donors. This behavior corresponds essentially to a dilution of the internal energy among modes in the hot donor molecule and is similar to the relaxation behavior of the “stiff” aromatic compounds. While the statistical correlation generally holds for the alkylated donors, we have preliminary evidence that increased floppiness due to longer chain lengths actually increases the likelihood of large  $\Delta E$  collisions. We are currently working to extend these studies to longer chain lengths.

### **Strong and weak collisions of pyrazine with HDO**

Transient IR probing has proven to be a powerful technique for investigating strong collisions where the appearance of scattered bath molecules is separated cleanly from the initial thermal distribution. However, it is often more difficult to obtain clean energy gain measurements for the low energy part of the energy transfer distribution function that corresponds to the weak collisions. Such information is desirable for a more complete description of the energy transfer dynamics. Complications in collecting data for low rotational states may include interference from atmospheric absorption and simultaneous appearance of population in the upper state of the probe transition. In a recent study, we have measured the energy gain profiles for HDO (000) molecules at 2.7  $\mu\text{m}$  in both low J and high J states that result from collisions with vibrationally excited pyrazine ( $E_{\text{vib}}=38000 \text{ cm}^{-1}$ ). The nascent Doppler-broadened lineprofiles of the low J states are dominated by depletion of the initial 300 K population but contain substantial contributions in the high velocity wings corresponding to appearance of HDO molecules in low J states. These data provide us the opportunity to test further the role of angular momentum constraints in collisional energy transfer of polyatomic molecules. By extending the water data to include a broader range of  $\Delta J$  for the bath molecule, a positive dependence is seen in the recoil velocity of the scattered molecules, with higher rotational states having larger recoil velocities. Comparable behavior has now been observed for three bath species: H<sub>2</sub>O (and HDO), DCl and CO<sub>2</sub>. The distribution of nascent HDO (000) rotational states with  $E_{\text{rot}} = 100$  to  $1400 \text{ cm}^{-1}$  are well described by a single temperature of  $T_{\text{rot}}=430 \text{ K}$ . In comparison with pyrazine/H<sub>2</sub>O collisions, HDO

exhibits substantially reduced rotational energies ( $T_{\text{rot}} = 920 \text{ K}$  for  $\text{H}_2\text{O}$ ). In addition, HDO undergoes energy transfer with integrated rates that are 50% larger than for  $\text{H}_2\text{O}$ . These results show that the relaxation is influenced by lowering the zero point energy of the intermolecular attraction. Additional studies are now underway using  $\text{D}_2\text{O}$  as a collision partner and future studies will look into potential contributions of H/D exchange reactions between highly excited pyrazine and  $\text{D}_2\text{O}$ .

### **“Supercollisions” of methylated pyridines with HDO**

Expanding on our previous studies of methylation effects in energy transfer, we have measured the collisional relaxation of pyridine, 2-methylpyridine and 2,6-dimethylpyridine ( $E_{\text{vib}} \sim 38500 \text{ cm}^{-1}$ ) with HDO. Nascent rotational and translational energy gain profiles were measured for HDO (000). For each donor molecule, the HDO rotational energy distribution is considerably narrower than that reported previously for  $\text{H}_2\text{O}$ . The accompanying J-dependent velocity distributions for HDO are slightly higher than for  $\text{H}_2\text{O}$ , as are consistent with the more closely spaced rotational levels of HDO. We are currently using this data to generate  $P(\Delta E)$  curves for these donor/acceptor pairs to provide an additional test of the role of state density in collisional energy transfer.

### **Transient IR absorption $\text{NH}_3$ as a molecular quencher**

One goal of our program is to identify the molecular properties that lead to efficient (or inefficient) collisional energy transfer involving highly vibrationally excited molecules. Many bulk relaxation studies show  $\text{NH}_3$  to be an especially effective quencher of vibrationally hot molecules. During this year, we have performed preliminary survey studies using transient diode laser absorption to probe  $\text{NH}_3$  as a collisional quencher of 2,6-dimethylpyridine ( $E_{\text{vib}} \sim 38500 \text{ cm}^{-1}$ ). The goal here is to measure the low and high J parts of the energy transfer distribution function and determine the partitioning of rotational, translational and vibrational energy in  $\text{NH}_3$ . Our initial studies used transient absorption of the  $\nu_4$  asymmetric bending mode near  $5 \mu\text{m}$ . Preliminary linewidth data suffered from low signal to noise ratios. We will now turn our attention to the NH stretching mode at  $2.8 \mu\text{m}$ .

### **DOE Supported Publications (2004-2006)**

1. “Trajectory study of supercollision relaxation in highly vibrationally excited pyrazine and  $\text{CO}_2$ ” Z. Li, R. Sansom, S. Bonella, D. F. Coker and A. S. Mullin, *J. Phys. Chem. A*. **109**, 7658-7666 (2005)
2. “Quenching dynamics of highly excited azabenzenes with DCl: The role of the energy acceptor,” Z. Li, E. Korobkova, K. Werner, L. Shum, A. S. Mullin, *J. Chem. Phys.* **123**, 174306 (2005).

3. "Relaxation dynamics of highly vibrationally excited picoline isomers ( $E_{\text{vib}} = 38300 \text{ cm}^{-1}$ ) with  $\text{CO}_2$ : The role of state density in impulsive collisions," E. M. Miller, L. Murat, N. Bennette, M. Hayes, and A. S. Mullin, *J. Phys. Chem. A.* 110, 3266-3272 (2006).
4. "Strong and weak collisions of vibrationally excited pyrazine with HDO" Z. Li, M. Elioff, J. Neudel and A. S. Mullin, in preparation.
5. "Methylation effects in state-resolved quenching of highly vibrationally excited azabenzenes ( $E_{\text{vib}} \sim 38500 \text{ cm}^{-1}$ ). III. Collisions with HDO" Z. Li and A. S. Mullin, in preparation.
6. "Strong collisions of vibrationally excited alkylated pyridines with  $\text{CO}_2$ " J. Du, Q. Liu, D. Havey, Z. Li and A. S. Mullin, in preparation.

# Reacting Flow Modeling with Detailed Chemical Kinetics

Habib N. Najm

Sandia National Laboratories  
P.O. Box 969, MS 9051, Livermore, CA 94551  
hnnajm@sandia.gov

## 1 Program Scope

The purpose of this research program is to understand the transient behavior of flames in reacting flow, thereby improving the state of the art in predictive modeling of combustion. The work involves: (1) Using computations to investigate the structure and dynamics of flames in unsteady vortical laboratory-scale flows; (2) Developing techniques for analysis of multidimensional reacting flow; (3) Developing numerical methods for discretizing large scale reacting flow systems of equations with detailed kinetics and transport; (4) Developing massively parallel codes for computing large scale reacting flow with detailed kinetics; and (5) Developing means for uncertainty quantification in reacting flow computations, including Bayesian methods for construction of uncertain chemical models from experimental data, and spectral polynomial chaos constructions for propagation of uncertainty in computations of chemical systems.

## 2 Recent Progress

### 2.1 Flame/Ignition Computations with CSP-Simplified Chemistry

We used Computational Singular Perturbation (CSP) theory for simplification of chemical mechanisms, based on ignition and/or one-dimensional (1D) flame computations with detailed mechanisms for methane-air and *n*Heptane-air combustion. We studied 2D premixed flame-vortex interaction using detailed and comprehensive simplified methane-air mechanisms. This was done over a range of reactants equivalence ratio, and for a range of transient strain-rate and curvature disturbances to the flame. The key objective of this study was to assess the impact of transient disturbances to the flame, by flow structures, on the fidelity of computed flame structure, using different simplified mechanisms under various operating conditions. Hitherto, we have found a generally small effect on the predictive accuracy of the various mechanisms due to even severe flow disturbances; e.g. transient tangential strain-rate values of the order of  $2500 \text{ s}^{-1}$ . For all but flames at the rich/lean stoichiometric limits, the error in predicted internal flame structure was largely unchanged from that observed with the steady-state planar premixed flame. The weaker flames at either stoichiometric limit ( $\Phi = 0.6, 1.4$ ) did exhibit increased relative error with increasing levels of transient strain-rate and curvature, as compared with the detailed mechanism solution. We also studied the ignition of *n*Heptane-air mixtures at various pressure, temperature, and stoichiometry conditions. The original detailed mechanism involves 560 species and 2538 reactions. Simplification with CSP led to a range of simplified mechanisms, down to 121 species, depending on specified error tolerances. Appropriately scaled CSP indices were used to achieve monotonic convergence of empirically observed simplified mechanism accuracy with variation of the CSP error tolerance. CSP analysis results were also used to shed light on *n*Heptane ignition physics, illustrating findings consistent with prior understanding of this system.

### 2.2 Bayesian Methods for Stochastic Inverse Problems

We have implemented Bayesian statistics for the solution of stochastic inverse problems. Such problems arise naturally in the context of model inference and parameter estimation from observations in the presence of noise and uncertainty. The Bayesian approach enables model construction with specified stochastic uncertainties in inferred model parameters. We developed new strategies for using Polynomial Chaos (PC) constructions to achieve dramatic acceleration of the evaluation of Bayes integrals using sampling, a key computational bottleneck in Bayesian inversion. We demonstrated this construction in the context of various sampling strategies, including both Monte-Carlo prior-sampling and Markov-Chain Monte Carlo (MCMC). The evaluation of the Bayes integral is related to a non-intrusive uncertainty

quantification (UQ) construction, which is sped-up substantially using an intrusive PC UQ approach. With the intrusive solution of the forward problem in hand, the cost of each sample in the evaluation of the integral is quite negligible. On a problem where the forward-problem involves a PDE solution, namely the solution of the transient heat-equation, we achieved speed-ups of the order of  $10^3\times$  in the inverse problem solution. We studied the dependence of the solution on the dimensionality and order of the PC construction, using Legendre-Uniform constructions, and demonstrated convergence of the implementation with PC expansion order. We also outlined a change of basis strategy that generalizes the approach by largely decoupling the intrusive problem solution from the specification of the Bayesian prior, except to the extent that the presumed distribution of the forward problem parameters in the UQ context generally encompasses the support of the prior, and that the form of this presumed distribution is invertible.

## 2.3 Bayesian Parameter Estimation

We used Bayesian parameter estimation constructions to analyze experimental measurements of the rate of quenching of NO  $A^2\Sigma^+(v' = 0)$  probed by two-photon laser-induced fluorescence using a picosecond laser. The goal was to arrive at rigorous estimates of uncertainties in quenching-rate parameter values inferred from the data. Besides their inherent value, these uncertainties, particularly when formulated probabilistically, are key pre-requisites for subsequent UQ studies that rely on models built with empirically-estimated parameters. In this particular experiment, a single exponential decay function was fitted to the data, including accounting for various sources of interference, such that the aggregate model fit involves six parameters. Using a component-wise MCMC sampling strategy, we explored and identified the joint posterior probability distribution for the model parameters, including a flexible two-parameter instrument noise model. The 1- and 2-dimensional marginal distributions for the six parameters in the model are shown in Figure 1. The model construction is given by:  $I(t) = I_f(t; i_o, \gamma_o, t_o) * f(t) * g(t; \Delta t_o) + b_o I_b(t) + y_o$ , where '\*' denotes a convolution;  $I_f$  is a single exponential decay function with an amplitude  $i_o$  and a decay rate  $\gamma_o$ , that starts at  $t_o$ ;  $f$  is an instrument response function;  $g$  is a Gaussian smoothing kernel with a full-width at half maximum of  $\Delta t_o$ ;  $I_b$  is a background fluorescence scaled by  $b_o$ ; and  $y_o$  is a baseline offset. The means of the marginal parameter distributions were close to their root mean square estimates, while the widths and shapes of these distributions quantify the uncertainty in each parameter. As can be seen in the figure, the 1D marginal distributions themselves were, all but one, nearly Gaussian, with the one parameter ( $t_o$ ) exhibiting an asymmetric distribution. This skewed PDF of  $t_o$  was not expected, but is in fact consistent with the role of  $t_o$  in the model. Moreover, examination of the two-dimensional marginal joint probability distributions of pairs of parameters, shown in the figure, exhibited some very clear correlations among some parameters (e.g.  $\gamma_o$  and  $t_o$ ), which is, again, consistent with the model construction. Such information, including non-gaussian probability density functions (PDFs) and parametric correlations are largely inaccessible with alternate parameter estimation methods, and provide ample demonstration of the utility of Bayesian methods in this context. [with T. Settersten]

## 2.4 High-Order Structured Adaptive Mesh Refinement

We have developed and demonstrated combinations of discretizations, interpolants, and filters for high-order computations on adaptive meshes. In particular, we investigated the requisite combinations of discretizations, interpolants, and filters to achieve solutions of a given order of convergence. These findings were demonstrated numerically with a number of relevant model problems. We also developed and implemented a high-order momentum solver on a uniform mesh, based on a velocity-projection construction, to be coupled with the adaptive mesh scalar solver. We are presently testing and validating the various software components of the momentum solver.

# 3 Future Plans

## 3.1 Flame Computations with CSP-Reduced Chemistry

We plan to extend the ongoing flame computations to other fuels and other vortex-flow configurations. We have started computations with vortical flow arrangements that involve significant compressive strain-

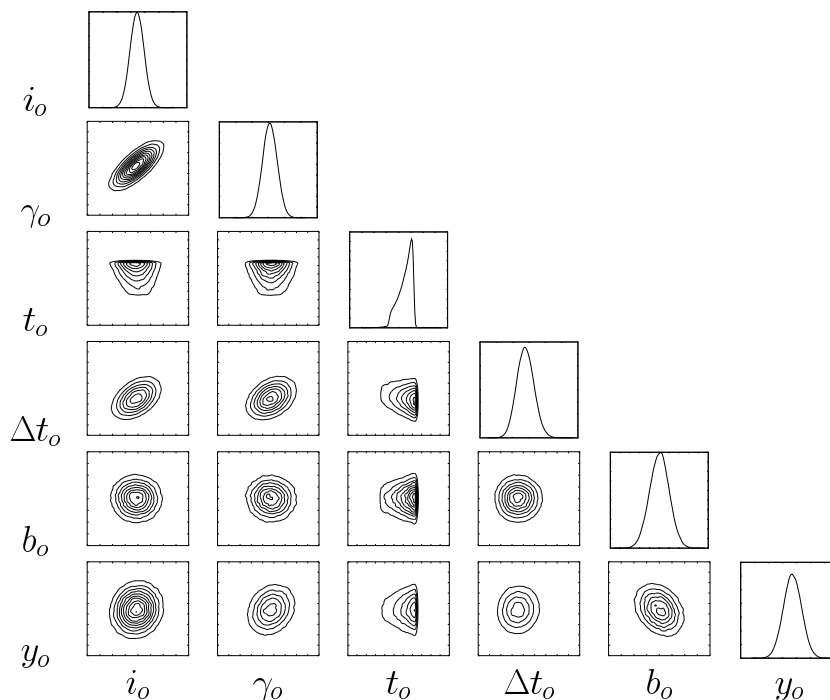


Figure 1: Results of the Bayesian parameter estimation study for the NO-quenching experiment of T. Settersten. Shown are 1D and 2D marginal PDFs of the six model parameters  $\{i_o, \gamma_o, t_o, \Delta t_o, b_o, y_o\}$ . The plots along the diagonal are the marginal PDFs of individual parameters. The 2D PDFs, shown as contour plots, are useful for exploring cuts of the higher dimensional posterior distribution of the parameters, and examining emergent correlations among pairs of parameters.

rate, versus the hitherto largely tensile strain-rate studies. We will continue these to examine the performance of simplified mechanisms under these conditions. We have also begun computations of *n*Heptane in homogeneous systems, and are proceeding towards 1D flame computations, again with a range of simplified mechanisms. We will also explore fuels of intermediate complexity, and will pursue 2D flame-vortex studies in each case as consistent with computational constraints.

### 3.2 Uncertainty Quantification (UQ) in Reacting Flow

The extension of the adaptive multi-wavelet based, Multi-Resolution Analysis (MRA) UQ construction to exothermic chemical models is key element of our future plans. This is a demonstration that needs to be done in order to arrive at a generally-demonstrated MRA UQ solution for reacting flow. Its main benefit is the locally adaptive spatial resolution of the parametric space, allowing for use of low order polynomial chaos constructions, and robust handling of non-linearities and bifurcations.

### 3.3 Bayesian Methods for Stochastic Inverse Problems

We are presently investigating Bayesian inverse problem solutions involving random fields. In this context, we will use model reduction strategies based on the Karhunen-Loève decomposition to represent random fields, and will couple that with polynomial chaos in a Bayesian framework. Subsequently, we also plan to address inference of chemical network structure from data using the Bayesian framework.

### 3.4 Bayesian Parameter Estimation

We will pursue application of Bayesian parameter estimation techniques to other combustion-relevant experimental data, with an eye towards exploring the general utility of the technique for construction of uncertain chemical models, as well as providing means of hypothesis testing where relevant.

### 3.5 High-Order Structured Adaptive Mesh Refinement (SAMR)

Our work on high-order SAMR development continues with the ongoing validation of the momentum solver. Once this is validated, we will demonstrate the coupled construction with the adaptive SAMR reaction-diffusion solvers, thereby arriving at the full reacting flow solver. Once in place, we will use this construction for investigations of unsteady laminar jet flames in laboratory-scale geometries.

### 3.6 CSP/PRISM Adaptive Chemistry

We are on our way towards developing a general implementation of CSP and PRISM-tabulation for enabling reacting flow computations with adaptive chemical reduction. Ongoing work, exploring strategies for construction of low-dimensional regression response surfaces in a given hypercube, will continue, towards a generally applicable construction, for arbitrary chemical systems. [with M. Frenklach].

## 4 BES-Supported Published/In-Press Publications [2004-2006]

- [1] Valorani, M., Creta, F., Donato, F., Najm, H.N., and Goussis, D.A., Skeletal Mechanism Generation and Analysis for *n*-Heptane with CSP, *Proc. Comb. Inst.* in press.
- [2] Valorani, M., Creta, F., Goussis, D.A., Lee, J.C., and Najm, H.N., An Automatic Procedure for the Simplification of Chemical Kinetics Mechanisms based on CSP, *Combustion and Flame* in press.
- [3] Singer, M.A., Pope, S.B., and Najm, H.N., Operator-Splitting with ISAT to Model Reacting Flow with Detailed Chemistry, *Combustion Theory and Modelling* in press.
- [4] Goussis, D.A., and Valorani, M., An Efficient Iterative Algorithm for the Approximation of the Fast and Slow Dynamics of Stiff Systems, *J. Comp. Phys.*, 214:316–346 (2006).
- [5] Najm, H.N., and Knio, O.M., Modeling Low Mach Number Reacting Flow with Detailed Chemistry and Transport, *J. Sci. Comp.*, 25(1):263–287 (2005).
- [6] Valorani, M., Goussis, D.A., Creta, F., and Najm, H.N., Higher Order Corrections in the Approximation of Low Dimensional Manifolds and the Construction of Simplified Problems with the CSP Method, *J. Comput. Phys.*, 209:754–786 (2005).
- [7] Lefantzi, S., Ray, J., Kennedy, C.A., and Najm, H.N., A Component-based Toolkit for Reacting Flows with Higher Order Spatial Discretizations on Structured Adaptively Refined Meshes, *Progress in Computational Fluid Mechanics*, 5(6):298–315 (2005).
- [8] Goussis, D.A., Valorani, M., Creta, F., and Najm, H.N., Reactive and Reactive/Diffusive Time Scales in Stiff Reaction-Diffusion Systems, *Progress in Computational Fluid Mechanics*, 5(6):316–326 (2005).
- [9] Reagan, M.T., Najm, H.N., Pébay, P.P., Knio, O.M., and Ghanem, R.G., Quantifying Uncertainty in Chemical Systems Modeling, *Int. J. Chem. Kin.*, 37(6):368–382 (2005).
- [10] Reagan, M.T., Najm, H.N., Debusschere, B.J., Maître, O.P. Le, Knio, O.M., and Ghanem, R.G., Spectral Stochastic Uncertainty Quantification in Chemical Systems, *Combustion Theory & Modeling*, 8:607–632 (2004).
- [11] Pébay, P.P., Najm, H.N., and Pousin, J., A Non-Split Projection Strategy for Low Mach Number Reacting Flows, *Int. J. Multiscale Computational Eng.*, 2(3):445–460 (2004).
- [12] Debusschere, B.J., Najm, H.N., Pébay, P.P., Knio, O.M., Ghanem, R.G., and Le Maître, O.P., Numerical challenges in the use of polynomial chaos representations for stochastic processes, *SIAM Journal of Scientific Computing*, 26(2):698–719 (2004).
- [13] Le Maître, O.P., Ghanem, R.G., Knio, O.M., and Najm, H.N., Uncertainty propagation using Wiener-Haar expansions, *Journal of Computational Physics*, 197(1):28–57 (2004).
- [14] Le Maître, O.P., Reagan, M.T., Debusschere, B.D., Najm, H.N., Ghanem, R.G., and Knio, O.M., Natural Convection in a Closed Cavity under Stochastic, Non-Boussinesq conditions, *SIAM J. Scientific Computing*, 26(2):375–394 (2004).
- [15] Le Maître, O.P., Najm, H.N., Ghanem, R.G., and Knio, O.M., Multi-resolution analysis of Wiener-type uncertainty propagation schemes, *Journal of Computational Physics*, 197:502–531 (2004).
- [16] Matta, A., Knio, O.M., Ghanem, R.G., Chen, C.-H., Santiago, J.G., Debusschere, B., and Najm, H.N., Computational Study of Band Crossing Reactions, *J. MEMS*, 13(2):310–322 (2004).

“Spectroscopy, Kinetics and Dynamics of Jet-Cooled Combustion Radicals”

Grant No. DE-FG02-05ERE15961, DOE Contractors Meeting 2006

Feng Dong, Chandra Savage, Melanie Roberts, Richard Walters and David J. Nesbitt  
JILA, National Institute of Standards and Technology and University of Colorado,  
and Department of Chemistry and Biochemistry, University of Colorado, Boulder,  
Colorado 80309

Our research program is directed toward elucidation of the kinetics, spectroscopy, kinetics and structural dynamics of combustion radicals, exploiting the powerful combination of i) slit supersonic discharge expansion, ii) high resolution direct laser absorption, and iii) and quantum shot noise limited detection methods. This poster will describe recent progress both developing and utilizing these methods, focusing primarily on the following three projects.

High-resolution infrared spectra of jet-cooled cyclopropyl radical are reported for the first time, specifically sampling the in-phase antisymmetric  $\text{CH}_2$  stretch ( $\nu_7$ ) vibration. In addition to yielding the first precise gas-phase structural information, the spectra reveal quantum level doubling into lower (+) and upper (-) states due to tunneling of the lone  $\alpha$ -CH with respect to the CCC plane. The bands clearly reveal intensity alternation due to H atom nuclear spin statistics (6:10 and 10:6 for even:odd  $K_a+K_c$  in lower (+) and upper (-) tunneling levels, respectively) consistent with  $C_{2v}$  symmetry of the cyclopropyl-tunneling transition state. The two *ground*-state-tunneling levels fit extremely well to a rigid asymmetric rotor Hamiltonian, but there is clear evidence for both local and global

state mixing in the vibrationally *excited*  $\nu_7$  tunneling levels. In particular, the upper (-) tunneling component of the  $\nu_7$  state is split by anharmonic coupling with a nearly isoenergetic dark state, which thereby acquires oscillator strength via intensity sharing with this bright state. From thermal Boltzmann analysis of fractional populations, tunneling splittings for cyclopropyl radical are estimated to be  $3.2 \pm 0.3 \text{ cm}^{-1}$  and  $4.9 \pm 0.3 \text{ cm}^{-1}$  in the ground and  $\nu_7$ -excited states, respectively. This analysis indicates ground state stereoracemization of the  $\alpha$ -CH radical center to be a very fast process [ $k \approx 2.0(4) \times 10^{11} \text{ s}^{-1}$ ], with the increase in tunneling rate upon  $\text{CH}_2$  in-phase asymmetric stretch excitation consistent with *ab initio* predictions of equilibrium vs transition-state zero-point energies. Modeling of the ground-state-tunneling splittings with high level *ab initio* 1D potentials indicates an improved  $V_0 = 1115 \pm 35 \text{ cm}^{-1}$  barrier height for  $\alpha$ -CH inversion through the cyclopropyl CCC plane.

High resolution IR absorption spectra have also been obtained for supersonically cooled ethyl radicals ( $T_{\text{rot}} = 20\text{K}$ ) in a slit supersonic jet discharge expansion, revealing first rotationally resolved data for CH-stretch excitation of the methyl group and complementing previous studies of the methylenic  $\text{CH}_2$  excitation. Three different vibrational bands are observed, one parallel ( $k = 0 \leftarrow 0$ ) and two perpendicular ( $|\Delta k| = 1 \leftarrow 0$ ), which for a nearly decoupled methyl rotor framework would correspond to symmetric and (nearly degenerate) asymmetric CH-stretch excitations. However, the splitting between the two asymmetric CH-stretch excitations is anomalously large ( $\approx 125 \text{ cm}^{-1}$ ), signaling the presence of interactions between the  $\text{CH}_2$  radical moiety and the opposing CH bond on the methyl group. This suggests an improved zeroth order vibrational description as an isolated CH stretch, strongly red shifted by

hyperconjugation, with localized vibrations in the remaining CH bonds split into symmetric and asymmetric stretches. Such a dynamical picture highlights the remarkably strong coupling between methyl CH-stretch vibrations and C–C torsional geometry and begins to elucidate discrepancies with previous matrix studies. The results from the present efforts also provide interesting comparison with high level theoretical *ab initio* potential surface studies by Harding and coworkers, with which the agreement is very good.

We are currently building up new capabilities with the discharge spectrometer for systematic kinetic control and study of the combustion radical chemistry. Specifically, we have designed and built pulsed "microinjector" inlets that are machined into the slit jaws, which most importantly allow us to inject reagents selectively into the post discharge region. This will be a particularly crucial advantage for "rational synthesis" of alkylperoxy radicals, which will be formed by dissociative detachment of low energy electrons to alkyl halides in the discharge, followed by microslit injector addition of O<sub>2</sub> to the corresponding alkyl radical species in the post discharge region. The value of spatial separation between i) alkyl radical formation and ii) O<sub>2</sub> microslit injector addition region is that O(<sup>3</sup>P) atom formation by the discharge is explicitly avoided. This permits, for example, one to look at the kinetics of methylperoxy radical formation from CH<sub>3</sub> + O<sub>2</sub>, without interferences from the corresponding fast radical-radical reaction of O + CH<sub>3</sub>. Progress toward our initial test system, specifically monitoring loss of methyl radical in the slit jet expansion via CH<sub>3</sub>+ O<sub>2</sub> → products, will be described.

---

## Radical Photochemistry and Photophysics

Daniel M. Neumark  
Chemical Sciences Division  
Lawrence Berkeley National Laboratory  
Berkeley, CA 94720  
Email: dneumark@berkeley.edu

The radical photochemistry and photophysics program is focused on fundamental studies of species and reactions relevant to combustion chemistry. This program is aimed at elucidating the photodissociation dynamics and bimolecular chemistry of free radicals and hydrocarbons. The experiments yield primary chemistry and photochemistry, bond dissociation energies, heats of formation, photoionization cross sections, and excited state dynamics. We are particularly interested in the photodissociation of alkoxy and peroxy radicals, both of which are critical intermediates in hydrocarbon oxidation, and in the dissociation of small aromatic radicals such as the phenyl and cyclopentadienyl radicals that are created in the early stages of soot formation. On a more fundamental level, one of the key conceptual issues that will be addressed is the competition between excited state and ground state dissociation in both radicals and closed-shell molecules. This issue is particularly relevant in light of recent considerable interest in conical intersections and the role they play in chemical dynamics. In general, free radicals have more lower-lying excited electronic states and dissociation channels than closed-shell molecules, and we expect the very different electronic state topologies in open vs. closed shell species to play a major role in the relative importance of excited vs. ground state dissociation.

We have developed a state-of-the-art fast beam dissociation instrument for studying the photodissociation dynamics of free radicals and negative ions. Recent installation of a photofragment coincident imaging detection system enables the study of three-body photodissociation events, and has facilitated the observation of photodissociation channels in which an H or D atom is ejected. A crossed molecular/laser beam instrument is used to investigate the primary chemistry and photochemistry of both closed-shell hydrocarbons and hydrocarbon radicals. A similar instrument on the Chemical Dynamics Beamline at the Advanced Light Source, in which scattered products are ionized with tunable synchrotron radiation, has been used to look at hydrocarbon photodissociation in more detail and to measure absolute photoionization cross sections for free radicals; this work will be continued on the beamline using a different apparatus based on photofragment imaging.

The photodissociation spectroscopy and dynamics of several free radicals were investigated using our fast beam photofragment translational spectroscopy instrument. In this experiment, radicals are generated by laser photodetachment of a fast (8–10 keV) beam of mass-selected negative ions. The radicals are then photodissociated by a second laser, and the photofragments are collected with high efficiency. We can measure the total dissociation signal as a function of excitation wavelength, thereby mapping out the photofragment yield spectrum of the radical. In addition, at fixed wavelengths, photofragment coincidence imaging yields the position and arrival times for all

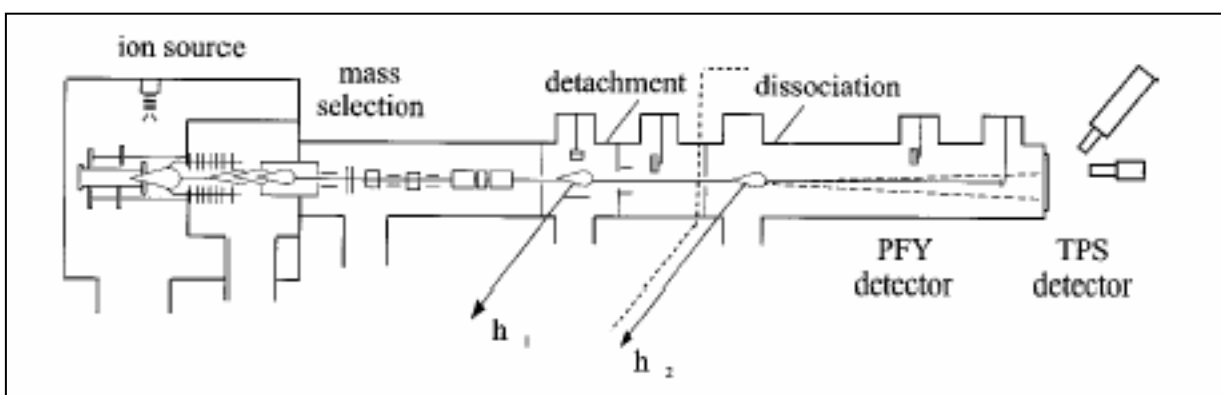
photofragments from each photodissociation event, from which the photofragment translational energy and angular distribution are obtained for each mass channel. New results were obtained for the ethoxy and DNCN radicals. The DNCN results show, for the first time, that  $D + \text{NCN}$  is an important dissociation channel, complementing earlier work in which we probed the  $\text{CD} + \text{N}_2$  channel. Both channels appear to result from internal conversion of electronically excited DNCN to its ground state prior to dissociation, thereby showing that there is a relatively facile pathway from  $\text{CD} + \text{N}_2$  to  $D + \text{NCN}$  on the ground state potential energy surface. This result supports the proposal by Lin and co-workers that the reaction  $\text{CH} + \text{N}_2 \rightarrow \text{H} + \text{NCN}$  plays a key role in NO production in flames.

The photofragment coincidence detection scheme also allows the detection and characterization of three-body dissociation processes, a phenomenon much less well understood than two-body dissociation. Thus far, we have successfully applied this method to negative ions as opposed to neutral radicals; the negative ion experiment is simpler as only a single laser is required. We have recently investigated the photodissociation of  $\text{I}_3^-$  and  $\text{I}(\text{H}_2\text{O})_n$  clusters with this method. In the case of  $\text{I}(\text{H}_2\text{O})_n$  ( $n \leq 5$ ) clusters, dissociation following either direct detachment or excitation of the charge-transfer-to-solvent (CTTS) bands was investigated. In both cases, the major product was two-fragment dissociation to  $\text{I} + (\text{H}_2\text{O})_n (+e^-)$  with three-fragment dissociation to  $\text{I} + (\text{H}_2\text{O})_{n-1} + \text{H}_2\text{O} (+e^-)$  observed as a minor (10%) channel. Analysis of the latter channel using Dalitz plots suggested this to be a sequential channel in which the I atom leaves first, and the neutral water cluster loses a water by evaporation.

Molecular beam photodissociation experiments have focused on closed shell molecules in the intermediate size regime (10–15 atoms), and using either electron impact or VUV photoionization to ionize and detect photoproducts. Molecular beam photofragment translational spectroscopy experiments elucidate the detailed photodissociation dynamics of molecules, yielding information on product branching ratios and whether dissociation occurs on the ground state via a statistical mechanism or by dissociation on excited state surfaces. In addition, we have developed a novel means of measuring absolute photoionization cross sections based on molecular beam photodissociation. The dissociation dynamics of allene, propyne, and propyne- $\text{d}_3$  at 193 nm were investigated with photofragment translational spectroscopy. The photoionization cross section of the phenyl radical ( $\text{C}_6\text{H}_5$ ) was determined via photolysis of phenyl chloride at both 248 and 193 nm, and comparison of the signal from VUV photoionization of momentum-matched Cl and phenyl products.

We have recently initiated radical photodissociation experiments on our molecular beam instrument with electron impact ionization, using a pulsed photolytic source to generate radicals and then photodissociating them with a second laser. Thus far, preliminary experiments have been obtained for the propargyl ( $\text{C}_3\text{H}_3$ ) radical in which kinetic energy and angular distribution for the  $\text{C}_3\text{H}_2$  product were measured. Our results are consistent with prior work by Fischer on this species in which the H atom channel was characterized by Doppler spectroscopy, thereby supporting the assignment of this earlier work (which has recently been questioned in a theoretical paper) to propargyl photodissociation.

In the near future, we are particularly interested in the photodissociation of alkoxy and peroxy radicals, both of which are critical intermediates in hydrocarbon oxidation, and in the dissociation of small aromatic radicals such as the phenyl and cyclopentadienyl radicals that are created in the early stages of soot formation. However, photodissociation studies will also be carried out on closed-shell molecules for which the issue of excited vs. ground state dissociation have been theoretically considered in detail; small biomolecules such as DNA bases are particularly attractive candidates in this regard. In addition, photoelectron and photofragment imaging experiments on radicals will be carried out at the Advanced Light Source to (a) further characterize radicals and the cations produced when they are ionized, and (b) determine their photoionization cross sections.



#### Recent publications:

J. C. Robinson, N. E. Sveum, and D. M. Neumark, "Determination of absolute photoionization cross sections for vinyl and propargyl radicals," *J. Chem. Phys.* 119, 5311 (2003).

J. C. Robinson, N. E. Sveum, and D. M. Neumark, "Determination of absolute photoionization cross sections for isomers of  $C_3H_5$ : allyl and 2-propenyl radicals," *Chem Phys Lett.* 383, 601 (2004).

A. A. Hoops, J. R. Gascooke, A. E. Faulhaber, K. E. Kautzman, and D. M. Neumark, "Two- and three-body photodissociation of gas phase  $I_3^-$ ," *J. Chem. Phys.* 120, 7901 (2004).

A. A. Hoops, J. R. Gascooke, K. E. Kautzman, and D. M. Neumark, "Photodissociation spectroscopy and dynamics of the  $CH_2CFO$  radical," *J. Chem. Phys.* 120, 8494 (2004).

J.C. Robinson, N.E. Sveum, S. J. Goncher and D.M. Neumark, "Photofragment translational spectroscopy of allene, propyne, and propyne- $d_3$  at 193 nm," *Mol. Phys.* 3, 1765 (2005).

A.E. Faulhaber, D. E. Szpunar, K. E. Kautzman, and D. M. Neumark, "Photodissociation dynamics of the ethoxy radical investigated by photofragment coincident imaging," J. Chem. Phys. A 109, 10239 (2005).

N. E. Sveum, S. J. Goncher, D. M. Neumark, "Determination of absolute photoionization cross sections of phenyl radical," Phys. Chem. Chem. Phys. 8, 592 (2006).

D. E. Szpunar, K. E. Kautzman, A. E. Faulhaber, and D. M. Neumark, "Photofragment coincidence imaging of small  $I(H_2O)_n$  clusters excited to the charge-transfer-to-solvent state," J. Chem. Phys. 124, 054318 (2006).

A. E. Faulhaber, J. R. Gascooke, A. A. Hoops, and D. M. Neumark, "Photodissociation dynamics of the HCNN radical," J. Chem. Phys. (in press).

# Determination of Accurate Energetic Database for Combustion Chemistry by High-Resolution Photoionization and Photoelectron Methods

C. Y. Ng

Department of Chemistry, University of California, Davis  
One Shields Avenue, Davis, California 95616  
E-mail Address: [cyng@chem.ucdavis.edu](mailto:cyng@chem.ucdavis.edu)

## Program Scope:

The main goal of this project is to obtain accurate thermochemical data, such as ionization energies (IEs), 0 K dissociative photoionization thresholds, 0 K bond dissociation energies ( $D_0$ ), and 0 K heats of formation ( $\Delta H^\circ_{f0}$ 's) for small and medium sizes molecular species and their ions of relevance to combustion chemistry. Accurate thermochemical data determined by high-resolution photoionization and photoelectron studies for selected polyatomic neutrals and their ions are also useful for benchmarking the next generation of *ab initio* quantum computational procedures.

## Recent Progress:

1. K. C. Lau and C. Y. Ng, "Accurate *ab initio* predictions of ionization energies of hydrocarbon radicals:  $\text{CH}_2$ ,  $\text{CH}_3$ ,  $\text{C}_2\text{H}$ ,  $\text{C}_2\text{H}_3$ ,  $\text{C}_2\text{H}_5$ ,  $\text{C}_3\text{H}_3$  and  $\text{C}_3\text{H}_5$ ", *J. Chem. Phys.* **122**, 224310 (2005).

The IEs for methylene ( $\text{CH}_2$ ), methyl ( $\text{CH}_3$ ), ethynyl ( $\text{C}_2\text{H}$ ), vinyl ( $\text{C}_2\text{H}_3$ ), ethyl ( $\text{C}_2\text{H}_5$ ), propargyl ( $\text{C}_3\text{H}_3$ ), and allyl ( $\text{C}_3\text{H}_5$ ) radicals have been calculated by the wavefunction based *ab initio* CCSD(T)/CBS approach, which involves the approximation to the complete basis set (CBS) limit at the coupled cluster level with single and double excitations plus a quasi-perturbative triple excitation [CCSD(T)]. When it is appropriate, the zero-point vibrational energy (ZPVE) correction, the core-valence (CV) electronic correction, the scalar relativistic (SR) effect correction, the diagonal Born-Oppenheimer (DBO) correction, and the high-order correlation (HOC) correction, have also been made in these calculations. The comparison between the computed IE values and the highly precise experimental IE values determined in previous pulsed field ionization-photoelectron (PFI-PE) studies indicates that the CCSD(T)/CBS method is capable of providing accurate IE predictions for these hydrocarbon radicals achieving error limits well within  $\pm 10$  meV. The benchmarking of the CCSD(T)/CBS IE predictions by the PFI-PE experimental results also lends strong support for the conclusion that the CCSD(T)/CBS approach with high-level energy corrections can serve as a valuable alternative for reliable IE determination of radicals, particularly for those radicals with very unfavorable Franck-Condon factors for photoionization transitions near their ionization thresholds.

2. X. N. Tang, Y. Hou, C. Y. Ng, and B. Ruscic, "Pulsed field ionization photoelectron-photoion coincidence study of the process  $\text{N}_2 + h\nu \rightarrow \text{N}^+ + \text{N} + e^-$ : Bond Dissociation Energies of  $\text{N}_2$  and  $\text{N}_2^{+*}$ ", *J. Chem. Phys.* **123**, 074330 (2005).

We have examined the dissociative photoionization reaction  $\text{N}_2 + h\nu \rightarrow \text{N}^+ + \text{N} + e^-$  near its threshold using the pulsed field ionization photoelectron-photoion coincidence (PFI-PEPICO) time-of-flight (TOF) method. By examining the kinetic energy release based on simulation of the  $\text{N}^+$  PFI-PEPICO TOF peak profile as a function of vacuum ultraviolet photon energy and by analyzing the breakdown curves of  $\text{N}^+$  and  $\text{N}_2^+$ , we have determined the 0 K threshold or appearance energy (AE) of this reaction to be  $24.2884 \pm 0.0010$  eV. Using this AE, together with known IEs of N and  $\text{N}_2$ , we have determined more precise values for the  $D_0$ 's of N-N ( $9.7543 \pm 0.0010$  eV) and N- $\text{N}^+$  ( $8.7076 \pm 0.0010$  eV) and the  $\Delta H^\circ_{f0}$ 's for N ( $112.469 \pm 0.012$  kcal/mol) and  $\text{N}^+$  ( $447.634 \pm 0.012$  kcal/mol). This  $\Delta H^\circ_{f0}(\text{N})$  has an error limit 6-fold smaller than that of the previous accepted  $\Delta H^\circ_{f0}(\text{N})$  value. Since the *ab initio* calculation of  $\Delta H^\circ_{f0}$  values of N-containing compounds using the atomization scheme requires the calibration with the

experimental  $\Delta H_{f0}^{\circ}(\text{N})$  value, this improved precision for the experimental  $\Delta H_{f0}^{\circ}(\text{N})$  will also improve the accuracy for *ab initio*  $\Delta H_{f0}^{\circ}$  calculations of N-containing compounds.

3. K.-C. Lau and C. Y. Ng, "Accurate *ab initio* predictions of ionization energies and heats of formation for the 2-C<sub>3</sub>H<sub>7</sub>, C<sub>6</sub>H<sub>5</sub>, and C<sub>7</sub>H<sub>7</sub> radicals", *J. Chem. Phys.* **124**, 044323 (2006).

The IEs for the 2-propyl (2-C<sub>3</sub>H<sub>7</sub>), phenyl (C<sub>6</sub>H<sub>5</sub>), and benzyl (C<sub>6</sub>H<sub>5</sub>CH<sub>2</sub>) radicals have been calculated by the wavefunction based *ab initio* CCSD(T)/CBS approach. The ZPVE correction, the CV electronic correction, and the SR effect correction have been also made in these calculations. Although a precise IE value for the 2-C<sub>3</sub>H<sub>7</sub> radical has not been directly determined before due to the poor Franck-Condon factor for the photoionization transition at the ionization threshold, the experimental value deduced indirectly using other known energetic data is found to be in good accord with the present CCSD(T)/CBS prediction. The comparison between the predicted value through the focal-point analysis and the highly precise experimental value for the IE(C<sub>6</sub>H<sub>5</sub>CH<sub>2</sub>) determined in the previous PFI-PE study shows that the CCSD(T)/CBS method is capable of providing an accurate IE prediction for C<sub>6</sub>H<sub>5</sub>CH<sub>2</sub>, achieving an error limit of 35 meV. The benchmarking of the CCSD(T)/CBS IE(C<sub>6</sub>H<sub>5</sub>CH<sub>2</sub>) prediction suggests that the CCSD(T)/CBS IE(C<sub>6</sub>H<sub>5</sub>) prediction obtained here has a similar accuracy of 35 meV. Taking into account this error limit for the CCSD(T)/CBS prediction and the experimental uncertainty, the CCSD(T)/CBS IE(C<sub>6</sub>H<sub>5</sub>) value is also consistent with the IE(C<sub>6</sub>H<sub>5</sub>) reported in the previous HeI photoelectron measurement. Furthermore, the present study provides support for the conclusion that the CCSD(T)/CBS approach with high-level energy corrections can be used to provide reliable IE predictions for C3-C7 hydrocarbon radicals with an uncertainty of  $\pm 35$  meV. Employing the atomization scheme, we have also computed the 0 K (298 K) heats of formation in kJ/mol at the CCSD(T)/CBS level for 2-C<sub>3</sub>H<sub>7</sub>/2-C<sub>3</sub>H<sub>7</sub><sup>+</sup>, C<sub>6</sub>H<sub>5</sub>/C<sub>6</sub>H<sub>5</sub><sup>+</sup>, and C<sub>6</sub>H<sub>5</sub>CH<sub>2</sub>/C<sub>6</sub>H<sub>5</sub>CH<sub>2</sub><sup>+</sup> to be 104.2/821.5 (88.9/805.3), 349.2/1146.3 (338.2/1136.6), and 223.6/926.4 (207.7/910.1), respectively. Comparing these values with the available experimental values, we find that the discrepancies for the 0 K and 298 K heats of formation values are  $\leq 1.4$  kJ/mol for 2-C<sub>3</sub>H<sub>7</sub>/2-C<sub>3</sub>H<sub>7</sub><sup>+</sup>,  $\leq 6.3$  kJ/mol for C<sub>6</sub>H<sub>5</sub>/C<sub>6</sub>H<sub>5</sub><sup>+</sup>, and  $\leq 2.8$  kJ/mol for C<sub>6</sub>H<sub>5</sub>CH<sub>2</sub>/C<sub>6</sub>H<sub>5</sub>CH<sub>2</sub><sup>+</sup>.

4. T. Zhang, X. N. Tang, K.-C. Lau, C. Y. Ng, C. Nicolas, D. S. Peterka, M. Ahmed, M. L. Morton, B. Ruscic, R. Yang, L. X. Wei, C. Q. Huang, B. Yang, J. Wang, L. S. Sheng, Y. W. Zhang, and F. Qi, "Direct identification of propargyl radical in combustion flames by VUV photoionization mass spectrometry", *J. Chem. Phys.* **124**, 074302 (2006).

We have developed an effusive laser photodissociation radical source, aiming for the production of vibrationally relaxed radicals. Employing this radical source, we have measured the VUV photoionization efficiency (PIE) spectrum of propargyl radical (C<sub>3</sub>H<sub>3</sub>) formed by 193 nm excimer laser photodissociation of propargyl chloride in the energy range of 8.5-9.9 eV using high-resolution multibunch synchrotron radiation. The VUV-PIE spectrum of C<sub>3</sub>H<sub>3</sub> thus obtained is found to exhibit pronounced autoionization features, which are tentatively assigned as members of two vibrational progressions of C<sub>3</sub>H<sub>3</sub> in excited autoionizing Rydberg states. The IE = 8.674 $\pm$ 0.001 eV of C<sub>3</sub>H<sub>3</sub> determined by a small steplike feature resolved at the photoionization onset of the VUV-PIE spectrum is in excellent agreement with the IE value reported in a previous pulsed field ionization-photoelectron study. We have also calculated the Franck-Condon factors (FCFs) for the photoionization transitions C<sub>3</sub>H<sub>3</sub><sup>+</sup>( $\nu_i$ ,  $i=1-12$ )  $\leftarrow$  C<sub>3</sub>H<sub>3</sub>. The comparison between the pattern of FCFs and the autoionization peaks resolved in the VUV-PIE spectrum of C<sub>3</sub>H<sub>3</sub> points to the conclusion that the resonance-enhanced autoionization mechanism is most likely responsible for the observation of pronounced autoionization features. We also present here the VUV-PIE spectra for the mass 39 ions observed in the VUV synchrotron photoionization mass spectrometric sampling of several premixed flames. The excellent agreement of the IE value and the pattern of autoionizing features of the VUV-PIE spectra observed in the photodissociation and flames studies has provided an unambiguous identification of propargyl radical as an important intermediate in the premixed combustion flames. The discrepancy found between the PIE spectra obtained in flames and photodissociation at energies above the IE(C<sub>3</sub>H<sub>3</sub>) suggests that the PIE spectra obtained in flames might have contributions from photoionization of vibrationally excited C<sub>3</sub>H<sub>3</sub> and/or dissociative photoionization processes involving larger hydrocarbon species formed in flames.

5. M. Hochlaf, T. Baer, X. M. Qian, and C. Y. Ng, "A Photoionization and Pulsed Field Ionization-Photoelectron Study of Cyanogen", *J. Chem. Phys.* **123**, 144302 (2005).

The VUV-PFI-PE and VUV-PIE spectra of NCCN in the energy region of 13.25-17.75 eV have been measured, covering the formation of  $\text{NCCN}^+(\tilde{X}^2\Pi_g, \tilde{A}^2\Sigma_g^+, \tilde{B}^2\Sigma_u^+, \tilde{C}^2\Pi_u, \text{ and } \tilde{D}^2\Pi_u)$ . The analysis of these spectra have provided accurate IE values of  $13.3705\pm 0.0010$ ,  $14.5288\pm 0.0010$ ,  $14.7697\pm 0.0010$ , and  $15.5158\pm 0.0010$  eV for the formation of  $\text{NCCN}^+$  in the  $\tilde{X}^2\Pi_g, \tilde{A}^2\Sigma_g^+, \tilde{B}^2\Sigma_u^+, \text{ and } \tilde{C}^2\Pi_u$  states, respectively. The  $\text{IE}[\text{NCCN}^+(\tilde{B}^2\Sigma_u^+)]$  value determined here indicates that the origin vibrational band of the  $\text{NCCN}^+(\tilde{B}^2\Sigma_u^+)$  state lies lower in energy by two quanta in the *cis* bending than previously reported. A set of spectroscopic parameters for  $\text{NCCN}^+(\tilde{X}^2\Pi_g)$  has been calculated using high level *ab initio* calculations. The experimental spectra are found to consist of ionizing transitions populating the vibronic levels of  $\text{NCCN}^+$  including pure vibronic progressions and combination modes involving the symmetric CN stretching, the CC and the even quanta of the anti-symmetric CN stretching, and the even quanta of the bending vibrations. Several bands arising from Renner-Teller, spin-orbit, and vibronic interactions between the valence electronic states of  $\text{NCCN}^+$  are also observed in the experimental PFI-PE spectrum. These bands are identified with the guidance of the present *ab initio* calculations.

### Future Plans:

We have established a state-of-the-art VUV laser photoion-photoelectron apparatus in our laboratory and have recently demonstrated sensitive VUV-PFI-PE and VUV-PFI-photoion (VUV-PFI-PI), and two-color laser infrared (IR)-VUV and VUV-IR photoion-photoelectron measurements. We plan to perform high-resolution VUV laser based PIE, PFI-PE, and PFI-PI measurements of selected hydrocarbon radicals. The PFI-PI measurements of radicals will allow the measurement of PFI-PE spectra covering not only the first IE, but also higher IEs of radicals without PFI-PE background interferences from impurities. We also plan to explore the application of the IR-VUV and VUV-IR schemes for PIE and PFI-PE studies of radicals.

### Publications of DOE sponsored research (2004-present)

1. H. K. Woo, P. Wang, K. C. Lau, X. Xing, and C. Y. Ng, "Vacuum Ultraviolet-Infrared Photo-Induced Rydberg Ionization Spectroscopy: C-H stretching frequencies for *trans*-2-butene and trichloroethene cations", *J. Chem. Phys.* **120**, 1756 (2004).
2. M. Hochlaf, K.-M. Weitzel, and C. Y. Ng, "Vacuum ultraviolet pulsed field ionization-photoelectron studies of  $\text{H}_2\text{S}$  in the range of 10-16 eV", *J. Chem. Phys.* **120**, 6944 (2004).
3. X.-M. Qian, K.-C. Lau, G.-Z. He, and C. Y. Ng, "Accurate Thermochemistry of the  $\text{ND}_2/\text{ND}_2^+$  and  $\text{ND}_3/\text{ND}_3^+$  Systems", *J. Chem. Phys.* **120**, 8476 (2004).
4. H. K. Woo, P. Wang, K.-C. Lau, X. Xing, and C. Y. Ng, "Single-photon vacuum ultraviolet laser pulsed field ionization-photoelectron studies of *trans*- and *cis*-bromopropenes", *J. Chem. Phys.* **120**, 9561 (2004).
5. X. M. Qian, K. C. Lau, and C.Y. Ng, "A High-Resolution Pulsed Field Ionization-Photoelectron-Photoion Coincidence Study of Vinyl Bromide", *J. Chem. Phys.* **120**, 11031-11041 (2004).
6. H. K. Woo, K.-C. Lau, and C. Y. Ng, "Vibrational spectroscopy of trichloroethene cation by vacuum ultraviolet pulsed field ionization-photoelectron method", *Chinese J. Chem. Phys.* (invited article) **17**, 292 (2004).
7. H. K. Woo, P. Wang, K.-C. Lau, X. Xing, and C. Y. Ng, "VUV pulsed field ionization-photoelectron and VUV-IR-photo-induced Rydberg study of *trans*- $\text{ClCH}=\text{CHCl}$ ", *J. Phys. Chem. A*, **108**, 9637 (2004).

8. P. Wang, X. Xing, K.-C. Lau, H. K. Woo, and C. Y. Ng, "Rovibrational-state-selected pulsed field ionization-photoelectron study of methyl iodide using two-color infrared-vacuum ultraviolet lasers", *J. Chem. Phys. (Communication)*, **121**, 7049 (2004).
9. Adam Brooks, Kai-Chung Lau, C.Y. Ng, and Tomas Baer, "The C<sub>3</sub>H<sub>7</sub><sup>+</sup> Appearance Energy from 2-Iodopropane and 2-Chloropropane Studied by Threshold Photoelectron Photoion Coincidence", *Eur. J. Mass Spectrom.* **10**, 819-827 (2004).
10. P. Wang, X. Xing, S. J. Baek, and C. Y. Ng, "Rovibrationally selected and resolved pulsed field ionization-photoelectron study of ethylene", *J. Phys. Chem. A (Communication)*, **108**, 10035 (2004).
11. C. Y. Ng, "Two-color photoionization and photoelectron studies by combining infrared and vacuum ultraviolet", *J. Electron Spectroscopy & Related Phenomena* (invited review), **142**, 179-192 (2005).
12. Jie Yang, Yuxiang Mo, K. C. Lau, Y. Song, X. M. Qian, and C. Y. Ng, "A combined vacuum ultraviolet laser and synchrotron pulsed field ionization study of BCl<sub>3</sub>", *Phys. Chem. Chem. Phys.* (Special issue for the 85th International Bunsen Discussion Meeting on Chemical Processes of Ions-Transport and Reactivity), **7**, 1518 (2005).
13. X. N. Tang, H. F. Xu, T. Zhang, Y. Hou, C. Chang, C. Y. Ng, Y. Chiu, R. A. Dressler, D. J. Levandier, "A pulsed field ionization photoelectron secondary ion coincidence study of the H<sub>2</sub><sup>+</sup>(X, v<sup>+</sup>=0-15, N<sup>+</sup>=1) + He proton transfer reaction", *J. Chem. Phys.* **122**, 164301 (2005).
14. K. C. Lau and C. Y. Ng, "Accurate *ab initio* predictions of ionization energies of hydrocarbon radicals: CH<sub>2</sub>, CH<sub>3</sub>, C<sub>2</sub>H, C<sub>2</sub>H<sub>3</sub>, C<sub>2</sub>H<sub>5</sub>, C<sub>3</sub>H<sub>3</sub> and C<sub>3</sub>H<sub>5</sub>", *J. Chem. Phys.* **122**, 224310 (2005).
15. T.-S. Chu, R.-F. Lu, K.-L. Han, X.-N. Tang, H.-F. Xu, and C. Y. Ng, "A time-dependent wave packet quantum scattering study of the reaction H<sub>2</sub><sup>+</sup>(v=0-2, 4, 6; j=1) + He → HeH<sup>+</sup> + H", *J. Chem. Phys.* **122**, 244322 (2005).
16. X. N. Tang, Y. Hou, C. Y. Ng, and B. Ruscic, "Pulsed field ionization photoelectron-photoion coincidence study of the process N<sub>2</sub> + hν → N<sup>+</sup> + N + e<sup>-</sup>: Bond Dissociation Energies of N<sub>2</sub> and N<sub>2</sub><sup>+</sup>", *J. Chem. Phys.* **123**, 074330 (2005).
17. M.-K. Bahng, X. Xing, Sun Jong Baek, and C. Y. Ng, "A two-color infrared-vacuum ultraviolet laser pulsed field ionization photoelectron study of NH<sub>3</sub>", *J. Chem. Phys.* **123**, 084311 (2005).
18. M. Hochlaf, T. Baer, X. M. Qian, and C. Y. Ng, "A Photoionization and Pulsed Field Ionization-Photoelectron Study of Cyanogen", *J. Chem. Phys.* **123**, 144302 (2005).
19. Tao Zhang, C. Y. Ng, Chow-Shing Lam, and Wai-Kee Li, "A 193 nm Laser Photofragmentation Time-of-Flight Mass Spectrometric Study of CH<sub>2</sub>ICI", *J. Chem. Phys.* **123**, 174316 (2005).
20. M.-K. Bahng, X. Xing, Sun Jong Baek, X.-M. Qian, and C. Y. Ng, "A combined VUV synchrotron pulsed field ionization-photoelectron and IR-VUV laser photoion depletion study of ammonia", *J. Phys. Chem. A*, web published Dec. 6, 2005.
21. Jingang Zhou, Kai-Chung Lau, Elsayed Hassanein, Haifeng Xu, Shan-Xi Tian, Brant Jones, and C. Y. Ng, "A photodissociation study of CH<sub>2</sub>BrCl in the A-band using the time-sliced velocity ion imaging method", *J. Chem. Phys.* **124**, 034309 (2006).
22. K.-C. Lau and C. Y. Ng, "Accurate *ab initio* predictions of ionization energies and heats of formation for the 2-C<sub>3</sub>H<sub>7</sub>, C<sub>6</sub>H<sub>5</sub>, and C<sub>7</sub>H<sub>7</sub> radicals", *J. Chem. Phys.* **124**, 044323 (2006).
23. P. Wang, H. K. Woo, K. C. Lau, X. Xing, C. Y. Ng, A. S. Zyubin, and A. M. Mebel, "Infrared vibrational spectroscopy of *cis*-dichloroethene in excited Rydberg states", *J. Chem. Phys.* **124**, 064310 (2006).
24. T. Zhang, X. N. Tang, K.-C. Lau, C. Y. Ng, C. Nicolas, D. S. Peterka, M. Ahmed, M. L. Morton, B. Ruscic, R. Yang, L. X. Wei, C. Q. Huang, B. Yang, J. Wang, L. S. Sheng, Y. W. Zhang, and F. Qi, "Direct identification of propargyl radical in combustion flames by VUV photoionization mass spectrometry", *J. Chem. Phys.* **124**, 074302 (2006).
25. K.-C. Lau and C. Y. Ng, "Accurate *ab initio* predictions of ionization energies and heats of formation for the cyclopropenylidene, propargylene and propadienylidene radicals", *Chinese Journal of Chemical Physics* (invited article) **19**, 29-38 (2006).

## Large Eddy Simulation of Turbulence-Chemistry Interactions in Reacting Flows

Joseph C. Oefelein  
Combustion Research Facility  
Sandia National Laboratories  
P.O. Box 969, Mail Stop 9051  
Livermore, California 94551-0969  
E-mail: [oefelei@sandia.gov](mailto:oefelei@sandia.gov)

### Program Scope:

Primary objectives are to apply a unique high-fidelity simulation capability based on the Large Eddy Simulation (LES) technique to a select set of advanced experiments currently under investigation at the Combustion Research Facility (CRF). This research augments existing expertise developed under the DOE Basic Energy Sciences (BES) program in the application of laser-diagnostics to turbulent flames. Key components include implementation of a unique theoretical-numerical framework, development of advanced models aimed at direct closure of detailed chemical mechanisms, rigorous model validation using data acquired from select target experiments, and detailed characterization of complex combustion processes through joint-analysis of data. The goal is to systematically focus on select science-based applications where the combination of LES and experiments can have a direct impact on scientific discovery. Information from validated LES solutions, combined with detailed laser-based experiments on well-defined benchmark cases, present new opportunities to understand the central physics of turbulence-chemistry interactions and for the development of accurate predictive models for advanced combustion systems. Each of the proposed tasks requires considerable high-level expertise, labor, and computational resources and are consistent with a National Laboratory's role of using high-performance computing.

### Recent Progress:

Application of LES provides the formal ability to treat the full range of multidimensional time and length scales that exist in turbulent reacting flows in a computationally feasible manner. The large energetic scales are resolved directly. The small "subgrid-scales" are modeled. This provides a way to simulate the complex multiple-time multiple-length scale coupling between processes in a time-accurate manner and facilitates analysis of all dynamic processes simultaneously. Treating the full range of scales is a critical requirement since phenomenological processes are inherently coupled through a cascade of nonlinear interactions. The baseline theoretical-numerical framework employed at the CRF combines a general treatment of the governing conservation and state equations with state-of-the-art numerical algorithms and massively-parallel programming paradigms. Our focus to-date has been on establishing a credible suite of verification and validation studies aimed at the simultaneous treatment of key turbulence and combustion phenomena typically present in contemporary power and propulsion systems. Recent results are given by Oefelein (2005, 2006a-c), Oefelein et al. 2006 and Segura et al. (2004).

The baseline theoretical-numerical framework combines a general treatment of the governing conservation equations with state-of-the-art numerical algorithms and massively-parallel programming paradigms. The theoretical framework handles both multicomponent and mixture-averaged systems, with a generalized treatment of the equation of state, thermodynamics, and transport processes. It can accommodate high-pressure real-gas/liquid phenomena, multiple-scalar mixing processes, finite-rate chemical kinetics and multiphase phenomena in a fully coupled manner. The current subgrid-scale closure is obtained using the mixed dynamic Smagorinsky model. There are no tuned constants used anywhere in the closure. The scheme has been optimized to account for thermodynamic nonidealities and transport anomalies over a wide range of pressures and temperatures. The numerical formulation treats the fully-coupled compressible form of the conservation equations, but can be evaluated in the incompressible limit using an implicit all-Mach-number time-advancement scheme. This scheme does not require the use of operating splitting methods and provides a fully coupled solution.

A unique dual-time-stepping approach is used with a generalized preconditioning methodology that treats convective, diffusive, geometric, and source term anomalies in an optimal manner. The implicit formulation allows one to set the physical-time step based solely on accuracy considerations. The spatial differencing scheme is optimized for LES using a staggered grid arrangement in generalized curvilinear coordinates. This provides non-dissipative spectrally clean damping characteristics and discrete conservation of mass, momentum and total-energy. The scheme can handle arbitrary geometric features, which inherently dominate the evolution of turbulence. A Lagrangian-Eulerian formulation is employed to accommodate particulates, sprays, or Lagrangian based combustion models, with full coupling applied between the two systems. The algorithm is massively-parallel and has been optimized to provide excellent parallel scalability attributes using a distributed multiblock domain decomposition with generalized connectivity. Distributed-memory message-passing is performed using MPI. This framework has been ported to all major platforms and provides highly efficient fine-grain scalability attributes. Sustained parallel efficiencies above 90-percent have been achieved with jobs as large as 4096 processors on the NERSC IBM SP platform.

The current focal point of our combustion modeling approach is on the direct treatment of reactive scalars and appropriately reduced finite-rate chemical mechanisms. The filtered energy and chemical source terms are closed using a moment-based reconstruction methodology, coupled with a stochastic treatment of fluctuating quantities, to obtain a modeled representation of the local instantaneous scalar field. Model coefficients are evaluated locally in closed form as a function of time and space using the dynamic modeling procedure. In the limit as the grid resolution and time-step approach the smallest relevant scales, contributions from the subgrid-scale models approach zero and the limit of a Direct Numerical Simulation (DNS) is achieved. This type of limiting behavior is highly desirable.

Activities to date have focused on establishing a credible suite of validation studies focused on the simultaneous treatment key phenomena present in typical systems, including wall-bounded three-dimensional flow, unsteady multiphase fluid dynamics, acoustics, transient broadband turbulence, scalar mixing of dense near-critical and supercritical fluid mixtures, high-pressure mixed-mode combustion dynamics, and breakup of hydrocarbon or cryogenic propellants over a wide Mach operating range (subsonic through supersonic). Following are examples of the recent studies conducted, with details provided in the references cited at the end of this document:

#### Premixed Flame Phenomena

As an extension of research currently underway at the CRF, we have begun to develop a joint program that combines high-fidelity LES and detailed experimental diagnostics, with emphasis placed on turbulent swirl-stabilized lean premixed flames. The baseline configuration is a laboratory-scale “dump-combustor.” The design has been optimized to provide non-ambiguous boundary conditions required for the validation of high-fidelity LES simulations while making optimal use of the advanced laboratory and diagnostic capabilities. The burner consists of an annular injector attached to a cylindrical chamber and nozzle assembly. The annular injector is designed to provide an acoustically clean, swirling, fully-developed turbulent profile with a uniform equivalence ratio, flow rate, and diminished wake effects due to the swirler. The cylindrical chamber is designed to provide clean, diagnostically accessible swirling flames without complicating factors such as wall impingement effects. Preliminary calculations have been performed to assist in identifying appropriate canonical studies required to advance our understanding of premixed flame phenomena at device relevant conditions.

#### Sprays and Multiphase Flow

Obtaining high-fidelity solutions of reacting sprays hinges on the application of methods and models that accurately describe momentum coupling and subgrid-scale modulation of turbulence, mass and energy coupling, subgrid-scale scalar mixing, and the combustion processes induced as a consequence. We have recently completed a detailed study aimed at validating LES subgrid-scale models for sprays in the dilute limit. Results were compared to the experimental data acquired by Sommerfeld et al. (International Journal of Heat and Fluid Flow, 12(1): 20-28, 1991; Journal of Fluids Engineering, 114: 648-656, 1992; International Journal of Multiphase Flow, 19(6): 1093-1127, 1993). This experiment provides detailed measurements of

swirling particle-laden flow in a chamber that consists of a sudden pipe expansion with a centered and annular jet discharging into a cylindrical test section. The agreement between the measured and calculated results is excellent and similar agreements have been obtained with respect to the entire experimental data set.

#### High-Pressure (Supercritical) Mixing and Combustion

To improve performance and efficiency, many power and propulsion systems operate at chamber pressures that approach or exceed the thermodynamic critical point of the fuel or oxidizer. Under these conditions, injected liquid jets undergo a transcritical change of state as interfacial fluid temperatures rise above the critical temperature of the local mixture. Several thermodynamic nonidealities and transport anomalies occur as a consequence. To investigate these issues, we have established one of the first quantitative characterizations of the flame structure and associated property variations in LOX–H<sub>2</sub> flames at supercritical pressure. For this situation, diminished inter-molecular forces promote diffusion dominated mixing prior to atomization. Liquid jets vaporize in the presence of exceedingly large thermophysical gradients and diffusion flames evolve as a consequence that are anchored by small but intensive recirculation zones just downstream of the respective injectors. Though continuous, gradients in the flame zone approach the behavior of a contact discontinuity. These phenomena, which are typical in modern gas-turbines and liquid-rockets, have not been considered within current modeling approaches. The goal of the current effort is to begin to quantify key phenomenological and modeling issues that must eventually be considered.

#### Treatment of Shocks and Detonations

As a last example, we have demonstrated that our theoretical-numerical framework can handle complex chemistry and thermophysical coupling over a wide range of conditions, and in particular those associated with detonations. We have performed a set of validation studies focused on a detonation wave in a cylindrical tube. The tube was charged with a stoichiometric mixture of hydrogen and oxygen, with initial conditions of 1 atm and 300 K. A 9-species, 24-step finite rate kinetics mechanism was employed with a generalized treatment of thermodynamic and transport properties. The classical regimes of interest were reproduced.

#### Nonpremixed Flame Phenomena

Our current efforts are a direct extension of joint research being conducted as part of International Workshop on Measurement and Computation of Turbulent Nonpremixed Flames (Barlow 1996-2007, [www.ca.sandia.gov/TNF](http://www.ca.sandia.gov/TNF)). Flames studied as part of this workshop have been selected to address a progression in chemical-kinetic and flow-field complexity. Specific experiments, as well as the overall progression of flames, have been designed to allow separate physical processes and individual submodels to be isolated. For example, a series of H<sub>2</sub> flames with helium dilution allowed detailed evaluation of NO predictions, independent of uncertainties in the radiation model. Jet flames of CO/H<sub>2</sub>/N<sub>2</sub> and CH<sub>4</sub>/N<sub>2</sub>/H<sub>2</sub> have added kinetic complexity while maintaining the simple attached jet-flame geometry. The piloted CH<sub>4</sub>/air jet flames include increasing degrees of localized extinction that tests the ability of models to treat strong interactions of turbulence and chemistry. Turbulent flames that are stabilized by the recirculation zones induced by bluff-bodies or swirling flows add fluid-dynamic complexity that is challenging to current models. Lifted jet flames in vitiated coflow serve to isolate the mixing/chemistry aspects of flame stabilization processes from the complex fluid dynamics of recirculating flows. This systematic progression is essential to the development of robust, predictive, models that have a solid basis in fundamental combustion science. Our major emphasis has been on performing complementary analysis to that currently being pursued by Barlow et al. (see Barlow's abstract). In particular, we are performing detailed calculations of the DLR-Sandia CH<sub>4</sub>/H<sub>2</sub>/N<sub>2</sub> jet flames using a progression of modeling approaches (from flamelet to reduced finite-rate chemistry) and grid resolutions (to within a factor of 4 of the measured Batchelor scale). The simulation incorporates the entire experimental test section and burner geometry using grids on the order of 5-10 million cells. These grids provide resolutions that approach the experimental data.

### **Future Plans:**

Given the current suite of verification and validation studies we have in place, we are now in a position to effectively combine the unique strengths of LES and experiments in an optimal manner. This will allow us to effectively focus on key scientific issues related to turbulence-chemistry interactions at relevant phenomenological conditions. It will also facilitate development and testing of advanced models and bridge the gap between basic research and engineering applications. We will continue to direct our attention toward joint activities being pursued in the Turbulent Combustion Laboratory and the International Workshop on Measurement and Computation of Turbulent Nonpremixed Flames ([www.ca.sandia.gov/TNF](http://www.ca.sandia.gov/TNF)), with emphasis placed on 1) investigating the fine-scale structure of mixture fraction and scalar dissipation fields in turbulent flames, 2) studying the instantaneous three-dimensional flame dynamics and orientation, and 3) investigating the influence of scalar dissipation on species mass fractions and temperature. Establishing a validated matrix of optimally selected studies will have a direct impact on scientific discovery at both the fundamental and applied levels. By following this approach we have a program that is focused on fundamental science in a manner that will directly impact applications of national interest.

### **BES Supported Publications (2004-2006):**

1. Apte, S. V., Mahesh, K., Moin, P. and Oefelein, J. C. (2003). Large eddy simulation of swirling particle-laden flows in a coaxial-jet combustor. *International Journal of Multiphase Flow*, **29**(8): 1311-1331.
2. Chiu, H.-H. and Oefelein, J. C. (2004). Chapter 6: Modeling liquid-propellant spray combustion processes (**invited**). Liquid rocket thrust chambers, aspects of modeling, analysis and design. *AIAA Progress in Astronautics and Aeronautics*, New York, New York.
3. Oefelein, J. C. (2005). Thermophysical characteristics of LOX-H<sub>2</sub> flames at supercritical pressure. *Proceedings of the Combustion Institute*, **30**: 2929-2937.
4. Oefelein, J. C. (2006a). Large eddy simulation of swirling particle-laden flow in a model axisymmetric combustor, *Proceedings of the Combustion Institute*, **31**, accepted.
5. Oefelein, J. C. (2006b). Large eddy simulation of turbulent combustion processes in power and propulsion systems (**invited**). *Progress in Aerospace Sciences*, in print.
6. Oefelein, J. C. (2006c). Mixing and combustion of cryogenic oxygen-hydrogen shear-coaxial jet flames at supercritical pressure. *Combustion Science and Technology*, **178**(1-3): 229-252.
7. Oefelein, J. C., Schefer, R. W. and Barlow, R. W. (2006). Toward validation of large eddy simulation for turbulent combustion (**invited**), *AIAA Journal*, **44**(3) 418-433.
8. Segura, J. C., Eaton, J. K. and Oefelein, J. C. (2004). *Predictive Capabilities of Particle-Laden Large Eddy Simulation*, Technical Report TSD-156, Department of Mechanical Engineering, Stanford University Stanford, California.

### **BES Supported Special Journal Issues (2004-2006):**

1. Special triple issue on Supercritical Fluid Transport and Combustion by J. C. Oefelein and V. Yang (guest editors). *Combustion Science and Technology*, **178**(1-3), 1-621 (20 topical papers), 2006.
2. Special sections on Combustion Modeling and Large Eddy Simulation, Development and Validation Needs for Gas Turbines by F. F. Grinstein, N.-S. Liu and J. C. Oefelein (guest editors). *AIAA Journal*, **44**(3), 417-468 (5 topical papers), and **44**(4), in-print (20 topical papers), 2006.

## KINETICS AND DYNAMICS OF COMBUSTION CHEMISTRY

David L. Osborn  
Combustion Research Facility  
Sandia National Laboratories  
P.O. Box 969, Mail Stop 9055  
Livermore, CA 94551-0969  
Telephone: (925) 294-4622  
E-mail: [dlosbor@sandia.gov](mailto:dlosbor@sandia.gov)

### PROGRAM SCOPE

The goal of this program is to elucidate mechanisms of elementary combustion reactions through the use of optical spectroscopy and mass spectrometry. Several techniques are employed. First, time-resolved Fourier transform spectroscopy (TR-FTS) is used to probe multiple reactants and products with broad spectral coverage ( $> 1000 \text{ cm}^{-1}$ ), moderate spectral resolution ( $0.1 \text{ cm}^{-1}$ ) and a wide range of temporal resolution (ns – ms). The inherently multiplexed nature of TR-FTS makes it possible to simultaneously measure product branching ratios, internal energy distributions, energy transfer, and spectroscopy of radical intermediates. Together with total rate coefficients, this additional information provides further constraints upon and insights into the potential energy surfaces that control chemical reactivity. Because of its broadband nature, the TR-FTS technique provides a global view of chemical reactions and energy transfer processes that would be difficult to achieve with narrow-band laser-based detection techniques.

Second, cavity-enhanced frequency modulation spectroscopy (a.k.a. NICE-OHMS) is used to provide an ultrasensitive, differential absorption spectroscopic probe. We have detected a time-resolved, transient absorption spectrum of the  $\text{NH}_2$  radical using this technique, which opens the door to measurements of chemical kinetics in flow cells and monitoring of species in flames. This cavity-enhanced FM spectroscopy technique provides very high sensitivity, the generality of absorption spectroscopy, and insensitivity to background absorptions that vary slowly with frequency. These advantages allow the suppression of secondary chemistry by increased dilution of reactive species while still retaining sufficient detection sensitivity.

Finally, photoionization mass spectrometry is used to sensitively and selectively probe unimolecular and bimolecular reactions. In the past year, we have brought online a new apparatus, the Multiplexed Chemical Kinetics Photoionization Mass Spectrometer. This apparatus utilizes tunable vacuum ultraviolet light from the Advanced Light Source synchrotron at Lawrence Berkeley National Laboratory for sensitive, isomer specific ionization of reactant and product molecules in chemical reactions.

### RECENT PROGRESS

#### Vinyl Iodide Photodissociation

The vinyl radical ( $\text{C}_2\text{H}_3$ ) is among the simplest unsaturated hydrocarbon free radicals and is an important intermediate in the combustion of aliphatic fuels. Vinyl halides are often used as convenient photolytic precursors to vinyl radicals, but they display interesting differences in thermochemistry and photodissociation dynamics as a function of the halogen

atom in  $C_2H_3X$  ( $X = F, Cl, Br, I$ ). While the first three systems have been studied quite extensively, there is relatively little information on  $C_2H_3I$ , which is the main subject of our study.

There are two product channels possible in  $C_2H_3X$  photodissociation at  $\lambda = 193 - 266$  nm:



The molecular elimination channel producing HX is the only channel observed in  $C_2H_3F$ ,<sup>1</sup> while the channel producing vinyl radicals is the only channel we observe in  $C_2H_3I$ . For the chloride and bromide, both channels are significant. We have studied this system using time-resolved Fourier emission spectroscopy to detect all four possible products in (1a) and (1b). We have measured the spin-orbit branching ratio of  $I / I^*$  using laser photolysis / multiple pass absorption spectroscopy. Finally, we measured the translational energy release and angular distribution of the products using velocity-mapped ion imaging.

A key question in the competition between atomic and molecular elimination is whether the dissociation occurs on the electronic ground or excited state surface(s). Our results, together with electronic structure calculations, highlight two important features of the potential energy surface that govern this branching. First, the degree of coupling between the excited electronic state (which is almost certainly of  $\pi^*\pi$  character) and the ground state changes as a function of the halogen atom. As the halogen atom becomes heavier, increasing overlap between the  $a''$   $p$ -orbital of the halogen and the C-C  $\pi$ -bond makes torsion about this C=C bond more difficult, leading to lower probabilities for internal conversion to the ground electronic state. Second, channel (1a) becomes significantly more exothermic with heavier halogen atoms, while the barriers on the ground electronic state to the elimination of HX are relatively insensitive to X. This change favors channel (1a) as the halogen atoms is changed from  $F \rightarrow Cl \rightarrow Br \rightarrow I$ .

### Time-resolved, ultrasensitive cavity-enhanced frequency modulation spectroscopy

We have built an ultra-sensitive laser absorption spectrometer based on the Noise Immune Cavity Enhanced Optical Heterodyne Molecular Spectroscopy technique (NICE-OHMS) developed by Ye, Hall and coworkers.<sup>2</sup> This technique utilizes frequency modulation (FM) spectroscopy to reduce sources of technical noise, coupled with a high-finesse sample cavity to provide long absorption pathlengths. Although NICE-OHMS is a differential technique, we can calibrate the spectrometer response to enable measurement of absolute absorption cross sections. The minimum detectable absorption is currently  $2 \times 10^{-11} \text{ cm}^{-1} \text{ Hz}^{-1/2}$ .

During the past year we have completed a study of the weak ( $7 \leftarrow 0$ ) vibrational band of NO, measuring intensities of 15 lines of P and R-branch transitions in the  ${}^2\Pi_{1/2} - {}^2\Pi_{1/2}$  sub-band. A vibrational transition moment of  $3.09(6) \mu\text{Debye} \pm 13\%$  and Herman-Wallis coefficients of  $a = -0.0078(26)$  and  $b = 0.00125(45)$  were found by fitting the line intensities. Based on our measured transition moment, and those of other transitions from the literature, a new parameterization for the electric dipole moment function (EDMF) of nitric oxide, valid for  $0.91 \leq r \leq 1.74 \text{ \AA}$ , has been extracted. The residuals of this fit demonstrate that the derived EDMF is the most accurate representation to date of the dipole moment function. The new EDMF will be valuable for accurate intensity prediction of transitions that cannot be easily measured experimentally.

### **The multiplexed chemical kinetics photoionization mass spectrometer**

We have recently completed the first year of experiments on a new photoionization mass spectrometer at the Chemical Dynamics Beamline of the Advanced Light Source (ALS) of LBNL. The chemical reactor is based on the Gutman design,<sup>3</sup> which allows the study of photodissociation and bimolecular reactions at pressures of  $\sim 3 - 10$  Torr and temperatures up to 1000 K.

While the study of chemical kinetics using PIMS is well-established, this apparatus has two unique features that make it especially powerful for chemical kinetics. First, the widely tunable, intense VUV radiation from the ALS enables isomer specific ionization of product species. For example, the ability to distinguish allene from propyne ( $C_3H_4$  isomers) and vinyl alcohol from acetaldehyde ( $C_2H_4O$  isomers) has already been demonstrated in the ALS low-pressure flame chamber.<sup>4</sup>

The second unusual feature of this experiment is the mass spectrometer. We employ a small magnetic sector instrument coupled to a time- and position-sensitive single-ion counting detector. This approach creates a mass spectrometer with 100% duty cycle (like a quadrupole instrument) and the multiplex advantage of measuring a broad range of masses simultaneously (as in time-of-flight spectrometry). This detector also measures the time dependence of each observed reactant and product molecule, which provides kinetic information on the reaction.

Our initial experiments investigated the  $CH_3 + O_2$  and  $C_2H_5 + O_2$  reactions. We succeeded in photoionizing the  $CH_3O_2$  radical, and have made the first measurement of its photoionization efficiency. We observe contributions from both the triplet and singlet electronic states of the cation. In the case of the  $C_2H_5 + O_2$  reaction, the  $C_2H_5O_2$  radical undergoes only dissociative ionization: its parent cation is not stable. The weakening of the  $OO-C_2H_5$  bond in the cation is consistent with the effects of hyperconjugation between the  $\sigma(C_\alpha-O)$  orbital and the  $\sigma(C_\beta-H)$  orbital that lies in the same plane.

### **The $C_3H_3 + C_3H_3 \rightarrow C_6H_6$ reaction**

A topic of substantial current interest is the formation of the first benzene ring in flames, or more generally, the formation of different  $C_6H_6$  isomers. The  $C_3H_3 + C_3H_3$  reaction is believed to be one of the most important reactions involved in the formation of the first aromatic rings in combustion. This reaction has been the focus of several theoretical studies.<sup>5,6</sup> In this reaction many isomeric forms of  $C_6H_6$  are energetically feasible (e.g., benzene, fulvene, 1,2 dimethylenecyclobutene, etc.), and the energy landscape that connects them has been explored theoretically. It is important to know which isomers are produced in each reaction step because some isomers are much more reactive than others, and therefore affect downstream chemistry in different ways. By determining which  $C_6H_6$  isomers are formed as a function of temperature and pressure, we can place experimental constraints on the size of barriers separating the many wells on this multi-dimensional potential surface.

Very recently we have made preliminary measurements at  $P = 4$  Torr and  $T = 305K$  of the propargyl self reaction using the new PIMS apparatus at the ALS. This experiment provides the first direct, time-resolved measurements of the isomer distribution of  $C_6H_6$  produced in this key reaction. The experiments are in rough agreement with the predictions of Miller and Klippenstein. Additional experiments at different  $T$  and  $P$  are planned to make more definitive comparisons.

## Future Directions

Using TR-FTS, we will investigate reactions of the vinyl ( $C_2H_3$ ) and propargyl ( $C_3H_3$ ) radicals to determine product channel identities and energy disposal. We will continue development of transient NICE-OHMS measurements for chemical kinetics. In particular, we plan to change as much of the NICE-OHMS spectrometer to fiber-coupled components as possible, which should increase the reliability and robustness of the apparatus, leading to more frequent utilization of this demanding technique.

One interesting problem to explore using the multiplexed chemical kinetics mass spectrometer apparatus instrument is the reaction  $C_3H_3 + C_2H_2$ . Previous work by Knyazev and Slagle<sup>7</sup> has shown that the initial product ( $C_5H_5$ ) can react with excess acetylene to form  $C_7H_7$ . This process continues to form  $C_9H_8$  and perhaps larger species. Measuring the isomeric forms of these products will provide information critical to the reaction mechanism for this molecular weight growth process.

## BES-sponsored publications, 2004 - present

1. "Time-dependent infrared emission following photodissociation of nitromethane and chloropicrin" E. A. Wade, K. E. Reak, S. L. Li, S. M. Clegg, P. Zou, and D. L. Osborn, *Journal of Physical Chemistry A*, **110**, 4405 (2006).
2. "Measurement of the sixth overtone band of nitric oxide, and its dipole moment function, using cavity-enhanced frequency modulation spectroscopy" J. Bood, A. McIlroy, and D. L. Osborn, *Journal of Chemical Physics*, **124**, 084311 (2006).
3. "The vinyl + NO reaction: determining the products with time-resolved Fourier transform spectroscopy," Peng Zou, Stephen J. Klippenstein, and David L. Osborn, *Journal of Physical Chemistry A*, **109**, 4921 (2005).
4. "Synchrotron photoionization measurements of combustion intermediates: the photoionization efficiency of HONO" C. A. Taatjes, D. L. Osborn, T. A. Cool, and K. Nakajima, *Chemical Physics Letters* **394**, 19 (2004).
5. "On the mechanism of the HCCO + O<sub>2</sub> reaction: Probing multiple pathways to a single product channel" P. Zou and D. L. Osborn, *Physical Chemistry Chemical Physics* **6**, 1697 (2004).

## References

1. <sup>1</sup> B. A. Balko, J. Zhang, Y. T. Lee, *J. Phys. Chem. A*, **101**, 6611 (1997).
2. <sup>2</sup> J. Ye, L. S. Ma, and J. L. Hall, *J. Opt. Soc. Am. B* **15**, 6 (1998).
3. <sup>3</sup> I. R. Slagle and D. Gutman, *J. Am. Chem. Soc.* **107**, 5342 (1985).
4. <sup>4</sup> T. A. Cool, K. Nakajima, T. A. Mostefaoui, F. Qi, A. McIlroy, P. R. Westmoreland, M. E. Law, L. Poisson, D. S. Peterka, and M. Ahmed *J. Chem. Phys.* **22**, 8356 (2003).
5. <sup>5</sup> J. A. Miller and S. J. Klippenstein, *J. Phys. Chem. A*, **105**, 7254 (2001).
6. <sup>6</sup> J. A. Miller and S. J. Klippenstein, *J. Phys. Chem. A*, **107**, 7783 (2003).
7. <sup>7</sup> V. D. Knyazev and I. R. Slagle, *J. Phys. Chem. A* **106**, 5613 (2002).

# ***Large amplitude motion and the birth of novel modes of vibration in energized molecules***

David S. Perry, Principal Investigator  
Department of Chemistry, University of Akron,  
Akron OH 44325-3601  
DPerry@UAkron.edu

## **Introduction**

In the presence of large amplitude motion, a molecular system no longer remains close to a well-defined reference geometry, which challenges the concepts of the traditional theory of molecular vibrations. Among the challenged concepts are normal modes and point group symmetry. The large amplitude coordinate may take on the character of a reaction coordinate along which one must continuously redefine the remaining “normal” coordinates. The consequences are that large amplitude motion can result in novel energy level structures and it can promote coupling between vibrations and hence accelerate intramolecular vibrational energy redistribution (IVR).

In this project, we examine the vibrational level structure and dynamics of molecules with a single internal rotor including methanol, nitromethane, and methylamine. Vibrational fundamental and overtone spectra of the jet-cooled molecules are examined by cavity ringdown, FTIR spectroscopy, and photofragment spectroscopy (IRLAPS). The ringdown experiments are done in our lab in Akron; the jet-FTIR is done in collaboration with Robert Sams at Pacific Northwest Labs (PNNL); the IRLAPS experiments are done in Thomas Rizzo’s lab at the EPFL in Switzerland. To understand the level structures and the vibrational mode coupling, we analyze high-resolution spectra, develop quantum mechanical models of the nuclear motion, and probe the potential surface with *ab initio* calculations.

### **A. IVR as a Non-adiabatic Effect in the CH Stretch – Torsion Manifold of Methanol.**

In previous work under this project,<sup>1</sup> we discovered the inverted torsional tunneling splitting in the asymmetric CH stretch vibrational states ( $\nu_2=1$  and  $\nu_9=1$ ). These results were successfully explained by our 4-dimensional model calculation that included the three CH stretch coordinates and the torsion.<sup>2</sup> Torsional motion interchanges the identities of the CH bonds *anti* and *gauche* to the OH, and the CH bonds in these positions have different force constants. A single lowest-order coupling term with the required symmetry ( $A_1$  in  $G_6$ ) was sufficient to reproduce the observed torsional structure. The inverted torsional structure is a general phenomenon that derives from molecular symmetry and the single coupling term results in a many mixed vibrational states throughout the CH stretch-torsion manifold. Subsequent spectroscopic reports<sup>3</sup> of other asymmetric vibrations have confirmed the generality of the effect, and a number of theoretical studies<sup>4</sup> have contributed to our understanding.

Fehrensen, Luckhaus, Quack, Willeke, and Rizzo<sup>5</sup> have used *ab initio* calculations, an adiabatic (Born-Oppenheimer-like) separation of the torsion from the other vibrations, and the concept of geometric phase to account for the torsional structure of excited methanol vibrational states. This insightful treatment gives an appealing conceptual unity with electronic spectroscopy and provides a criterion for when such inverted torsional structure should be expected. We have been able to use our fully coupled 4-D model to test the limits of applicability of the adiabatic approximation and to explore the non-adiabatic effects.

In this adiabatic approximation, the CH stretches are the “fast” degrees of freedom solved at each torsional angle, and the “slow” degree of freedom is torsion motion in the effective potential defined by

the CH stretch vibrations. By definition, such an approximation does not allow exchange of energy between the torsion and the CH stretch vibrations. Such energy transfer (IVR) is therefore a non-adiabatic effect. Even though our model contains only a single coupling term in the local-mode – free-rotor basis, the same Hamiltonian, when expressed in the adiabatic basis, contains a myriad of off-diagonal IVR coupling matrix elements. In agreement with Pearman and Gruebele<sup>7</sup>, we find that the scaling behavior of torsionally-mediated IVR is such that the coupling strength falls off only slowly ( $a = 0.3 - 0.5$ ) with increasing coupling order. This scaling behavior dictates a more important role for direct high-order coupling in the presence of large-amplitude torsional motion than in more rigid molecules. Our model calculations indicate that the extended high-order coupling derives fundamentally from the form of the torsional potential and the nature of the 1-dimensional torsional motion and is therefore expected to be general property of torsional molecules.

At high energies, our model reveals new patterns of approximate torsion-vibration degeneracies: (i) At high torsional energy but low CH stretch excitation, the  $\nu_2$  and  $\nu_9$  normal modes merge into an E-type degenerate asymmetric stretch, which is combined with the degenerate free internal rotation. (ii) At high CH stretch but low torsion, torsional tunneling is quenched (Fig. 1) and the three CH normal modes morph into two distinct local modes  $\nu_a$  and  $\nu_b$ . (iii) When both are highly excited, the two local CH stretches converge to a triply degenerate local mode that combines with free internal rotation to yield six-fold near-degeneracies.

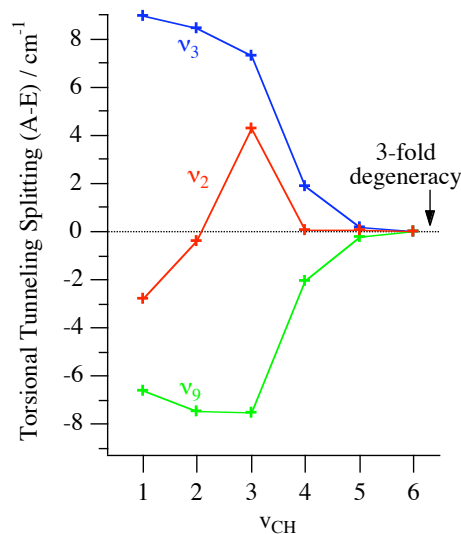


Fig. 1. Torsional tunneling in methanol is quenched at high CH stretch excitation.

## B. Multistage Torsion-Vibration-Rotation Coupling in the $\nu_6$ NO Stretch of Nitromethane

In nitromethane ( $\text{CH}_3\text{NO}_2$ ), the planarity of the heavy atoms results in a very low ( $2 \text{ cm}^{-1}$ ) 6-fold torsional barrier. Thus, we have the opportunity to extend the stretch-torsion model discussed above to this new situation. Slit-jet FTIR spectra from PNNL have enabled detailed rotational assignments of the lowest 4 internal-rotation states of the  $\nu_6$  asymmetric NO stretch. The comparison of the observed pattern of the torsional levels with our model calculation indicates that the torsion-vibration coupling parameter in nitromethane is much smaller than in methanol. We also find that the rotational lines of lowest torsional state ( $m=0$ ) are each fragmented into clumps of 3 – 6 transitions, which are the spectroscopic signature of IVR. Because of a favorable combination of spectroscopic parameters, we are able to follow each IVR interaction as a function of  $J$ ,  $K_a$ , and  $K_c$ , and thereby assign each as anharmonic or Coriolis type  $a$ ,  $b$ , or  $c$ . Four stages of vibration-torsion-rotation coupling are identified: (i) sub-picosecond  $c$ -axis Coriolis coupling to a torsionally excited state dark vibration ( $\nu_7+\nu_{10}$  or  $\nu_5$ ), (ii)  $a$ -axis Coriolis coupling between  $A_1'$  and  $A_2'$  torsional states of the dark vibration, (iii)  $c$ -axis Coriolis coupling of the dark vibration back to dark rotational states of the  $\nu_6$  N-O stretch, and (iv) at  $J'=8$  and higher an additional strong coupling to a second torsionally excited dark vibration.

## C. Conformational Dependence of IVR in Methanol

Methanol molecules with one or two quanta of torsional excitation have a significant probability of being at or near the eclipsed conformation, whereas molecules without torsional excitation have geometries near the minimum energy (staggered) conformation. In previous work,<sup>8</sup> we have recorded and assigned IRLAPS spectra representing the direct excitation of torsionally excited states in the OH manifold. This capability has made it possible to study the conformational dependence of IVR in the OH

overtone manifold of methanol. Results for staggered and partially eclipsed methanol excited to the OH stretch overtone  $5\nu_1$  are presented in Fig. 2.

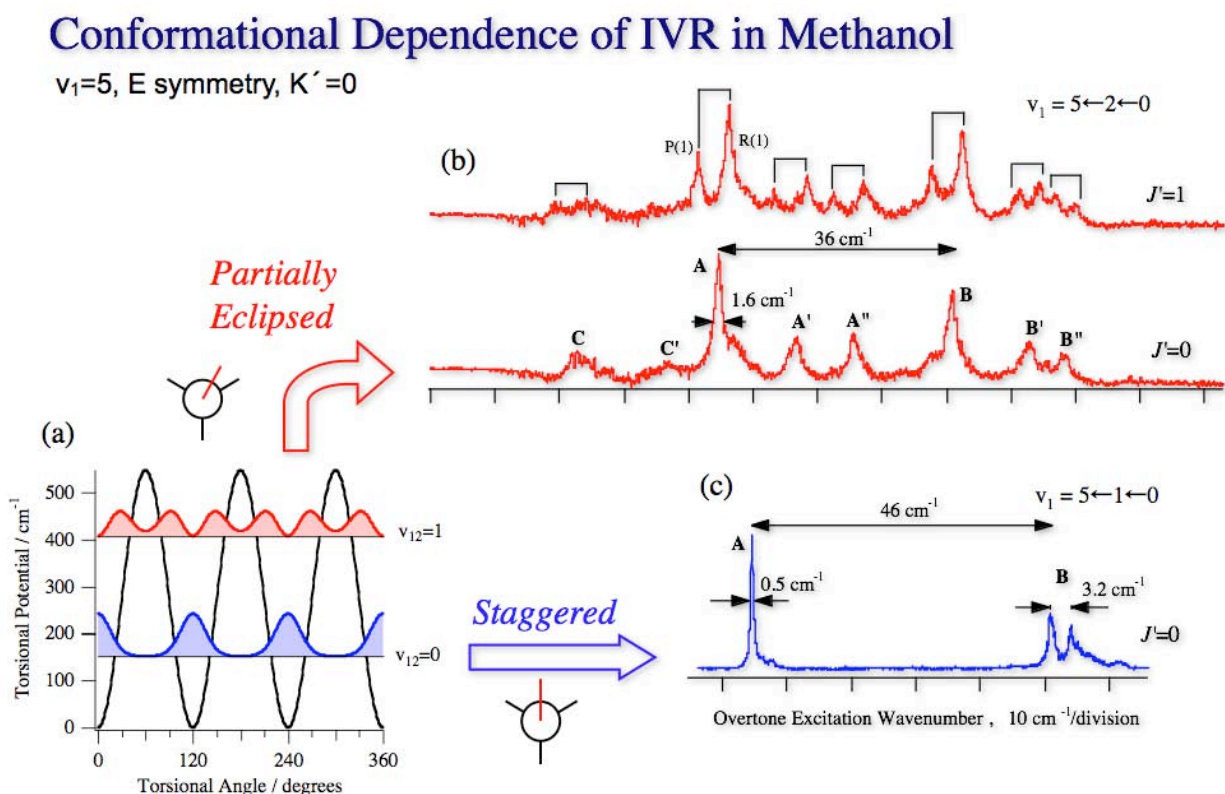


Fig. 2. (a) Calculated torsional angle probability distribution of the lowest two torsional states in methanol in the  $\nu_1=5$  vibrational state. (b) Spectra of partially eclipsed methanol. (c) Spectra of staggered methanol.

Our previous IRLAPS spectra of the OH overtones (Fig. 2(c)) showed structure on three frequency scales, which was interpreted in terms of three IVR timescales. The fastest timescale, which corresponds to the  $46 \text{ cm}^{-1}$  splitting in Fig 2(c), is the coupling of the OH overtone  $5\nu_1$  with the CH combination  $4\nu_1+\nu_2$ . In the partially eclipsed conformation, the splitting is reduced to  $36 \text{ cm}^{-1}$ , which means that the OH – CH coupling has become slower than in the staggered conformation. We believe that this change can be explained by the misalignment of the atomic orbitals involved in coupling the OH bond to the *anti* CH bond. In contrast, the narrowest features in the partially eclipsed methanol spectra are broader than in staggered methanol. This indicates that the third timescale, which corresponds to coupling to a dense manifold of dark vibrational states, is faster.

#### Plans for the Next Year

Our continuous-wave cavity ringdown technique (CW-CRDS) was developed and tested on the OH ( $\nu_1$ ) + CH ( $\nu_3$ ) stretch combination band of methanol between  $6510$  and  $6550 \text{ cm}^{-1}$  [2]. In order to test the concepts, presented in section A. above, at a higher level of CH stretch excitation, this technique will be extended to the CH overtone region ( $2\nu_{\text{CH}}$ ). For this purpose a new laser source, a CW PPLN OPO, has been acquired and a CW slit jet is under construction. The PPLN OPO has both broader tunability and narrower bandwidth than the previously used external cavity diode laser; however scanning and control are much more complicated and will require a significant developmental effort. The CW jet will allow the much higher data collection rates needed for extensive high resolution scans.

Analysis of the data outlined in the sections above will continue and manuscripts will be prepared for publication.

### Cited References

- <sup>1</sup> L.-H. Xu, X. Wang, T. J. Cronin, D. S. Perry, G. T. Fraser, and A. S. Pine, *J. Mol. Spectrosc.* **185**, 158 (1997).
- <sup>2</sup> X. Wang and D. S. Perry, *J. Chem. Phys.* **109**, 10795 (1998).
- <sup>3</sup> R. M. Lees and L.-H. Xu, *Phys. Rev. Lett.* **84**, 3815 (2000).
- <sup>4</sup> J. T. Hougen, *J. Mol. Spectrosc.* **181**, 287 (1997); J. T. Hougen, *J. Mol. Spectrosc.* **207**, 60 (2001); M. A. Tamsamani, L.-H. Xu, and D. S. Perry, *Can. J. Phys.* **79**, 467 (2001).
- <sup>5</sup> B. Fehrensen, D. Luckhaus, M. Quack, M. Willeke, and T. R. Rizzo, *J. Chem. Phys.* **119**, 5534 (2003).
- <sup>6</sup> D. Madsen, R. Pearman, and M. Gruebele, *J. Chem. Phys.* **106** (14), 5874 (1997).
- <sup>7</sup> R. Pearman and M. Gruebele, *Z. Phys. Chem. (Muenchen)* **214** (11), 1439 (2000).
- <sup>8</sup> D. Rueda, O. V. Boyarkin, T. R. Rizzo, I. Mukhopadhyay, and D. S. Perry, *J. Chem. Phys.* **116** (1), 91 (2002).

### Publications from this Project, 2003-2006

- [1] L. Wang, Y.-B. Duan, R. Wang, G. Duan, I. Mukhopadhyay, D.S. Perry, K. Takagi, Determination of reduced Hamiltonian parameters for the CD<sub>3</sub>OH isotopomers of methanol, *Chem. Phys.*, **292**, 23-29, (2003).
- [2] Shucheng Xu, Jeffrey J. Kay, and David S. Perry, Doppler-limited CW infrared cavity ringdown spectroscopy of the  $\nu_1+\nu_3$  OH+CH stretch combination band of jet-cooled methanol, *J. Mol. Spectrosc.* **225**, 162-173 (2004).
- [3] David Rueda, Oleg V. Boyarkin, Thomas R. Rizzo, Andrei Chirokolava and David S. Perry, Vibrational overtone spectroscopy of jet-cooled methanol from 5,000 to 14,000 cm<sup>-1</sup>, *J. Chem. Phys.*, **122**, 044314 (2005).

# INVESTIGATION OF NON-PREMIXED TURBULENT COMBUSTION

Grant: DE-FG02-90ER14128

Stephen B. Pope  
Sibley School of Mechanical & Aerospace Engineering  
Cornell University  
Ithaca, NY 14853  
pope@mae.cornell.edu

## 1 Scope of the Research Program

The focus of the current work is on the development of computational approaches which allow our detailed knowledge of the chemical kinetics of combustion to be applied to the modeling and simulation of combustion devices. In the past year, the work has been focused in three general areas: PDF model calculations of the Barlow & Frank non-premixed turbulent jet flames; application of the *in situ* adaptive tabulation (ISAT) algorithm to the efficient calculation of laminar flames; and investigations of dimension reduction of combustion chemistry.

## 2 Recent Progress

The principal research results from this program are described in the publications listed in the final Section. Some of these results are highlighted in the following subsections.

### 2.1 Investigation of non-premixed piloted jet flames

The Barlow & Frank piloted methane/air jet flames (flames D, E, and F) are designed to examine the important processes of extinction and reignition. It is a challenge for turbulent combustion models to account accurately for these phenomena. We have performed two studies, both based on PDF method calculations, in which the importance of chemical mechanisms and turbulent mixing models are examined.

In the first study (Cao & Pope 2005), seven different chemical mechanisms for methane are used in PDF model calculations of the Barlow & Frank flames D, E and F in order to investigate the ability of these mechanisms to represent the local extinction and reignition observed in these flames. The mechanisms studied range from a 5-step reduced mechanism to the GRI3.0 mechanism which involves 53 species. As in several other recent studies, we use the PDF method based on the joint probability density function of velocity, turbulence frequency and composition. Extensive tests are performed to ensure the numerical accuracy of the calculations, to relate them to previous calculations based on the same model, and to re-examine the sensitivity of the calculations (especially of flame F) to uncertainties in the pilot temperature and the treatment of radiation.

As has been observed in other studies of laminar and turbulent non-premixed flames, we find that the GRI3.0 mechanism overpredicts the levels of  $NO$ , typically by a factor of two. Apart from this, the GRI3.0 and GRI2.11 mechanisms yield comparably good agreement with the experimental data for all three flames, including the level of local extinction and the conditional means of major and other minor species. Two augmented reduce mechanisms (ARM1 and ARM2) based on GRI2.11 and containing 16 and 19 species are slightly less accurate; while the 5-step reduced mechanism and two  $C_1$  skeletal mechanisms containing 16 species display significant inaccuracies. An examination of the autoignition and laminar-flame behavior of the different mechanisms confirms (with some exceptions) expected trends: there is an association between long ignition delay times, small extinction strain rates, and high levels of local extinction. This study again demonstrates the ability of the joint PDF method to represent accurately the strong turbulence-chemistry interactions in these flames, and it clarifies the necessary level of description of the chemical kinetics.

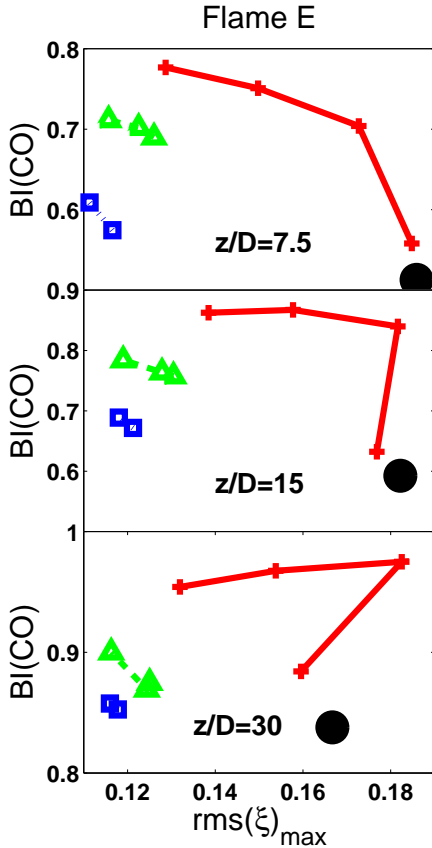


Figure 1: Burning indexes of  $CO$  against the maximum r.m.s. of mixture fraction  $\xi$  obtained using the EMST, IEM, and MC mixing models. The solid circles represent the experimental data (Barlow & Frank) and lines with symbols represent the PDF calculations using different mixing models: red solid with plus: EMST; green dashed with triangle: IEM; blue dotted with square: MC.

In the second study (Cao *et al.* 2006) further PDF model calculations (using GRI3.0) are performed of the Barlow & Frank flames in order to investigate the performance of three commonly-used turbulent mixing models. These models are the IEM (interaction by exchange with the mean), MC (modified Curl), and EMST (Euclidean minimum spanning tree) mixing models. In each of these models, the rate of mixing is controlled by the model constant  $C_\phi$ . It is found that all three models are capable of yielding levels of local extinction (quantified by a burning index) comparable to the experimental observations, but this is achieved using  $C_\phi = 3.3$  for IEM, and  $C_\phi = 3.8$  for MC (compared to  $C_\phi = 1.5$  for EMST). However, in these calculations with IEM and MC, the mixture fraction variance is significantly underpredicted: only the EMST model is capable of calculating both the observed burning indexes and the mixture fraction variance.

This finding is demonstrated in Fig.1, which shows the burning index based on  $CO$  plotted against the peak value of the r.m.s. of mixture fraction at three axial locations. The experimental data are shown as the single point at each axial location, whereas, for each mixing model, the calculations correspond to a curve parameterized by the value of  $C_\phi$ . Blow-off occurs shortly after the lowest points shown. As may be seen, only the EMST mixing model is capable of yielding both the correct values of burning index and of mixture fraction r.m.s.

## 2.2 Implementing ISAT for efficient flame computations with detailed chemistry.

The *in situ* adaptive tabulation algorithm (ISAT, Pope 1997) is a storage/retrieval methodology which can greatly speed up the chemistry calculations involved in the computation of reactive flows. The method has been effectively used in PDF method calculations (e.g., Cao *et al.* 2006) in which the chemistry and mixing are separated into different fractional steps. The works of Singer, Pope and Najm (2006a,b) apply ISAT to the calculation of laminar flames with detailed chemistry and transport.

This work is a collaboration between Cornell and Sandia, in which the ISAT algorithm is combined with the **dflame** code of Najm, which implements the operator-splitting scheme of Najm & Knio (2004). This is accomplished through a Strang sub-splitting method which further separates the reaction processes

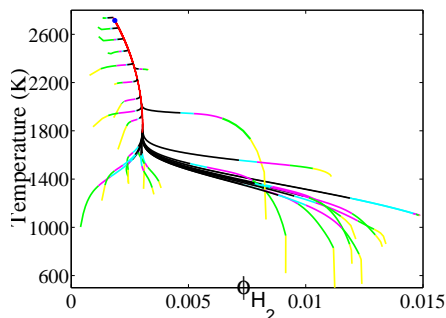


Figure 2: Projection onto the temperature-hydrogen plane of the reaction trajectories for the  $H_2$ /air system. The initial compositions are chosen randomly from the composition space and have the same amount of elements and enthalpy. Each trajectory is colored by the dimension of the attracting manifold. Yellow: 6-dimensional; green: 5-dimensional; magenta: 4-dimensional; cyan: 3-dimensional; black: 2-dimensional; red: 1-dimensional; blue: 0-dimensional. The blue dot is the equilibrium point.

from transport processes. For the pure reaction sub-steps, the adaptive tabulation scheme ISAT is used which makes use of a stiff ODE solver. The non-stiff equations in the sub-splitting scheme are computed using a single-stage, second-order Runge-Kutta scheme. The scheme is then applied to a one-dimensional laminar premixed methane-air flame propagation problem with detailed chemistry. For this problem, second-order temporal convergence is demonstrated and results are compared with those obtained using the original **df**lame code. The impact of the ISAT error tolerance on solution accuracy is demonstrated and it is shown that solution error can be controlled by changing the ISAT tolerance. The CPU time savings obtained by using ISAT rather than direct integration (DVODE) is examined. It is found that with GRI3.0, after an initial ISAT table build-up, the use of ISAT speeds the reaction sub-steps of the computations by roughly a factor of 13 and the overall scheme achieves a speed-up of approximately 7.5. For problems involving more complex chemistry and flow conditions, greater speed-ups are anticipated.

In Singer *et al.* (2006b) this work is extended to unsteady two-dimensional flames using parallel processing. The scheme was applied to the case of a laminar flame front interacting with a counter-rotating vortex-pair: this configuration has been studied extensively both experimentally and numerically and the results obtained here are consistent with previous work. ISAT performance was examined and compared to that of the original DVODE-based scheme. Here it was found that the ISAT scheme provides an overall code speed-up of approximately 2.5-3.

### 2.3 Dimension reduction of combustion chemistry

In numerical simulations of combustion processes, the use of dimension reduction to simplify the description of the chemical system has the advantage of reducing the computational cost, but it is important also to retain accuracy and adequate detail. Most existing dimension reduction methods assume the existence of low-dimensional attracting manifolds in the full composition space and try to approximate or directly identify the low-dimensional attracting manifolds. However, questions remain about the geometry of the reaction trajectories in the full composition space, the existence of the low-dimensional attracting manifolds in low-temperature regions, and the minimum dimension of the attracting manifold required for describing a particular chemical system. These issues are addressed by Ren & Pope (2006) for  $H_2$ /air and  $CH_4$ /air systems.

An interesting result of this work is shown in Fig. 2. Reaction trajectories for the  $H_2$ /air system are obtained by integrating the ordinary differential equations given by the chemical kinetics (at fixed pressure and enthalpy) from many different initial conditions, all of the same elemental composition. The figure shows these trajectories projected only the plane of temperature and specific moles of  $H_2$ . Given that enthalpy, pressure and elements are conserved, there are 6 degrees of freedom in the system. The color coding along the trajectories gives the “effective” dimension (initially 6) along the trajectory. As may be seen, the dimension progressively decreases along the trajectories until the (zero-dimensional) point of chemical equilibrium is reached.

## 3 Future Plans

Current work and that in the immediate future is focused on two topics. The first is to extend our dimension-reduction investigations to more complex fuels. So far we have applied the ICE-PIC method

(Ren *et al.* 2006) to hydrogen and methane, with up to 35 species. We shall proceed to apply ICE-PIC to skeletal *n*-heptane mechanisms with of order 200 species. Second, we are developing computationally efficient implementation of “local” turbulent mixing models, starting with VCIEM (velocity-conditioned interaction by exchange with the mean). Such conditioning arises in several current models and has a strong physical basis. However, it poses challenges to numerical implementations which we are addressing.

## 4 Publications from DOE Research 2004-2006

1. R.W. Bilger, S.B. Pope, K.N.C. Bray and J.F. Driscoll (2005) “Paradigms in Turbulent Combustion Research,” Proceedings of the Combustion Institute, **30**, 21–42. (Plenary lecture at the Thirtieth International Symposium on Combustion.)
2. R. Cao and S.B. Pope (2005) “The influence of chemical mechanisms on PDF calculations of non-premixed piloted jet flames,” *Combustion and Flame* **143**, 450–470.
3. R.R. Cao, H. Wang and S.B. Pope (2006) “The effect of mixing models in PDF calculations of piloted jet flames,” Proceedings of the Combustion Institute, **31** (to be published).
4. B.J.D. Liu and S.B. Pope (2005) “The Performance of *In Situ* Adaptive Tabulation in Computations of Turbulent Flames,” *Combustion, Theory & Modelling* **9**, 549–568.
5. K. Liu, S.B. Pope and D.A. Caughey (2005) “Calculations of Bluff-Body Stabilized Flames using a Joint PDF Model with Detailed Chemistry,” *Combustion and Flame* **141**, 89–117.
6. S. B. Pope (2004) “Accessed Compositions in Turbulent Reactive Flows”, *Flow, Turbulence and Combustion* **72**, 219–243.
7. S.B. Pope (2004) “Gibbs function continuation for the stable computation of chemical equilibrium,” *Combustion and Flame* **139**, 222–226.
8. S.B. Pope (2004) “Advances in PDF Methods for Turbulent Reactive Flows,” in *Advances in Turbulence X*, H.I. Andersson and P.-A. Krogstad (Eds.), CIMNE, pp. 529-536.
9. S.B. Pope (2005) “Computational modeling of turbulent flames,” in *Frontiers of Computational Fluid Dynamics 2006*, World Scientific Publishing.
10. Z. Ren and S.B. Pope (2004) “An investigation of the performance of turbulent mixing models.” *Combustion and Flame* **136**, 208–216.
11. Z. Ren and S.B. Pope (2004) “Entropy production and element conservation in the quasi-steady-state approximation,” *Combustion and Flame* **137**, 251–254.
12. Z. Ren and S.B. Pope (2005) “Species reconstruction using pre-image curves,” Proceeding of the Combustion Institute, **30**, 1293–1300.
13. Z. Ren and S.B. Pope (2006) “The geometry of reaction trajectories and attracting manifolds in composition space,” *Combustion Theory and Modelling* (to be published).
14. M.A. Singer and S.B. Pope (2004) “Exploiting ISAT to solve the equations of reacting flow,” *Combustion Theory and Modelling* **8**, 361–383.
15. M.A. Singer, S.B. Pope and H.N. Najm (2006a). “Operator-Splitting with ISAT to Model Reacting Flow with Detailed Chemistry,” *Combustion, Theory & Modelling* (to be published).
16. M.A. Singer, S.B. Pope and H.N. Najm (2006b) “Modeling unsteady reacting flow with operator-splitting and ISAT,” *Combustion and Flame* (submitted).

## OPTICAL PROBES OF ATOMIC AND MOLECULAR DECAY PROCESSES

S.T. Pratt  
Building 200, B-125  
Argonne National Laboratory  
9700 South Cass Avenue  
Argonne, Illinois 60439  
E-mail: spratt@anl.gov

### PROJECT SCOPE

Molecular photoionization and photodissociation dynamics can provide considerable insight into how energy and angular momentum flow among the electronic, vibrational, and rotational degrees of freedom in isolated, highly energized molecules. This project involves the study of these dynamics in small polyatomic molecules, with an emphasis on understanding the mechanisms of intramolecular energy flow and determining how these mechanisms influence decay rates and product branching ratios. It is also aimed at understanding how internal energy can influence photoionization cross sections. The experimental approach combines double-resonance laser techniques, which are used to prepare selected highly excited species, with mass spectrometry, ion-imaging, and high-resolution photoelectron spectroscopy, which are used to characterize the decay of the selected species. Additional techniques, including vuv photoionization, excited-state absorption spectroscopy by fluorescence-dip techniques, and zero-kinetic energy-photoelectron spectroscopy are also used.

### RECENT PROGRESS

In the past year, we have focused on using a combination of ion imaging and vuv single-photon ionization to probe the internal energy dependence of the relative photoionization cross sections of a number of small free radicals. This work is important because vuv photoionization is increasingly being used to detect products of photodissociation and reactive scattering, as well as to characterize species in flames, and because the internal energy dependence of the ionization cross sections has not been characterized. This work builds on the approach discussed by Gross et al.<sup>1</sup> to address the internal energy dependence of the photoionization cross section of the 2-butyl radical at 157 nm. It is also similar in spirit to experiments by Neumark and coworkers<sup>2,4</sup> in which vuv photoionization of momentum matched fragments produced by photodissociation was used to determine absolute photoionization cross sections of a number of radicals.

In a typical experiment, a suitable precursor is photodissociated giving rise to the radical of interest and an atomic fragment. In some cases, the photodissociation dynamics, along with the internal energy distribution of the radical fragment, have been previously characterized. In other cases, ionization of the atomic fragment by single- or resonant multi-photon ionization, followed by ion imaging, allows the determination of the total translational energy,  $P(E_T)$ . Using the conservation of energy, a knowledge of the photon energy and the bond dissociation energy yields the internal energy distribution of the radical,  $P(E_{int})$ . Single-photon ionization and ion imaging of the radical fragment can then be used to extract a second distribution,  $P_R(E_T)$ , as well as  $P_R(E_{int})$ . Unlike the  $P(E_T)$  distribution determined from the atomic fragment, the radical distribution does not necessarily reflect the true  $P(E_T)$  distribution, because each value of  $E_T$  corresponds to a different internal energy of the radical, and the photoionization cross section may depend on this internal energy. Thus,  $P_R(E_{int})$  corresponds to the true  $P(E_{int})$  weighted by the

internal-energy dependent, relative photoionization cross section of the radical,  $\sigma(E_{\text{int}})$ . As a result, knowledge of  $P(E_{\text{int}})$ , along with a determination of  $P_{\text{R}}(E_{\text{int}})$ , allows the extraction of  $\sigma(E_{\text{int}})$ .

Initial work focused on the photodissociation of  $\text{CH}_3\text{I}$  and  $\text{CF}_3\text{I}$  and the photoionization of  $\text{CH}_3$  and  $\text{CF}_3$ . The ground states of  $\text{CH}_3$  and  $\text{CH}_3^+$  are both planar and have similar geometries, suggesting that ionization would preserve the internal energy of the neutral and that the photoionization cross section near threshold would not depend strongly on internal energy. The imaging experiments fulfilled these expectations. In contrast, because the ground state of  $\text{CF}_3$  is pyramidal and the ground state of  $\text{CF}_3^+$  is planar, it was expected that excitation of the umbrella mode in the  $\text{CF}_3$  would produce a strong dependence of the photoionization cross section on internal energy. Previous studies suggested that excited vibrational levels of the umbrella mode of  $\text{CF}_3$  were significantly populated in the near uv photodissociation of  $\text{CF}_3\text{I}$ . Somewhat surprisingly, although our imaging studies did show significant vibrational excitation of the  $\text{CF}_3$ , in agreement with previous studies, the photoionization cross section showed no internal energy dependence. Recent calculations by Bowman et al.<sup>5</sup> have shown convincingly that previous assignments of the umbrella and symmetric stretching vibrational modes of  $\text{CF}_3$  were incorrect and should be reversed. These calculations then imply that the vibrational excitation observed in both the present and previous experiments corresponds to the symmetric stretch and not the umbrella mode. This reassignment provides an explanation for the lack of internal energy dependence of the photoionization cross sections, because the symmetric stretch is not expected to improve the overlap between the pyramidal  $\text{CF}_3$  and the planar cation. This reassignment also suggests that models for the photodissociation dynamics of  $\text{CF}_3\text{I}$  should be re-examined.

Similar studies have now been performed on the internal energy dependence of the relative photoionization cross sections of a number of additional free radicals including ethyl, n-propyl, i-propyl, allyl, and propargyl. In these studies, the internal energy, and thus the density of states, is sufficiently high that individual vibrational levels cannot be resolved in the  $P(E_{\text{int}})$  distributions; nevertheless, information can still be gained on the internal energy dependence of the cross section. Two themes appear to emerge from these studies.

(1) Often for hot radicals, very little internal energy dependence of the photoionization cross section is observed. This is a result of a number of factors, two of which are mentioned here. For simplicity, it is assumed that the photoionization cross section is primarily determined by the summed Franck-Condon factors between a given initial state and all of the energetically accessible ionic levels at the photon energy. The first factor is that the internal energy can be distributed among both the vibrational and rotational degrees of freedom of the radical, which has the effect of smearing out any dependence of the cross section on vibrational energy. The second factor is that for high internal energy, intramolecular vibrational energy redistribution (IVR) will often be important, and spread the vibrational excitation throughout all the vibrational modes of the molecule. A strong internal energy dependence is only expected for Franck-Condon active vibrations whose character changes significantly upon ionization. The number of these is generally relatively small and, as a result of IVR, the average population in these modes will tend to be relatively small. As a result, any internal energy dependence of the cross section for those specific modes will tend to be smeared out by averaging with other modes.

(2) In some cases, the detection efficiency of very hot radicals significantly reduced even if the neutral radical is stable. Often, the dissociation pathways for the corresponding cations have significantly lower thresholds than the neutral radical. Thus, if a significant fraction of the internal energy of the neutral

radical is preserved upon ionization, the ion may have sufficient energy to dissociate, leading to loss of the parent ion signal. Thus, even "soft" ionization near threshold can result in fragmentation of sufficiently hot radicals. Of course, fragmentation of the parent ion will produce a signal at the daughter ion mass, and thus allow it to be taken into account.

## FUTURE PLANS

Our immediate plans are to continue our imaging studies of the internal energy dependence of relative photoionization cross sections of selected free radicals. We intend to focus on smaller radicals with lower levels of vibrational excitation. In such systems, it should be possible to resolve the vibrational levels of the ion in the imaging experiments, and thus gain more detailed information on the photoionization cross sections. We will also pursue the possibility of recording images as a function of wavelength, thus enabling us to multiplex the recording of photoionization spectra for different initial vibrational levels. We are currently in the process of analyzing our initial results from such experiments on vibrationally excited methyl radicals. In the coming year we are also planning to use vuv light for the pump transition in double-resonance experiments on some small polyatomic molecules such as H<sub>2</sub>O and NH<sub>3</sub>. This approach will allow us to perform experiments using intermediate states that are difficult to study with multiphoton pump transitions. (Double-resonance experiments can be difficult with a multiphoton pump step because the intensity of the pump beam often saturates the ionization of the intermediate level.)

In the past year, we have focused on characterizing the internal energy dependence of the photoionization cross sections of a number of different hydrocarbon radicals, and as a result, construction of a new apparatus to allow slice imaging and photoelectron imaging was postponed. Progress on the construction of this machine is expected in the coming year. This imaging electron spectrometer will provide an important complement to the magnetic bottle electron spectrometer currently in use. Imaging studies of superexcited states that undergo both autoionization and predissociation are planned, and the ability to examine both the ionization and dissociation processes in a complementary manner should be particularly revealing.

I will continue to collaborate with Christian Jungen on theoretical models of vibrational autoionization in polyatomic molecules. We are working to extend our earlier study of simple polyatomic molecules to situations involving degenerate electronic states. In particular, we are currently working on a paper that shows how to extract information about autoionization rates for triatomic molecules from spectroscopic information on the Renner-Teller interactions in low-lying Rydberg states.

## References

1. R. L. Gross, X. Liu, and A. G. Suits, *Chem. Phys. Lett.* **362**, 229 (2002).
2. J. C. Robinson, N. E. Sveum, and D. M. Neumark, *J. Chem. Phys.* **119**, 5311 (2003).
3. J. C. Robinson, N. E. Sveum, and D. M. Neumark, *Chem. Phys. Lett.* **383**, 601 (2004).
4. N. E. Sveum, S. J. Gonchev, and D. M. Neumark, *Phys. Chem. Chem. Phys.* **8**, 592 (2006).
5. J. M. Bowman, X. Huang, L. B. Harding, and S. Carter, *Mol. Phys.* **104**, 33 (2006).

This work was supported by the U.S. Department of Energy, Office of Science, Office of Basic Energy Sciences, Division of Chemical Sciences, Geosciences, and Biosciences, under Contract W-31-109-Eng-38.

## DOE-SPONSORED PUBLICATIONS SINCE 2004

1. S. T. Pratt  
PHOTOIONIZATION OF EXCITED STATES OF MOLECULES  
Radiation Physics and Chemistry, **70**, 435 (2004).
2. P. Bell, F. Aguirre, E. R. Grant, and S. T. Pratt  
MODE-DEPENDENT VIBRATIONAL AUTOIONIZATION OF RYDBERG STATES OF NO<sub>2</sub>.  
II. COMPARING THE SYMMETRIC STRETCHING AND BENDING VIBRATIONS  
J. Chem. Phys., **120**, 2667-2676 (2004).
3. W. L. Glab and S. T. Pratt  
ION ROTATIONAL DISTRIBUTIONS FOLLOWING VIBRATIONAL AUTOIONIZATION  
OF RYDBERG STATES OF WATER  
J. Chem. Phys., **120**, 8555-8566 (2004).
4. Patrice Bell, F. Aguirre, E. R. Grant, S. T. Pratt  
STATE-SELECTIVE PRODUCTION OF VIBRATIONALLY EXCITED NO<sub>2</sub><sup>+</sup> BY DOUBLE-  
RESONANT PHOTOIONIZATION  
J. Phys. Chem. A, **108**, 9645-9651 (2004).
5. F. Aguirre and S. T. Pratt  
PHOTOIONIZATION AND PHOTODISSOCIATION DYNAMICS OF THE B <sup>1</sup>Σ<sub>u</sub><sup>+</sup> AND  
C <sup>1</sup>Π<sub>u</sub> STATES OF H<sub>2</sub> and D<sub>2</sub>  
J. Chem. Phys., **121**, 9855-9864 (2004).
6. S. T. Pratt  
VIBRATIONAL AUTOIONIZATION IN POLYATOMIC MOLECULES  
Ann. Rev. Phys. Chem., **56**, 281-308 (2005).
7. F. Aguirre and S. T. Pratt  
PHOTOIONIZATION OF VIBRATIONALLY HOT CH<sub>3</sub> AND CF<sub>3</sub>  
J. Chem. Phys. **122**, 234303 (2005) (13 pages).
8. L. R. McCunn, D. I. G. Bennett, L. J. Butler, H. Fan, F. Aguirre, and S. T. Pratt  
PHOTODISSOCIATION OF PROPARGYL CHLORIDE AT 193 NM  
J. Phys. Chem. A. **110**, 843-850 (2006).
9. Haiyan Fan and S. T. Pratt  
PHOTOIONIZATION OF HOT RADICALS: C<sub>2</sub>H<sub>5</sub>, n-C<sub>3</sub>H<sub>7</sub>, and i-C<sub>3</sub>H<sub>7</sub>  
J. Chem. Phys. **123**, 204301 (2005).
10. Haiyan Fan and S. T. Pratt  
NEAR THRESHOLD PHOTOIONIZATION OF HOT ISOPROPYL RADICALS  
J. Chem. Phys. **124**, 114312 (2006).
11. Haiyan Fan and S. T. Pratt  
PHOTODISSOCIATION OF PROPARGYL BROMIDE AND  
PHOTOIONIZATION OF PROPARGYL RADICAL  
J. Chem. Phys. in press (2006).

## Photoinitiated Reactions of Radicals and Diradicals in Molecular Beams

Hanna Reisler

Department of Chemistry, University of Southern California

Los Angeles, CA 90089-0482

reisler@usc.edu

### Program Scope

Open shell species such as radicals and diradicals are central to reactive processes in combustion and environmental chemistry. Hydroxyalkyl radicals and carbenes are important, because cleavage of C-H and O-H bonds is implicated in reactions of atoms and radicals with alcohols and alkanes. For the alkoxy  $\leftrightarrow$  hydroxyalkyl and hydroxycarbene  $\leftrightarrow$  aldehyde structural isomers, competition between isomerization and dissociation on the ground potential energy surface (PES) may be significant. Our long-term goal is to investigate the dynamics of predissociation of free radicals for which multiple pathways, including molecular rearrangements, compete. The chosen systems are amenable to treatment by high-level theory. The detailed measurements on simple systems will serve as benchmarks that will be extended to larger systems in a homologous series.

### Recent Progress

#### I. Overtone Predissociation of CH<sub>2</sub>OH via Tunneling

In our 2005 DOE abstract we reported on the action spectroscopy of the third overtone of the OH stretch of CH<sub>2</sub>OH obtained by monitoring H photofragments. Because this radical decomposes to H + CH<sub>2</sub>O with an activation barrier calculated at 14,000-16,000 cm<sup>-1</sup>, it was remarkable that we could pump the reaction coordinate directly up to at least 13,600 cm<sup>-1</sup>. Below we report additional results that establish the predissociation mechanism.

##### (a) Hydrogen fragment yield spectra of CH<sub>2</sub>OH and CD<sub>2</sub>OH

Following excitation of the hydroxymethyl radical in the region of the third overtone, 4v<sub>1</sub>, no depletion or double-resonance ionization signals were observed, in contrast to the rather large signals observed when exciting to the 1v<sub>1</sub> - 3v<sub>1</sub> states. As the energy of 4v<sub>1</sub> is well above the thermochemical threshold for dissociation to H + CH<sub>2</sub>O, the detection method was switched to monitoring hydrogen fragments. The spectra could be fit with band origins of 13,598 cm<sup>-1</sup> and 13,617 cm<sup>-1</sup> for CH<sub>2</sub>OH and CD<sub>2</sub>OH, respectively. The linewidth was  $\sim$  1.3 cm<sup>-1</sup> for both. No D fragment signal could be detected from CD<sub>2</sub>OH. The pump laser frequency was scanned over a range of  $\pm$  600 cm<sup>-1</sup> around the third overtone transition but transitions other than the OH stretch overtone could not be identified. Thus, the OH overtone transitions appear to be well localized up to 4v<sub>1</sub> and their Birge-Sponer plot is linear.

##### (b) Time-of-flight (TOF) analysis of hydrogen fragments

One concern in carrying out overtone excitation is that the observed dissociation signal is due to a 2-photon transition to a low-lying excited electronic state mediated by the overtone transition. In the case of CH<sub>2</sub>OH this would be the 3s(2A') state, whose one-

photon onset is at  $\sim 26\,000\text{ cm}^{-1}$ . In order to evaluate the contribution of 1- and 2-photon processes, TOF analysis of the hydrogen translational energy was carried out.

Figure 1 shows TOF spectra of hydrogen fragments obtained from  $\text{CH}_2\text{OH}$  for two pump laser frequencies: (a) one-photon excitation at  $\sim 27,000\text{ cm}^{-1}$ , where dissociation from the  $3s$  state gives rise to fast H atoms, and (b) excitation to the  $4v_1$  state. The arrows mark the position of the maximum (minimum) TOF for H atoms allowed in this case. In trace (b) the arrows correspond to the maximum H-atom translational energy allowed in pumping the third overtone for  $D_0(\text{CH}_2\text{O-H})=1.19\text{ eV}$ . We conclude that excitation to the  $4v_1$  level leads to predissociation and that the contribution of vibrationally-mediated photodissociation from  $3s$  is negligible. TOF measurements carried out for hydrogen fragments from  $\text{CD}_2\text{OH}$  gave similar results. The absence of signal from D-fragments indicates that isomerization is not important.

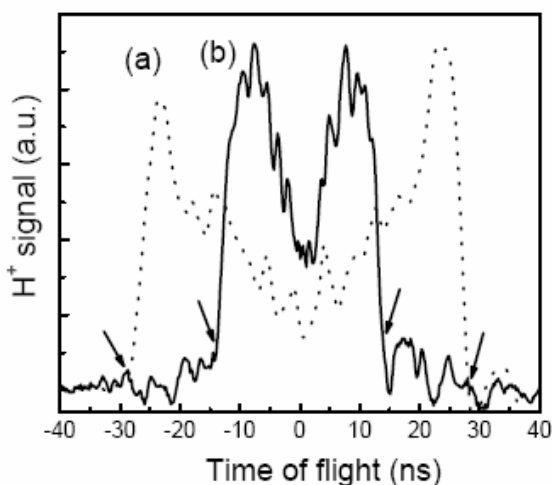


Fig. 1: Time of flight spectra of H fragments produced in the dissociation of  $\text{CH}_2\text{OH}$  by one photon excitation at (a)  $27,210\text{ cm}^{-1}$ ; and (b)  $13,605\text{ cm}^{-1}$ . Zero TOF indicates no recoil energy. The arrows show the maximum and minimum values allowed by the thermochemistry for one-photon dissociation.

The similarity of the spectral linewidths in  $\text{CH}_2\text{OH}$  and  $\text{CD}_2\text{OH}$  suggests that lifetime broadening is dominant and the rates of the unimolecular processes in the two species are similar. The linear Birge-Sponer plot indicates that the reaction barrier to direct OH bond fission is higher than the  $4v_1$  energy. Therefore, fragmentation must take place by tunneling through the O-H dissociation barrier. This process may be treated to a first approximation as a one-dimensional semiclassical tunneling through an Eckart potential. If we assume that the linewidth results only from lifetime broadening and use an imaginary frequency of  $1712\text{ cm}^{-1}$  (as calculated by Larry Harding),<sup>1</sup> we obtain a dissociation barrier of  $15,200\text{ cm}^{-1}$ , close to the calculated values of  $14,000\text{--}16,000\text{ cm}^{-1}$ .

## II. Electronic Spectroscopy of the Hydroxyethyl Radical

The ionization energy of the hydroxyethyl radical,  $\text{CH}_3\text{CHOH}$ , is much lower than that of the hydroxymethyl radical ( $6.85$  vs.  $7.50\text{ eV}$ ); therefore, its Rydberg states are expected to lie lower in energy. In work in progress we have used REMPI and H-photofragment yield spectroscopy to assign the electronic spectrum of the radical and compare the assignments to calculations that take into account quantum defects for Rydberg states. Using 2+2 REMPI, we identified a progression of broad bands separated by  $\sim 1600\text{ cm}^{-1}$ , which in analogy with the narrower bands observed in the hydroxy-

methyl radical, were assigned to the CO-stretch progression (see Fig. 2). The band origin was found at 309 nm ( $32,300\text{ cm}^{-1}$ ), close to the 296 nm predicted by assuming the same quantum defect value as for the  $3p_z$  state of  $\text{CH}_2\text{OH}$ . Thus, we assign the upper state of the observed REMPI transition of the hydroxyethyl radical as the  $3p_z$  state.

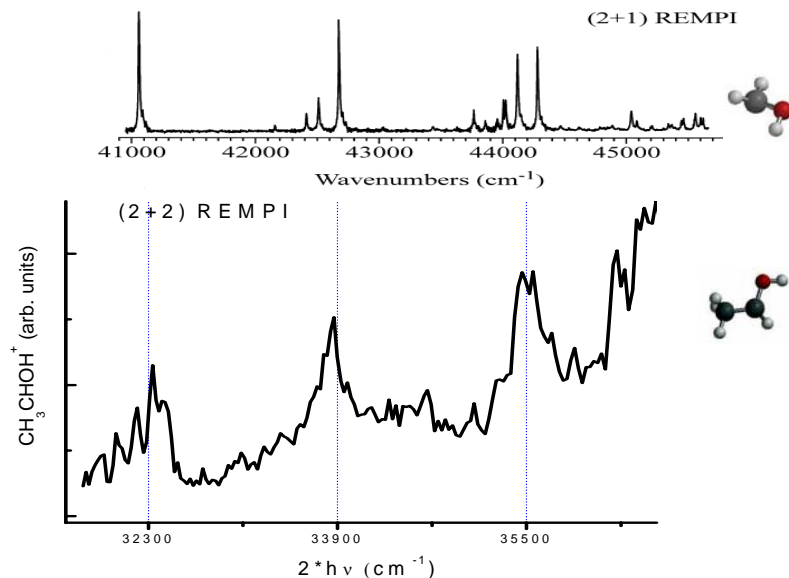


Fig. 2. REMPI spectrum of the hydroxyethyl radical (bottom trace) compared to that of the hydroxymethyl radical excited to the  $3p_z$  state (upper trace). Note the progression of  $\sim 1600\text{ cm}^{-1}$ , which is similar in both radicals. Also notice the greater lifetime broadening in hydroxyethyl.

The  $3s$  state of hydroxyethyl is predicted to lie around 537 nm, assuming a quantum defect identical to  $\text{CH}_2\text{OH}$  ( $3s$ ). As with  $\text{CH}_2\text{OH}$ , no REMPI spectrum could be detected in the region of  $3s$ , because dissociation is too fast. By using H-photofragment yield spectroscopy, the onset of the absorption to the  $3s$  state was found at 520 nm ( $19,200\text{ cm}^{-1}$ ). The quantum defects for the  $3p_z$  states of hydroxymethyl and hydroxyethyl radicals are 0.65 and 0.72, respectively, whereas for the  $3s$  state, the corresponding values are 1.23 and 1.21. Recently, Krylov and coworkers calculated the energies of low-lying Rydberg states in a homologous series of hydrocarbon radicals derived from vinyl, and showed a dependence of the quantum defects of the different  $p$  Rydberg states on changes in charge distributions in the ion core.<sup>2</sup> We will analyze differences in quantum defects in hydroxyalkyl radicals using similar considerations.

Dynamical studies are also in progress. For these studies we use partially deuterated hydroxyethyl radicals. Our preliminary results show that near the origin of the transition to the  $3s$  state, only the OH bond is broken, whereas at higher energies, the C-H bond is broken as well. Experiments to determine whether isomerization to ethoxy takes place are underway.

### III. Photoelectron Imaging and REMPI Spectroscopy of Diazomethane

In our attempts to develop efficient sources of methylene radicals in molecular beams, we have considered diazomethane as a potential precursor. We developed a procedure to prepare diazomethane safely and transport it to the molecular beam without decomposition. We also developed sensitive diagnostics of diazomethane by using a well-

resolved 2+1 REMPI transition via an upper Rydberg state, which we assign as  $2^1A_2(3p)$ . The  $2^1A_2(3p) \leftarrow 1^1A_1$  transition, which was not seen in the absorption spectrum obtained by Merer,<sup>3</sup> is forbidden in one-photon but allowed in two-photon absorption.

In order to characterize the vibronic spectrum of diazomethane in this region ( $\sim 53,000 \text{ cm}^{-1}$ ), we use photoelectron imaging from selected vibronic states. The photoelectron images show that the  $2^1A_2(3p)$  state is mostly of Rydberg character, but several of the vibronic states are coupled to other states. These couplings are shown clearly as additional rings in the photoelectron images obtained by ionizing the excited state and also as velocity-dependent photoelectron angular distributions. In collaboration with Anna Krylov and her student Lucasz Koziol, we identified one perturber as the Rydberg  $1^1B_1(3p)$  state. These studies are ongoing and demonstrate the advantage of combining REMPI with excited-state photoelectron imaging in assigning electronic spectra and unraveling dynamics and nonadiabatic interactions. Our next step is to assess diazomethane as a source of methylene radicals.

### Future Work

In the future we plan to finish our work on the dynamics of  $\text{CH}_3\text{CHOH}$  on the ground and excited electronic states and extend the work to other hydroxyalkyl radicals, such as  $\text{CH}_2\text{CH}_2\text{OH}$  and hydroxypropyl. Our emphasis is on elucidating the roles of conical intersections and isomerization. We will also finish our study on the two-photon spectroscopy and dynamics of diazomethane and characterize its photolysis and pyrolysis as possible sources of methylene in the lowest singlet and triplet states. Work on the photodissociation dynamics of small carbenes will then begin.

### References

1. L. Harding, private communication.
2. L. Koziol, S.V. Levchenko and A.I. Krylov, *J. Phys. Chem. A.*, in press (2006).
3. Merer, A.J. *Can. J. Phys.* 42, 1242 (1964).

### Publications, 2003-2005

Competitive C–H and O–D bond fission channels in the UV photodissociation of the deuterated hydroxymethyl radical ( $\text{CH}_2\text{OD}$ ), L. Feng, A. V. Demyanenko, and H. Reisler, *J. Chem. Phys.* **120**, 6524-6530 (2004).

Rotationally resolved infrared spectroscopy of the hydroxymethyl radical ( $\text{CH}_2\text{OH}$ ), L. Feng, J. Wei, and H. Reisler, *J. Phys. Chem. A*, **108**, 7903 (2004).

Photodissociation of the  $3p_z$  state of the hydroxymethyl radical ( $\text{CH}_2\text{OH}$ ):  $\text{CH}_2\text{O}$  and  $\text{HCOH}$  products, L. Feng and H. Reisler, *J. Phys. Chem. A.*, **108** (45): 9847-9852 (2004).

## High Accuracy Calculation of Electronic Structure, Molecular Bonding and Potential Energy Surfaces

Klaus Ruedenberg

Ames Laboratory USDOE, Iowa State University, Ames, Iowa, 50011  
ruedenberg@iastate.edu

### Scope

Essential for the theoretical treatment of molecular reactions, dynamics, kinetics, spectra and other problems is the accurate knowledge of potential energy surfaces – not only at those geometries where a system is in equilibrium, i.e. at the minima, but also in other coordinate space regions that are traversed during reactive geometry changes. The major impediment in achieving high accuracy (i.e. better than a kcal/mol) in these regions is the difficulty of describing the non-relativistic electron correlations. For systems involving several atoms other than hydrogen, this has so far been achieved only for molecules at equilibrium geometries. Along reaction paths, difficulties arise because the effectiveness of most current methods is tied to the dominance of a *single* configuration in the wavefunction, a feature that is lost on many reaction paths and at kinetically important transition states of combustion reactions. The configuration interaction method reported here offers a way to overcome this difficulty.

### Recent Results

Recently, we have developed a new *ab initio* approach for calculating full CI energies with greater efficiency than had been previously possible: The *correlation energy extrapolation by intrinsic scaling (CEEIS)*, whereby such energies become accessible in cases where that did not used to be possible. It is configuration-interaction based and complemented by a complete basis set extrapolation as well as relativistic corrections. Applications to C<sub>2</sub>, N<sub>2</sub>, O<sub>2</sub>, F<sub>2</sub> have yielded the dissociation energies of these molecules within one kcal/mol of the experimental values. The enthalpy of formation of water was obtained with an error of 0.03 kcal/mol.

We have now demonstrated that the method is also effective in achieving high accuracy in the energy along a reaction path where the dominant zeroth-order reference function is multi-configurational and undergoes marked changes in its composition.

Specifically, we have calculated the potential energy curve of F<sub>2</sub> at a dozen points along its entire dissociation path. From them, we determined an analytic representation in the novel form of an even-tempered Gaussian expansion, augmented by a long-range  $r^{-6}$  decay, by a least-mean-squares fit with a root-mean-square deviation of 0.1 millihartree (See the figure below). We calculated the vibrational spectrum of this potential energy curve using the discrete-variable-representation method. The agreement between these theoretical and the experimental spectroscopic values of Colbourn, Dagenais, Douglas and Raymonda (1976), which is exhibited in the table below, for the first time achieves wavenumber accuracy by an *ab-initio* approach for systems of this size: The dissociation energy is obtained within 28 cm<sup>-1</sup> of the spectroscopic value, which itself has an uncertainty of  $\pm 50$  cm<sup>-1</sup>. The 23 observed energy levels are obtained with a mean absolute deviation of 0.9 cm<sup>-1</sup> from the experimental values. The corresponding 23 rotational constants B<sub>v</sub> are obtained with a mean absolute deviation of 0.0015 cm<sup>-1</sup> from the experimental values. At least two additional vibrational levels are predicted.

The analysis also yields a spectroscopic determination of the coefficient  $C_6$  of the long-range ( $r^{-6}$ ) dispersion term. It is found within less than 10% of the value previously deduced from a frequency integration of the atomic polarizability of fluorine, calculated by a time-dependent density functional method (Chu and Dalgarno, 2004).

### Future Work

The CEEIS method will be applied to reaction paths of other dissociations and reactions. The method will be adapted to the treatment of core-related correlations. The use of localized orbitals will be developed for the treatment of larger reactive systems.

### Publications in 2004, 2005, 2006

*Molecule Intrinsic Minimal Basis Sets. I. Exact Resolution of Ab-Initio Optimized Molecular Orbitals in terms of Deformed Atomic Minimal-Basis Orbitals.*

W.C. Lu, C.Z. Wang, M.W. Schmidt, L. Bytautas, K.M. Ho, K. Ruedenberg  
J. Chem. Phys. **120**, 2629-2637 (2004)

*Molecule Intrinsic Minimal Basis Sets. II. Bonding Analyses for  $Si_4H_6$  and  $Si_2$  to  $Si_{10}$ .*

W. C. Lu, C. Z. Wang, M. W. Schmidt, L. Bytautas, K. M. Ho, K. Ruedenberg  
J. Chem. Phys. **120**, 2638-2651 (2004)

*Exact Representation of Electronic Structures in Crystals in Terms of Highly Localized Quasiatomic Minimal Basis Orbitals.*

W. C. Lu, C. Z. Wang, T. L. Chan, K. Ruedenberg, and K. M. Ho  
Phys. Rev. B **70**, 04110(R) (2004)

*Correlation Energy Extrapolation Through Intrinsic Scaling. I. Method.*

L. Bytautas and K. Ruedenberg  
J. Chem. Phys. **121**, 10905 (2004)

*Correlation Energy Extrapolation Through Intrinsic Scaling II. Nitrogen and Water.*

L. Bytautas and K. Ruedenberg  
J. Chem. Phys., **121**, 10919 (2004)

*Correlation Energy Extrapolation Through Intrinsic Scaling III. Compact Wavefunctions.*

L. Bytautas and K. Ruedenberg  
J. Chem. Phys. **121**, 10852 (2004)

*Correlation Energy Extrapolation Through Intrinsic Scaling. IV. Accurate Binding Energies of the Homonuclear Diatomic Molecules  $C_2$ ,  $N_2$ ,  $O_2$  and  $F_2$ .*

L. Bytautas and K. Ruedenberg  
J. Chem. Phys. **122**, 154110 (2005)

*Transferability of the Slater-Koster Tight-Binding Scheme from a First-Principles Perspective.*

W. C. Lu, C. Z. Wang, K. Ruedenberg and K. M. Ho,  
Phys. Rev. B **72**, 205123 (2005).

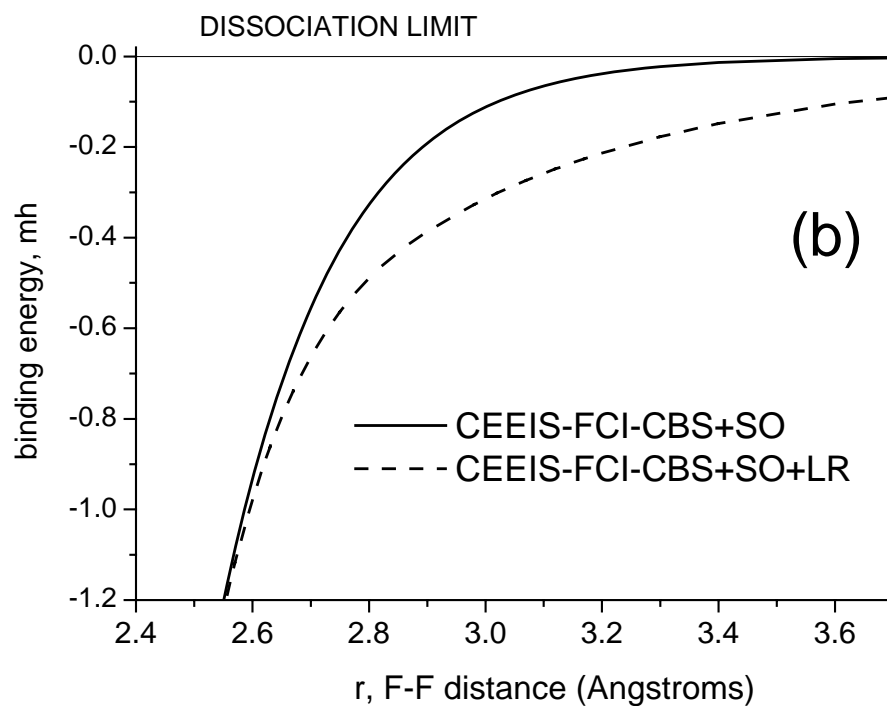
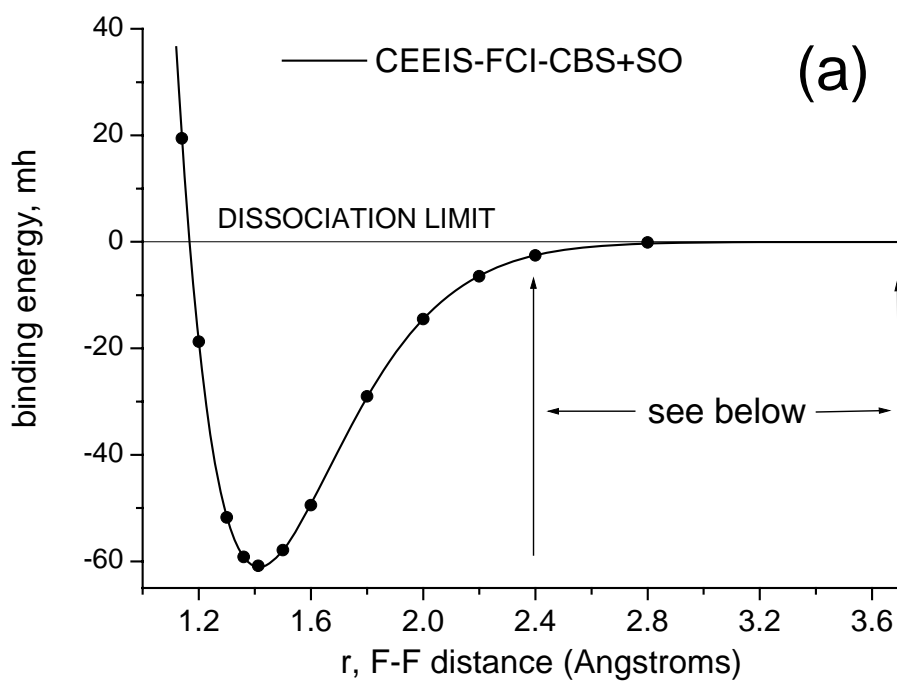
*Correlation Energy Extrapolation Through Intrinsic Scaling. V. Electronic Energy, Atomization Energy and Enthalpy of Formation of Water.*

L. Bytautas and K. Ruedenberg  
J. Chem. Phys. accepted for publication

*Full ab initio Determination of the Potential Energy Curve and the Vibrational Energy Spectrum of  $F_2$  to Wavenumber Accuracy by a New Quantum Chemical Method*

L. Bytautas, N. Matsunaga, T. Nagata, M. S. Gordon, K. Ruedenberg  
Phys. Rev. Letts. submitted for publication

v	Vibrational levels of F <sub>2</sub>			Rotational constants of F <sub>2</sub>		
	Experiment	Theory	Δ	Experiment	Theory	Δ
0	0.00	0.00	0.00	0.8833	0.8799	0.0034
1	893.90	893.91	0.01	0.8696	0.8672	0.0024
2	1764.15	1764.14	-0.01	0.8560	0.8541	0.0019
3	2610.22	2610.12	-0.10	0.8423	0.8407	0.0016
4	3431.53	3431.25	-0.28	0.8284	0.8268	0.0016
5	4227.43	4226.89	-0.54	0.8142	0.8124	0.0018
6	4997.19	4996.36	0.83	0.7996	0.7975	0.0021
7	5740.05	5738.93	-1.12	0.7844	0.7821	0.0023
8	6455.17	6453.82	1.35	0.7685	0.7661	0.0024
9	7141.63	7140.18	-1.45	0.7518	0.7493	0.0025
10	7798.48	7797.10	-1.38	0.7343	0.7318	0.0025
11	8424.67	8423.58	-1.09	0.7156	0.7135	0.0021
12	9019.11	9018.51	-0.60	0.6958	0.6941	0.0017
13	9580.63	9580.67	0.04	0.6747	0.6736	0.0011
14	10108.02	10108.68	0.66	0.6522	0.6518	0.0004
15	10599.62	10601.00	1.38	0.6282	0.6283	-0.0001
16	11053.90	11055.83	1.93	0.6025	0.6030	-0.0005
17	11468.96	11471.11	2.15	0.5750	0.5753	-0.0003
18	11842.62	11844.36	1.74	0.5449	0.5445	0.0004
19	12172.25	12172.58	0.33	0.5094	0.5097	-0.0003
20	12452.98	12451.88	-1.10	0.4711	0.4690	0.0021
21	12678.00	12676.13	-1.88	0.4185	0.4173	0.0012
22	12830.38	12830.46	0.08	0.3365	0.3365	0.0000
23	-	12902.86	-	0.2402	0.2402	
24	-	12934.12	-	0.0964	0.0964	
25	-	12945.90	-	0.0964	0.0964	
ZPE	455.51	455.37	-0.14			
DI sSE	12918.88±50	12948.15	29.27			



- Panel (a) : The twelve ab-initio calculated energies (solid dots) and the fitted analytic (eventempered Gaussian) potential energy curve of  $F_2$ .
- Panel (b) : Enlargement of the long-range region. Solid line: The same curve as in (a)  
Dashed line: Potential energy curve including the long-range augmentation.

## Active Thermochemical Tables – Progress Report

Branko Ruscic

Chemistry Division, Argonne National Laboratory,  
9700 South Cass Avenue, Argonne, IL 60439  
ruscic@anl.gov

### Program Scope

The *spiritus movens* of this program is the need to provide the scientific community with accurate and reliable thermochemical, spectroscopic and structural information on chemical species that are relevant in energy-producing processes, such as combustion, or play prominent roles in the related post-combustion environmental chemistry, thus contributing to the global comprehension of the underlying chemical reactions and/or providing benchmark values for test and development of advanced theoretical approaches. The program has recently developed a novel approach that aims to optimally extract the knowledge content from thermochemically relevant measurements and hence produce not only *the best currently available* thermochemical values for the target species, but also provide *critical tests of new experimental or theoretical data*, as well as develop *pointers to future determinations that will most efficiently improve the thermochemical knowledge base*. The experimental portion of this program uses photoionization mass spectrometry and related methods to study ephemeral species that are produced *in situ* using various suitable techniques. The effort of this program is coordinated with related experimental and theoretical efforts within the Argonne Chemical Dynamics Group to provide a broad perspective of this area of science.

### Recent Progress

#### Development of Active Thermochemical Tables and the Core (Argonne) Thermochemical Network

Active Thermochemical Tables (ATcT) are a new paradigm of how to derive accurate, reliable, and internally consistent thermochemical values that properly reflect all the available thermochemically-relevant knowledge, and are becoming the archetypal approach to thermochemistry in the age of cyber science. The current development of ATcT has several related components: The conceptual advances in the underlying approach to thermochemistry, and the construction and evaluation of the Core (Argonne) Thermochemical Network, together with the resulting delivery of new thermochemistry for stable and ephemeral species are a direct product of this project (funded by DOE BES), while the accompanying computer-science developments involved in bringing to life a practical instance of ATcT as a web-service was highly leveraged by an additional funding source (DOE MICS).

As opposed to traditional sequential thermochemistry, ATcT is based on the Thermochemical Network (TN) approach. The TN approach allows a thorough statistical analysis of the available knowledge, solving it for the desired thermochemical properties of all the target species simultaneously. The TN Graph is constructed by utilizing the multitude of all available thermochemically-relevant experimental determinations. This is followed by a statistical analysis of the TN that critically examines its self consistency. The goal of the statistical analysis is to isolate “optimistic” uncertainties that may have been associated with some of the original determinations and that invariably occur in practice for a long list of reasons. The statistical evaluation of the knowledge present in the TN is made possible by the very nature of the thermochemical interdependencies embodied in the TN, which are in practice manifested both as competing determinations and alternate thermochemical cycles through the TN. Once the TN is statistically evaluated and adjusted to be self-consistent, it is utilized by ATcT to simultaneously produce the thermochemistry of all the target chemical species. For further details on the ATcT approach please consult Ruscic et al., *J. Phys. Chem. A*, **108**, 9979, (2004); for a more succinct description see B. Ruscic, *Active Thermochemical Tables*, in: *2004 Yearbook of Science and Technology*, McGraw-Hill, 2004, pp 3.

The ATcT suite consists of the ATcT Kernel and the underlying data libraries. While additional

commodity features are still under development, the current ATcT Kernel is at a sufficiently mature stage to perform all the necessary manipulations of the TN Graph and produce new thermochemistry. Except for several minor bug (nuisance, not miscomputation) fixes, the Kernel did not undergo any other changes during the past year.

The principal part of the development effort was focused on fortifying the Core (Argonne) Thermochemical Network, C(A)TN, which is the central data library of ATcT and the source of new and improved thermochemical values from ATcT. During the past year, C(A)TN (current ver. 1.056) has grown to encompass ~700 species linked by ~6000 thermochemically relevant determinations. While the growth in the number of species was a quite substantial ~40% in a year, the number of determinations spanning the TN Graph was expanded by a rather impressive factor of ~2.4. The primary reason for this somewhat disproportional growth is that the central focus of our effort at this point of development is not so much on simply expanding the coverage of C(A)TN, as much as fortifying and polishing the knowledge content of the TN Graph for the extant species. A substantial fraction of new links in the TN Graph comes from targeted composite theoretical computations that are now conveniently available using commodity computers (G3, G3//B3LYP, CBS-Q, CBS-QB3, CBS-APNO, W1); these computations serve as the routine core definition for gaseous species and add to the redundancy of C(A)TN that is one of the needed ingredients for the high performance of ATcT. Thus, we are finalizing the results for a number of related chemical species. We are currently in the process of writing up a string of several papers that will report the newly derived ATcT thermochemistry for these species (grouped in convenient sets amenable to congruent and correlated scientific discussion). HO<sub>2</sub> and the related NO and NO<sub>2</sub> have just appeared in press, and other manuscripts (N, NO<sub>x</sub>, C, CH<sub>n</sub>, etc.) will be prepared shortly. In the interim, the latest unpublished thermochemical values for any species currently contained in the Core (Argonne) TN (together with referencing instructions that provide links to archived sets of values) will continue to be available (and quotable) as private communication(s) by contacting the PI via e-mail.

We have also embarked on a process of refurbishing the polynomialized Burcat's Thermochemical Library for Combustion (extensively used around the world by Chemkin users and other modelers) and assimilating it as one of the Auxiliary ATcT Libraries. In collaboration with A. Burcat (Technion), who spent his sabbatical year with us, we have systematically replaced those species that were based on group-additivity estimates in previous editions of Burcat's Library, with high-quality composite ab initio computations at the G3 level of theory (using mostly the G3//B3LYP variant). Also, those species that are currently available from the fully-networked C(A)TN have been refurbished in Burcat's Library by utilizing directly the ATcT data. These improvements resulted in the new edition (both hard-copy and electronic), now entitled "*Third Millennium Ideal Gas and Condensed Phase Thermochemical Database for Combustion with Updates from Active Thermochemical Tables*". This is likely to be the last edition prepared in the old-fashioned way, which involves substantial manual labor. The aim of the absorption/merger into ATcT is two-fold. Once the translation into one of the Auxiliary ATcT Libraries is complete, Burcat's Library (which contains ~1300 species) will be one of the sources of non-networked thermochemical data, very valuable for species not yet covered by C(A)TN. At the same time, once the full integration with ATcT is completed, the polynomialized library will be automatically updated with every new ATcT solution of the C(A)TN and the latest version electronically distributed around the world.

We have also started a joint pilot project with NIST that probes the revision of the NBS Tables of Chemical Thermodynamic Properties using the ATcT approach. The NBS Tables have not been updated since their publication in 1982. An obvious barrier to revising a critical evaluation of thermochemical data is the immense effort that is entailed in such undertaking. With the appearance of Active Thermochemical Tables (ATcT), a new possibility for revising the NBS Tables has emerged, which is currently being explored by this joint project. For the pilot stage of this project, a target list of about two dozen "key" thermochemical species has been developed. The revision process involves the construction of the related portions of the Thermochemical Network (TN) Graph by mining the extensive archives of information that were utilized and critically evaluated during the construction of the original NBS Tables, further augmented by introducing all available thermochemically-relevant determinations that appeared

since. The project leverages from the ability of ATcT to simultaneously evaluate massive amounts of interdependent information, as well as from the ATcT capability to accept incremental updates to the TN Graph and painlessly propagate the new knowledge through all affected values.

### Other progress

As part of the IUPAC Task Group on Thermochemistry of Radicals (where the Argonne effort is central to the success of the project), we are in the process of performing critical and meticulous evaluations of the thermochemistry of a number of small radicals and intermediate species that are important in combustion and atmospheric chemistry. The resulting "IUPAC recommended values" are being published in a series of papers. We have an ongoing long-term collaboration with C.-Y. Ng (U. C. Davis) and T. Baer (UNC Chapel Hill) to perform a number of thermochemically relevant photoionization measurements at the Chemical Dynamics Beamline at ALS Berkeley, which are driven by deficiencies or inconsistencies in some basic thermochemical quantities that are being uncovered as we are building and analyzing the Core (Argonne) Thermochemical Network. We have an ongoing long-term collaboration with J. Stanton and J. Boggs (U. Texas Austin), A. Csaszar (Eötvös U. Budapest), and J. M. L. Martin (Weizmann) on computing critical thermochemistry for small radicals via state-of-the art theory (where the selection of targets is via ATcT), as well as the development of new and even more accurate theoretical approaches (where the accuracy requirements are again driven by ATcT). We have also an ongoing collaboration with the group of T. Turany (Eötvös U. Budapest) on extending the ATcT approach to Monte Carlo analysis of reaction mechanisms.

### Future Plans

Future plans of this program pivot around further developments and expansive use of Active Thermochemical Tables, coupled to targeted theoretical and laboratory experimental investigation of radicals and transient species that are intimately related to combustion processes. Of particular interest are species that potentially define the initial attack of O<sub>2</sub> on hydrocarbon moieties during combustion, as well as other ephemeral species that are implicated in subsequent atmospheric chemistry (particularly hydrocarbon moieties that contain oxygen and/or nitrogen). In collaboration with theorists in the Argonne Chemical Dynamics Group, we plan on determining in quantitative ways the effects of hindered rotations and soft and/or coupled internal modes on thermochemical quantities of both transient and stable species. We also intend to further enhance our fitting methods for accurate determination of fragment appearance energies from photoionization measurements.

*This work is supported by the U.S. Department of Energy, Office of Basic Energy Sciences, Division of Chemical Sciences, Geosciences, and Biosciences, under Contract W-31-109-ENG-38. Development of certain underlying computer-science components of Active Thermochemical Tables were supported by the Office of Advanced Scientific Computing Research, Division of Mathematical, Information and Computational Sciences, under the same Contract.*

### Publications resulting from DOE sponsored research (2004 - )

- *Introduction to Active Thermochemical Tables: Several "Key" Enthalpies of Formation Revisited*, B. Ruscic, R. E. Pinzon, M. L. Morton, G. von Laszewski, S. J. Bittner, S. G. Nijsure, K. A. Amin, M. Minkoff, and A. F. Wagner, *J. Phys. Chem. A* **108**, 9979 (2004).
- *Active Thermochemical Tables*, B. Ruscic, in: *2005 Yearbook of Science and Technology* (yearly update to *Encyclopedia of Science and Technology*), McGraw-Hill, New York, pp 3-7 (2004).
- *Refinements of the Bond Dissociation Energy of Carbon Monoxide and of the Enthalpy of Formation of Carbon Atom in Gas Phase Using the Active Thermochemical Tables Approach*, B. Ruscic, R. E. Pinzon, M. L. Morton, A. G. Csaszar, J. F. Stanton, M. Kallay, and G. von Laszewski, *Proc. 59<sup>th</sup> Int. Symp. Mol. Spectrosc.*, Columbus, OH (2004).
- *From Theoretical Calculations to Experimental Assignment of NMR Spectra*, T. J. Kupka, B. Ruscic, R. E. Botto, L. Curtiss, G. Pasterna, P. Lodowski, and W. Szeja, *Proc. 36<sup>th</sup> Great Lakes Regional Meeting Amer.*

- Chem. Soc., Peoria, IL (2004).
- *Theoretical Calculations on the Reaction of Ethylene with Oxygen*, H. Hua, B. Ruscic, and B. Wang, *Chem. Phys.* **311**, 335 (2005).
  - *A Collaborative Informatics Infrastructure for Multi-scale Science*, J. D. Myers, T. C. Allison, S. Bittner, B. Didier, M. Frenklach, W. H. Green, Jr., Y.-L. Ho, J. Hewson, W. Koegler, C. Lansing, D. Leahy, M. Lee, R. McCoy, M. Minkoff, S. Nijsure, G. von Laszewski, D. Montoya, L. Oluwole, C. Pancerella, R. Pinzon, W. Pitz, L. A. Rahn, B. Ruscic, K. Schuchardt, E. Stephan, A. Wagner, T. Windus, and C. Yang, *Cluster Computing* **8**, 243 (2005).
  - *IUPAC Critical Evaluation of Thermochemical Properties of Selected Radicals: Part I*, B. Ruscic, J. E. Boggs, A. Burcat, A. G. Csaszar, J. Demaison, R. Janoschek, J. M. L. Martin, M. L. Morton, M. J. Rossi, J. F. Stanton, P. G. Szalay, P. R. Westmoreland, F. Zabel, and T. Berces, *J. Phys. Chem. Ref. Data* **34**, 573 (2005).
  - *Pulsed Field-Ionization Photoelectron-Photoion Coincidence Study of the Process  $N_2 + h\nu \rightarrow N^+ + N + e^-$ : Bond Dissociation Energies of  $N_2$  and  $N_2^+$* , X. Tang, Y. Hou, C. Y. Ng, and B. Ruscic, *J. Chem. Phys.* **123**, 074330 (2005).
  - *Active Thermochemical Tables: Thermochemistry for the 21st Century*, B. Ruscic, R. E. Pinzon, G. von Laszewski, D. Kodeboyina, A. Burcat, D. Leahy, D. Montoya, and A. F. Wagner, *J. Phys. Conf. Ser.* **16**, 561 (2005).
  - *Third Millennium Ideal Gas and Condensed Phase Thermochemical Database for Combustion with Updates from Active Thermochemical Tables*, A. Burcat and B. Ruscic, ANL-05/20, Argonne National Laboratory, Argonne, IL, USA, and TAE 960, Technion – Israel Institute of Technology, Haifa, Israel (2005).
  - *Active Thermochemical Tables: Thermochemistry for the 21st Century*, B. Ruscic, R. E. Pinzon, G. von Laszewski, D. Kodeboyina, A. Burcat, D. Leahy, D. Montoya, and A. F. Wagner, *Proc. 6<sup>th</sup> Int. Conf. Chem. Kinet.*, Gaithersburg, MD (2005).
  - *On the Heats of Formation for NO, NO<sub>2</sub>, and HO<sub>2</sub>, and Rate Constants for OH + NO<sub>2</sub> → HO<sub>2</sub> + NO and OH + HO<sub>2</sub> → H<sub>2</sub>O + O<sub>2</sub>*, B. Ruscic, N. K. Srinivasan, M.-C. Su, J. W. Sutherland, and J. V. Michael, *Proc. 6<sup>th</sup> Int. Conf. Chem. Kinet.*, Gaithersburg, MD (2005).
  - *Investigating Internal Rotation in Molecules and Radicals*, A. Burcat and B. Ruscic, *Proc. 6<sup>th</sup> Int. Conf. Chem. Kinet.*, Gaithersburg, MD (2005).
  - *Direct Identification of Propargyl Radical in Combustion Flames by VUV Photoionization Mass Spectrometry*, T. Zhang, X. N. Tang, K.-C. Lau, C. Y. Ng, C. Nicolas, D. S. Peterka, M. Ahmed, M. L. Morton, B. Ruscic, R. Yang, L. X. Wei, C. Q. Huang, B. Yang, L. S. Sheng, Y. W. Zhang, and F. Qi, *J. Chem. Phys.* **124**, 074302 (2006).
  - *Active Thermochemical Tables: Thermochemistry for the 21<sup>st</sup> Century*, B. Ruscic, *Proc. 21<sup>st</sup> Austin Symp. Mol. Struct.*, Austin, TX (2006).
  - *Active Thermochemical Tables: Accurate Enthalpy of Formation of Hydroperoxyl Radical, HO<sub>2</sub>*, B. Ruscic, R. E. Pinzon, M. L. Morton, N. K. Srinivasan, M.-C. Su, J. W. Sutherland, and J. V. Michael, *J. Phys. Chem.* **110**, 0000 (2006) (in press, available on the web through *J. Phys. Chem. A ASAP*, <http://dx.doi.org/10.1021/jp056311j>).
  - *Reflected Shock Tube Studies of High-Temperature Rate Constants for OH + NO<sub>2</sub> → HO<sub>2</sub> + NO and OH + HO<sub>2</sub> → H<sub>2</sub>O + O<sub>2</sub>*, N. K. Srinivasan, M.-C. Su, J. W. Sutherland, J. V. Michael, and B. Ruscic, *J. Phys. Chem.* **110**, 0000 (2006) (in press, available on the web through *J. Phys. Chem. A ASAP*, <http://dx.doi.org/10.1021/jp057461x>).
  - *Active Thermochemical Tables: On the Accurate Sequential Bond Dissociation Energies of Water*, B. Ruscic, R. E. Pinzon, A. Fernandez, M. L. Morton, D. Kodeboyina, and G. von Laszewski, *Proc. 61<sup>st</sup> Int. Symp. Mol. Spectrosc.*, Columbus, OH (2006) (in press).
  - *Cyber Thermochemistry: The New Active Thermochemical Tables Paradigm*, B. Ruscic, R. E. Pinzon, A. Fernandez, M. L. Morton, D. Kodeboyina, and G. von Laszewski, *Abstr. Pap. 232<sup>nd</sup> ACS National Meeting*, San Francisco, CA (2006) (in press).
  - *Revision of Several "Key" Thermochemical Species from the NBS Tables Using the Active Thermochemical Tables Approach: A NIST-Argonne Pilot Project*, A. Fernandez, B. Ruscic, D. G. Archer, R. D. Chirico, M. Frenkel, and J. W. Magee, *Abstr. Pap. 232<sup>nd</sup> ACS National Meeting*, San Francisco, CA (2006) (in press).

# Theoretical Studies of Elementary Hydrocarbon Species and Their Reactions

Henry F. Schaefer III and Wesley D. Allen  
Center for Computational Chemistry  
University of Georgia  
Athens, GA 30602-2525  
E-mail: hfs@uga.edu and wdallen@uga.edu

## Mechanisms of soot formation: the allyl + propargyl system

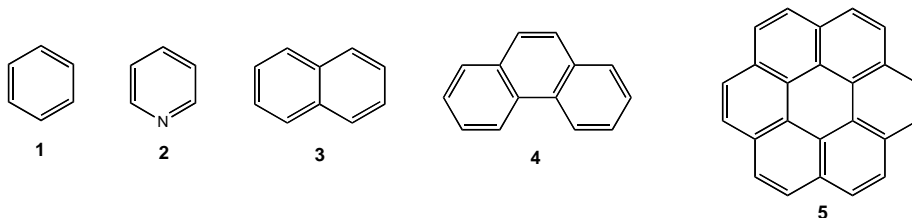
Environmental, toxicological, technical, and inherent scientific concerns continue to stimulate both experimental and theoretical research on soot formation during hydrocarbon combustion. Current models for soot formation center around the planar growth of polycyclic aromatic hydrocarbons (PAHs), some of which are carcinogenic and/or mutagenic. The formation of the first aromatic ring in the pyrolysis of aliphatic fuels is widely believed to be the rate-limiting step in soot formation, and thus a large body of research has been devoted to the elucidation of this mechanism. The best candidate precursors are resonance stabilized free radicals (RSFRs), whose enhanced stability and resistance to attack by O<sub>2</sub> allows the buildup of significant populations of these species under typical flame conditions, enhancing the probability of their recombination to form larger hydrocarbons. While there is a growing consensus that the predominant route to benzene formation is generally the self-reaction of propargyl radicals, significant contributions may also arise from other reactions. A combustion model constructed by Pope and Miller [*Proc. Combust. Inst.* **28**, 1519 (2000)] indicates that virtually all benzene is formed from either C<sub>3</sub>H<sub>3</sub> + C<sub>3</sub>H<sub>3</sub> → phenyl + H or C<sub>3</sub>H<sub>5</sub> + C<sub>3</sub>H<sub>3</sub> → fulvene, with the branching ratio depending strongly on the fuel mixture.

To improve combustion models for benzene formation, we are executing an exhaustive study of the complicated, multistate allyl + propargyl reaction surface, including the paths for formation of 1,2,5-hexatriene, 1,3,5-hexatriene, 1-hexene-5-yne, fulvene + H<sub>2</sub>, benzene, 3-methylene-4-methylcyclobutene, 3- and 4-methylenecyclopentene, and H + 3-methyl-cyclopentene-4- or -5-yl. Our exploratory computations with B3LYP/DZP density functional theory have already revealed a number of reaction possibilities, as shown by the structures in Figure 1. A viable (multistep) pathway from allyl + propargyl to fulvene + H<sub>2</sub> is the following (energies relative to reactants): (1) direct combination to singlet 1,2,5-hexatriene (**3**) at -57 kcal mol<sup>-1</sup>; (2) ring closure over a transition state **8** at -8 kcal mol<sup>-1</sup> to cyclic diradical **5**, whose triplet state lies at -43 kcal mol<sup>-1</sup>; (3) traversing a barrier (**12**) of uncertain height to 4-methylenecyclopentene (**11**) at -84 kcal mol<sup>-1</sup>; (4) H-atom loss to 4-methylenecyclopenten-3-yl (**15**) radical at -13 kcal mol<sup>-1</sup>; and (5) further H-atom loss and recombination to fulvene (**16**) + H<sub>2</sub> at -65 kcal mol<sup>-1</sup>. The formation of **15** can be promoted via attack on **11** by existing radicals in the flame, or **11** can equilibrate with **10**, from which concerted elimination of H<sub>2</sub> to form fulvene is possible. The path from 1,2,5-hexatriene (**3**) to 4-methylenecyclopentene (**11**) by way of **5** is critical to fulvene (and hence benzene) formation from allyl + propargyl, and we are thus pursuing this process with multireference electronic wavefunction methods. We should emphasize that the scheme in Figure 1 by no means represents a complete scan of the possible allyl + propargyl pathways.

## Nonplanarity of aromatic hydrocarbons: Dramatic failures of popular theoretical methods

We have recently discovered remarkable anomalies in electronic structure predictions for a sizable number of aromatic compounds, including benzene (**1**), pyridine (**2**), naphthalene (**3**), anthracene

(4), and coronene (5). At electron-correlated MP2, MP3, CISD, and CCSD levels of theory with a host of popular Pople basis sets, these molecules are not planar! These failures serve as a stark warning for black-box *ab initio* applications for aromatic hydrocarbons, particularly large, polycyclic species for which only limited basis sets are feasible.



In the case of benzene, the planar  $D_{6h}$  optimum structure is predicted by the methods in question to have an imaginary frequency for the  $b_{2g}$  out-of-plane bending mode that distorts into a  $D_{3d}$  chair conformation. Examples of harmonic frequencies (in  $\text{cm}^{-1}$ ) computed with Pople basis sets for this mode are: 6-31++G/(MP2, MP3, CISD),  $\omega_4 = (943i, 892i, 435i)$ ; 6-31++G(d)/(MP2, MP3, CISD),  $\omega_4 = (961i, 884i, 295i)$ ; 6-31++G(d,p)/(MP2, MP3, CISD),  $\omega_4 = (936i, 862i, 247i)$ ; 6-311+G/(MP2, CISD),  $\omega_4 = (1087i, 709i)$ ; 6-311+G(d,p)/MP2,  $\omega_4 = 399i$ ; 6-311++G/(MP2, CISD),  $\omega_4 = (1844i, 1385i)$ ; and 6-311++G(d,p)/(MP2, CISD),  $\omega_4 = (1181i, 511i)$ . In contrast, MP2 theory with the [6-311G(d,p), cc-pVDZ, ANO4321] basis sets yields only real frequencies,  $\omega_4 = (413, 634, 709) \text{ cm}^{-1}$ , and none of the Dunning basis sets (DZP, TZP, DZP+, TZ2P, TZ2Pf, cc-pVXZ) we tested give MP2 frequencies that are imaginary, or real and below  $400 \text{ cm}^{-1}$ . Only correlated wavefunctions are prone to the  $\omega_4$  basis set anomalies; the Hartree-Fock, B3LYP, and BLYP frequencies with the same Pople basis sets are in the expected ranges.

Our technical analysis of the spurious benzene out-of-plane vibrational frequencies has excluded several possible causes of the computed imaginary vibrational frequencies: (1) With particularly stringent settings for numerical accuracy, the peculiar frequencies are reproducible, generally to within  $1 \text{ cm}^{-1}$ , across diverse computational platforms and with four different electronic structure packages. (2) The effect is not due to deficiencies in MP2 theory but is also observed with higher-order CC, CI, and  $MP_n$  electron correlation methods. (3) The RHF reference wavefunctions for the correlated methods exhibit no *spatial* orbital instabilities in the immediate vicinity of the  $D_{6h}$  structure of benzene, so that the spurious vibrational frequencies are not attributable to nearby singularities in force constants and surrounding envelopes of unphysical mathematical behavior. (4) Variational collapse of wavefunction solutions upon distortion from  $D_{6h}$  symmetry is not a problem, and the modes of imaginary frequency given by the correlated methods can be smoothly followed to locate lower-energy minima. For example, the  $1101i \text{ cm}^{-1} b_{2g}$  mode from MP2/6-311+G theory leads to a  $D_{3d}$  minimum  $0.562 \text{ kcal mol}^{-1}$  lower in energy, with ring torsional angles of  $5.81^\circ$ , and a lowest frequency of  $388 \text{ cm}^{-1}(e_u)$ .

To clarify the origin of the benzene nonplanarity failure, Table 1 lists some basis sets (Group A) that yield imaginary OOP frequencies for the planar structure at the MP2 level, as well as similar basis sets (Group B) that give all real frequencies. The presence of diffuse functions on hydrogen (++ augmentation) is associated with the appearance of OOP modes of negative curvature, but several variations of the 6-311G basis give imaginary frequencies without spatially extended hydrogen functions. Analysis of individual MP2 pair correlation energies reveals that the predominant driving force for distortion of benzene into  $D_{3d}$  symmetry with Group A basis sets is a large, collective enhancement of the correlation energy for  $\sigma$ - $\pi$  electron pairs. Distorting from planarity provides a better basis set for recovering electron correlation, which in the severe Group A cases overcomes the familiar molecular orbital preference for planarity arising from  $\pi$  delocalization. We have mathematically documented and

quantified this phenomenon by means of a two-electron basis set incompleteness diagnostic, evaluated using our integral codes for performing explicitly-correlated R12 computations. The diagnostic confirms that the source of the anomalous benzene frequencies is an insidious intramolecular basis set incompleteness error (BSIE) that varies strongly with geometry over the potential energy surface.

Table 1. Classification of basis sets according to MP2 out-of-plane vibrational frequencies for  $D_{6h}$  benzene

Group A: At least one imaginary frequency			
3-21++G	6-31++G(d,p)	6-311+G(d,p)	[C(8s7p)/H(7s)]
3-21++G(d,p)	6-311G	6-311++G	
6-31++G	6-311+G	6-311++G(d)	[C(8s7p6d)/H(7s6p)]
6-31++G(d)	6-311+G(d)	6-311++G(d,p)	
Group B: All real frequencies			
3-21G	6-31G	6-311G	DZVP
3-21G(d)	6-31G(d)	6-311G(d,p)	TZVP
3-21G(d,p)	6-31G(d,p)	DZ	cc-pVDZ
3-21+G	6-31+G	DZP	aug-cc-pVDZ
3-21+G(d)	6-31+G(d)	DZP+	cc-pVTZ
3-21+G(d,p)	6-31+G(d,p)	TZ	aug-cc-pVTZ

The success of any practical basis set for benzene and other arenes hinges on minimizing the *differential* planar vs. nonplanar BSIE, recognizing that the resulting predictions will be far from the atomic-orbital limit for the corresponding angular momentum cutoff. In maintaining this balance, the basis should not be made rich in  $s$ ,  $p$ , or even  $d$  functions if no higher angular momentum functions (particularly carbon  $f$  manifolds) are present. Otherwise, the nuclear framework may distort from planarity to mimic the effect of the missing higher polarization functions. The correlation-consistent (aug)-cc-pVnZ basis sets of Dunning and co-workers, which contain functions with all angular momentum values allowed for principal quantum number  $n$ , are fundamentally constructed to provide the necessary balance. Existing NASA atomic-natural orbital (ANO) basis sets are an even better choice in this regard because their large primitive sets further reduce basis set superposition errors.

### Retro-Diels-Alder fragmentation of *o*-benzyne

The most facile path for benzene pyrolysis involves sequential hydrogen abstraction/loss to *o*-benzyne. Recent experiments in the Ellison laboratory at the University of Colorado have investigated the thermal decomposition of *o*-benzyne in a supersonic hyperthermal nozzle. The thermal dissociation products were detected using photoionization time-of-flight mass spectrometry, matrix-isolated infrared absorption spectroscopy, and chemical ionization mass spectrometry. At the threshold dissociation temperature, *o*-benzyne cleanly decomposes into acetylene and diacetylene via a retro-Diels-Alder mechanism. We have performed definitive *ab initio* electronic structure computations of this process using cc-pVXZ ( $X = 2-6$ ) basis sets and a series of increasingly rigorous coupled-cluster methods, CCSD, CCSD(T), CCSDT, and CCSDT(Q). In the retro-Diels-Alder transition state for *o*-benzyne decomposition, the breaking C-C bond has a distance of 2.207 Å and the lowest harmonic vibrational frequencies are  $\omega_9(a_1) = 621i \text{ cm}^{-1}$  and  $\omega_{24}(b_2) = 40 \text{ cm}^{-1}$ , all at the CCSD(T)/cc-pVTZ level. The minuscule  $\omega_{24}$  frequency reveals that the potential energy surface is extremely flat with respect to distortions toward a stepwise decomposition path. Focal-point extrapolations of the barrier for concerted

fragmentation yield  $88.5 \text{ kcal mol}^{-1}$  for the CBS CCSDT limit, in accord with the Ellison experiments and previous G2M computations by Moskaleva, Madden, and Lin [*Phys. Chem. Chem. Phys.* **1**, 3967 (1999)]. Our computations also yield an improved 298 K enthalpy of formation of diacetylene,  $109.7 \text{ kcal mol}^{-1}$ .

### Next-generation, explicitly correlated electronic structure methods

All common wavefunction methods of electronic structure theory have a fundamental and troublesome flaw: the inability to correctly describe the exact mathematical cusp behavior of many-electron wavefunctions in the vicinity of coalescence points (Coulomb singularities), and hence to fully account for instantaneous, short-range correlation among electrons. Achieving high thermochemical accuracy requires *next-generation* methodologies that solve the electron cusp problem by explicitly incorporating interelectronic variables ( $r_{12}$ ) into molecular wavefunctions. We have continued to pursue a long-term research program to further develop highly accurate *explicitly correlated* methods, to create attendant state-of-the-art computer codes, to undertake practical chemical applications of unprecedented size, and to disseminate such expertise to the scientific community. Our computer codes have been used in numerous chemical applications that conjoin conventional CCSD(T) and explicitly correlated MP2 methods within a focal point extrapolation scheme for pinpointing the *ab initio* limit of electronic structure theory. Unprecedented accuracy has thus been achieved for contemporary problems in combustion and other areas. Most recently we have programmed R12-UMP2 theory into our codes and are progressing toward the first implementation of *open-shell* explicitly-correlated perturbation theories built upon restricted Hartree-Fock (ROHF) orbitals.

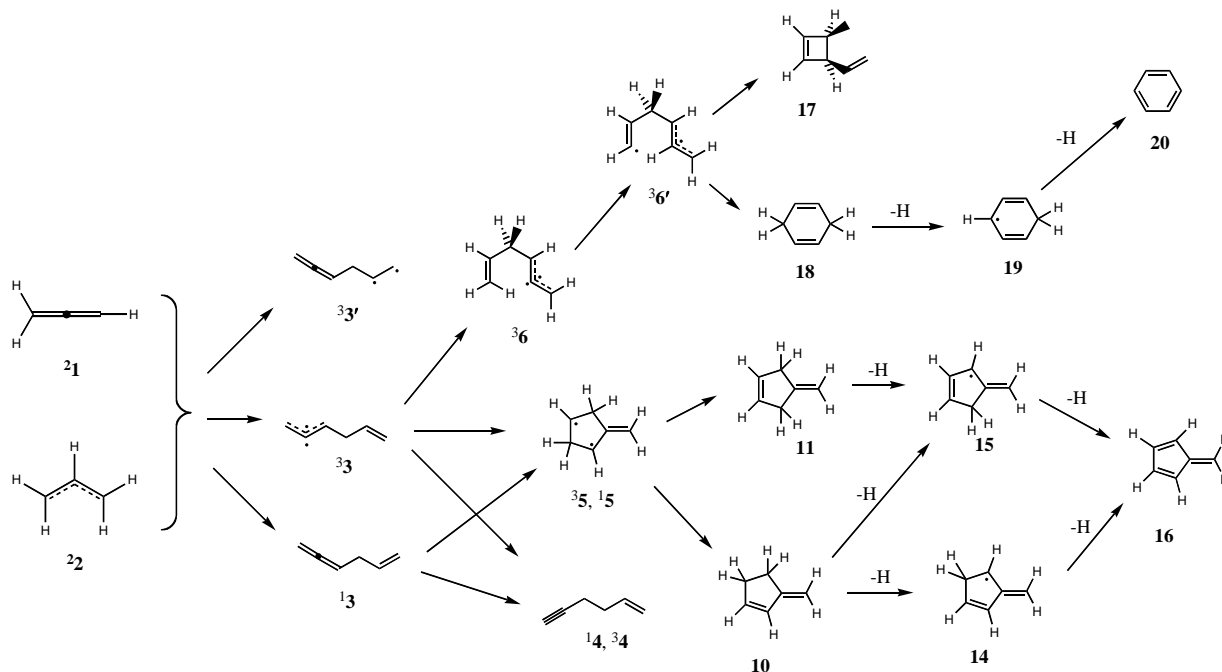


Figure 1. Pathways for the reaction of propargyl and allyl radicals.

## Publications Supported by DOE: 2004, 2005, 2006

1. K. W. Sattelmeyer, Y. Yamaguchi, and H. F. Schaefer, "Energetics of the Low-Lying Isomers of HCCO," *Chem. Phys. Lett.* **383**, 266 (2004).
2. L. D. Speakman, B. N. Papas, H. L. Woodcock, and H. F. Schaefer, "A Reinterpretation of Microwave and Infrared Spectroscopic Studies of Benzaldehyde," *J. Chem. Phys.* **120**, 4247 (2004).
3. R. D. DeKock, M. J. McGuire, P. Piecuch, W. D. Allen, H. F. Schaefer, K. Kowalski, S. A. Spronk, D. B. Lawson, and S. L. Laursen, "The Electronic Structure and Vibrational Spectrum of *trans*-HNOO," *J. Phys. Chem. A* **108**, 2893 (2004).
4. M. Schuurman, S. Muir, W. D. Allen, and H. F. Schaefer, "Toward Subchemical Accuracy in Computational Thermochemistry: Focal Point Analysis of the Heats of Formation of NCO and [H, N, C, O] Isomers," *J. Chem. Phys.* **120**, 11586 (2004).
5. Y. Yamaguchi and H. F. Schaefer, "The Diazocarbene (CNN) Molecule: Characterization of the  $\tilde{X}^3\Sigma^-$  and  $\tilde{A}^3\Pi$  Electronic States," *J. Chem. Phys.* **120**, 9536 (2004).
6. S. E. Wheeler, W. D. Allen, and H. F. Schaefer, "Thermochemistry of Disputed Soot Formation Intermediates  $C_4H_3$  and  $C_4H_5$ ," *J. Chem. Phys.* **121**, 8800 (2004).
7. R. K. Sreeruttun, P. Ramasami, G. Yan, C. S. Wannere, P. v. R. Schleyer, and H. F. Schaefer, "The Alkylethynyl Radicals,  $\cdot C\equiv C-C_nH_{2n+1}$  ( $n=1-4$ ), and their Anions," William L. Hase Special Issue, *Int. J. Mass Spec.* **241**, 295 (2005).
8. M. S. Schuurman, W. D. Allen, and H. F. Schaefer, "The Highly Anharmonic  $BH_5$  Potential Energy Surface Characterized in the *Ab Initio* Limit," *J. Chem. Phys.* **122**, 104302 (2005).
9. M. Schuurman, W. D. Allen, and H. F. Schaefer, "The *Ab Initio* Limit Quartic Force Field of  $BH_3$ ," *J. Comput. Chem.* **26**, 1106 (2005).
10. B. N. Papas and H. F. Schaefer, "Concerning the Precision of Standard Density Functional Programs: GAMESS, GAUSSIAN, MOLPRO, NWCHEM, and Q-CHEM," Debashis Mukherjee Special Issue, *J. Mol. Struct.*
11. R. K. Sreeruttun, P. Ramasami, A. Paul, C. S. Wannere, and H. F. Schaefer, "Effects of Fluorine on the Structures and Energetics of the Propynal and Propargyl Radicals and their Anions," *J. Org. Chem.* **70**, 8676 (2005).
12. N. J. DeYonker, S. Li, Y. Yamaguchi, and H. F. Schaefer, "Applications of Equation-of-Motion Coupled Cluster Methods to Low-Lying Singlet and Triplet Electronic States of HBO and BOH," *J. Chem. Phys.* **122**, 234316 (2005).
13. X. Zhang, Q. Li, J. B. Ingels, A. C. Simmonett, S. E. Wheeler, Y. Xie, R. B. King, H. F. Schaefer, and F. A. Cotton, "Remarkable Electron Accepting Properties of the Simplest Benzenoid Cyanocarbons: Hexacyanobenzene, Octacyanonaphthalene, and Decacyano-anthracene," *J. Chem. Soc. (London) Chem. Comm.*, **758** (2006).
14. D. Moran, A. C. Simmonett, F. E. Leach, W. D. Allen, P. v. R. Schleyer, and H. F. Schaefer, "Popular Theoretical Methods Predict Arenes to be Nonplanar," *J. Am. Chem. Soc.*
15. X. Zhang, A. T. Maccarone, M. R. Nimlos, S. Kat, V. M. Bierbaum, B. K. Carpenter, G. B. Ellison, B. Ruscic, A. C. Simmonett, W. D. Allen, and H. F. Schaefer, "Unimolecular Thermal Fragmentation of Ortho-Benzyne," *J. Chem. Phys.*

# Gas Phase Molecular Dynamics: Spectroscopy and Dynamics of Transient Species

Trevor J. Sears([sears@bnl.gov](mailto:sears@bnl.gov)),

*Department of Chemistry, Brookhaven National Laboratory, Upton, NY 11973-5000*

## Program Scope

This research is carried out as part of the Gas Phase Molecular Dynamics Group program in the Chemistry Department at Brookhaven National Laboratory. High resolution spectroscopy, augmented by theoretical and computational methods, is used to investigate the structure and reactivity of chemical intermediates in the elementary gas phase reactions involved in combustion chemistry and in chemical processes occurring at or near surfaces of heterogeneous catalysts. Techniques to improve the sensitivity of laser absorption spectroscopy are developed as are models of intra-and inter-molecular interactions in molecular free radicals and other reactive species. The results lead to improved understanding and modeling of processes involving these species and are applicable to a wide variety of practical problems.

## Recent Progress

### *CH<sub>2</sub> c- state double resonance measurements*

Double resonance spectra have been measured to confirm several tentative theoretical assignments of rovibrational states belonging to the previously uncharacterized c (singlet) electronic state of CH<sub>2</sub>. Direct excitation from the singlet a state is very weak, nominally a two-electron excitation. In a two-step excitation via the b state, a sequence of two fully allowed transitions permit detection by transient FM spectroscopy of the c-b lines following a pulsed laser preparation of selected b state levels by b-a transitions. The experiment as first conducted used the higher power, but lower resolution, ns-pulsed laser to saturate a known rovibrational transition in the CH<sub>2</sub> b-a system. Transitions from the prepared b-state level to previously unknown c-state levels resulted in transient absorption of light from a frequency-modulated c.w. tunable Ti:sapphire ring laser. For experimental reasons it would be desirable to employ the more easily scanned pulsed laser system to search for the unknown transitions, however there is insufficient power in the c.w. laser to saturate a transition in the extended sample used in these experiments. However, we have recently shown that a.c. Stark level shifts and broadening induced by moderate (~5mJ) unfocused ns-pulses can be sensitively detected by the c.w. probe laser beam monitoring the known b-a transition. This new scheme for detecting optical-optical double resonance spectra has a large number of exciting potential applications, some of which are discussed below (with Hall & Kim).

### *Reversible kinetics of intersystem crossing in CH<sub>2</sub>*

Time resolved FM absorption permits high dynamic range measurement of singlet methylene decay kinetics, revealing double exponential decays for the first time. The relative amplitudes of fast and slow decay components are observed to vary with the nuclear spin state of CH<sub>2</sub> in the vibrationless singlet state, confirming distinct, uncoupled decay pathways in the two nuclear spin modifications. The pattern of singlet-triplet mixed gateway levels differs for these nuclear spin manifolds, and the vibrational energies of the zero-order triplet states responsible for the mixing is the key variable responsible for the differences in reversibility. These results are being extended with measurements on vibrationally excited singlet CH<sub>2</sub> and temperature dependent kinetics using pump-probe spectroscopy to measure population transfer kinetics directly (with Hall & Kim).

### *Hot bands in the electronic spectrum of HCCl*

New jet-cooled and ambient temperature spectra of HCCl at wavelengths to the red of the band origin of the A-X system have revealed that the C-Cl stretching vibration in the excited state was previously mis-assigned. The revised frequency corrects an anomalously large apparent anharmonicity in this mode and permitted a recalibration of the *ab initio* potential energy surface for the state. This, in turn, allowed the

assignment of many shorter wavelength bands observed by other workers and an accurate calculation of vibronic band positions and intensities in this spectrum (with Kobayashi (Japan), Hall & Yu).

#### *Zeeman measurements on FeH*

In collaboration with Prof. Tim Steimle (Arizona State), we have begun experiments to examine the electronic spectroscopy of transition metal hydrides. Initial measurements were made at ASU, resulting in the first measurements of the Zeeman effect in FeH, which is of interest to Astronomy as a potential probe of magnetic fields in the sun. At BNL, we have very recently begun experiments on transition metal hydrides, targeted towards understanding the electronic structure of possible hydrogen storage materials (with Steimle (ASU), Muckerman & Wang).

#### *Calculation of ground and excited electronic states of transition metal hydrides*

We have calculated the energies, bond lengths, vibrational frequencies and dipole moments for the low-lying electronic states of several first transition metal series hydrides at a very high level of theory (MRCI-SD from a very large CASSCF reference function). The results for FeH are compared to the experimental results for this, the best characterized of these small, but very complicated, systems. The state ordering and relative energies compare very well with experiment. More importantly, the wavefunctions also correctly predict electric dipole moments, where they have been measured. Previously published calculations have poor agreement with the experimentally measured dipole moments, because they take insufficient account of the low-lying  $3d^7 4s^1$  excited configuration of the Fe atom which is important in the description of the bonding in the lowest states of the FeH molecule. Similar calculations on VH predict another complicated set of low-lying states with quintet and triplet multiplicities. The strongest spectroscopic transitions are predicted to lie at wavelengths longer than 1 micron. As the work was being completed, we heard that unpublished data recorded in a furnace source near 1.4 microns by the Kitt Peak astronomy group support our results. Work is proceeding in our laboratory to record the spectrum in a lower temperature source which will make spectral assignment simpler (with Muckerman & Wang).

### **Future Plans**

#### *Transient AC Stark effect optical-optical double resonance*

Our discovery that the transient FM absorption experiment can be used to sensitively detect small a.c. Stark-induced broadenings and shifts in levels induced by modest pulsed ns-laser power levels opens the way to a number of exciting new measurements. In  $\text{CH}_2$ , for example, it should be possible to spectroscopically measure the onset of absorption to the dissociation continuum calculated to lie slightly more than  $30\,000\text{ cm}^{-1}$  above the a-state origin. By folding the double resonance scheme, transitions from known a-state levels of mixed triplet and singlet character to pure triplet ground state levels would provide a direct spectroscopic measurement of the  $\text{CH}_2$  singlet-triplet splitting,  $\Delta E_{\text{st}}^0$ , for the first time. Other problems requiring the detection of weak absorptions from a known excited state level to unknown or ill-defined higher electronic states, such as those involving isomers or dissociations will also be amenable to attack using this technique (with Hall & Kim).

#### *Spectroscopy of transition metal hydrides*

Using a laser ablation / supersonic expansion source, we are beginning an effort to detect electronic spectra of small hydride molecules and clusters. Calculations suggest that all the simple hydrides have multiple low-lying ( $<1\text{ eV}$ ) excited electronic states, so these systems represent examples of extreme breakdown of the Born-Oppenheimer approximation. First experiments will be directed towards vanadium hydride, which is the least well-known of all 3d metal hydrides. Subsequent measurements will attempt to measure the spectra of mixed metal clusters including magnesium hydrides, that have shown potential as future hydrogen storage materials (with Muckerman & Wang).

#### *Ionization spectroscopy of highly excited aromatic radicals*

In collaboration with Phil. Johnson (Stony Brook), we are developing methods to calculate Franck-Condon band intensities in the spectra of these species. For allowed vibronic bands, existing publicly-available

Franck-Condon computer codes combined with ab initio calculation of the vibrational force field for the electronic states generally permits a reasonable calculation of the band intensities. For band systems that become allowed only through vibronic coupling via mode or modes of a particular symmetry, it is less straightforward. We are developing a model in which the electronic transition moment is expanded in a Taylor series in the mode(s) in question, then the spectrum computed by combining this result with standard Franck-Condon calculations for the symmetric modes. Initial results for benzonitrile and phenylacetylene look promising and the technique promises to make vibronic assignment of such spectra much more secure than methods based on matching to computed frequencies alone. Lifetime measurements have also suggested a triplet-triplet fluorescence step may be involved in the relaxation of  $S_1$  in these systems and we will search for this emission in the near-infrared (with Johnson (SBU)).

### Publications 2004-2006

P. Zou, J. Shu, T. J. Sears, G. E. Hall and S. W. North, The photodissociation of bromoform at 248 nm: Single and multiphoton processes, *J. Phys. Chem A* **108**, 1482-1488 (2004).

G. E. Hall, A. Komissarov and T. J. Sears, Doppler-resolved spectroscopy as an assignment tool in the spectrum of singlet methylene *J. Phys. Chem A*. **108** 7922-7927 (2004).

Y. Kim, A. Komissarov, G. E. Hall and T. J. Sears, Observation of the c1A1 state of methylene by optical-optical double resonance, *J. Chem. Phys.* **123**, 024306 (2005).

H. G. Yu, G. E. Hall, J. T. Muckerman and T. J. Sears, The vibrational dependence of axis-switching in triatomic spectra, *Molec. Phys.* **104**, 47-53 (2006).

H.-G. Yu, T.J. Sears and J.T. Muckerman, Potential energy surfaces and vibrational energy levels of DCCl and HCCl in three low-lying states, *Mol. Phys.* **104**, 47 (2006).

G. E. Hall, T. J. Sears and H.-G. Yu, Rotationally Resolved Spectrum of the A(060) -- X(000) Band of HCB<sub>r</sub>, *J. Molec. Spectrosc.* **235**, 125-131 (2006).

Z. Wang, R.G. Bird, H.-G. Yu and T.J. Sears, Hot bands in jet-cooled and ambient temperature spectra of chloromethylene, *J. Chem. Phys.* **124**, 074314 (2006).

H. Xu, P. M. Johnson and T. J. Sears, Photoinduced Rydberg ionization spectroscopy of phenylacetylene: vibrational assignments of the C state of the cation, *J. Phys. Chem. A*. (submitted, Mar 2006).

K. Kobayashi, G. E. Hall and T. J. Sears, The spectrum of CH<sub>2</sub> near 1.36 and 0.92 microns: Re-evaluation of rotational level structure and perturbations in a(010). *J. Chem. Phys.* (submitted, Mar. 2006).

Z. Wang, T. J. Sears and J. T. Muckerman, Multi-reference configuration interaction calculations of the low-lying states of iron and vanadium monohydride, FeH and VH, *J. Chem. Phys.* (submitted April 2006).

# Picosecond Nonlinear Optical Diagnostics

Thomas B. Settersten  
Combustion Research Facility, Sandia National Laboratories  
P.O. Box 969, MS 9056  
Livermore, CA 94551-0969  
tbsette@sandia.gov

## Program Scope

This program focuses on the development of innovative laser-based detection strategies for important combustion radicals and the investigation of the fundamental physical and chemical processes that directly affect quantitative application of these techniques. These investigations include the study of fundamental spectroscopy, energy transfer, and photochemical processes. This aspect of the research is essential to the correct interpretation of diagnostic signals, enabling reliable comparisons of experimental data and detailed combustion models. Many of these investigations use custom-built tunable picosecond (ps) lasers, which enable efficient nonlinear excitation, provide high temporal resolution for pump/probe studies of collisional processes, and are amenable to detailed physical models of laser-molecule interactions.

## Recent Progress

*Detection of atomic hydrogen and investigation of population kinetics in  $n=2$ .* We previously demonstrated the detection of atomic hydrogen in flames using picosecond two-color polarization spectroscopy (TC-PS) in collaboration with Sukesh Roy (Innovative Scientific Solutions, Inc.) and Robert Lucht (Purdue). In recent work with Bob Lucht and Waruna Kulatilaka (Purdue), we extended this wave-mixing diagnostic approach to the full grating geometry using two independent laser sources. Hydrogen is two-photon excited from 1S to 2S using 243-nm laser pulses and probed via  $H_\alpha$  lines with a 656-nm laser pulse. The relative timing of the pump and probe pulses is controlled electronically. The versatile experimental configuration enables detailed investigation of the polarization dependence of the wave mixing signal and is rapidly switched to the TC-PS configuration for direct comparison of signals generated in the two configurations. Independent pump and probe lasers enable detailed investigation of collisional effects as well as laser-induced broadening and shifting of the pump transition.

In this collaboration, DNI-based calculations were used to develop an understanding of the effects of collisions, saturation, and Doppler broadening on ps TC-PS. The calculations treat the two-photon excitation step to H(2S) nonperturbatively and include pathways through bound  $nP$  intermediate states. The modeling results indicated that while two-photon excitation to H(2S) is very effective, it produces negligible anisotropy in the angular momentum distribution. The model indicates that TC-PS signal are produced by coherences generated between hyperfine states in 2S and hyperfine states in 2P. The experimentally measured polarization dependence of the signal is generally reproduced by the model, but experimental signals observed with linearly polarized pump photons are in contradiction to the model. We are currently working to include Stark mixing of the hyperfine

states, which may help to explain the observation of TC-PS signal excited by a linearly polarized pump laser.

Taking advantage of the effective 1S-2S pumping to produce population gratings in  $n=2$ , we demonstrated a signal-level improvement of two-orders of magnitude compared to that observed with TC-PS. This significant improvement in signal level justifies the more complex experimental configuration of the grating geometry compared to TC-PS for some sensing applications. Based on strong signals previously observed by the Lucht group using TC-PS in diamond-forming and other flames, we feel that the grating configuration of this technique shows great potential for hydrogen detection applications in reacting flows. More extensive experiments to characterize the saturation and collisional dependence of the signal in flames are planned.

The DNI code has recently been modified to include the effect of spatial coherence necessary to properly model wave mixing in the grating geometry. The greater complexity of the code comes with significant computational cost. In collaboration with Philippe Pebay (Sandia), we are parallelizing the code to run on local computer clusters to enable rapid turnaround, accelerating our development.

***Electronic spectroscopy of propargyl.*** In collaboration with Jeff Gray and William Humphries (Ohio Northern University), we set up a coherent IR-UV double-resonance spectrometer to investigate the electronic spectroscopy of propargyl ( $C_3H_3$ ). The UV absorption bands of propargyl lie between 300 and 340 nm, and recent claims attribute UV absorption features around 240 nm to propargyl. There is, however, some contention surrounding the assignment of the 240-nm feature. We attempted to address this controversy with double resonance spectroscopy. Propargyl was photolytically produced using a 193-nm pulse to dissociate propargyl chloride. We used IR excitation in the well-characterized  $\nu_1$  band at 3  $\mu\text{m}$  and UV probing around 332 nm and 242 nm. The polarization spectroscopy configuration and the grating geometry were both used. Unfortunately neither configuration produced measurable signals due to the unfavorable combination of quantum state dilution at 300 K and the quantum-state specificity of the technique. Filtered UV radiation from a deuterium lamp was used to investigate the transient absorption following photolysis of propargyl chloride. The absorption near 330 nm was prompt with the photolysis pulse and matched the structure of the UV bands of propargyl. Significantly stronger absorption at 240 nm was observed, but this signal rose more slowly than that at 330-nm, leaving the assignment of this band still in question.

***Fluorescence quenching.*** We have started a substantial effort to develop accurate predictive models for the quenching of fluorescence from CO  $B^1\Sigma^+(v=0)$ , NO  $A^2\Sigma^+(v=0)$ , H( $n=3$ ), and O ( $3p^3P$ ). This research builds on our previous success using time-resolved ps laser-induced fluorescence (LIF) to measure temperature- and species-dependent quenching cross sections in a heated cell. We are extending our measurements to temperatures approaching 2000 K using premixed, low-pressure flames. Initial work has focused on the design, construction, and characterization of a low-pressure flame facility, which is nearing completion. A variety of premixed low-pressure flames, using various fuels, oxidizers, diluents, and flow rates will be utilized to achieve the desired conditions. The time-resolved LIF apparatus uses a ps laser to two-photon excite the species on the burner centerline and micro-channel plate photomultipliers to detect the fluorescence. Using our time-resolved ps-LIF apparatus, we can very accurately measure fluorescence lifetimes, which will be on the order of 2 ns or longer under the low-pressure flame conditions.

## Future Plans

**Fluorescence quenching.** We will complete the construction and characterization of our new low-pressure flame facility and start experiments to systematically investigate quenching in a series of flames. Using a design-of-experiments approach, we will determine an appropriate matrix of flames, measure the quenching rates, and infer species- and temperature-dependent quenching cross sections. The higher-temperature data will enable the development and validation of comprehensive quenching models.

We propose to investigate fluorescence lifetime imaging and the feasibility of prompt ps-LIF imaging for quantitative concentration measurements of NO. These experiments will use a gated ( $<100$  ps FWHM) intensified camera to detect the LIF signal generated by 50-ps excitation of NO in flames. By scanning the gate with respect to the laser pulse, a two-dimensional image of the time-resolved fluorescence can be obtained in steady or periodically forced flames. Measured lifetimes will be compared to those predicted by a quenching model that we are developing. Furthermore, it should be possible to obtain single-shot “quench-free” images by gating the detection to overlap with the laser pulse. We propose to evaluate critically the feasibility of this application.

**Hydroxyl ground-state population kinetics.** We previously used two-color resonant four-wave mixing spectroscopy (TC-RFWM) in the full grating geometry to demonstrate its ability to probe both inelastic and elastic collisions affecting OH ground-state populations. Single-mode laser pulses of approximately 50-ps duration provided adequate temporal resolution for time-domain studies of rotational energy transfer (RET) and sufficient spectral resolution for state-resolved excitation in an atmospheric-pressure flame. The decays of the first three multipole moments in  $X^2\Pi_{3/2}(v'=1, N')$  were observed directly using a time-delayed probe. By tuning the probe laser to transitions originating from collisionally populated levels, we were also able to observe rates of population, alignment, and orientation transfer in the RET process.

We will use this technique to probe OH ground-state collisions in a series of atmospheric-pressure flames. Measurements of total RET rates and orientation and alignment destruction rates will be measured for  $1 \leq N' \leq 12$ . State-to-state RET rates will be determined by probing collisionally populated levels. Using these data in conjunction with a perturbative model for TC-RFWM, we will test scaling laws for RET due to collisions with the major collision partners. Similarly, we will investigate the use of anisotropy measurements for the determination of  $m_J$  propensity rules.

In conjunction with the experiments, we will continue our collaboration with Bob Lucht to develop a fully  $m_J$ -resolved, non-perturbative density-matrix-based model describing TC-RFWM of OH in the grating geometry. Our results will be used to develop, validate, and test RET models in this simulation. This work will dramatically improve our ability to describe accurately laser-based detection (LIF as well as WM) of OH in the saturating limit.

**Detection of atomic hydrogen in flames.** We will continue our collaboration with Bob Lucht to develop non-perturbative models describing two-color wave-mixing in atomic hydrogen. The code is currently being parallelized in collaboration with Philippe Pebay, and we will have the code running on a local cluster this year. Using the picosecond wave-mixing experiment, we will continue investigations to determine appropriate collisional rates in flames and validate the model dependencies on polarization and saturation.

**Nitric oxide quenching pathways.** We have substantially improved our empirical models for quenching of NO  $A^2\Sigma^+$  by important collision partners in flames. Recently, we observed significant branching of the quenching process to the ground vibrational level in  $X^2\Pi$ . This finding may have important implications to the saturated detection of NO in high-pressure systems. We will extend our quenching studies to probe more completely the product state distributions for important room-temperature collision partners, including CO<sub>2</sub>, H<sub>2</sub>O, and O<sub>2</sub> using step-scan Fourier transform infrared spectroscopy in collaboration with David Osborn (Sandia). Results of these investigations will be used in conjunction with our cross-section measurements to provide an improved understanding of the quenching mechanisms and the role of the quenched molecules in saturation.

**Photolytic interference to CO and O detection.** We have shown compelling evidence for the photolytic production of atomic oxygen from vibrationally excited CO<sub>2</sub> in flames and demonstrated the significance of this interference to two-photon LIF detection of atomic oxygen using excitation at 226 nm. This process also interferes with two-photon detection of CO using excitation at 230 or 217 nm. Continuing to collaborate with Jonathan Frank, we will measure the temperature- and wavelength-dependent photolysis yields of O( $2p^3P$ ) and CO( $X^1\Sigma$ ) from CO<sub>2</sub>. The experiment will employ either an excimer laser at 193 nm or a tunable ns laser to photodissociate CO<sub>2</sub> in a high-temperature fluorescence cell. A delayed ps laser will probe the products with two-photon LIF detection of CO and O. Time-resolved fluorescence detection will be employed to correct for the effect of fluorescence quenching. Absolute calibration of the CO LIF detection will be determined by seeding the flow with a known concentration of CO. Because the photodissociation of CO<sub>2</sub> results in equal concentration of CO and O, this absolute calibration can be used to calibrate the O LIF detection scheme. Saturation with increasing laser energy of the photolysis processes will be characterized. We will compile these results in the form of a model that can be incorporated in comprehensive two-photon LIF models for the detection of CO and O.

### **BES-Supported Publications (2004-present)**

A. N. Karpetsis, T. B. Settersten, R. W. Schefer, and R. S. Barlow, "Laser imaging system for determination of three-dimensional scalar gradients in turbulent flames," *Opt. Lett.* **29**, 355 (2004).

X. Chen, B. D. Patterson, T. B. Settersten, "Time-domain investigation of OH ground-state energy transfer using picosecond two-color polarization spectroscopy," *Chem. Phys. Lett.* **388**, 358 (2004).

J. H. Frank, B. D. Patterson, X. Chen, T. B. Settersten, "Comparison of nanosecond and picosecond excitation for two-photon LIF imaging of atomic oxygen in flames," *Appl. Opt.*, **43**, 2588 (2004).

J. H. Frank, T. B. Settersten, "Two-photon LIF imaging of atomic oxygen in flames with picosecond excitation," *Proc. Combust. Instit.*, **30**, 1527 (2005).

J. W. Daily, W. G. Bessler, C. Schulz, V. Sick, T. B. Settersten, "Role of non-stationary collisional dynamics in determining nitric oxide LIF spectra," *AIAA J.*, **43**, 458 (2005).

T. B. Settersten, B. D. Patterson, J. A. Gray, "Temperature- and species-dependent quenching of NO  $A^2\Sigma^+(v'=0)$  probed by two-photon laser-induced fluorescence using a picosecond laser," *J. Chem. Phys.*, submitted (2006).

T. B. Settersten, B. D. Patterson, H. Kronmayer, V. Sick, C. Schulz, J. Daily, "Branching ratios for quenching of nitric oxide  $A^2\Sigma^+(v'=0)$  to  $X^2\Pi(v''=0)$ ," in preparation (2006).

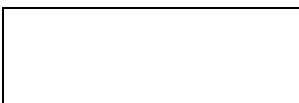
X. Chen, T. B. Settersten, "Investigation of OH ground-state energy transfer using picosecond two-color resonant four-wave-mixing spectroscopy," in preparation (2006).

# Theoretical Studies of Potential Energy Surfaces and Computational Methods

Ron Shepard  
Chemistry Division  
Argonne National Laboratory  
Argonne, IL 60439  
[email: shepard@tcg.anl.gov]

**Program Scope:** This project involves the development, implementation, and application of theoretical methods for the calculation and characterization of potential energy surfaces (PES) involving molecular species that occur in hydrocarbon combustion. These potential energy surfaces require an accurate and balanced treatment of reactants, intermediates, and products. This difficult challenge is met with general multiconfiguration self-consistent-field (MCSCF) and multireference single- and double-excitation configuration interaction (MR-SDCI) methods. In contrast to the more common single-reference electronic structure methods, this approach is capable of describing accurately molecular systems that are highly distorted away from their equilibrium geometries, including reactant, fragment, and transition-state geometries, and of describing regions of the potential surface that are associated with electronic wave functions of widely varying nature. The MCSCF reference wave functions are designed to be sufficiently flexible to describe qualitatively the changes in the electronic structure over the broad range of molecular geometries of interest. The necessary mixing of ionic, covalent, and Rydberg contributions, along with the appropriate treatment of the different electron-spin components (e.g. closed shell, high-spin open-shell, low-spin open shell, radical, diradical, etc.) of the wave functions are treated correctly at this level. Further treatment of electron correlation effects is included using large scale multireference CI wave functions, particularly including the single and double excitations relative to the MCSCF reference space. This leads to the most flexible and accurate large-scale MR-SDCI wave functions that have been used to date in global PES studies.

**Electronic Structure Code Maintenance, Development, and Applications:** A major component of this project is the development and maintenance of the COLUMBUS Program System. The COLUMBUS Program System computes MCSCF and MRSDCI wave functions, MR-ACPF (averaged coupled-pair functional) energies, MR-AQCC (averaged quadratic coupled cluster) energies, spin-orbit CI energies, and analytic energy gradients. Geometry optimizations to equilibrium and saddle-point structures can be done automatically for both ground and excited electronic states. The COLUMBUS Program System is maintained and developed collaboratively with several researchers including Isaiah Shavitt (University of Illinois), Russell M. Pitzer (Ohio State University), Thomas Mueller (Central Institute for Applied Mathematics, Juelich, Germany), and Hans Lischka (University of Vienna, Austria). The COLUMBUS Program System of electronic structure codes is maintained on the various machines used for production calculations by the Argonne Theoretical Chemistry Group, including Macintosh personal computers, IBM RS6000 workstations, DEC/COMPAC ALPHA workstations, the parallel IBM SP at NERSC, and the Group's 64-CPU Linux cluster. Most recently, the codes have been ported to the 320-CPU JAZZ Teraflop facility at Argonne. Ports to the Cray X1 and to the IBM Blue Gene machines are in progress. The parallel sections of the code are based on the single-program multiple-data (SPMD) programming model with explicit message passing using the portable MPI library, and the portable Global Array Library is used for data distribution. These computer codes are used in the production-level molecular applications by members and visitors of the Argonne Theoretical Chemistry Group. The next major release of the COLUMBUS codes will begin to incorporate the newer language features of F90/F95. This will facilitate future development and maintenance effort.



**Computation of Eigenvalue Bounds:** During the development of the Subspace Projected Approximate Matrix (SPAM) diagonalization method (described last year), it was necessary to compute bounds of approximate eigenvalues and eigenvectors. This work resulted in the development of a general computational procedure to compute rigorous eigenvalue bounds for general subspace eigenvalue methods. This method consists of the recursive application of a combination of the Ritz Bound, the Residual Norm Bound, the Gap Bound, and the Spread Bound. In addition to application within the SPAM method, this method may also be applied to the Davidson method as used in CI calculations and to the Lanczos method as used in the computation of vibrational eigenvalues. This software will be distributed using anonymous ftp and through the *Computer Physics Communications* program library.

**Linear Combination of Product Wavefunctions:** A practical limitation of standard MCSCF wave function optimization is the extension to active orbital spaces beyond the 12 to 14 orbital range. This range is sufficient for small molecules and for particular molecular reactions of larger molecules for which the orbitals involved in the reaction are localized and with relative unchanging nature. However, when the nature of the active orbitals changes significantly (e.g. strong valence-Rydberg mixing, or strong charge redistribution), then larger active orbital spaces are necessary. In this abstract last year, we introduced a new approach to MCSCF and CI wave function calculations. This method is based on the graphical unitary group approach (GUGA) of Shavitt. This approach uses an expansion basis that depends on a relatively small set of nonlinear parameters. The important feature of this approach is that the computational effort depends on this small number of variables  $N_\phi$  rather than the much larger dimension of the linear expansion space  $N_{\text{csf}}$ . Table I shows some statistics for singlet full-CI wave functions with  $n=N$  where  $n$  is the number of orbitals and  $N$  is the number of electrons.  $N_{\text{csf}}$  is the dimension of the underlying linear expansion space,  $N_\phi$  is the number of free variables in a single product basis function,  $t(H_{MN})$  is time in seconds required to compute a hamiltonian matrix element  $H_{MN} = \langle M | \hat{H} | N \rangle$  involving two product functions  $|M\rangle$  and  $|N\rangle$ , and  $t(E')$  is the time required to compute an analytic gradient of the energy with respect to the full set of nonlinear parameters  $\phi_{(mM)}$  (quantities that are used in the optimization of the energy). Note in particular that the last row of this table corresponds to an expansion space of about  $5.5 \cdot 10^{24}$  CSFs; this is about  $9.2N_A$ , or over 9 moles, of CSFs, many orders of magnitude larger than can be treated with traditional CI methods, yet only a modest effort of a few seconds is required to compute  $H_{MN}$  for this expansion. To appreciate the significance of these timings, we show in Fig. 1 a comparison with the effort that would be required for this same matrix element computed with traditional full-CI technology. For the largest wave function expansion, only a few seconds are required to compute  $H_{MN}$  with our new method, whereas about  $10^{24}$  seconds would be required with the traditional approach; as noted in Fig. 1, this latter number corresponds to about a million times the age of the universe. These timings show the tremendous potential of our new method.

At present, we have the ability to optimize wave functions only for small wave functions expansions such as those at the top of Table I. Figure 2 shows some computed dissociation curves for our new method using optimized wave function parameters for the ground state  $^1\Sigma_g^+$  of the  $N_2$  molecule. The incorrect dissociation for the RHF wave function is clearly shown in this figure; the computed  $D_e$  is about 1h too large, and the curve displays an incorrect  $\sim 1/R$  asymptotic behavior. The three-parameter PP-GVB wave function, which is a special case of our general approach based on a  $2^2 2^2 2^2$  PPMC Shavitt graph with no singly-occupied orbitals, is sufficiently flexible to dissociate to neutral N atom fragments with no spurious ionic contamination. However, it is not sufficiently flexible to dissociate to ground state  $^4S$  atom fragments; it dissociates instead to a mixture of ground and excited neutral fragments. The product functions based on the more flexible  $6^6$  Shavitt graph do dissociate correctly to  $^4S$  RHF ground state atom fragments. The  $N_\alpha=1$ ,  $N_\alpha=2$ , and  $N_\alpha=3$  wave functions all dissociate to the (exact in this model)

CASSCF limit as  $R \rightarrow \infty$ . The  $N_\alpha=3$  wave function is identical to the CASSCF wave function at all bond distances. The  $N_\alpha=1$  and  $N_\alpha=2$  curves are intermediate between the PP-GVB curve and the CASSCF curve; this is consistent with the fact that the PPMC Shavitt graph is a subgraph of the  $6^6$  full-CI graph and with the variational nature of the wave function for increasing values of  $N_\alpha$ . Fig. 3 shows an expanded view of the same curves near the  $R_e$  region. It is clear from these curves that even the  $N_\alpha=1$  wave function does a reasonably good job of describing the bond-breaking and spin-recoupling involved in the dissociation of the  $N \equiv N$  triple bond. The  $N_\alpha=2$  curve is slightly above the CASSCF curve, from about 0.3mh difference near  $R_e$ , increasing to about 3.1mh near  $R=3a_0$ , and then approaching 0.0mh as  $R \rightarrow \infty$ .

**Table I.** Statistics for Singlet Full-CI Wave Function Expansions

$n=N$	$N_{csf}$	$N_{row}$	$N_\phi$	$t(H_{MN})^a$	$t(E')^b$
2	3	5	2	0.00	0.00
4	20	14	13	0.00	0.00
6	175	30	39	0.00	0.00
8	1,764	55	86	0.00	0.01
10	19,404	91	160	0.00	0.05
12	226,512	140	267	0.00	0.16
14	2,760,615	204	413	0.01	0.44
16	34,763,300	285	604	0.04	1.24
18	449,141,836	385	846	0.07	3.48
20	5,924,217,936	506	1145	0.13	9.29
22	79,483,257,308	650	1507	0.21	25.67
24	1,081,724,803,600	819	1938	0.34	65.49
26	14,901,311,070,000	1015	2444	0.54	140.61
28	207,426,250,094,400	1240	3031	0.82	250.45
30	2,913,690,606,794,775	1496	3705	1.21	423.87
32	41,255,439,318,353,700	1785	4472	1.75	676.76
34	588,272,005,095,043,500	2109	5338	2.49	1.07E3
36	8,441,132,926,294,530,000	2470	6309	3.46	1.62E3
38	121,805,548,126,430,067,900	2870	7391	4.66	2.38E3
40	1,766,594,752,418,700,032,400	3311	8590	6.27	3.48E3
42	25,739,723,541,439,406,257,200	3795	9912	8.25	4.93E3
44	376,607,675,256,599,252,232,000	4324	11363	11.19	6.88E3
46	5,531,425,230,331,301,517,157,500	4900	12949	14.43	9.47E3

a) Times are in seconds on a 2.5GHz PowerMac G5 to construct a single  $H_{MN}$  matrix element.

b) Times in seconds to construct the analytic gradient vector  $E'(\boldsymbol{\phi}_0) \equiv \partial E(\boldsymbol{\phi}) / \partial \phi_{(mM)} \big|_{\boldsymbol{\phi}_0}$  for  $N_\alpha=1$  using the  $\mathbf{G}^{[u]}$  and  $\mathbf{S}^{[u]}$  arrays.

Our new method is characterized by several important features. First, open-shell functions may be included in our expansions, which are formulated directly in terms of spin-eigenfunctions. This allows our new method to be used for the reactions that are important to combustion chemistry (i.e. involving radicals and other open-shell electronic states) without introducing spin contamination. Second, we place no intrinsic restrictions on the orbital occupations, so our product functions are not restricted to only geminals or to other molecular fragments. Third, we use linear combinations of  $N_\alpha$  product wave functions rather than a single expansion term. This allows our method to be used for both ground and excited electronic states, the increased wave function flexibility will lead to more accurate wave functions, and it will allow the computation of transition moments, nonadiabatic coupling, and other properties that at present can only be computed reliably with MCSCF and MRCI approaches. This method will be included in the COLUMBUS Program System distribution. Our present focus is on the efficient optimization of the nonlinear wave function parameters for larger wave function expansions, such as those near the bottom of Table I.

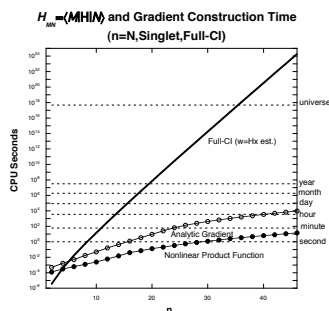


Fig. 1

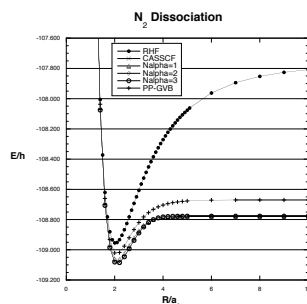


Fig. 2

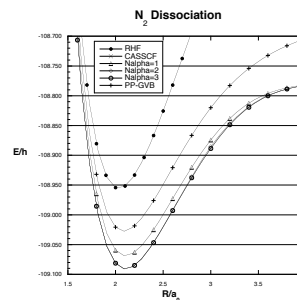


Fig. 3

**Public Distribution of Software:** The COLUMBUS Program System is available using the *anonymous ftp* facility of the internet. The codes and online documentation are available from the web address <http://www.univie.ac.at/columbus/>. In addition to the source code, the complete online documentation, installation scripts, sample calculations, and numerous other utilities are included in the distribution. A partial implementation of an IEEE POSIX 1009.3 library has been developed and is available from <ftp://ftp.tcg.anl.gov/pub/libpxf>. This library simplifies the porting effort required for the COLUMBUS codes, and also may be used independently for other Fortran programming applications. The SPAM code described above is available from <ftp://ftp.tcg.anl.gov/pub/spam>.

This work was supported by the U.S. Department of Energy by the Office of Basic Energy Sciences, Division of Chemical Sciences, Geosciences and Biosciences, under contract W-31-109-ENG-38.

#### Publications:

- “Analytic Evaluation of Nonadiabatic Coupling Terms at the MR-CI Level. I: Formalism,” H. Lischka, M. Dallos, P. G. Szalay, D. R. Yarkony, and R. Shepard, *J. Chem. Phys.* **120**, 7322-7329 (2004).
- “Analytic Evaluation of Nonadiabatic Coupling Terms at the MR-CI Level. II. Minima on the Crossing Seam: Formaldehyde and the Photodimerization of Ethylene,” M. Dallos, H. Lischka, R. Shepard, D. R. Yarkony, and P. G. Szalay, *J. Chem. Phys.* **120**, 7330-7339 (2004).
- “An Ab Initio Study of AmCl<sup>+</sup>: f-f Spectroscopy and Chemical Binding,” J. L. Tilson, C. Naleway, M. Seth, R. Shepard, A. F. Wagner, and W. C. Ermler, *J. Chem. Phys.* **121**, 5661-5675 (2004).
- “Computing Eigenvalue Bounds for Iterative Subspace Methods,” Y. Zhou, R. Shepard, and M. Minkoff, *Computer Physics Comm.* **167**, 90-102 (2005).
- “Software for Computing Eigenvalue Bounds for Iterative Subspace Methods,” R. Shepard, M. Minkoff, and Y. Zhou. *Computer Physics Comm.* **170**, 109-114 (2005).
- “Advanced Software for The Calculation of Thermochemistry, Kinetics, and Dynamics,” D. M. Medvedev, S. K. Gray, A. F. Wagner, M. Minkoff, and R. Shepard, *J. Physics: Conference Series* **16**, 247-251 (2005).
- “A General Nonlinear Expansion Form for Electronic Wave Functions,” R. Shepard, *J. Phys. Chem. A* **109**, 11629-11641 (2005).
- “Hamiltonian Matrix and Reduced Density Matrix Construction with Nonlinear Wave Functions,” R. Shepard, (*submitted*).
- “Optimization of Nonlinear Wave Function Parameters,” R. Shepard and M. Minkoff, (*submitted*).

## COMPUTATIONAL AND EXPERIMENTAL STUDY OF LAMINAR FLAMES

M. D. Smooke and M. B. Long  
Department of Mechanical Engineering  
Yale University  
New Haven, CT 06520  
[mitchell.smooke@yale.edu](mailto:mitchell.smooke@yale.edu)

### Program Scope

Our research has centered on an investigation of the effects of complex chemistry and detailed transport on the structure and extinction of hydrocarbon flames in coflowing axisymmetric configurations. We have pursued both computational and experimental aspects of the research in parallel. The computational work has focused on the application of accurate and efficient numerical methods for the solution of the boundary value problems describing the various reacting systems. Detailed experimental measurements were performed on axisymmetric coflow flames using two-dimensional imaging techniques. Spontaneous Raman scattering and laser-induced fluorescence were used to measure the temperature, major and minor species profiles. Laser-induced incandescence has been used to measure soot volume fractions. A new approach to optical pyrometry has been developed to measure temperatures where the other techniques fail due to the presence of soot. Our goal has been to obtain a more fundamental understanding of the important fluid dynamic and chemical interactions in these flames so that this information can be used effectively in combustion modeling.

### Recent Progress

The major portion of our work during the past year has focused on a combined computational and experimental study of time varying, axisymmetric, laminar unconfined methane-air diffusion flames and on a combined computational and experimental study of sooting and nonsooting axisymmetric, laminar diffusion flames. The time varying systems can bridge the gap between laminar and fully turbulent systems. In addition, time varying flames offer a much wider range of interactions between chemistry and fluid dynamics than do steady-state configurations. The sooting flames can enable the investigator to understand the detailed inception, oxidation and surface growth processes by which soot is formed in hydrocarbon flames.

*Heat Release:* A non-sooting, lifted, methane/air, coflowing, non-premixed flame was studied experimentally and computationally. The flame structure was computed by solving the fully elliptic governing equations with detailed transport coefficients and an optically thin radiation submodel. Gas temperature, major species mole fractions, and non-fuel hydrocarbon concentrations were experimentally mapped in two dimensions with both probe techniques (coupled to infrared absorption spectroscopy and on-line mass spectrometry) and *in situ* optical diagnostics (Rayleigh and Raman scattering). Contour plots of measured and computed formaldehyde concentrations agree reasonably well and both revealed a region of intense formaldehyde production near the lifted flame base. High formaldehyde production rates correlated well with regions of high heat release. Further, regions of the dominant formaldehyde formation reaction,  $\text{CH}_3 + \text{O} = \text{HCHO} + \text{H}$ , also correlated with areas of maximum heat release rate. The work will be transitioned to our soot formation and time-dependent flame studies.

*Soot Modeling:* We model the soot kinetics as coalescing, solid carbon spheroids undergoing surface growth in the free molecule limit. The particle mass range of interest is divided into sections and an equation is written for each section including coalescence, surface growth, and

oxidation. For the smallest section, an inception source term is included. The transport conservation equation for each section includes thermophoresis, an effective bin diffusion rate, and source terms for gas-phase scrubbing. The gas and soot equations are additionally coupled through non-adiabatic radiative loss in the optically-thin approximation. The inception model employed here is based on an estimate of the formation rate of two- and three-ringed aromatic species (naphthalene and phenanthrene), and is a function of local acetylene, benzene, phenyl and molecular hydrogen concentrations. Oxidation of soot is by  $O_2$  and  $OH$ . The surface growth rate is based upon that of Harris and Weiner [1] with an activation energy as suggested by Hura and Glassman [2]. Using planar laser imaging, we obtain two-dimensional fields of temperature, fuel concentration, and soot volume fraction in the  $C_2H_4/N_2$  flames. The temperature field is determined using the two scalar approach of Stårner *et al.* [3]. The soot volume fraction field is determined by laser-induced incandescence (LII). In our initial work, probe measurements of the soot volume fraction were used for calibration. More recently, absorption measurements are being coupled with the LII measurements both as a check for the calibration and as an independent measurement of the soot volume fraction profile. The use of multiple measurement techniques should improve our overall confidence in the results as well as provide better estimates of the accuracy of the measurements.

Fuel and nitrogen are introduced through the center tube (4 mm id) and air through the outer coflow with plug flow velocity profiles. Both velocity profiles were those employed in the experiments. Flames containing 32% (68%), 40% (60%), 60% (40%) and 80% (20%) mole fractions of ethylene (nitrogen) with a bulk-averaged velocity of 35 cm/sec were studied. The coflow air velocity was 35 cm/sec. Reactant temperatures were assumed to be 298 K. Calculations were performed on an AMD Dual Opteron 240 system.

We have investigated the changing soot field as the dilution fuel fraction in the central tube changed [5,6]. We were able to predict soot volume fractions along the wings of the flame in good agreement with experimental measurements; but we underpredicted soot volume fractions along the centerline. This deficiency was particularly true for the flames with higher fuel mole fractions. The transition from peak soot along the centerline to peak soot volume fractions along the wings (observed both in our experiments and our modeling) is qualitatively consistent with the early work of Santoro and coworkers [e.g., 7,8], although in the prior work, the fuel jet was undiluted and the transition in the soot field was observed by increasing the fuel jet velocity.

To help understand the reasons for the transition of soot from the centerline to the wings of the flame as the fuel fraction increases, we began an investigation of the relative rates of inception, surface growth, and oxidation, along with a particle residence time analysis as a function of fuel fraction. While inception tends to peak on the centerline, the maximum in surface growth migrates from the centerline to the wings of the flame as the fuel fraction increases. Concurrently, the relative importance of surface growth and inception reverses. This change in the relative importance of these two subprocesses is due to the significant increase in residence time available for soot growth in the flame wings. Moreover, even with a significant increase in residence time along the centerline (and the local increase in fuel fraction) associated with the less diluted flames, the ageing of the soot particles and the lower temperatures inhibit the enhanced soot inception and growth along the centerline.

*Time-Varying Flames:* Atmospheric pressure, overventilated, axisymmetric, coflowing, nonpremixed laminar flames were generated with a burner in which the fuel flows from an uncooled 4.0 mm inner diameter vertical brass tube (wall thickness 0.038 mm) and the oxidizer flows from the annular region between this tube and a 50 mm diameter concentric tube. The oxidizer is air while the fuel is a mixture containing methane (nitrogen) 65% (35%) by volume, to

eliminate soot. The burner includes a small loudspeaker in the plenum of the fuel jet, which allows a periodic perturbation to be imposed on the exit parabolic velocity profile. Perturbations of 30% and 50% of the average velocity have been investigated. Because the flame is slightly lifted, there is no appreciable heat loss to the burner.

Experimentally, Rayleigh and Raman scattering were used to obtain two-dimensional fields of temperature, and of mole fractions of  $N_2$ ,  $CO_2$ ,  $CH_4$ ,  $H_2$ ,  $O_2$ ,  $CO$ , and  $H_2O$ . Measurements of excited-state  $CH$  ( $CH^*$ ) emission were used to determine overall flame shape during the initial cycles after the forcing is initiated. Particle image velocimetry (PIV) was used to determine the fuel tube exit velocity and phase over a cycle of the forcing modulation. Computationally, we solved the transient equations for the conservation of total mass, momentum, energy and species mass with detailed transport and finite rate chemistry submodels. The governing equations are written using a modified vorticity-velocity formulation and are solved on an adaptively refined grid using implicit time stepping and Newton's method nested with a Bi-CGSTAB iterative linear system solver. Results of the study included an investigation of the start-up features of the time-dependent flames and the time it takes for initial transients to dissipate. We included a detailed description of the fluid dynamic-thermochemical structure of the flame at a 20 Hz forcing frequency for both 30% and 50% sinusoidal velocity perturbations. Comparisons of experimentally-determined and calculated temperature,  $CO$  and  $H_2O$  mole fraction profiles provided verification of the accuracy of the model.

As we move toward the investigation of soot formation in these time-varying flames, we will need to adopt different diagnostics in sooty regions of the flame, since the presence of soot will interfere with the Raman- and Rayleigh-based diagnostics that we have used previously. We have investigated the potential application of a relatively low-cost, color digital camera, for use as a three-color optical pyrometer for measuring soot temperatures within the flame. The use of the built-in color filter array (CFA) of the digital camera allows for two-dimensional imaging of flame emission at the wavelengths of the color filters. The image data provide pixel-by-pixel spectral and spatial information, which are then used to calculate the two-dimensional flame temperatures. The filter profiles of the CFA were characterized to provide a calibration for the two-color method used to calculate the temperatures. Images were taken of sooting, axisymmetric laminar ethylene flames, and the two-dimensional temperature field was calculated. Comparisons were made to temperature and soot distributions provided by our calculations.

## **Future Plans**

During the next year we hope to expand our research in several areas. We will continue our study of sooting hydrocarbon flames with the goal of understanding the interaction of soot formation and  $NO_x$  production with an emphasis on the effects of soot radiation on thermal and prompt  $NO_x$ . We also plan on including the model in our time-dependent flame systems with the goal of being able to predict soot volume fractions as a function of time. Experimentally we will continue our work on improving the accuracy of our soot volume fraction measurements, as well as applying other diagnostic techniques that can provide information on the soot such as primary particle size and aggregation. We also plan on using LIF to measure  $NO_x$  in sooting ethylene-air flames and we will continue to develop the soot pyrometry by improving the characterization of the camera's color filter array. Finally, in the time-varying flames, we will perform phase-averaged particle image velocimetry to allow a comparison of measured and computed velocity fields

## References

1. Harris, S.J., and Weiner, A.M., *Combust. Sci. Tech.*, **31**, p. 155, (1983).
2. Hura, H.S. and Glassman, I., *Proceedings of the Combustion Institute*, **22**, p. 371, (1988).
3. Starner, S., Bilger, R. W., Dibble, R. W., Barlow, R. S., *Combust. Sci. Tech.*, **86**, p. 223, (1992).
4. Sun, C. J., Sung, C. J., Wang, H., and Law, C. K., *Comb and Flame*, **107**, p. 321, (1996).
5. Smooke, M. D., McEnally, C. S., Pfefferle, L. D., Hall, R. J., and Colket, M. B., *Comb. Flame*, **117**, p. 117, (1999).
6. Smooke, M. D., Hall, R. J., Colket, M. B., Fielding, J., Long, M. B., McEnally, C. S., and Pfefferle, L. D., *Comb. Theory and Modelling*, **8**, p. 593, (2004).
7. Santoro, R. J., Semerjian, H. G., and Dobbins, R. A., *Comb. Flame*, **51**, p. 203, (1983).
8. Santoro, R. J. and Semerjian, H. G., *Proceedings of the Combustion Institute*, **20**, p. 997, (1984).

## DOE Sponsored Publications since 2004

1. F. Laurent, V. Santoro, M. Noskov, M. D. Smooke, A. Gomez and M. Massot, "Accurate Treatment of Size Distribution Effects in Polydisperse Spray Diffusion Flames: Multi-Fluid Modelling, Computations and Experiments," *Comb. Theory and Modelling*, **8**, (2004).
2. M.D. Smooke, R.J. Hall, M.B. Colket, J. Fielding, M.B. Long, C.S. McEnally, and L.D. Pfefferle, "Investigation of the Transition from Lightly Sooting towards Heavily Sooting Coflow Ethylene Diffusion Flames," *Comb. Theory and Modelling* **8**, (2004).
3. J. A. Cooke, M. D. Smooke, M. Bellucci, A. Gomez, A. Violi, T. Faravelli and E. Ranzi, "Computational and Experimental Study of a JP-8 Counterflow Diffusion Flame," *Proceedings of the Combustion Institute*, **30**, (2005).
4. V. V. Toro, A. V. Mokhov, H. B. Levinsky and M. D. Smooke, "Combined Experimental and Computational Study of Laminar, Axisymmetric Hydrogen-Air Diffusion Flames," *Proceedings of the Combustion Institute*, **30**, (2005).
5. K.T. Walsh, J. Fielding, M.D. Smooke, A. Linan and M.B. Long, "A Comparison of Computational and Experimental Lift-Off Heights of Coflow Laminar Diffusion Flames," *Proceedings of the Combustion Institute*, **30**, (2005).
6. M. Noskov and M. D. Smooke, "An Implicit Compact Scheme Solver with Application to Chemically Reacting Flows," *J. Comp. Physics*, **203**, (2005).
7. M. J. H. Anthonissen, B. A. V. Bennett and M. D. Smooke, "An Adaptive Multilevel Local Defect Correction Technique with Application to Combustion," *Comb. Theory and Modelling*, **9**, (2005).
8. S. A. Kaiser, J. H. Frank, and M. B. Long, "Use of Rayleigh Imaging and Ray Tracing to Correct for Beam-Steering Effects in Turbulent Flames," *Appl. Opt.* (2005).
9. J. H. Frank, S. A. Kaiser, and M. B. Long, "Multiscalar Imaging in Partially Premixed Jet Flames with Argon Dilution," *Combust. Flame*, **143**, (2005).
10. M.D. Smooke, M.B. Long, B.C. Connelly, M.B. Colket and R.J. Hall, "Soot Formation in Laminar Diffusion Flames," *Combust. Flame* **143**, (2005).
11. M. Noskov, M. Benzi and M. D. Smooke, "An Implicit Compact Scheme Solver for Two-Dimensional Multicomponent Flows," to be published *Comp. and Fluids*, (2006).
12. S. Dworkin, B. A. V. Bennett and M. D. Smooke, "A Mass-Conserving Vorticity-Velocity Formulation with Application to Nonreacting and Reacting Flow," to be published *J. Comp. Phys.*, (2006).

## Universal and State-Resolved Imaging Studies of Chemical Dynamics

Arthur G. Suits  
*Department of Chemistry, Wayne State University*  
5101 Cass Ave  
Detroit, MI 48202  
asuits@chem.wayne.edu

### Program Scope

The focus of this program is on combining universal ion imaging probes providing global insight, with high-resolution state-resolved probes providing quantum mechanical detail, to develop a molecular-level understanding of chemical phenomena. Particular emphasis is placed upon elementary reactions important in understanding and predicting combustion chemistry. This research is conducted using state-of-the-art molecular beam machines, photodissociation, reactive scattering, and vacuum ultraviolet lasers in conjunction with ion imaging techniques. An ongoing parallel effort is made to develop new tools and experimental methods with which to achieve these goals.

### Recent Progress

Roaming atoms. Last year we reported evidence for a novel “roaming atom” mechanism in formaldehyde photodissociation. Our high-resolution slice imaging experiments featured detection of single rotational levels of CO produced in dissociation of formaldehyde in the vicinity of the threshold for H atom loss. The results showed, in addition to the conventional molecular elimination channel known to give rise to vibrationally cold H<sub>2</sub> in conjunction with rotationally excited CO, a second channel yielding highly vibrationally excited H<sub>2</sub> with rotationally cold CO. Dynamical calculations from the Bowman group confirmed this as an intramolecular H abstraction process in which one of the H atoms roams around the molecule, bypassing the usual transition state entirely. We have completed an intensive imaging study of formaldehyde dissociation along three lines: first, we have explored the dynamics of the roaming atom mechanism in detail. Our model of this involves dissociation of the HCO in the “field” of the roaming atom, giving highly vibrationally excited H<sub>2</sub> that also gives substantial rotational excitation as seen in the experiments. Remarkably, the roaming H<sub>2</sub> rotational excitation is higher than in the impulsive dissociation in the conventional molecular elimination process. The roaming atom dynamics are summarized in the trajectory from Bowman’s calculations shown in Fig. 1.

The second aspect of our formaldehyde investigation currently under analysis concerns the energy dependence of the roaming mechanism. We have obtained photofragment excitation spectra and countless sliced images for single CO rotational levels following dissociation at energies up to several thousand wavenumbers above the radical threshold, and find the importance of roaming relative to the molecular channel continues to grow. This provides strong support of the view that the roaming channel is directly related to the radical dissociation process, and exhibits similar excitation behavior. On the other hand, despite the increase in available energy, the product rotational state distributions for the roaming mechanism show little change, as expected given the model sketched above.

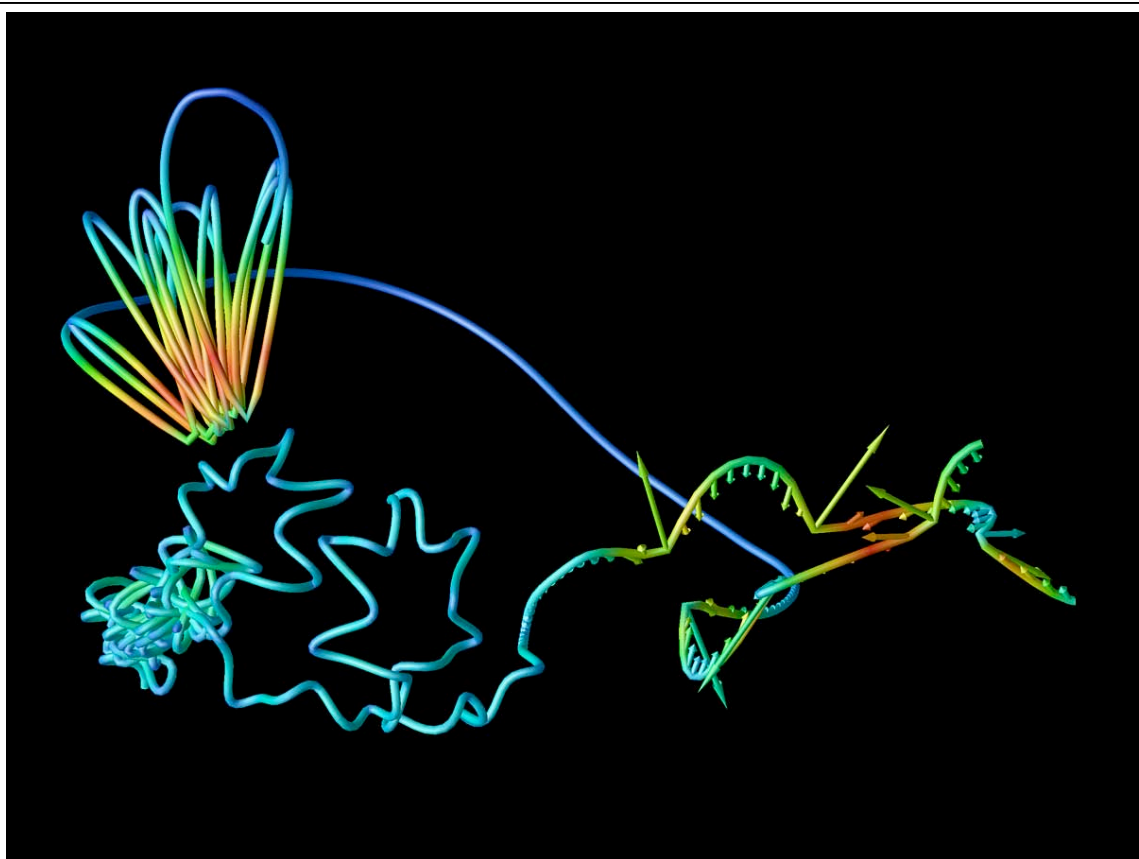


Figure 1 . A sample roaming trajectory yielding  $\text{H}_2$   $v=6$  and  $j_{\text{CO}}=5$ . H atom speeds are encoded in trajectory color, and forces (direction and magnitude) are shown in the abstraction region. Only the H atoms are shown. The trajectory begins at left and ends with departure of  $\text{H}_2$  at right.

Finally, we have used our high-resolution measurements of the conventional molecular channel to give total correlated  $\nu_{\text{H}_2}$  and  $j_{\text{CO}}$  product state distributions. The photolysis energy ranged from 1800 to 4100  $\text{cm}^{-1}$  above the molecular elimination threshold, and included the  $2^14^1$ ,  $2^14^3$ ,  $2^24^1$ ,  $2^24^3$ , and  $2^34^1$  transitions to  $S_1$ . These detailed measurements allowed determination of the  $\nu_{\text{H}_2}$ -specific CO rotational distributions even though the data was obtained in an orthogonal dimension. We find a strong correlation between the  $\text{H}_2$  vibration and the CO rotation due to the dynamical influence of the highly repulsive exit channel. A simple model which estimates the impact parameters for each  $\text{H}_2$  product vibrational level determined by calculating the molecular transition/displacement vectors at various points along the reaction coordinate can partially account for the trends in the correlated distributions. Rotational correlations between  $\text{H}_2$  and CO products have been confirmed to be very weak.

*State-resolved crossed-beam slice imaging.* We have recently achieved DC slice imaging of single product rovibrational states in crossed-beam reactive scattering. Our results for the  $\text{HCl}$  ( $v=0$ ,  $J=2$ ) product of the  $\text{Cl}+\text{C}_2\text{H}_6$  reaction are shown in Fig. 2. The image shows strongly coupled angular and translational energy distributions revealing features of the reaction not seen in previous studies. The overall distribution is mainly forward scattered with respect to the Cl beam, with a translational energy distribution peaking

near the collision energy. However, there is a substantial backscattered contribution that is very different. It shows a sharp peak at 8.0 kcal/mol, but extends to much lower energy, implying substantial internal excitation in the ethyl radical co-product. We have recently extended this to a range of collision energies and to the full range of product rotational states. These results provide new insight into the reaction, and they have been examined in terms of alternative models of the dynamics. This work represents the first genuine crossed-beam study in which a product other than the methyl radical was detected with quantum state specificity, and shows the promise of the approach generally for high resolution state-resolved reactive scattering.

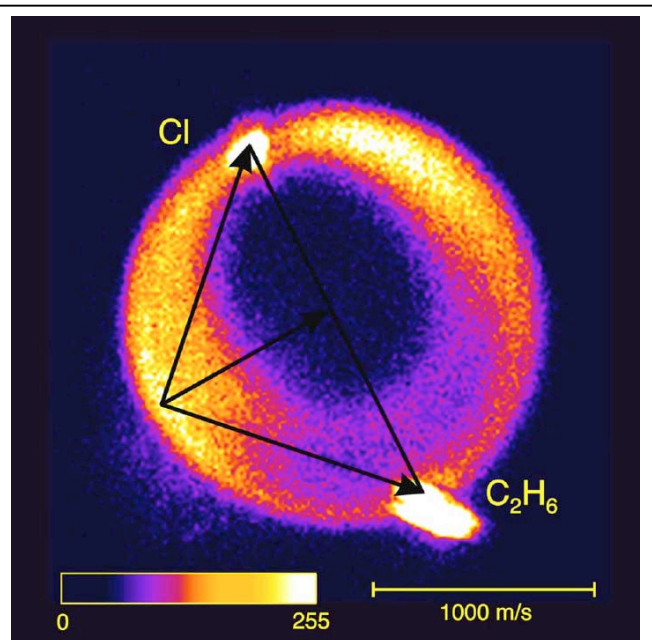


Figure 2. Raw image of HCl ( $v=0, J=2$ ) from reaction of Cl + C<sub>2</sub>H<sub>6</sub> at 6.7 kcal/mol, with Newton diagram superimposed.

### Selected Future Plans

Roaming atom reaction dynamics. We will perform DC slice imaging a range of systems to investigate the generality of the roaming mechanism. Current effort is focused on acetaldehyde, in which either CH<sub>3</sub> or H atom may be the roaming species, and in acetophenone, in which methyl or phenyl radicals will be the roaming species. Again, we will use state-resolved slice imaging detection of CO and look for the characteristic bimodal distributions and low product rotational levels to identify the roaming process.

State-resolved and universal crossed-beam DC slice imaging. We have plans to pursue a range of studies using our crossed-beam sliced imaging approach. We will continue study of the Cl abstraction reactions, both with a range of target alkanes and with deuterated systems to understand the details of the dynamics that have emerged in the initial studies above. We also plan to examine O atom reactions, in particular the reactions with unsaturated hydrocarbons, in which state resolved slice imaging may reveal correlated product information and details not seen in the well-known universal studies of Y. T. Lee and coworkers. Finally, we have recently developed an intense CN source and have had preliminary success in crossed-beam reaction of CN with alkanes. We will examine these reactions, both with universal VUV detection of the radical, and for the reaction CN+CH<sub>4</sub> we will use state resolved detection of CH<sub>3</sub>.

State-correlated photochemistry of HCCO. We propose state-correlated imaging of the ketylenyl radical, HCCO. There is a marvelous body of work on the spectroscopy and

dynamics of this system. Although the dynamics measurements were obtained at fairly low translational energy resolution, they provide a roadmap for rich correlated state imaging measurements of the CO. This radical system has the advantage that metastable levels of the state may be excited state-specifically so we need not worry about contamination by dissociation of unknown species. Small changes in photolysis energy were seen to change the branching between dissociation on the doublet and quartet surfaces quite dramatically. Again, quantum state specific probing of the CO product will provide correlated internal state information on the rovibrational levels of both ground state ( $X^2\Pi$ ) and electronically excited ( $a^4\Sigma^-$ ) CH product, allowing investigation of ground state dissociation and intersystem crossing dynamics.

### DOE Publications 2004-present

W. Li, R. Lucchese, A. Doyuran, Z. Wu, H. Loos, G. E. Hall and A. G. Suits, "Superexcited state dynamics probed with an extreme ultraviolet free electron laser," *Phys. Rev. Lett.*, **92** 083002 (2004).

X. Liu and A. G. Suits, "The dynamics of hydrogen abstraction in polyatomic molecules," in **Modern Trends in Chemical Reaction Dynamics**, X. M. Yang, K. Liu, eds. (World Scientific, Singapore: 2004)

D. Townsend, S. A. Lahankar, S. K. Lee, S. D. Chambreau, A. G. Suits, X. Zhang, J. Rheinecker, L.B. Harding and J. M. Bowman, "The roaming atom: Straying from the reaction path in formaldehyde decomposition," *Science* **306**, 1158 (2004) (10.1126/ science.1104386).

S. K. Lee, D. Townsend, O. S. Vasyutinskii and A. G. Suits, " $O(^1D)$  orbital orientation in the ultraviolet photodissociation of ozone," *Phys. Chem. Chem. Phys.*, **7**, 1650, (2005).

D. Townsend, W. Li, S. K. Lee, R. L. Gross and A. G. Suits, "Universal and State resolved imaging of chemical dynamics," (Invited feature article) *J. Phys. Chem. A*, **109**, 8661 (2005) 10.1021/jp0526086.

S. D. Chambreau, D. Townsend, S. A. Lahankar, S. K. Lee and A. G. Suits, "Novel molecular elimination mechanism in formaldehyde photodissociation: The roaming H atom pathway," *Phys. Scr.* **73** C89-C93 (2006).

Brian D. Leskiw, Myung Hwa Kim, Gregory E. Hall and Arthur G. Suits, "Reflectron Velocity Map Ion Imaging," *Rev. Sci. Instr.* **76**, 104101 (2005).

W. Li, C. Huang, M. Patel, D. Wilson and A. G. Suits, "State-Resolved Reactive Scattering by Slice Imaging: A New View of the  $Cl+C_2H_6$  Reaction," *J. Chem. Phys.* **124**, 011102 (2006).

A. Komissarov, M. Minitti, A. G. Suits and G. E. Hall, "Correlated product distributions from ketene dissociation measured by dc sliced ion imaging" *J. Chem. Phys.* **124**, 014303 (2006).

Steven D. Chambreau, Sridhar A. Lahankar, and Arthur G. Suits, "Correlated  $v_{H_2}$  and  $j_{CO}$  product states from formaldehyde photodissociation: Dynamics of molecular elimination," *J. Chem. Phys.* (in press).

C. Huang, W. Li and A. G. Suits, "Rotationally-Resolved Reactive Scattering: Imaging Detailed  $Cl + C_2H_6$  Reaction Dynamics," *J. Chem. Phys.* (in press).

# Elementary Reaction Kinetics of Combustion Species

Craig A. Taatjes

*Combustion Research Facility, Sandia National Laboratories,*

*P.O. Box 969, Mail Stop 9055*

*Livermore, CA 94551-0969*

*cataatj@sandia.gov [www.ca.sandia.gov/CRF/staff/taatjes.html](http://www.ca.sandia.gov/CRF/staff/taatjes.html)*

## SCOPE OF THE PROGRAM

This program aims to develop new optical methods for studying chemical kinetics and to apply these methods to the investigation of fundamental chemistry relevant to combustion science. The central goal is to perform accurate measurements of the rates at which important free radicals react with stable molecules. Understanding the reactions in as much detail as possible under accessible experimental conditions increases the confidence with which modelers can treat the inevitable extrapolation to the conditions of real-world devices. Another area of research is the investigation and application of new detection methods for precise and accurate kinetics measurements. Absorption-based techniques are emphasized, since many radicals critical to combustion are not amenable to fluorescence detection. Finally, measurements of species in flames (see also the abstract of Nils Hansen) are used to reveal important reactions or species for individual laboratory investigation.

An important part of our strategy is using experimental data to test and refine detailed calculations (working in close cooperation with Stephen Klippenstein and Jim Miller), drawing on the calculational results to gain insight into the interpretation of our results and to guide experiments that will probe key aspects of potential energy surfaces. This methodology has been applied in our investigations of the reactions of alkyl radicals with O<sub>2</sub>, where the combination of rigorous theory and validation by detailed experiments has made great strides toward a general quantitative model for alkyl oxidation. Reactions of unsaturated hydrocarbon radicals that may play a role in soot formation chemistry, and reactions that may produce or consume enols in flames are also targets of investigation.

## PROGRESS REPORT

The current efforts of the laboratory center on developing high-sensitivity absorption-based techniques for kinetics measurements, and on applying these techniques to investigate important combustion reactions. A major focus continues to be the application of cw infrared frequency-modulation (FM) spectroscopy to measurements of product formation in reactions of alkyl radicals with O<sub>2</sub> and the exploitation of visible absorption spectroscopy of the vinyl radical for kinetics measurements. A new multiplexed photoionization mass spectrometric reactor has also been installed at the Advanced Light Source, in collaboration with Stephen Leone and Musa Ahmed at Lawrence Berkeley National Laboratory and David Osborn at Sandia.

**Enols as Combustion Intermediates.** Carbonyl (keto) compounds are well-established combustion intermediates. However, their less-stable enol tautomers, bearing OH groups adjacent to carbon-carbon double bonds, are not included in standard models. The power of the synchrotron photoionization method allowed us to observe substantial quantities of 2, 3, and 4-carbon enols in flames of many different fuels. Investigation of the concentration profiles demonstrated that the chemistry of enols in the flames cannot be accounted for purely by keto-enol tautomerization. Explaining enol formation and describing the consequences of these unexpected compounds will require revision to current hydrocarbon oxidation mechanisms. However, little is known about enols' flame chemistry. Enol formation in low-pressure flames takes place in the preheat zone and its precursors are most likely fuel species or the early products of fuel decomposition. We have correlated the mole fraction profiles of ethenol in several representative low-pressure flames with those of possible precursor species as a means for judging likely formation pathways in flames. These correlations and modeling suggest that the reaction of OH with ethene is in fact the dominant source of ethenol in many hydrocarbon flames, and that addition-elimination reactions of OH with other alkenes are also likely to be responsible for enol formation in flames. On this basis, enols are predicted to be minor intermediates in most flames and should be most prevalent in olefinic flames where reactions of the fuel with OH can produce enols directly.

A new reactor coupled to a novel photoionization mass spectrometer (PIMS) is operational at the Chemical Dynamics Beamline of the Advanced Light Source (ALS). The first set of experiments yielded the photoionization efficiency curve of  $\text{CH}_3\text{O}_2$ , giving the first experimental adiabatic ionization energy of an alkylperoxy radical (see David Osborn's abstract). Other experiments have confirmed the production of ethenol in the reaction of hydroxyl with ethene and production of ethenol and propenol in the reaction of hydroxyl with propene.

**Measurements of Product Formation in Alkyl +  $\text{O}_2$  Reactions.** In the previous year, quantitative comparisons of  $\text{HO}_2$  formation measurements with master equation models revealed discrepancies in the *i*-propyl oxidation. The production of  $\text{DO}_2$  in the deuterated *i*-propyl +  $\text{O}_2$  reaction showed systematic deviation of the experimental  $\text{DO}_2$  production and the predictions of the master equation solution, with the experiment showing higher prompt  $\text{DO}_2$  yields and faster secondary  $\text{DO}_2$  production. Reconciliation of model with experiment has been obtained by lowering the transition state to formation of  $\text{HO}_2$  from *i*-propylperoxy radical, producing a new "best fit" model. This agreement comes at the cost of making the calculated rate coefficient for *i*-propyl +  $\text{O}_2$  to form propene about a factor of 7 higher than the value derived in the experimental work of Gulati and Walker (Gulati, S. K.; Walker, R. W. *J. Chem. Soc. Faraday Trans. 2* **1988**, *84*, 401), but maintains good agreement with the equilibrium constant determinations of Knyazev and Slagle.

**Laser Photolysis/cwLPA Measurements of C<sub>2</sub>H<sub>3</sub> Reactions.** The vinyl radical and the allyl radical are formed promptly from the 193 nm photolysis of their respective trichlorosilane precursors. By comparison of the transient visible absorption and the 1315 nm I atom absorption from 266 nm photolysis of vinyl iodide and allyl iodide, the absorption cross sections at 404 nm of vinyl radical ( $(3.0 \pm 0.5) \times 10^{-19} \text{ cm}^2$ ) and allyl radical ( $(3.6 \pm 0.5) \times 10^{-19} \text{ cm}^2$ ) have been derived. Using these cross sections, the vinyl radical yield from trichlorovinylsilane is determined to be  $\phi = (0.89 \pm 0.20)$  per 193 nm photon absorbed, and the allyl radical yield from allyltrichlorosilane  $\phi = (0.7 \pm 0.20)$  per 193 nm photon absorbed. The vinyl radical cross section appears inconsistent with a measurement from the Koshi group. The vinyl radical cross section measurements in Koshi's group relied on a second-order fit to the vinyl radical decay, in conjunction with the literature measurement of the vinyl radical self-reaction, to derive the C<sub>2</sub>H<sub>3</sub> concentration. It is our present contention that the literature rate coefficient for the vinyl radical self-reaction is in error.

As discussed in last year's abstract, we have applied long-path absorption spectroscopy in the (A-X) band of C<sub>2</sub>H<sub>3</sub> to investigations of the C<sub>2</sub>H<sub>3</sub> self-reaction. Photolysis of vinyl iodide at 266 nm produced vinyl radicals and I atoms; the I atom is measured by infrared absorption on the spin-orbit transition, and the initial vinyl radical concentration is assumed to be equal to the initial I atom concentration. The present results are almost a factor of three below the literature determinations, with a slight negative temperature dependence. In the past year we have begun to make confirmatory measurements of the vinyl radical absorption cross section and the self-reaction rate constant, using different vinyl precursors (hence the trichlorovinylsilane work). The definitive confirmation of these results, including direct measurement of the I atom absorption cross section and kinetics measurements at various probe laser wavelengths, will be one of the earliest targets of the next year.

#### **FUTURE DIRECTIONS**

Characterization of R + O<sub>2</sub> reactions will continue, both in the infrared absorption work and in the new PIMS apparatus. The ability to simultaneously probe various reactants and products will play a key role in extending these measurements. One important extension of the deuterated alkane oxidation work will be to probe OD formation. Because the reaction coordinate for the internal isomerization to QOOH (the precursor to OH formation) involves a large degree of H-atom motion, the deuterium kinetic isotope effect may be larger for OH formation than for HO<sub>2</sub> formation. Further in the future, oxidation of selectively deuterated alkanes may make it possible to distinguish among different internal abstraction pathways in R + O<sub>2</sub> reactions. Interpretation of isotopic labeling experiments will require detection of both HO<sub>2</sub> and DO<sub>2</sub> and an

understanding of the kinetic isotope effects on the overall reaction. In the long term, detection of the hydroperoxy radical intermediate in the  $R + O_2 \rightarrow RO_2 \rightarrow QOOH \rightarrow QO + OH$  mechanism might be possible in the infrared or conceivably by photoionization.

The application of synchrotron photoionization mass spectrometry to chemical kinetics will continue. The ready tunability of the ALS photon energy permits isotopic discrimination similar to that enjoyed in the current ALS flame experiments, and the kinetics measurements will be exploit this capability. Further characterization of enol formation in reactions of OH with alkenes, kinetics of reactions of combustion radicals with ethenol, addition reactions of propargyl radicals with unsaturated hydrocarbons, and oxidation of cycloalkyl radicals are possible targets of future investigations.

Publications acknowledging BES support 2004-present

1. Frank Striebel, Leonard E. Jusinski, Askar Fahr, Joshua B. Halpern, Stephen J. Klippenstein and Craig A. Taatjes, "Kinetics of the Reaction of Vinyl Radicals with NO: Ab Initio Theory, Master Equation Predictions, and Laser Absorption Measurements," *Phys. Chem. Chem. Phys.* **6**, 2216 - 2223 (2004).
2. Craig A. Taatjes, David L. Osborn, Terrill A. Cool, Koichi Nakajima, "Synchrotron Photoionization of Combustion Intermediates: The Photoionization Efficiency of HONO," *Chem. Phys. Lett.* **394**, 19-24 (2004).
3. Marc J. L. de Lange, Steven Stolte, Craig Taatjes, Jacek Klos, Gerrit C. Groenenboom, and Ad van der Avoird, "Steric Asymmetry and Lambda-Doublet Propensities in Rotationally Inelastic Scattering of NO ( $^2\Pi_{1/2}$ ) with He," *J. Chem. Phys.*, **121**, 11691-11701 (2004).
4. Terrill A. Cool, Koichi Nakajima, Craig A. Taatjes, Andrew McIlroy, Phillip R. Westmoreland, Matthew E. Law and Aude Morel, "Studies of a Fuel-Rich Propane Flame with Photoionization Mass Spectrometry," *Proc. Combust. Inst.* **30**, 1631-1638 (2005).
5. Craig A. Taatjes, Stephen J. Klippenstein, Nils Hansen, James A. Miller, Terrill A. Cool, Juan Wang, Matthew E. Law, and Phillip R. Westmoreland, "Synchrotron Photoionization Measurements of Combustion Intermediates: Photoionization Efficiency of C<sub>3</sub>H<sub>2</sub> Isomers," *Phys. Chem. Chem. Phys.* **7**, 806-813 (2005).
6. Edgar G. Estupiñán, Stephen J. Klippenstein, and Craig A. Taatjes, Measurements and Modeling of HO<sub>2</sub> Formation in the Reactions of *n*-C<sub>3</sub>H<sub>7</sub> and *i*-C<sub>3</sub>H<sub>7</sub> Radicals with O<sub>2</sub>," *J. Phys. Chem. B* **109**, 8374-8387 (2005).
7. Craig A. Taatjes, Nils Hansen, Andrew McIlroy, James A. Miller, Juan P. Senosiain, Stephen J. Klippenstein, Fei Qi, Liusi Sheng, Yunwu Zhang, Terrill A. Cool, Juan Wang, Phillip R. Westmoreland, Matthew E. Law, Tina Kasper, and Katharina Kohse-Höinghaus, "Enols are Common Intermediates in Hydrocarbon Oxidation," *Science*, 308, 1887-1889, published online May 12, 2005 [DOI: 10.1126/science.1112532] (2005).
8. Terrill A. Cool, Juan Wang, Koichi Nakajima, Craig A. Taatjes, and Andrew McIlroy, "Photoionization Cross Sections for Reaction Intermediates in Hydrocarbon Combustion," *Int. J. Mass. Spectrom.* **247**, 18-27 (2005).
9. John D. DeSain, Leonard E. Jusinski, and Craig A. Taatjes, "Temperature Dependence and Deuterium Kinetic Isotope Effects in the HCO + NO Reaction," *J. Photochem. Photobiol. A: Chem.*, **176**, 149-154 (2005)
10. Craig A. Taatjes, Nils Hansen, James A. Miller, Terrill A. Cool, Juan Wang, Phillip R. Westmoreland, Matthew E. Law, Tina Kasper, Katharina Kohse-Höinghaus, "Combustion Chemistry of Enols: Possible Ethenol Precursors in Flames," *J. Phys. Chem. A* **110**, 3254-3260 (2006).
11. Nils Hansen, Stephen J. Klippenstein, Craig A. Taatjes, James A. Miller, Juan Wang, Terrill A. Cool, Bin Yang, Rui Yang, Lixia Wei, Chaoqun Huang, Jing Wang, Fei Qi, Matthew E. Law and Phillip R. Westmoreland, "The Identification and Chemistry of C<sub>4</sub>H<sub>3</sub> and C<sub>4</sub>H<sub>5</sub> Isomers in Fuel-Rich Flames," *J. Phys. Chem. A* **110**, 3670- (2006).
12. Craig A. Taatjes, "Uncovering the Fundamental Chemistry of Alkyl + O<sub>2</sub> Reactions via Measurements of Product Formation," *J. Phys. Chem. A* **110**, 4299-4312 (2006).
13. John D. DeSain, Leonard E. Jusinski, and Craig A. Taatjes, "Ultraviolet Absorption Cross Section of Vinyl Trichlorosilane and Allyl Trichlorosilane and the Branching Fraction of the Vinyl Radical and Allyl Radical Channels in 193 nm Photolysis," *Phys. Chem. Chem. Phys.*, in press (2006).
14. Eric R. Hudson, Christopher Ticknor, Brian Sawyer, Craig A. Taatjes, Heather J. Lewandowski, Jason Bochinski, John Bohn, and Jun Ye, "Production of cold formaldehyde molecules for study and control of chemical reaction dynamics with hydroxyl radicals," *Phys. Rev. A*, in press (2006).

# Theoretical Chemical Dynamics Studies of Elementary Combustion Reactions

Donald L. Thompson

Department of Chemistry, University of Missouri, Columbia, MO 65211

thompsondon@missouri.edu

## Program Scope

The speed with which quantum chemistry calculations can now be done makes the direct use of *ab initio* forces in MD simulations feasible. However, high-level quantum calculations are often too costly in computer time for practical applications and the levels of theory that must be used are often inadequate for reactions. Thus, among the immediate pressing problems are the efficiency in using expensive high-level quantum chemistry methods (which often do not provide the necessary gradients directly) and ways to correct the errors in *ab initio* energies when necessary. A critical part of the solution is better methods for fitting global potential energy surfaces (PESs) and techniques for making direct dynamics more efficient (e.g., reducing the number of points that must be computed). Within the context of modern quantum chemistry capabilities it is sensible to focus on local fitting schemes. Originally, we proposed using cubic splines,<sup>1</sup> however, they require a fairly high density of points for a good fit. A more useful approach is the interpolating moving least squares (IMLS) introduced by Ischtwan and Collins.<sup>2</sup> It is based on a modified Shepard interpolation, the simplest case of IMLS. We are exploring higher-order IMLS, which do not require derivatives, and thus can be used to with the highest-level quantum chemistry methods for which forces are not directly obtainable. The initial goal is to develop efficient methods for generating global PESs, but the long-term goal is develop methods in which software for rate calculations direct quantum chemistry codes to produce *ab initio* predictions of reaction rates and related dynamics quantities.

## Recent Progress

In our initial study,<sup>3</sup> we developed the basic IMLS method for efficient and accurate local fitting of discrete energy values to provide global representations of PESs, which demonstrated with 1-, 2-, 3-D fits of the Koizumi *et al.*<sup>4</sup>  $\text{HN}_2 \rightarrow \text{N}_2 + \text{H}$  PES. We showed that this fitting scheme accurately describes the PES, is not computationally time-consuming, can be improved using higher degrees and larger numbers of basis functions, and is straightforward to apply. Subsequently, we examined the basic formal and numerical aspects of higher-degree IMLS.<sup>5</sup> For simplicity we chose applications to two 1-D cases: the Morse oscillator and a 1-D cut of the  $\text{HN}_2$  PES. We systematically examined the effects of the weight function parameters, the degree of IMLS, and the number and location of the energy points. We discovered compact and accurate representations of potentials and gradients for first through ninth degree IMLS fits. We showed how the number of *ab initio* points needed for a given accuracy declines with the degrees of the IMLS. We outlined automatic procedures for point selection to minimize this decline. In the next study, we applied various-degree IMLS to a 6-D PES for  $\text{HOOH}$ .<sup>6</sup> We did a systematic study of the effects of weight function parameters, the degree and partial degree of IMLS, the number of data points allowed, and the optimal

automatic point selection of data points up to full third-degree IMLS (TD-IMLS) fits. With partial reduction of cross terms and automatic point selection the full 6-D PES could be fit up to 100 kcal/mol to an accuracy of less than 1 kcal/mol with ~1350 *ab initio* points.

We have developed a method in which a zeroth-order PES  $V_0$  is used as a reference surface and IMLS is used to fit the difference  $V-V_0$  in it and the *ab initio* PES  $V$ .<sup>7</sup> This allows for the fitting of a much smoother topology than that of the real PES. It is relatively easy to formulate an approximate analytical PES to serve as  $V_0$ , since the main consideration is that it accurately fit the critical points (which can be determined by high-level quantum chemistry calculations). We demonstrated it by using the analytical PES developed by Kuhn *et al.*<sup>8</sup> for HOOH. The root-mean-square error in the fitting of the 6-D PES is reduced by ~50% for a given number of *ab initio* points by using the reference PES. This approach has great potential for use in an automatic procedure for constructing accurate PES based on *ab initio* results.

The standard IMLS method for fitting PESs uses all available *ab initio* points for fitting. Since remote points negligibly influence accuracy but the time-to-solution increases linearly with the number of points, schemes to exclude remote points from the fitting can improve efficiency. We have devised two cutoff methods to locally restrict the number of included *ab initio* points.<sup>9</sup> The fixed radius cutoff (FRC) method includes points within a hypersphere of *fixed* radius that is an input variable. The density adaptive cutoff (DAC) method includes points within a hypersphere of *variable* radius depending on the point density. The DAC involves a self-consistent step in which the appropriate radius of the hypersphere necessary to contain the selected number of points is determined by a Newton iteration procedure. Both the FRC and DAC methods are smoothed to avoid any discontinuities in value or slope. The DAC method is found to be both more robust and efficient than the FRC method and is the recommended cutoff method. In addition to testing the efficacy of cutoff methods, this study shows that typical plain weight functions used in IMLS studies are not as optimal as they could be. For large regions of weight parameter space, DAC and FRC cutoff methods produced rms errors in energy and gradients that are significantly better than the standard method with no cutoffs. In other words, excluding more remote points significantly improves the fit obtained with a non-optimal plain weight function. These results indicate the benefit of finding more flexible weight functions that optimally balance near and far *ab initio* points. The cutoff procedures developed can then be directly applied to dramatically improve the efficiency of IMLS fitting.

### **Future Work**

Our studies have demonstrated that remarkable accuracy with relatively few points can be achieved with IMLS. This is because a least-squares procedure is carried out every time an IMLS fit is evaluated. The effective cost of a fitted surface is some balance between the number of expensive *ab initio* points required to define it and the number of mathematical operations necessary to evaluate it. We are carrying out studies on both fronts. To reduce the number of *ab initio* points, we are developing ways to use *ab initio* gradients in IMLS fitting. To reduce the time-to-solution we are examining more sophisticated, including non-linear, basis functions.

We are currently pursuing three projects. First, we are using IMLS to produce a new H<sub>2</sub>CN surface for dynamics studies. The equilibrium and transition state frequencies of the IMLS fit compare favorably to the *ab initio* force field. We have completed classical trajectory calculations of the rates for H<sub>2</sub>CN → H + HCN. The rates converge rapidly with the number of included *ab initio* points.<sup>10</sup> We are now extending the H<sub>2</sub>CN surface to cover all relevant configurations. Second, we are incorporating gradients as well as energies into the IMLS framework. Since many electronic structure methods can produce the vector gradients at the same computational cost as the scalar energy the cost of producing a multidimensional IMLS fit could be dramatically reduced by incorporating gradients. Since the function minimized in the least squares step is composed of information (energies and gradients) with different units that affect minimization, scaling is an issue for gradient incorporation. Several scaling methods are being investigated. Third, we are developing a sequence of general automatic PES generation codes. These codes include permutation symmetry for the common case where the PES represents a system with chemically identical atoms. Proper treatment of permutation produces proper fits with the added benefit of more compact basis sets that improve time to solution. These codes are being tested on analytic PES libraries. Once perfected, the call to an analytic PES routine will be replaced by electronic structure calls for automatic generation of *ab initio* PESs. In addition, with entire PES libraries as test beds, new basis sets, coordinate systems, and sampling methods for IMLS can be more universally and rigorously tested.

All of this work will be done in collaboration with Drs. A. Wagner and M. Minkoff at ANL.

---

## References

- <sup>1</sup> D. R. McLaughlin and D. L. Thompson, *J. Chem. Phys.* **59**, 4393 (1973).
- <sup>2</sup> J. Ischtwan and M. A. Collins, *J. Chem. Phys.* **100**, 8080 (1994).
- <sup>3</sup> G. G. Maisuradze and D. L. Thompson, *J. Phys. Chem. A* **107**, 7118 (2003).
- <sup>4</sup> H. Koizumi, G. C. Schatz, and S. P. Walch, *J. Chem. Phys.* **95**, 4130 (2003).
- <sup>5</sup> G. G. Maisuradze, D. L. Thompson, A. F. Wagner, and M. Minkoff, *J. Chem. Phys.* **119**, 10002 (2003).
- <sup>6</sup> G. G. Maisuradze, A. Kawano, D. L. Thompson, A. F. Wagner, and M. Minkoff, *J. Chem. Phys.* **121**, 10329 (2004).
- <sup>7</sup> A. Kawano, Y. Guo, D. L. Thompson, A. F. Wagner, and M. Minkoff, *J. Chem. Phys.* **120**, 6414 (2004).
- <sup>8</sup> B. Kuhn, T. R. Rizzo, D. Luckhaus, M. Quack, and M. A. Suhm, *J. Chem. Phys.* **111**, 2565 (1999).
- <sup>9</sup> A. Kawano, I. Tokmakov, D. L. Thompson, A. F. Wagner, and M. Minkoff, *J. Chem. Phys.* **124**, 054105(1-13) (2006).
- <sup>10</sup> Y. Guo, L. B. Harding, A. F. Wagner, M. Minkoff, and D. L. Thompson, in preparation.

---

**Publications (2004-present):**

- Akio Kawano, Yin Guo, Donald L. Thompson, Albert F. Wagner, and Michael Minkoff, “*Improving the Accuracy of Interpolated Potential Energy Surfaces by Using an Analytical Zeroth-Order Potential Function*,” J. Chem. Phys. **120**, 6414-6422 (2004).
- Yin Guo, Akio Kawano, Donald L. Thompson, Albert F. Wagner, and Michael Minkoff, “*Interpolating Moving Least-Squares Methods for Fitting Potential Energy Surfaces: Applications to Classical Dynamics Calculations*,” J. Chem. Phys. **121**, 5091-5097 (2004).
- Gia G. Maisuradze, Akio Kawano, Donald L. Thompson, Albert F. Wagner, and Michael Minkoff, “*Interpolating Moving Least-Squares Methods for Fitting Potential Energy Surfaces: Analysis of an Application to a Six-Dimensional System*,” J. Chem. Phys. **121**, 10329-10338 (2004).
- Akio Kawano, Igor Tokmakov, Donald L. Thompson, Albert F. Wagner, and Michael Minkoff, “*Interpolating Moving Least-Squares Methods for Fitting Potential Energy Surfaces: Further Improvement of Efficiency via Cutoff Strategies*,” J. Chem. Phys. **124**, 054105(1-13) (2006).

## Elementary Reactions of PAH Formation

Robert S. Tranter  
Chemistry Division  
Argonne National Laboratory  
Argonne, IL-60439  
tranter@anl.gov

### Program scope

This program is focused on the elucidation of kinetic and mechanistic parameters of elementary reactions involved in the formation and destruction of the building blocks for aromatic species. The approach involves using a low pressure fast flow reactor equipped with a quadrupole MS and a shock tube equipped with laser schlieren diagnostics and a time-of-flight mass spectrometer to span a wide range of reaction temperatures and pressures in complementary studies. A series of experiments have been started with the TOF-MS shock tube on the decomposition of fluorinated hydrocarbons including 1,1,1-trifluoroethane, TFE. Not only will this serve as a test reaction for the apparatus but the reaction pressure can be varied from around 150 torr to 1000 torr (reflected shock pressures) allowing fall-off in this unimolecular decomposition reaction to be studied. This will complement the laser schlieren experiments of John Kiefer and co-workers who have proposed a nonstatistical decomposition of TFE. Additional experiments have been started on phenyl iodide decomposition as a prelude to studying the reactions of the phenyl radical including the recombination to biphenyl. At the present time phenyl iodide decomposition has been studied using the new laser schlieren apparatus to characterize the decomposition prior to using it as a source of radicals in TOF-MS experiments.

### Recent Progress

The TOF-MS apparatus had been constructed in John Kiefer's shock tube laboratory at UIC where the initial testing and early experiments were performed. In late November 2005 the TOF-MS and shock tube interface were moved from UIC to the new shock tube laboratory at Argonne where the TOF-MS is now coupled to a shock tube that can be operated both with diaphragms and without diaphragms. The shock tube has also been equipped for laser schlieren experiments.

During the development of this apparatus numerous improvements to the TOF-MS and interface have been made that greatly improve the performance of the instrument. Within the interface between the TOF-MS and shocktube the major changes include redesigning the interface so that the skimmer exit approaches within a few millimeters of the ion source and using spacer pins to set and maintain the nozzle/skimmer alignment and separation. Additional modifications have been recently made which greatly improve the gas flow in the interface and allow the gases streaming out of the shock tube to be evacuated more efficiently. The net result of these changes has been a large improvement in sensitivity which has permitted smaller nozzles and skimmers to be used. These are advantageous as the smaller nozzles perturb the gas in the shock tube less and smaller skimmers reduce the pressure build up in the MS.

To obtain concentration time profiles from which kinetic data can be extracted it is necessary to have well defined profiles at short reaction times where the concentrations are changing rapidly. For a TOF-MS/shock tube experiment this implies having short flight times for the heavy ions in the drift section of the TOF-MS so that ion packets can be injected and analyzed rapidly. In the original configuration the flight time for neon ions was about 24  $\mu$ s and for  $m/z = 100$  was about 50  $\mu$ s. This implied that for the majority of the planned experiments that an ion generation/injection frequency of about 20kHz would have to be used to prevent intermingling of spectra. This in turn implied that spectra could only be obtained every 50 $\mu$ s which is not adequate for defining the concentration time profiles well enough for kinetic studies. The flight time for neon has been reduced to 9.7 $\mu$ s when the TOF-MS is operating in reflectron mode by installing a shortened drift section and making small increases in the repeller/extractor voltages. Now in a 20  $\mu$ s period  $m/z$  up to 83 can be observed. With the shortened flight tube and reflectron operation the mass resolution remains adequate for the current experiments. To obtain even shorter sampling intervals the ion source can be pulsed at higher frequencies (max. 195kHz, 5.129 $\mu$ s between samples) under these conditions the lighter ions from an ionization event overtake the heavier ions from the prior event in the drift tube and the spectra become intermingled. However with accurate knowledge of the ion flight times

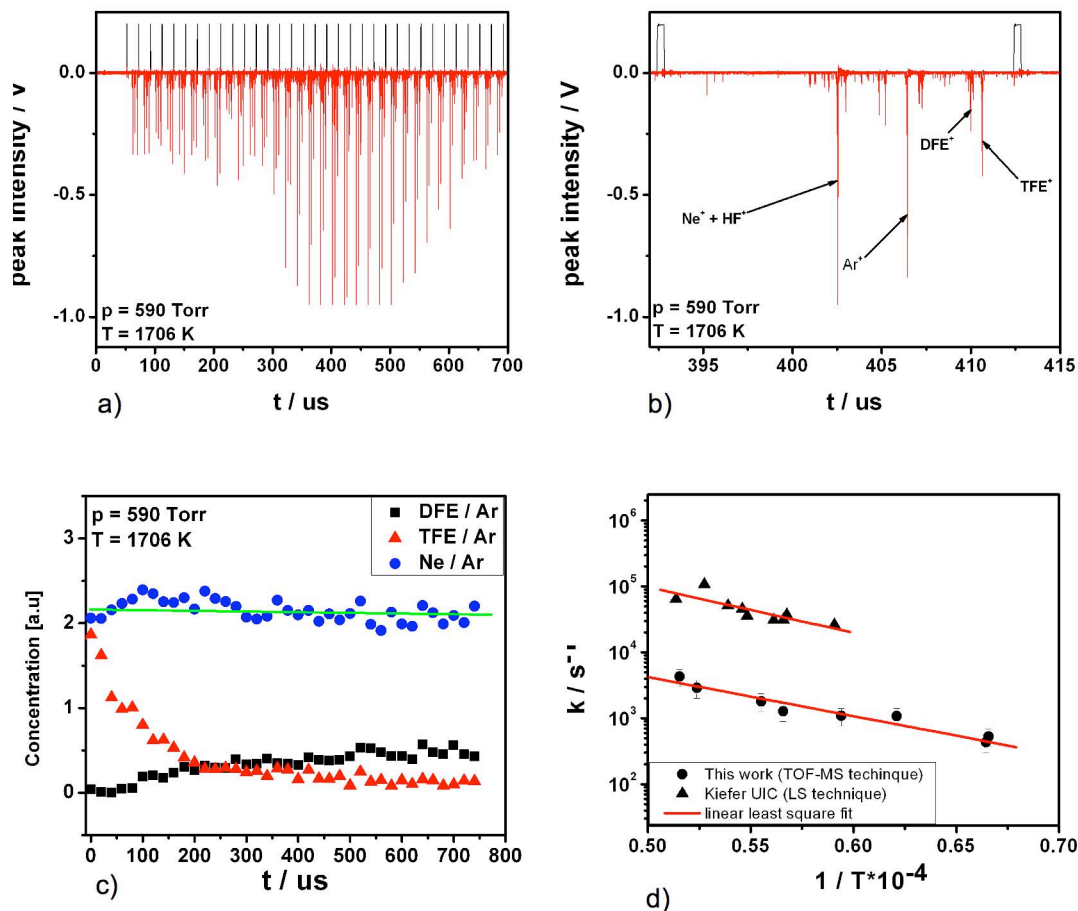


Figure 1: a) Mass spectra at 20  $\mu\text{s}$  intervals behind reflected shock wave. Upper line is ion gate timing signal, negative spikes are the detector output. Times are relative to the start of data acquisition not the generation of the reflected shock b) Individual mass spectrum. Ion generation occurs on rising edge of square wave and injection on falling edge. c) Extracted concentration time profiles from mass spectra. Times are relative to the generation of the reflected shock wave d) Extracted rate coefficients for vinyl fluoride decomposition see text for comments.

the spectra can be deconvoluted and software has been written to do this. For most operations so far, pulsing the ion source at 50kHz has given well defined concentration time profiles without the complications of overlapping spectra.

With the TOF-MS coupled to Kiefer's shock tube a number of experiments were performed to study the decomposition of fluorinated hydrocarbons including 1,1,1-trifluoroethane (TFE), 1,1-difluoroethane (DFE), and vinyl fluoride (VF). TFE and VF eliminate HF and provide simple clean systems for testing the TOF-MS/shock tube setup. DFE eliminates HF at low temperatures but rapidly degenerates to a chain reaction at moderate temperatures. During these experiments the background noise in the TOF-MS was relatively high and could not be reduced. Thus the sensitivity of the detector was reduced to a level where the random noise spikes were minimized but good peaks for the reagents and products were observed. This reduction in sensitivity required that the reagent concentrations were increased and for all these experiments the mixture consisted of 10% reagent, 10% argon with the balance neon. The argon acts as an internal standard. Of course there will be a strong temperature drop due to the exothermicity of the reactions with such concentrated mixtures and this can be accounted for by simulation.

Some results from the VF and TFE experiments are shown in fig. 1 where raw spectra and the extracted concentration/time profiles are shown (all taken at 20  $\mu\text{s}$  intervals). In fig. 1a the transition from preshock to reflected shock can be seen and this point can be accurately determined by triggering the data acquisition system from the passage of the incident shock wave under a pressure transducer and measuring the time of arrival of the shock wave at the endwall. Of particular interest is the low scatter in the data which is particularly important at short times where the concentrations are changing rapidly, fig. 1c. From the TFE data and the literature rate coefficients the reaction temperature was obtained and compared with the calculated reflected shock temperature,  $T_5$  and a large difference between these temperatures (200-300K) was observed. A similar problem was observed with the VF experiments. This is

demonstrated by the plot of rate coefficients, fig.1d, extracted from the vinyl fluoride TOF-MS experiments which are compared with the results of laser schlieren data taken in the same series of experiments (not simultaneously). In the VF experiments the activation energies determined by the LS and TOF-MS experiments appear to be in good agreement which is encouraging however the offset between the datasets indicate that there is a problem with the temperature measurement in the TOF-MS experiments. It was suspected that the source of this discrepancy was due to the extrapolation of the shock velocity from the point of measurement to the endwall of the driven section where sampling into the TOF-MS occurs. In the setup at UIC this distance was about 50 inches and while shock wave attenuation was taken into account the extrapolation may not have been accurate enough.

When the TOF-MS was moved from UIC to Argonne the opportunity was taken to install four additional pressure transducers within 12” of the endwall of the driven section and a fifth was located in the endwall. These transducers allow the incident shock velocity to be accurately measured close to the endwall thereby avoiding the extrapolation problem and greatly reducing the errors in calculating T5. After reassembly and cleaning of all parts of the ion source and ion optics the background noise in the MS was greatly reduced permitting the sensitivity of the detector to be increased and the reagent concentration in the mixtures to be correspondingly decreased. Currently the experiments with TFE and VF are being repeated.

The shock tube at Argonne was constructed as a diaphragmless shock tube specifically for coupling to the TOF-MS. The main advantages of this are that there are no fragments from diaphragms, the tube does not need to be opened to air, the shocks are reproducible and the turn around time is short which can make a tremendous increase in the number of experiments that can be run particularly if the apparatus is automated (feasible as there are no diaphragms to change). The diaphragmless shock tube is of a new design which should allow even better control of the firing of the shock tube leading to more reproducible shock wave experiments and better control for the generation of weak shock waves which are desirable for some reflected shock experiments where low temperatures and pressures are needed and relaxation studies in laser schlieren experiments. At the present time the diaphragmless shock tube produces very good, weak shocks. Laser schlieren has been used to monitor the shock waves in rare gases and these experiments show very clean shock waves being formed that are superior to those seen with diaphragms. A couple of problems in generating strong shock waves have been identified which are related to the time taken to move the plate sealing the driver section of the shock tube from the driven section out of the way. Currently this movement is relatively slow and thus flow of gas from the driver to driven sections is impeded and the shock strength reduced. These problems are being addressed and in the near future the diaphragmless shock tube should be operating as intended. Currently the tube has been modified to use aluminium diaphragms that are punctured with a knife blade. This compromise retains many of the desirable features of the diaphragmless shock tube (no fragments, reproducible shocks) but permits much stronger shocks to be generated than can be achieved at this time with the diaphragmless arrangement.

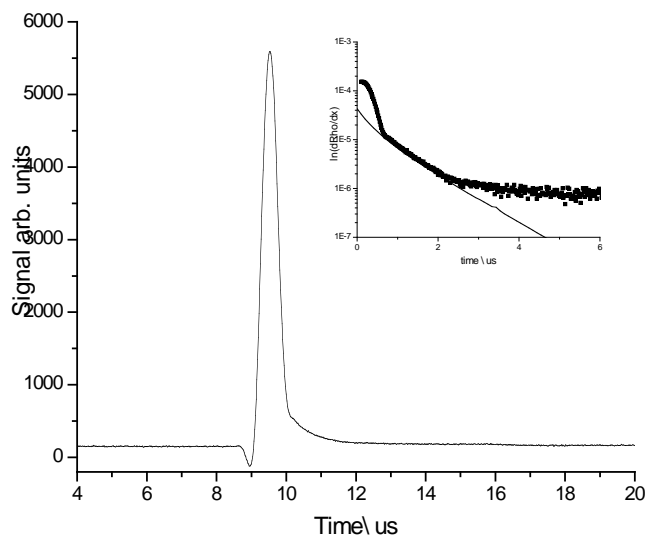


Figure 2: Laser schlieren profile of 2% cyclohexene in argon. T=1694 k, P=124 torr. Inset shows simulation of the early density gradient.

In the last year a new design of the split photodiode detector used in laser schlieren experiments was completed and a laser schlieren diagnostic system was added to the shock tube. In addition to performing normal LS studies the schlieren system is used to monitor the shock waves generated in TOF-MS experiments and with the diaphragmless shock tube. It is clear from these studies that the diaphragmless shock tube produces very clean, well formed shock waves. Fig. 2 shows a plot of a schlieren experiment on the decomposition of cyclohexene

which was used as a test reaction and the associated simulation.

## Future Plans

Further experiments are being performed to ensure that accurate kinetic data can be recovered from the shock tube/TOF-MS experiments and the low pressure flow reactor is being constructed to augment the facilities available and extend the range of reaction conditions. Experiments focused around the oxidation of the phenyl radical and the competition with pyrolysis and reaction of the radical with other species such as acetylene are planned. The reaction of phenyl radicals shifts mechanism from the stabilization of the peroxy adduct at low temperatures to decomposition via two channels at high temperatures. The two literature studies at high temperature show broad agreement but the activation energies for the two channels differ significantly and at low temperatures the shift in mechanism has not been mapped out. Both the TOF-MS and the low pressure flow tube will be used to tackle these problems. With regard to the recombination of phenyl radicals recent theoretical calculations by Haring and Klippenstein predict rate coefficient that is several times greater than the available literature values. The available data for this reaction is sparse and the TOF-MS/ shock tube will be used to obtain direct measurements of this reaction at elevated temperatures.

## Publications

1. K. S. Gupte, J. H. Kiefer, R.S. Tranter, S. J. Klippenstein, and L. B. Harding, "Decomposition of Acetaldehyde: Experiment and Detailed Theory", Accepted 31<sup>st</sup> international Symposium on Combustion.
2. Miller, C. H., Tang W., Tranter R.S., Brezinsky K., "Shock tube pyrolysis of 1,2,4,5-hexatetraene", *J. Phys. Chem. A* 110, 3605-3613, 2006.
3. Sivaramakrishnan R., Vasudevan H., Tranter R. S., Brezinsky K., "A Shock Tube Study of the High Pressure Thermal Decomposition of Benzene", *Combustion Science and Technology*, 178, 285-305, 2006.
4. Weiyong Tang, Robert S. Tranter and Kenneth Brezinsky, "An optimized semi-detailed sub-mechanism of benzene formation from propargyl recombination", *J. Phys. Chem. A*, 110, 2165-2175, 2006.
5. Sivaramakrishnan R., Tranter R. S., Brezinsky K., "A High Pressure Model for the Oxidation of Toluene", *Proceedings of the Combustion Institute*, 30, 1165-1173, 2005.
6. Sivaramakrishnan R., Tranter R. S., Brezinsky K., "Ring Conserved Isodesmic Reactions: A New Method for Estimating the Heats of Formation of Aromatics and PAHs", *J. Phys. Chem. A*, 109, 1621-1628, 2005.
7. Tranter R. S., Raman A., Sivaramakrishnan R., Brezinsky K., "Ethane Oxidation and Pyrolysis from 5 bar to 1000 bar: Experiments and Simulation", *Int. J. Chem. Kin.*, 37, 306-331, 2005.
8. Weiyong Tang, Libin Zhang, Andreas A. Linninger, Robert S. Tranter and Kenneth Brezinsky, "Solving Kinetic Inversion Problems via a Physical Trust Region Gauss-Newton (PGN) Method", *Ind. Engr. Chem. Res.*, 44, 3626-3637, 2005.
9. Weiyong Tang, Robert S. Tranter and Kenneth Brezinsky, "Isomeric Product Distributions of the Recombination of Propargyl Radicals", *J. Phys. Chem. A*, 109 (27), 6056-6065, 2005.

## VARIATIONAL TRANSITION STATE THEORY

### Principal investigator, mailing address, and electronic mail

Donald G. Truhlar  
Department of Chemistry, University of Minnesota, 207 Pleasant Street SE,  
Minneapolis, Minnesota 55455  
truhlar@umn.edu

### Program scope

This project involves the development of variational transition state theory (VTST) with multidimensional tunneling (MT) contributions and its application to gas-phase reactions. The further development of VTST/MT as a useful tool for combustion kinetics also involves developing and applying new methods of electronic structure calculations for the input potential energy surfaces and methods to interface reaction-path and reaction-swath dynamics calculations with electronic structure theory. The project also involves the development and implementation of practical techniques and software for applying the theory to various classes of reactions and transition states and applications to specific reactions, with special emphasis on combustion reactions and reactions that provide good test cases for methods needed to study combustion reactions.

### Recent progress

A theme that runs through our current work is the development of consistently and generally defined electronic structure methods with empirical elements ("semiempirical model chemistries," in the language of late John Pople), including molecular mechanics, density functionals, and scaled-electron-correlation components and the use of these methods in direct or dynamics calculations of chemical reaction rates or efficient interpolation schemes. Direct dynamics denotes that, instead of using a pre-defined potential energy functions, all required energies and forces for each geometry that is important for evaluating dynamical properties are obtained directly from electronic structure calculations. Development of exchange and correlation functionals for Density functional theory (DFT), when it is accurate enough, is very attractive as an electronic structure method for direct dynamics because of its relatively low cost and analytic gradients and Hessians. Development of improved exchange and correlation functionals is an active research area in theoretical chemistry and physics, but most of this research has neglected the important issues of barrier height prediction and noncovalent interactions, and as a consequence the functionals have not been accurate for quantitative kinetics. We have now developed new functionals, especially the M05-2X functional (Minnesota 2005 functional with double nonlocal exchange), that are quite accurate for these properties, and we have also developed multi-coefficient correlation methods (MCCMs) for using wave function theory for these properties.

In order to generate reactive potential energy surfaces with minimal computational effort, we have introduced an algorithm called multiconfiguration molecular mechanics (MCMM). MCMM describes polyatomic potential energy surfaces by several interacting molecular mechanics (MM) configurations (each of which is the analog of a valence bond configuration) and can thus be viewed as an extension of standard MM to chemical reactions or as an extension of empirical valence bond theory to include systematically improvable interpolation. MCMM fitting is accomplished by combining molecular mechanics potentials for the reactant and product wells

with electronic structure data (energy, gradient, and Hessian) at the saddle point and a small number of non-stationary points. We developed a general strategy for placement of the non-stationary points for fitting potential energy surfaces in the kinetically important regions and for calculating rate constants for atom transfer reactions by variational transition state theory with multidimensional tunneling. Then we improved the efficiency of the MCMM method by using electronic structure calculations only for certain critical elements of the Hessians at the non-stationary points and by using interpolation for the other elements at the non-stationary points. We tested this new MCMM strategy for a diverse test suite of reactions involving hydrogen-atom transfer. The new method yields quite accurate rate constants as compared with straight (uninterpolated) direct dynamics calculations at the same electronic structure level.

### Software distribution

We have developed several software packages for applying variational transition state theory with optimized multidimensional tunneling coefficients to chemical reactions and for carrying out MCCM calculations, combined quantum mechanical molecular mechanical calculations, density functional theory calculations with new density functionals, direct dynamics, and MCMM applications. The URL of our software distribution site is [comp.chem.umn.edu/Truhlar](http://comp.chem.umn.edu/Truhlar). The license requests that we fulfilled during the period Jan. 1, 2004–Mar. 1, 2005 for software packages developed wholly or partially under DOE support is as follows:

	<i>Total</i>	<i>academic</i>	<i>government/DoD</i>	<i>industry</i>
POLYRATE	162	148	8	6
GAMESSPLUS	76	67	4	5
SMXGAUSS	63	55	3	5
GAUSSRATE	56	54	1	1
MOPAC-mn	41	36	3	2
HONDOPLUS	34	28	5	1
QMMM	29	25	1	3
MULTILEVEL	12	12	0	0
GAMESSPLUSRATE	10	10	0	0
6 others	32	30	1	1

### Future plans

We have several objectives for the next few years: (1) incorporate dividing surfaces appropriate for association reactions into POLYRATE, and we will integrate these methods with master equation solvers to treat the stabilization of intermediate complexes by energy transfer collisions; (2) further improve density functionals and multi-coefficient correlation methods for potential energy surfaces; (3) further develop the multi-configuration molecular mechanics approach as an efficient tool for the semiautomatic fitting of potential energy surfaces; (4) develop more reliable methods for including anharmonicity at variational transition states, especially for torsions; (5) calculate reactions rates of peroxides and enols; (6) enhance our user-friendly packages that allow more researchers to carry out calculations conveniently by the new methods.

### Publications, 2004-present

#### *Journal articles*

1. “Small Basis Sets for Calculations of Barrier Heights, Energies of Reaction, Electron Affinities, Geometries, and Dipole Moments,” B. J. Lynch, D. G. Truhlar, *Theoretical Chemistry Accounts* **111**, 335-344 (2004).

2. "Small Representative Benchmarks for Thermochemical Calculations," B. J. Lynch, D. G. Truhlar, *Journal of Physical Chemistry A* **107**, 8996-8999 (2003); erratum: **108**, 1460 (2003).
3. "Benchmark Results for Hydrogen Atom Transfer Between Carbon Centers and Validation of Electronic Structure Methods for Bond Energies and Barrier Heights," A. Dybala-Defratyka, P. Paneth, J. Pu, D. G. Truhlar, *Journal of Physical Chemistry A* **108**, 2475-2486 (2004).
4. "Tests of Second-Generation and Third-Generation Density Functionals for Thermochemical Kinetics," Y. Zhao, J. Pu, B. J. Lynch, D. G. Truhlar, *Phys. Chem. Chem. Phys.* **6**, 673-676 (2004).
5. "Development and Assessment of a New Hybrid Density Functional Method for Thermochemical Kinetics," Y. Zhao, B. J. Lynch, D. G. Truhlar, *J. Phys. Chem. A* **108**, 2715-2719 (2004).
6. "Efficient Molecular Mechanics for Chemical Reactions: Multiconfiguration Molecular Mechanics using Partial Electronic Structure Hessians," H. Lin, J. Pu, T. V. Albu, D. G. Truhlar, *Journal of Physical Chemistry A* **108**, 4112-4124 (2004).
7. "Doubly Hybrid DFT: New Multi-Coefficient Correlation and Density Functional Methods for Thermochemistry and Thermochemical Kinetics," Y. Zhao, B. J. Lynch, D. G. Truhlar. *Journal of Physical Chemistry A* **108**, 4786-4791 (2004).
8. "Hybrid Meta Density Functional Theory Methods for Thermochemistry, Thermochemical Kinetics, and Noncovalent Interactions: The MPW1B95 and MPWB1K Models and Comparative Assessments for Hydrogen Bonding and van der Waals Interactions," Y. Zhao, D. G. Truhlar, *Journal of Physical Chemistry A* **108**, 6908-6918 (2004).
9. "Use of Block Hessians for the Optimization of Molecular Geometries," *Journal of Computational and Theoretical Chemistry* **1**, 54-60 (2005).
10. "The 6-31B(d) Basis Set and the BMC-QCISD and BMC-CCSD Multi-Coefficient Correlation Methods," B. J. Lynch, Y. Zhao, D. G. Truhlar, *Journal of Physical Chemistry A* **109**, 1643-1649 (2005).
11. "Multi-Coefficient Extrapolated Density Functional Theory for Thermochemistry and Thermochemical Kinetics," Y. Zhao, B. J. Lynch, D. G. Truhlar, *Physical Chemistry Chemical Physics* **7**, 43-52 (2005).
12. "Benchmark Calculations of Reaction Energies, Barrier Heights, and Transition State Geometries for Hydrogen Abstraction from Methanol by a Hydrogen Atom," and D. G. Truhlar, *Journal of Physical Chemistry A* **109**, 773-778 (2005).
13. "Benchmark Database of Barrier Heights for Heavy Atom Transfer, Nucleophilic Substitution, Association, and Unimolecular Reactions and Its Use to Test Theoretical Methods," Y. Zhao, N. González-García, D. G. Truhlar, *Journal of Physical Chemistry A* **109**, 2012-2018 (2005).
14. "Temperature Dependence of Carbon-13 Kinetic Isotope Effects of Importance to Global Climate Change," H. Lin, Y. Zhao, B. A. Ellingson, J. Pu, D. G. Truhlar, *Journal of the American Chemical Society* **127**, 2830-2831 (2005).
15. "Redistributed Charge and Dipole Schemes for Combined Quantum Mechanical and Molecular Mechanical Calculations," H. Lin, D. G. Truhlar, *Journal of Physical Chemistry A* **109**, 3991-4004 (2005).
16. "Benchmark Databases for Nonbonded Interactions and Their Use to Test Density Functional Theory," Y. Zhao D. G. Truhlar, *Journal of Chemical Theory and Computation* **1**, 415-432 (2005).
17. "Databases for Transition Element Bonding: Metal-Metal Bond Energies and Bond Lengths and Their Use to Test Hybrid, Hybrid Meta, Meta Density Functionals and Generalized Gradient Approximations," N. E. Schultz, Y. Zhao, D. G. Truhlar, *Journal of Physical Chemistry A* **109**, 4388-4403 (2005).

18. "Design of Density Functionals that are Broadly Accurate for Thermochemistry, Thermochemical Kinetics, and Nonbonded Interactions," Y. Zhao, D. G. Truhlar, *Journal of Physical Chemistry A* **109**, 5656-5667 (2005).
19. "Multi-Coefficient Extrapolated DFT Studies of  $\pi\cdots\pi$  Interactions: The Benzene Dimer," Y. Zhao, D. G. Truhlar, *Journal of Physical Chemistry A* **109**, 4209-4212 (2005).
20. "How Well Can New-Generation Density Functional Methods Describe Stacking Interactions in Biological Systems?" Y. Zhao, D. G. Truhlar, *Phys. Chem. Chem. Phys.* **7**, 2701-2705 (2005).
21. "Infinite-Basis Calculations of Binding Energies for the Hydrogen Bonded and Stacked Tetramers of Formic Acid and Formamide and Their use for Validation of Hybrid DFT and Ab Initio Methods," Y. Zhao, D. G. Truhlar, *Journal of Physical Chemistry A* **109**, 6624-6627 (2005).
22. "How Well Can Density Functional Methods Describe Hydrogen Bonds to Pi Acceptors?" Y. Zhao, O. Tishchenko, D. G. Truhlar, *Journal of Physical Chemistry B* **109**, 19046-19051 (2005).
23. "A New Algorithm for Efficient Direct Dynamics Calculations of Large-Curvature Tunneling and Its Application to Radical Reactions with 9–15 Atoms," A. Fernández-Ramos, D. G. Truhlar, *Journal of Chemical Theory and Computation* **1**, 1063-1078 (2005).
24. "Density Functionals for Inorganometallic and Organometallic Chemistry," N. E. Schultz, Y. Zhao, D. G. Truhlar, *Journal of Physical Chemistry A* **109**, 11127-11143 (2005).
25. "Combined Valence Bond-Molecular Mechanics Potential Energy Surface and Direct Dynamics Study of Rate Constants and Kinetic Isotope Effects for the H + C<sub>2</sub>H<sub>6</sub> Reaction," A. Chakraborty, Y. Zhao, H. Lin, D. G. Truhlar, *Journal of Chemical Physics* **124**, 044315/1-044315/14 (2006).
26. "Design of Density Functionals by Combining the Method of Constraint Satisfaction with Parametrization for Thermochemistry, Thermochemical Kinetics, and Noncovalent Interactions," Y. Zhao, N. E. Schultz, D. G. Truhlar, *Journal of Chemical Theory and Computation*, in press.
27. "Finding Saddle Points by Using the Nudged Elastic Band Method: An Implementation for Application to Gas-Phase Systems," N. Gonzalez-Garcia, J. Pu, A. Gonzalez-Lafont, J. M. Lluch, D. G. Truhlar, *Journal of Chemical Theory and Computation*, submitted.
28. "Modeling of Bimolecular Reactions," A. Fernández-Ramos, J. A. Miller, S. J. Klippenstein, D. G. Truhlar, *Chemical Reviews*, submitted.

#### **Book chapters**

1. "Variational Transition State Theory and Multidimensional Tunneling for Simple and Complex Reactions in the Gas Phase, Solids, Liquids, and Enzymes," D. G. Truhlar, in *Isotope Effects in Chemistry and Biology*, A. Kohen, H.-H. Limbach, eds. (Marcel Dekker, Inc., New York, 2006), pp. 579-620.
2. "Multilevel Methods for Thermochemistry and Thermochemical Kinetics," B. J. Lynch, D. G. Truhlar, in *Recent Advances in Electron Correlation Methodology*, edited by A. K. Wilson, K. A. Peterson, eds. (American Chemical Society Symposium Series, Washington, DC, 2006), in press.
3. "Variational Transition State Theory in the Treatment of Hydrogen Transfer Reactions," B. C. Garrett, D. G. Truhlar, in *Physical and Chemical Aspects of Hydrogen Transfer*, edited by J. T. Hynes, H. H. Limbach; Vol. 1 of *Handbook of Hydrogen Transfer*, R. L. Schowen, ed. (Wiley-VCH, Weinheim, Germany, 2006), in press.
4. "Variational Transition State Theory," B. C. Garrett, D. G. Truhlar, in *Theory and Applications of Computational Chemistry: The First Forty Years*, C. E. Dykstra, G. Frenking, K. Kim, G. Scuseria, eds. (Elsevier, Amsterdam, 2005), pp. 67-87.
5. "Variational Transition State Theory with Multidimensional Tunneling," A. Fernandez-Ramos, B. A. Ellingson, B. C. Garrett, D. G. Truhlar, in *Reviews in Computational Chemistry*, K. B. Lipkowitz, ed. (Wiley-VCH, Hoboken, NJ), in press.

## Chemical Kinetic Data Base for Combustion Modeling

Wing Tsang  
National Institute of Standards and Technology  
Gaithersburg, MD 20899  
Wing.tsang@nist.gov

**PROGRAM SCOPE AND DEFINITION:** Combustion is the consequence of chemical changes. The details of these chemical changes are embodied in the set of single step reactions that can be used to describe the temporal behavior of a combustion system. Changes in physical conditions such as pressure, temperature and the species environment can effect the rates and directions of the overall processes. These physical conditions are brought about not only by the chemistry but by the fluid dynamics of the system. The underlying science that is the basis of combustion are fluid dynamics and chemical kinetics. Recent progress in fluid dynamics have led the development of Computational Fluid Dynamics (CFD) codes that can handle increasing amounts of chemistry. It is possible to envision the time when simulations will become a powerful design tool with the capability of supplementing and expanding the range of physical testing. Simulations are the basis of modern technology. One could scarcely design an airplane or a computer chip without such tools. The aim of this project is to help develop the chemical kinetic databases for use in such reactive flow programs.

There has been much interest in applying these powerful new CFD tools for the description of real systems involving real fuels. This inevitably means larger organic fuels. All of our recent work has been focussed in this area. Larger molecules have been generally avoided by combustion kineticists since it is usually assumed that smaller molecules are more amenable to detailed treatment. Our exploration into the combustion chemistry of larger fuels suggest that our understanding of chemical reactivity has reached a stage that important uncertainties have been removed. There is now the capability of making full use of earlier data and applying this understanding to larger molecules with multiple reaction channels.

Unlike other databases, a kinetics database for combustion modeling of real fuels has almost no direct measurements. Combustion is carried out over enormous ranges of reaction conditions; from lower temperatures characteristic of cool flames to the adiabatic flame temperatures when reaction is essentially complete. Pressures can range from less than 1 bar for scram jets to close to 100 bars in diesels. The best conditions for making correct experimental determinations are rarely those of real situations. As a result there must be major emphasis on predictions from theory or correlations. The quality of a kinetics database is a measure of how well the chemistry is quantitatively understood.

**RECENT PROGRESS:** A complete combustion kinetics database can be visualized as made up of 4 distinct modules. They are, (a) pyrolysis of fuel molecules (b) oxidative degradation of fuel molecules, (c) PAH/Soot formation and (d) oxidation of light hydrocarbons. The first two modules deal directly with the specific fuel. The other two modules are universal since they contain reactions that involve the breakdown products of any organic fuel. Although there is need for more work in all the modules, considerable efforts have been devoted to the building of databases for these last three modules [1-6]. To a certain extent they have been validated by comparison with experimental measurements on combustion properties. Pyrolytic reactions (a) represent the competitive channel to module (b) and has largely been neglected. Work during the past year has focused on unimolecular reactions in pyrolysis and oxidation modules. In the former area the emphasis has been on the completion of our earlier work on heptane pyrolysis. In the oxidation area we have been interested in examining the data with respect to the initial oxidation process. Unimolecular reactions are the processes that reduce a fuel molecule to the smaller unsaturated and oxygenated fragments that are the inputs to modules (c) and (d). Much of the modern

developments are not reflected in current databases. Many of the reactions are effected by energy transfer. The existence of pressure dependences in the rate constants and branching ratios means that rate constants cannot be expressed in the standard Arrhenius or modified Arrhenius form..

**A: Unimolecular reactions during pyrolysis:** A focus of the present work was to set the stage for extensions into larger molecules. Figure 1 contains data on the beta bond scission rate constants for a number of normal alkyl radicals and is illustrative of the possibilities. The data includes a direct measurement of n-butyl radical decomposition[7] and the decomposition of n-pentyl and n-hexyl was derived[8] from the reverse radical addition process and through detailed balance. It can be seen that the rate constants are virtually equal to each other. This is not surprising since it is known that methylene insertion beta or further away from the bond being broken has almost no effect on rate constants. These results demonstrate the local nature of the transition state for beta bond scission. Hence, to a good approximation, the same rate expression can be used regardless of the size of the molecules. Also included in Figure 1 is a recent ab initio calculations by Jitariu et al [9] for 1-pentyl radical decomposition and isomerization. Although at high temperatures the predictions are satisfactory, there appears to be wider divergences at lower temperature. The capability of such calculations to reproduce the properties of transition states are uncertain. The well documented 4-6 kJ/mol uncertainty in the heats of formation of even small organic compounds can result in unacceptably large errors in the lower temperature ranges.

As much as possible all our recommendations will be based on experimental results. Figure 2 is a plot of the rate constants for 1-4 hydrogen transfer for 1-hexyl radical isomerization. We have shown that low and high temperature data for 1-5 hydrogen transfer in hexyl radical isomerization can be accounted for by the assumption of tunneling and fitted results with an unsymmetrical Eckart potential with a width of 1.15 Angstroms. We have made the same assumption regarding the width of the Eckart potential for 1-4 hydrogen transfer and been able to fit experimental results. This suggests that it may be possible to fit other 1-n isomerization processes in the same manner. This is necessary since there is no low temperature data for H-transfer isomerization for  $n > 5$ . The strongly curved nature of the Arrhenius plot makes necessary taking tunneling effects into consideration. Its neglect would have resulted in gross

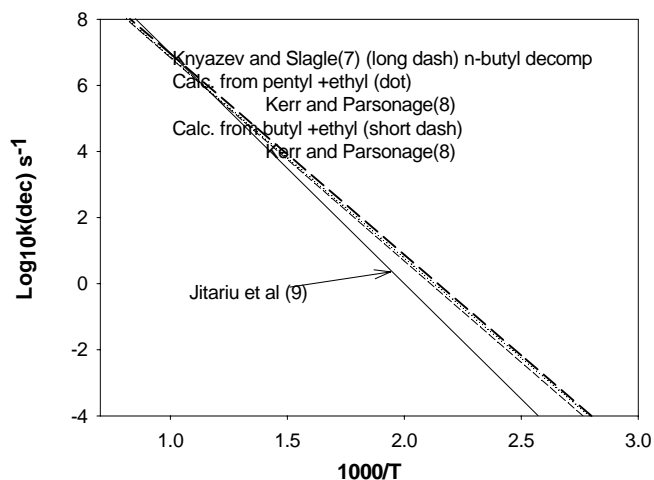


**Figure 1: Rate constants for beta bond cleavage for 1-alkyl radicals**

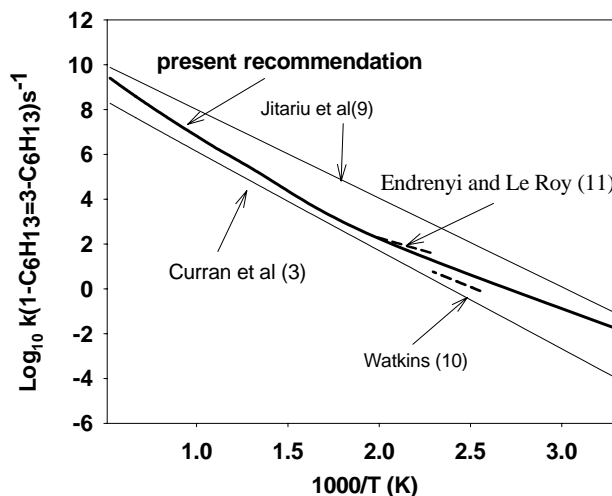


**Figure 2: Rate constants for 1-4 hydrogen transfer isomerization in 1-hexyl radical decomposition**

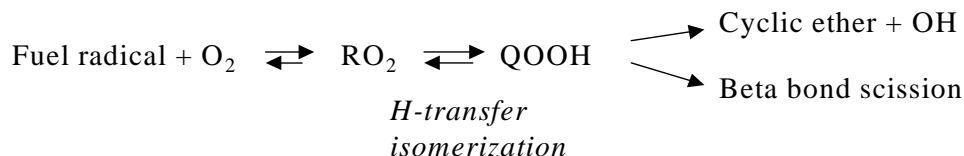


**Figure 3: Mechanism for the initial oxidation of fuel radicals treated in the present work**

underestimates of the rate constants for isomerization at low temperature. A fundamental problem is that rate constants for any of the radicals are dependent on the starting radical. There is thus the need for keeping track of the antecedent of a particular radical. Fortunately the spread of results are no more than a factor of 2 over the 1-100 bar pressure of interest. It may thus be possible to use average values.

**B: Chemically activated reactions following oxygen molecule addition to heptyl radicals.** In practically all combustion kinetics databases, the sequence of reactions beginning with oxygen molecule addition to a fuel radical is treated as a series of thermal reactions. The addition reaction leads to a hot molecule with 155 kJ/mol of excess energy. The subsequent processes involve the internal abstraction of hydrogens from the carbon backbone, the formation of 3, 4 and 5 member oxygenated ring compounds together with the ejection of an OH radical and the competitive beta bond scission process. A general mechanism for any fuel can be found in Figure 3. For heptyl radicals there are four peroxy radicals. The complexity of this process is similar to that for the chemically activated decomposition of the radical formed from terminal addition of hydrogen to 1-heptene. There are no direct measurements on the rate constants of the individual processes for these reactions. Even the required thermodynamic data is only being developed through ab initio calculations[12]. This has its own uncertainties. It is suspected that in many of the fuel oxidation databases even the thermodynamics is in error. Much of the current effort was devoted to estimating molecular properties of the oxygenates. This is in contrast to the situation with hydrocarbons[13] and is illustrative of the benefits arising from reliable databases

Although for the smaller hydrocarbon fuels data on OH and HO<sub>2</sub> radical formation have now been published [14], there is a serious lack of data on the rate constants of many of the processes listed in Figure 3. Wijaya et al [15] have published estimates of the rate constants for the formation of the oxygenated cyclic ethers. Others have made estimates for the H-atom transfer isomerization reactions.

As noted earlier, our preference is to fit as closely as possible experimental measurements. Unfortunately, the data in the literature on heptane oxidation have considerable uncertainties. Large number of products are formed. It is never clear that failure to report a product is really due to its absence. Reaction extents are large so there are uncertainties whether product yields reflect initial processes. Since oxidation is taking place the reaction conditions are not clearly defined. There is no temperature dependent data. Nevertheless there is large amount of data and the mechanism that is given in Figure 3 represents the general consensus [16,17]. Our task is to give numbers to these mechanisms. The following represents our procedure. There are no problems with the oxygen molecule addition reaction radical + O<sub>2</sub> since this is a radical combination process and there are extensive literature values for the rate constants for smaller alkyl radicals. Rate constants for the last process will be estimated by first using the rate constants for beta bond scission determined in the hydrocarbon pyrolysis work and then selecting a rate constant for the cyclic ether formation that is compatible with the product distributions. The rate expression will be determined by using the A-factor determined by Wijaya et al and selecting an activation energy that will lead to the desired rate constants. Finally for the isomerization reaction we will select rate constants that will reproduce the distribution of all the products and the absolute yields. It is interesting that the thermodynamics favor the oxygen adduct overwhelmingly. We will then correct for energy transfer effects and with the new high pressure rate expressions project results to all combustion conditions through the solution of the time dependent master equation. We are in the process of carrying out this

work. Unfortunately, there is a great deal of speculative details that need to be verified and we do not have the same confidence of the results as for the pyrolytic situation. Actually, with the better understanding of the behavior of these systems, the experimental database could be vastly improved.

**PLANNED WORK:** We will complete and submit for publication a paper containing the reactions involved in the pyrolysis of heptane. This will cover module (a). We will complete work on the rate constants for the initial steps in heptane oxidation. All of these studies will take into account energy transfer effects. It will be extremely interesting to compare the new values of the rate constants with those from earlier databases in established models of heptane oxidation.

### RECENT PUBLICATIONS

- Babushok, V. and Tsang, W. "Kinetic Modeling of Heptane Combustion and PAH Formation", *J. Prop. and Power.*, 2004, 20, 403-412
- Tsang, W., "Progress in the Development of Combustion Databases for Liquid Fuels" *Data Science Journal*, 2004, 3, 1-9
- Baulch DL, Bowman CT, Cobos CJ, Cox RA, Just T, Kerr JA, Pilling MJ, Stocker D, Troe J Tsang W, Walker RW, Warnatz J. "Evaluated kinetic data for combustion modeling" Supplement II, *Journal of Phys. Chem. Ref. Data.* 4 (3): 757-1397 2005
- Tsang, W., Mechanism and Rate Constants for the Decomposition of 1-Pentenyl Radicals" *J. Phys. Chem.* In press

### REFERENCES

1. GRI-Mech, Smith, G. P., Golden, D. M., Frenklach, M., Moriarty, N.W., Eiteneer, B., Goldenberg, M., Bowman, C. T., Hanson, R. K., Song, S., Gardiner, W. C., Jr., Lissianski, V. V., and Qin, Z., [http://www.me.berkeley.edu/gri\\_mech/](http://www.me.berkeley.edu/gri_mech/)
2. Appel, J., Bockhorn, H., and Frenklach, M., *Combust.Flame*, 121, 2000, 122.
3. Curran, H. J., Gaffuri, P., Pitz, W. J., and Westbrook, C. K., *Comb. Flame*. 114:149, 1998
4. Lindstedt, R.P., Maurice, L.Q. . *Combust.Sci.Tech.*, 1995, 107: 317-353.
5. Bakali, A.E., Delfau, J-L., Vovelle, C., . *Combust.Flame*, 1999, 118:381-389.
6. Fournet, R., Warth, V., Glaude, P.A., Battin-Leclerc, F., Scacchi, G., Come, G.M., *Int.J.Chem.Kinet.*, 2000, 32:36-51.
7. Knyazev, V. D. and Slagle, I. R., *J. Phys. Chem.*, 1996, 100, 5318-5328
8. Kerr, J. A., and Parsonage, M. J., "Evaluated Kinetic Data on Gas Phase Addition Reactions, Reactions of Atoms and Radicals with Alkenes, Alkynes and Aromatic Compounds, CRC Press, 18901 Cranwood
9. Jitariu, L. C., Jones, L. D., Robertson, S. H., Pilling, M. J., and Hillier, I. H., *J. Phys. Chem.*, A 2003, 107, 8607-8617
10. Watkins, K.W., *Can. J. Chem.*, 1972, 50, 3738-3749
11. Endrenyi L. and Le Roy, D. J., *J. Phys. Chem.*, 1966, 4081-4084
12. Sumathi, R. and Green W. H. , *Phys. Chem. Chem. Phys.*, 2003, 5, 3403-3417
13. API
14. DeSain J.D., Klippenstein S.J., Miller J.A., Taatjes, C. A., *J. Phys. Chem. A* 107:2003, 4415-4427,
15. Wijaya, C. J., Sumathi, R. and Green W. H., *J. Phys. Chem.*, A 2003, 4908-4920
16. Griffith, J. F. and Mohamed, C. "Experimental and numerical studies of oxidation chemistry and spontaneous ignition phenomenon " in *Comprehensive Chemical Kinetics*, Vol 35, "Low Temperature Combustion and Autoignition" (M. J. Pilling, ed) Elsevier, Amsterdam, 1997. Pg9g. 545-643
17. Pollard, R. T. "Hydrocarbons" in "Comprehensive Chemical Kinetics, Vol 17, "Gas Phase Combustion" (G. H. Bamford, ed) Elsevier, Amsterdam, 1977, pg 249-361

## SINGLE-COLLISION STUDIES OF ENERGY TRANSFER AND CHEMICAL REACTION

James J. Valentini  
Department of Chemistry  
Columbia University  
3000 Broadway, MC 3120  
New York, NY 10027  
jjv1@columbia.edu

### PROGRAM SCOPE

This research program aims to develop an understanding of the dynamics of bimolecular reactions. We are interested in many reactions—ones that are actually important in combustion, those that are prototypes of such reactions, and those that illustrate fundamental dynamical principles that govern combustion reactions. The principal question that we pose in our current work is how "many body" effects influence bimolecular reactions. By many-body effects we mean anything that results from having a reaction with a potential energy surface of more than three mathematical dimensions. For the reactions that we study now there are actually many more than three dimensions, at least 12 and usually many more, and part of our effort is to determine how many of them actually participate in the important dynamics of the reactions. These are polyatomic reactions, that is, reactions in which one or both of the reactants and one or both of the products are molecules with from 4 to 20 atoms. Our major current interest is in reactions for which the reactants offer multiple, identical reaction sites. Though sometimes we are interested in the details particular to one specific reaction, our approach is more commonly to study an entire class of reactions to develop a general understanding of how the factors of energetics, kinematics, and reactant/product structure control the dynamics in a series of analogous systems. As part of developing that understanding we devise and test models that explicate the interplay of these different influences.

Our effort is primarily experimental, but supplemented by computational simulations that help reveal details not accessible to experiments. Our experiments are measurements of quantum-state-resolved partial cross sections under single-collision conditions. We use pulsed uv lasers to produce reactive radical species and thereby initiate chemical reactions. The reaction products are detected and characterized by resonant multi-photon ionization (REMPI) and time-of-flight mass spectroscopy. We have a new capability with an ion imaging detector that allows measurement of partial cross sections resolved by scattering angle and velocity, and provides determination of the correlation of the quantum state of one product with the quantum state of the other.

In a collaborative effort with David Chandler we are studying ways to produce molecules at ultra-low temperatures, and study collisions at the low energies associated with these temperatures.

### RECENT PROGRESS

In the past year we constructed and assembled an ion imaging apparatus, and tested and calibrated it with photofragmentation measurements. We have studied photodissociation of HBr, HI, and H<sub>2</sub>S to give a known velocity and angle distribution of product H, with which we could determine the distance-velocity scale factor of our detector. These measurements also allow us to test the effectiveness of our ion "slicing" in recovering the speed-angle distribution as a function of ion flight time through the temporally expanded ion TOF distribution. We use small extraction fields to expand the ions in time by a significant amount and short-pulse gating of the detector to cut through the resultant ion packet. These calibration experiments were successful, showing a consistent image scale factor, one that agrees with that obtained from ion trajectory simulations. We also saw good velocity resolution.

Since our planned bimolecular reaction experiments frequently will involve the detection of fast moving H<sub>2</sub> product we need to compress the ion image to keep it within the spacial extent of the detector. To do so we use a large-aperture, long-axial-length einzel lens, to create a positive lens. This allows us to slice the velocity distribution of the high-velocity H<sub>2</sub> product quite effectively.

To test our apparatus for detection of H<sub>2</sub> with a dynamical process giving a wide range of H<sub>2</sub> speed and recoil angle we chose photodissociation of butadiene. We previously characterized the H<sub>2</sub> rovibrational state distribution for photodissociation of butadiene, and Neumark et al. have extracted the H<sub>2</sub> speed distribution from conventional crossed beam TOF measurements of the coproduct of H<sub>2</sub> formation. Somewhat surprising to us is that we get H<sub>2</sub> product that is somewhat faster than what Neumark et al. concluded, even though our photolysis is done at longer wavelength than theirs. We think our measurements are correct, but we are repeating the experiments under different conditions to be sure. This is a good test of bimolecular reaction measurements because the H<sub>2</sub> REMPI signal from butadiene photolysis, which is a very minor channel, is comparable to what we get for H<sub>2</sub> from the reactions.

In the computational part of our work we completed an extensive series of quasiclassical trajectory calculations aimed at testing a kinematic model of energy constraints in bimolecular reactions. We developed that model as a way of explaining a particularly interesting feature of the energy disposal in atom abstraction reactions, namely the observation that only a fraction, sometimes a very small fraction, of the energetically-allowed product quantum states are actually populated, even in cases in which the collision energy is far above the reaction barrier height. We were able to show that a simple kinematic constraint could explain the bounding of the product rovibrational energy. We were able to quantitatively predict the highest energy populated quantum state in all reactions for which state-to-state dynamics measurements had been made. Our QCT results show that some aspects of the model are correct, but key elements of it are not supported by the trajectory results. We are puzzled by this outcome. The model is getting quite a few applications beyond our own work, and seems very valuable in interpreting the results of state-to-state dynamics experiments.

We have continued the collaboration with David Chandler to produce ultra-cold molecules by velocity cancellation in molecular collisions. The experiment takes advantage of the fact that in some molecular collisions the velocity vector of a scattered product in the center-of-mass frame is exactly the negative of the velocity vector of the center-of-mass, yielding a lab-frame product velocity that is identically zero. Current efforts are aimed at trapping the cold molecules. Other, possibly simpler, routes to making cold molecules that can be trapped are also being explored.

#### FUTURE PLANS

We will begin to use our ion imaging capability study bimolecular reactions. The immediate focus will be on the  $\text{H} + \text{alkane} \rightarrow \text{H}_2 + \text{alkyl}$  reactions for which we have already determined the  $\text{H}_2$  product rovibrational state distributions. Here our aim is to determine the joint probability of forming  $\text{H}_2$  in a particular quantum state correlated with the alkyl radical in a particular internal energy. This is chosen to test a local reaction model we have developed of atom + polyatom reactions that says that the rovibrational state is coupled to the internal energy of the alkyl radical in a specific way. The most important such reaction is  $\text{H} + \text{CH}_4 \rightarrow \text{H}_2 + \text{CH}_3$  reaction. We believe that we will have enough velocity resolution to observe the population of individual vibrational states of the  $\text{CH}_3$  product in the translational energy distribution of the  $\text{H}_2(v',j')$ . On the other hand, we can detect the  $\text{CH}_3$  product and use its measured angular and speed distribution to infer the rovibrational state of the  $\text{H}_2$  with which it is formed. Since REMPI of  $\text{CH}_3$  is quite straightforward this should be no problem. Recent theoretical work shows that the cross section for this reaction is larger at lower collision energies (around 0.65 eV) than at higher energies (around 1.5 eV). This makes a study of this reaction at an energy nearer to threshold tractable, and the development of a lower energy hot atom source for H atoms by the Wittig group makes getting down to these energies feasible. Lower energy experiments are both more interesting and more accessible to theoretical treatment with which to compare results.

We will continue our cold molecule studies with David Chandler attempting to trap the cold molecules that we have already produced.

#### PUBLICATIONS – 2004 -PRESENT

1. N.S. Shuman, M. Mihok, M. Fistik, and J.J. Valentini, "Quasiclassical Trajectory Calculations to Evaluate a Kinematic Constraint on Internal Energy in Suprathreshold Collision Energy Abstraction Reactions," *Journal of Chemical Physics* 123, 074312 (2005).
3. M.S. Elioff, J.J. Valentini, and D.W. Chandler, "Formation of  $\text{NO}(j'=7.5)$  Molecules with Sub-Kelvin Translational Energy via Molecular Beam Collisions with Argon using the Technique of Molecular Cooling by Inelastic Collisional Energy-Transfer," *European Physical Journal D: Atomic, Molecular and Optical Physics* 31, 385-393 (2004).

# Time-resolved Structural Probes of Molecular Dynamics

Peter M. Weber  
Department of Chemistry  
Brown University, Providence, Rhode Island 02912  
Peter\_Weber@brown.edu

## 1. Program Scope

Our research explores new time-resolved probes of molecular dynamics and applies them to model systems. The two techniques that we concentrate on are time-resolved electron diffraction and time-resolved Rydberg spectroscopy. Both use electrons as tools to characterize the transient molecular structures.

In the electron diffraction experiment we use ultrashort electron pulses to probe molecular structures in the Fourier plane. A laser pulse initiates a structural rearrangement, either by exciting the molecule to an excited state with a different geometry, or by inducing a chemical reaction. The electron pulse arrives some well-defined time after the pump pulse, and probes the instantaneous molecular structure, or distribution of structures. Careful consideration of the challenges of this experiment leads us now to use relativistic (megavolt) electrons for this experiment. The first demonstration experiments have been extremely promising.

In the second technique, we use electrons that are loosely bound in Rydberg orbitals as structural probes. We have found that the phase shifts that Rydberg electrons encounter when passing the molecular ion core are sensitive measures of the molecular structure. The phase shifts are spectrally observed as deviations of the Rydberg peak positions from the corresponding positions of the peaks in hydrogen atoms. This leads to a method to characterize molecular structures that we call Rydberg Fingerprint Spectroscopy (RFS). One of the great advantages of RFS is that it is very insensitive to thermal congestion, making it a very intriguing choice for the study of molecular dynamics and combustion processes.

To implement RFS in the context of time-resolved molecular structure measurements, we use a pump-probe multi-photon ionization/photoelectron experiment: a first laser pulse excites the molecule to a Rydberg state, and a time-delayed probe pulse ionizes it. The photoelectron spectrum reveals the binding energy of the electron, and thereby reveals the molecule's time-dependent structural fingerprint. In the example described in this abstract, we apply the method to explore the fragmentation dynamics of the  $\alpha$  bonds in tertiary amines.

## 2. Recent Progress

### *Megavolt electron diffraction with ultrashort electron pulses*

Electron diffraction with ultrashort electron pulses has emerged as a promising tool to explore time-dependent molecular structures. Traditionally, electron diffraction on gas

phase samples is performed using electron energies of 20 to 60 keV. At that energy, space-charge interactions between the electrons within a pulse greatly limit the electron beam current, and thereby put severe constraints on the achievable signal-to-noise ratio of the experiment. In our collaboration with J. Hastings at the Stanford Linear Accelerator, we solve the space-charge problem by using ultrashort electron pulses with much higher energy. Using existing RF electron gun technology, it is possible to generate electron pulses with durations as short as 400 fs. With a beam energy of 5 MeV, such short durations can be maintained even when as many as  $10^7$  electrons are in a single pulse. This should afford the opportunity to perform single-shot, highly time-resolved electron diffraction experiments.

We have pursued the application of RF photocathode sources to ultra-fast electron diffraction (UED) using the Gun Test Facility at the Stanford Linear Accelerator Center, which provides a well-characterized 5.4 MeV electron beam. As a test target we used a polycrystalline 160 nm aluminum foil. The experiments were conducted using electron pulses containing a total charge of 3 pC, or  $1.9 \cdot 10^7$  electrons. The electron bunch was collimated with a solenoid, and intersected the sample about 0.75 m from the photocathode. The diffraction pattern was observed using quadrupole magnetic lenses to produce a parallel-to-point image of the sample on a phosphor screen placed 3.95 m downstream of the target. Previous studies have shown that the pulse duration of this electron bunch is less than 500 fs rms at the target. Figure 1 shows both the experimentally measured and the simulated diffraction patterns from the polycrystalline foil. It is clear that even the single, ultrashort electron pulse is sufficient to record the powder pattern of the foil.

Simulations show that the electron pulse duration is limited by the duration of the laser pulse that generates the electrons, which is 2 picoseconds. (The acceleration of the electron pulse in the RF gun entails a pulse compression by a factor of 5). The simulations also suggest that using shorter laser pulses for the RF photocathode gun, electron pulses as short as 100 fs should be readily obtainable.

The breakthrough application of RF photocathode guns for UED at MeV energies points towards experiments on a 100 femtosecond time scale on

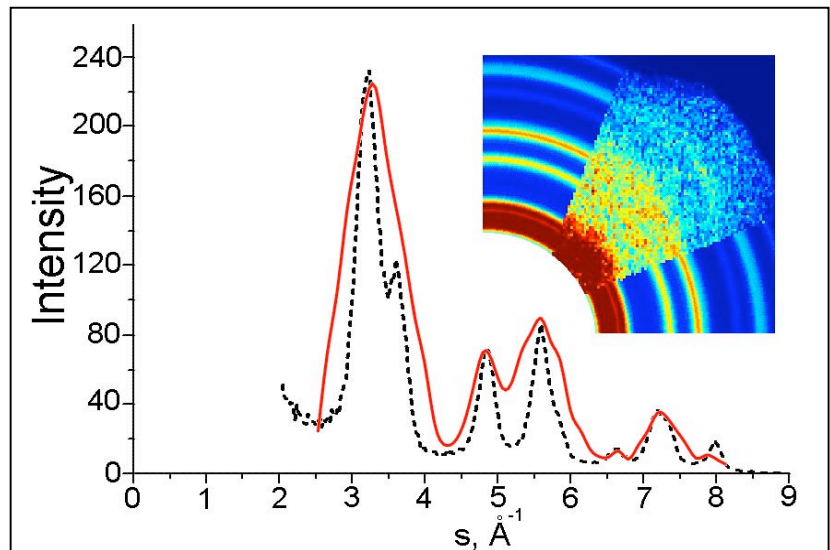


**Figure 1:** Diffraction patterns of 160 nm polycrystalline aluminum foil. The experimental and simulated radial traces are represented by solid and dashed lines, respectively. The inset shows, in the center slice, the experimental pattern taken with a single 500 fs electron pulse, flanked by the simulated diffraction pattern.

both condensed phases and gas phase samples. We have shown that diffraction patterns are obtainable from a single ultrashort pulse with MeV energy, bringing atomic scale ‘movies’ of molecular structures, phase transitions in solid films and liquid dynamics within reach.

### Time-resolved Rydberg fingerprint spectroscopy of tertiary amines

Our past work has shown that the energies of Rydberg states are sensitive probes of molecular structure. This sensitivity is traced to the phase shifts that the Rydberg electron suffers when passing through the ion core. Since RFS can be easily coupled with pump-probe methodology, it can be employed in a time-resolved manner to probe the dynamics of chemical reactions.

In the present experiments, Rydberg fingerprint spectroscopy was applied to study the photofragmentation dynamics of tertiary amines. N,N dimethylisopropylamine is excited to the 3p Rydberg state by a laser pulse with a wavelength of 208.5 nm. A time delayed probe pulse at 417 nm ionizes the molecule. The mass spectrum shows at very short delay times the parent ion only. At longer delay one observes a fragment with mass 72, corresponding to the cleavage of the  $\alpha$  bond. This appears to indicate that fragmentation of the molecule on the Rydberg surface is revealed in the time-resolved mass spectrum. The mass spectrum is not unambiguous, however, since it does not rule out the possibility that the ionization is out of the Rydberg state of the parent ion, with a later fragmentation of the ion on its way to the mass spectrometer.

While this ambiguity is impossible to resolve with mass spectrometry, the time-resolved RFS shows clearly that the fragmentation does not occur on the Rydberg surface. As shown in figure 2, at a time of 120 ps the mass spectra of N,N dimethylisopropylamine and dimethyl 2-butylamine show the same fragments. The RFS reveal, however, that the fingerprint spectra at that delay time are quite distinct. Clearly, at the time of the ionization the molecules have not yet fragmented.

RFS is able to resolve the ambiguity of the mass spectra even though the molecules are very hot at the time of ionization. The optical excitation to high-lying vibrational states, and the relaxation from the initially excited 3p state to 3s releases about 1.4 eV into vibrational coordinates. In spite of this large energy, the RFS show reasonably well-resolved spectra. This

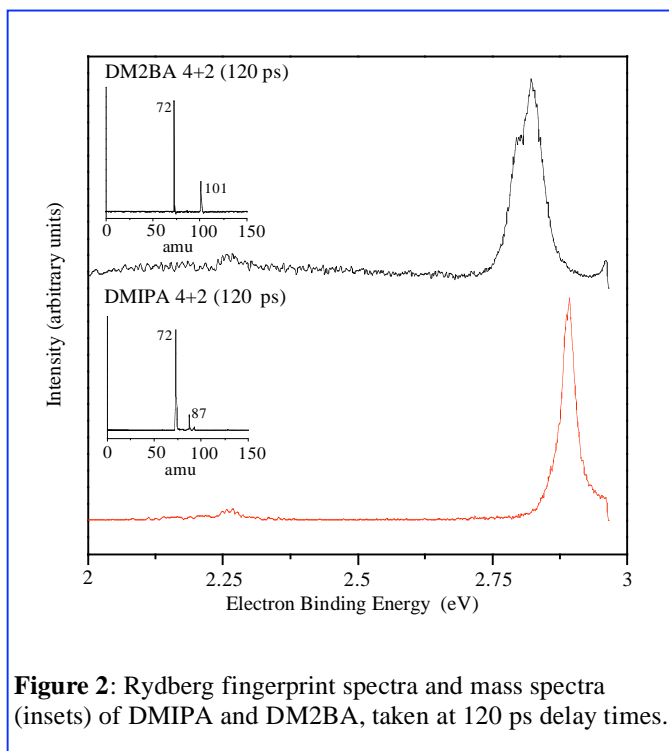


**Figure 2:** Rydberg fingerprint spectra and mass spectra (insets) of DMIPA and DM2BA, taken at 120 ps delay times.

suggests that RFS is capable of providing useful structural fingerprints in cases where many other spectroscopic techniques are overwhelmed by thermal congestion.

### 3. Future Plans

The Rydberg fingerprint spectroscopy and the pump-probe electron diffraction provide complementary views of molecular structure. Both techniques are amenable to highly time-resolved experiments. We continue to explore the unique strengths and weaknesses of both techniques by performing experiments on model systems. Current efforts are directed toward building up the MeV electron source for permanent chemical dynamics experiments. The Rydberg fingerprint spectroscopy is applied to probe the dynamics in small cyclic molecules, and to explore its applicability in large, flexible molecular systems with many degrees of freedom.

### 4. Publications resulting from DOE sponsored research (2004 - 2006)

1. "The Ultrafast Photofragmentation Pathway of N,N-Dimethylisopropylamine," M.P. Minitti, J.L. Gosselin, T.I. Sølling and P.M. Weber, in print, *FemtoChemistry VII*.
2. "Megavolt electron beams for ultrafast time-resolved electron diffraction," F. M. Rudakov, J. B. Hastings, D. H. Dowell, J. F. Schmerge, and P. M. Weber, In print, "Shock Compression of Condensed Matter – 2005," the Proceedings of the 14th APS Topical Conference on Shock Compression of Condensed Matter.
3. "Structure sensitive photoionization via Rydberg levels," N. Kuthirummal and P. M. Weber, in print, *J. Mol. Spect.*
4. "Energy Flow and Fragmentation Dynamics of N, N, Dimethyl-isopropyl amine," Jaimie L. Gosselin, Michael P. Minitti, Fedor M. Rudakov, Theis I. Sølling and Peter M. Weber, *Journal of Physical Chemistry A*, **2006**, *110*, 4251-4255.
5. "Ultrafast Electron Microscopy in Materials Science, Biology, and Chemistry," Wayne E. King, Geoffrey H. Campbell, Alan Frank, Bryan Reed, John Schmerge, Bradley J. Siwick, Brent C. Stuart, and Peter M. Weber, *Journal of Applied Physics*, **97**, 111101 (2005).
6. "Rydberg Fingerprint Spectroscopy: A New Spectroscopic Tool With Local And Global Structural Sensitivity," J. L. Gosselin and Peter M. Weber, *J. Phys. Chem. A*, *109*, pp 4899 – 4904 (2005).
7. "Control of local ionization and charge transfer in the bifunctional molecule 2-phenylethyl-N,N-dimethylamine using Rydberg fingerprint spectroscopy," W. Cheng, N. Kuthirummal, J. Gosselin, T. I. Sølling, R. Weinkauff, and P. M. Weber, *Journal of Physical Chemistry*, *109*, pp 1920 – 1925 (2005).
8. "Experimental and theoretical studies of pump-probe electron diffraction: time-dependent and state-specific signatures in small cyclic molecules," Peter M. Weber, Ray C. Dudek, Seol Ryu, and Richard M. Stratt, in "*Femtochemistry and Femtobiology: Ultrafast Events in Molecular Science*," Eds. M. Martin and J. T. Hynes, Elsevier, p. 19, (2004).
9. "Probing reaction dynamics with Rydberg states: The ring opening reaction of 1, 3-cyclohexadiene," N. Kuthirummal and P. M. Weber, in "*Femtochemistry and Femtobiology: Ultrafast Events in Molecular Science*," Eds. M. Martin and J. T. Hynes, Elsevier, p. 37 (2004).
10. "Centering of ultrafast time-resolved pump-probe electron diffraction patterns" J. D. Cardoza, R. C. Dudek, R. J. Mawhorter, and P. M. Weber. *Chemical Physics*, *299*, 307 – 312 (2004).
11. "Electron diffraction of molecules in specific quantum states: a theoretical study of vibronically excited s-tetrazine" S. Ryu, R. M. Stratt, K. K. Baeck and P. M. Weber, *Journal of Physical Chemistry A*, *108*, 1189 – 1199 (2004).

## Chemical Kinetic Modeling of Combustion Chemistry

William J. Pitz and Charles K. Westbrook  
Lawrence Livermore National Laboratory

### Program Scope

Our research project focuses on developing detailed chemical kinetic reaction mechanisms for the combustion of a wide variety of hydrocarbon and other chemical species. These reaction mechanisms are intended to be applicable over extended ranges of operating conditions, including temperature, pressure, and fuel/oxidizer ratio, making them so-called “comprehensive” reaction mechanisms. They can then be systematically reduced in size and complexity as needed for specific types of modeling applications. We also use these detailed kinetic mechanisms to carry out modeling studies of practical combustion systems, and we also contribute basic chemical information on thermochemical and kinetic data.

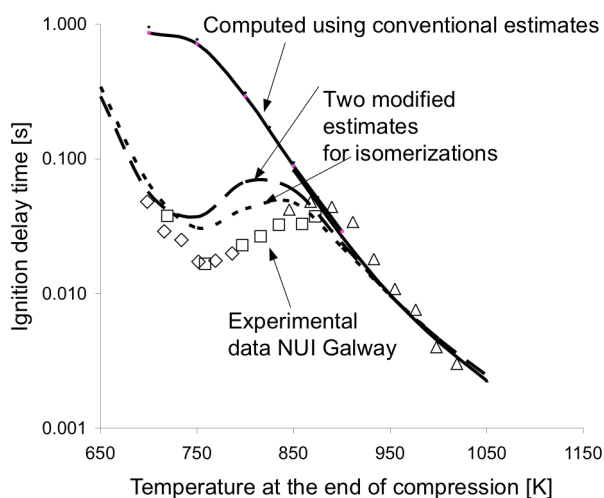
### Recent Progress

During the past year, we have developed detailed kinetic mechanisms and carried out kinetic modeling studies in several interconnected areas, including kinetics of oxygenated hydrocarbons and their importance in diesel soot production, as well as detailed chemical kinetic mechanisms for new chemical species, including a high temperature mechanism for di-isobutylene and a comprehensive mechanism for methyl cyclohexane.

An important new source of petroleum for transportation and other uses is the enormous reserves in Canada that exists in the form of oil sands. This petroleum, when refined for diesel fuel, contains unusually high levels of polycyclic paraffins, and previous and present kinetic models for practical fuels have never taken this class of hydrocarbons into account. To solve this problem, we have been developing full-range kinetic reaction mechanisms for representative cyclic and polycyclic paraffins, most recently for methyl cyclohexane or MCH. Combining a recent high temperature reaction mechanism for MCH oxidation with new low and intermediate reaction pathways, we have used both shock tube and rapid compression machine experimental data for MCH to provide and validate the new reaction mechanism.

At high temperature, the mechanism for ignition and oxidation consists of the familiar processes of H atom abstraction and radical decomposition via  $\beta$ -scission, and the major chain branching pathway is via the reaction of H atoms with molecular oxygen. At low and intermediate temperatures, the chain branching reaction pathways are quite similar in concept with reactions of n-paraffins and iso-paraffins, with a major role played by isomerization of MCH-peroxy radicals. The 6-membered transition state ring pathways play the same branching role for MCH as for the other alkanes, and the 5-membered and 7-membered transition state ring compounds provide chain propagation, and the

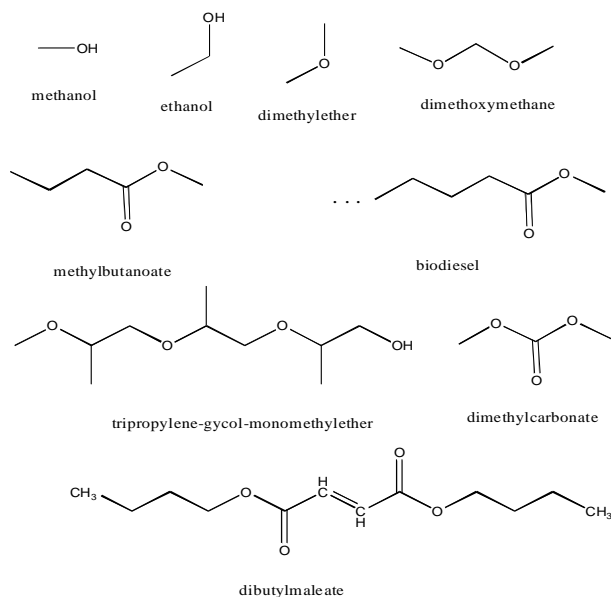
observed negative temperature coefficient phenomena that are observed experimentally depend sensitively on the balance between these chain branching and propagation rates. However, we have found that the activation energy barriers to these isomerization reactions cannot be predicted from their analogous reactions with n-alkane and iso-alkane hydrocarbons. We have interpreted this by proposing that the presence of the non-aromatic ring provides another contribution to the activation energy barrier for the transfer of the H atom, in addition to the contributions from the C-H bond that is being broken and the transition state ring strain that common to all of the n-paraffin, iso-paraffin, and cyclo-paraffin species. If we do not include this additional factor, the observed NTC region is not predicted to occur, as shown in the accompanying figure.



Our studies of the use of oxygenated hydrocarbon as additives to reduce soot production in diesel engines have continued [8] and have shown that the placement of atomic oxygen in the oxygenated hydrocarbon can influence the effectiveness of the additive to reduce sooting. Some of the oxygenates we have studied, and for which we have developed kinetic reaction mechanisms, are shown on the next page. In particular, oxygenates with an alkyl methyl ester structure are distinctly less effective in their use of oxygen atoms in reducing soot production, and this has been traced to the decomposition of the methoxy formyl radical. This radical preferentially decomposes to produce  $\text{CO}_2$  directly, which removes one C atom from the soot producing pool of carbon, rather than have the two O atoms each produce CO and thereby remove two carbon atoms from that pool.

There are many recent experimental studies of soot formation in laminar premixed and diffusion flames. Those studies consistently show that addition to the fuel of the same oxygenates we have examined in diesel environments result in soot reduction in premixed flames and soot increase in diffusion flames. We are currently working to identify the kinetic reasons for this behavior and to

extend this work to examine further factors, such as hydrocarbon fuel structure, that also modify sooting behavior in combustion systems.



We have developed a new kinetic mechanism for diisobutylene, a large olefin related to iso-octane. This species has two structural isomers which react at different rates, complicating both modeling and experimental analyses. This large olefin is expected to be used as part of the olefinic fraction of surrogate models for practical transportation fuels, particularly diesel fuel and gasoline.

Kinetic models for explosives and energetic materials have been developed [11], and the recommendations from those studies for reductions in emissions of harmful chemical species, especially soot, during their incineration remain to be tested in real experiments. Extensions of these models to new propellants such as ammonium perchlorate are planned for the future.

### Future Plans

We will continue to carry out chemical kinetic modeling studies of a wide variety of combustion problems, developing new kinetic reaction mechanisms when they do not already exist. We will focus in particular on the very early phases of soot production in flames and diesel engines, looking towards identifying unifying principles that provide fundamental kinetic understanding of this important chemical process.

William J. Pitz  
LLNL, L-091  
P. O. Box 808  
Livermore, CA 94550

pitz1@llnl.gov  
925-422-7730

## References to publications of DOE sponsored research in 2004-2006

1. Buchholz, B.A., Mueller, C.J., Upatnieks, A., Martin, G.C., Pitz, W.J., and Westbrook, C.K., "Using Carbon-14 Isotope Tracing to Investigate Molecular Structure Effects of the Oxygenate Dibutyl Maleate on Soot Emissions from a DI Diesel Engine", **Soc. Auto. Eng.** 2004-01-1849 (2004).
2. Jayaweera, T.M., Melius, C.F., Pitz, W.J., Westbrook, C.K., Korobeinichev, O.P., Shvartsberg, V.M., Shmakov, A.G., Rybitskaya, I.V., and Curran, H.J., "Flame inhibition by phosphorus-containing compounds over a range of equivalence ratios", **Combust. Flame** 140, 103-115 (2005).
3. Korobeinichev, O.P., Shvartsberg, V.M., Shmakov, A.G., Bolshova, T.A., Jayaweera, T.M., Melius, C.F., Pitz, W.J., and Westbrook, C.K., "Flame Inhibition by Phosphorus-Containing Compounds in Lean and Rich Propane Flames", **Proc. Combust. Inst.** 30, 2350-2357 (2005).
4. Glaude, P.-A., Pitz, W.J., and Thomson, M.J., "Chemical Kinetic Modeling of Dimethyl Carbonate in an Opposed-Flow Diffusion Flame", **Proc. Combust. Inst.** 30, 1111-1118 (2005).
5. O'Conaire, M., Curran, H.J., Simmie, J.M., Pitz, W.J., and Westbrook, C.K., "A Comprehensive Modeling Study of Hydrogen Oxidation", **Int. J. Chem. Kinet.** 36, 603-622 (2004).
6. Zheng, X.L., Lu, T.F., Law, C.K., Westbrook, C.K., and Curran, H.J., "Experimental and computational study of nonpremixed ignition of dimethyl ether in counterflow", **Proc. Combust. Inst.** 30, 1101-1109 (2005).
7. Westbrook, C.K., Mizobuchi, Y., Poinso, T., Smith, P.A., and Warnatz, J., "Computational Combustion", **Proc. Combust. Inst.** 30, 125-157 (2005).
8. Westbrook, C.K., Pitz, W.J., and Curran, H.J., "Chemical Kinetic Modeling Study of the Effects of Oxygenated Hydrocarbons on Soot Emissions from Diesel Engines", *J. Phys. Chem. A*, published on the Web 03/29/2006.
9. Pitz, W.J., Naik, C.V., Ni Mhaoldúin, T., Westbrook, C.K., Curran, H.J., Orme, J.P., and Simmie, J.M., "Modeling and Experimental Investigation of Methylcyclohexane Ignition in a Rapid Compression Machine", Accepted for publication, *Proc. Combust. Inst.* 31 (2006).
10. Metcalfe, W.K., Pitz, W.J., Curran, H.J., Simmie, J.M., and Westbrook, C.K., "The Development of a Detailed Chemical Kinetic Mechanism for Diisobutylene and Comparison to Shock Tube Ignition Times", Accepted for publication, *Proc. Combust. Inst.* 31 (2006).
11. Pitz, W.J., and Westbrook, C.K., "A Detailed Chemical Kinetic Model for Gas Phase Combustion of TNT", Accepted for publication, *Proc. Combust. Inst.* 31 (2006).

## PROBING FLAME CHEMISTRY WITH MBMS, THEORY, AND MODELING

Phillip R. Westmoreland

Department of Chemical Engineering  
University of Massachusetts Amherst  
159 Goessmann Laboratory, 686 N. Pleasant  
Amherst, MA 01003-9303

Phone 413-545-1750  
FAX 413-545-1647  
westm@ecs.umass.edu  
<http://www.ecs.umass.edu/che/westmoreland.html>

### Program scope

Our objective is obtaining kinetics of hydrocarbon combustion and molecular-weight growth in flames. Our approach combines molecular-beam mass spectrometry (MBMS) experiments on low-pressure flat flames; *ab initio* thermochemistry and transition-state structures; rate constants predicted by transition-state and chemical activation theories; and whole-flame modeling using mechanisms of elementary reactions. The MBMS technique is particularly powerful because it can be used to measure a wide range of species quantitatively, including radicals.

Our electron-ionization quadrupole MS at UMass provides species profiles with high signal sensitivity and mass resolution. In a multi-investigator collaboration at the Advanced Light Source (ALS) at LBNL, we also are obtaining extraordinarily specific isomer identifications and their profiles using a time-of-flight MS with VUV photoionization; we co-developed this system with fellow DOE-BES contractors Terry Cool, Andy McIlroy, Nils Hansen, and Craig Taatjes. Additional collaborators in making measurements include Katharina Kohse-Höinghaus of Universität Bielefeld and Fei Qi of the National Synchrotron Radiation Laboratory in Hefei, China, while DOE-BES contractors Jim Miller, Stephen Klippenstein, and Fred Dryer have been collaborators in the modeling.

### Recent progress

A series of papers in the past year has focused on data, reactive-flow modeling, and new identification of species, their ionization energies, and their thermochemistry on flames. The ALS collaboration has investigated a number of flames experimentally, giving special attention for this contract to measurements in stoichiometric and fuel-rich cyclohexane and toluene flames.

*Stoichiometric cyclohexane flame.* Last year, I described our mapping of a stoichiometric cyclohexane flame with 32.5% argon at 30.00 torr and 35.0 cm/s feed gas velocity (at 300 K). By combining the capabilities of the UMass and ALS systems, we measured profiles of 70 species from masses 1 to 98. References 6 and 12 give further details, including additional species identification and modeling.

Particular insights have been discovered in the pathways for oxidation and aromatics formation, greatly aided by the ability to identify isomers of the hydrocarbon intermediates.

Destruction of the fuel was by OH and H abstraction to form cyclohexyl, decomposing / isomerizing to 5-hexenyl, decomposing to 3-butenyl, decomposing to 1,3-butadiene + H and to  $C_2H_3 + C_2H_4$ . All of these hydrocarbons were identified and mapped. The dominant hydrocarbon intermediates proved to be ethene, going to  $CH_3+CHO$  via  $O+C_2H_4$ ; vinyl, going to  $CH_2O+CHO$  via  $O_2+C_2H_3$  with some decomposition to  $C_2H_2$ ; and 1,3-butadiene, which was more important than expected and was destroyed by a mix of abstraction and O-atom addition.

Aromatics formation was not from the  $C_3H_3$  routes observed in ethene flames but rather from successive dehydrogenation reactions.  $C_6H_6$  was almost all benzene, 99.5% vs. 0.5% fulvene. In contrast, the stoichiometric allene-doped  $C_2H_4$  flame had 20% fulvene, 45% benzene and 35%

1,5-hexadiyne. Modeling showed that  $C_3H_3$  combination was not sufficient to predict benzene in the cyclohexane flame, although it had been in the allene-doped  $C_2H_4$  flame. Instead, benzene production was described quantitatively by a cyclo- $C_6$  dehydrogenation sequence of H-abstractions, H beta-scissions, and disproportionation steps.

*Fuel-rich cyclohexane flame.* We now have mapped a  $\phi=2.0$  cyclohexane flame with 30.4% argon at 30.00 torr. The intent was to enhance the molecular-weight growth pathways. We are in the process of analyzing profiles and currently have profiles of 66 species, including indene and naphthalene. Again, benzene dominates at  $m/z=78$  although fulvene is present. Initial modeling shows good agreement for the major species.

*Toluene flames.* We also have mapped stoichiometric and fuel-rich ( $\phi=1.8$ ) toluene flames, and those data are being analyzed. Species detected in the fuel-rich flame range up to the three-ring aromatics acenaphthylene and fluorene.

*Identification of widespread occurrence of enols.* We first identified the presence of ethenol, vinyl alcohol in a fuel-rich ethylene flame (*J. Chem. Phys.* **119**:16, 8356-8365, 2003), but in Ref. 5, we were able to show further that the enols are widespread in combustion. We studied 24 flames of 14 fuels, resolving ethenol, propenols, and butenols from aldehydes and other isomers. Enols were detected in most of the flames. The ethenol/acetaldehyde ratio reached as high as 0.9 (benzene flame,  $\phi=1.66$ ), while ethenol was below detectable limits in methane, ethane, and propane flames studied. Fast equilibration mechanisms by keto-enol tautomerization in solution do not apply in the gas-phase, and direct isomerization has a high activation energy.

Subsequent work has focused on modeling the chemistry and assessing how important these new pollutants are. Our recent paper (Ref. 9) identified chemically activated OH+olefin reactions as the apparent source of enols. When an adduct is formed, the bond energy released into the nascent radical allows it to decompose if energetically accessible routes are available. In the case of  $C_2H_4+OH$ , the rovibrationally excited  $\bullet CH_2CH_2OH$  adduct can revert to reactants or can eliminate H by beta-scission to form ethenol,  $CH_2=CHOH$ . Calculated rate constants were used in flame models to make acceptable predictions of the ethenol profiles in flames of  $C_2H_4$  ( $\phi=1.9$ ), allene ( $\phi=1.8$ ),  $C_3H_6$  ( $\phi=2.3$ ), and  $C_2H_6$  ( $\phi=1.4$ ), where it was predicted to be below the limit of detection as had been observed experimentally.

*Identification of  $C_3H_2$  species.* We had detected  $C_3H_2$  as a significant signal 20 years ago in  $C_2H_2$  flames, but the identity or identities could not be determined until now. In Ref. 3, the ALS collaborators identified the dominant  $C_3H_2$  isomers using recent data from the ALS apparatus, our past measurements at MIT and UMass, and quantum-chemistry calculations by our Sandia colleagues and us. Triplet propargylene (HCCCH, prop-2-ynylidene, the lowest-energy isomer) and singlet propadienylidene ( $H_2CCC$ ) were dominant in different flames. Furthermore, we established their thermochemistry persuasively by using different high-level calculations.

With their identities resolved, my group is now developing different reaction sets for each isomer. The first isomer is formed primarily by abstraction of H from  $C_3H_3$  and is involved in radical pathways like abstraction and addition, while the second is formed by  $H_2$  elimination and participates in carbene insertion reactions.

*Resolution of  $C_4H_3$  and  $C_4H_5$  isomers.* For over 50 years,  $C_4H_3$  and  $C_4H_5$  have been of interest as reactants that could possibly form aromatics. This interest reached a high point in the early 1980's when  $C_2H_2$  addition routes were proposed with thermal isomerization from  $C_4H_5$  by Cole *et al.*, with thermal isomerization from  $C_4H_3$  by Frenklach *et al.*, and by fast, chemically activated isomerization from both  $C_4H_3$  and  $C_4H_5$  by Westmoreland *et al.* These routes required the radical to be at the end vinylic position:  $\bullet CH=CH-CCH$  ( $n-C_4H_3$ ) and  $\bullet CH=CH-CH=CH_2$  ( $n-$

C<sub>4</sub>H<sub>5</sub>). These species are thermodynamically less favored than having the radicals at the allylic, stabilized 2- position (*i*-C<sub>4</sub>H<sub>3</sub> and *i*-C<sub>4</sub>H<sub>5</sub>), but there was substantial dispute over whether the thermodynamic penalty was sufficient to overcome kinetic advantages and the isomers could not be resolved experimentally. The advent of experimental evidence and reasonable routes for C<sub>3</sub>H<sub>3</sub> combination by Kern, Stein, Miller, Melius, and others decreased the interest in C<sub>4</sub>H<sub>3</sub> and C<sub>4</sub>H<sub>5</sub>.

In Ref. 10, we used data from the ALS MBMS with computed thermochemistry to establish the presence of *i*-C<sub>4</sub>H<sub>3</sub>, *i*-C<sub>4</sub>H<sub>5</sub>, and a combination of butynyl isomers (CH<sub>3</sub>-CC-CH<sub>2</sub> and CH<sub>3</sub>-CH-CCH) in allene, propyne, cyclopentene, and benzene flames. There was no evidence for *n*-isomers, whether due to low mole fractions or to their low Franck-Condon factors. Again, thermochemistry was persuasively established by accurate calculations and ionization-energy measurements.

*Identification of C<sub>5</sub>H<sub>x</sub> species.* In Ref. 11, we have identified the C<sub>5</sub>H<sub>x</sub> species in fuel-rich allene, propyne, cyclopentene, and benzene flames. We reported profiles for masses 63 to 66 in fuel-rich C<sub>2</sub>H<sub>2</sub> combustion in 1986, but these species have largely been left out of flame models because species identities were not established. Cyclopentadienyl is recognized as a possible phenyl+O product, and its combination has been proposed as a route to naphthalene. Thus, identifying it and resolving the various C<sub>5</sub> isomers is important. Using the techniques established for C<sub>3</sub>H<sub>2</sub>, C<sub>4</sub>H<sub>3</sub>, and C<sub>4</sub>H<sub>5</sub> isomers:

- C<sub>5</sub>H<sub>2</sub> was identified predominantly to be the cyclic isomer -CCHCCCH-.
- For C<sub>5</sub>H<sub>3</sub>, both H<sub>2</sub>CCCCCH (*i*-C<sub>5</sub>H<sub>3</sub>) and HCCCHCCH (*n*-C<sub>5</sub>H<sub>3</sub>) isomers were present.
- C<sub>5</sub>H<sub>4</sub> was made up of contributions from 1,2,3,4-pentatetraene, 1,2-pentadiene-4-yne, and 1,3-pentadiyne. 1,4-pentadiyne was detected in cyclopentene and benzene flames.
- For C<sub>5</sub>H<sub>5</sub>, only the cyclopentadienyl radical was detected.
- C<sub>5</sub>H<sub>6</sub> had contributions from cyclopentadiene, 1-penten-3-yne, and 1-penten-4-yne.
- C<sub>5</sub>H<sub>7</sub> was obscured by isotopic contributions from *m/z*=66.
- Cyclopentene, 1,3-pentadiene, 2-pentyne, and 1,4-pentadiene contributed to C<sub>5</sub>H<sub>8</sub>.

The study also established ionization energies for *i*-C<sub>5</sub>H<sub>3</sub> [(8.20±0.05) eV], *n*-C<sub>5</sub>H<sub>3</sub> [(8.31±0.05) eV], 1,2-pentadiene-4-yne [(9.22±0.05) eV], 1-penten-4-yne [(9.90±0.05) eV], and C<sub>5</sub>H<sub>6</sub> [(9.95±0.05) eV] using the data and QCISD(T) calculations.

### Future plans

We will map stoichiometric and fuel-rich methane and acetylene flames at the ALS and at UMass, exploiting the respective strengths of both systems. These flames are classic targets of modeling, but the ALS system offers new opportunities to answer unresolved questions about kinetics and identities of key isomers in those flames, including CH<sub>3</sub>O/CH<sub>2</sub>OH, C<sub>3</sub>H<sub>2</sub>'s, C<sub>3</sub>H<sub>4</sub>'s, HCCO/C<sub>3</sub>H<sub>5</sub>, CH<sub>2</sub>CO/C<sub>3</sub>H<sub>6</sub>, CH<sub>2</sub>CHO/ CH<sub>3</sub>CO/C<sub>3</sub>H<sub>7</sub>'s, CH<sub>2</sub>CHOH/ CH<sub>3</sub>CHO, C<sub>4</sub>H<sub>3</sub>, C<sub>4</sub>H<sub>5</sub>, C<sub>4</sub>H<sub>6</sub>'s, C<sub>4</sub>H<sub>7</sub>'s, C<sub>5</sub>'s, C<sub>6</sub>'s, C<sub>7</sub>'s, C<sub>8</sub>'s, and oxygenates in the range of mass 54 to 110.

Other ALS flames have been picked by the collaboration, including alcohols, dimethyl ether, aldehydes, ketones, blended fuels like propene and ethanol, and ester fuels relevant to biodiesel, such as methyl and ethyl formate. As we steadily increase the resolving power of the instrument and develop new data-analysis techniques, we also re-map selected data.

Accurate modeling of these data is increasingly important in our work. We are mapping temperatures and area-expansion ratios for these flames, so we will be able to deliver more accurate modeling and extraction of selected rate constants from the flame data. We are also

working with the PrIME cyberinfrastructure initiative in a pilot effort to set up raw MBMS data and data-analysis software in archival forms and availability.

### Publications citing DOE-sponsored Research, 2004-2006

1. M.E. Law, T. Carrière, P.R. Westmoreland, "Allene Addition to a Fuel-Lean Ethylene Flat Flame," *Proceedings of the Combustion Institute* **30**(1), 1353-1361 (2004).
2. T.A. Cool, K. Nakajima, C.A. Taatjes, A. McIlroy, P.R. Westmoreland, M.E. Law, A. Morel, "Studies of a Fuel-Rich Propane Flame with Photoionization Mass Spectrometry," *Proceedings of the Combustion Institute* **30**(1), 1681-1688 (2004).
3. Hansen, J.A. Miller, T.A. Cool, J. Wang, M.E. Law, P.R. Westmoreland, "Synchrotron Photoionization Measurements of Combustion Intermediates: Photoionization Efficiency of C<sub>3</sub>H<sub>2</sub> Isomers," *Phys. Chem. Chem. Phys.* **7**, 806-813 (2005).
4. Ruscic, J. E. Boggs, A. Burcat, A. G. Czászár, J. Demaison, R. Janoschek, J. M. L. Martin, M. L. Morton, M. J. Rossi, J. F. Stanton, P. G. Szalay, P. R. Westmoreland, F. Zabel, T. Bérces, "IUPAC critical evaluation of thermochemical properties of selected radicals - Part I," *J. Phys. Chem. Ref. Data* **34**(2), 573-656 (2005).
5. C.A. Taatjes, N. Hansen, A. McIlroy, J.A. Miller, J.P. Senosiain, S.J. Klippenstein, F. Qi, L. Sheng, Y. Zhang, T.A. Cool, J. Wang, P.R. Westmoreland, M.E. Law, T. Kasper, K. Kohse-Höinghaus, "Enols Are Common Intermediates in Hydrocarbon Oxidation," *Science* **308**(5730), 1887-1889 (2005).
6. M. E. Law, *Molecular-Beam Mass Spectrometry of Ethylene and Cyclohexane Flames*, Ph.D. Dissertation, University of Massachusetts Amherst (2005).
7. T.A. Cool, A. McIlroy, F. Qi, P.R. Westmoreland, L. Poisson, D.S. Peterka, M. Ahmed, "A Photoionization Mass Spectrometer for Studies of Flame Chemistry with a Synchrotron Light Source," *Rev. Sci. Instr.* **76**, 094102-1 to 094102-7 (Sept 2005).
8. P. R. Westmoreland, M.E. Law, T.A. Cool, J. Wang, C.A. Taatjes, N. Hansen, T. Kasper. "Analysis of Flame Structure by Molecular-Beam Mass Spectrometry Using Electron-Impact and Synchrotron-Photon Ionization," *Fizika goreniya i vzryva (Russian) / Combustion, Explosion and Shock Waves (English)* (in press, 2006).
9. C.A. Taatjes, N. Hansen, J.A. Miller, T.A. Cool, J. Wang, P.R. Westmoreland, M.E. Law, T. Kasper, K. Kohse-Höinghaus. "Combustion Chemistry of Enols: Possible Ethenol Precursors in Flames," *J. Phys. Chem. A* **110**(9), 3254-3260 (2006). DOI: 10.1021/jp0547313
10. N. Hansen, S.J. Klippenstein, C. A. Taatjes, J.A. Miller, J. Wang, T.A. Cool, B. Yang, R. Yang, L. Wei, C. Huang, J. Wang, F. Qi, M.E. Law, P.R. Westmoreland, T. Kasper, K. Kohse-Höinghaus. "Identification and Chemistry of C<sub>4</sub>H<sub>3</sub> and C<sub>4</sub>H<sub>5</sub> Isomers in Fuel-Rich Flames," *J. Phys. Chem. A* **110**(10), 3670-3678 (2006). DOI: 10.1021/jp0567691
11. N. Hansen, S.J. Klippenstein, J.A. Miller, J. Wang, T.A. Cool, M.E. Law, P.R. Westmoreland, T. Kasper, K. Kohse-Höinghaus, "Identification of C<sub>5</sub>H<sub>x</sub> Isomers in fuel-rich flames by photoionization mass spectrometry and electronic structure calculations", *J. Phys. Chem. A* **110**(13), 4376-4388 (2006). DOI: 10.1021/jp0569685.
12. M.E. Law, P.R. Westmoreland, T. A. Cool, J. Wang, N. Hansen, T. Kasper. "Benzene Precursors and Formation Routes in a Stoichiometric Cyclohexane Flame," *Proceedings of the Combustion Institute* **31** (accepted).
13. T. A. Cool, J. Wang, N. Hansen, P. R. Westmoreland, F. L. Dryer, Z. Zhao, A. Kazakov, T. Kasper, K. Kohse-Höinghaus. "Photoionization mass spectrometry and modeling studies of the chemistry of fuel-rich dimethyl ether flames," *Proc. Combustion Institute* **31** (accepted).
14. K. Kohse-Höinghaus, Patrick Oßwald, Ulf Struckmeier, T. Kasper, N. Hansen, C. A. Taatjes, J. Wang, T.A. Cool, S. Gon, P.R. Westmoreland. "The influence of ethanol addition on a premixed fuel-rich propene-oxygen-argon flame," *Proceedings of the Combustion Institute* **31** (accepted).
15. N. Hansen, J.A. Miller, C. A. Taatjes, J. Wang, T.A. Cool, M.E. Law, P.R. Westmoreland. "Photoionization Mass Spectrometric Studies and Modeling of Fuel-Rich Allene and Propyne Flames," *Proceedings of the Combustion Institute* **31** (accepted).

## Photoinitiated processes in small hydrides

Curt Wittig  
Department of Chemistry  
University of Southern California  
Los Angeles, CA 90089  
(213) 740-7368  
wittig@usc.edu

During the past year, we have concentrated on the role of curve crossings in small polyatomic species and relativistic effects in hydrides that contain heavy atoms. In such systems, spin and electronic angular momentum cease to have good quantum numbers due to spin-orbit interaction. This can facilitate transitions between potential energy surfaces, complicating the intramolecular dynamics. Relativistic effects observed in heavy atom systems have no counterparts with lighter molecules. Our previous experimental study of the  $\text{H}_2\text{Te}$  system yielded results that are in excellent agreement with recent high-level theoretical calculations.<sup>1</sup> This system provides low energy H atoms whose translational energy can be tuned continuously, down to almost zero kinetic energy. This work inspired us to initiate experiments with  $\text{SbH}_3$ . We have also started experiments with  $\text{AsH}_3$ . In continuing with our studies of  $\text{H}_2\text{O}$  and  $\text{C}_2\text{H}$ , we have begun to integrate a four-wave mixing scheme for the generation of tunable VUV light.

### Results and future work

#### I. $\text{H}_2\text{Te}$ absorption spectrum and photodissociation dynamics

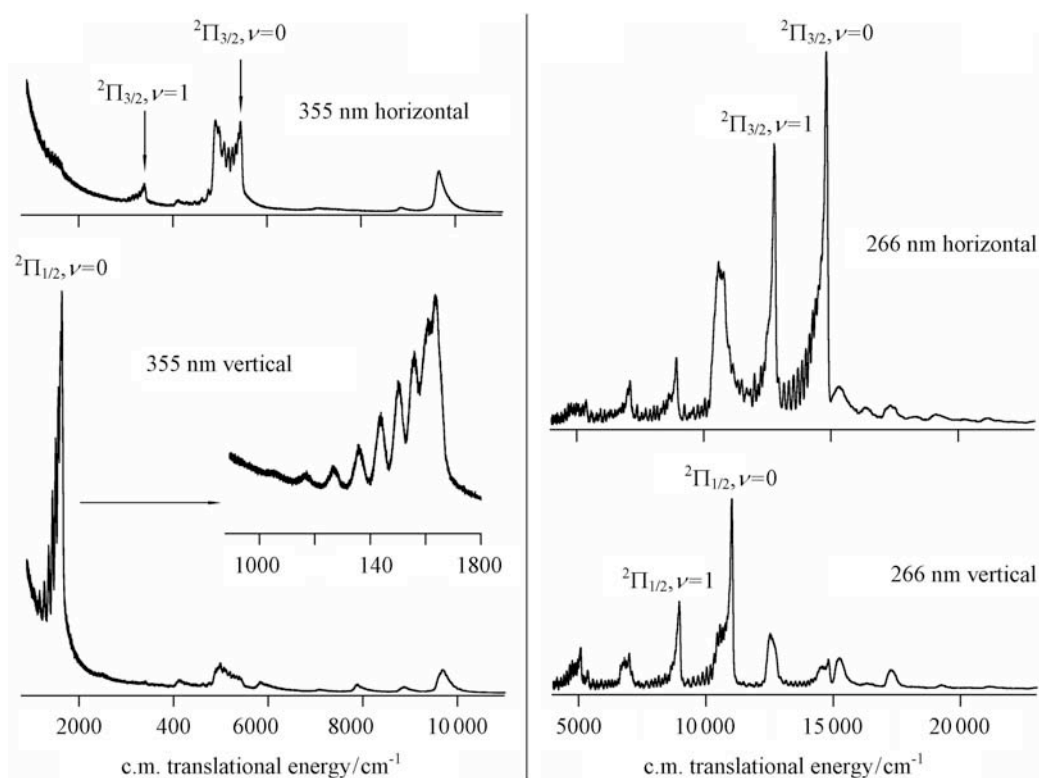
A detailed analysis of the absorption spectrum and photodissociation experiments (both primary and secondary processes) has been carried out,<sup>1,2</sup> and the most important results are summarized here.  $\text{H}_2\text{Te}$  is a model system for studying relativistic effects. It is isoelectronic with HI, and the lighter isovalent dihydrides in the group,  $\text{H}_2\text{O}$ ,  $\text{H}_2\text{S}$ , and  $\text{H}_2\text{Se}$ , have been studied in varying degrees of detail. Three product channels are energetically accessible in the first absorption band of  $\text{H}_2\text{Te}$ : (i)  $\text{H}_2 + \text{Te}$ ; (ii)  $\text{H} + \text{TeH}(^2\Pi_{3/2}, v, N)$ ; (iii)  $\text{H} + \text{TeH}(^2\Pi_{1/2}, v, N)$ . Spin-orbit excited  $\text{TeH}(^2\Pi_{1/2})$  lies  $3815 \text{ cm}^{-1}$  above the  $\text{TeH}$  ground state. Our photodissociation experiments are sensitive only to channels (ii) and (iii). Center-of-mass translational energy distributions for photolysis at 266 and 355 nm obtained with high- $n$  Rydberg time-of-flight (HRTOF) spectroscopy are shown below.

These experiments are also sensitive to secondary photolysis of the  $\text{TeH}$  products that are formed via the primary photolysis channels (ii) and (iii) described above. Following  $\text{H}_2\text{Te}$  photolysis, the nascent  $\text{TeH}$  diatoms can absorb a second photon and dissociate, yielding  $\text{H} + \text{Te}(^3P_{2,1,0})$  and/or  $\text{H} + \text{Te}(^1D_2)$ . Analyses of the secondary photolysis products in this study determined that  $D_0 = 64.8 \pm 0.4 \text{ kcal/mole}$  ( $22,300 \text{ cm}^{-1} \pm 150 \text{ cm}^{-1}$ ), in good agreement with the theoretical predictions.

Alekseyev *et al.* have recently calculated the low-lying potential energy surfaces and transition dipole moments in the H–TeH coordinate.<sup>1</sup> One of the most striking features is the

weakly bound  $3A'$  surface. Its large- $r$  shape is remarkably similar to that of the  $^3\Pi_{0+}$  curve in the isoelectronic HI system.

In an earlier publication [J. Underwood, D. Chastaing, S. Lee, P. Boothe, T. C. Flood, and C. Wittig, Chem. Phys. Lett. **362**, 483 (2002)] we proposed that there should exist a state that is similar to the HI( $^3\Pi_{0+}$ ) curve in the H–TeH coordinate.<sup>5</sup> Because the  $\Omega = 1/2$  state has a larger degree of spherical symmetry than the  $\Omega = 3/2$  state, TeH( $^2\Pi_{1/2}$ ) is not inclined to form either strongly bonding or anti-bonding orbitals with a H-atom. This results in a shallow van der Waals-like well on the  $3A'$  surface at large  $r$  that leads to spin-orbit excited products. Calculations in the H–TeH coordinate predict that the  $3A'$  surface is bound by  $\sim 1600$  cm<sup>-1</sup>. We attribute the long-wavelength structure observed in the absorption spectrum taken in our labs to vibrations of H<sub>2</sub>Te on the  $3A'$  surface.

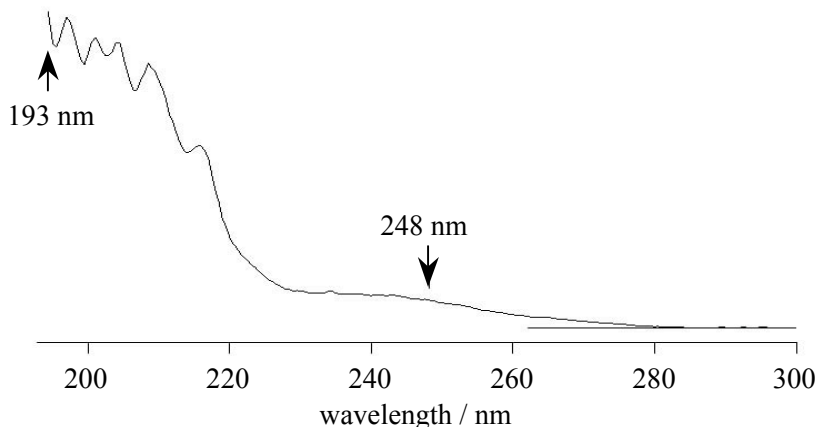


Photodissociation with horizontally polarized 266 nm radiation yields primarily TeH( $^2\Pi_{3/2}$ ). This transition is due to a transition dipole moment out of the plane of the molecule, and this is assigned to the  $4A'' \leftarrow \tilde{X}A'$  transition. The large anisotropy indicates that the TeH( $^2\Pi_{1/2}$ ) channel results from a transition to a distinct electronic state, rather than from coupling of  $4A''$  to another state in the exit channel that leads to the spin-orbit excited products. The  $3A'$ ,  $4A'$ , and  $3A''$  states correlate with the spin-orbit excited channel, but the  $3A' \leftarrow \tilde{X}A'$  transition moment is in the plane of the molecule, so  $3A'$  is unlikely to be involved. Near the Franck-Condon region, the  $4A''$  state has a larger transition dipole moment, but absorption to  $3A'$  is also possible.

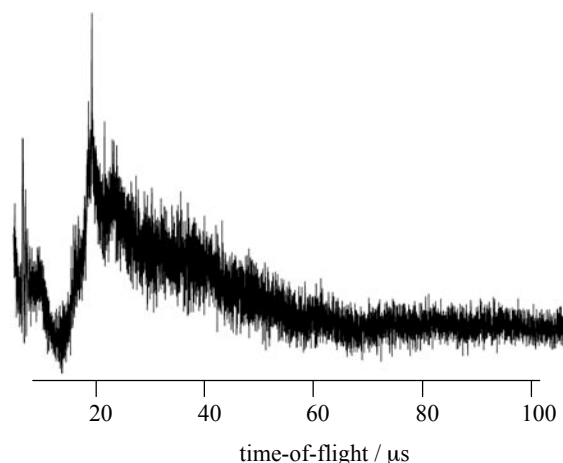
At 355 nm,  $\sim 65\%$  of the photoproducts are due to the excited spin-orbit channel. This is due to the role of the  $3A'$  state. In the Franck-Condon region,  $3A' \leftarrow \tilde{X}A'$  and  $2A' \leftarrow \tilde{X}A'$  transition dipole moments are weak, as both transitions are of primarily singlet to triplet character.<sup>1</sup> The preference for long-wavelength photodissociation via the spin-orbit excited channel is due to the behavior of the transition dipole moment outside the Franck-Condon region. The  $3A' \leftarrow \tilde{X}A'$  transition moment increases quickly with H-TeH distance, due primarily to increasing singlet character at large  $r$  of the  $3A'$  state.

## II. SbH<sub>3</sub>

One of the challenges of working with systems containing heavy atoms is that they can be unstable and SbH<sub>3</sub> is no exception. We have succeeded in synthesizing it and are currently carrying out HRTOF experiments with 193 nm. A 300 K absorption spectrum from our lab is shown below. As in H<sub>2</sub>Te, a long wavelength tail is observed.



Experiments are underway to photolyze SbH<sub>3</sub> at 193 nm and probe the H atoms. The energy is sufficient to break two Sb-H bonds. Calculations predict  $D_e$  values of 63.3, 55.8 and 53.9 kcal/mole for successive Sb-H bonds.<sup>7</sup> Despite severe sample stability issues, we have observed a small HRTOF signal from 193 nm photolysis of SbH<sub>3</sub> (on the right). A peak is apparent in the TOF spectrum at  $\sim 20 \mu\text{s}$ . Using the theoretical  $D_e$  value for breaking the first Sb-H bond, the time of arrival of the H atom is predicted to be  $\sim 16.4 \mu\text{s}$ .



A large amount of internal excitation in the SbH<sub>2</sub> cofragment or an underestimate of the calculated  $D_e$  value might explain the discrepancy between our prediction and the HRTOF result.

Based on our experience with the  $\text{H}_2\text{Te}$  system,  $\text{SbH}_3$  appears to be more unstable, despite the fact that the absorption spectrum does not indicate that it is light sensitive. It is likely that, as with  $\text{H}_2\text{Te}$ , a surface catalyzed decomposition process is degrading the sample to  $2\text{Sb} + 3\text{H}_2$  even when the sample is maintained at the temperature of liquid nitrogen. Namely, our future success relies upon whether sufficient  $\text{SbH}_3$  can be expanded through the pulsed nozzle in the face of sample degradation throughout the foreline and within the General Valve nozzle. We have recently coated all the metal in the foreline and nozzle with Sulfinert, in order to increase the signal to noise ratio. We hope these improvements will lengthen the lifetime of our  $\text{SbH}_3$  sample and enable us to gain a clearer picture of the dissociation dynamics as well as determine an accurate  $D_0$  for two of the Sb–H bonds.

Photolysis at 248 nm should prove to be interesting as well. At this wavelength, not only will the long wavelength tail of the absorption spectrum be accessed, but the energy in the system will be near the region where only one of the Sb–H bonds can be broken. Photodissociation dynamics in this region may be quite different than those observed at higher energies.

### III. $\text{AsH}_3$

Following the progression towards heavy atoms in the Group V hydrides,  $\text{AsH}_3$  is another system in which to explore relativistic effects. Certain experimental details are simplified in using  $\text{AsH}_3$  for it requires no complicated synthesis on our part and possesses a large absorption cross section ( $1.8 \times 10^{-17} \text{ cm}^2$ ) at 193 nm. A much earlier study of  $\text{AsH}_3$  using a low resolution spectroscopic technique [B. Koplitz, Z. Xu, and C. Wittig, *Appl. Phys. Lett.* **52**, 860 (1988)] determined that  $\text{AsH}_2$  contains significant internal energy upon 193 nm photodissociation. The HRTOF technique offers superior resolution and will yield the  $\text{AsH}_2$  internal energy distribution.

### IV. $\text{H}_2\text{O}$ , $\text{C}_2\text{H}$ , and VUV generation

Tunable VUV is desirable to probe the  $\tilde{X}/\tilde{B}$  conical intersection in  $\text{H}_2\text{O}$  at energies lower than those studied to date.<sup>4</sup> We are integrating a four-wave mixing scheme to generate radiation from  $\sim 140$  to 133 nm. An added benefit of such a system is that it can also replace the current method we use for generation of the Lyman- $\alpha$  probe radiation (non-resonant tripling in Kr). The four-wave mixing scheme has significantly higher efficiencies, thereby increasing our sensitivity in the heavy atom studies. In parallel, we plan to prepare  $\text{C}_2\text{H}$  by the photolysis of  $\text{C}_2\text{H}_2$  or another suitable precursor, and then photolyze  $\text{C}_2\text{H}$ , recording the H atom translational energy distribution using HRTOF.

### Publications supported by DOE: 2004-2006

1. A. B. Alekseyev, H.-P. Liebermann, and C. Wittig, *J. Chem. Phys.* **121**, 9389 (2004).
2. J. Underwood, D. Chastaing, S. Lee, and C. Wittig, *J. Chem. Phys.* **123**, 84312 (2005).
3. C. Wittig, *J. Phys. Chem. B* **109**, 8428 (2005).
4. J. Underwood and C. Wittig, *Chem. Phys. Lett.* **386**, 190 (2004).

THEORETICAL STUDIES OF THE REACTIONS AND SPECTROSCOPY OF RADICAL SPECIES  
RELEVANT TO COMBUSTION REACTIONS AND DIAGNOSTICS

DAVID R. YARKONY

DEPARTMENT OF CHEMISTRY, JOHNS HOPKINS UNIVERSITY, BALTIMORE, MD 21218  
yarkony@jhu.edu

We use computational techniques to study electronically nonadiabatic processes involving radical species that are relevant to combustion reactions and combustion diagnostics. During the past year we have considered the role of the  $1^2A - 2^2A$  conical intersection seam on *ground state* of vinoxy.<sup>1</sup> However our most enduring work may be our treatment of the ethoxy radical, being prepared for publication and described below. Recently we developed a perturbation theory based approach for representing of two<sup>2</sup> (or even three<sup>3</sup>) *coupled* potential energy surfaces in the vicinity of two or three state conical intersections. The approach treats *all* internal coordinates correctly to second order in nuclear displacements and determines a quasi diabatic representation using a limited number of *ab initio* data points. In the ethoxy radical the lowest energy two state conical intersection is quite close to the minimum on the ground state potential energy surface. In this challenging situation, our approach enabled us to readily determine coupled potential energy surfaces, including the spin-orbit interaction, suitable for describing the vibronic levels of the  $1^2A$ ,  $2^2A$  coupled electronic states of the ethoxy radical.

### I. Nonadiabatic Effects in Molecular Spectra

#### A. An 18 dimensional representation of the coupled $1,2^2A$ electronic states of ethoxy including spin-conserving nonadiabatic effects and the spin-orbit interaction

The ethoxy radical  $\text{CH}_3\text{-CH}_2\text{-O}$  is important from a practical perspective as a combustion intermediate in, for example, the oxidation of alkanes. From a theoretical perspective, this radical occupies a unique position in the molecular sequence R-O where R = H,  $\text{CH}_3$ ,  $\text{CH}_3\text{-CH}_2$ , and higher alkyls. Hydroxyl, OH, is known to have a significant fine structure splitting owing to the partial quenching of the  $\text{O}(^3P_J)$  spin-orbit interaction. The well-studied methoxy radical,<sup>4</sup>  $\text{CH}_3\text{O}$ , adds the complication of nonadiabatic interactions owing to an Exe Jahn-Teller effect.<sup>5</sup> In hydroxyl and methoxy, symmetry plays a key role in describing and interpreting the vibronic wave functions, arising from the  $^2\Pi$  and  $^2E$  electronic states, respectively. In the  $1^2A$  and  $2^2A$  electronic states of ethoxy, the analogues of the  $^2\Pi$  and  $^2E$  states, these nonadiabatic effects, the spin-orbit interaction and the interstate couplings resulting from conical intersections, involving, are operative. However in ethoxy symmetry is of little or no help in the analysis. The expected close proximity of the minimum energy point on the conical intersection seam of the  $1^2A$  and  $2^2A$  states and the minimum on the ground  $1^2A$  state potential energy surface ( confirmed by detailed calculations ) further complicates the situation as does the large number of internal modes, 18, compared to 1 and 9 in OH and  $\text{CH}_3\text{O}$ .

It was in this somewhat daunting context that we undertook to consider the electronic structure aspects of determining the low-lying vibronic levels of the nonadiabatically coupled  $1^2A$  and  $2^2A$  electronic states of the ethoxy radical. In a manuscript being prepared for publication we employed our recently introduced methods for accurately describing the vicinity of two and three state conical intersections, using data obtained from reliable multireference configuration interaction wave functions at a minimal number of nuclear configurations,<sup>2,3</sup> to develop coupled potential energy surfaces to describe the low-lying states of ethoxy. These results were obtained in the full  $N^{\text{int}}=18$  space of

internal nuclear coordinates. Thus in ethoxy we used the ostensibly complicating factor of the close proximity of the conical intersection seam and ground state equilibrium structure to advantage. The Hamiltonian we developed to describe the region of the conical intersection is sufficiently accurate in the vicinity of the equilibrium structure to analyze the low-lying vibronic states. These calculations were supplemented with the determination of the spin-orbit coupling interactions in the full 1- and 2-electron Breit-Pauli spin-orbit operator.

## II. Nonadiabatic Effects in Photodissociation

### A. $H_2CCOH$ : The role of $1^2A' - 2^2A$ conical intersection

The vinoxy radical is of significant import in combustion chemistry being a major product in the reaction of  $O(^3P)$  with hydrocarbons. Three electronic states have been studied the  $\tilde{X}^2A'$ ,  $\tilde{A}^2A'$  and  $\tilde{B}^2A''$  states. Currently we are concerned with the  $\tilde{X}^2A'$  and  $\tilde{A}^2A'$  states. Vinoxy dissociates to either  $CH_2CO+H$  or  $CH_3 + CO$ . The bottleneck for the latter product is the rearrangement step  $CH_2COH \rightarrow CH_3CO$ . The branching ratio for the products depends on the precursor state. When the  $\tilde{B}^2A''$  state is initially excited significant quantities of both products are observed.<sup>6</sup> However when the  $\tilde{X}^2A'$  state is produced directly  $H + H_2CCO$  is not observed. This failure to observe  $H + CH_2CO$  had been attributed to nonadiabatic recrossing.<sup>7</sup> In nonadiabatic recrossing<sup>8</sup> a nonadiabatic transition near a saddle point on the lower surface, 'blocks' that channel. Previously we have shown that tilted conical intersections can facilitate nonadiabatic recrossing.<sup>9</sup>

We considered the  $1, 2^2A'$  accidental conical intersections in the vinoxy radical could block the  $H +$  ketene channel. We identified a novel conical intersection topography, anticipated from a determination of the characteristic parameters as continuous functions of the seam coordinates, that greatly facilitates lower state to upper state nonadiabatic transitions, can enhance nonadiabatic recrossing, and for upper state to lower state transitions, routes all wave packets onto a single broad path on the lower half of the double cone. This final point should be contrasted with the more standard situation where two, three or even four distinct paths down the cone are expected. While the prevalence of this combination of characteristic parameters remains to be established, it is interesting to note that this combination can also be found in our recent study of photodissociation of  $H_2COH$  to  $H_2CO + H$ .<sup>10</sup> We considered the possibility that this conical intersection seam blocks the  $H +$  ketene dissociation channel by facilitating nonadiabatic recrossing. Our analysis of the conical topographies and the proximity of the conical intersections to the transition state for dissociation to ketene does not support nonadiabatic recrossing as a dynamical bottleneck for the  $H +$  ketene channel. Our calculations suggest that a more careful determination of the barrier to  $H +$  ketene dissociation, using the extended active space described in our work, is in order and is key to understanding branching ratios on the ground state surface.

### III. Future Directions

In the coming year, we intend to use the coupled potential energy surfaces including the spin-orbit interaction described in section I to determine the low-lying vibronic levels in ethoxy. To this end we have written time-independent and time-dependent Lanczos based diagonalization and wave packet propagation algorithms that exploit the details of our coupled quasi diabatic state representation of electronic states. These algorithms are specifically designed to exploit parallel architectures.

The ability to accurately describe a significant region of coupled multidimensional potential energy surfaces will enable us to address questions concerning near conical intersection dynamics.

One of the first problems we will address with this new technology is the mode specific behaviour observed by Crim in the vibrationally mediated photodissociation of  $\text{NH}_3$ .<sup>11</sup>

#### Literature Cited

- 1 R. A. Young Jr and D. R. Yarkony, *J. Chem. Phys.* **123**, 084315 (2005).
- 2 D. R. Yarkony, *J. Chem. Phys.* **123**, 204101 (2005).
- 3 M. Schuurman and D. R. Yarkony, *J. Chem. Phys.* **124**, 124109 (2006).
- 4 S. C. Foster, P. Misra, T.-Y. D. Lin, C. P. Damo, C. C. Carter, and T. A. Miller, *J. Phys. Chem.* **92**, 5914 (1988).
- 5 R. Englman, *The Jahn-Teller Effect in Molecules and Crystals*. (Wiley-Interscience, New York, 1972).
- 6 D. L. Osborn, H. Choi, D. H. Mordant, R. T. Bise, D. M. Neumark, and C. M. Rohlfing, *J. Chem. Phys.* **106**, 3049 (1997).
- 7 J. L. Miller, L. R. McCunn, M. J. Kirsch, and L. J. Butler, *J. Chem. Phys.* **121**, 1830 (2004).
- 8 G. C. G. Waschewsky, P. W. Kash, T. L. Myers, D. C. Kitchen, and L. J. Butler, *J. Chem. Soc. Faraday Trans* **90**, 1581 (1994).
- 9 D. R. Yarkony, *J. Chem. Phys.* **114**, 2601 (2001).
- 10 D. R. Yarkony, *J. Chem. Phys.* **112**, 084316 (2005).
- 11 A. Bach, J. M. Hutchison, R. J. Holiday, and F. F. Crim, *J. Chem. Phys.* **118**, 7144 (2003); A. Bach, J. M. Hutchison, R. J. Holiday, and F. F. Crim, *J. Chem. Phys.* **116**, 4955 (2002).

#### PUBLICATIONS SUPPORTED BY DE-FG02-91ER14189: 2004 - present

- 1 *Conical Intersections: Their description and consequences*, D. R. Yarkony, in *Conical Intersections: Electronic Structure, Dynamics and Spectroscopy*, Wolfgang Domcke, David R. Yarkony and Horst Köppel, eds. World Scientific Publishing, Singapore, (2004).
- 2 *Determination of potential energy surface intersections and derivative couplings in the adiabatic representation* D. R. Yarkony, in *Conical Intersections: Electronic Structure, Dynamics and Spectroscopy*, W. Domcke, D. R. Yarkony and H. Köppel, eds. World Scientific Publishing, Singapore, (2004)
- 3 *The analytic evaluation of nonadiabatic coupling terms at the MR-CI level I; Determination of minima on the crossing seam*  
Dallos, M.; Lischka, H.; Szalay, P.; Shepard, R.; Yarkony, D. *J. Chem. Phys.* **120**, 7330 (2004).
- 4 *Marching along ridges. Efficient location of energy minimized conical intersections of two states using extrapolatable functions*  
D. R. Yarkony, *J. Phys. Chem. A* **108**, 3200-3205 (2004).
5. *Exploring Molecular Complexity: The Role of Conical Intersections in  $\text{NH}_3$  Photodissociation*  
David R. Yarkony, *J. Chem. Phys.* **121**, 628-631 (2004)
6. *A Continuous Representation of the Branching Spaces of Two State Conical Intersections Along their Seams. A Group Homomorphism Approach*  
S. Han and D. Yarkony, in *Conical Intersections*, G. Worth and S. Althorpe, eds. (CCP6, 2004)
7. *Statistical and Nonstatistical Nonadiabatic Photodissociation from the first excited state of the hydroxymethyl radical*  
David R. Yarkony, *J. Chem. Phys.* **112**, 084316 (2005)
8. *A Novel Conical Intersection Topography and its Consequences. The  $1, 2^2\text{A}$  Conical Intersection Seam of the Vinyoxy Radical*,  
R. Andrew Young, Jr. and David R. Yarkony, *J. Chem. Phys.* **123**, 084315 (2005).

# GAS-PHASE MOLECULAR DYNAMICS: QUANTUM MOLECULAR DYNAMICS OF COMBUSTION REACTIONS AND MOLECULAR SPECTROSCOPY CALCULATIONS

Hua-Gen Yu

Chemistry Department, Brookhaven National Laboratory

Upton, NY 11973-5000

hgy@bnl.gov

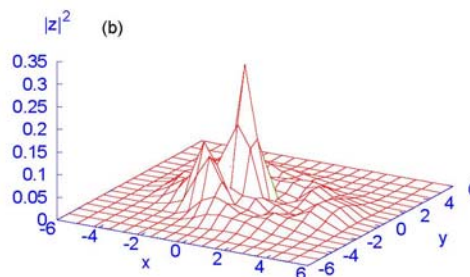
## Program Scope

The goal of this program is the development of computational methods for studying chemical reaction dynamics and molecular spectroscopy in the gas phase. We are interested in developing rigorous quantum dynamics algorithms for small polyatomic systems and in implementing approximate approaches for complex ones. Particular focuses are on the dynamics and kinetics of chemical reactions and on the rovibrational spectra of species involved in combustion processes. This research also explores the potential energy surfaces of these systems of interest using state-of-the-art quantum chemistry methods.

## Recent Progress

### A coherent discrete variable representation method

A coherent discrete variable representation (ZDVR) method has been developed for constructing a multidimensional potential-optimized DVR basis. In this approach, inspired by a coherent-state formalism in momentum and conjugate coordinates, the multidimensional quadrature pivots are obtained by diagonalizing a complex coordinate operator matrix in a finite basis set, which is spanned by the lowest eigenstates of a two-dimensional reference Hamiltonian. Here a *c-norm* condition is used in the diagonalization procedure. The orthonormal eigenvectors define a collocation matrix connecting the localized ZDVR basis functions and the finite basis set. The method has been applied to two vibrational models for computing the lowest bound states. Results show that the ZDVR method provides exponential convergence and accurate energies. In addition, a zeroth order approximation method has been derived and tested.



A typical two-dimensional coherent discrete variable representation (ZDVR) basis function

### Vibronic energies of DCCI and HCCI in three low-lying states

Three low-lying electronic states ( $X^1A'$ ,  $a^3A''$ ,  $A^1A''$ ) and the spin-orbit coupling matrix between the  $X$  and  $a$  states of HCCI have been calculated with an *ab initio* multi-reference configuration interaction (MRCI) method. The three-dimensional potential energy surfaces are interpolated using a general DVR interpolation technique from 6075 MRCI energy points. The vibronic energy levels of the DCCI and HCCI molecules are computed using a variational  $K$ -dependent quantum dynamics approach in hyperspherical coordinates. As a result, the Renner-Teller effect and the spin-orbit coupling in the system are treated in detail. In addition, the relative position of

the triplet state of HCCl to the singlet ground state is predicted to be  $2122\text{ cm}^{-1}$  (with Sears & Muckerman).

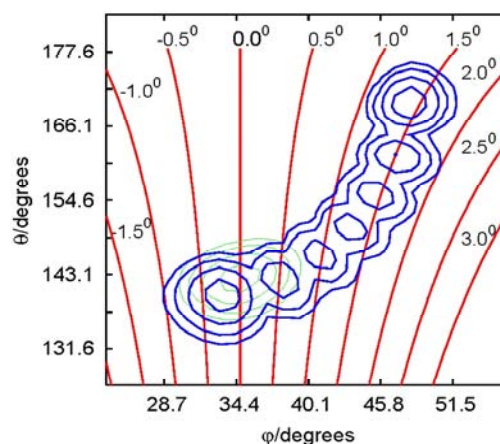
### Transition intensity calculation of the $A^1A''-X^1A'$ band of HCCl

Recently, our group has measured several hot bands lying to the red of the origin of the  $A^1A''-X^1A'$  transition of HCCl. These new bands may reveal a clue to the fundamental C-Cl stretching frequency of HCCl in the  $A$  state. In order to confirm this, following the energy level calculations described above, we further studied the transition intensities of the  $A^1A''-X^1A'$  bands based on a MRCI/aug-cc-pVTZ dipole moment surface. In a manner similar to the potential energy surfaces, the dipole moment surface was interpolated from a set of grid points. Results show that there exist apparent intensities for the  $A(0, \nu_2, \nu_3)-X(100)$  transitions of HCCl due to the fact that the  $X(012)$  vibrational state lies very close in energy to the  $X(100)$  state (with Sears).

### Exploring the intensity of the parallel sub-bands of the $A(060)-X(000)$ transition of HCB

In our group the rotationally resolved spectrum of the  $A(006)-X(000)$  has been recorded recently.

The spectrum contains both perpendicular and parallel rotational sub-band structures, where the latter are partially due to axis-switching in the transition as shown in the figure. However, the relative intensity of the parallel rotational bands to the perpendicular ones is not well explained by solely using the axis-switching model. The calculated intensities are substantially smaller than observed. In this work we propose another possible explanation by considering Coriolis coupling in the excited state and the non-adiabatic effect due to the electronic coupling between the  $B^1A'$  and  $X^1A'$  states, based on the calculated transition dipole moment matrices in four low-lying electronic states included the  $B^1A'$  excited state (with Hall & Sears).



Contour plots of the  $A(060)$  and  $X(000)$  vibrational states for HCB in the hyperangle plane. The axis-switching angles with respect to the equilibrium geometry of the  $X$  state are explicitly labeled in the figure.

### Quantum molecular dynamics study of radical-radical reactions

We have improved our dual-level *ab initio* direct dynamics program, and applied it to study two combustion-related reactions: the  $^1\text{CH}_2 + \text{C}_2\text{H}_2$  and  $\text{OH} + \text{HOCO}$  reactions. The  $^1\text{CH}_2 + \text{C}_2\text{H}_2$  reaction has been studied using the dual-level “scaling all correlation” (SAC) *ab initio* method of Truhlar et al, i.e., the UCCSD(SAC)/cc-pVDZ theory. Results show that the reaction occurs via long-lived complexes. The lifetime of the cyclopropene intermediate is obtained as  $3.2 \pm 0.4$  ps. It is found that the intermediate propyne can be formed directly from reactants through the insertion of  $^1\text{CH}_2$  into one C-H bond of  $\text{C}_2\text{H}_2$ . However, compared to the major mechanism in which the propyne is produced through a ring-opening of the cyclopropene complex, this reaction pathway is much less favorable.

The dynamics study of the  $\text{OH} + \text{HOCO}$  reaction has been carried out using the UMP2(SAC)/6-31G(d) method. This method was selected by minimizing the root-mean-squares errors of the relative SAC energies of the stationary points corresponding to the CCSD(T)/CBS results. The

reaction is shown to proceed through an addition intermediate, HOC(O)OH, which then passes through a four-centered transition state as it produces the products H<sub>2</sub>O and CO<sub>2</sub>. The energetics suggest that the reaction is effectively barrierless. The calculated thermal rate constant of  $1.03 \times 10^{-11} \text{ cm}^3 \text{ molecule}^{-1} \text{ s}^{-1}$  at room temperature shows that it is a fast radical reaction, and the intermediate HOC(O)OH is short-lived (with Muckerman & J. Francisco).

## Future Plans

### Kinetics and dynamics study of the reaction of HOCO with oxygen

We will apply our direct *ab initio* molecular dynamics program for studying some important combustion reactions. Currently, of particular interest is the reactivity of the HOCO radical reaction with oxygen atom and molecule. For the O + HOCO reaction, in collaboration with J. Francisco (Purdue), we will address the energies, geometries, and vibrational frequencies of the stationary points on the ground-state doublet potential energy surface, and the reaction mechanism by using a SAC/UCCD method. For the O<sub>2</sub> + HOCO reaction, on the other hand, the *ab initio* direct dynamics study will be carried out using the UB3PW91 density functional theory (DFT). This DFT method is selected by minimizing the errors of the relative energies of the stationary points on the ground-state electronic surface of HOC(O)O<sub>2</sub> with respect to the best *ab initio* values of Poggi and Francisco (*J. Chem. Phys.* 120 (2004) 5073). Besides the kinetics and dynamics studies of the reaction, we also hope to predict the lifetime of the HOC(O)O<sub>2</sub> intermediate produced through the reaction course, and the energy disposal in the HO<sub>2</sub> + CO<sub>2</sub> products. For both reactions, the temperature dependence of the thermal rate constants will be calculated (with Muckerman & J. Francisco).

### Rovibrational tunneling spectroscopy of weakly bound molecular clusters

Significant experimental progress has been made on understanding the structure and dynamics of weakly bound clusters from very simple van der Waals molecules, *e.g.*, Ar-H<sub>2</sub> and Ne-HF, to systems of real chemical interest such as the OH<sup>-</sup>(H<sub>2</sub>O)<sub>n</sub> clusters. These experimental advances present a major challenge to theory both in calculating the potential energy surface of clusters, and in developing the dynamics methods to compute the rovibrational bound states. In the dynamics aspect, the challenge arises from the shallowness of the potential well of the weakly bound molecular clusters that gives rise to strong anharmonic effects in their ground-state dynamics. This consideration precludes the applicability of the widely used vibrational normal mode approach. Furthermore, the vibrational energy level spacings are also very small, and one needs to calculate them to a very high accuracy. In this research, we plan to apply the two-layer Lanczos algorithm for studying the rovibrational spectra of the HF(H<sub>2</sub>)<sub>n</sub> and OH<sup>-</sup>(H<sub>2</sub>O)<sub>n</sub> clusters, implemented with the diffusion Monte Carlo technique. In these calculations, we are particularly interested in studying tunneling dynamics in the spectroscopy of the hydrogen-containing molecular clusters (with Z. Bacic and J. Bowman).

## Acknowledgment

This work was performed at Brookhaven National Laboratory under Contract DE-AC02-98CH10886 with the U.S. Department of Energy and supported by its Division of Chemical Sciences, Office of Basic Energy Sciences.

### Publications since 2004

- H.-G. Yu and J.T. Muckerman, *MRCI calculations of the lowest potential energy surface for CH<sub>3</sub>OH and direct ab initio dynamics calculations of the O(<sup>1</sup>D) + CH<sub>4</sub> and OH + CH<sub>3</sub> reactions*, J. Phys. Chem. A **108**, 8615 (2004).
- H.-G. Yu and J.T. Muckerman, *Exploring the multiple reaction pathways for the H + cyc-C<sub>3</sub>H<sub>6</sub> reaction*, J. Phys. Chem. A **108**, 10844 (2004).
- H.-G. Yu, *Full-dimensional quantum calculations of vibrational spectra of six-atom molecules. I. Theory and numerical results*, J. Chem. Phys. **120**, 2270 (2004).
- H.-G. Yu, *Converged quantum dynamics calculations of vibrational energies of CH<sub>4</sub> and CH<sub>3</sub>D using an ab initio potential*, J. Chem. Phys. **121**, 6334 (2004).
- H.-G. Yu and J.T. Muckerman, *Ab initio and direct dynamics studies of the reaction of singlet methylene with acetylene, and the lifetime of the cyclopropene complex*, J. Phys. Chem. A **109**, 1890 (2005).
- H.-G. Yu, J.T. Muckerman and J.S. Francisco, *Direct ab initio dynamics study of the OH + HOCO reaction*, J. Phys. Chem. A **109**, 5230 (2005).
- H.-G. Yu, *A coherent discrete variable representation method for multidimensional systems in physics*, J. Chem. Phys. **122**, 164107 (2005).
- H.-G. Yu, T.J. Sears and J.T. Muckerman, *Potential energy surfaces and vibrational energy levels of DCCL and HCCL in three low-lying states*, Mol. Phys. **104**, 47 (2006).
- G. E. Hall, T. J. Sears and H.-G. Yu, *Rotationally Resolved Spectrum of the A(060) -- X(000) Band of HCB<sub>r</sub>*, J. Molec. Spectrosc. **235**, 125 (2006).
- Z. Wang, R.G. Bird, H.-G. Yu and T.J. Sears, *Hot bands in jet-cooled and ambient temperature spectra of chloromethylene*, J. Chem. Phys. **124**, 74314 (2006).
- H.-G. Yu and J.T. Muckerman, *Quantum molecular dynamics study of the reaction of O<sub>2</sub> with HOCO*, J. Phys. Chem. A (in press, 2006).

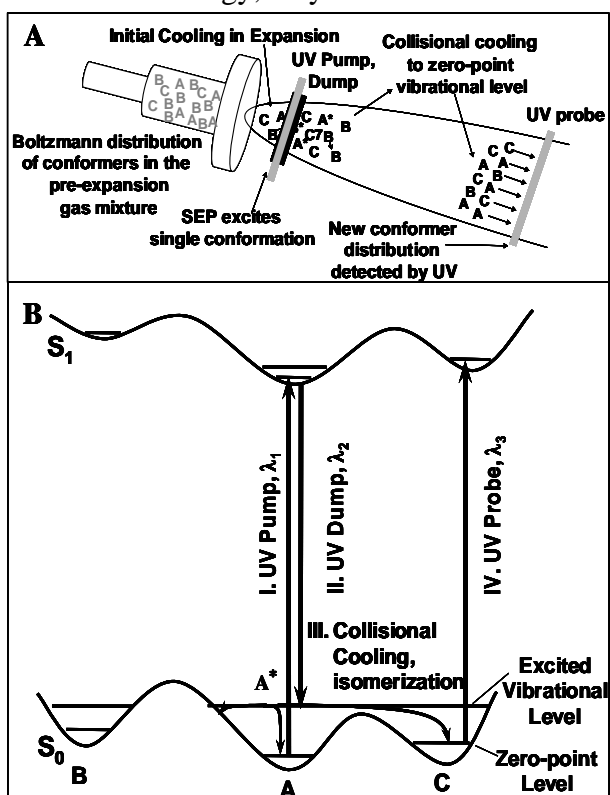
# Experimental Characterization of the Potential Energy Surfaces for Conformational Isomerization in Aromatic Fuels

Timothy S. Zwier

Department of Chemistry, Purdue University, West Lafayette, IN 47907-2084  
zwier@purdue.edu

## Program Definition and Scope

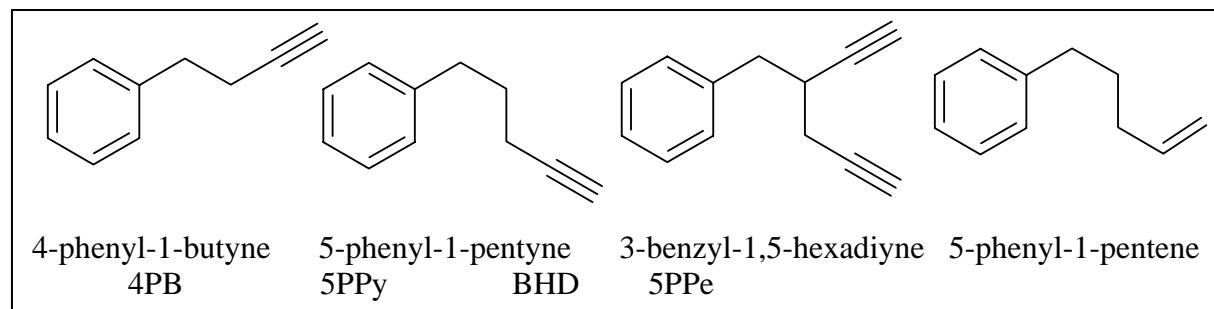
Gasoline and diesel fuels are complicated mixtures containing about 30% aromatics, including alkylbenzene, alkenylbenzene, and alkynylbenzenes of various chain lengths. The combustion of these molecules is influenced by their structural and conformational make-up, and by the rates of isomerization between them. The objective of this research program is to develop and utilize laser-based methods to characterize the spectroscopy and isomerization dynamics of conformational isomers of aromatic derivatives that play a role in soot formation. As a first step in all these studies, UV-UV hole-burning and resonant ion-dip infrared (RIDIR) spectroscopy are being used to determine the number and identity of the conformations present, based on their ultraviolet and infrared spectral signatures. These structural studies then serve as a foundation for studies of the dynamics of conformational isomerization using SEP population transfer spectroscopy (SEP-PTS). Stimulated emission pumping (SEP) is used to selectively excite a single conformation of the molecule of interest to a well-defined vibrational energy early in the supersonic expansion. If the excited molecules have sufficient energy, they can isomerize before being re-cooled in the expansion to allow isomer-specific detection in LIF or R2PI. By tuning the SEP dump laser in a 20-10-20 Hz laser configuration, it is possible to directly measure the energy thresholds separating individual A→B reactant-product isomer pairs, thereby mapping out key stationary points on the multi-dimensional potential energy surface for isomerization. We are using these methods to study conformational isomerization in substituted benzenes spanning a range of types and degrees of conformational flexibility. From near-threshold intensity measurements we hope to explore the rate of isomerization relative to collisional cooling as a function of energy above threshold. These results can provide new tests of RRKM descriptions of isomerization in large molecules.



## Recent Progress

### A. The single-conformation spectroscopy of a series of alkynylbenzenes

During the past year, we completed a detailed study of the single-conformation spectroscopy of 4-phenyl-1-butyne, 5-phenyl-1-pentyne, 3-benzyl-1,5-hexadiyne, and 5-phenyl-1-pentene, whose structures are shown below.

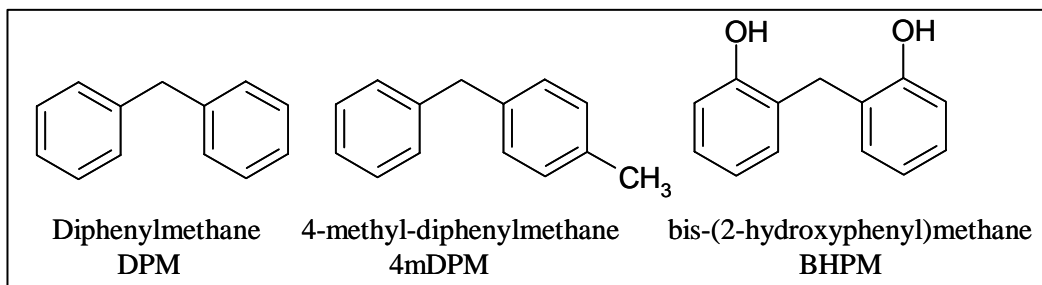


This series of molecules spans an interesting range of size and conformational complexity. A combination of vibronic level R2PI spectroscopy, rotational band contour analysis, UV-UV hole-burning, and RIDIR spectroscopy have been employed to obtain firm conformational assignments. There are two conformations of 4PB, in which the acetylenic group is anti or gauche with respect to the ring. Three conformations of 5PPy are observed, while five conformations are present in BHD. In all cases, the  $S_1 \leftarrow S_0$  origin transitions of the conformers are spread over about  $150 \text{ cm}^{-1}$ . The magnitude and direction of the electronic frequency shift reflect the types of interactions of the side chains with the phenyl ring. CIS calculations correctly predict the direction of the transition moment in these alkylbenzenes, aiding in the rotational band contour fitting of the observed bands. In BHD, the two acetylenic groups produce acetylenic CH stretch fundamentals that reflect the relative orientation of these groups in the hexadiyne side chain. We are currently engaged in SEP-population transfer studies on this triad of molecules.

5-phenyl-1-pentene (5PPE) is a close analog of 5-phenyl-1-pentyne, substituting a vinyl group for the acetylenic group at the end of the 5-carbon chain. Previous photochemical studies have identified unusual photochemistry associated with addition of the vinyl group across the phenyl ring to form bicyclic products (C.D.D. Ho and H. Morrison, *J. Am. Chem. Soc.* **127**, 2114 (2005)). We have subjected 5PPE to our methods in order to determine the conformations present and to search for conformation-specific behavior in the excited state lifetimes or isomerization dynamics. Five conformational isomers were identified in the R2PI spectrum, and the observed transitions were assigned to specific conformers based on rotational band contour analysis of the  $S_1 \leftarrow S_0$  origin transitions and a comparison with 5-phenyl-1-pentyne.

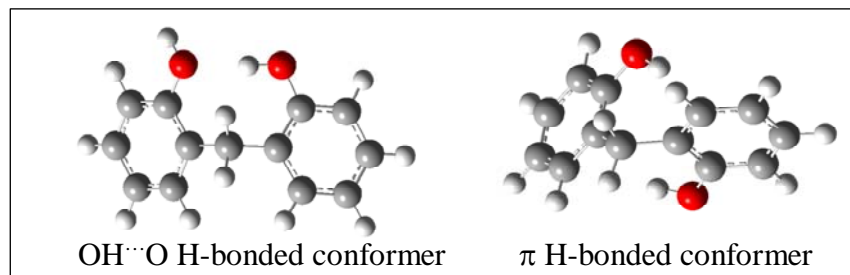
### B. Diphenylmethane, 4-methyldiphenylmethane, and bis-(2-hydroxyphenyl)methane

Diphenylmethane (DPM), 4-methyldiphenylmethane (4-mDPM), and bis-(2-hydroxyphenyl)methane (BHPM) form another series of molecules which possess increasing conformational complexity, with two torsional coordinates in DPM (specifying the torsional angles of the two phenyl rings), three in 4-mDPM (two phenyl torsions plus a methyl internal rotor), and four in BHPM (two phenyl torsions and two OH torsions). In this series, additional interest is fueled by the fact that the conformational flexibility occurs between two ultraviolet chromophores, which complicate and enrich the ultraviolet spectroscopy, and show promise for providing novel insight to the unique vibronic coupling that accompanies such a circumstance.



According to calculations, in the ground states of DPM and 4mDPM, the two phenyl rings are able to internally rotate with respect to one another with only modest barriers of about  $200\text{ cm}^{-1}$  separating the  $C_2$  minima. We are able to follow torsional progressions in the vibronic spectrum that reach near to the top of the computed barrier. In DPM, the  $S_0$ - $S_1$  and  $S_0$ - $S_2$  origins are split by  $123\text{ cm}^{-1}$ . More than a year ago, we collaborated with D. Plusquellic at NIST to record the high resolution electronic spectrum of the  $S_1 \leftarrow S_0$  origin transition of DPM. The rotational constants are consistent with a  $C_2$  geometry for DPM with a  $60^\circ$  angle between the two phenyl rings. The direction of the transition moment is different than in toluene (70:30 a:c hybrid band), indicating that the coupling across the methylene group is sufficient to rotate the transition moment from the direction anticipated based on toluene. Unable to fit the  $S_2$  origin due to an overlap of two bands, we have now returned to NIST to record the spectra of the fully deuterated isotopomer, DPM- $d_{12}$ . We are currently working on fitting these spectra. In 4-mDPM, the electronic excitation is localized on either of the two rings, with a splitting between  $S_1$  and  $S_2$  states of  $662\text{ cm}^{-1}$ . At the  $S_2$  origin of 4-mDPM, electronic energy transfer to  $S_1$  is complete on the timescale of the fluorescence.

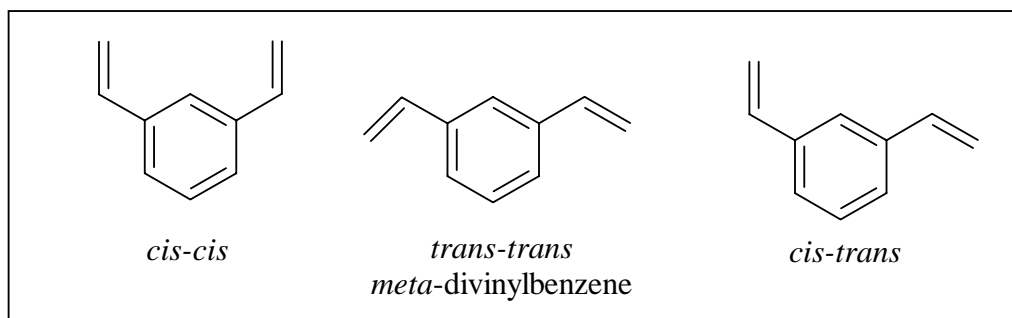
Finally, the addition of the two OH groups in the ortho positions on the two rings leads to the formation of two distinct conformational isomers, one in which the two OH groups H-bond to one another, and the other in which the two OH groups each form  $\pi$  H-bonds with the other ring. This is borne out by fluorescence-dip infrared spectra in the OH stretch region. Excited state FDIR spectra were also recorded, revealing the effects of electronic excitation on the H-bonding. In the OH $\cdots$ O H-bonded conformer, the  $S_1$  and  $S_2$  states are localized on the two rings, as one would expect based on the distinct donor and acceptor roles played by the two rings. However, even in the  $\pi$ -bond conformer, the excited state infrared spectrum reflects at least a partial localization in the excited states of this conformer as well.



### Spectroscopy and isomerization of *ortho*-, *meta*-, and *para*-divinylbenzene

Having just completed a study of *ortho*-, *meta*-, and *para*-ethynylstyrene (*o*ES, *m*ES, and *p*ES), we have now extended our work on structural and conformational isomers of substituted aromatics to include *ortho*-, *meta*-, and *para*-divinylbenzene, shown below. The spectroscopic studies have included resonant two photon ionization (R2PI), UV-UV hole-burning spectroscopy (UVHB), and resonant ion-dip infrared spectroscopy (RIDIRS). Building off of previous work

by the Pratt group (T.V. Nguyen, J.W. Ribblett, and D.W. Pratt, Chem. Phys. **283**, 279-287 (2002)), we have now identified the missing conformers of *meta*-DVB and *para*-DVB. In addition, stimulated emission pumping-population transfer spectroscopy (SEP-PTS) was used to place direct experimental bounds on the barrier to conformational isomerization between the three isomers of *m*DVB (*cis-cis*, *cis-trans*, and *trans-trans*). These studies used the new dispersed fluorescence chamber with its high-efficiency fluorescence collection optics and high throughput pumping capacity designed for hole-filling studies. We have proven that the isomerization pathway between *cis-cis* and *trans-trans* involves sequential isomerization of the two vinyl groups traversing over two barriers each of about 1200 cm<sup>-1</sup> (~3.5 kcal/mol) rather than concerted motion over one barrier of about twice that size. Both the barrier heights and relative energies of the minima are close to those determined by DFT Becke3LYP/6-31+G\* calculations.



### Publications acknowledging DOE support, 2004-present

Talitha M. Selby and Timothy S. Zwier, "Conformation-specific spectroscopy of 4-phenyl-1-butyne and 5-phenyl-1-pentyne, J. Phys. Chem. A **109**, 8487-8496 (2005).

Talitha M. Selby, Alope Das, T. Bekele, H. Daniel Lee, and Timothy S. Zwier, Conformation-specific spectroscopy of 3-benzyl-1,5-hexadiyne, J. Phys. Chem. A **109**, 8497-8506 (2005).

Bruce C. Garrett, et al., "The Role of Water on Electron-Initiated Processes and Radical Chemistry: Issues and Scientific Advances", Chemical Reviews **105**, 355-389 (2005).

Talitha M. Selby, Jasper R. Clarkson, Diane Mitchell, James A.J. Fitzpatrick, and Timothy S. Zwier, "Isomer-specific spectroscopy and conformational isomerization energetics of o-, m-, and p-ethynylstyrenes", J. Phys. Chem. A **109**, 4484-96 (2005).



## Author Index

Allen, Wesley D.....	256	Lester, M.I.....	155	Truhlar, D.G.....	292
Baer, T.....	1	Lester, Jr., W.A. ....	158	Tsang, W.....	296
Barlow, R.S.....	5	Lignell, D.....	29	Valentini, J.J.....	300
Bowman, C. T.....	103	Light, J.C.....	161	Walters, R. ....	213
Bowman, J. M. ....	9	Lin, M.C.....	165	Weber, P.M. ....	303
Brown, N.J. ....	13	Long, M.B.....	272	Westbrook, C.K. ....	307
Butler, L. J.....	17	Lucht, R.P. ....	169	Westmoreland, P.R. ....	311
Carpenter, B.K. ....	21	Macdonald, R.G. ....	173	Wittig, C.....	315
Chandler, D.W. ....	25	Mebel, A. ....	177	Yarkony, D.R. ....	319
Chen, J.H.....	29,119	Michael, J.V.....	181	Yoo, C.S.....	29
Continetti, R.E. ....	33	Michelsen, H.A. ....	185	Yu, H.G.....	322
Cool, T.A. ....	37	Miller, J.A. ....	189	Zwier, T.S. ....	326
Crim, F.F.....	41	Miller, T.A. ....	193		
Dai, H.L. ....	44	Miller, W.H.....	197		
Davis, H.F. ....	48	Muckerman, J.T. ....	201		
Davis, M.J. ....	52	Mullin, A.S.....	205		
Dong, F. ....	213	Najm, H.N.....	209		
Dryer, F.L.....	56	Nesbitt, D. J.....	213		
Ellison, G.B.....	60	Neumark, D.M. ....	216		
Ervin, K.M. ....	65	Ng, C.Y. ....	220		
Field, R.W.....	69	Oefelein, J. ....	224		
Flynn, G. ....	73	Osborn, D.L. ....	228		
Frank, J.H.....	77	Perry, D.S.....	232		
Frenklach, M. ....	81	Pitz, W.J.....	307		
Gray, S.K. ....	85	Pope, S.B.....	236		
Green, Jr., W.H. ....	89	Pratt, S.T. ....	240		
Guo, H.....	93	Reisler, H. ....	244		
Hall, G.E. ....	95	Roberts, M.....	213		
Hansen, N.....	99	Ruedenberg, K. ....	248		
Hanson, R.K.....	103	Ruscic, B.....	252		
Harding, L.B. ....	107	Rutland, C.J.....	119		
Hawkes, E.R.....	29	Sankaran, R. ....	29		
Head-Gordon, M.....	111	Savage, C. ....	213		
Hershberger, J.F. ....	115	Schaefer III, H.F. ....	256		
Im, H.G. ....	119	Sears, T.J.....	261		
Johnson, P.M.....	123	Settersten, T.A. ....	264		
Kaiser, R.I.....	127	Shepard, R.....	268		
Kellman, M.E.....	131	Smooke, M.D.....	272		
Kerstein, A.R. ....	135	Suits, A.G.....	276		
Kiefer, J.H.....	139	Taatjes, C.A. ....	280		
Klippenstein, S.J. ....	143	Thompson, D.L. ....	284		
Krylov, A.I.....	147	Tranter, R.S.....	288		
Leone, S.R.....	151	Trouvé, A. ....	119		



## Participants

Wesley Allen  
Center for Computational Chemistry  
University of Georgia  
Athens, GA 30622  
Phone: 706-542-7729  
E-Mail: wdallen@ccqc.uga.edu

Tomas Baer  
Chemistry Department  
University of North Carolina  
Chapel Hill, NC 27599-3290  
Phone: 919-962-1580  
E-Mail: baer@unc.edu

Robert Barlow  
P.O. Box 969, MS9051  
Sandia National Laboratories  
Livermore, CA 94550  
Phone: 925-294-2688  
E-Mail: barlow@ca.sandia.gov

Joel Bowman  
1515 Dickey Drive  
Dept. of Chemistry, Emory University  
Atlanta, GA 30322  
Phone: 404-727-6592  
E-Mail: jmbowma@emory.edu

Bastiaan Braams  
Dept. MathCS, 400 Dowman Drive #W401  
Emory University  
Atlanta, GA 30322  
Phone: 404-727-1980  
E-Mail: braams@mathcs.emory.edu

Nancy Brown  
One Cyclotron Road, MS: 90K-113  
Lawrence Berkeley National Laboratory  
Berkeley, CA 94720  
Phone: 510-486-4241  
E-Mail: NJBrown@lbl.gov

Laurie Butler  
5640 S. Ellis Avenue  
The James Franck Institute  
The University of Chicago  
Chicago, IL 60637  
Phone: 773-702-7206  
E-Mail: L-Butler@uchicago.edu

David Chandler  
7011 East Ave.  
Sandia National Laboratories  
Livermore, CA 94550  
Phone: 925-294-3132  
E-Mail: eharpel@sandia.gov

Jackie Chen  
7011 East Avenue, MS 9051  
Sandia National Laboratories  
Livermore, CA 94550  
Phone: 925-294-2586  
E-Mail: jhchen@sandia.gov

Robert Continetti  
Dept. Chem. 0340, 9500 Gilman Drive  
University of California San Diego  
La Jolla, CA 92093-0340  
Phone: 858-534-5559  
E-Mail: rcontinetti@ucsd.edu

Terrill Cool  
228 Clark Hall  
Cornell University  
Ithaca, NY 14853  
Phone: 607-255-4191  
E-Mail: tac13@cornell.edu

Fleming Crim  
1101 University Ave.  
University of Wisconsin, Madison  
Madison, WI 53706  
Phone: 608-263-7364  
E-Mail: fcrim@chem.wisc.edu

Hai-Lung Dai  
Department of Chemistry  
University of Pennsylvania  
Philadelphia, PA 19104  
Phone: 215-898-5077  
E-Mail: dai@sas.upenn.edu

H. Floyd Davis  
Dept. of Chem. & Chem. Bio., Baker Lab.  
Cornell University  
Ithaca, NY 14853-1301  
Phone: 607-255-0014  
E-Mail: hfd1@cornell.edu

## Participants

Michael Davis  
Chemistry Division  
Argonne National Laboratory  
Argonne, IL 60439  
Phone: 630-252-4802  
E-Mail: davis@tcg.anl.gov

Frederick Dryer  
D-329-D Engineering Quadrangle  
Princeton University  
Princeton, NJ 08544-5263  
Phone: 609-258-5280  
E-Mail: fldryer@princeton.edu

Barney Ellison  
Department of Chemistry  
University of Colorado  
Boulder, CO 80309-0215  
Phone: 303 492-8603  
E-Mail: barney@jila.colorado.edu

Kent M. Ervin  
Dept. of Chemistry/216  
University of Nevada, Reno  
Reno, NV 89557  
Phone: 775-784-6676  
E-Mail: ervin@chem.unr.edu

Robert Field  
Room 6-219, 77 Massachusetts Avenue  
MIT  
Cambridge, MA 02139  
Phone: 617-253-1489  
E-Mail: rwfield@mit.edu

George Flynn  
MC 3109 Havemeyer, 3000 Broadway  
Columbia University  
New York, New York 10027  
Phone: 212-854-4162  
E-Mail: gwfl1@columbia.edu

Jonathan Frank  
PO Box 969, MS 9051  
Sandia National Labs  
Livermore, CA 94551-0969  
Phone: 925-294-4645  
E-Mail: jhfrank@ca.sandia.gov

Michael Frenklach  
Department of Mechanical Engineering  
University of California at Berkeley  
Berkeley, CA 94720-1740  
Phone: 510-643-1676  
E-Mail: myf@me.berkeley.edu

David Golden  
Building 520  
Stanford University  
Stanford, CA 94305  
Phone: 650-723-5009  
E-Mail: david.golden@stanford.edu

Stephen Gray  
Chemistry Division  
Argonne National Laboratory  
Argonne, IL 60439  
Phone: 630-252-3594  
E-Mail: gray@tcg.anl.gov

William Green  
77 Massachusetts Ave. Rm. 66-270  
MIT  
Cambridge, MA 02139  
Phone: 617-253-4580  
E-Mail: whgreen@mit.edu

Hua Guo  
Department of Chemistry  
University of New Mexico  
Albuquerque, New Mexico 87131  
Phone: 505-277-1716  
E-Mail: hguo@unm.edu

Gregory Hall  
Chemistry Department  
Brookhaven National Laboratory  
Upton, NY 11973-5000  
Phone: 631-344-4376  
E-Mail: gehall@bnl.gov

Nils Hansen  
PO Box 969 MS 9055  
Sandia National Laboratories  
Livermore, CA 94551  
Phone: 925-294-6272  
E-Mail: nhansen@sandia.gov

## Participants

Ronald Hanson  
Mechanical Engineering  
Stanford University  
Stanford, CA 94305-3032  
Phone: 650-723-6850  
E-Mail: rkhanson@stanford.edu

John Hershberger  
Department of Chemistry  
North Dakota State University  
Fargo, ND 58105  
Phone: 701-231-8225  
E-Mail: john.hershberger@ndsu.edu

Philip Johnson  
Department of Chemistry  
Stony Brook University  
Stony Brook, NY 11794  
Phone: 631-632-7912  
E-Mail: philip.johnson@sunysb.edu

Michael Kellman  
Department of Chemistry  
University of Oregon  
Eugene, OR 97403  
Phone: 541-346-4196  
E-Mail: kellman@uoregon.edu

Stephen Klippenstein  
9700 S. Cass Ave.  
Argonne National Laboratory  
Argonne, IL 60439  
Phone: 630-252-3596  
E-Mail: sjk@anl.gov

Allan Laufer  
100 Bureau Drive: Stop 8380  
Retired - NIST Guest Scientist  
Gaithersburg, MD 20899  
Phone: 301-975-2062  
E-Mail: allan.laufer@nist.gov

Marsha Lester  
231 South 34th Street  
University of Pennsylvania, Department of Chemistry  
Philadelphia, PA 19104-6323  
Phone: 215-898-4640  
E-Mail: milester@sas.upenn.edu

Lawrence Harding  
9700 South Cass Avenue  
Argonne National Laboratory  
Argonne, IL 60439  
Phone: 630-252-3591  
E-Mail: harding@anl.gov

Richard Hilderbrandt  
SC-22.1 Office of Basic Energy Sciences  
19901 Germantown Road  
Department of Energy  
Germantown, MD 20874  
Phone: 301-903-0035  
E-Mail: richard.hilderbrandt@science.doe.gov

Ralf Kaiser  
2545 The Mall  
University of Hawaii  
Honolulu, HI 96822  
Phone: 808-956-5731  
E-Mail: kaiser@gold.chem.hawaii.edu

John Kiefer  
810 S. Clinton  
University of Illinois at Chicago  
Chicago, IL 60680  
Phone: 312-996-5711  
E-Mail: kiefer@uic.edu

Anna Krylov  
Dept. of Chemistry  
University of Southern California  
Los Angeles, CA 90089  
Phone: 213-740-4929  
E-Mail: krylov@usc.edu

Stephen Leone  
209 Gilman Hall  
University of California at Berkeley  
Berkeley, CA 94720  
Phone: 510-643-5467  
E-Mail: srl@berkeley.edu

William A. Lester Jr.  
Department of Chemistry  
University of California at Berkeley  
Berkeley, CA 94720-1460  
Phone: 510-643-9590  
E-Mail: walester@lbl.gov

## Participants

John Light  
929 E 57th St.  
University of Chicago  
Chicago, IL 60637  
Phone: 773-702-7197  
E-Mail: j-light@uchicago.edu

M. C. Lin  
805 Clifton Road  
Emory University  
Atlanta, GA 30322  
Phone: 404-727-2825  
E-Mail: chemmcl@emory.edu

Robert Lucht  
School of Mechanical Engineering  
Purdue University  
West Lafayette, IN 47907-2088  
Phone: 765-494-5623  
E-Mail: lucht@purdue.edu

Robert Macdonald  
9700 South Cass Ave  
Argonne National Laboratory  
Argonne, IL 60439  
Phone: 630-252-7742  
E-Mail: rgmacdonald@anl.gov

Dawn Manley  
7011 East Avenue, MS 9051  
Sandia National Laboratories  
Livermore, Ca 94550  
Phone: 925-294-4589  
E-Mail: dmanley@sandia.gov

Diane Marceau  
SC 22.1 Office of Basic Energy Sciences  
19901 Germantown Road  
Department of Energy  
Germantown, MD 20874  
Phone: 301-903-0235  
E-Mail: diane.marceau@science.doe.gov

Andrew McIlroy  
7011 East Ave.  
Sandia National Laboratories  
Livermore, CA 94550  
Phone: 925-294-3054  
E-Mail: amcrlr@sandia.gov

Alexander Mebel  
11200 SW 8th Street  
Florida International University  
Miami, FL 33193  
Phone: 305-348-1945  
E-Mail: mebela@fiu.edu

Joe Michael  
9700 S. Cass Avenue  
Argonne National Laboratory  
Argonne, IL 60439  
Phone: 630-252-3171  
E-Mail: jmichael@anl.gov

Hope Michelsen  
P. O. Box 969; MS 9055  
Sandia National Laboratory  
Livermore, CA 94551  
Phone: 925-294-2335  
E-Mail: hamiche@ca.sandia.gov

James A. Miller  
Combustion Research Facility  
Sandia National Laboratories  
Livermore, CA 94551-0969  
Phone: 925-294-2759  
E-Mail: jamille@sandia.gov

Terry Miller  
Dept. of Chemistry, 120 W 18th  
Ohio State University  
Columbus, OH 43210  
Phone: 614-292-2569  
E-Mail: tamiller@chemistry.ohio-stte.edu

William H. Miller  
Dept. of Chemistry  
University of California Berkeley  
Lawrence Berkeley National Laboratory  
Berkeley, CA 94720  
Phone: 510-642-0653  
E-Mail: millerwh@berkeley.edu

James Muckerman  
Chemistry Department  
Brookhaven National Laboratory  
Upton, NY 11973-5000  
Phone: 631-344-4368  
E-Mail: muckerma@bnl.gov

## Participants

Amy Mullin  
Department of Chemistry and Biochemistry  
University of Maryland  
College Park, MD 20742  
Phone: 301-405-6569  
E-Mail: mullin@umd.edu

Habib Najm  
7011 East Avenue, MS 9051  
Sandia National Laboratories  
Livermore, CA 94550  
Phone: 925-294-2054  
E-Mail: hnnajm@sandia.gov

David Nesbitt  
440 UCB  
JILA / NIST, University of Colorado  
Boulder, CO 80309-0440  
Phone: 303-492-7791  
E-Mail: cshaw@jila.colorado.edu

Daniel Neumark  
Department of Chemistry, B64A Hildebrand Hall  
Lawrence Berkeley National Laboratory  
University of California Berkeley  
Berkeley, CA 94720-1460  
Phone: 510-643-3850  
E-Mail: dneumark@berkeley.edu

Cheuk-Yiu Ng  
Department of Chemistry, One Shields Ave.  
University of California at Davis  
Davis, CA 95616  
Phone: 530-754-9645  
E-Mail: cyng@chem.ucdavis.edu

Joseph Oefelein  
7011 East Avenue, MS 9051  
Sandia National Laboratories  
Livermore, CA 94550  
Phone: 925-294-2648  
E-Mail: oefelei@sandia.gov

David Osborn  
7011 East Avenue  
Sandia National Laboratories  
Livermore, CA 94551-0969  
Phone: 925-294-4622  
E-Mail: dlosbor@sandia.gov

David Perry  
The Department of Chemistry  
The University of Akron  
Akron, OH 44325-3601  
Phone: 330-972-6825  
E-Mail: dperry@uakron.edu

William Pitz  
P.O. Box 808  
Lawrence Livermore National Laboratory  
Livermore, CA 94551  
Phone: 925-422-7730  
E-Mail: pitz1@llnl.gov

Stephen Pope  
254 Upson Hall  
Cornell University  
Ithaca, NY 14853  
Phone: 607-255-4314  
E-Mail: pope@mae.cornell.edu

Stephen Pratt  
Building 200, 9700 S. Cass Avenue  
Argonne National Laboratory  
Argonne, IL 60439  
Phone: 630 252-4199  
E-Mail: stpratt@anl.gov

Hanna Reisler  
Department of Chemistry, MC 0482  
University of Southern California  
Los Angeles, CA 90089-0482  
Phone: 213-740-7071  
E-Mail: reisler@usc.edu

Branko Ruscic  
9700 S Cass Ave - CHM 200  
Argonne National Laboratory  
Argonne, IL 60439  
Phone: 630-252-4079  
E-Mail: ruscic@anl.gov

Henry Schaefer III  
1004 Cedar St.  
Center for Computational Chemistry  
University of Georgia  
Athens, GA 30602  
Phone: 706 542-2067  
E-Mail: hfs@uga.edu

## Participants

Trevor Sears  
Chemistry Dept.  
Brookhaven National Laboratory  
Upton, NY 11973  
Phone: 631-344-4374  
E-Mail: sears@bnl.gov

Tom Settersten  
PO Box 969 MS 9056  
Sandia National Laboratories  
Livermore, CA 94551  
Phone: 925-294-4701  
E-Mail: tbsette@sandia.gov

Ron Shepard  
9700 S. Cass Ave.  
Argonne National Laboratory  
Argonne, IL 60439  
Phone: 630-252-3584  
E-Mail: shepard@tcg.anl.gov

Philip Smith  
50 S Central Campus Dr., Room 3290 MEB  
The University of Utah  
Salt Lake City, UT 84112-9203  
Phone: 801-585-3129  
E-Mail: smith@crsim.utah.edu

Mitchell Smooke  
15 Prospect Street  
Yale University  
New Haven, CT 06520-8284  
Phone: 203-432-4344  
E-Mail: mitchell.smooke@yale.edu

Arthur Suits  
5101 Cass Ave.  
Wayne State University  
Detroit, MI 48202  
Phone: 313 577 9008  
E-Mail: asuits@chem.wayne.edu

Craig Taatjes  
7011 East Ave., MS 9055  
Sandia National Laboratories  
Livermore, CA 94551  
Phone: 925-294-2764  
E-Mail: cataatj@sandia.gov

Donald Thompson  
601 S. College Ave.  
University of Missouri, Columbia  
Columbia, MO 65211  
Phone: 573-882-0051  
E-Mail: thompsondon@missouri.edu

Alison Tomlin  
ERRI, University of Leeds  
University of Leeds  
Leeds, W. Yorks LS6 4LE  
Phone: +44 113 3432500  
E-Mail: A.S.Tomlin@leeds.ac.uk

Robert Tranter  
9700 S Cass Ave.  
Argonne National Laboratory  
Argonne, IL 60439  
Phone: 630-252-6505  
E-Mail: tranter@anl.gov

Wing Tsang  
100 Bureau Drive  
National Institute of Standards and Technology  
Gaithersburg, MD 20899  
Phone: 301-975-2507  
E-Mail: wing.tsang@nist.gov

Frank Tully  
SC-22.1/19901 Germantown Road  
US DOE Office of Basic Energy Sciences  
Germantown, MD 20874  
Phone: 301-903-5998  
E-Mail: frank.tully@science.doe.gov

James Valentini  
3000 Broadway, MC 3120  
Department of Chemistry  
Columbia University  
New York, NY 10027  
Phone: 212-854-7590  
E-Mail: jjv1@columbia.edu

Albert Wagner  
9700 S. Cass Avenue, Bldg. 200  
Chemistry Division  
Argonne National Laboratory  
Argonne, IL 60439  
Phone: 630-252-3570  
E-Mail: wagner@tcg.anl.gov

## Participants

Peter Weber  
Box H  
Brown University  
Providence, RI 02912  
Phone: 401-863-3767  
E-Mail: Peter\_Weber@brown.edu

Charles Westbrook  
P. O. Box 808  
Lawrence Livermore National Laboratory  
Livermore, CA 94550  
Phone: 925-422-4108  
E-Mail: westbrook1@llnl.gov

Phillip Westmoreland  
Chemical Engineering, 159 Goessmann  
University of Massachusetts, Amherst  
Amherst, MA 01003  
Phone: 413-545-1750  
E-Mail: westm@ecs.umass.edu

Kevin Wilson  
One Cyclotron Road, MS: 6R2100  
Lawrence Berkeley National Laboratory  
Berkeley, CA 94720  
Phone: 510-495-2474  
E-Mail: KRWilson@lbl.gov

Curt Wittig  
Department of Chemistry  
University of Southern California  
Los Angeles, CA 90089  
Phone: 213-740-7368  
E-Mail: wittig@usc.edu

David Yarkony  
3400 N. Charles Street  
Department of Chemistry  
Johns Hopkins University  
Baltimore, MD 21218  
Phone: 415 516-4663  
E-Mail: yarkony@jhu.edu

Hua-Gen Yu  
Chemistry Department  
Brookhaven National Laboratory  
Upton, NY 11973  
Phone: 631-344 4367  
E-Mail: hgy@bnl.gov

Timothy Zwier  
Department of Chemistry  
Purdue University  
West Lafayette, IN 47907-2084  
Phone: 765-494-5278  
E-Mail: zwier@purdue.edu